

# Thèse de Doctorat

\* (instructions page en annexe)

## Matthieu GARNIER

*Mémoire présenté en vue de l'obtention du  
grade de Docteur de l'Université de Nantes  
sous le label de L'Université Nantes Angers Le Mans*

École doctorale : *Végétal, Environnement, Nutrition, Agroalimentaire, Mer (VENAM).*

Discipline : *Physiologie, biologie des organismes, populations, interactions*

Spécialité : *Biologie marine et microbiologie.*

Unité de recherche : *IFREMER, Unité BRM, Laboratoire PBA*

Soutenue le 29 juin 2016

Thèse N° :

## Allocation du carbone et métabolisme azoté chez l'haptophyte *Tisochrysis lutea*.

### JURY

Rapporteurs : **Angela FALCIATORE**, Chercheur HDR, CNRS - UMR 7238 - Université Pierre et Marie Curie Paris 06  
**Thierry TONON**, Maître de conférences HDR, Université Pierre et Marie Curie Paris 06

Examineurs : **Bernard OFFMANN**, Professeur HDR, Université de Nantes-FRE 3478  
**Benoît SCHOEFS**, Professeur HDR, Université du Maine- IUML -IFR 3473  
**Raffaele SIANO**, Chercheur, IFREMER  
**Philippe SOUDANT**, Directeur de recherche CNRS, UBO-LEMAR-UMR6539

Directeur de Thèse : **Jean-Paul CADORET**, Directeur de recherche, Greensea  
Co-directeur de Thèse : **Bruno SAINT-JEAN**, Chercheur IFREMER



Allocation du carbone et métabolisme  
azoté chez l'haptophyte *Tisochrysis*  
*lutea*.

---



*Pour Armand.*

*Pour Jason*

*Pour Emilien*

*Pour Hyacinthe*



## Remerciements

D'une manière générale, je souhaite remercier l'organisme IFREMER au sein duquel j'ai le plaisir de travailler depuis plus de 15 ans, et qui m'a permis de me former tout au long de ces années et de présenter aujourd'hui ce travail de thèse. Merci aux femmes et hommes qui y travaillent et œuvrent avec passion pour la connaissance du monde marin.

Je remercie Jean-Paul Cadoret, de m'avoir accueilli au laboratoire BPA et soutenu dans l'engagement et la réalisation de cette thèse sur les microalgues. Merci à Gaël Bougaran d'avoir préservé jusqu'au bout les conditions sereines pour l'accomplissement de ce travail.

Ce travail a été encadré par Bruno Saint-Jean. Un très grand merci à toi.

Merci à Angela Falciatore et Thierry Tonon d'avoir accepté d'être rapporteur de cette thèse et merci à Raffaele Siano, Philippe Soudant, Benoît Schoefs et Bernard Hofmann d'avoir accepté de l'examiner.

Merci à Catherine Leblanc et David Macherel d'avoir accompagné ce travail au sein du comité de thèse.

**L'ensemble de cette thèse est le fruit d'un travail collectif, cohésif et exaltant réalisé au sein du laboratoire PBA.** Cette dynamique fructueuse est possible grâce à l'implication active et bienveillante de tous les participants à ce laboratoire que je remercie.

Je remercie notamment la Patateam : Bruno Saint-Jean, Jean- Baptiste Berard, Gregory Carrier, Nathalie Schreiber, et Aurelie G-Charrier d'avoir collectivement participé à l'élaboration des expériences, à leur déroulement et à leur valorisation. Merci à Ewa Lukomska, Catherine Rouxel, Stanislas Thiriet-Rupert, Raymond Kaas, Aurelie Charrier, Christelle Château, Caroline Baroukh et Alice Rimbault pour leur contribution à ce travail. Merci aussi à Loic Le Dean, Elodie Nicolau, Judith Rumin, Myriam Le Chevanton, Hansy Haberkorn. Et enfin merci Isabelle Richard qui sait rendre la vie au laboratoire plus simple.

Merci aux copains.

Merci Jean François et Christiane.

Merci Magali.

# Table des matières

|   |           |
|---|-----------|
| Liste des publications et communications orales .....   | 9         |
| Liste des figures .....   | 1         |
| <b>Introduction générale.....</b>   | <b>17</b> |
| 1. Le phytoplancton.....  | 17        |
| 2. La limitation minérale et production primaire océanique .....  | 19        |
| 3. Histoire évolutive et diversité des microalgues .....  | 21        |
| 4. Les haptophytes. ....  | 25        |
| 5. Les microalgues, des usines cellulaires pour les biotechnologies.....  | 31        |
| 6. Métabolisme de l'azote chez les microalgues.....   | 35        |
| A. Absorption et assimilation de l'azote.....   | 35        |
| B. Limitations et carences azotées : définitions et outils d'étude.....   | 37        |
| C. Impact de la limitation et de la carence sur le métabolisme de l'azote. ....   | 42        |
| 7. Le métabolisme du carbone chez les microalgues.....  | 45        |
| A. La fixation autotrophe du carbone.....   | 45        |
| B. La fixation hétérotrophe du carbone.....   | 49        |
| C. Les voies métaboliques cœur.....   | 49        |
| 8. Le stockage du carbone.....  | 53        |
| A. Les sucres de réserve.....   | 53        |
| B. Les lipides de réserve.....  | 55        |
| C. Recyclage métabolique du carbone. ....   | 63        |
| 9. Impact de la carence azotée sur le métabolisme du carbone.....   | 65        |
| A. Carence azotée et stockage du carbone. ....  | 65        |
| B. Baisse de la fixation du carbone.....  | 66        |
| C. Origine des lipides lors de la carence azotée: Remobilisation intracellulaire du carbone ou<br>synthèse de novo ? .....  | 67        |
| 10. <i>Tisochrysis lutea</i> , espèce modèle pour l'étude du métabolisme des haptophytes. ....  | 68        |
| 11. Présentation de l'étude.....  | 71        |
| <b>Chapitre I : Identification et régulation des transporteurs d'azote de <i>Tisochrysis</i><br/><i>lutea</i>.....</b>  | <b>76</b> |
| 1. Introduction.....  | 76        |
| 2. Résultats principaux et perspectives.....  | 77        |
| 3. Article .....  | 79        |
| <b>Chapitre II : Les bases moléculaires de <i>Tisochrysis lutea</i>. Analyses<br/>transcriptomiques comparatives entre la souche sauvage (WT) et souche mutante<br/>hyper-lipidique S2M2 en carence azotée.....</b> | <b>9</b>  |
| 1 Introduction.....   | 99        |
| 2 Résultats principaux et perspectives.....   | 100       |
| 3. Article .....  | 101       |



### **Chapitre III : Effets de la carence azotée chez *Tisochrysis lutea*. Analyses protéomiques comparatives entre la souche sauvage (WT) et une souche mutante hyper lipidique (S2M2) sous différentes conditions de disponibilité en azote. ...11**

|   |     |
|---|-----|
| 1 Introduction.....   | 119 |
| 2 Résultats principaux .....  | 120 |
| 3 Résultats complémentaires : Etude des kinases et phosphatases mutées..... | 123 |
| 4 Bilan et perspectives .....   | 126 |
| 3. Article .....  | 127 |

### **Chapitre IV : Limitation azotée et allocation du carbone chez *Tisochrysis lutea*.**

#### **Approche intégrative appliquée en chémostat.....14**

|  |     |
|--|-----|
| 1 Introduction.....  | 14  |
| 2 Caractérisation des souches clonales en culture batch .....  | 14  |
| 3 Hypothèses et modèles écophysologiques. ....   | 14  |
| 4 Validation des hypothèses: Etude dynamique de la limitation azotée et de l'allocation du carbone.<br>..... | 1   |
| 5 Identification du protéome de <i>T. lutea</i> et analyses comparatives.....                                | 1   |
| 6 Expression génique des protéines identifiées.....  | 1   |
| 7. Article .....   | 184 |

### **Chapitre V : CSAP & PLAAOX, deux protéines majeures régulées par l'azote.**

#### **Annotation et étude de leur régulation. ....18**

|   |     |
|---|-----|
| 2 Matériel et méthodes.....   | 188 |
| <i>Matériel biologique</i> .....                                    | 188 |
| <i>Extraction des ARNs et production d'ADN complémentaire</i> ..... | 188 |
| <i>Clonage et séquençage des régions codantes.</i> .....            | 190 |
| <i>Mesures d'expression</i> .....                                   | 190 |
| <i>Analyses bio-informatiques</i> .....                             | 191 |
| 3 Résultats .....   | 192 |
| <i>Clonage et séquençage</i> .....                                  | 192 |
| <i>Analyses de séquence protéique</i> .....                         | 192 |
| <i>Recherche de protéines orthologues</i> .....                     | 193 |
| <i>Structures génomiques</i> .....                                  | 194 |
| <i>Régulation transcriptionnelle</i> .....                          | 197 |
| 4 Discussion .....  | 197 |

#### **Conclusions générales et perspectives. ....20**

|  |     |
|--|-----|
| Des transporteurs d'azote identifiés.....                            | 203 |
| Vers la caractérisation fonctionnelle des transporteurs .....        | 203 |
| Les voies métaboliques principales : avancées et perspectives.....   | 204 |
| Limitation azotée et orientation métabolique .....                   | 205 |
| Les niveaux de régulation.....                                       | 206 |
| Limitation azotée et métabolisme du carbone : Clés métaboliques..... | 206 |
| Perspectives.....  | 207 |
| Bilan .....  | 208 |



## Liste des publications et communications orales

### ✓ Publications soumises incluses dans cette thèse

**Garnier M**, Bougaran G, Pavlovic M, Berard JB, Carrier G, Charrier A, Le Grand F, Lukomska E, Rouxel C, Schreiber N, Nicolau E, Cadoret JP, Rogniaux H, Saint-Jean B, (Submitted in January 2016) Use of a lipid rich strain reveals mechanisms of nitrogen limitation and carbon partitioning in the haptophyte *Tisochrysis lutea*. Submitted to algal research.

### ✓ Publications publiées incluses dans cette thèse

**Garnier M**, Carrier G, Rogniaux H, Nicolau E, Bougaran G, Saint-Jean B, Cadoret JP (2014) Comparative proteomics reveals proteins impacted by nitrogen deprivation in wild-type and high lipid-accumulating mutant strains of *Tisochrysis lutea*. J Proteomics 105: 107–120

Cadoret J-P, **Garnier M**, Saint-Jean B (2012) Chapter Eight - Microalgae, Functional Genomics and Biotechnology. In Gwenaël Piganeau, ed, Adv. Bot. Res. Academic Press, pp 285–341

Carrier G, **Garnier M**, Le Cunff L, Bougaran G, Probert I, De Vargas C, Corre E, Cadoret J-P, Saint-Jean B (2014) Comparative Transcriptome of Wild Type and Selected Strains of the Microalgae *Tisochrysis lutea* Provides Insights into the Genetic Basis, Lipid Metabolism and the Life Cycle. PLoS ONE 9: e86889

Cadoret J-P, Bougaran G, Bérard J-B, Carrier G, Charrier A, Coulombier N, **Garnier M**, Kaas R, Le Déan L, Lukomska E, et al (2014) Microalgae and Biotechnology. In A Monaco, P Prouzet, eds, Dev. Mar. Resour. John Wiley & Sons, Inc., pp 57–115

Charrier A, Bérard J-B, Bougaran G, Carrier G, Lukomska E, Schreiber N, Fournier F, Charrier AF, Rouxel C, **Garnier M**, et al (2015) High-affinity nitrate/nitrite transporter genes (Nrt2) in *Tisochrysis lutea*: identification and expression analyses reveal some interesting specificities of Haptophyta microalgae. Physiol Plant. doi: 10.1111/ppl.12330

### ✓ Publications en lien avec les sujets de la thèse

Le Chevanton M, **Garnier M**, Bougaran G, Schreiber N, Lukomska E, Bérard J-B, Fouilland E, Bernard O, Cadoret J-P (2013) Screening and selection of growth-promoting bacteria for *Dunaliella* cultures. Algal Res 2: 212–222

Vasseur C, Bougaran G, **Garnier M**, Hamelin J, Leboulanger C, Chevanton ML, Mostajir B, Sialve B, Steyer J-P, Fouilland E (2012) Carbon conversion efficiency and population dynamics of a marine algae–bacteria consortium growing on simplified synthetic digestate: First step in a bioprocess coupling algal production and anaerobic digestion. Bioresour Technol 119: 79–87

### ✓ Communications orales sur le sujet de thèse

Garnier Matthieu (2015). *Tisochrysis lutea* 2Xc1 strain is so fat. Why? EPC6 - 6th European Phycological Congress. 23-28 August 2015, London. Poster

Garnier Matthieu (2013). *Tisochrysis lutea* 2X strain is so fat. Why? Journées Société Phycologique de France. 24-25 septembre 2015, Vannes. Présentation orale 15mn

Garnier Matthieu (2014). Use of selected strain to study nitrogen physiology in relation to lipid accumulation. *Tisochrysis lutea* as a promising model? Journées scientifiques de l'école de doctorale VENAM. 20-21 janvier 2014, Angers. Présentation orale 15mn

Garnier Matthieu, Cadoret Jean-Paul (2014). Comparative proteomics reveals proteins impacted by nitrogen deprivation in wild-type and high lipid-accumulating mutant strains of *Tisochrysis lutea*. Alg'n' Chem 2014 : Which future for algae in industry? 31 March – 3 April 2014. Présentation orale 15mn

Garnier Matthieu (2013). Use of selected strain to study nitrogen physiology in relation to lipid accumulation. *Tisochrysis lutea* as a promising model? Journées Société Phycologique de France. 16-18 décembre 2013, Roscoff. Présentation orale 15mn

Garnier Matthieu (2013). Use comparative proteomics on a selected microalgae provides candidates for biofuel production. EuPA 2013, 14-17 Octobre 2013, Saint-Malo, France. Poster

#### ✓ **Autres publications**

**Garnier M**, Matamoros S, Chevret D, Pilet M, Leroi F, Tresse O (2010) Adaptation to Cold and Proteomic Responses of the Psychrotrophic Biopreservative Lactococcus piscium Strain CNCM I-4031. Appl Environ Microbiol 76: 8011–8018

Azandegbe A, **Garnier M**, Andrieux-Loyer F, Kerouel R, Philippon X, Nicolas J (2010) Occurrence and seasonality of *Vibrio aestuarianus* in sediment and *Crassostrea gigas* haemolymph at two oyster farms in France. Dis Aquat Organ 91: 213–221

**Garnier M**, Labreuche Y, Garcia C, Robert A, Nicolas J (2007) Evidence for the involvement of pathogenic bacteria in summer mortalities of the Pacific oyster *Crassostrea gigas*. Microb Ecol 53: 187–196

**Garnier M**, Labreuche Y, Nicolas J (2008) Molecular and phenotypic characterization of *Vibrio aestuarianus* subsp. *francensis* subsp. nov., a pathogen of the oyster *Crassostrea gigas*. Syst Appl Microbiol 31: 358–365

Andreani A, Cavalli A, Granaiola M, Leoni A, Locatelli A, Morigi R, Rambaldi M, Recanatini M, **Garnier M**, Meijer L (2000) Imidazo[2,1-b]thiazolymethylene- and indolymethylene-2-indolinones: a new class of cyclin-dependent kinase inhibitors. Design, synthesis, and CDK1/cyclin B inhibition. Anticancer Drug Des 15: 447–452

Jeong H, Kim M, Son K, Han M, Ha J, **Garnier M**, Meijer L, Kwon B (2000) Cinnamaldehydes inhibit cyclin dependent kinase 4/cyclin D1. Bioorg Med Chem Lett 10: 1819–1822

Leclerc S, **Garnier M**, Hoessel R, Marko D, Bibb J, Snyder G, Greengard P, Biernat J, Wu Y, Mandelkow E, et al (2001) Indirubins inhibit glycogen synthase kinase-3 beta and CDK5/P25, two protein kinases involved in abnormal tau phosphorylation in Alzheimer's disease - A property common to most cyclin-dependent kinase inhibitors? *J Biol Chem* 276: 251–260

Meijer L, Leost M, **Garnier M**, Leclerc S (1999) The search for and potential therapeutic applications of chemical inhibitors of cyclin dependant protein kinases. *Eur J CANCER* 35: 1574

Meijer L, Leost M, Leclerc S, **Garnier M** (2000a) Cyclin-dependent kinases and their chemical inhibitors: New targets and tools for the study of the testis? *TESTIS EPIDIDYMIS Technol YEAR 2000* 39–58

Meijer L, Thunnissen A, White A, **Garnier M**, Nikolic M, Tsai L, Walter J, Cleverley K, Salinas P, Wu Y, et al (2000b) Inhibition of cyclin-dependent kinases, GSK-3 beta and CK1 by hymenialdisine, a marine sponge constituent. *Chem Biol* 7: 51–63

Mettey Y, Gompel M, Thomas V, **Garnier M**, Leost M, Ceballos-Picot I, Noble M, Endicott J, Vierfond J, Meijer L (2003) Aloisines, a new family of CDK/GSK-3 inhibitors. SAR study, crystal structure in complex with CDK2, enzyme selectivity, and cellular effects. *J Med Chem* 46: 222–236

Pouvreau S, Gangnery A, Tiapari J, Lagarde F, **Garnier M**, Bodoy A (2000a) Gametogenic cycle and reproductive effort of the tropical blacklip pearl oyster, *Pinctada margaritifera* (Bivalvia : Pteriidae), cultivated in Takapoto atoll (French Polynesia). *Aquat LIVING Resour* 13: 37–48

Pouvreau S, Tiapari J, Gangnery A, Lagarde F, **Garnier M**, Teissier H, Haumani G, Buestel D, Bodoy A (2000b) Growth of the black-lip pearl oyster, *Pinctada margaritifera*, in suspended culture under hydrobiological conditions of Takapoto lagoon (French Polynesia). *AQUACULTURE* 184: 133–154

## Liste des figures

|   |    |
|---|----|
| Figure 1 Production primaire océanique de 1997 à 2000.....  | 16 |
| Figure 2 Shéma de la pompe biologique du carbone.....   | 16 |
| Figure 3 Limitation nutritive dans les océans.....  | 18 |
| Figure 4 Vue schématique de l'évolution des plastes dans l'histoire des eucaryotes .....  | 20 |
| Figure 5 Exemples de variations morphologiques chez les haptophytes. ....   | 23 |
| Figure 6 Exemple d'haptophyte munie d'un haptonème développé. ....  | 23 |
| Figure 7 Phylogénie actuelle des haptophytes.....   | 24 |
| Figure 8 Falaise de calcaire datant du crétacé supérieur.....   | 24 |
| Figure 9 Image satellite de blooms attribués à <i>Emiliana huxleyi</i> .....  | 26 |
| Figure 10 Contribution relative des (A) haptophytes, (B) diatomées, et (C) procaryotes photosynthétiques à la production primaire au cours de l'année 2000..... | 28 |
| Figure 11 Analyse bibliométrique des lipides de microalgues. ....   | 33 |
| Figure 12 Schéma de l'absorption et assimilation de l'azote chez les microalgues.....   | 24 |
| Figure 13 Schéma de l'assimilation de l'azote (forme ammoniacale) par le couple enzymatique GS-GOGAT.....   | 36 |
| Figure 14 Relation entre taux de croissance ( $\mu$ ) et quotas cellulaire azoté (QN) dans un chemostat selon Droop (1968).....                                 | 39 |
| Figure 15 Représentation schématique d'une culture en mode batch.....   | 40 |
| Figure 16 Représentation schématique d'une culture en mode chemostat. ....  | 40 |
| Figure 17 Représentation schématique de concentration du carbone chez <i>Chlamydomonas reinhardtii</i> .....  | 44 |
| Figure 18 Représentation schématique de la chaîne photosynthétique .....  | 47 |
| Figure 19 Représentation schématique du cycle de Calvin.....  | 47 |
| Figure 20 Schéma simplifié de l'absorption et assimilation du carbone organique sous forme acétate, glycerol et glucose.....                                    | 28 |
| Figure 21 Schéma simplifié de la glycolyse et néoglucogenèse .....  | 51 |
| Figure 22 Schéma simplifié de la voie des pentoses phosphates .....   | 51 |
| Figure 23 : Localisation cellulaire des réactions de glycolyse et de la voie des pentoses phosphates (PPP) chez les plantes et les microalgues.....             | 51 |
| Figure 24 Schéma simplifié du cycle de Krebs.....   | 52 |
| Figure 25 Schéma simplifié du cycle du glyoxylate .....   | 52 |
| Figure 26 Structures de l'amidon (A) et de la chrysolaminarine (B) et du mannitol (C) .....   | 54 |
| Figure 27 Structures d'acides gras spécifiques de microalgues. ....   | 54 |
| Figure 28 Représentation simplifiée des voies de biosynthèse des lipides chez les microalgues .....   | 58 |
| Figure 29 : Observation au microscope électronique à transmission des vésicules lipidiques (LD) chez <i>Chlamydomonas reinhardtii</i> . ....                    | 60 |
| Figure 30 Schéma d'un vésicule lipidique de plante. ....  | 60 |
| Figure 31 Schéma simplifié de la dégradation des TAG et $\beta$ -oxydation.....   | 64 |
| Figure 32 Phylogénie des Isochrysidales sur la base des séquences 18S.....  | 69 |
| Figure 33 <i>Tisochrysis lutea</i> observé au microscope électronique à transmission. ....  | 69 |
| Figure 34 flux de carbone simplifié utilisé par Mairet <i>et al.</i> pour modélisation (Mairet <i>et al.</i> , 2011)..  | 70 |

|   |     |
|---|-----|
| Figure 35 : Résultats d'amélioration du contenu en acide gras de <i>T. lutea</i> dans le cadre du projet Shamash. ....  | 70  |
| Figure 36 Représentation du transporteur NRT2 chez <i>Hordeum vulgare</i> (Forde, 2000) .....   | 75  |
| Figure 37 Cultures batch limitées par l'azote <i>T. lutea</i> en début de phase stationnaire. ....  | 98  |
| Figure 38 Suivi de cultures batch des souches WT et S2M2. ....  | 98  |
| Figure 39 Analyse de ploïdie : .....  | 102 |
| Figure 40 : Suivi de cultures batch des souches WT et S2M2. ....  | 118 |
| Figure 41: Modifications posttraductionnelles observées sur gel 2-DE.....   | 122 |
| Figure 42 Structure tridimensionnelle d'une serine thréonine phosphatases PP2Cc humaine. ....   | 125 |
| Figure 43 Structure tridimensionnelle de la Cycline Dependant Kinase 2 humaine. ....  | 125 |
| Figure 44 Suivi de croissance en mode batch limité par l'azote des souches multiclonales WT et S2M2 (2X) et des souches clonales WTc1 et 2Xc1.....                                | 145 |
| Figure 45 Présentation schématique d'un model écophysologique.....  | 147 |
| Figure 46 Photobioréacteur 10L utilisé pour les cultures en chemostat limités par l'azote. ....   | 149 |
| Figure 47 Protéomes des souches WTc1 et 2Xc1 analysés sur gel SDS-Page 12%.....   | 150 |
| Figure 48 Cycle du Mannitol.....  | 153 |
| Figure 49 Abondance des protéines CSAP et PLAAOx chez les souches WTc1 et 2Xc1 en limitation azotée. ....   | 158 |
| Figure 50 Corrélation entre analyses RNAseq et quantification protéique « label free ». ....  | 186 |
| Figure 51 Proteome de <i>T. lutea</i> WT en carence azotée observé sur gel 2D-E. ....   | 186 |
| Figure 52 Distribution de l'abondance protéique des 4332 protéines de <i>T. lutea</i> WTc1 identifiées par spectrométrie de masse lors de la limitation azotée (Chapitre IV)..... | 186 |
| Figure 53 Caractérisation des échantillons pour mesures d'expression des gènes des protéines CSAP et PLAAOx. ....   | 189 |
| Figure 54 Structures primaires des protéines PLAAOx et CSAP de <i>T. lutea</i> . ....   | 195 |
| Figure 55 Représentation schématique du scaffold 1920 du génome de <i>T. lutea</i> . ....   | 195 |
| Figure 56 Cinétique d'expression relative des gènes PLAAOx et CSAP1 après spike azoté. ....   | 196 |
| Figure 57 Hypothèse d'action conjointe de la CSAP et de la PLAAOx dans la remobilisation des acides aminés vers le métabolisme du carbone et de l'azote.....                      | 200 |





# Introduction générale

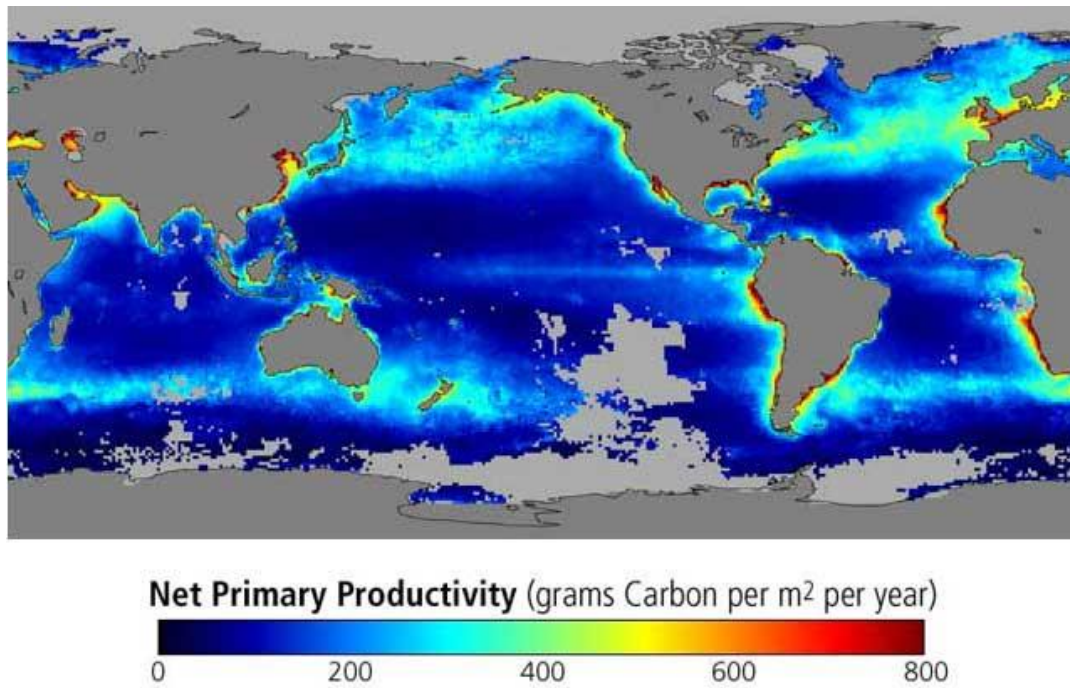


Figure 1 Production primaire océanique de 1997 à 2000. (Source : <http://oceancolor.gsfc.nasa.gov/SeaWiFS/>).

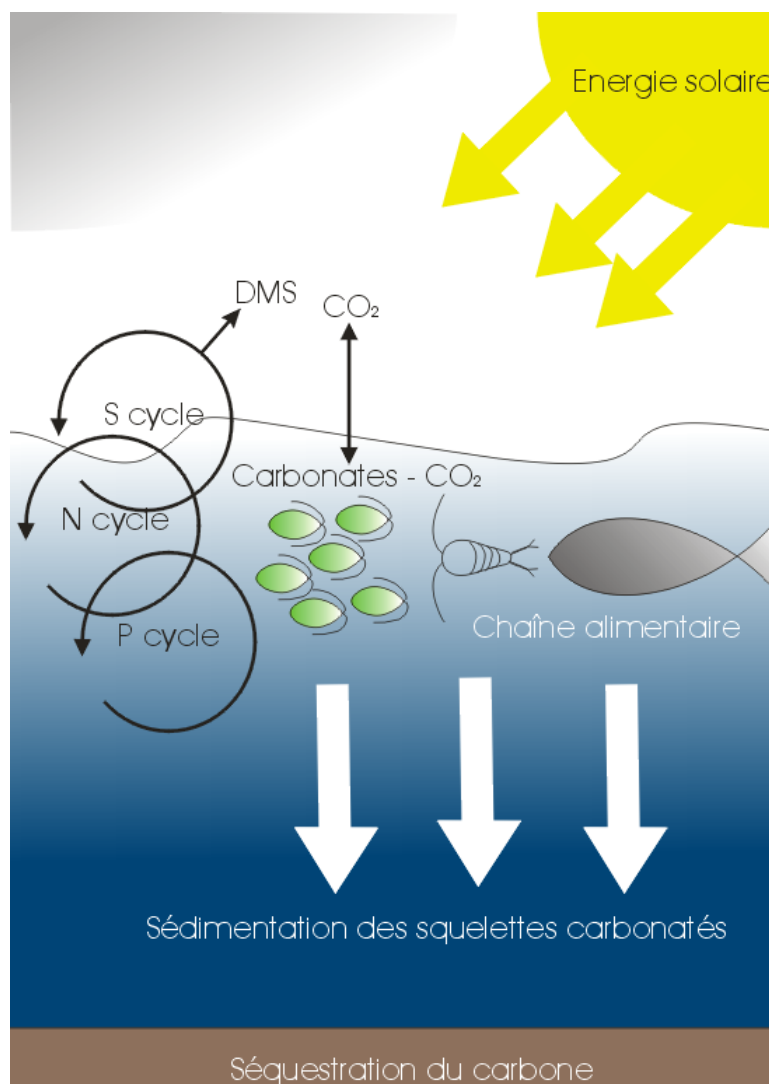


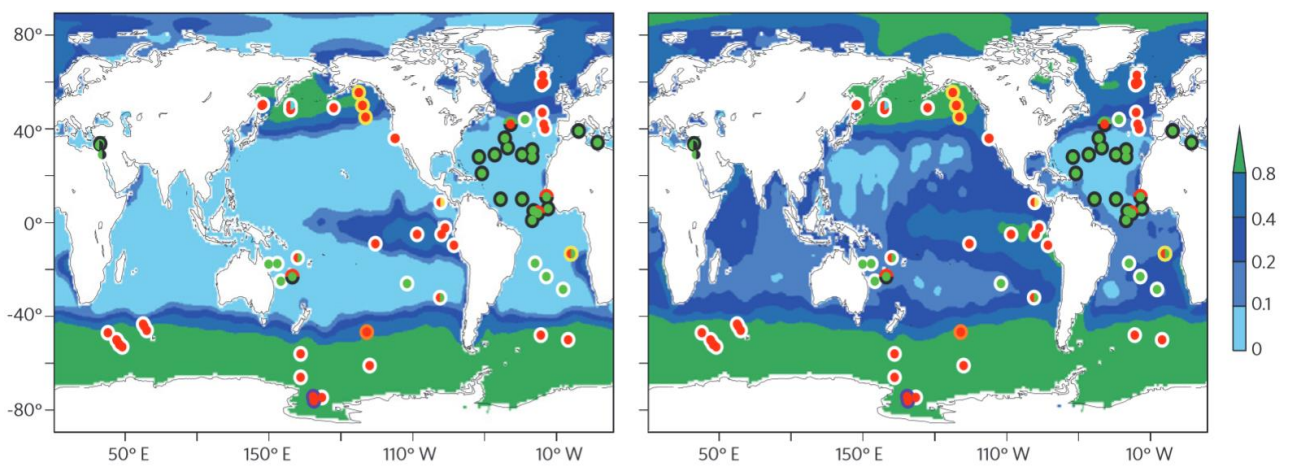
Figure 2 Schéma de la pompe biologique du carbone océanique.

## Introduction générale.

### 1. Le phytoplancton.

Le terme phytoplancton englobe l'ensemble des micro-organismes photosynthétiques eucaryotes et procaryotes (cyanobactéries) qui vivent dans la zone euphotique des océans et des milieux aquatiques dulcicoles. Le phytoplancton est à la base de l'ensemble des réseaux trophiques en milieu marin, à l'exception des écosystèmes hydrothermaux profonds où elle est assurée par des bactéries et archaeobactéries chimiolithoautotrophes. Il ne représente que 1 % de la biomasse photosynthétique de la planète, et pourtant, il assure plus de 45 % de la production primaire mondiale et plus de 90% de la production primaire du milieu aquatique (Geider *et al.*, 2001) (**Figure 1**). Le phytoplancton contribue considérablement aux processus biogéochimiques et climatiques de la planète, tels que la production d'oxygène, le recyclage des nutriments, et la séquestration du carbone atmosphérique responsable de l'effet de serre. Chaque année, près de 10 milliards de tonnes de carbone fixés par le phytoplancton sous forme de matière organique ou de squelettes carbonatés sont exportés vers les zones profondes de l'océan par sédimentation des cadavres et autres particules organiques. Il joue ainsi un rôle primordial de puits de carbone de l'atmosphère vers le fond des océans (**Figure 2**). L'étude des mécanismes impliqués dans la séquestration et l'allocation du carbone par le phytoplancton est donc primordiale pour la compréhension des cycles biogéochimiques de la planète.

La grande majorité du phytoplancton océanique est composée de micro-organismes procaryotes (ou cyanobactéries), relativement peu diversifiés, et appartenant aux genres *Prochlorococcus* et *Synechococcus* que l'on retrouve dans les eaux de surface de l'ensemble des océans. Il est généralement considéré que les communautés des eaux oligotrophes subtropicales sont largement dominées par les cyanobactéries, puis, par des eucaryotes photosynthétiques de taille inférieure à deux micromètres (Scanlan *et al.*, 2009). Les eucaryotes photosynthétiques sont beaucoup plus diversifiés que les cyanobactéries (Finazzi *et al.*, 2010). Ils dominent les communautés dans les zones plus riches en sels nutritifs, près des côtes, des pôles, et dans les zones d'« upwelling ». Il est considéré que les eucaryotes photosynthétiques les plus abondants sont les diatomées, responsables à elles seules de 20% de la fixation de dioxyde de carbone (CO<sub>2</sub>) par photosynthèse sur notre planète (Field *et al.*, 1998), viennent ensuite les dinoflagellés puis les haptophytes.



**Figure 3 Limitation nutritive dans les océans.** (Source : Moore et al., 2013)

Le fond de carte indique les concentrations en azote sur la carte de gauche et en phosphore sur la carte de droite (en  $\mu\text{mol.kg}^{-1}$ ). Les cercles indiquent les natures du premier et du deuxième élément limitant : le disque interne est coloré selon la nature du premier élément limitant et la coloration du contour périphérique indique la nature du second élément limitant. En cas de co-limitation, le disque central est bicolore. Azote en vert ; Phosphore en noir ; Fer en rouge, Silicates en orange, Cobalt en jaune, Zinc en bleu et vitamine B12 en violet.

L'ensemble de ces microorganismes interagissent par des échanges trophiques, allopathiques et physiques au sein de communautés dont les structures sont étroitement guidées par des facteurs biotiques (relations trophiques, mutualismes, symbioses, infections virales) et abiotiques (température et limitation trophique) (Vargas *et al.*, 2015).

## 2. La limitation minérale et production primaire océanique

Le développement des organismes phytoplanctoniques nécessite l'apport par l'environnement d'un ensemble d'éléments minéraux utilisés pour la production de matière organique grâce à la photosynthèse. Les composants de l'appareil photosynthétique, les enzymes et autres protéines de structure sont riches en azote et en fer. Le phosphore est un des principaux constituants des acides nucléiques et des lipides membranaires. Il est également impliqué dans le transfert de l'énergie et le métabolisme cellulaire car c'est un composant de métabolites énergétiques (nucléotides phosphates ATP et ADP) et métabolites du pouvoir réducteur (NADP, NADPH). Les silicates sont utilisés par les diatomées pour la construction de leur squelette externe siliceux. Dans les océans, la production primaire est généralement limitée par la disponibilité en l'un de ces éléments minéraux de base ou plus rarement de cofacteur enzymatique comme la vitamine B12 (Boyd *et al.*, 2010). Les concentrations en éléments nutritifs dans l'environnement dépendent d'apports exogènes (précipitations, proximité des estuaires et des sources hydrothermales, mise en suspension des sédiments), des flux de masse d'eau (« upwellings », courants océaniques) et des activités biologiques qui participent au cycle de la matière organique (reminéralisation bactérienne, sécrétion par des organismes hétérotrophes). De ce fait, la concentration des éléments nutritifs est hétérogène en fonction des zones géographiques. On mesure ainsi des productivités primaires différentes en fonction des zones océaniques (**Figure 1**). La nature de l'élément limitant est également un élément variable en fonction des zones géographiques (**Figure 3**). D'une manière générale, l'azote est considéré comme étant le premier élément limitant dans une grande partie de l'océan. Cependant, et bien que les configurations spatiales restent assez floues, le fer est l'élément limitant dans les eaux proches des pôles et dans les zones d'« upwelling » de l'océan Austral et de l'est du Pacifique. Le phosphore, la vitamine B12 et d'autres oligo-éléments peuvent aussi co-limiter la production primaire (Moore *et al.*, 2013). L'impact de la limitation des éléments nutritifs, et notamment de l'azote, sur la production primaire et le métabolisme du carbone est donc un sujet important pour évaluer les rôles du phytoplancton dans la séquestration du carbone.

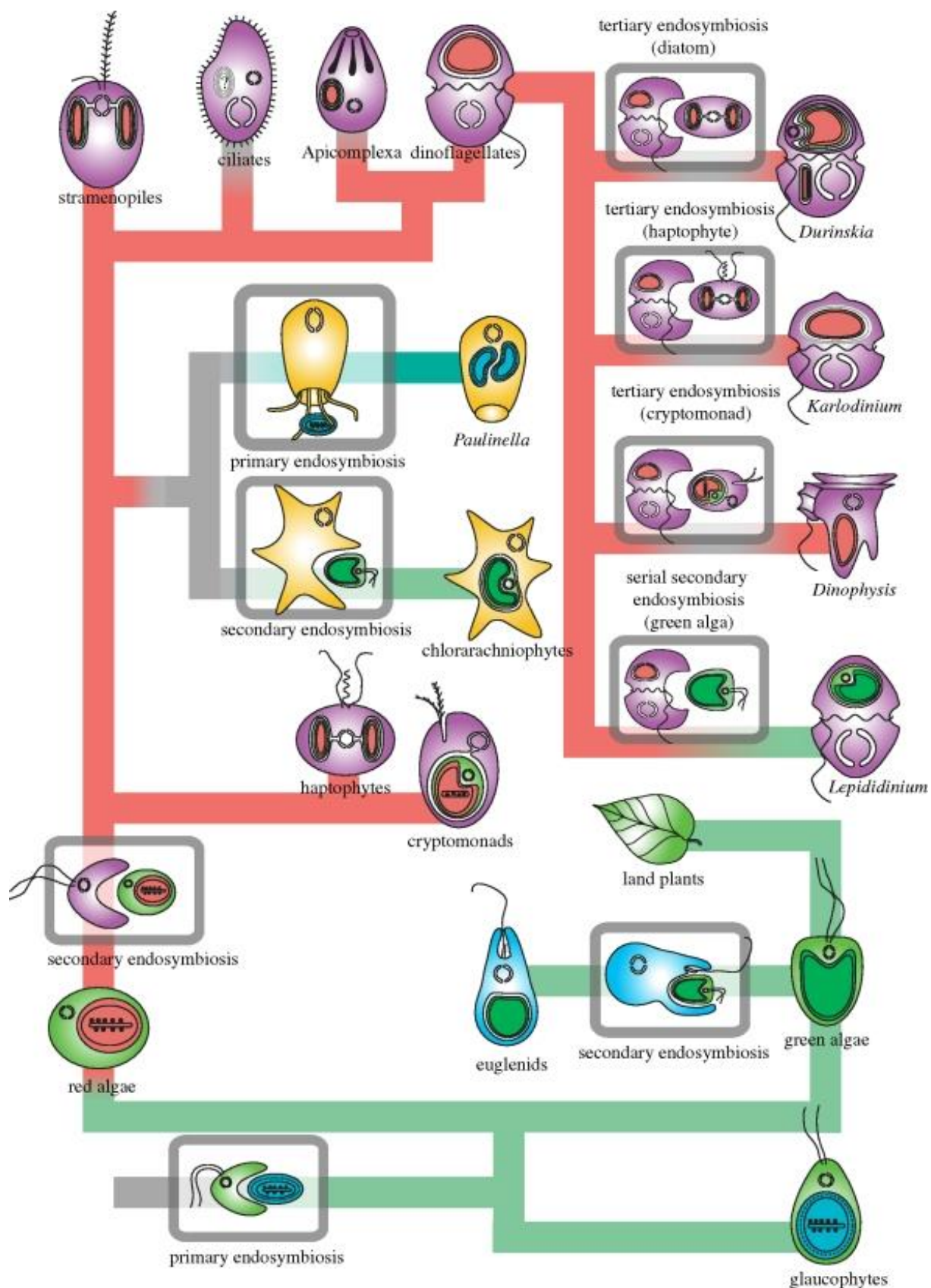


Figure 4 Vue schématique de l'évolution des plastes dans l'histoire des eucaryotes. (Source : Keeling et al, 2010)

### 3. Histoire évolutive et diversité des microalgues

Le terme « microalgue » est employé dans certains cas pour définir l'ensemble des microorganismes photosynthétiques et dans d'autres cas pour définir uniquement les microorganismes eucaryotes photosynthétiques. Nous retiendrons cette dernière définition dans la suite de ce document.

Les microalgues constituent un groupe très diversifié, de par leur morphologie, leur composition biochimique ou leur métabolisme. L'origine polyphylétique ou monophylétique des microalgues a largement été débattue dans la communauté spécialisée. L'analyse des données moléculaires, accessibles depuis seulement quelques années, tend à montrer une origine monophylétique de ces organismes (Keeling, 2010). Les premiers eucaryotes photosynthétiques oxygénés seraient apparus il y a environ 1,8 milliards d'années à partir d'un événement d'endosymbiose d'un organisme procaryote photosynthétique, proche des cyanobactéries actuelles, par un organisme eucaryote unicellulaire. Cette première endosymbiose aurait donné lieu au groupe des archaeplastidae (Woese and Fox, 1977; Delwiche, 1999; Curtis *et al.*, 2012). Une succession de perte de gènes, d'échanges géniques et de changements structurels auraient peu à peu fait évoluer l'organisme photosynthétique phagocyté en un organite responsable de la photosynthèse : le chloroplaste. L'évolution divergente du chloroplaste au sein de la cellule aurait donné lieu à trois embranchements: Les glaucophytes, proches de l'ancêtre commun des archaeplastidae, les chlorophycées ou algues vertes, et les rhodophycées ou algues rouges. Ces embranchements divergent notamment par la nature des pigments chloroplastiques et par la structure de la Rubisco, protéine clé de la photosynthèse. Il y a 500 millions d'années, les embryophytes auraient divergé des chlorophycées pour donner naissance aux plantes terrestres (Hedges *et al.*, 2004, Keeling *et al.*, 2005).

C'est suite à différents événements d'endosymbiose des archaeplastidae par des organismes unicellulaires eucaryotes que serait apparu le groupe polyphylétique des microalgues. Les chlorarachniophytes et euglènes proviendraient de l'endosymbiose de microalgues vertes. L'endosymbiose de microalgues rouges aurait donné lieu à une très grande diversité d'organismes parmi lesquels sont retrouvés : les chrysophytes, les cryptomonads, les haptophytes, les dinoflagellés, les ciliés et les straménopiles (**Figure 4**). La question de savoir si un ou plusieurs événements indépendants d'endosymbiose d'algue rouge sont à l'origine de ce groupe a été longtemps débattue dans la communauté spécialisée.

Ainsi, Cavalier-Smith (2002), sur la base de la composition pigmentaire des espèces, regroupe les haptophytes, les straménopiles et les cryptophytes au sein d'un même groupe monophylétique appelé chromalvéolates, terme couramment employé pour définir les algues dites « brunes ». Cependant, la monophylie de ce super-groupe ne semble pas être supportée par les études phylogénétiques (Baurain *et al.* 2010). Les nombreux évènements d'endosymbioses tertiaire, de pertes de plastides, et de transferts géniques horizontaux qui ont eu lieu et qui sont toujours en cours, complexifient fortement la reconstruction phylogénique des microalgues. Les estimations du nombre d'espèces d'algues vont de 30 000 à plus

d'un million selon les auteurs, une étude prudente et récente avançant le nombre à 72500 (Guiry, 2012).

Cette très grande diversité phylogénique se reflète par une très grande diversité de métabolismes, de morphologies cellulaires, de contenus pigmentaires, ou de type de cycles de vie. A titre d'exemple, notons les très nombreux types morphologiques des frustules siliceux chez les diatomées ou des thèques de carbonate de calcium chez les haptophytes coccolithophores (Figure 6). Les évènements d'endosymbioses secondaires ont conduit à des structures chloroplastiques diversifiées. Par exemple, les chloroplastes de cryptophytes comme les haptophytes et les straménopiles sont séparés du cytoplasme par quatre membranes, issues de l'assemblage de la membrane plasmique et de la membrane chloroplastique de l'algue rhodophycée phagocytée. Contrairement aux haptophytes, les cryptophytes et les chlorarachniophytes ont conservé le noyau de l'algue phagocytée sous forme vestigiale (le nucléomorphe)(Archibald, 2007). Ces différences de structures internes impliquent l'existence de transporteurs spécifiques pour assurer les flux à travers les quatre membranes des straménopiles (Archibald, 2012). Les métabolismes sont eux aussi extrêmement variés. Si la plupart des microalgues sont photo-autotrophes, c'est à dire qu'elles synthétisent leur matière organique à partir de substances minérales qu'elles puisent dans le milieu grâce à l'énergie photosynthétique, de nombreuses espèces sont capables d'hétérotrophie, puisant alternativement leur énergie à partir de l'hydrolyse de la matière organique ou de la photosynthèse. Certaines microalgues comme les dinoflagellés ont développé des mécanismes de prédation et peuvent vivre plusieurs mois dans l'eau de mer sans recourir à l'énergie photosynthétique (Sherr and Sherr, 2007). Ces espèces se rapprochent, par certains points de vue, du monde animal.



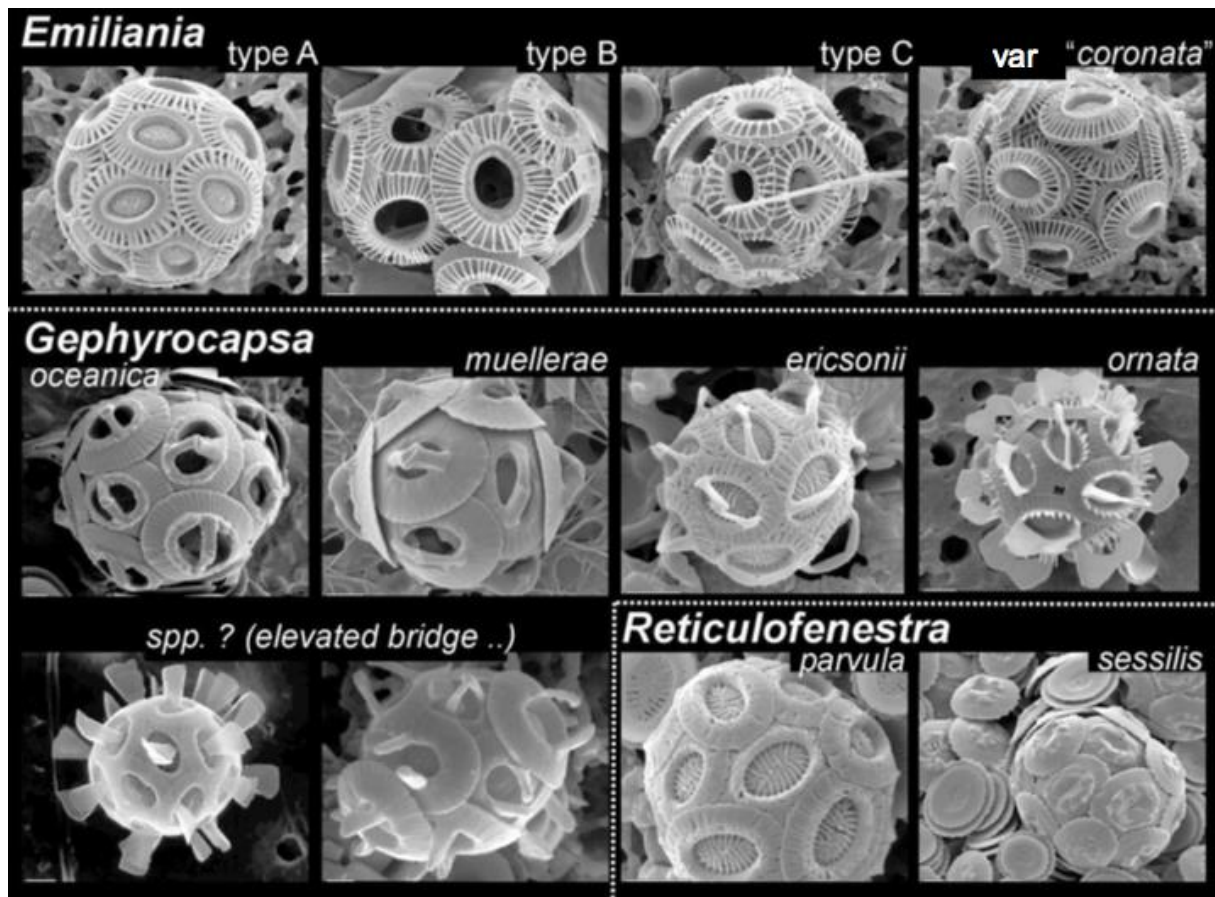


Figure 5 Exemples de variations morphologiques chez les haptophytes. (Source : Young et al., 2003)

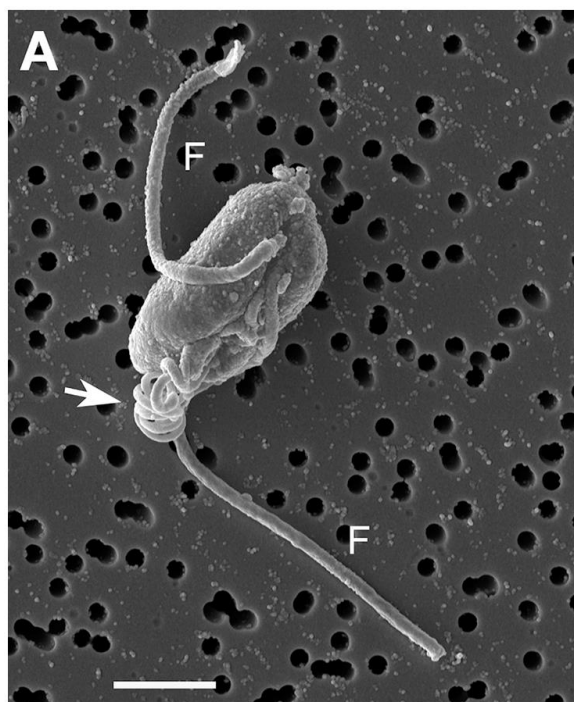


Figure 6 Exemple d'haptophyte munie d'un haptonème développé. (Source : Hovde et al., 2015)

La souche *Chrysmulina tobin* observée au microscope électronique à balayage. La flèche indique l'haptonème.

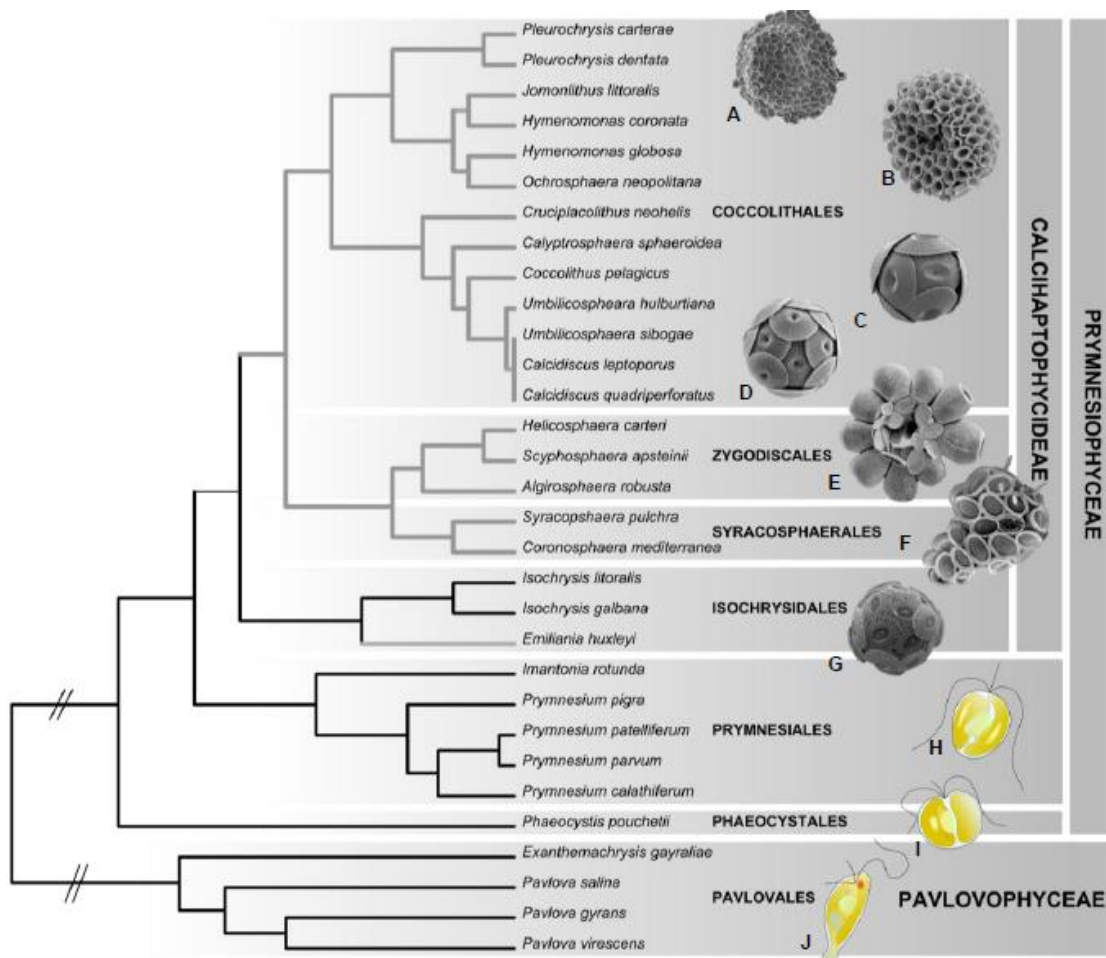


Figure 7 Phylogénie actuelle des haptophytes sur la base de leurs séquences 18S. (Source : Vargas et al., 2007)



Figure 8 Stratifications calciques issues de la sédimentation des squelettes de microalgues coccolithophores durant le crétaé supérieur.

Falaise d'Étretat (Normandie, France) (©Moirent Camille).

#### 4. Les haptophytes.

Les haptophytes, autrement nommés prymnésiophytes, sont des petites microalgues de 2 à 8  $\mu\text{m}$  contenant un ou deux chloroplastes, et caractérisés par la présence d'un haptonème plus ou moins développé à un moment donné de leur cycle de vie. L'haptonème est un appendice filiforme spécifique des haptophytes, inséré entre les deux flagelles. Il permettrait l'adhésion au substrat, le déplacement de particules, voire la capture de proies (Figure 6). Les haptophytes sont divisés en deux groupes qui diffèrent par la taille de leurs flagelles: les Pavlovophyceae et les Coccolithophyceae. Les membres les plus connus, les coccolithophores, se trouvent au sein de ce dernier groupe et sont caractérisés par la présence de plaques extracellulaires plus ou moins calcifiées appelés coccolites. La présence de coccolites dépend cependant des espèces et du cycle de vie et n'est donc plus considéré comme un critère de classification (Brownlee *et al.*, 2015).

De nombreuses espèces présentent un cycle de vie haplodiplophasique, qui alterne des générations diploïdes et haploïde caractérisées par deux morphotypes différents. Ces morphotypes peuvent se développer de façon indépendante par reproduction asexuée. Par exemple, Chez *Emiliania huxleyi*, les cellules diploïdes sont non-mobiles et présentent des coccolites à leur surface alors que les cellules haploïdes ne contiennent pas de coccolite et sont mobiles grâce à la présence de deux flagelles. Le cycle de vie de certaines haptophytes non coccolithophores comme celles appartenant aux genres *Isochrysis* et *Tisochrysis* reste à ce jour très mal connu.

Les haptophytes constituent un groupe monophylétique ancien et diversifié issu de l'endosymbiose secondaire d'une microalgue rouge (Andersen, 2004; Vargas *et al.*, 2007) (**Figure 7**). Les membres de ce taxon étaient présents dès l'ère du Néoprotérozoïque, il y a environ 520 à 1000 millions d'années (Medlin *et al.*, 2008). Les espèces coccolithophores ont commencé à proliférer dans les océans et à impacter de manière significative le cycle du carbone dès la fin du Jurassique il y a environ 150 millions d'années. Ainsi, certains bassins sédimentaires et falaises de craie datant de cette époque sont composés principalement des tests calcaires (ou coccolites) qui encapsulent certains de ces organismes (**Figure 8**). Les océans actuels contiennent une très grande quantité d'haptophytes, souvent de petite taille (pico-haptophytes), et répandues sur l'ensemble des eaux de surface. D'après leurs études, Liu et co-auteurs estiment à plus de 1000 le nombre d'espèces génétiques différentes dans quelques litres d'eau de mer tropicale (Liu *et al.*, 2009).



**Figure 9** Image satellite d'un bloom phytoplanctonique attribué à la souche *Emiliana huxleyi*. (Source : <http://oceancolor.gsfc.nasa.gov/SeaWiFS/>)

Image satellite prise à l'ouest des côtes bretonnes le 26 juin 2000.

Les haptophytes tirent principalement leur énergie de la production primaire mais certaines espèces sont également mixotrophes et sont capables de prédation (Tillmann, 1998). Cette grande flexibilité trophique des haptophytes leur confère un avantage écologique majeur. Certaines espèces comme *Emiliania huxleyi* et *Phaeocystis sp* peuvent former des efflorescences phytoplanctoniques considérables lorsque les conditions environnementales sont favorables. Visibles par images satellites, ces blooms peuvent dépasser les 100 000 km<sup>2</sup> de surface avec des concentrations cellulaires supérieures à 10 000 cellules / ml (**Figure 9**). Les haptophytes participent aux échanges gazeux entre les océans et l'atmosphère. La bio-minéralisation du calcium par les cellules coccolithophores impacte l'alcalinité des eaux de la zone photique des océans. Ainsi, on estime que 50% de la sédimentation du carbonate de calcium dans les océans provient des coccolithes des haptophytes (Milliman, 1993; Shiraiwa, 2003). Ils pourraient aussi jouer un rôle non négligeable dans le cycle du soufre à travers la production de diméthylsulfure (DMS), principale composé organique sulfuré volatile émis par les océans (Li *et al.*, 2010a). Les coccolithophores jouent donc un rôle primordial dans les cycles biogéochimiques de la planète.

Les haptophytes caractérisent notamment le phytoplancton tropical mais sont présents dans tous les écosystèmes photosynthétiques océaniques. Les espèces les plus étudiées sont les espèces coccolithophores et principalement *Emiliania huxleyi*, une coccolithophore de l'ordre des Isochrysidales et de la famille des Noelaerhabdaceae. Il s'agit de l'haptophyte la plus fréquemment identifiée dans les blooms océaniques qui participe considérablement à la séquestration du carbone atmosphérique (Paasche, 2001).

Certaines études suggèrent que le rôle écologique des haptophytes non coccolithophores, plus difficiles à détecter que les organismes calcifiés, est souvent fortement sous-estimé (Liu *et al.*, 2009). Les haptophytes sont les uniques producteurs d'un pigment photosynthétique (le 19'-hexanoyloxyfucoxanthin) omniprésent dans l'eau de mer (**Figure 10**). Un bilan quantitatif de l'importance de ce pigment à l'échelle globale au cours de l'année 2000 suggère que la biomasse de ces organismes serait jusqu'à deux fois plus importante que celle des cyanobactéries ou des diatomées, et que les haptophytes pourraient contribuer de 30 à 50 % à la production primaire océanique (Liu *et al.*, 2009).

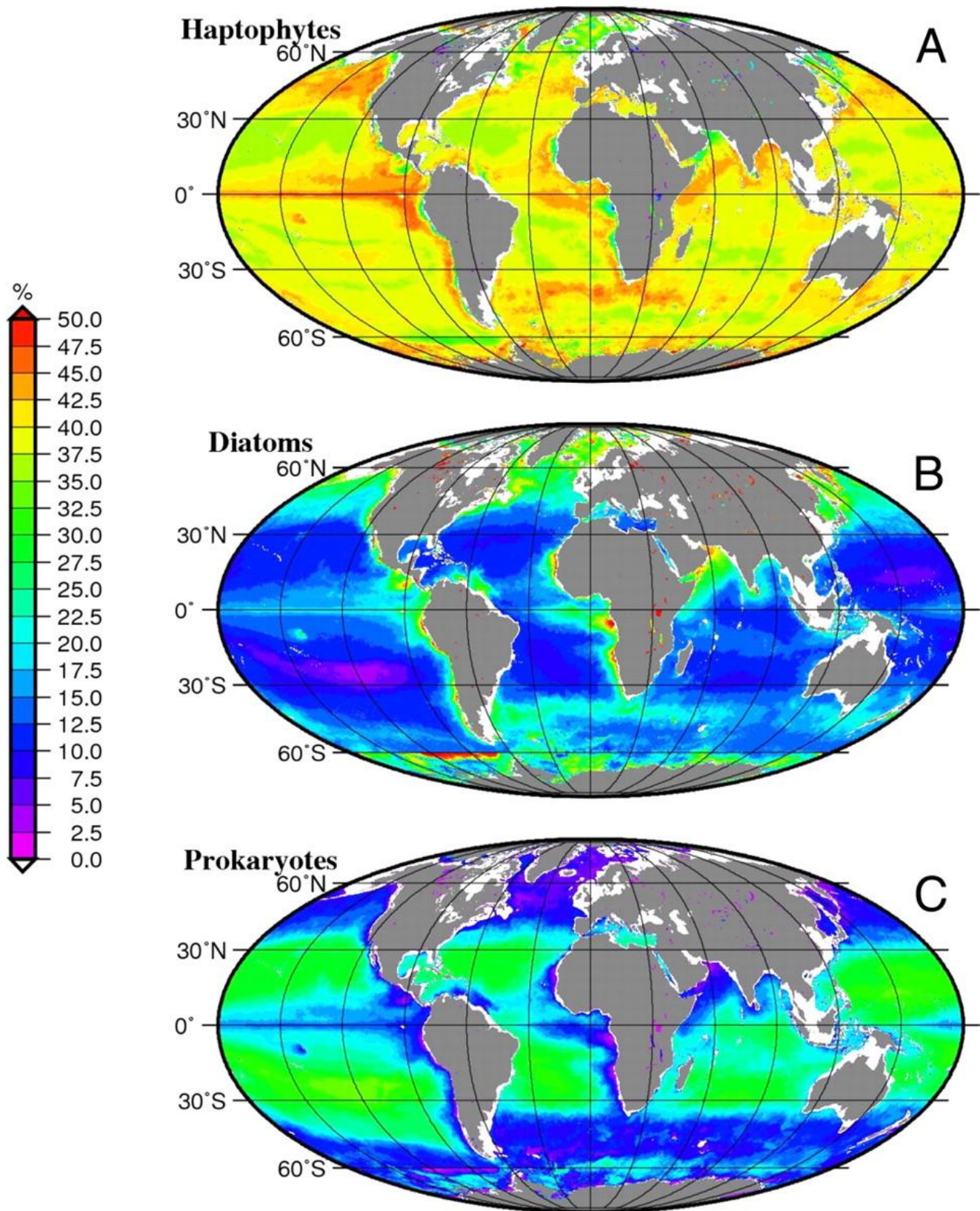


Figure 10 Contribution relative des (A) haptophytes, (B) diatomées, et (C) procaryotes photosynthétiques à la production primaire au cours de l'année 2000. (Source : Liu et al. 2009)

D'autre part, les haptophytes de l'ordre des isochrysidales produisent des alkénones, lipides neutres à très longue chaînes (C37-C39) impliqués dans le stockage du carbone (Eltgroth *et al.*, 2005). (Eltgroth *et al.*, 2005). Suite à la sédimentation des haptophytes, ces lipides, dont le niveau d'insaturation dépend de la température, sont emprisonnés dans les sédiments marins et sont utilisés comme bio-marqueurs par les paléo-climatologues pour la datation des sédiments marins (Eglinton and Eglinton, 2008).

Par ailleurs, certaines espèces non coccolithophores telles que *Isochrysis galbana*, *Tisochrysis lutea* et *Pavlova lutheri* sont cultivées depuis plusieurs décennies pour la nutrition de larves et juvéniles d'organismes marins pour l'aquaculture et l'aquariologie (Hemaiswarya *et al.*, 2011). Ces espèces produisent de fortes quantités d'acides gras polyinsaturés à longue chaîne (AGPI-LC) et notamment l'acide docosahexaénoïque (DHA) et l'acide eicosapentaénoïque (EPA) d'intérêt pour la nutrition et la santé (Meireles *et al.*, 2003; Ryckebosch *et al.*, 2014). Certaines espèces dites oléagineuses comme *Tisochrysis lutea* accumulent de fortes quantités de lipides de réserve d'intérêt pour la production d'agro-carburants de troisième génération. Les haptophytes ont donc un rôle écologique primordial et leur culture présentent un intérêt biotechnologique pour plusieurs domaines d'application tels que l'aquaculture, l'énergie, et la santé.

Les connaissances physiologiques et métaboliques concernant les haptophytes sont relativement parcellaires et concernent essentiellement l'espèce *E. huxleyi*. Les premières données transcriptomiques sur cette espèce ont été acquises dès 2009 et son génome publié en 2013 (von Dassow *et al.*, 2009; Rokitta *et al.*, 2011; Read *et al.*, 2013). A ce jour le génome d'une seule autre haptophyte, *Chrysochromulina tobin*, a été publié (Hovde *et al.*, 2015). Les révélations récentes sur le rôle primordial des haptophytes non coccolithophores sur les cycles biogéochimiques et l'intérêt biotechnologique que présentent certaines de ces espèces, suscitent un besoin de connaissances accru sur le métabolisme et la physiologie de ces microalgues.





## 5. Les microalgues, des usines cellulaires pour les biotechnologies.

Parmi la très grande diversité des espèces identifiées dans les environnements aquatiques, certaines espèces de microalgues ont été isolées et sont cultivées pour différentes applications biotechnologiques. On considère que les perspectives de valorisation sont à l'échelle de l'extraordinaire diversité métabolique de ces microorganismes très peu exploités jusqu'à présent. Ces valorisations touchent les domaines de la phyto-remédiation, la nutrition humaine, l'industrie agroalimentaire, la santé et l'énergie. Les microalgues sont traditionnellement cultivées dans des systèmes assez simples pour la nutrition d'espèces aquacole (mollusques, crustacés, poissons), mais les techniques de culture évoluent très rapidement pour s'adapter aux nouvelles applications. Des photobioréacteurs de plus en plus instrumentés sont développés pour améliorer les rendements, orienter les métabolismes et sécuriser les productions contre les contaminants. Le potentiel de valorisation des microalgues, les modes de culture ainsi que les moyens de recherches à mettre en œuvre pour le développement de cette filière ont fait l'objet d'un travail collectif présenté dans un chapitre de l'ouvrage : « Development of Marine Ressources » et accessible en annexes de ce document (Cadoret *et al.*, 2014).

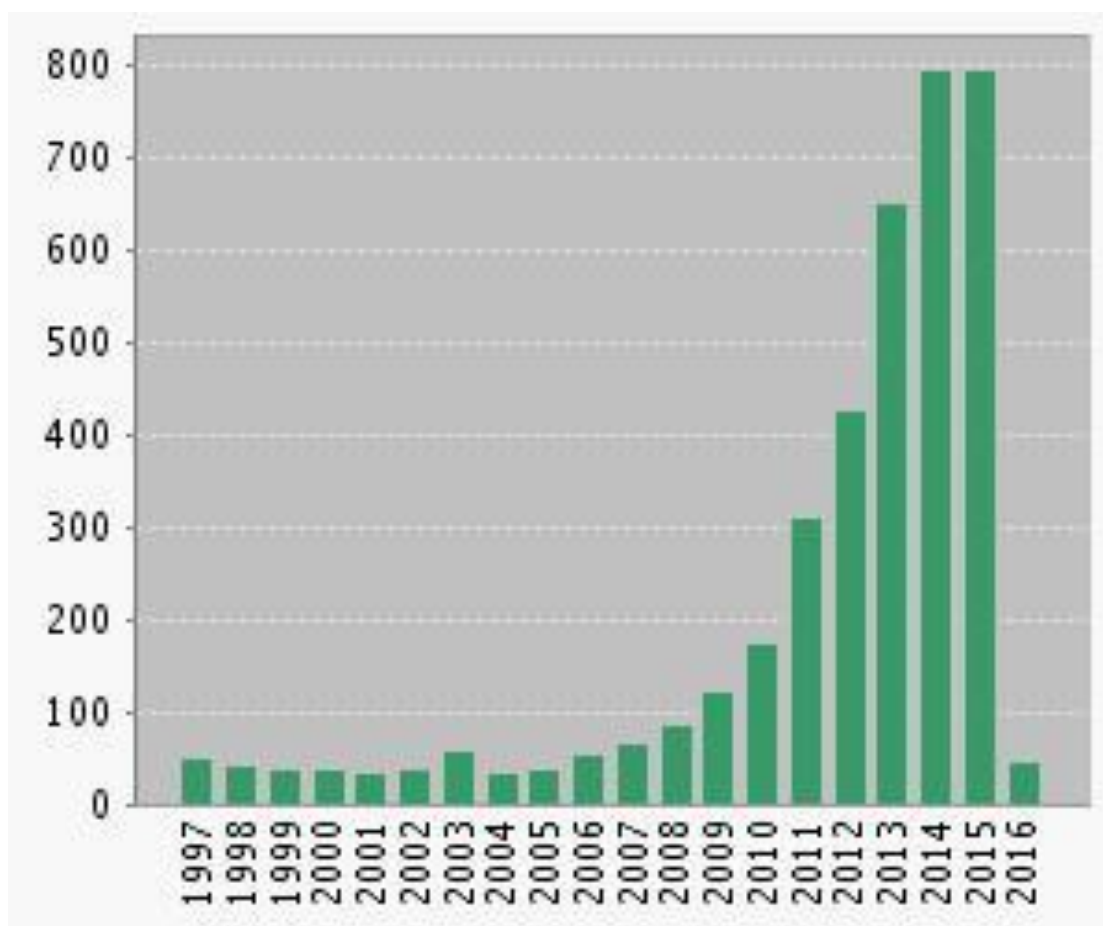
Le développement de la filière microalgues est limité, entre autre, par des coûts de production relativement élevés par rapport aux autres sources de molécules organiques (Slade and Bauen, 2013). En effet, l'azote et le phosphore représentent des entrants cruciaux pour leur culture et les coûts induits par l'utilisation de ces engrais impactent considérablement les rentabilités de productions. De plus, l'utilisation intensive de ces engrais remet en question l'équilibre de l'analyse du cycle de vie des productions algales (Lardon *et al.*, 2009). La gestion de l'azote au sein des unités de production fait donc parti des points importants à optimiser pour améliorer la rentabilité et durabilité de cette industrie en plein essor.

Grâce au développement considérable des techniques de séquençage à haut débit dans les années 2000, il est désormais possible d'accéder relativement facilement aux données moléculaires des organismes vivants. Cette révolution technologique permet le séquençage de génomes et de transcriptome de microalgues dont le nombre ne cesse de croître. Ces données moléculaires ont été utilisées pour étudier les relations phylogéniques et l'histoire évolutive des espèces, pour mieux comprendre le métabolisme spécifique des différents *phyla*, pour identifier des gènes et voies métaboliques spécifiques, et pour développer l'utilisation des microalgues pour la production de protéines recombinantes. L'apport de la génomique pour le développement des biotechnologies des

microalgues a fait l'objet d'un travail collectif publié dans l'ouvrage « Genomic Insights Into The Biology of Algae » en 2012 et accessible en annexes de ce document (Cadoret *et al.*, 2012).

Parmi les molécules d'intérêt issu de microalgues, les lipides font l'objet d'un intérêt particulier. En effet, les microalgues convertissent, grâce à la photosynthèse, l'énergie lumineuse en énergie stockable sous forme de sucres ou de lipides. Chez certaines microalgues, ces lipides sont riches en acides gras polyinsaturés à très longue chaîne (AGPI-LC) d'intérêt majeur pour la santé (Mühlroth *et al.*, 2013). Parmi les espèces productrices de AGPI-LC en autotrophie, les haptophytes sont sans doute les plus productives (Meireles *et al.*, 2003; Ryckebosch *et al.*, 2014).

L'étude des enzymes impliquées dans la synthèse de ces acides gras a fait l'objet de nombreux travaux (Tonon *et al.*, 2004; Lu *et al.*, 2009; Lu *et al.*, 2010; Zhang *et al.*, 2010; Yu *et al.*, 2011; Zäuner *et al.*, 2012; Guiheneuf and Stengel, 2013; Mühlroth *et al.*, 2013; Vaezi *et al.*, 2013; Huerlimann *et al.*, 2014a; Kotajima *et al.*, 2014; Dolch and Maréchal, 2015). D'autre part, des pigments lipidiques tels que le  $\beta$ -carotène et l'astaxanthine sont produits en fortes concentrations par certaines espèces de microalgues, comme respectivement *Dunaliella salina* et *Haematococcus pluvialis*, et sont couramment utilisés pour l'industrie agroalimentaire. Enfin, certaines microalgues dites oléagineuses peuvent produire de très fortes quantité de lipides de réserve, jusqu'à 80% de leur biomasse dans certaines conditions physiologiques, qui peuvent être utilisées comme agro-carburant de troisième génération (Hu *et al.*, 2008). Etant donné l'intérêt potentiel énergétique et économique des agro-carburants, les études ayant trait aux lipides de microalgues ont montré une croissance exponentielle ces 6 dernières années comme le montre l'étude bibliométrique Figure 11. Or, le niveau de limitation azotée des cultures représente un levier intéressant pour guider la production de lipides neutres. L'étude de l'effet de la limitation azotée sur le métabolisme du carbone et des mécanismes régulateurs chez les microalgues présente donc un intérêt biotechnologique primordial.



**Figure 11 Analyse bibliométrique des publications portant sur l'étude des lipides de microalgues.**

Recherche réalisée par les mots clés « Lipid\* » et « Microalg\* » dans le Web Of Science (<https://apps.webofknowledge.com>). Etude réalisée le 02/02/2016.

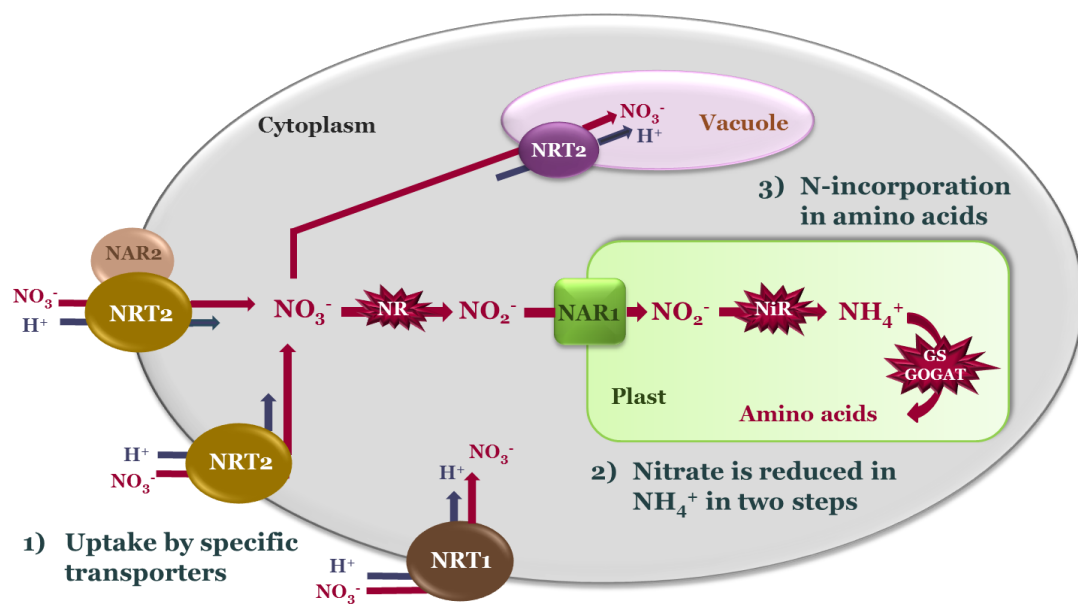


Figure 12 Schéma de l'absorption et de l'assimilation de l'azote chez les microalgues.

## 6. Métabolisme de l'azote chez les microalgues

### A. Absorption et assimilation de l'azote

Dans les océans, l'azote dissous est retrouvé sous forme minérale et organique, ceci à des concentrations très différentes en fonction des zones géographiques. L'utilisation de l'azote organique par les microalgues a longtemps été ignorée. Or, plusieurs travaux ont montré que les micro-organismes hétérotrophes eucaryotes pouvaient accéder à cette ressource azotée grâce à l'action de protéases et d'amino-acid oxydases localisées à la surface des cellules qui convertissent les acides aminés en azote minéral, (Palenik and Morel, 1990a; Palenik and Morel, 1991; Mulholland *et al.*, 2002; Stoecker and Gustafson, 2003). D'autre part, des diatomées comme *Phaeodactylum tricornutum* sont capables d'absorber l'urée et de le convertir en source d'azote minéral par des uréases (Bowler *et al.*, 2010; Valenzuela *et al.*, 2012; Alipanah *et al.*, 2015). L'azote minéral dans les océans est composé majoritairement de nitrates ( $\text{NO}_3^-$ ) et, dans une moindre mesure, d'ammonium ( $\text{NH}_4^+$ ). Malgré des concentrations en nitrate de 10 à 1000 fois plus importante que l'ammonium, la forme ammoniacale est préférentiellement absorbée par les microalgues. Dans les cultures de microalgues, les deux formes d'azote minéral sont utilisées. Chez les plantes, les nitrates et l'ammonium sont absorbés grâce à des transporteurs actifs spécifiques (NRT et AMT respectivement). Il existe deux types de NRTs qui diffèrent par leur affinité au nitrate. Les HATS pour « high-affinity transport system » et les LATS pour « low-affinity transport system ». L'expression de certains de ces transporteurs est régulée par les concentrations en nitrate environnantes. Quatre systèmes de transport haute affinité ont été identifiés chez *Chlamydomonas reinhardtii* et trois chez la diatomée *Thalassiosira pseudonana* (Song and Ward, 2007; Fernandez and Galvan, 2008) (**Figure 12**). Chez les plantes et les chlorophycées, ces systèmes se distinguent par leur efficacité (vitesse de transport), et par leur régulation. Certains de ces systèmes requièrent un partenaire protéique (NAR2) pour être fonctionnels (**Figure 12**) (Galvan and Fernández, 2001; Rexach *et al.*, 2002). Du fait des faibles concentrations en nitrate dans l'eau de mer, ces transporteurs à haute affinité ont un rôle primordial dans l'accès à l'azote minéral. En ce qui concerne les transporteurs d'ammonium, plusieurs isoformes de la famille des AMT1 ont été identifiés dans la plupart des *phyla* de microalgues (Kang and Chang, 2014 ; Gonzalez-Ballester *et al.*, 2004; Yan *et al.*, 2012).

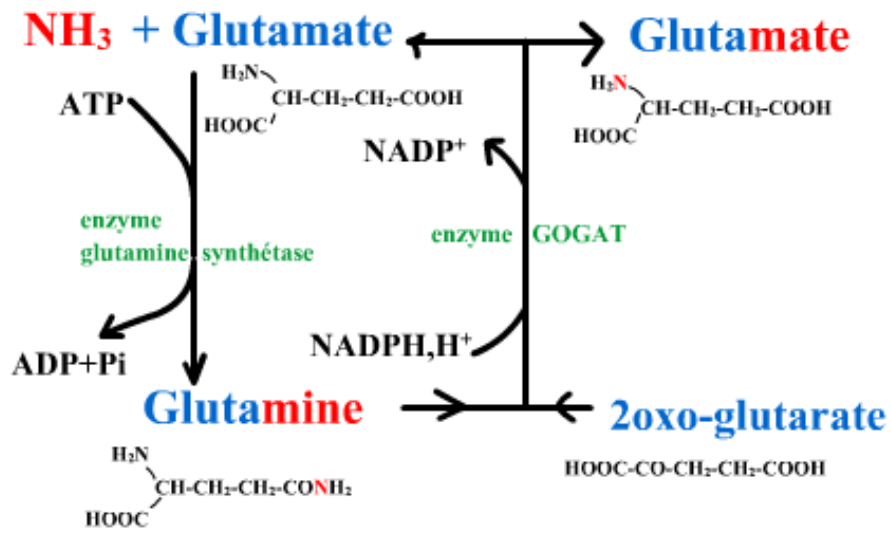


Figure 13 Schéma de l'assimilation de l'azote ammoniacal par le couple enzymatique GS-GOGAT.

Après absorption, les nitrates localisés dans le cytoplasme sont soit réduits en nitrites par des nitrates réductases (NR), soit transportés à l'intérieur de vacuoles pour y être stockés (**Figure 12**). Bien que des vacuoles aient été observées chez certaines microalgues, leur rôle dans le stockage des nitrates reste à démontrer. Les nitrites sont transportés dans les chloroplastes par des transporteurs NAR1, puis réduits en ammonium par la nitrite réductase (NiR) (**Figure 12**).

L'ammonium est ensuite assimilé en molécules organiques azotées grâce à l'action de la glutamate déshydrogénase ou bien de l'action combinée de la glutamine synthétase (GS) et de la glutamate synthase (GOGAT) (**Figure 13**). La glutamate déshydrogénase convertit l' $\alpha$ -cétoglutarate produit par le cycle de Krebs en glutamate par réaction d'amination réductrice. Cette réaction utilise du NADPH. Dans le cas du cycle GS/GOGAT, les deux enzymes agissent conjointement, la GS permettant l'incorporation de l'azote et la GOGAT du squelette carboné (**Figure 13**). La GS converti le glutamate en glutamine et la GOGAT produit du glutamate à partir de la glutamine et de l'oxoglutarate. Le glutamate et la glutamine vont ensuite servir de donneurs de groupements amines par transamination pour la synthèse des acides aminés et autre bases azoté. Les squelettes carbonés alors utilisés (pyruvate, oxaloacétate, l'érythrose-4-phosphate, ribose) proviennent des voies métaboliques du carbone décrites dans le paragraphe 7 de cette introduction.

## **B. Limitations et carences azotées : définitions et outils d'étude**

L'azote est un des principaux éléments limitant la production primaire des océans (Davey *et al.*, 2008; Browning *et al.*, 2014). Les méthodologies couramment employées en océanographie pour identifier l'élément limitant consistent à mesurer les éléments nutritifs dans le milieu extracellulaire, à mesurer les quotas cellulaires et réaliser des expériences d'enrichissement en microcosme ou mésocosme (Beardall *et al.*, 2001). Alors que les notions de limitation et de carence sont difficiles à définir dans l'environnement car les milieux sont constamment soumis à des flux de matières difficiles à mesurer (activité biologique, arrivées de contaminants, homogénéisation des masses d'eau, etc...) ces notions peuvent être bien déterminées dans des systèmes de culture contrôlée. Pour étudier l'impact de la limitation azotée sur le métabolisme, des expériences en culture pures sont donc très généralement utilisées.

### ✓ **Méthodes de mesure de croissance**

En fonction des publications, la croissance des cultures de microalgues est évaluée soit par le suivi de la concentration cellulaire (CC), soit par le suivi de la concentration de carbone particulaire (C). Chacune de ces deux méthodes présente ses avantages et limites et sont employées dans des

contextes différents. En générale, les études écophysiologiques emploient le suivi du carbone particulaire car il reflète à lui seul l'ensemble de la biomasse organique synthétisée dans la culture et rends compte du rendement global de la culture. Il permet de modéliser la croissance en fonction des différents paramètres (lumière, température, concentration en éléments limitants...). Cependant, ce proxy reflète difficilement l'évolution des processus cellulaires durant la croissance (division cellulaire, taille des cellules, mise en place des réserves). Pour ces raisons, les études qui portent sur le métabolisme et ses régulations utilisent la CC pour évaluer la croissance. Ce proxy sera employé dans la suite du paragraphe pour décrire deux modes de culture employés pour l'étude de la limitation azotée.

#### ✓ **Modèle de croissance.**

Le modèle de croissance décrit par Droop en 1968 postule que le taux de croissance ( $\mu$ ) des microalgues suit une fonction hyperbolique dépendante du quota de l'élément limitant (Droop, 1968) (Figure 14). Le quota  $Q$  d'un élément correspond à l'ensemble des formes de cet élément dans la cellule. Dans le cas d'une culture limitée par l'azote le taux de croissance suit donc la fonction suivante.

$$\mu = \bar{\mu} \left( 1 - \frac{QN_0}{QN} \right)$$

Avec  $\bar{\mu}$ =constante,  $QN$  quotas d'azote;  $QN_0$  quotas d'azote minimal.

Ce modèle sera utilisé par la suite pour définir le taux de croissance en fonction du quota d'azote.

#### ✓ **Limitation et carence azotée**

La limitation et la carence azotée ont des effets différents sur la physiologie des microalgues (Parkhill *et al.*, 2001). La carence azotée correspond à un état pour lequel l'absence d'azote empêche la croissance de la culture. A ce stade,  $QN$  est égale à  $QN_0$  et  $\mu$  est égale à 0. La limitation azotée correspond à un état de croissance pour lequel le taux de croissance ( $\mu$ ) est limité par la disponibilité en azote (Parkhill *et al.*, 2001). En condition de limitation azotée, le taux de croissance ( $\mu$ ) est supérieur à zéro et inférieur au taux de croissance maximum ( $\mu_{max}$ ) observé lorsque l'azote ne limite aucunement la croissance. La limitation azotée réfère donc à une grande variabilité de niveaux de limitations et les microalgues peuvent détecter avec une très grande sensibilité des baisses modérées d'azote dans le milieu (Lee *et al.*, 2012). Pour estimer le niveau de limitation, le rapport  $QN/QC$  (ou  $N/C$ ) du quota d'azote  $QN$  divisé par le quota de carbone  $QC$  est généralement utilisé comme proxy. Plus la valeur de ce rapport  $N/C$  est faible, plus la limitation est forte.



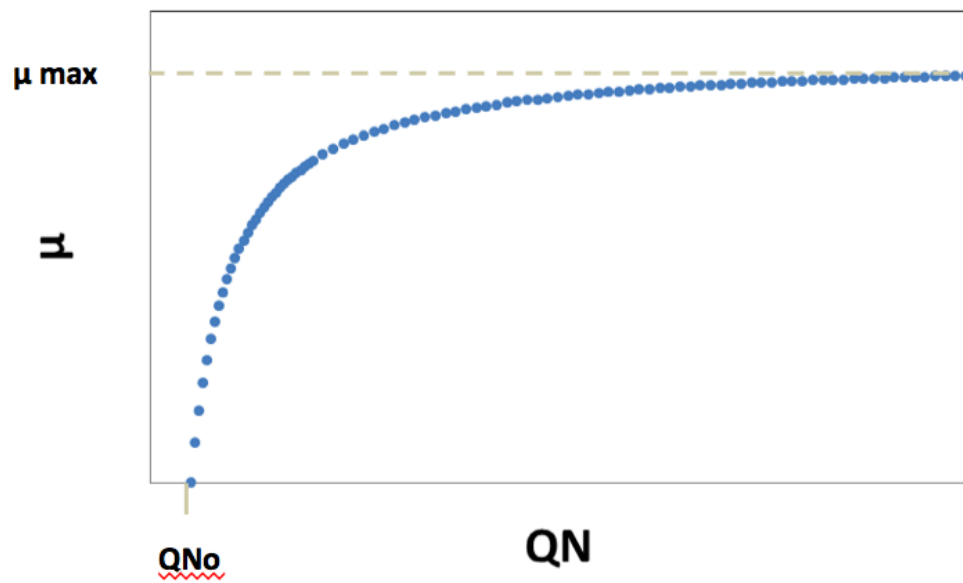


Figure 14 Relation entre le taux de croissance ( $\mu$ ) et les quotas cellulaires en azote ( $QN$ ) dans un chemostat selon Droop (1968).

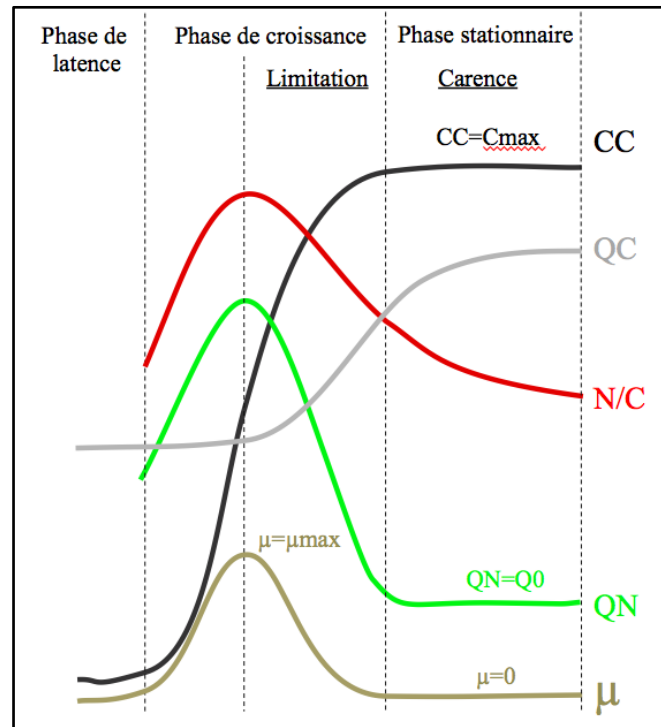


Figure 15 Représentation schématique d'une culture en mode batch.

CC : concentration cellulaire, QC : quotas de carbone par cellule ; QN : quotas d'azote par cellule,  $\mu$  : taux de croissance.

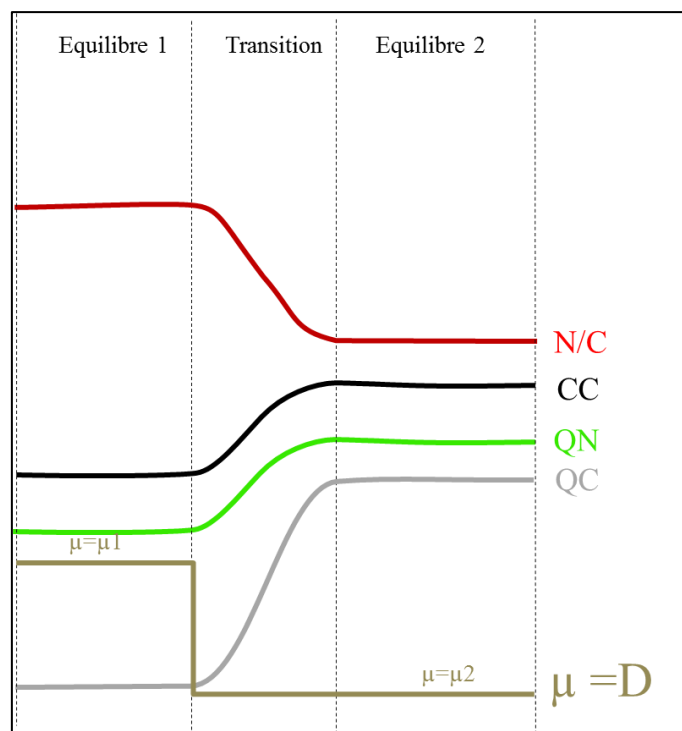


Figure 16 Représentation schématique d'une culture en mode chemostat soumise à deux taux de dilution successifs

CC : concentration cellulaire, QC : quotas de carbone par cellule ; QN : quotas d'azote par cellule,  $\mu$  : taux de croissance ; D : taux de dilution.

### ✓ **Limitation et carence en cultures batch**

Dans les cultures en mode batch limitées par l'azote, tous les éléments nécessaires à la croissance des microalgues sont apportés au temps initial dans la culture. Ils sont absorbés au cours du temps jusqu'à ce que seule la disponibilité en azote impacte le développement de la culture. Dans ce type de culture, une première phase d'acclimatation appelée phase de latence est généralement observée, puis une phase de croissance pendant laquelle les cellules se divisent grâce aux nutriments apportés, et enfin une phase stationnaire due à l'épuisement total de l'azote. Une phase de décroissance due à une mortalité cellulaire intervient ensuite si la phase stationnaire est prolongée.

Au cours de la croissance,  $N/C$  ainsi que  $\mu$  augmentent et atteignent un maximum ( $N/C_{max}$  ;  $\mu_{max}$ ) à l'instant «  $t$  » au-delà duquel la raréfaction de l'azote contraint le taux de croissance. Le quota d'azote ( $Q_N$ ) baisse ensuite et tend vers une valeur minimale ( $Q_0$ ). Lors de cette phase, nous parlerons de limitation azotée. Au-delà de cette phase, la croissance est nulle ( $\mu=0$ ) et  $Q_N$  atteint la valeur minimale  $Q_N=Q_0$ . Cet état physiologique correspond alors à la carence azotée. L'absence de division cellulaire due à la carence azotée n'implique pas nécessairement l'arrêt de la production primaire et de l'absorption du carbone. De ce fait, le quota carbone  $Q_C$  peut continuer à augmenter pour un  $Q_N$  constant ( $=Q_0$ ). Il en découle alors une baisse du rapport  $N/C$  lors de la phase de carence azotée. Le rapport  $N/C$  rend ainsi compte donc et de la raréfaction de l'azote dans la cellule, et de l'accumulation de carbone pendant la culture. Dans une culture en mode « batch », la physiologie des algues suit une dynamique qui passe par des phases d'absence de limitation, à une limitation croissante puis une carence azotée (**Figure 15**).

### ✓ **Limitation en mode chemostat**

Dans les cultures en mode continu de type chémostat, les éléments nécessaires à la croissance des microalgues sont apportés en continu grâce à un flux entrant de milieu de culture constant. Ce flux est apporté à un taux de dilution  $D$  ( $j^{-1}$ ). Le volume de culture est maintenu par un flux sortant équivalent. La culture atteint un équilibre écophysologique qui peut être maintenu en principe indéfiniment (**Figure 16**). Cet équilibre est caractérisé par

- Des concentrations cellulaires stables, des quotas cellulaires constants et donc un ratio  $N/C$  constant.
- Un taux de croissance ( $\mu$ ) constant et égal au taux de dilution ( $D$ ).

- L'élément limitant (N) est absorbé en totalité par les microalgues. De ce fait la concentration en azote algale est égale à la concentration en azote du milieu de culture en entrée du chemostat.

Dans un chémostat à l'équilibre limité par l'azote, la limitation est d'autant plus élevée que le débit est faible. Différents niveaux de limitation azotée peuvent ainsi être étudiés en modulant le débit. Contrairement au mode batch, il n'y a pas d'arrêt de division cellulaire.

Les cultures en chémostat présentent donc l'avantage d'accéder à des états physiologiques stables et parfaitement caractérisables contrairement aux cultures en mode batch qui sont dynamiques et dans lesquels la physiologie des cellules évolue au cours du temps.

Malgré ses avantages, le chémostat reste peu employé pour étudier la limitation azotée chez les microalgues, sans doute car plus difficile à mettre en œuvre. Le mode opératoire employé pour provoquer le stress azoté consiste généralement à prélever des algues dans une culture en mode batch et à les faire croître dans un nouveau milieu sans azote. Les échantillons sont ensuite analysés après différentes durées de cultures dans ce milieu carencé. Ainsi, les résultats des études publiées sont souvent difficiles à comparer car les caractères écophysologiques (QN, QC, N/C) et les cinétiques permettant d'évaluer le niveau de limitation ou de carence ne sont généralement pas mentionnés.

### **C. Impact de la limitation et de la carence sur le métabolisme de l'azote.**

La limitation et la carence azotée induisent un comportement cellulaire comparable dans ses grandes lignes chez les différentes espèces de microalgues étudiées, et notamment chez la chlorophycée *Chamydomonas reinhardtii*, la diatomée *P. tricornutum* et l'eustigmatophyceae *Nannochloropsis gaditana*. Les différentes études montrent que la raréfaction de l'azote dans le milieu induit une augmentation de l'efficacité de l'absorption d'azote par la régulation de l'expression des transporteurs membranaires (Hildebrand and Dahlin, 2000; Kang *et al.*, 2007; Song and Ward, 2007). De plus, elle induit une baisse de l'activité photosynthétique grâce à la sous accumulation de protéines de synthèse de la chlorophylle (Dong *et al.*, 2013; Alipanah *et al.*, 2015) et le ralentissement de la synthèse de composés azotés de type protéique grâce à une baisse de l'activité transcriptionnelle et traductionnelle (Dong *et al.*, 2013; Alipanah *et al.*, 2015). Dans certains cas, le ralentissement de la synthèse de composés azotés de type nucléique *via* la sous-expression d'enzymes de la voie des pentoses phosphate est observée (Rismani-Yazdi *et al.*, 2012). Enfin, elle induit la remobilisation de l'azote au sein de la cellule *via* l'augmentation de l'activité protéolytique

et la régulation de l'ensemble des voies du métabolisme azoté à l'intérieur de la cellule (Dong *et al.*, 2013; Alipanah *et al.*, 2015). Chez les diatomées cette remobilisation intracellulaire fait intervenir le cycle de l'urée (Allen *et al.*, 2011). Les études réalisées sur les haptophytes et principalement sur *E huxleyi* montrent que la raréfaction de l'azote inorganique dans le milieu induit l'utilisation de l'azote organique extracellulaire (McKew *et al.*, 2015), la baisse de l'activité d'assimilation de l'azote (Kaffes *et al.*, 2010), et la remobilisation de l'azote intracellulaire en faisant intervenir, à l'instar des diatomées, le cycle de l'urée (Rokitta *et al.*, 2011).

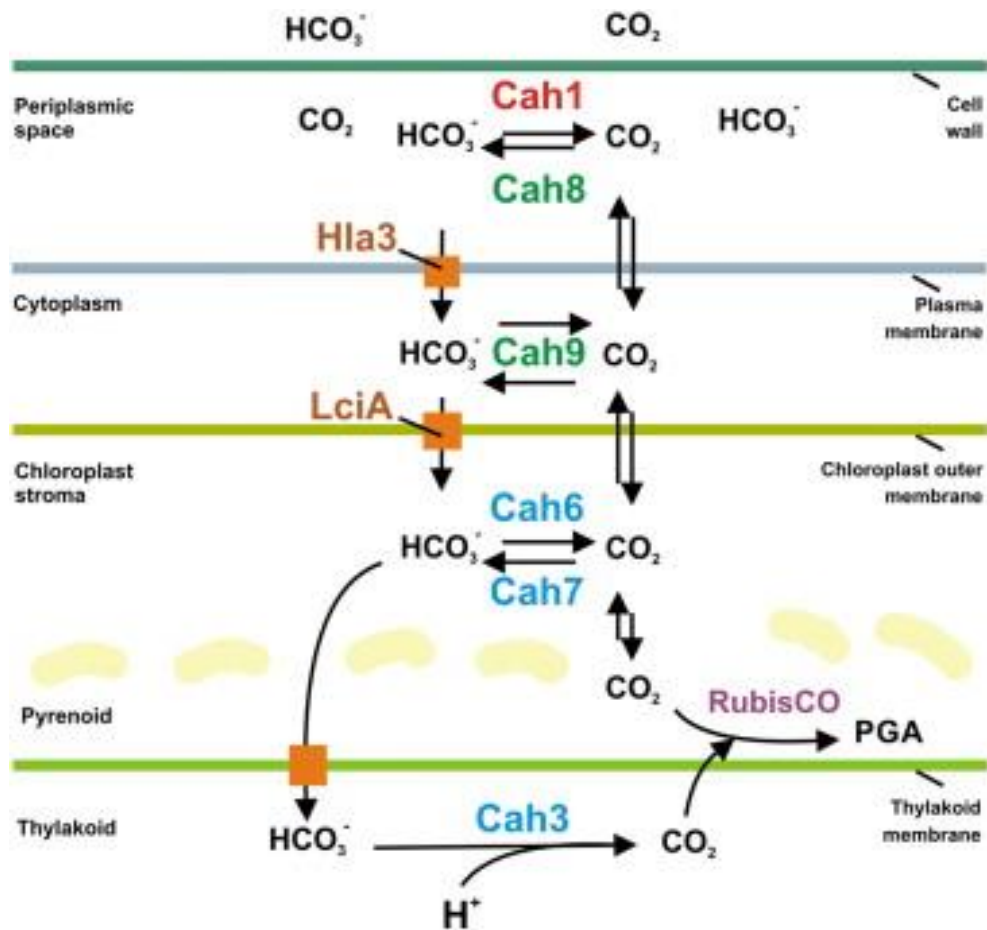


Figure 17 Représentation schématique de la concentration du carbone chez *Chlamydomonas reinhardtii*. (Source : Wink et al 2013)

Cah : anhydrase carbonique; Hla et LciA sont des transporteurs de carbonate.

## 7. Le métabolisme du carbone chez les microalgues.

### A. La fixation autotrophe du carbone

Chez les organismes photosynthétiques, la première étape de fixation du carbone inorganique est assurée par la ribulose-1,5-bisphosphate carboxylase/oxygénase ou Rubisco qui carboxyle le D-Ribulose-1,5-bisphosphate par incorporation d'une molécule de CO<sub>2</sub>. Cette première étape du cycle de Calvin est localisée dans le stroma des chloroplastes. Un ratio CO<sub>2</sub>/O<sub>2</sub> trop faible à proximité de la Rubisco aboutit à une réaction inverse d'oxydation du ribulose-1,5-bisphosphate et donc à un phénomène de photo-respiration induisant une perte net de carbone. La fixation du carbone par la photosynthèse nécessite une concentration minimale de CO<sub>2</sub> à proximité de la Rubisco. Le carbone inorganique dans l'eau est retrouvé essentiellement sous la forme de carbonates (HCO<sub>3</sub><sup>-</sup>) et le dioxyde de carbone (CO<sub>2</sub>) dissous qui s'équilibrent en fonction du pH de l'eau. Le CO<sub>2</sub> diffuse 10 000 fois plus lentement dans l'eau que dans l'air.

Pour assurer une concentration minimale de CO<sub>2</sub> à proximité de la Rubisco, les microalgues mettent en place des processus de concentration et d'acheminement du carbone inorganique de l'extérieur de la cellule vers le stroma des chloroplastes (Winck et al ; Kroth et al, 2008). Les mécanismes de concentration du carbone (MCC) font intervenir des transporteurs membranaires actifs du carbone inorganique et des enzymes de la famille des anhydrases carboniques qui convertissent les formes HCO<sub>3</sub><sup>-</sup> en CO<sub>2</sub> (**Figure 17**). Ces mécanismes sont retrouvés chez la plupart des algues et plantes aquatiques et chez quelques plantes terrestres (Raven et al 2008). Chez les diatomées, un système parallèle de concentration du carbone de type C4 a été mis en évidence (Reinfelder *et al.*, 2000; Bowler *et al.*, 2010). Ce système a été initialement identifié chez certaines plantes et permet d'augmenter l'efficacité d'assimilation du CO<sub>2</sub>. Il consiste à synthétiser de l'oxaloacétate (métabolite précurseur constitué de 4 carbones) (OAA) à partir du phosphoénolpyruvate (PEP) et du CO<sub>2</sub> par l'action de la phosphoénolpyruvate carboxylase (PEPC). L'OAA est alors transporté vers le chloroplaste, puis carboxylé pour fournir du CO<sub>2</sub> à la Rubisco (Tanaka *et al.*, 2014). Les résultats de certains travaux suggèrent que ce système pourrait exister dans d'autres *phyla* de microalgues comme chez les haptophytes (Tsuji *et al.*, 2012). Les voies principales de fixation du carbone sont relativement bien conservées entre les microalgues et les plantes supérieures. La photosynthèse est divisée en deux phases et a lieu dans les thylacoïdes des chloroplastes.

- La phase claire consiste à générer de l'ATP et du pouvoir réducteur, sous la forme de NADPH, grâce à l'énergie photochimique de la lumière captée par les antennes photosynthétiques ancrées aux membranes des thylacoïdes sur les photosystèmes I et II de la chaîne photosynthétique (**Figure 18**). Si le principe de cette phase est conservé chez les eucaryotes photosynthétiques, la nature des pigments utilisés par les antennes varie sensiblement en fonction des *phyla* et des conditions environnementales. Par exemple, alors que la chlorophylle a est utilisée par tous les *phyla* comme pigment central des antennes collectrices, la chlorophylle b n'est retrouvée que chez les chlorophycées et les espèces issues de l'endosymbiose secondaire des chlorophycées. La chlorophylle c est retrouvée chez les rhodophycées et les espèces issues de l'endosymbiose secondaire des rhodophycées. De nombreux autres pigments impliqués dans la photosynthèse ont été identifiés en fonction des *phyla* analysés (Mulders *et al.*, 2014).
- La phase sombre de la photosynthèse (cycle de Calvin) débute par la carboxylation de la ribulose-1,5-bisphosphate par la Rubisco. Il s'ensuit 7 autres réactions qui permettent de produire une molécule de glycéraldéhyde 3-phosphate (G 3-P) à partir de 2 molécules de CO<sub>2</sub>. Le NADPH et l'ATP utilisés pour ce cycle sont générés par la phase claire de la photosynthèse (**Figure 19**). Le G 3-P est un carrefour métabolique essentiel pour l'ensemble des réactions des organismes.



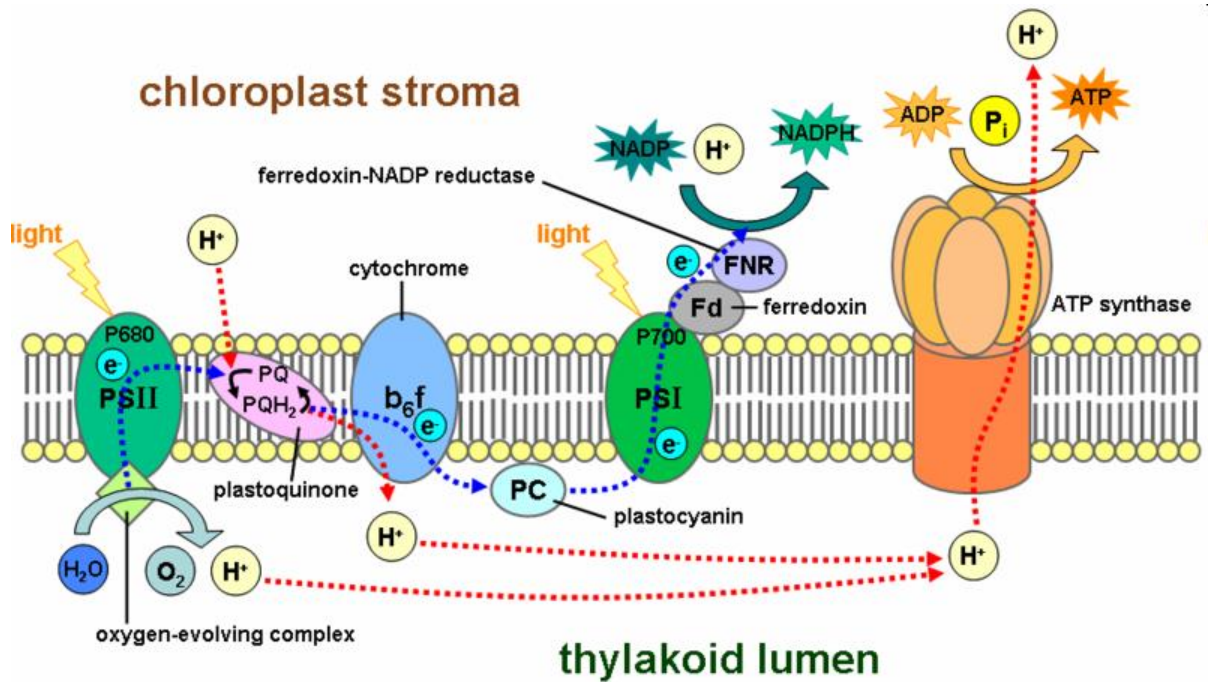


Figure 18 Représentation schématique de la chaîne photosynthétique. (Source : <https://en.wikipedia.org/wiki/Photosynthesis>)

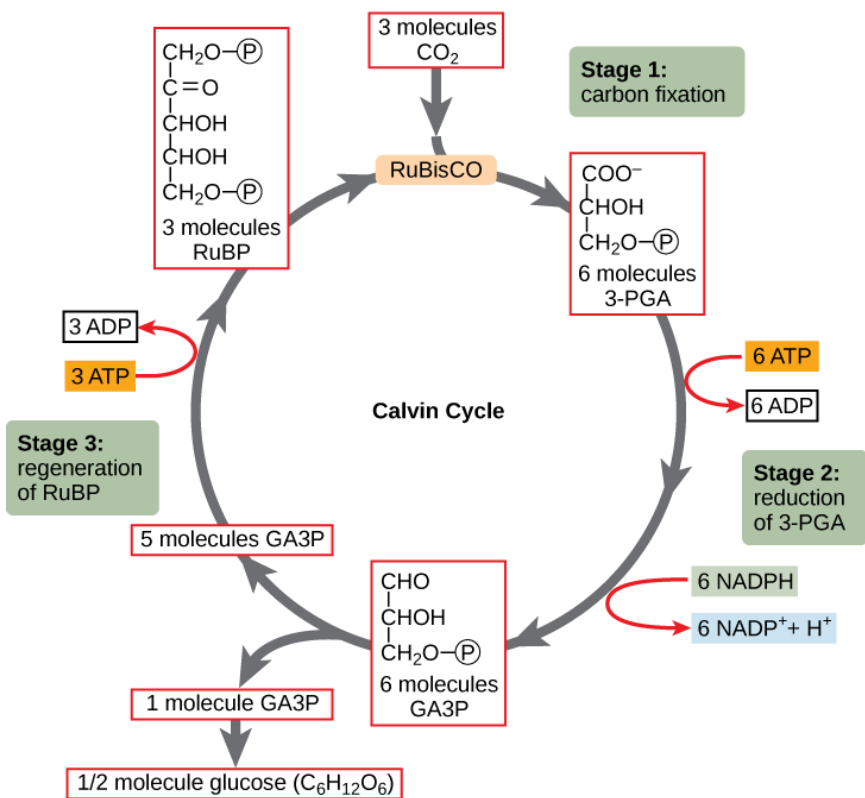


Figure 19 Représentation schématique du cycle de Calvin. (Source : "OpenStax College, Using Light Energy to Make Organic Molecules. October 16, 2013.")

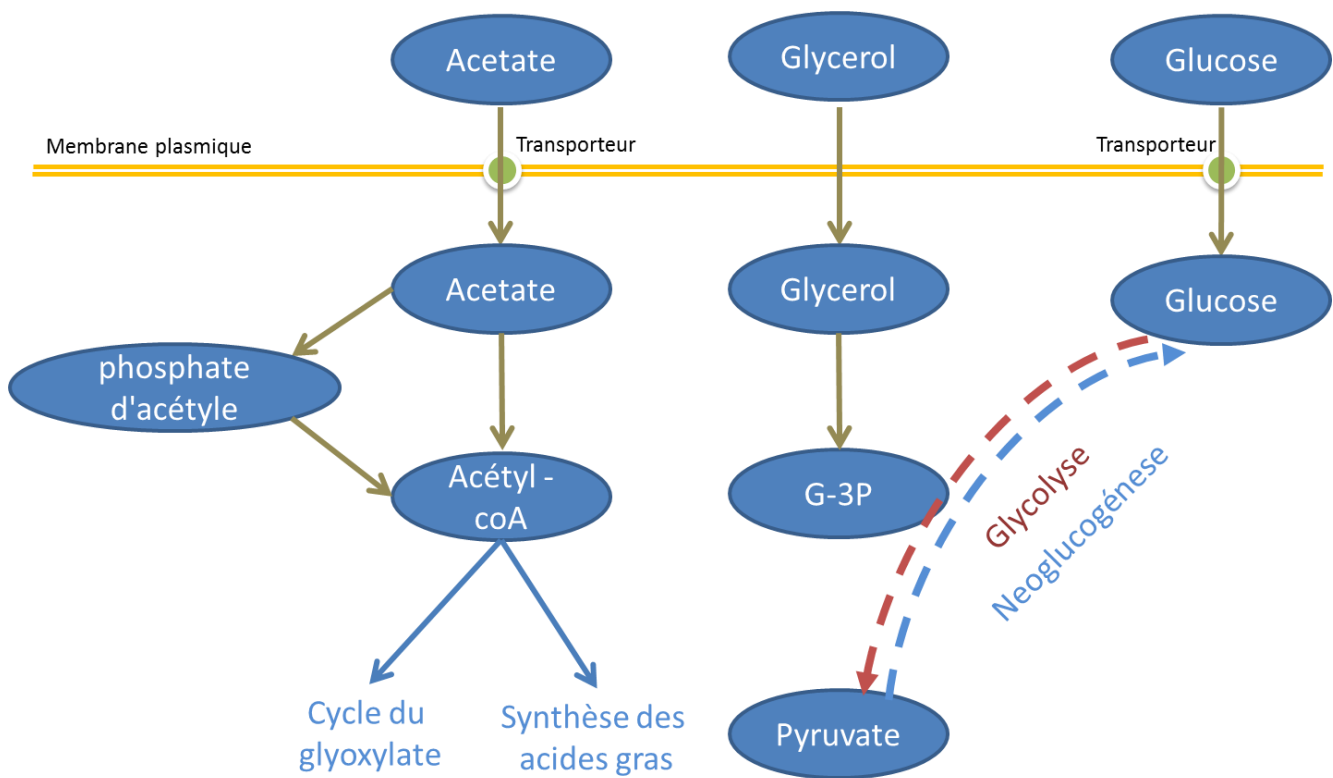


Figure 20 Schéma simplifié de l'absorption et de l'assimilation du carbone organique sous forme d'acétate, de glycérol et de glucose. (Modifié d'après Perez-Garcia et al., 2011)

## B. La fixation hétérotrophe du carbone.

En absence de lumière, les microalgues doivent trouver une alternative à la photosynthèse pour générer de l'énergie et les métabolites précurseurs. Elles peuvent notamment puiser dans leurs réserves glucidiques et lipidiques pour alimenter les voies énergétiques (glycolyse, cycle de Krebs). Ces mécanismes seront développés au paragraphe suivant. Certaines espèces mixotrophes (autotrophes et hétérotrophes) sont capables de puiser leur énergie et leur source carbonée à partir de la dégradation de molécules organiques (acétate, glucose, glycérol, etc.) puisées dans le milieu environnant (Perez-Garcia *et al.*, 2011) (**Figure 20**). Dans le cas de l'acétate, cette molécule est absorbée grâce à des transporteurs spécifiques, puis métabolisée en acétyl-CoA. Cette réaction fait intervenir soit une seule enzyme : l'acétyl-CoA synthétase, soit deux enzymes : l'acétate kinase, qui converti l'acétate en phosphate d'acétyle, puis la phosphate acétyltransferase, qui converti le phosphate d'acétyle en acétyl-CoA. L'acétyl-CoA alimente ensuite la synthèse *de novo* des acides gras, et/ou le cycle du glyoxylate.

Le glycérol est quant à lui converti directement en G 3-P. Le glucose est importé dans la cellule et intégré directement dans la glycolyse. Les voies citées ci-dessus seront présentées dans le chapitre suivant.

## C. Les voies métaboliques cœur.

Le carbone fixé sous forme de G 3-P est alloué soit à la biomasse fonctionnelle c'est à dire à l'ensemble des molécules impliquées dans le fonctionnement et la structure cellulaire (ADN, ARN, protéines, lipides membranaires), soit aux réserves carbonées, essentiellement les sucres et les lipides de réserve. Quatre voies métaboliques principales sont distinguables et présentées d'une manière schématique sur les figures 21 ,22, 24 et25. Ces voies centrales permettent de générer les précurseurs métaboliques pour l'ensemble des voies métaboliques de la cellule, ceci à partir du carbone fixé.

- La glycolyse et ses réactions inverses (néoglucogenèse) (Figure 21) : Les réactions enzymatiques ont généralement lieu dans le cytoplasme des cellules. Le glucose est synthétisé à partir du G 3-P en 5 étapes réactionnelles. Le G 3-P peut provenir soit directement du cycle de Calvin, soit à partir du pyruvate *via* la néoglucogenèse. La glycolyse, à proprement parler, consiste à dégrader le glucose en 10 étapes réactionnelles et à produire du pyruvate, de l'énergie sous forme d'ATP et du pouvoir réducteur sous forme NADH. Le pyruvate généré est un précurseur de nombreuses réactions métaboliques comme la

production de l'acétyl-CoA par l'intermédiaire du complexe pyruvate déshydrogénase, et la synthèse d'acides aminés (alanine, leucine et valine).

La glycolyse et la néoglucogenèse font intervenir un ensemble d'enzymes bidirectionnelles communes aux deux voies, et des enzymes spécifiques de chacune des deux voies.

- La voie des pentoses phosphates (PPP) (Figure 22) utilise le glucose 6 phosphate (G 6-P), un intermédiaire entre le glucose et le G 3-P. Elle permet en premier lieu la synthèse en 3 étapes du ribose-5-phosphate (Ri 5-P) et la production de pouvoir réducteur sous forme de NADPH. Le Ri 5-P est ensuite converti soit en phosphoribosylpyrophosphate (PRPP), précurseur activé pour la synthèse des bases puriques et pyrimidiques, soit en érythrose 4-phosphate, précurseur des acides aminés aromatiques : phénylalanine, tyrosine et tryptophane.

Si la glycolyse et la voie des pentoses phosphates sont conservées chez les différents organismes photosynthétiques eucaryotes, les réactions enzymatiques mises en œuvre peuvent être localisées différemment en fonction des *phyla*, soit dans le cytoplasme soit dans le chloroplaste (Moriyama *et al.*, 2014). (Figure 23)

- Le cycle de Krebs (Figure 24) est localisé dans les mitochondries et permet de produire de l'énergie sous forme ATP, et du pouvoir réducteur sous forme NADH et FADH. De plus, il converti les produits de la glycolyse (acétyl-CoA, pyruvate (Pyr) ou phosphoénolpyruvate (PEP)) en précurseurs métaboliques qui peuvent être utilisés pour la production des acides aminés et notamment l' $\alpha$ -cétoglutarate et l'oxaloacétate. L' $\alpha$ -cétoglutarate est à la base des acides aminés glutamate et des dérivés. L'oxaloacétate est à la base des acides aminés aspartate, lysine, asparagine, méthionine, thréonine, and isoleucine. Le pouvoir réducteur ainsi que le fumarate produits par le cycle de Krebs sont utilisés par la respiration oxydative localisée sur les membranes des mitochondries pour générer de l'énergie sous forme d'ATP.
- Le cycle du glyoxylate est une voie métabolique dérivée du cycle de Krebs qui court-circuite les étapes de décarboxylation (Figure 25). Contrairement au cycle de Krebs, ce cycle permet de fixer du carbone mais ne génère pas d'ATP. D'une manière schématique, l'acétyl-CoA est converti en succinate qui alimente la synthèse d'une grande variété de sucres et autres précurseurs métaboliques. Cette voie est utilisées pour la croissance à partir de lipides de réserves ou à partir de molécules organiques pour les microalgues mixotrophes (Perez-Garcia *et al.*, 2011). Chez *C. reinhardtii*, les réactions enzymatiques de ce cycle ont lieu dans les peroxysomes (Lauersen *et al.*, 2016).

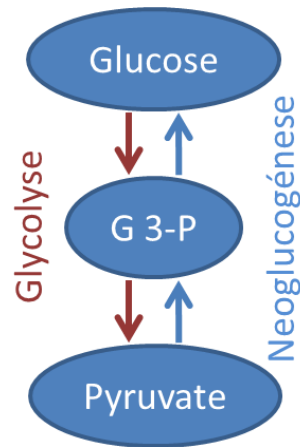


Figure 21 Schéma simplifié de la glycolyse et de la néoglucogénèse.

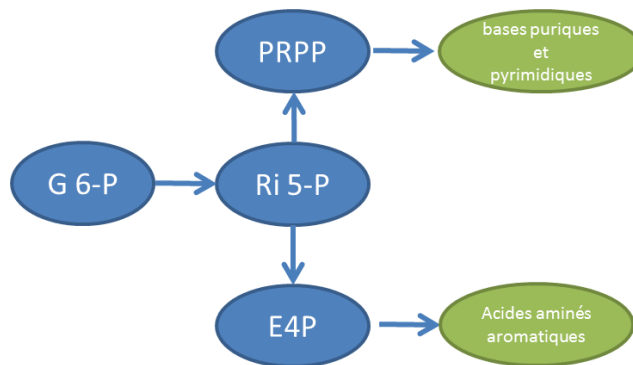


Figure 22 Schéma simplifié de la voie des pentoses phosphates.

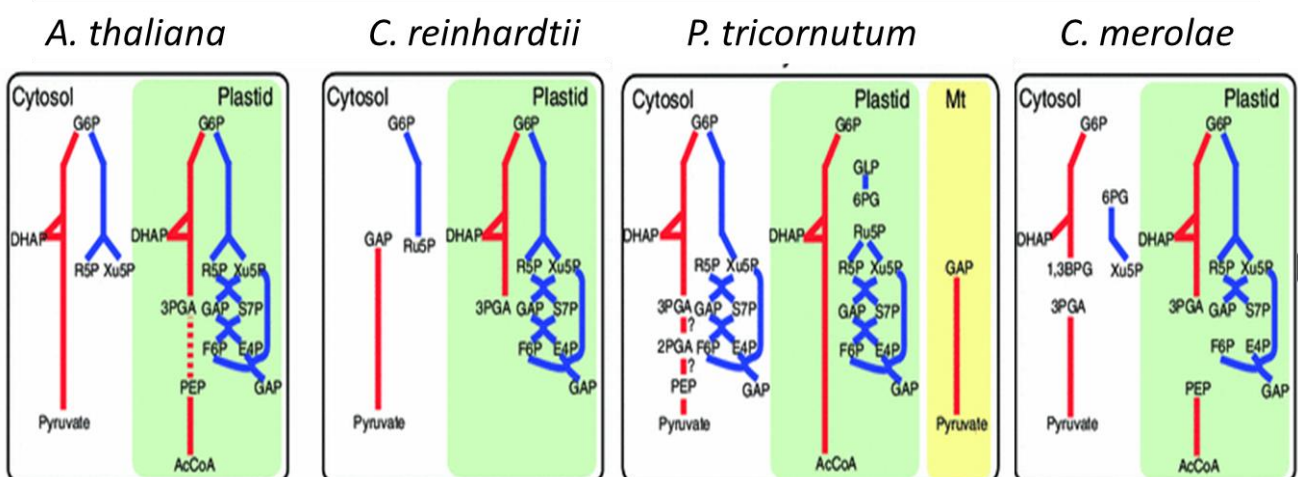


Figure 23 : Localisation cellulaire des réactions de la glycolyse et de la voie des pentoses phosphates (PPP) chez les plantes et les microalgues. (Source : Moriyama et al, 2014)

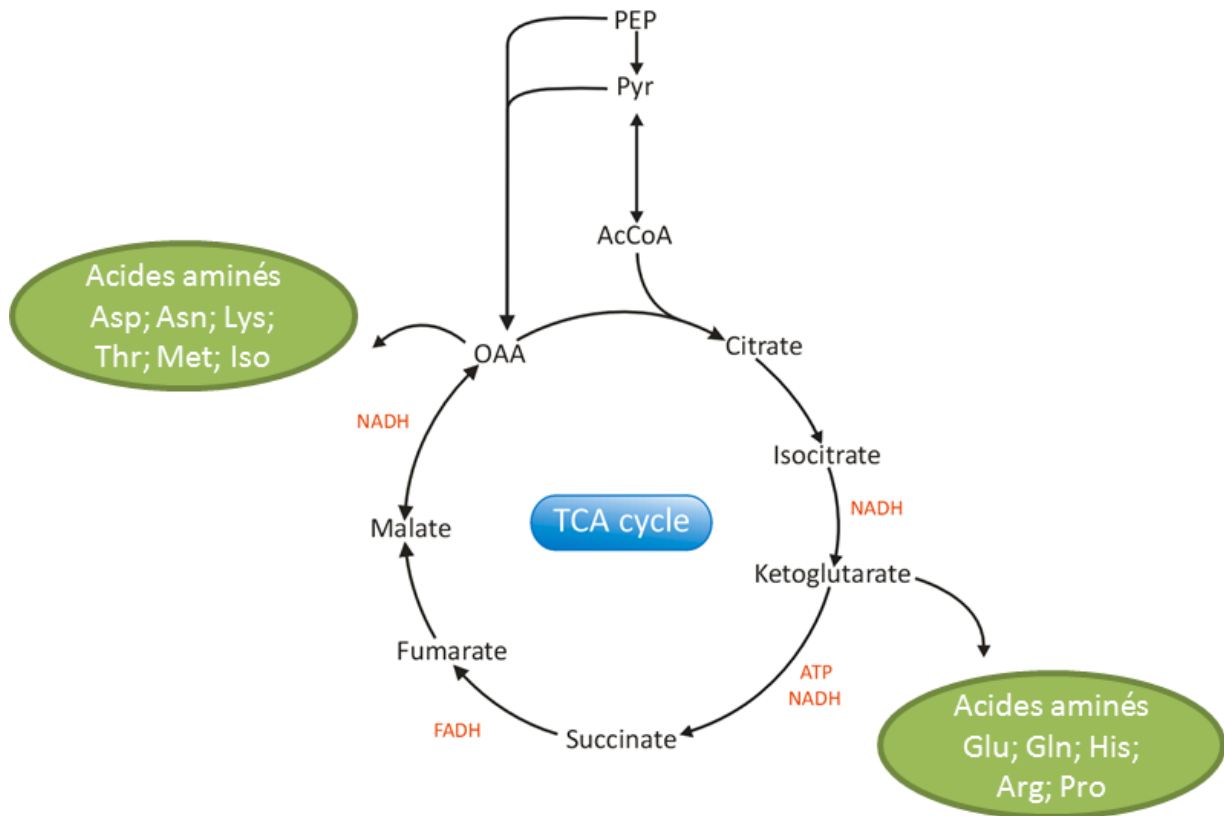


Figure 24 Schéma simplifié du cycle de Krebs.

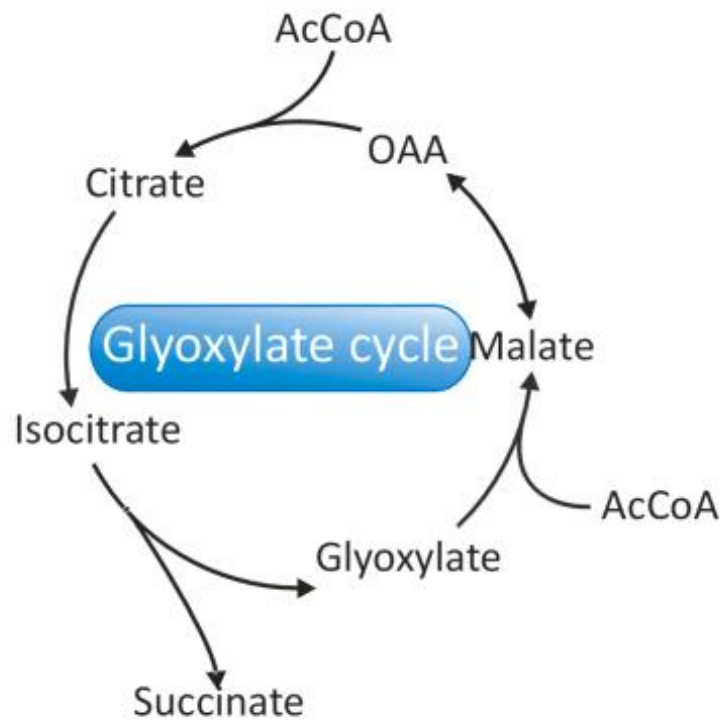


Figure 25 Schéma simplifié du cycle du glyoxylate.

## 8. Le stockage du carbone.

Lorsque les conditions nutritives sont défavorables au développement des populations phytoplanctoniques, certaines espèces de microalgues constituent des réserves carbonées riches en énergie sous forme de sucres ou de lipides de réserve. Ces réserves pourront être utilisées comme source de carbone, d'ATP et de pouvoir réducteur lorsque les conditions favorables à la croissance seront restaurées. La forme majoritaire sous laquelle les microalgues stockent leur carbone dépend des espèces considérées. Chez *C. reinhardtii*, le carbone est essentiellement accumulé sous forme de granules d'amidon. La production de TAGs ne se produit que lorsque la disponibilité en carbone dépasse la capacité de synthèse de l'amidon, par exemple lors de l'ajout d'acétate dans des cultures mixotrophes, ou lorsque la voie de synthèse de l'amidon est modifiée par mutagenèse (Fan *et al.*, 2011; Goodson *et al.*, 2011; Ramazanov and Ramazanov, 2006; Wang *et al.*, 2009; Li *et al.*, 2010b; Siaux *et al.*, 2011; Blaby *et al.*, 2013; Wang, 2008; Work *et al.*, 2010). Certaines espèces de diatomées comme *Odontella aurita* accumulent de la chrysolaminarine lors d'un stress azoté alors que d'autres espèces comme *P. tricornutum* accumulent plutôt des lipides (Valenzuela *et al.*, 2012; Valenzuela *et al.*, 2013; Xia *et al.*, 2014). Chez les haptophytes *T. lutea* et *Isochrysis zhangjiangensis*, le carbone est accumulé sous forme de TAGs et sous forme de chrysolaminarine (Lacour *et al.*, 2012; Wang *et al.*, 2014).

### A. Les sucres de réserve.

Chez les microalgues en générale, les sucres de réserve majoritaires sont des polymères de glucose. Chez les chlorophycées, les rhodophycées et glaucophytes il s'agit de l'amidon. Ce polymère est un mélange de deux homopolymères, l'amylose et l'amylopectine, composés de chaînes glucanes liées par des liaisons  $\alpha$  (1-4) et  $\alpha$  (1-6) (Busi *et al.*, 2014) (**Figure 26**). La synthèse de l'amidon et son stockage sous forme de granules se fait dans le chloroplaste des plantes et des chlorophycées. Chez les rhodophycées et des glaucophytes, la synthèse et le stockage de l'amidon (appelé communément amidon floridéen) ont lieu dans le cytoplasme (Zeeman *et al.*, 2010).

Chez les straménopiles et les haptophytes, le sucre de réserve principal est la chrysolaminarine. Ce polymère a une structure basée sur un squelette glucane de liaisons  $\beta$  (1-3), souvent ramifié par des liaisons  $\beta$  (1-6) (**Figure 26**). Chez les diatomées, la chrysolaminarine est synthétisée dans le cytoplasme et accumulée dans des vacuoles (Kroth, 2008). Bien que certaines enzymes aient été identifiées récemment chez les diatomées (Zhu *et al.*, 2015), Les voies de biosynthèse de la chrysolaminarine restent à ce jour très mal connues.

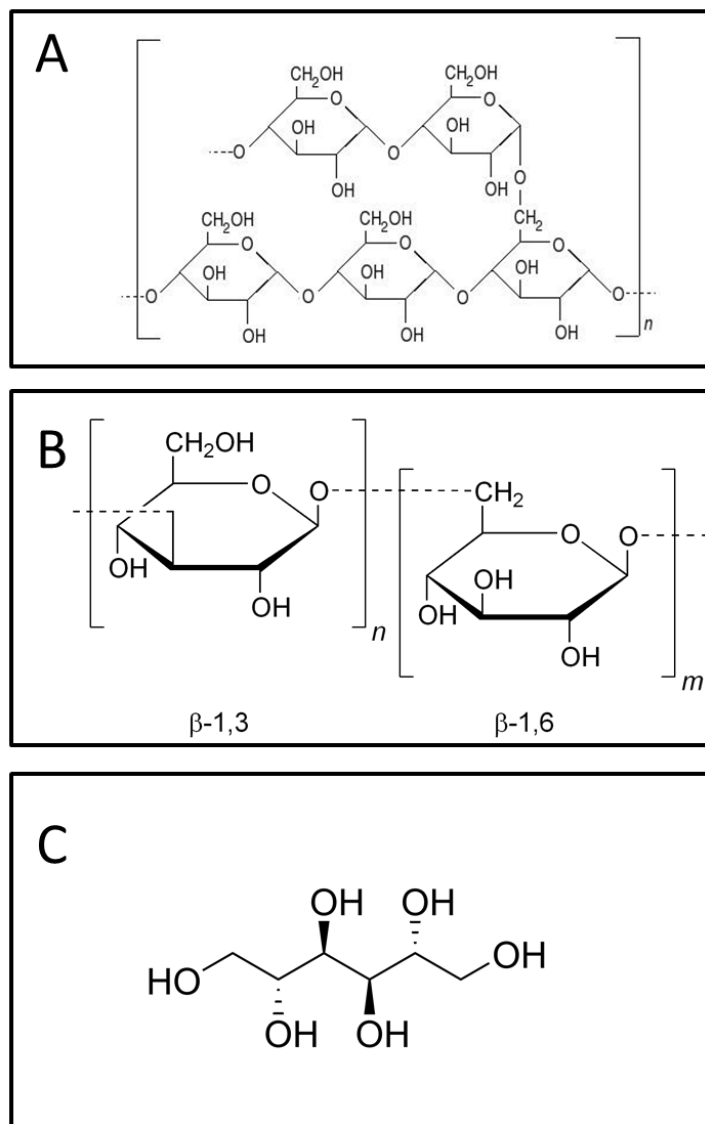


Figure 26 Structures de l'amidon (A) de la chrysolaminarine (B) et du mannitol (C).

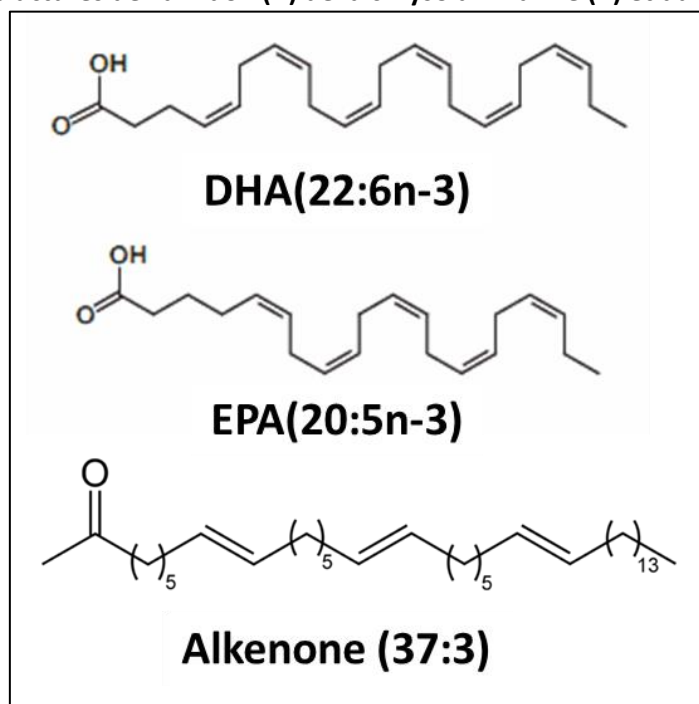


Figure 27 Structures d'acides gras spécifiques de microalgues.



Chez les algues en général, le fructose-6-phosphate (F6P) produit par le cycle de Calvin n'est pas converti en saccharose comme chez les plantes supérieures. Chez les macroalgues straménopiles, le F6P est principalement converti en mannitol qui, dans certaines conditions s'accumule fortement dans le cytosol et se comporte comme un moyen de stockage du carbone (**Figure 26**). Le métabolisme du mannitol est désormais bien connu chez les macroalgues du genre *Ectocarpus* (Michel *et al.*, 2010; Groisillier *et al.*, 2014; Bonin *et al.*, 2015). La présence de mannitol ainsi que certains gènes associés à son métabolisme ont été détectés chez des diatomées, des haptophytes et des chlorophycées (Dittami *et al.*, 2011; Mausz and Pohnert, 2015). Son rôle et son importance dans le stockage du carbone chez les microalgues est à ce jour très mal connu.

## B. Les lipides de réserve.

- **Les lipides de microalgues.**

Les lipides en général peuvent être classés en 3 catégories : 1) Les lipides membranaires qui englobent principalement les phospholipides et glycolipides ; 2) Les terpénoïde auxquels appartiennent caroténoïdes les chlorophylles et certaines plastoquinones qui sont impliqués généralement dans la photosynthèse, la photoprotection et la défense contre le stress oxydatif. 3) Les triacylglycérides (TAGs) et diacylglycérides (DAGs) qui constituent les principales réserves énergétiques chez les microalgues. Les lipides de microalgues présentent de nombreuses spécificités par rapport aux lipides de plantes telles que les acides gras polyinsaturés à très longue chaîne tels l'EPA et le DHA mobilisés dans les lipides membranaires et les lipides de réserve, les alkenones utilisées pour le stockage du carbone chez certaines haptophytes (**Figure 27**), ou le diacylglyceryltrimethylhomoserine (DGTS) fortement mobilisé au sein des membranes (Moore *et al.*, 2001; Guschina and Harwood, 2006).

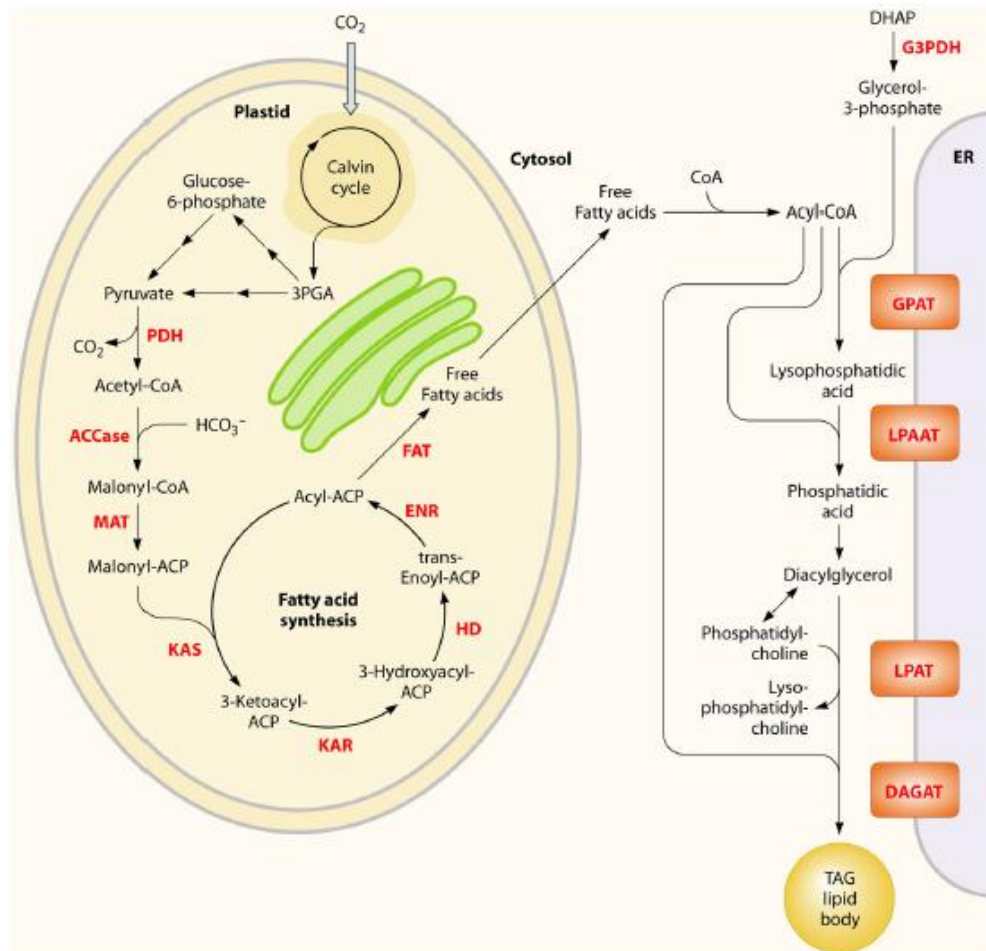
Les voies de biosynthèse des lipides de réserve chez les plantes ont été fortement étudiées pour des intérêts agronomiques, la plante non oléagineuse *Arabidopsis thaliana* étant généralement utilisée comme modèle biologique (Wallis and Browse, 2010). Jusqu'aux années 2010, le métabolisme des lipides des algues était relativement peu connu par rapport aux plantes. L'intérêt biotechnologique croissant pour certains lipides de microalgues a bénéficié ces dernières années du développement du séquençage à haut débit pour révéler les bases moléculaires des métabolismes spécifiques à ces microorganismes.



A ce jour, les études sur le métabolisme des lipides portent majoritairement sur les chlorophycées *C. reinhardtii* et en moindre mesure *Nannochloropsis sp.* et les diatomées *Oceanica pseudonana* et *P. tricornutum*. Les analyses *in silico* des données génomiques montrent de fortes homologies entre le métabolisme lipidique des plantes et des microalgues séquencées, (Guschina and Harwood, 2006; Moellering *et al.*, 2010; Khozin-Goldberg and Cohen, 2011; Merchant *et al.*, 2011). Cependant, il existe selon plusieurs aspects des différences significatives entre le métabolisme lipidique des plantes et des algues, et entre les microalgues elles-mêmes. A titre d'exemple, deux voies métaboliques alternatives de la synthèse des terpénoïde ont été identifiées en fonction des espèces microalgales (Lohr *et al.*, 2012). La voie du mévalonate utilise l'acétyl-CoA et a lieu dans le cytoplasme. La voie du méthylérythritol phosphate utilise le pyruvate et le G3P et a lieu dans le chloroplaste (Lohr *et al.*, 2012). Encore à titre d'exemple, des études ont permis d'identifier des désaturases et élongases impliquées dans la synthèse des AGPI-LC (Tonon *et al.*, 2004; Lu *et al.*, 2009; Lu *et al.*, 2010; Zhang *et al.*, 2010; Yu *et al.*, 2011; Zäuner *et al.*, 2012; Guiheneuf and Stengel, 2013; Mühlroth *et al.*, 2013; Vaezi *et al.*, 2013; Huerlimann *et al.*, 2014a; Kotajima *et al.*, 2014; Dolch and Maréchal, 2015). Il existe encore à ce jour de nombreuses lacunes concernant les enzymes impliquées dans la synthèse des lipides spécifiques de microalgues. Ainsi, il n'existe aucune donnée sur les mécanismes de synthèse des alkenones chez les haptophytes (Laws *et al.*, 2001; Eltgroth *et al.*, 2005; Toney *et al.*, 2012). Dans la suite de ce document, nous nous focaliserons sur le métabolisme des lipides de réserve de type TAG qui constituent la principale forme de stockage chez la plupart des microalgues.

- **Biosynthèse des acides gras.**

Sur les bases des analyses *in silico* des données génomiques, la synthèse *de novo* des acides gras chez les microalgues semble se dérouler comme chez les plantes (**Figure 28**). Elle a lieu dans le chloroplaste et fait intervenir différentes enzymes au lieu d'un complexe protéique multienzymatique comme chez animaux. La pyruvate kinase chloroplastique convertit le phosphoénolpyruvate en pyruvate. Le complexe chloroplastique pyruvate déshydrogénase (PDC) convertit le pyruvate en acétylcoenzyme A (acétyl-CoA) et l'acétyl-CoA est converti en malonyl-CoA par l'acétyl-CoA carboxylase (ACCase) afin d'alimenter la voie métabolique de biosynthèse des acides gras. Le groupe malonyl du malonyl -CoA est greffé sur un transporteur (ACP) par la malonyl-CoA:ACP transacylase (MAT). La biosynthèse des acides gras consiste en une succession de quatre réactions de condensation successives catalysées par des enzymes non complexées chez les algues : La 3-ketoacyl-ACP synthase (KAS), la 3-ketoacyl-ACP réductase (KAR), la 3-hydroxyacyl-ACP déshydratase (HD) et la enoyl-ACP réductase (ENR).



**Figure 28 Représentation simplifiée des voies de biosynthèse des lipides chez les microalgues. (Source : Radakovits et al, 2010)**

Les acides gras sont synthétisés dans le chloroplaste alors que l'assemblage des TAGs se produit au niveau du réticulum endoplasmique (RE). Les enzymes de biosynthèse des acides gras et de l'assemblage des TAGs sont indiquées en rouge. PDH, pyruvate déshydrogénase ; ACCase, acétyl-CoA-carboxylase ; MAT, malonyl-CoA:ACP transférase ; KAS, 3-cétoacyl-ACP transférase ; KAR, 3-cétoacyl-ACP réductase ; HD, 3-hydroxyacyl-ACP déshydratase ; ENR, énoyl-ACP réductase ; FAT, acyl-ACP thioestérase ; G3PDH, glycérol-3-phosphate déshydrogénase ; GPAT, glycérol-3-phosphate acyl-transférase ; LPAAT, acide lysophosphatidique acyltransférase ; LPAT, acide phosphatidylcholine acyltransférase ; DAGAT, diacylglycérol transférase.

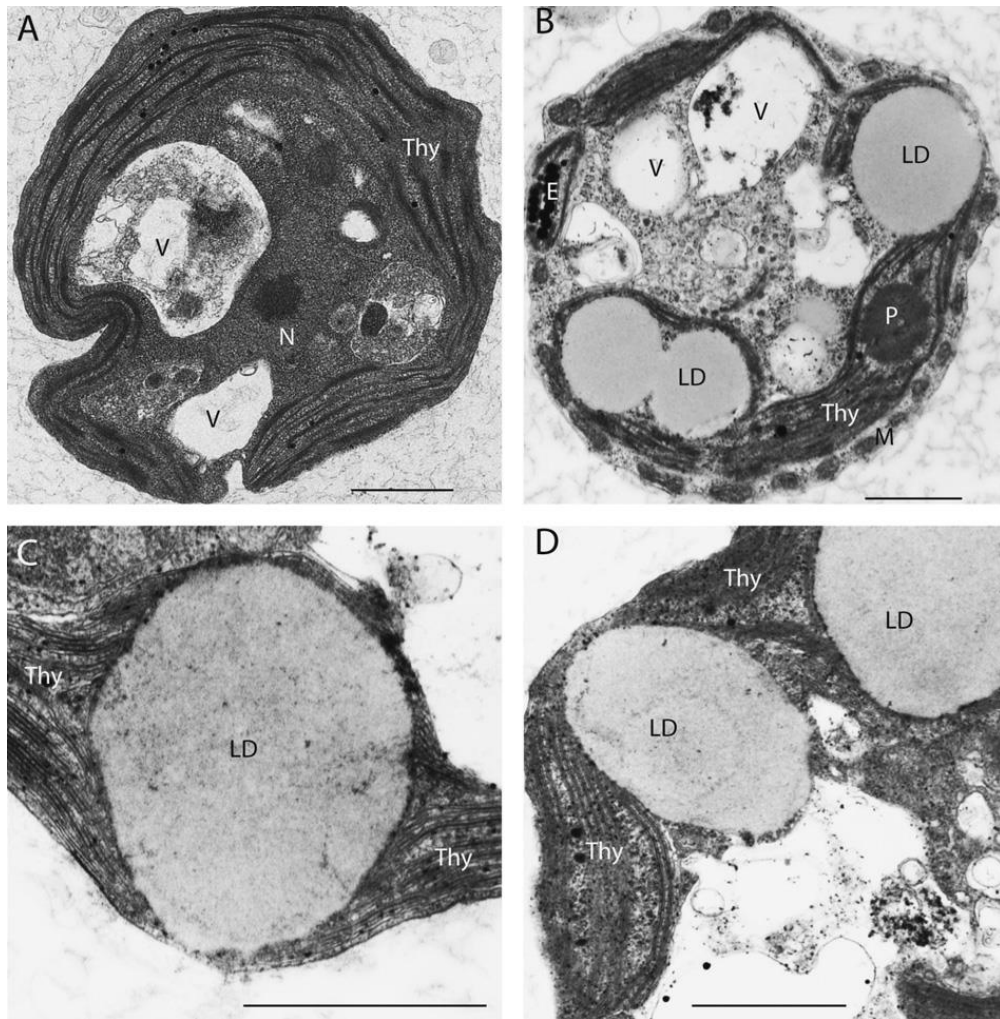
La 3-ketoacyl-ACP synthase (KAS), la 3-ketoacyl-ACP réductase (KAR), la 3-hydroxyacyl-ACP déshydratase (HD) et la enoyl-ACP réductase (ENR). Chaque cycle de condensation permet d'allonger de deux carbones la chaîne précurseur d'Acyl-ACP. En fin d'élongation, l'acide gras est « libéré » de l'ACP par l'acyl-ACP thioestérase (FAT). Ceci conduit à la formation d'acide gras à chaîne hydrocarbonée de 16 et/ou 18 atomes de carbone. La synthèse des acides gras nécessite une source de carbone (Acétyl-CoA) une source d'énergie (l'ATP) et une source de pouvoir réducteur (NADH et NADPH) qui sont fournies par les réactions photosynthétiques réalisées à proximité dans le chloroplaste (**Figure 28**). Les acides gras peuvent ensuite être transportés vers différents compartiments cellulaires et éventuellement allongés et désaturés par des élongases et des désaturases respectivement. Les acides gras sont ensuite utilisés pour la synthèse des lipides membranaires (phospholipides et glycolipides) et des lipides de réserve par greffage sur une base glycérol.

Chez les plantes, la première étape de synthèse *de novo* des acides gras assurée par l'ACCase est considérée comme la réaction limitant la production de lipides de réserve. Chez les microalgues, bien que cette étape soit cruciale à la synthèse des acides gras (Huerlimann *et al.*, 2014b), la surexpression de l'ACCase n'aboutit pas nécessairement à la suraccumulation de TAGs (Dunahay *et al.*, 1996). Malgré des voies métaboliques similaires entre plantes et microalgues, il existe donc des spécificités notables à chacun des *phyla* considérés.

- **Biosynthèse des triglycérides.**

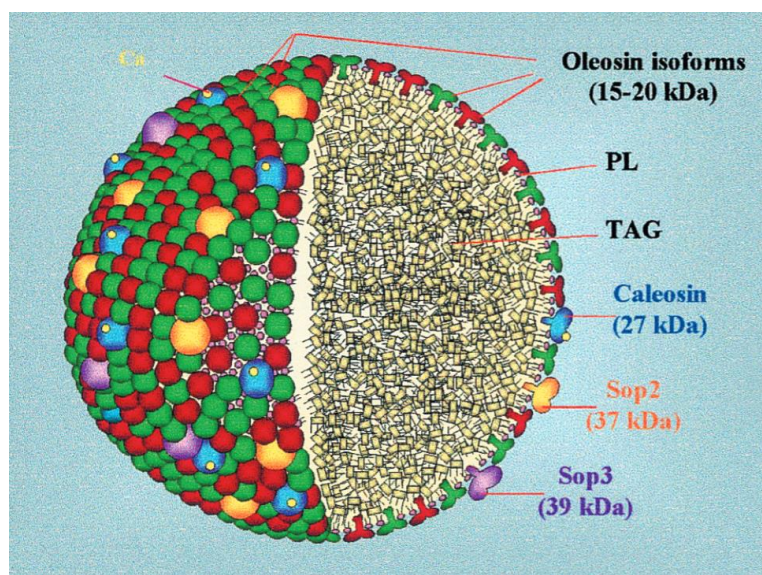
Les triglycérides ou triacylglycérols (TAGs) constituent la majeure partie des lipides de réserve des microalgues. Les enzymes clé de la biosynthèse des TAGs ont été identifiées chez l'espèce modèle *C. reinhardtii* par analyses transcriptomiques (Miller *et al.*, 2010; Boyle *et al.*, 2011; Merchant *et al.*, 2011; Boyle *et al.*, 2012; Msanne *et al.*, 2012). Le nombre d'homologue pour chacune des enzymes varie considérablement en fonction des *phyla* (Merchant *et al.*, 2011). Le rôle de ces homologues reste à ce jour mal identifié.

D'une manière générale, chez les plantes et les microalgues, les TAGs sont assemblés au niveau de réticulum endoplasmique par greffage des acides gras sur une base de G 3-P pour former successivement de l'acide phosphatidic (PA), du diacylglycérol (DAG) et du triacylglycérol (TAG) (**Figure 28**). Ces réactions font intervenir différentes acyltransférases (GPAT : glycérol-3-phosphate acyl-transférase ; LPAAT : acide lysophosphatidique acyltransférase ; LPAT : acide phosphatidylcholine acyltransférase ; DAGAT : diacylglycérol transférase). Il s'agit de la voie Kennedy décrite dans les graines de plantes oléagineuse en 1961 par Kennedy (Kennedy 1961).



**Figure 29 : Observation au microscope électronique à transmission des vésicules lipidiques (LD) chez *Chlamydomonas reinhardtii*.** (Source : Fan et al., 2011)

(A) Cellule non carencée et (B) carencée en azote. (C) observation d'un LD dans le chloroplaste. (D) LD à la jonction chloroplaste-cytosol. Thy : Thylacoïdes ; E : eyespot ; M : mitochondrie ; V : vacuoles ; N : noyau.



**Figure 30 Schéma d'une vésicule lipidique de plante.** (Source : Frandsen et al., 2001)

Une voie de synthèse de TAGs alternative a été mise en évidence chez les chlorophytes et chez les diatomées. Cette voie consiste à utiliser les acides gras de la phosphatidylcholine, lipides membranaires majoritaire, et de les greffer sur le diacylglycérol grâce à l'action de la phospholipid:diacylglycérol acyltransferase (PDAT) (Yoon *et al.*, 2012).

D'autre part, chez les chlorophycées et contrairement aux plantes, la synthèse de TAGs se produit conjointement au niveau du réticulum endoplasmique et dans le chloroplaste. Les vésicules lipidiques formées dans le chloroplaste par accumulation de TAGs sont ensuite secrétées dans le cytoplasme (Fan *et al.*, 2011; Goodson *et al.*, 2011) (**Figure 29**). A ce jour, il existe peu d'information à ce sujet chez les autres *phyla* de microalgues.

- **Les vésicules lipidiques.**

Les vésicules lipidiques (VL) sont des organites spécialisés dans le stockage des lipides de réserve. Chez les plantes, ils sont composés d'un cœur lipidique riche en TAGs encapsulé par une membrane monocouche phospholipidique associées à des protéines membranaires majoritaires, les oléosines et caléosines, qui agissent comme des agents structurants et stabilisants (Frandsen *et al.*, 2001) (Figure 30). Bien que la structure des vésicules lipidiques soit similaire entre plantes et microalgues, il existe certaines différences notables. D'une part, les vésicules lipidiques de microalgues contiennent des pigments de type caroténoïdes contrairement aux plantes. D'autre part, les vésicules lipidiques de microalgues ne contiennent ni oléosine ni caléosine. Chez les chlorophycées *C. reinhardtii*, *Dunaliella salina*, *Dunaliella Bardawil*, *Haematococcus pluvialis*, et *Volvox carteri*, une protéine majoritaire caractérisée par un motif peptidique conservé, la « major lipid droplet protein » (MLDP), joue un rôle structurant de ces vésicules (Moellering and Benning, 2010; Davidi *et al.*, 2012). Des protéines majoritaires de fonction similaire mais de nature différente ont été décrites chez les straménopiles *Nannochloropsis sp* et *Fistulifera solaris* (Vieler *et al.*, 2012; Maeda *et al.*, 2014). Malgré l'absence d'homologie de séquence entre les protéines majoritaires des différents *phyla* de microalgues, il semblerait que les structures tridimensionnelles restent conservées. Par ailleurs, de nombreuses protéines impliquées dans la synthèse des TAGs et dans leur dégradation sont présentes dans les vésicules lipidiques de *C reinhardtii* ce qui suggère une activité métabolique à l'intérieur de ces vésicules chez de microalgues (Nguyen *et al.*, 2011).

La mise en réserve de TAGs sous forme de vésicules lipidiques permet le stockage d'acides gras qui seront utilisés ultérieurement soit pour la synthèse de lipides membranaires, soit pour la production de précurseurs métaboliques *via* la  $\beta$ -oxydation et le cycle du glyoxylate.





D'autre part, lors de stress nutritifs comme une carence azotée, les cellules soumises à la lumière poursuivent une activité photosynthétique qui génère des composés oxydatifs non intégrés dans les composés azotés. La synthèse de TAGs pourrait permettre d'assimiler l'excès de composés photo-assimilés et de se prémunir du stress oxydatif (Solovchenko, 2012). D'autre part, les caroténoïdes présents dans les vésicules lipidiques peuvent également avoir un rôle de photoprotection lorsque les algues sont soumises à un excès d'énergie photochimique (Solovchenko, 2012; Klok *et al.*, 2013).

### C. Recyclage métabolique du carbone.

Lors de changement de conditions physiologiques, le carbone alloué sous différentes formes au sein de la cellule peut être réorienté pour la production de molécules d'intérêt pour les nouvelles conditions. Schématiquement, lors d'un stress nutritionnel, le carbone est orienté majoritairement vers le stockage sous forme de sucres et lipides de réserve, ceci au détriment de la production de biomasse fonctionnelle (protéines, acides nucléique, lipides membranaires). Généralement les microalgues accumulent dans un premier temps des sucres de réserve, puis dans un second temps des lipides de réserve. Dans certains cas de stress prolongé, une partie du carbone des sucres de réserve peut être utilisé pour la production de lipides de réserve (Wang *et al.*, 2015). Lorsque les conditions redeviennent favorables, les lipides et sucres de réserves sont dégradés pour produire de l'énergie sous forme d'ATP, du pouvoir réducteur sous forme de NADPH et NADH et des précurseurs métaboliques pour la synthèse de biomasse fonctionnelle. Ces mécanismes de réallocation du carbone au sein de la cellule font intervenir le catabolisme, et les voies métaboliques cœur qui se croisent au niveau de carrefours métaboliques.

- **Utilisation des sucres de réserve**

Les sucres de réserves sont dégradés en unité glucose par différentes glycoside-hydrolases (GH), plus ou moins spécifiques des substrats, et répertoriées sur le site internet <http://www.cazy.org/>. Les unités glucoses peuvent être converties en métabolites précurseurs par la voie de la glycolyse et alimenter l'ensemble des voies anaboliques. Le pyruvate issu de la glycolyse peut être converti en Acétyl-CoA par le complexe pyruvate déshydrogénase (PDH). Chez les microalgues, la PDH mitochondriale permet d'alimenter le cycle de Krebs alors que la PDH chloroplastique permet d'alimenter en Acétyl-CoA la biosynthèse des acides gras. La dégradation des sucres de réserve peut ainsi alimenter soit la synthèse de lipides de réserve, soit la synthèse de biomasse fonctionnelle.

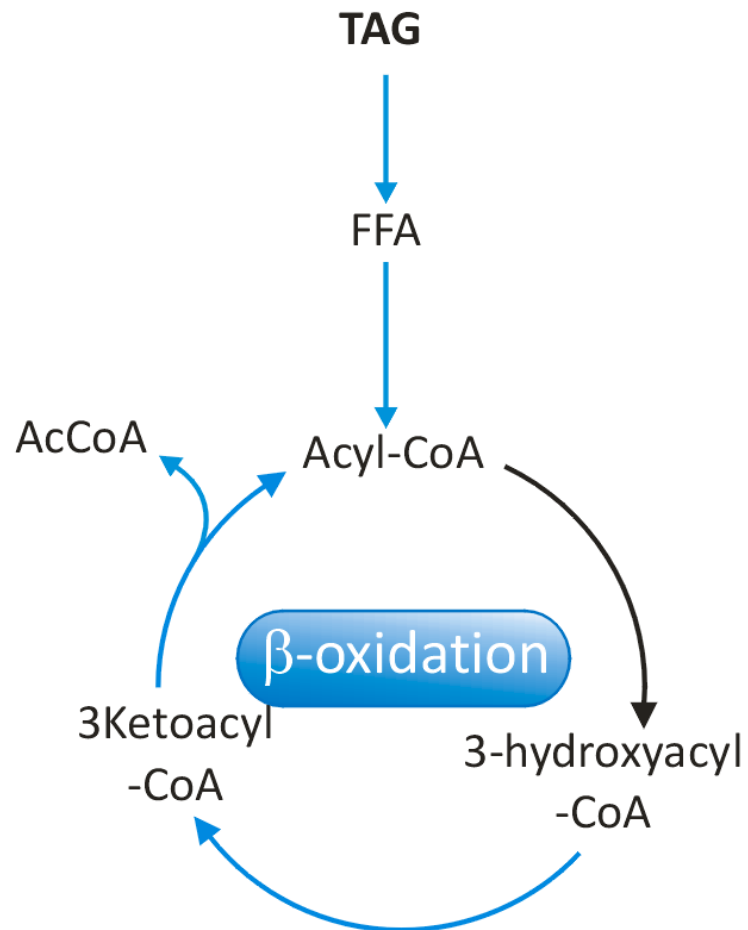


Figure 31 Schéma simplifié de la  $\beta$ -oxydation des TAGs.

- **Utilisation des lipides de réserve**

Les TAGs sont hydrolysés en acides gras libres par l'action d'enzymes de type triacylglycérols hydrolases (TAGH) localisées à l'intérieur des vésicules lipidiques. Puis les acides gras sont dégradés par  $\beta$ -oxydation en Acétyl-CoA (**Figure 31**). Cet Acétyl-CoA peut ensuite alimenter le cycle de Krebs dans la mitochondrie pour générer de l'énergie, du pouvoir réducteur ou des acides aminés. Il peut aussi être métabolisé par le cycle du glyoxylate, seule voie métabolique permettant la synthèse de glucides à partir d'acides gras. Lors de la germination des graines chez les plantes oléagineuses, ces voies permettent de dégrader les lipides de réserve pour la production de métabolites primaires puis de biomasse fonctionnelle nécessaire à la croissance. Chez les plantes, la  $\beta$ -oxydation et le cycle du glyoxylate ont lieu dans les glyoxysomes. L'ensemble des enzymes impliquées dans ces voies ont été identifiées dans les génomes de microalgues mais la localisation cellulaire des réactions reste à confirmer (Hayashi *et al.*, 2015). A l'instar des sucres de réserve, la dégradation des lipides de réserve permet d'alimenter en métabolites précurseurs l'ensemble des voies anaboliques de la cellule.

## 9. Impact de la carence azotée sur le métabolisme du carbone

### A. Carence azotée et stockage du carbone.

La disponibilité de l'azote est un des moteurs principaux du stockage du carbone chez microalgues. Lors de la limitation azotée, le rapport N/C des microalgues baisse et le carbone fixé est alloué à des composés énergétiques carbonés pauvres en azote : les sucres et les lipides de réserve (Spoehr and Milner, 1949; Shifrin and Chisholm, 1981; Guschina and Harwood, 2006).

Les publications portant sur les mécanismes moléculaires impliqués dans la réponse au stress azoté ont vu leur nombre fortement augmenter ces cinq dernières années. Ces travaux portent essentiellement sur des espèces oléagineuses et sur l'algue modèle *C. reinhardtii*. Cependant, les résultats de ces études sont souvent difficiles à comparer du fait de la grande diversité des conditions écophysiologiques entre les études. Ainsi, à l'exception des travaux de Msanne *et al.* (2012) et Shtaida *et al.* (2014) réalisés en en photo-autotrophie avec le CO<sub>2</sub> pour seule source de carbone, les études sur *C. reinhardtii* sont réalisées dans des conditions de mixotrophie pour augmenter l'accumulation de TAGs (Miller *et al.*, 2010; Fan *et al.*, 2011; Fan *et al.*, 2012; Lee *et al.*, 2012; Ramanan *et al.*, 2013; Schmollinger *et al.*, 2014; Valledor *et al.*, 2014; Wase *et al.*, 2014; Gargouri *et al.*, 2015; Park *et al.*, 2015). Les autres espèces telles que *P. tricornutum*, *Micractinium pusillum*, *N. oceanica* et *N. gaditana* sont cultivées en photo-autotrophie (Valenzuela *et al.*, 2012; Dong *et al.*, 2013; Simionato *et al.*, 2013; Valenzuela *et al.*, 2013; Yang *et al.*, 2014; Alipanah *et al.*, 2015). D'autre

part, les modes opératoires utilisés pour générer une limitation azotée consistent dans certains cas à réaliser des cultures en mode batch et attendre la phase stationnaire, dans d'autre cas à reprendre les cellules dans un milieu exempt d'azote, ou plus rarement à cultiver les cultures en chemostat. Enfin, le niveau de limitation azotée est rarement défini pour comparer les études entre elles.

Néanmoins, d'une manière générale, l'ensemble de ces travaux montrent que la raréfaction de l'azote affecte profondément le métabolisme du carbone, de sa fixation à sa remobilisation au sein de la cellule.

### **B. Baisse de la fixation du carbone.**

La carence azotée affecte profondément les mécanismes photosynthétiques de fixation du carbone chez les microalgues. La photosynthèse est affectée à travers la dégradation de la chlorophylle a et la sous-expression des protéines de l'appareil photosynthétique (Miller *et al.*, 2010; Lee *et al.*, 2012; Msanne *et al.*, 2012; Wase *et al.*, 2014; Alipanah *et al.*, 2015; Gargouri *et al.*, 2015). Chez *C. reinhardtii*, les protéines impliquées dans les mécanismes de concentration du carbone, le cycle de Calvin et de la traduction chloroplastique sont généralement sous-exprimées. Des résultats similaires concernant le cycle de Calvin et de la traduction chloroplastique ont été obtenus chez *P. tricornutum* (Valenzuela *et al.*, 2012). La baisse de la fixation photosynthétique du carbone permet de limiter le déséquilibre entre l'absorption de l'azote et du carbone. Cependant, malgré une baisse d'activité photosynthétique, les microalgues oléagineuses continuent d'assimiler du carbone. Ainsi, chez *P. tricornutum*, les gènes impliqués dans les mécanismes de concentration du carbone sont surexprimés lors de la carence azotée (Valenzuela *et al.*, 2013). Chez *N. gaditana*, le stress azoté provoque une profonde modification de l'appareil photosynthétique lui permettant de réduire sans pour autant stopper complètement sa fixation du carbone (Simionato *et al.*, 2013).

L'effet de la limitation azotée sur l'assimilation du carbone organique semble controversé selon les auteurs. Dans le cas particulier des cultures mixotrophes de *C. reinhardtii*, les enzymes de l'assimilation de l'acétate sont surexprimées lors de la carence azotée dans les études de Gargouri *et al.* (2015) mais sous-exprimées dans les travaux de Lee *et al.* (2012) et Wase *et al.* (2014). Selon Miller *et al.* (2010), l'acétyl-CoA produit à partir de l'acétate n'intégrerait pas le cycle de glyoxylate mais serait converti directement en acide gras pour la production de TAGs. D'autre part, Fan *et al.* (2012) montrent que la présence de lumière et donc d'activité photosynthétique est indispensable pour la production de TAGs dans des cultures mixotrophes. En conclusion, *C. reinhardtii* assimile du carbone sous forme acétate et le convertit en TAGs par des voies métaboliques de nature encore mal connues mais qui font intervenir l'activité photosynthétique.

### C. Origine des lipides lors de la carence azotée: Remobilisation intracellulaire du carbone ou synthèse de novo ?

La provenance des acides gras utilisés pour la synthèse des TAGs lors de la carence azotée est encore débattue dans la communauté scientifique. Chez les plantes oléagineuses, les enzymes de la synthèse *de novo* des acides gras sont fortement surexprimées dans les graines lors de la biosynthèse des TAGs (Lee *et al.*, 2002; O'Hara *et al.*, 2002; Ruuska *et al.*, 2002). Certains auteurs suggèrent que la synthèse *de novo* est la principale source d'acides gras chez les microalgues pour l'assemblage des TAGs (Fan *et al.*, 2011; Li *et al.*, 2012b; Simionato *et al.*, 2013; Wang *et al.*, 2015). Cependant, selon certaines études contradictoires chez *C. reinhardtii*, *N. gaditana*, *P. tricornutum* et *N. oleoabundans*, ces enzymes ne sont pas surexprimées lors de la carence azotée (Lee *et al.*, 2012; Li *et al.*, 2012b; Msanne *et al.*, 2012; Valenzuela *et al.*, 2012; Dong *et al.*, 2013; Simionato *et al.*, 2013; Gao *et al.*, 2014; Shtaida *et al.*, 2014; Valledor *et al.*, 2014; Huerlimann *et al.*, 2014b; Alipanah *et al.*, 2015). Ces résultats suggèrent que les acides gras utilisés pour la synthèse des lipides de stockage peuvent provenir non seulement de la synthèse *de novo* des acides gras dans certains cas, mais également de la remobilisation intracellulaire du carbone.

Dans l'ensemble des études, la carence azotée provoque un bouleversement global de l'allocation du carbone de la cellule ceci *via* la régulation des enzymes de l'ensemble des voies métaboliques du carbone. Lors de la carence azotée, *C. reinhardtii*, *P. tricornutum* et *N. gaditana*, sur-expriment des enzymes de dégradation des lipides membranaires (Simionato *et al.*, 2013; Li *et al.*, 2014; Schmollinger *et al.*, 2014; Valledor *et al.*, 2014; Alipanah *et al.*, 2015). A l'inverse, les enzymes du catabolisme des TAGs, de la  $\beta$ -oxydation et du cycle du glyoxylate sont sous-exprimées ce qui provoque une conservation du carbone des TAGs (Wase *et al.*, 2014; Gargouri *et al.*, 2015). Ces résultats suggèrent une conservation des lipides de réserve, et une remobilisation des acides gras des lipides membranaires.

D'autre part, chez *C. reinhardtii* et *P. tricornutum*, une carence azotée supérieur à 24H conduit à une activation de la dégradation des sucres de réserve et de la glycolyse (Valenzuela *et al.*, 2012; Wase *et al.*, 2014; Alipanah *et al.*, 2015; Gargouri *et al.*, 2015). Ceci conduit à une remobilisation du carbone des sucres de réserve pour la production de l'acétyl-CoA, métabolite précurseurs pour la synthèse lipidique. De la même manière, lors d'un stress azoté chez *P. tricornutum*, la suraccumulation d'enzymes de dégradation des acides aminés branchés intervient dans la remobilisation du carbone des protéines vers l'acétyl-CoA (Ge *et al.*, 2014). Selon ces mêmes auteurs, l'acétyl-CoA formé à partir de la dégradation des acides aminés branchés est intégré au cycle de Krebs et le malate formé

est transporté des mitochondries vers le chloroplaste pour être converti en pyruvate puis acétyl-CoA et alimenter ainsi la synthèse des acides gras.

## 10. *Tisochrysis lutea*, espèce modèle pour l'étude du métabolisme des haptophytes.

*T. lutea* est une haptophyte de la famille des Isochrysidaceae et de l'ordre des isochrysidales (**Figure 32**). Cette espèce planctonique océanique tropicale a été isolée pour la première fois en Polynésie Française dans les années 1980 et a été identifiée depuis en atlantique, dans le Pacifique et en Mer du Nord (Bendif *et al.*, 2013). Sur la base de critères morphologiques, elle a longtemps été associée à l'espèce *Isochrysis galbana* sous le nom *Isochrysis affinis galbana* souche Tahiti ou T-ISO (**Figure 33**). Des approches phylogénétiques ont récemment permis de définir un nouveau genre *Tisochrysis* qui inclue pour l'instant une seule espèce *T. lutea* (Bendif *et al.*, 2013). Les deux espèces *T. lutea* et *I. galbana* sont donc souvent confondues dans la littérature malgré des optimums de température différents. A l'exception des Noelaerhabdaceae auxquels appartiennent *Geophyrocapsa oceanica* et *E. huxleyi*, les isochrysidales ne forment pas de coccolite et l'existence d'un cycle haplodiplophasique n'a encore jamais été mise en évidence. *T. lutea* est une des microalgues les plus couramment cultivée dans pour l'aquaculture, soit pour la nutrition de larves de mollusques et crustacés marins dans les écloséries, soit pour la nutrition de proies vivantes pour la pisciculture et l'aquariologie (lire pour exemple (Okauchi, 1990; Thinh, 1994; Ferreira *et al.*, 2008; Reitan, 2011). Elle produit de fortes quantités de DHA et est donc considérée comme une source d'AGPI-LC intéressante pour la santé animale et humaine (Swift and Taylor, 1974; Tzovenis *et al.*, 1997; Gouveia *et al.*, 2008; Fradique *et al.*, 2013). D'autre part, elle accumule, suite à une limitation azotée, de fortes quantités de sucres et lipides de réserve et est considérée par plusieurs auteurs comme une algue oléagineuse (Rieley *et al.*, 1998; Lin *et al.*, 2007; Feng *et al.*, 2011; Lacour *et al.*, 2012; Eltgroth *et al.*, 2005; Feng *et al.*, 2011; Stephenson *et al.*, 2011; Roleda *et al.*, 2013; Song *et al.*, 2013; Huerlimann *et al.*, 2014b; Nalder *et al.*, 2015). D'autre part, *T. lutea* et de sa cousine *Isochrysis galbana* sont des espèces couramment utilisée pour des études écophysiologiques (Flynn *et al.*, 1992; Saoudihelis *et al.*, 1994 (Bougaran *et al.*, 2003; Bougaran *et al.*, 2010; Lacour *et al.*, 2012; Marchetti *et al.*, 2013).

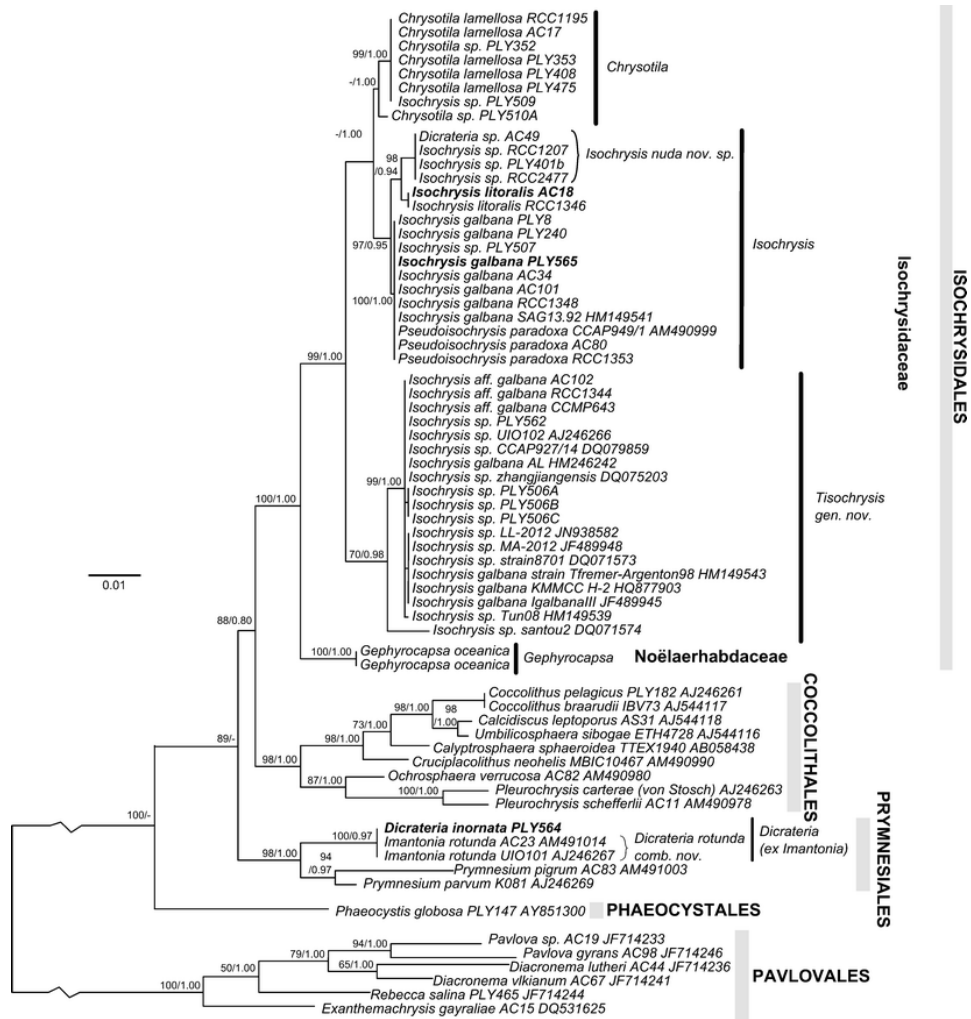


Figure 32 Phylogénie des Isochrysidales sur la base de leurs séquences 18S. (Source : Bendif et al., 2013)

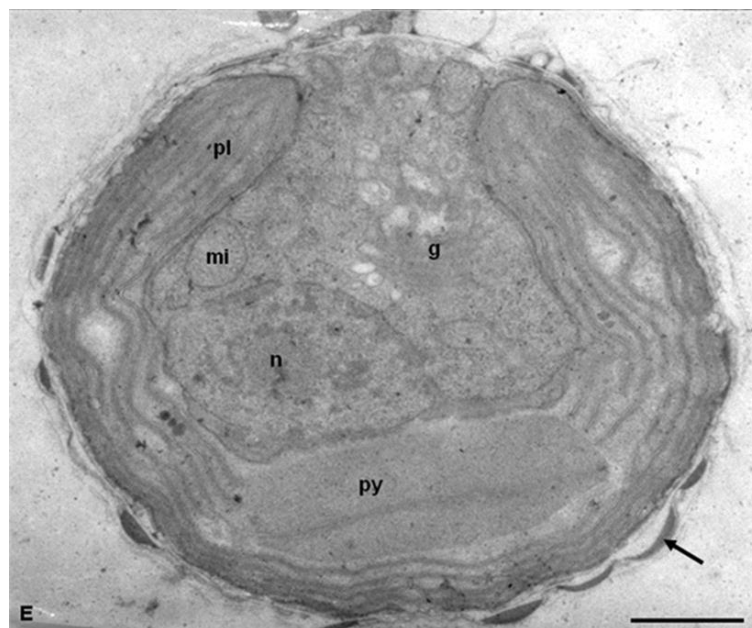


Figure 33 Cellule de *Tisochrysis lutea* observée au microscope électronique à transmission. (Source : Bendif et al., 2013)

La barre d'échelle représente 1  $\mu\text{m}$ . pl : plaste pariétal ; n : noyau ; mi : mitochondrie ; py : pyrénoloïde ; g : golgi.

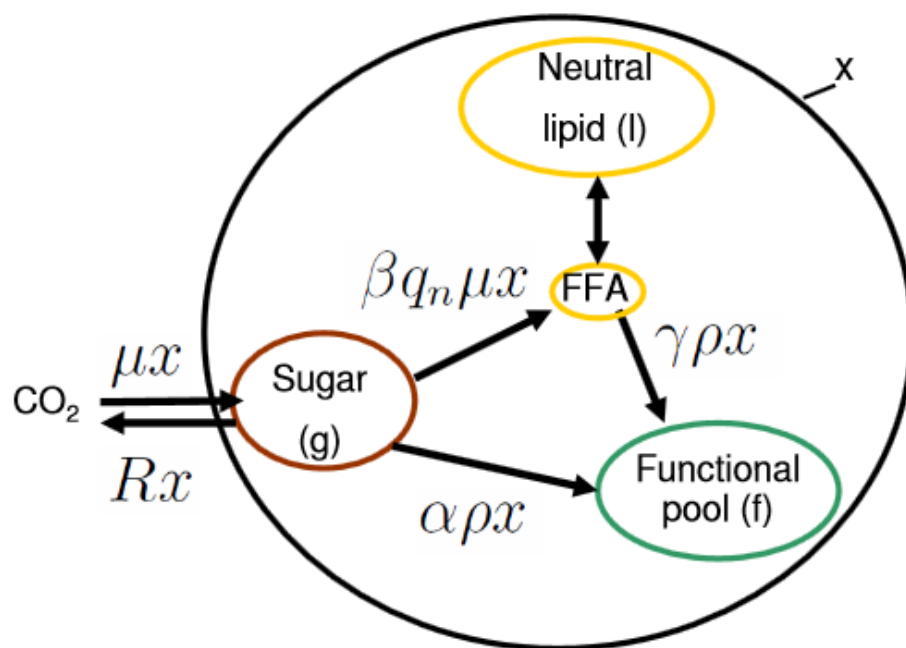


Figure 34 Représentation simplifié du flux de carbone utilisé par Mairet et al. (Mairet et al., 2011)

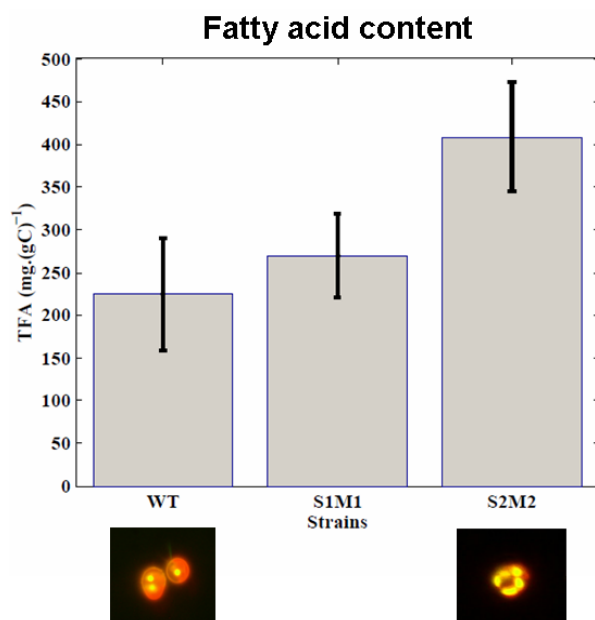


Figure 35 : Résultat d'amélioration du contenu en acide gras de *T. lutea* dans le cadre du projet Shamash. (Source : Bougaran et al, 2012)



Sur la base de flux intracellulaires de carbone simples (**Figure 34**), Mairet et co-auteurs ont proposé un modèle de croissance de *T. lutea* permettant de prédire la productivité de biomasse, de lipides et de sucres (Mairet *et al.*, 2011). Ces modèles globaux basés sur des approches écophysiologicals ne tiennent pas compte de données moléculaires qui étaient très parcellaires en début de ce travail (Qi *et al.*, 2002; Pereira *et al.*, 2004; Petrie *et al.*, 2010; Li *et al.*, 2012a; Shi *et al.*, 2012).

Lors du projet Shamash (financement ANR 2006-2009), une stratégie de sélection variétale non OGM (Organisme Génétiquement Modifié) basée sur la mutation UV et de tri cellulaire d'amélioration des espèces de microalgues a permis l'obtention d'une souche de *T. lutea* accumulant deux fois plus de lipides neutres que la souche originelle lors de la carence azotée (Figure 35) (Bougaran *et al.*, 2012). Les connaissances concernant les mécanismes moléculaires impliqués dans le métabolisme de l'azote et l'allocation du carbone chez les haptophytes sont très fragmentées fragmentaires et concernent essentiellement l'espèce coccolithophore *E. huxleyi*. Du fait des applications biotechnologiques avérées et potentielles de *T. lutea* et du rôle primordial des haptophytes sur les cycles biogéochimiques, notre choix d'étude s'est tout naturellement portée sur la compréhension du métabolisme azoté et de l'allocation du carbone chez cette espèce. nous avons posé comme stratégie scientifique d'utiliser cette espèce comme modèle pour étudier le métabolisme azote et l'allocation du carbone.

## 11. Présentation de l'étude.

L'objectif de ce travail de thèse est de contribuer à une meilleure connaissance du métabolisme des haptophytes non coccolithophores. Plus précisément, il vise à mieux cerner les mécanismes d'adaptation à la limitation azotée et les mécanismes d'allocation du carbone chez *T. lutea*. Ces questions, déjà abordées chez certaines espèces de diatomées et chlorophycées ne l'ont jamais été chez les haptophytes non coccolithophores dont l'étude présente des implications tant au niveau écologique que biotechnologique. La stratégie générale consiste à intégrer des approches de génomique fonctionnelles et des approches écophysiologicals pour comprendre les mécanismes moléculaires associés à différentes conditions azotées et à différents phénotypes.

Dans un premier temps, nous avons initié des travaux sur le transport de l'azote en identifiant les transporteurs haute affinité de *T. lutea* et en caractérisant leur expression en fonction de la limitation azotée.

Nous avons ensuite profité de souches mutantes hyper-lipidiques pour identifier les mécanismes impliqués dans l'accumulation lipidique chez *T. lutea*. L'utilisation de mutants est une pratique

couramment utilisée pour décrire les mécanismes moléculaires associés à un phénotype. Les stratégies de « reverse génomique » consistent à muter un gène cible pour identifier sa fonction par caractérisation du phénotype. A l'inverse, les stratégies de « forward génomique » consistent à identifier les gènes impliqués dans les différences phénotypiques préalablement obtenue de manière non contrôlée. Cette dernière stratégie sera mise en œuvre par différentes approches pour comprendre les mécanismes impliqués dans l'accumulation des lipides en comparant la souche sauvage et les souches mutantes obtenues par mutation aléatoire et sélection, ceci dans différentes conditions de limitation et carence azotée. Nous avons cherché à savoir pourquoi des souches mutantes accumulent plus de lipides de réserve que la souche sauvage et comment la limitation azotée intervient dans l'accumulation des lipides.

**Chapitre I :** Le chapitre I est consacré à l'identification et à la caractérisation des 4 transporteurs d'azote de haute affinité de *T. lutea*. Ces travaux ont été publiés dans la revue *Physiologia Plantarum* en 2015 (Charrier *et al.*, 2015).

**Chapitre II :** Dans une première étude de génomique fonctionnelle, nous avons identifié et comparé les transcriptomes de la souche sauvage (WT ; CCAP927/14) et de la souche hyper-lipidique S2M2 (2X ; CCAP926/14) lors de la carence azotée, en début de phase stationnaire d'une culture en mode batch. Cette étude a permis d'acquérir les premières bases moléculaires de *T. lutea*, et d'identifier certains gènes candidats pouvant intervenir dans la suraccumulation lipidique chez la souche mutante. Ces travaux font l'objet d'un article publié dans la revue *PLoS One* en 2013 (Carrier *et al.*, 2014).

**Chapitre III :** Ce chapitre présente la première étude protéomique réalisée chez *T. lutea*. Il vise d'une part à identifier les protéines différenciellement accumulées entre les deux souches dans les mêmes conditions physiologiques que l'étude transcriptomique, c'est à dire lors de la carence azotée. D'autre part, il vise à étudier l'effet de la carence azotée sur le protéome de chacune des deux souches en comparant un état peu limité par l'azote et un état carencé. Ces analyses ont permis d'identifier des protéines de fonction connues ou inconnues régulées par l'azote et potentiellement impliquées dans l'accumulation des lipides. L'ensemble des techniques et les résultats principaux de cette étude ont été publiés dans « *Journal of Proteomics - Elsevier* » en 2014 (Garnier *et al.*, 2014). Une analyse complémentaire des enzymes potentiellement impliquées dans des modifications post traductionnelles observées sera également présentée dans ce chapitre.

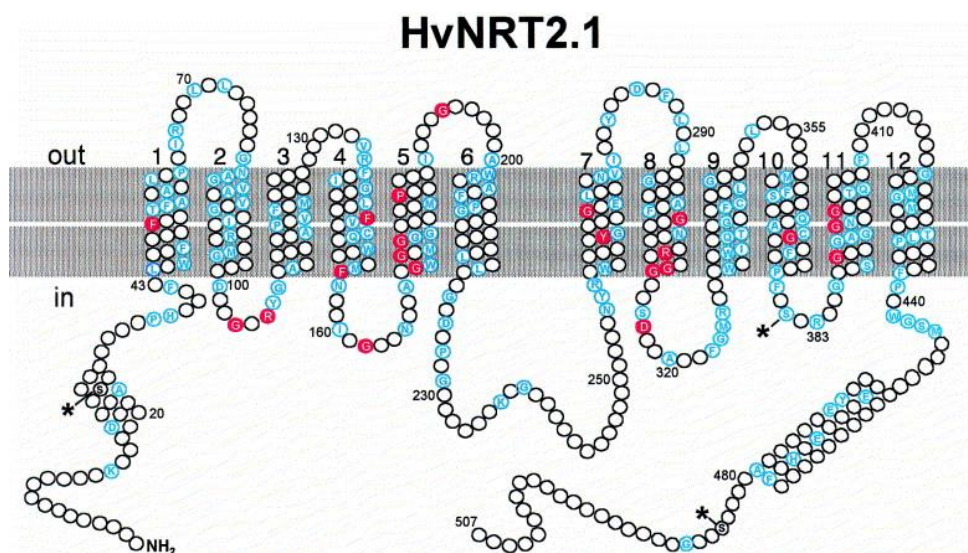
**Chapitre IV** Ce chapitre présente une étude dynamique et intégrative de l'effet de la limitation azotée sur l'allocation du carbone chez les souches WT et S2M2 (2X). Dans ce travail, les deux souches ont été cultivées en mode chemostat et étudiées lors de variations fines et contrôlées de la limitation azotée. Des approches écophysiologiques, biochimiques, transcriptomiques et protéomiques ont été employées pour comparer les deux souches et les différents niveaux de limitation. Les voies métaboliques potentiellement impliquées dans la sur accumulation lipidique de la souche mutante ont été identifiées par des approches protéomiques haut débit. Une partie des résultats de ces travaux a été proposé pour publication au journal *Algal Research* en janvier 2016 sous le titre « Use of a lipid rich strain reveals mechanisms of nitrogen limitation and carbon partitioning in the haptophyte *T.lutea* » (Garnier *et al.*, en soumission) . Les modèles écophysiologiques proposé ainsi que les résultats d'analyses transcriptomiques font l'objet de paragraphes dédiés dans ce chapitre.

**Chapitre V** Ce dernier chapitre est consacré exclusivement à l'étude de deux protéines CSAP et PLAAOx, qui sont des protéines majoritaires, de fonction mal connue et qui ont été sélectionnées sur la base des résultats des chapitres précédents. Dans ce chapitre, nous présentons des résultats d'annotation fonctionnelle, d'expression en fonction de la limitation azotée, et faisons une synthèse sur la régulation et le rôle potentiel de ces deux protéines d'intérêt.

Enfin, Le dernier chapitre est consacré aux conclusions générales de ce travail et aux perspectives de recherches qui en découlent



Chapitre I :  
Identification et régulation des  
transporteurs d'azote de *Tisochrysis*  
*lutea*.



**Figure 36** Représentation schématique du transporteur NRT2 chez *Hordeum vulgare*. (Source : Forde, 2000)

Les résidus conservés dans les plantes et les algues sont indiqués en bleu.

## Chapitre I : Identification et régulation des transporteurs d'azote de *Tisochrysis lutea*.

---

### 1. Introduction.

L'étude du transport de l'azote chez les haptophytes présente des intérêts pour la gestion des ressources minérales dans les cultures de microalgues ainsi que pour l'étude du cycle de l'azote au sein des masses d'eau océaniques. Dans ce chapitre, nous présentons la première caractérisation moléculaire des gènes de transporteurs d'azote (nitrates / nitrites) à haute affinité de type *Nrt2* chez la microalgue *T. lutea*, et d'une manière plus générale, chez les haptophytes. Les protéines NRT2 sont des protéines transmembranaires de 500 à 600 acides aminés impliquées dans le transport à haute affinité du nitrate. Elles présentent une structure conservée de 12 hélices transmembranaires et d'une boucle cytosolique centrale. Cette famille de transporteurs présentent des motifs peptidiques conservés présents au sein de l'hélice 5 et entre l'hélice 2 et 3 (**Figure 36**) (Forde, 2000). Généralement, plusieurs membres de cette même famille ont été identifiés chez les plantes et les algues. Ainsi quatre membres de la famille de gènes *Nrt2* ont été identifiés chez la chlorophycée *C. reinhardtii* (Galvan and Fernández, 2001), et 3 chez la diatomée *T. pseudonana* (Song & Ward 2007). Jusqu'alors, la plupart des études d'expression chez les microalgues montrent que les *Nrt2* sont globalement surexprimés lors de la raréfaction de l'azote. Cependant, l'ensemble de ces travaux s'intéressent à l'expression globale des gènes *Nrt2* et non à l'expression individuelle des gènes (Hildebrand and Dahlin, 2000; Kang et al., 2007; Song and Ward, 2007). Alors qu'il n'existe aucune donnée chez les algues sur les mécanismes de régulation des gènes *Nrt2*, chez les plantes, la régulation de l'expression des gènes *Nrt2* est associée à la quantité de métabolites azotés intracellulaires. En effet, de fortes concentration intracellulaires inhibent l'expression de ces gènes (Forde, 2000). L'objectif de l'étude présentée dans ce chapitre consiste à mieux comprendre le rôle et la régulation des quatre gènes *Nrt2* chez *T. lutea* (*TINrt1*, *TINrt2*, *TINrt3*, *TINrt4*).

Dans un premier temps, les séquences génomiques des quatre gènes ont été séquencées et analysées pour étudier la structure des gènes. La structure putative des protéines codées a été étudiée par annotation experte en utilisant différents outils bio-informatiques. Une étude d'homologie a été entreprise par approche phylogénétique entre les NRT2s de microalgues, de cyanobactéries et de plantes supérieures. Cette étude a notamment permis de mettre en évidence la

présence de quatre gènes codant pour des transporteurs de type NRT2 chez la microalgue *T. lutea*. Dans un second temps, la régulation des quatre gènes *Nrt2* a été étudiée en fonction de la disponibilité en azote. La souche *T. lutea* WT a été cultivée en culture batch limitée par l'azote en utilisant soit l'ammonium ( $\text{NH}_4^+$ ) ou le nitrate ( $\text{NO}_3^-$ ) comme source d'azote. L'expression de chacun des quatre gènes a été mesurée par RT-qPCR au cours de la raréfaction de l'azote dans le milieu afin d'étudier la régulation de ces gènes. Enfin, pour étudier l'inhibition de leur expression respective par les métabolites azotés intracellulaires, des expériences ont été effectuées en ajoutant à des cellules carencées en azote, différentes sources d'azote métabolisable ( $\text{NH}_4^+$ ,  $\text{NO}_3^-$ ,  $\text{NO}_2^-$ ) dans le but de générer l'accumulation intracellulaire de ces métabolites. L'expression des gènes *Nrt2*, mesurée par RT-qPCR, a été suivie au cours du temps pendant les 2 heures qui suivent l'ajout d'azote.

## 2. Résultats principaux et perspectives.

Les résultats principaux sont présentés dans l'article « High-affinity nitrate/nitrite transporter genes (Nrt2) in *Tisochrysis lutea*: identification and expression analyses reveal some interesting specificities of Haptophyta microalgae » publié en 2015 et présenté en fin de ce chapitre (Charrier *et al.*, 2015).

Lors de ce travail, nous avons montré que la structure générale des transporteurs NRT2 restait conservée chez *T. lutea*. Cependant, les quatre protéines NRT2 de *T. lutea* (TINRT2) présentent des spécificités tant au niveau de la structure des gènes qu'au niveau des protéines. Contrairement aux gènes *Nrt2* de l'haptophyte *E. huxleyi*, aucun intron n'a été identifié dans les gènes de *T. lutea*. Les analyses de séquence protéiques montrent une similarité forte au sein des haptophytes et suggèrent que les quatre formes des gènes *Nrt2s* proviennent d'événements de duplications géniques au sein de l'espèce *T. lutea*. D'autre part les protéines TINRT2 contiennent tous une boucle extracellulaire située entre les domaines transmembranaires 9 et 10 (voir fig. 1 de Charrier *et al.*, 2015). Cette boucle est spécifique des haptophytes et pourrait être impliquée dans la liaison au substrat en remplacement de la protéine NAR2. De nouvelles études sont nécessaires pour élucider le rôle de ces boucles spécifiques chez *T. lutea*.

Nous avons également montré que les profils d'expression des différents gènes *TINrt2* au cours de cultures batch limitées par l'azote étaient spécifiques à chacun des quatre gènes. Ceci suggère que ces gènes possèdent probablement des rôles différents (voir fig. 3,4 et 5 de Charrier *et al.*, 2015). Le gène *TINrt2.2* est exprimé de façon constitutive mais à un niveau relativement bas par rapport aux autres *TINrt2*, et cela, quelle que soit la source d'azote extracellulaire et le niveau de limitation des cellules. Le rôle fonctionnel de ce transporteur reste encore à identifier mais semble peu important au regard du niveau d'expression très faible. A l'inverse, l'expression des gènes *TINrt2.1* et *TINrt2.3*



est induite à des concentrations de nitrate relativement élevées mais est totalement inhibée par la présence d'ammonium. L'expression de ces deux gènes semble liée au niveau de limitation azoté des cellules. Elle est augmentée lors de la carence azotée. Ce type de régulation a été montré à plusieurs reprises chez les plantes et les chlorophycées et permet d'augmenter le potentiel d'absorption d'azote lors de sa raréfaction dans le milieu. Enfin, un comportement très original a été montré pour le gène *TINrt2.4* dont l'expression est généralement inversement corrélée à celles des gènes *TINrt2.1* et *TINrt2.3*. L'expression de ce gène semble davantage dépendre du niveau de limitation intracellulaire de la cellule révélé par le rapport N/C particulière, et non de la réelle disponibilité en azote extracellulaire. En conséquence, ce gène *TINrt2.4* ne semblerait pas directement impliqué dans l'accès à l'azote extracellulaire mais plutôt dans le trafic intracellulaire de l'azote minéral. L'ensemble de ces résultats d'expression au niveau transcriptomique devra être confirmé par des mesures d'abondance protéiques.

Les résultats de l'étude de la régulation des gènes par les métabolites intracellulaires montrent que les gènes *TINrt2.1* et *TINrt2.3* sont réprimés par les 3 formes de métabolites azotés testés. Cette régulation est d'autant plus forte que le type de métabolite est assimilable ( $\text{NH}_4^+ > \text{NO}_3^- > \text{NO}_2^-$ ) (voir fig. 6 de Charrier et al., 2015). Ces résultats suggèrent ainsi que le taux répression génique dépend de la position du substrat dans la voie d'assimilation du nitrate. Cela conforte l'idée que l'accumulation de métabolites intracellulaires azotés provenant de la voie d'assimilation du nitrate est impliquée dans la régulation des gènes *TINrt2.1* et *TINrt2.3*. A l'inverse des gènes *TINrt2.1* et *TINrt2.3*, l'expression du gène *TINrt2.4* semble activée par la présence intracellulaire de  $\text{NH}_4^+$ . Ces résultats suggèrent que le gène *TINrt2.4* pourrait avoir un rôle différent de ceux de *TINrt2.1* et *TINrt2.3*. A l'instar du gène *Nrt2.7* de *A. thaliana*, le gène *TINrt2.4* pourrait être impliqué dans des processus de stockage de l'azote intracellulaire à l'intérieur de vacuoles (Chopin et al., 2007). Cette hypothèse est supportée par la présence d'un motif peptidique additionnel en C-terminal de cette protéine pouvant éventuellement être impliqué dans l'adressage de cette protéine vers une localisation subcellulaire spécifique telle que le système vacuolaire. Cependant, bien que la présence d'une vacuole chez *T. lutea* ait été observée par microscopie électronique, son rôle dans le stockage de l'azote reste encore à démontrer.

Ces travaux ouvrent des perspectives de recherche intéressantes sur le rôle de ces transporteurs dans la gestion de l'azote par les haptophytes. Des travaux complémentaires sont maintenant nécessaires pour confirmer les résultats d'analyses d'expression génique au niveau des protéines et pour caractériser le rôle spécifique de chacun de ces 4 transporteurs dans l'absorption et le stockage de l'azote.



# High-affinity nitrate/nitrite transporter genes (*Nrt2*) in *Tisochrysis lutea*: identification and expression analyses reveal some interesting specificities of Haptophyta microalgae

Aurélie Charrier, Jean-Baptiste Bérard, Gaël Bougaran, Grégory Carrier, Ewa Lukomska, Nathalie Schreiber, Flora Fournier, Aurélie F. Charrier, Catherine Rouxel, Matthieu Garnier, Jean-Paul Cadoret and Bruno Saint-Jean\*

Physiology and Biotechnology of Algae Laboratory, IFREMER, Nantes 44311, France

## Correspondence

\*Corresponding author,  
e-mail: bruno.saintjean@ifremer.fr

Received 24 September 2014;  
revised 27 January 2015

doi:10.1111/ppl.12330

Microalgae have a diversity of industrial applications such as feed, food ingredients, depuration processes and energy. However, microalgal production costs could be substantially improved by controlling nutrient intake. Accordingly, a better understanding of microalgal nitrogen metabolism is essential. Using *in silico* analysis from transcriptomic data concerning the microalgae *Tisochrysis lutea*, four genes encoding putative high-affinity nitrate/nitrite transporters (*TiNrt2*) were identified. Unlike most of the land plants and microalgae, cloning of genomic sequences and their alignment with complementary DNA (cDNA) sequences did not reveal the presence of introns in all *TiNrt2* genes. The deduced *TiNRT2* protein sequences showed similarities to *NRT2* proteins of other phyla such as land plants and green algae. However, some interesting specificities only known among Haptophyta were also revealed, especially an additional sequence of 100 amino acids forming an atypical extracellular loop located between transmembrane domains 9 and 10 and the function of which remains to be elucidated. Analyses of individual *TiNrt2* gene expression with different nitrogen sources and concentrations were performed. *TiNrt2.1* and *TiNrt2.3* were strongly induced by low  $\text{NO}_3^-$  concentration and repressed by  $\text{NH}_4^+$  substrate and were classified as inducible genes. *TiNrt2.2* was characterized by a constitutive pattern whatever the substrate. Finally, *TiNrt2.4* displayed an atypical response that was not reported earlier in literature. Interestingly, expression of *TiNrt2.4* was rather related to internal nitrogen quota level than external nitrogen concentration. This first study on nitrogen metabolism of *T. lutea* opens avenues for future investigations on the function of these genes and their implication for industrial applications.

**Abbreviations** – AA, amino acids; AN, ammonium nitrate; cDNA, complementary DNA; cHATS, constitutive high-affinity transport system; cLATS, constitutive low-affinity transport system; CT, threshold cycle; GAPDH, glyceraldehyde 3-phosphate dehydrogenase; GS/GOGAT, glutamine synthetase/glutamine oxoglutarate aminotransferase; HATS, high-affinity transport system; iHATS, inducible high-affinity transport system; iLATS, inducible low-affinity transport system; LATS, low-affinity transport system; MFS, major facilitator superfamily; mRNA, messenger RNA; NAR, nitrite transporter; NiR, nitrite reductase; NNP, nitrate/nitrite porter; NR, nitrate reductase; NRT, nitrate transporter; PTR, peptide transporter; Q-RT-PCR, quantitative real-time polymerase chain reaction.

## Introduction

Nitrogen is an essential element for all living organisms. It participates in many crucial biological processes, including the formation of amino acids, proteins and chlorophyll. Nitrogen is preferentially absorbed in the ammonium form, however, this form is scarce in the environment and nitrate is the most commonly used source of nitrogen (Forde 2000).

Many reports have described the nitrate assimilation pathway in higher plants and certain microalgae (Ullrich 1983, Crawford and Forde 2002, Fernandez and Galvan 2008). The first step of nitrate assimilation involves nitrate uptake across the plasma membrane by different types of nitrate transporters (NRTs) and seems to be a major step in controlling nitrogen assimilation (Daniel-Vedele et al. 1998, Fernandez and Galvan 2008). In cells, nitrate is reduced to nitrite in the cytoplasm by nitrate reductase (NR). Nitrite is transported into the chloroplast by a nitrite transporter (NAR1) for its reduction to ammonia by nitrite reductase (NiR). Ammonia is then incorporated into carbon skeletons by the glutamate dehydrogenase or the combined action of glutamine synthetase and glutamate synthase (Ahmad and Hellebust 1984). In plants, nitrate can also be stored in vacuoles by the action of nitrate antiporters and NRTs located on the tonoplast (De Angeli et al. 2006, Dechorgnat et al. 2012). In green microalgae, different storage structures (contractile vacuoles and intracellular granules) have been described but their origins and their functions remain unclear (Becker 2007). Studies have shown that the transport capacities of the tonoplast membranes in green algae are similar to those of land plants (Becker 2007). However, no NRTs have yet been located on intracellular organelles of microalgae. Moreover, although many processes in nitrate assimilation are common to both algae and higher plants, Ullrich (1983) suggested that some differences could exist due to differential evolution, differences in the structural properties of the enzymes among these species and, most importantly, the large surface area of contact that algal cells have with external nutrients.

In recent years, the mechanisms that respond to nitrate availability have been the subject of much research. Previous studies indicate that  $\text{NO}_3^-$  uptake requires an active transport system (Forde 2000, Galvan and Fernández 2001). Molecular investigations in land plants have shown that four types of transport systems exist depending on the concentration of nitrate in the environment (Crawford and Glass 1998). Two high-affinity transport systems (HATS) coexist and can take up  $\text{NO}_3^-$  at very low external concentrations ( $<250\ \mu\text{M}$ ). The first system [inducible high-affinity transport system

(iHATS)] is inducible by  $\text{NO}_3^-$  and characterized by high values of  $K_m$  and  $V_{\max}$  (for plants, typically  $20\text{--}100\ \mu\text{M}$  and  $3\text{--}8\ \mu\text{mol g}^{-1}\ \text{h}^{-1}$ , respectively). The second system [constitutive high-affinity transport system (cHATS)] is constitutively expressed and does not depend on the nitrogen concentration, having low values of both  $K_m$  and  $V_{\max}$  (for plants  $6\text{--}20\ \mu\text{M}$  and  $0.3\text{--}0.82\ \mu\text{mol g}^{-1}\ \text{h}^{-1}$ , respectively) (Crawford and Glass 1998). When the  $\text{NO}_3^-$  external concentration reaches values around the  $500\ \mu\text{M}$  range, two other transport systems with low-affinity for nitrate [constitutive low-affinity transport system (cLATS) and inducible low-affinity transport system (iLATS)] become involved in the absorption flux (Siddiqi et al. 1990, Glass et al. 1992, Crawford and Glass 1998, Galvan and Fernández 2001). The low-affinity transport system (LATS) is unsaturable.

The peptide transporter (PTR) and the nitrate/nitrite porter (NNP) gene families, belonging to the major facilitator superfamily (MFS), have been identified as encoding putative NRTs (Forde 2000, Tsay et al. 2007). The MFS proteins have a typical membrane topology of 12 transmembrane domains arranged as two sets of six, connected by a cytosolic loop (Forde 2000, Galvan and Fernández 2001). The amino acid sequences share a conserved sequence motif [G-X<sub>3</sub>-D-X<sub>2</sub>-G-X-R] between transmembrane domains 2 and 3, and another motif [I-X<sub>2</sub>-R-X<sub>3</sub>-G-X<sub>3</sub>-G] within transmembrane domain 4. The PTR family is a multi-genic family found in a wide variety of plants and algae (Steiner et al. 1995). It includes several members characterized as low-affinity NRTs (*Npf* genes, formerly named *Nrt1* genes) (Crawford and Glass 1998, Forde 2000, Lérán et al. 2014). One exception is observed for *Nrt1.1*, which possesses a double affinity for  $\text{NO}_3^-$  (HATS/LATS) (Wang et al. 1998, Liu et al. 1999). The NNP family includes high-affinity nitrate/nitrite transporters (*Nrt2* genes). The NRT2 proteins have between 500 and 600 AA and present a consensus motif [FYK]-X<sub>3</sub>-[ILQRK]-X-[GA]-X-[VASK]-X-[GASN]-[LIVFQ]-X<sub>1,2</sub>-G-X-G-[NIM]-X-G-[GTA] within the fifth putative transmembrane domain. This motif is proposed as the signature for the NNP family (Forde 2000). A portion of this sequence [A-G-W/L-G-N-M-G] has been also suggested as the substrate recognition motif. The members of the *Nrt2* gene family show substrate specificity for nitrate and/or nitrite with different affinities. The first member of the NNP family to be cloned was the *CrnA* gene from *Aspergillus nidulans* (Brownlee and Arst 1983, Unkles et al. 1991) and was identified to be a functional nitrate/nitrite transporter when expressed in *Xenopus* oocytes (Zhou et al. 2000). Then, *Nrt2* genes from *Chlamydomonas reinhardtii* were identified to mediate high affinity nitrate transport like *CrnA* gene.

Subsequently, many studies identified *Nrt2* genes in different species of land plants and microalgae (e.g. *Arabidopsis thaliana*, *Nicotiana tabacum*, *Oryza sativa* and *Dunaliella salina*) based on sequence homology analysis (Krapp et al. 1998, Orsel et al. 2002, He et al. 2004, Cai et al. 2008). The number of high-affinity nitrate/NRTs varies between species. Recent studies on the green microalga *C. reinhardtii* have provided information on the properties of NRT2 (Quesada et al. 1994, 1998, Galván et al. 1996, Fernandez and Galvan 2007). In fact, *C. reinhardtii* have four NO<sub>3</sub><sup>-</sup> or/and NO<sub>2</sub><sup>-</sup> uptake systems, each with distinctive kinetic and regulatory properties, and some of these systems require the presence of an accessory protein (NAR2) to be functional (Galván et al. 1996, Rexach et al. 1999, 2002). Thereafter, other NAR2 proteins have since been identified in land plants (Tong et al. 2005, Orsel et al. 2006).

The high-affinity NRTs in marine microalgae are of particular interest due to the low nitrate concentrations available in seawater (Collos et al. 2005, Song and Ward 2007). Research has been conducted on marine microalgae for many years for the economic development of its biomass and various molecules that have high added value such as antioxidants, pigments and polysaccharides. However, microalgae have significant nitrogen needs to develop and produce their biomass. In the future, the price of nitrogen fertilizer will tend to increase in relation to the price of energy. Therefore, it is important to improve our knowledge of nitrogen absorption and assimilation mechanisms in these species. Haptophyta represent a major phylum of marine eukaryotic phytoplankton, ecologically dominant in ocean euphotic zones. A culture strain originally isolated from Tahiti and named *Tisochrysis lutea* (formerly *Isochrysis affinis galbana*) has been extensively studied due to its widespread use in aquaculture as feed for shellfish and shrimps (Bougaran et al. 2003, Bendif et al. 2013). *Tisochrysis lutea* remains very difficult to transform and genetic tools suitable for the study of the regulation of the N-metabolism pathway in this taxon are scarce. This study used integrative physiological and molecular approaches to improve our understanding of nitrogen metabolism in *T. lutea*. In this article, we present the first molecular characterization of individual genes encoding putative high-affinity nitrate/nitrite transporters (*Nrt2*) in the Haptophyta. Using transcriptomic data, we identified four *Nrt2* genes in *T. lutea*. Analyses of the *Tisochrysis* NRT2 sequences reveal some interesting specificities compared with NRT2 proteins of other phyla such as land plants and green algae. Moreover, several experimental investigations revealed gene expression profiles similar to land plants for three genes in *T. lutea* and,

unexpectedly, one gene that presents a very atypical expression profile, never observed in any other phylum.

## Materials and methods

### Strain and strain maintenance

Wild-type *T. lutea* was provided by the Culture Centre of Algae and Protozoa (CCAP 926/14). An axenic *T. lutea* strain was grown in a Conway medium (Walne 1966) prepared with seawater, in a controlled environment with a constant irradiance of 150 μmol m<sup>-2</sup> s<sup>-1</sup> at 22°C. Population densities were estimated by cell counting and by spectrophotometry measuring the OD<sub>680</sub> and OD<sub>800</sub>.

### Elementary analyses

Particulate nitrogen (N) and carbon (C) concentrations (μM) were estimated by filtering given volumes of cells on precombusted 25 mm GF/C filters (Whatman, Buckinghamshire, UK, 1.2 μm). The filters were then dried for 24 h at 70°C and further analyzed using a CN Elemental Analyzer (Flash 2000, Thermo Fisher Scientific, Waltham, MA, USA). Particulate N/C ratios were calculated by dividing the particulate N concentration by the particulate C concentration.

### Residual nitrogen analysis

Residual NO<sub>3</sub><sup>-</sup>, NO<sub>2</sub><sup>-</sup> and NH<sub>4</sub><sup>+</sup> concentration in 1.2 μm filtrates was measured using an AA3 HR autoanalyzer (Serlabo Technologies, Vedene, France) according to an automated spectrophotometric method (Aminot and Kérouel 2007).

### Identification and cloning of nitrate/nitrite transporter genes in *T. lutea*

Transcriptomic data (Carrier et al. 2014) were used to identify nitrate/nitrite transporter genes in *T. lutea*. The gene-specific primers were designed for each *TINrt2* gene and used for polymerase chain reaction (PCR) amplification (Table S1, Supporting Information). The amplified products were examined on agarose gels by electrophoresis and were purified using QIAquick PCR Purification Kit (Qiagen, Helden, Germany) following the manufacturer's instructions. The clean PCR products were cloned using a TOPO TA Cloning Kit (Invitrogen, Carlsbad, CA, USA) and the ligated plasmids were transformed into *Escherichia coli* (One Shot<sup>®</sup> TOP10 Chemically Competent *E. coli*, Carlsbad, CA, USA). The transformed cells were spread on Luria–Bertani medium containing 50 μg ml<sup>-1</sup> kanamycin with agar

on plates. The full-length complementary DNA (cDNA) were resequenced using the Sanger method by GATC Biotech (Konstanz, Germany).

### Sequence analyses

Several programs were used to analyze the *T. lutea* NRT2 sequences. The prediction of transmembrane domains was performed with TMPRED software (Hofmann and Stoffel 1993). WOLFPsORT was used to predict the subcellular localization of the proteins (Horton et al. 2007) and iPSORT software was used as the subcellular localization site predictor for N-terminal sorting signals (signal peptide, mitochondrial targeting peptide or chloroplast transit peptide) (Bannai et al. 2002). The NETPHOSK program was used to predict putative kinase phosphorylation sites in the amino acid sequences (Blom et al. 1999). The sequence alignments were performed with CLUSTALW or MUSCLE software. The homology analyses were performed by using the BLAST program on the NCBI database and *T. lutea* transcriptome.

### Homology trees of NRT2 proteins

Reference amino acid sequences were obtained from the GenBank database: *A. thaliana* (NP\_190092; AEE28241), *Brassica napus* (CAC05338), *Glycine max* (NP\_001236444), *Nicotiana glauca* (CAA69387), *Oryza sativa* (BAA33382), *Solanum lycopersicum* (NP\_001234127), *Triticum aestivum* (AAK19519), *Zea mays* (NP\_001105780), *Chlorella sorokiniana* (AAK02066), *Chlorella variabilis* (EFN52690), *Cylindrotheca fusiformis* (AAD49572), *Dunaliella salina* (AAU87579), *Dunaliella tertiolecta* (ABP01763), *Chlamydomonas reinhardtii* (CAD60538; CAA80925), *Emiliania huxleyi* CCMP1516 (EOD39011), *E. huxleyi* (ABP01765), *Tetraselmis chui* (ADU76799), *Thalassiosira pseudonana* (ACI64621), *Ostreococcus tauri* (XP\_003091529), *Skeletonema costatum* (AAL85928), *Volvox carterii* (EFJ43757), *Aspergillus nidulans* (AAA76713), *Hebeloma cylindrosporum* (CAB60009), *Neurospora crassa* (CAD71077), *Hansenula polymorpha* (CAA11229), *Agrobacterium* sp. H13-3 (YP\_004277958), *Burkholderia rhizoxinica* (YP\_004022689), *Pseudomonas stutzeri* (WP\_003298315), *Calothrix* sp. PCC 6303 (AFZ00090), *Chroococcidiopsis thermalis* PCC 7203 (YP\_007092893) and *Cyanobacterium stanieri* PCC 7202 (AFZ48362). The amino acid sequences were aligned using MUSCLE software and the resulting alignment file was used to construct a homology tree using PHYML software through the phylogeny.fr website (Dereeper et al. 2008). The homology tree was drawn with TREEDYN software.

### Quantification of abundance transcripts by quantitative real-time polymerase chain reaction

#### RNA extraction and reverse transcription

The samples were centrifuged (20 min, 5000 g, 4°C). The supernatant was discarded and the sea water was taken up to remove the salt. The pellets were resuspended in Trizol reagent (Invitrogen, Carlsbad, CA, USA) and chloroform. After centrifugation, the upper phases were collected and 0.5 volume of absolute EtOH was added. The samples were transferred to a column of the RNeasy Plant mini kit (Qiagen, Helden, Germany) and the manufacturer's instructions were followed thereafter. A DNase treatment (RQ1 DNase, Promega, Madison, WI, USA) was applied and total RNA was purified using the RNeasy Plant Mini Kit with the RLT buffer and EtOH. The quality and concentration of RNA were determined with a spectrophotometer (ND-1000; NanoDrop Technologies, Wilmington, DE) at wavelengths of 260 and 280 nm. The PCR amplification of an RNA sample served as a check for genomic DNA contamination. Total RNA was stored at -80°C. Reverse transcription of RNA was performed using the High Capacity cDNA Reverse Transcription kit (Applied Technologies, Foster, CA, USA) following the manufacturer's instructions.

#### Real-time PCR and SYBR Green detection

Quantitative PCR reactions were initiated by adding the cDNA to the SYBR Green PCR master mix (Applied Biosystems, Foster, CA, USA) and 300 nM of forward and reverse primers. Ubiquitin and GAPDH (glyceraldehyde 3-phosphate dehydrogenase) genes were chosen as reference genes and remained stable in our experiments. These primer sets were specifically designed to amplify a 100–150 bp fragment from the genes *TlUbi*, *TlGAPDH*, *TlNrt2.1*, *TlNrt2.2*, *TlNrt2.3* and *TlNrt2.4* in *T. lutea* (Table S2). The reactions were carried out on an Agilent Mx3000P QPCR System (Agilent Technologies, Santa Clara, CA, USA). PCR settings were 95°C for 10 min and then 95°C for 15 s, and 60°C for 1 min for 40 cycles. The fluorescence intensity from the complex formed by SYBR Green and the double-stranded PCR product was continuously monitored from cycles 1–40. The threshold cycle (CT) at which the fluorescence intensity became higher than a preset threshold was used to calculate the gene transcript level.

To obtain the gene expression data, the comparative CT method and standard curve method were combined to calculate an RNA molar ratio between a target gene and a reference gene, as previously described by Chung

et al. (2005). Standard curves of each gene were generated to calibrate the PCR efficiency, and the slopes of standard curves were  $-3.2$  [*TIUbi* messenger RNA (mRNA)],  $-3.4$  (*TIGAPDH* mRNA),  $-3.2$  (*TINrt2.1*),  $-3.28$  (*TINrt2.2*), and  $-3.33$  (*TINrt2.3*) and  $-3.353$  (*TINrt2.4*), respectively. The relative mRNA abundance [ $X_0/R_0$ , in mmol of the target gene (mol *TIUbi* mRNA) $^{-1}$ ], was calculated by the following equation:  $\log(X_0/R_0) = \log(M_r/M_x) + (C_{t_x}/b_x) - (C_{t_r}/b_r)$ , where  $X_0$  and  $R_0$  are the initial numbers of target and reference molecules,  $M_r$  and  $M_x$  are the molecular weights of the target and reference amplicons,  $C_{t_x}$  and  $C_{t_r}$  are the CT numbers of X and R, and  $b_x$  and  $b_r$  are the standard curve slopes of X and R, respectively. The specificity of the quantitative reverse-transcription polymerase chain reaction (Q-RT-PCR) products was confirmed by melting temperature analysis.

## Experimental protocols

### *Expression studies of Tisochrysis Nrt2 genes during batch culture with NaNO<sub>3</sub>*

An axenic preculture of *T. lutea* was grown in a Conway medium with 1 mM NaNO<sub>3</sub>. During exponential phase, which corresponds to a high nitrogen quota, cells were inoculated into a new modified Conway medium containing 200 μM NaNO<sub>3</sub>. The initial cellular density in the new batch culture was about  $2 \times 10^6$  cells ml<sup>-1</sup>. The irradiance and temperature were set at 200 μmol m<sup>-2</sup> s<sup>-1</sup> and 22°C, respectively. The cultures were aerated with 0.2-μm filtered air and pH was adjusted to 8.0 with CO<sub>2</sub> injections. Discrete sampling was realized and three parameters were monitored throughout the experiment: the nutritional status (particulate nitrogen and carbon), the composition of the medium (residual NO<sub>3</sub><sup>-</sup>) and the abundance of *TINrt2* transcripts.

### *Expression studies of Tisochrysis Nrt2 genes during batch culture with NH<sub>4</sub>Cl*

The axenic preculture of *T. lutea* was grown in a modified Conway medium with 200 μM NH<sub>4</sub>Cl. In the stationary phase, corresponding to a low nitrogen quota, cells were inoculated into non-enriched seawater for 24 h in order to lower the natural nitrogen content of the seawater. Then, a new modified Conway medium with 200 μM NH<sub>4</sub>Cl was added. The initial cellular density in the new batch culture was about  $1.5 \times 10^6$  cells ml<sup>-1</sup>. The irradiance and temperature were fixed at 200 μmol m<sup>-2</sup> s<sup>-1</sup> and 22°C, respectively. The cultures were aerated with 0.2-μm filtered air and pH was adjusted to 8.0 with CO<sub>2</sub>

injections. A discrete sampling was performed and three parameters were monitored throughout the experiment: the nutritional status (particulate nitrogen and carbon), the composition of the medium (residual NO<sub>3</sub><sup>-</sup>) and the abundance of *TINrt2* transcripts.

Concerning the *TINrt2* relative mRNA abundance as a function of the N/C ratio (N status) in cells, N/C ratios were calculated by dividing the particulate N concentration by the particulate C concentration.

### *Regulation of TINrt2 expression by different N-substrate conditions*

To study the short-term regulation of *TINrt2* expression by N metabolites, 3 l of axenic cultures growing in continuous culture with N-limiting conditions were transferred into sterilized bottles. The cultures were aerated with 0.2-μm filtered air and received a constant irradiance of 200 μmol m<sup>-2</sup> s<sup>-1</sup> and the pH was adjusted to 8.0 with CO<sub>2</sub> injections. Cells were left without any nutritional supply for the time necessary to clear their internal nitrogen quotas. It was considered that the cells had the lowest nitrogen quotas when the algal growth was at stationary phase. Different types of Conway media were prepared from different forms of nutrients [NaNO<sub>3</sub>; NaNO<sub>2</sub> and (NH<sub>4</sub><sup>+</sup>)(NO<sub>3</sub><sup>-</sup>)], but all containing 1 mM of total nitrogen, and were added to the different cultures independently. Samples were collected and total RNA extractions were performed at 0, 15, 30, 60 and 120 min after N depletion. All experiments were performed in triplicate.

## Statistics

Statistical analyses were performed with Matlab<sup>®</sup> (Mathworks, Natick, MA) using Kruskal–Wallis test ( $\alpha = 0.05$ ).

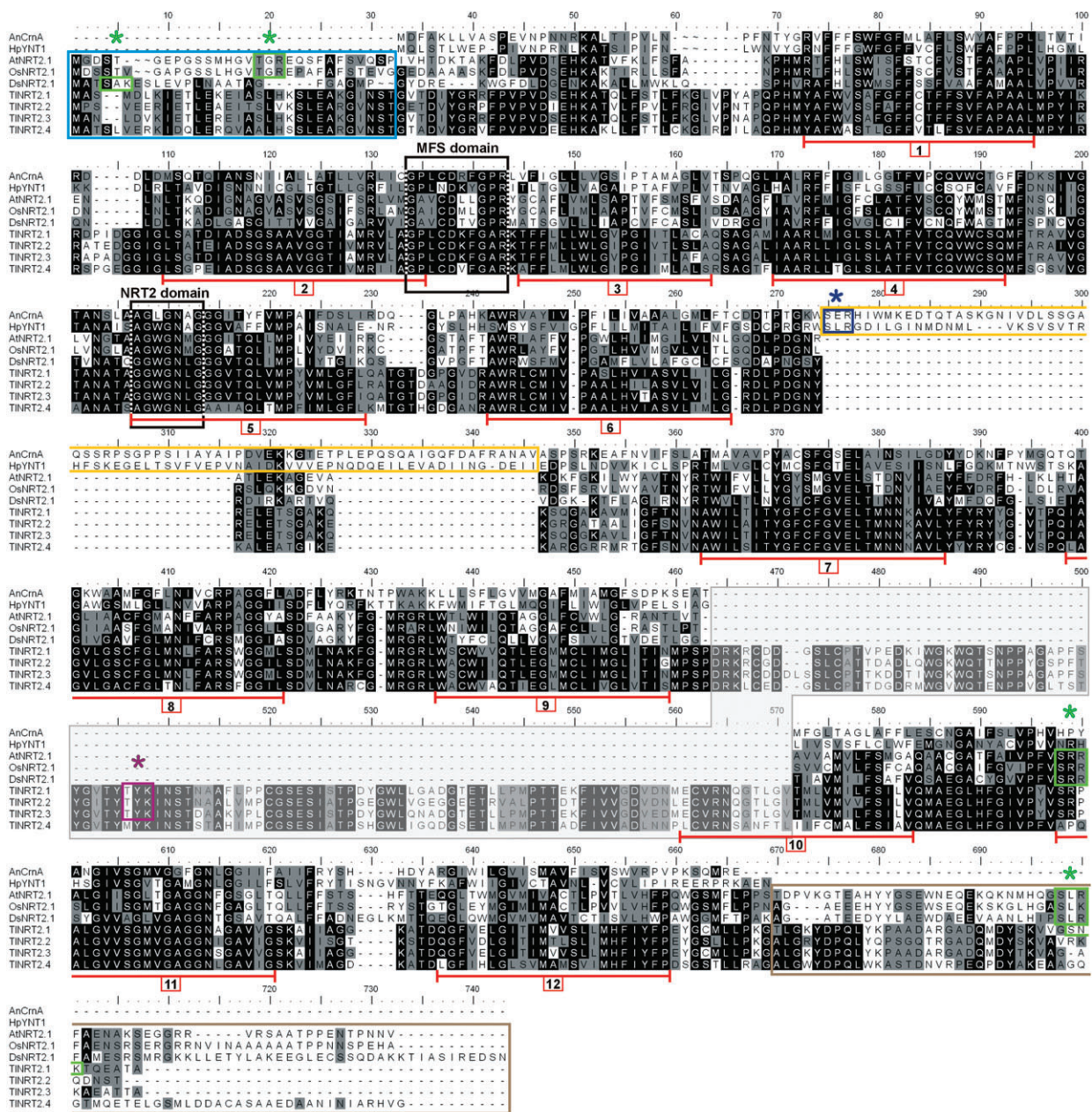
## Results

### *Identification of T. lutea Nrt2 transcripts*

In this study, four genes, encoding putative high-affinity nitrate/nitrite transporters, have been identified in *T. lutea* based on our transcriptomic data (Carrier et al. 2014) and were named *TINrt2.1*, *TINrt2.2*, *TINrt2.3* and *TINrt2.4*. The *TINrt2* gene identification was performed by similarity searches, using several NRT2 sequences from different species (*A. nidulans*, *H. polymorpha*, *A. thaliana*, *O. sativa* and *D. salina*), against the transcriptome database of *T. lutea* (Fig. 1). The respective *TINrt2* full-length cDNAs were cloned and resequenced to confirm sequence reliability.

In addition, *T. lutea* was checked for the presence of any NAR2 accessory protein. Nevertheless,

# CHAPITRE I : Identification et caractérisation des transporteurs d'azote.



**Fig. 1.** Alignment of NRT2 protein sequences from *Aspergillus nidulans*, *Hansenula polymorpha*, *Arabidopsis thaliana*, *Oryza sativa*, *Dunaliella salina* and *Tiwochrysis lutea*. Alignment was performed with CLUSTALW. Sequence identities are indicated by a black background and homologies by a grey background.



despite numerous homology searches using various NAR2 sequences from several species [*A. thaliana* (AED95911.1), *Cucumis sativus* (ACV33078.2), *Micromonas* sp. RCC299 (ACO68771.1) and *C. reinhardtii* (A8J4P7)], no gene encoding a putative NAR2 protein was detected in *T. lutea*.

### Intron–exon structure of the *T. lutea* *Nrt2* genes

Amplifications of genomic sequences were performed using primers designed in the 5' untranslated region (5'UTR) and 3'UTR regions (Table S1). The amplicons were sequenced using the Sanger method (GATC Biotech). To report the genomic and cDNA sequences of the *TlNrt2* genes, a full alignment of the cDNA sequences and the genomic sequences was performed using CLUSTALW software. No introns were detected in the genomic sequences using the alignments with the respective cDNA sequences.

Concerning the sequence comparison, the highest value of nucleotide sequence identity was found between *TlNrt2.1* and *TlNrt2.3*, with a value up to 82.8% identity (Table S3). However, strong identities were also observed between all of the *TlNrt2* nucleotide sequences (from 68.4 to 79.1%).

### Characteristics of deduced TINRT2 amino acid sequences obtained using bioinformatic tools

The deduced TINRT2.1, TINRT2.2, TINRT2.3 and TINRT2.4 proteins have 633, 630, 634 and 661 amino acid residues, respectively. These protein sequences showed strong similarities, with identity scores ranging up to 92.9% (Table S3). The WOLF PSORT program (Horton et al. 2007) for prediction of protein subcellular localization placed the four *T. lutea* NRT2 on the plasma membrane. The iPSORT software (Bannai et al. 2002) did not detect the presence of any signal, mitochondrial targeting, or chloroplast transit peptides.

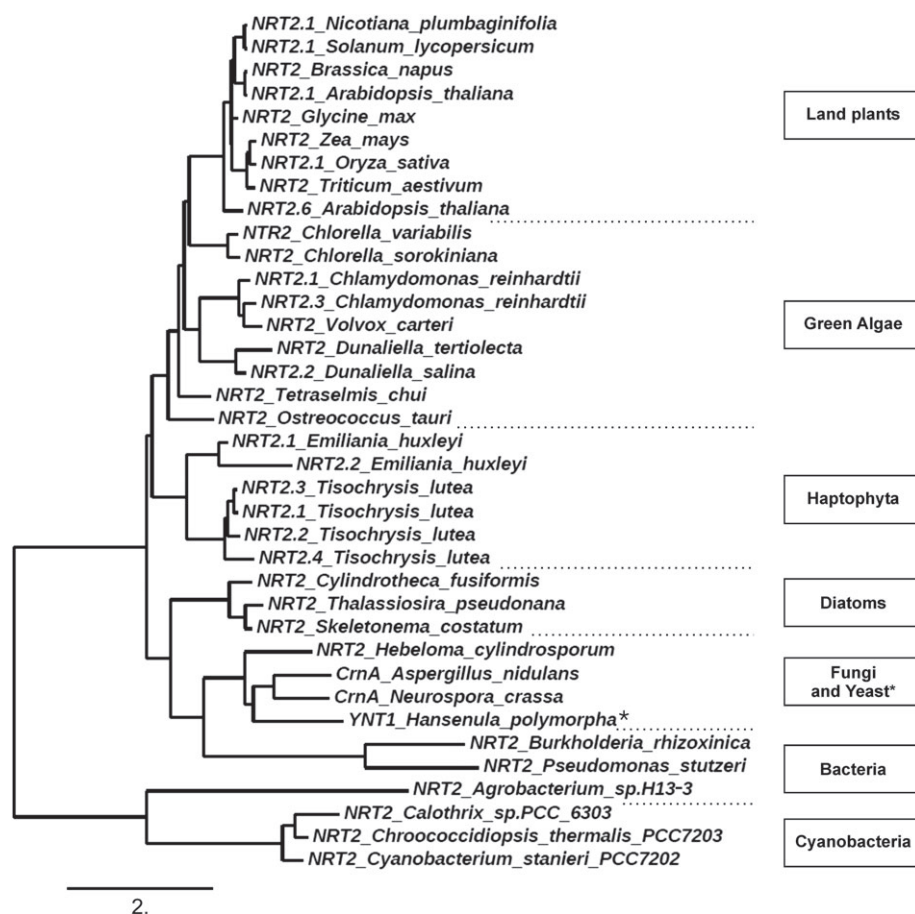
Hydropathic analysis was performed with the TMPRED program and predicted the presence of 12 transmembrane domains. A first cytosolic loop was observed between transmembrane domains 6 and 7, and is specific to the MFS family. Contrary to the fungal and yeast NRT2 sequences, that have a large central cytosolic loop (90 AA), *Tisochrysis* NRT2 sequences show a short cytosolic loop (20–30 AA) as observed in land plants and green algae (Fig. 1). The specific domain (G-X<sub>3</sub>-D-X<sub>2</sub>-G-X-R) characteristic of the MFS is identified between transmembrane domains 2 and 3 in *T. lutea* NRT2 sequences (Fig. 1). The signature motif for the nitrate/nitrite transporters family (A-G-W/L-G-N-M-G), which is suggested as a recognition substrate motif, was also found in the fifth transmembrane domain.

A second loop is observed only in *Tisochrysis* NRT2 sequences and is located between transmembrane domains 9 and 10. This loop is extracellular and has about 100 AA, which is highly atypical compared with the NRT2 sequences from other species (Fig. 1). Homology researches were made on this atypical loop. The results of BLAST analysis showed that this additional sequence is not found in NRT2 sequences of other species, except in the NRT2 sequences of another haptophyte, *E. huxleyi*. Analysis of a shotgun proteomic experiment (not shown in this article) confirmed the presence of these proteins and, more precisely, the additional amino acid sequence (Fig. S1). Indeed, two peptides were identified in this additional loop of *Tisochrysis* NRT2 sequences. BLAST analyses then confirmed that these peptides did not match with other proteins from *T. lutea* and were specific to TINRT2 proteins.

The deduced TINRT2 proteins show an extended N-terminal domain (30 AA) and an extended C-terminal domain as described in plants and green algae. However, the alignment in Fig. 1 shows that TINRT1, TINRT2.2 and TINRT2.3 sequences harbor C-terminal domains smaller (40 AA) than all others (60–70 AA). Using NETPHOSK program (Blom et al. 1999), several protein kinase C recognition motifs are detected for only three TINRT2 sequences (TINRT2.1, TINRT2.2 and TINRT2.3), but at a different position to those found in other organisms. In contrast, no protein kinase C recognition motif was detected in TINRT2.4. Furthermore, the conserved protein kinase C recognition motifs in land plants and green algae are not found for all TINRT2 proteins except for TINRT2.1, which harbors this motif type in the C-terminal domain (Fig. 1). Nevertheless, the same motif of phosphorylation by protein kinase C is predicted within the additional sequences in three TINRT2 proteins (TINRT2.1, TINRT2.2 and TINRT2.3). Contrary to the yeast and fungal NRT2 sequences, no protein kinase C recognition motifs were detected in the central cytosolic loop.

### Similarity scores and homology tree

The amino acid sequences of TINRT2 have fairly low homologies with NRT2 proteins of other species (Table S4). Indeed, the identity scores obtained with AsCrnA (*A. nidulans*) and HpYNT1 (*H. polymorpha*) were only about 26 and 23%, respectively. Nevertheless, the identity scores seem to be greater with sequences of land plants and algae. For example, between 28.5 and 34.3% identity and up to 47.2% similarity was found with AtNRT2.1 (*A. thaliana*). Moreover, it was also shown that the protein sequences of *T. lutea* NRT2 have up to 35%



**Fig. 2.** Homology tree of high-affinity nitrate transporters (NRT2) composed of 37 NRT2 sequences from bacteria, yeast, fungi, algae and land plants. Accession numbers are given in the Materials and methods section. The amino acid sequences were aligned using MUSCLE software and the phylogeny tree built in PHYLIP software (Dereeper et al. 2008).

identity with other NRT2 of algae (between 31 and 35% identity with *C. reinhardtii* NRT2.3).

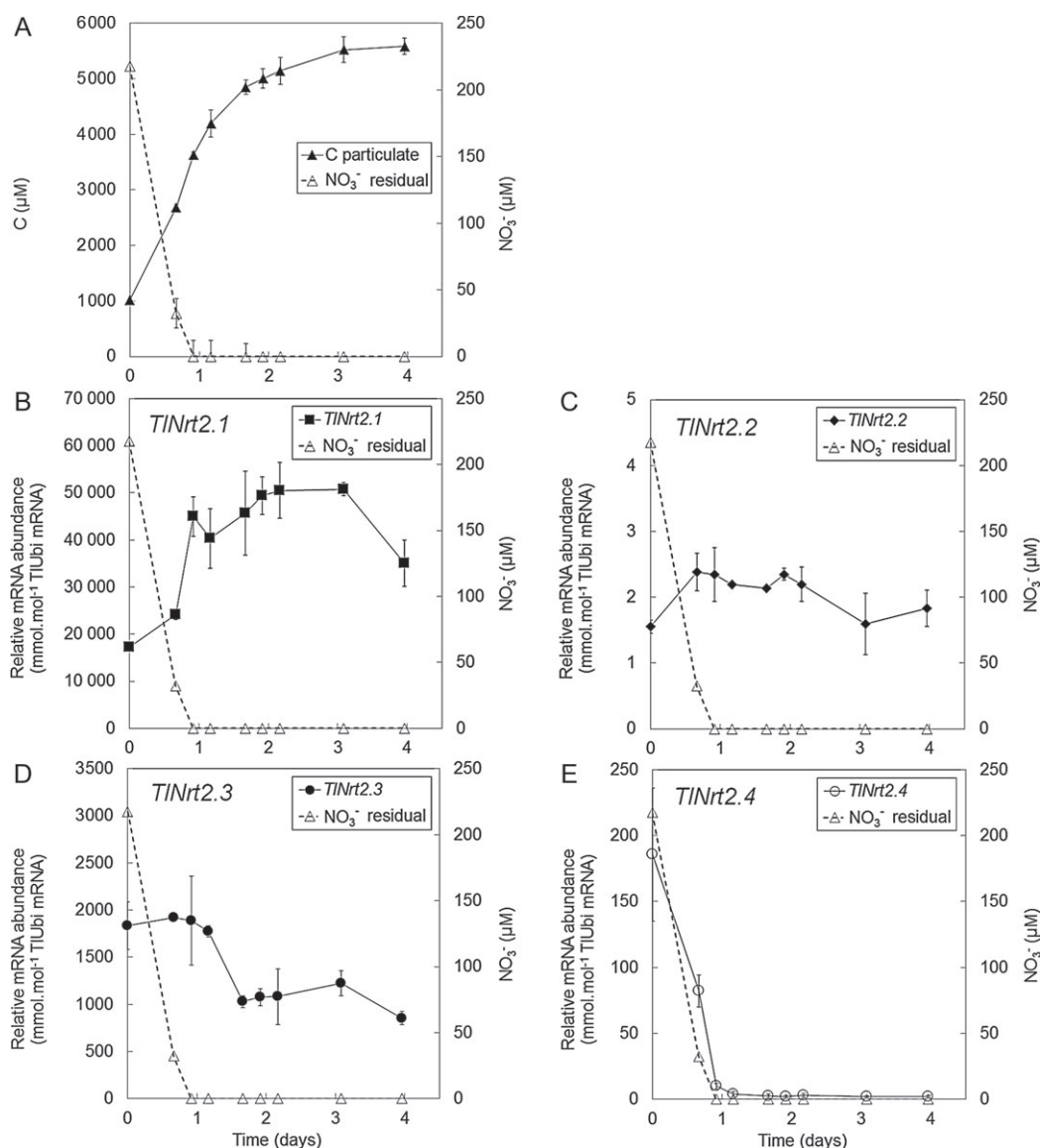
In the same way, the homology tree highlights the fact that the *Nrt2* genes from this haptophyte cluster with the *Nrt2* genes from land plants and green algae (Fig. 2). This group, containing the *Nrt2* genes of land plants, green algae and haptophytes, differs completely from other phyla (diatoms, fungi, cyanobacteria and bacteria). However, inside this group, results showed that the *Nrt2* genes of green algae are closely related to the *Nrt2* genes of land plants, while the *Nrt2* genes of the Haptophyta are distinct to the green lineage. In addition, *T. lutea* *Nrt2* seems to form a single clade, separate from those of *E. huxleyi*.

### Transcriptional responses of *TINrt2* genes during nitrate batch culture

In order to observe the expression of individual *TINrt2* genes during batch culture, cells with high nitrogen

quotas (i.e. at the exponential phase) were inoculated in a modified Conway medium containing 200  $\mu$ M nitrate as the sole source of nitrogen. Cell density exponentially increased for 2 days before reaching the stationary phase (Fig. 3A). Residual nitrate provided at 200  $\mu$ M at day 0 was almost exhausted after 16h, and totally depleted from 22h until day 4. The transcript level of the NRTs genes was monitored throughout the batch culture. The relative mRNA abundance was normalized using the reference gene (ubiquitin).

The relative abundance of *TINrt2.1* transcripts showed an average of 17.2 mol mol<sup>-1</sup> *TIUbi* mRNA when external nitrate was still abundant (Fig. 3B). Thereafter, the residual concentration of nitrate began to drop and an increase of the *TINrt2.1* gene expression (24.1 mol mol<sup>-1</sup> *TIUbi* mRNA) was observed when the external nitrate concentration was around 30  $\mu$ M. However, the *TINrt2.1* mRNA abundance expression peaked after the nitrate had been totally depleted from



**Fig. 3.** Various parameters of *Tisochrysis lutea* cells grown in nitrate batch culture. Axenic preculture of *Tisochrysis lutea* was grown in a Conway medium with 1 mM NaNO<sub>3</sub>. During exponential phase, cells were inoculated into a new modified Conway medium containing 200 μM NaNO<sub>3</sub>. (A) Concentrations of particulate carbon (measured using a CN elemental analyzer) and residual nitrate (measured using an automated spectrophotometric method) (μM) during the batch culture. (B) Relative mRNA abundance of *TINrt2.1*. (C) Relative mRNA abundance of *TINrt2.2*. (D) Relative mRNA abundance of *TINrt2.3*. (E) Relative mRNA abundance of *TINrt2.4*. Each value represents the mean ± SE of three independent experiments.

the medium (45.6 mol mol<sup>-1</sup> TIUbi mRNA, or 2.6-fold). This maximal transcript level of *TINrt2.1* remained stable until the cells reached the stationary phase.

The transcript level of *TINrt2.2* was relatively stable, with an average of 2.1 mmol mol<sup>-1</sup> TIUbi mRNA throughout the experimental period (Fig. 3C). The results suggested that *TINrt2.2* was constitutively expressed in these culture conditions.

For *TINrt2.3* gene, the transcript level remained stable until 28 h with an average of 1857 mmol mol<sup>-1</sup> TIUbi

mRNA and declined at 40 h (1105 mmol mol<sup>-1</sup> TIUbi mRNA) when the residual nitrate was undetectable (Fig. 3D). The *TINrt2.3* transcript level then reached 853 mmol mol<sup>-1</sup> TIUbi mRNA by the end of the experiment.

In contrast to other *TINrt2* genes, *TINrt2.4* transcript level was high (185 mmol mol<sup>-1</sup> TIUbi mRNA) when the external nitrate concentration was 200 μM (Fig. 3E). Its expression decreased during nitrate consumption by algal cells to an average of 82.2 mmol mol<sup>-1</sup> TIUbi

mRNA. When the nitrate was totally depleted after 22h, no gene expression was detected until the end of the experiment.

### Transcriptional responses of *TlNrt2* genes during ammonium batch culture

To determine the expression profile of each *TlNrt2* gene when the nitrate in the medium is replaced by ammonium as the sole nitrogen source, cells were inoculated in non-enriched seawater for 24 h in order to lower the natural nitrogen content of the seawater. In addition, to observe a strong repression of *TlNrt2* genes in the presence of ammonium, it was necessary that their expressions were high at the beginning of the experiment. For this reason, prior to their inoculation, cells with empty nitrogen quotas were preconditioned under nitrogen starvation. Once the initial physiological conditions were met, a modified Conway medium with 200  $\mu\text{M}$   $\text{NH}_4\text{Cl}$  was added. The growth pattern of the population showed that cell density increased exponentially for 3.8 days and then entered the stationary phase (Fig. 4A). The ammonium supplied was totally depleted after 20 h (day 0.8) and remained undetectable until day 4.8. The transcript level of the NRTs genes was monitored throughout the batch culture.

In the nitrogen-starved cultures of *T. lutea*, the relative transcript levels of *TlNrt2.1* and *TlNrt2.3* were high, with average values of 64.8  $\text{mol mol}^{-1}$  *TIUbi* mRNA and 1808  $\text{mmol mol}^{-1}$  *TIUbi* mRNA, respectively (Fig. 4B, D).

When  $\text{NH}_4^+$  was added to the nitrogen-starved cultures, the relative transcript levels of *TlNrt2.1* drastically declined to 80.5  $\text{mmol mol}^{-1}$  *TIUbi* mRNA (700-fold) observed 7 h after the addition of the  $\text{NH}_4^+$  (Fig. 4B). Thereafter, a very strong induction to an average value of 4473  $\text{mmol mol}^{-1}$  *TIUbi* mRNA was observed when the ammonium was totally depleted. The increase of relative transcript abundance continued until the end of the experiment (46 500  $\text{mmol mol}^{-1}$  *TIUbi* mRNA) in the nitrogen-starved cells.

For *TlNrt2.3* expression, the relative transcript abundance declined very quickly 328-fold (5.5  $\text{mmol mol}^{-1}$  *TIUbi* mRNA) in 4 h after the addition of  $\text{NH}_4^+$  (Fig. 4D). Thereafter, the transcript level increased when the external ammonium was completely depleted (309.9  $\text{mmol mol}^{-1}$  *TIUbi* mRNA). The increase of relative transcript abundance continued until the end of the experiment (1526.6  $\text{mmol mol}^{-1}$  *TIUbi* mRNA in day 2) in the nitrogen-starved cells.

The *TlNrt2.2* gene transcript level was low and remained relatively constant at an average of 2.7  $\text{mmol mol}^{-1}$  *TIUbi* mRNA throughout the experiment (Fig. 4C).

Finally, the *TlNrt2.4* expression profile was very atypical. In the nitrogen-starved cultures of *T. lutea*, the transcript level was low, with an average value of 1.5  $\text{mmol mol}^{-1}$  *TIUbi* mRNA (Fig. 4E). Following the addition of  $\text{NH}_4^+$  to the nitrogen-starved cultures, the *TlNrt2.4* transcript level significantly increased by 6.6-fold after 4 h (10  $\text{mmol mol}^{-1}$  *TIUbi* mRNA) and remained approximately stable until day 1. Thereafter, the transcript level of *TlNrt2.4* fell dramatically in day 2 in the nitrogen-starved cells with an average of 1.76  $\text{mmol mol}^{-1}$  *TIUbi* mRNA.

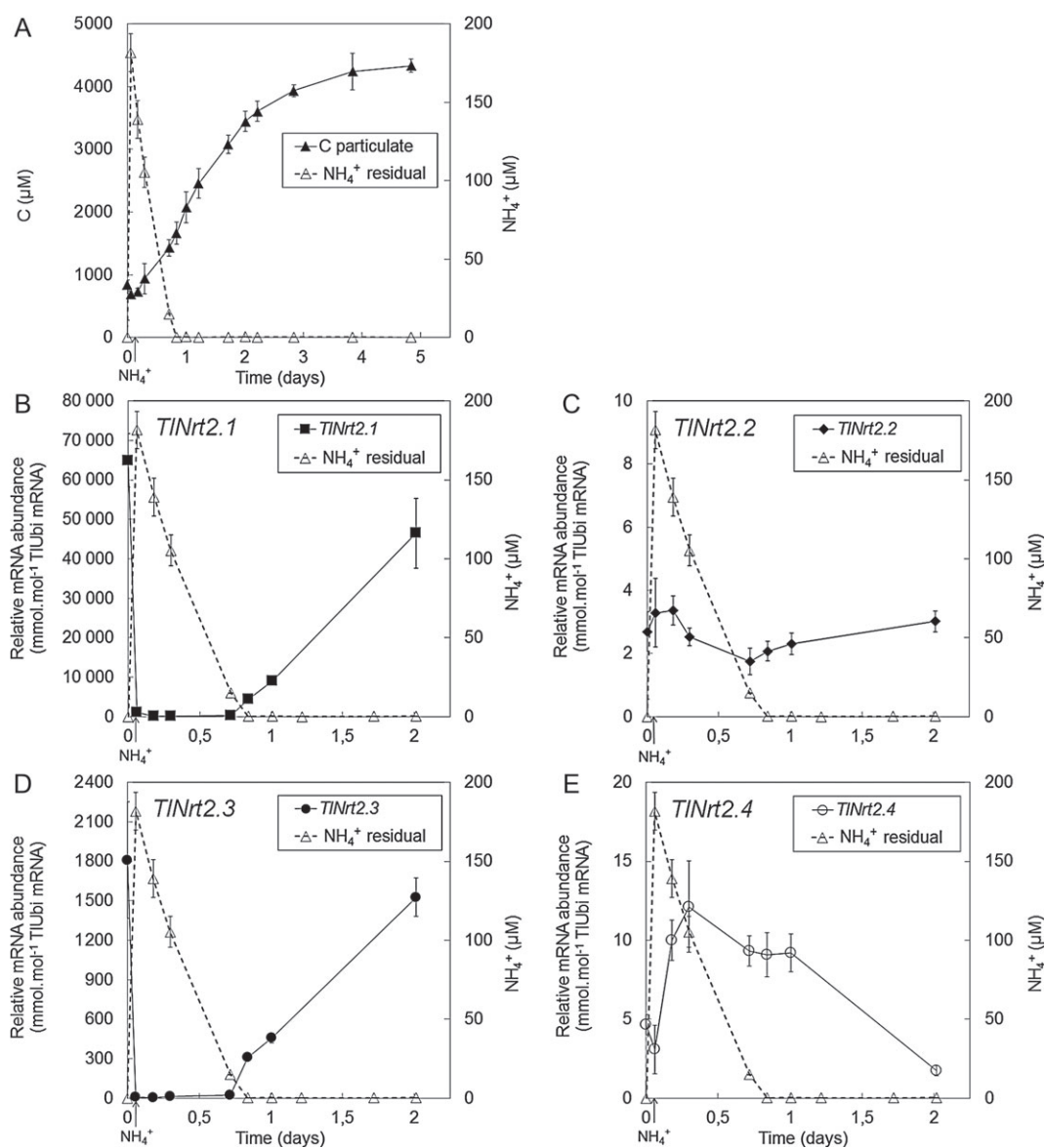
### Transcriptional responses of *TlNrt2* genes according to N/C cell ratio

N and C cell quotas have been analyzed during the sampling of the ammonium batch culture in order to determine the N/C cell ratio. Thus the transcriptional responses of *TlNrt2* genes have been highlighted according to the N status of *T. lutea* cells (Fig. 5). In concordance with the results, three distinct expression profiles are observed as indicated in Fig 5A–C, respectively. *TlNrt2.1* and *TlNrt2.3* inducible genes responded with a same pattern, which is uncorrelated to the N/C cell ratio. For instance at the highest N/C values the expression of these two genes is only dependent of the residual nitrogen concentration (Fig. 5A). This non-correlation to the N/C cell ratio is signed by a 'loop' pattern on the graph. As expected, the expression of *TlNrt2.2* constitutive gene was independent of N/C ratios as the residual nitrogen depletion (Fig. 5B). On the other hand, the *TlNrt2.4* gene was expressed regardless to the presence of ammonium substrate (Fig. 5C). A high expression of *TlNrt2.4* gene was observed for both residual nitrogen levels when the cell quota was full. In contrast, its gene expression was strongly repressed for empty cell quota (fivefold). Moreover a significant threshold near to  $\text{N/C} = 0.11$  ( $P < 0.05$ ;  $n = 21$ ) was observed.

### Regulation of *T. lutea Nrt2* genes by nitrate and different reduced nitrogen sources

In our earlier experiment, we observed an expression of three *TlNrt2* genes in nitrogen-starvation conditions (Figs 3 and 4). In order to investigate the impact of high concentrations of different nitrogen sources (1 mM of total nitrogen) on *TlNrt2* gene expression, a short-term incubation experiment (lasting 2 h) using different sources of nitrogen was performed after nitrogen-starvation preconditioning.

Under nitrate-repletion, the mRNA abundance of *TlNrt2.1* decreased until reaching a value equal to 0.5-fold the value of the mRNA abundance observed

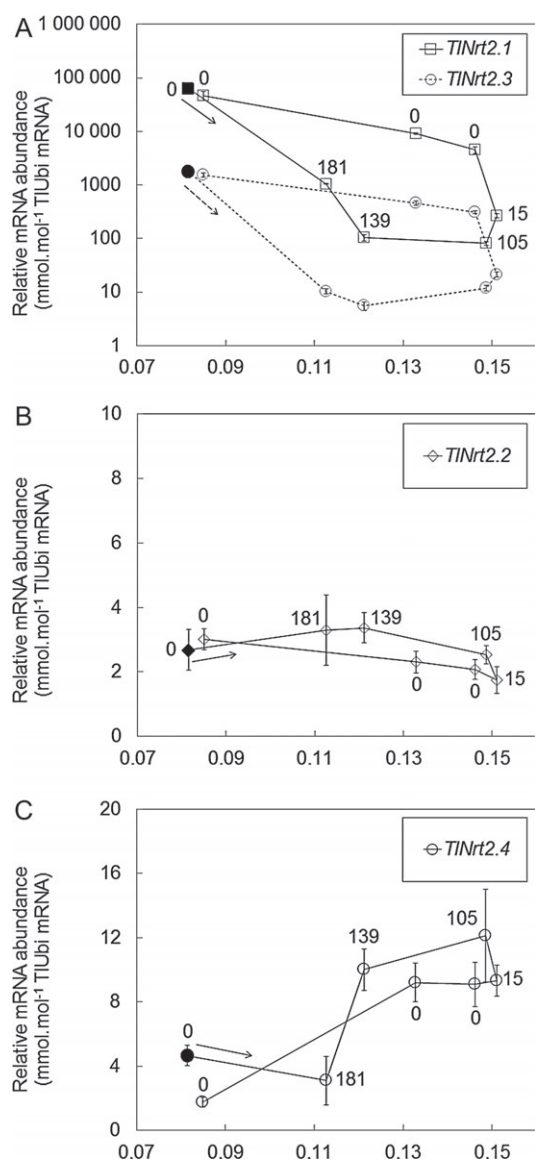


**Fig. 4.** Various parameters of *Tisochrysis lutea* cells grown in ammonium batch culture. Axenic preculture was grown in a modified Conway medium with  $200 \mu\text{M}$   $\text{NH}_4\text{Cl}$ . In stationary phase, cells with an empty quota were inoculated into non-enriched seawater for 24 h in order to lower the natural nitrogen content of the seawater. Then, a new modified Conway medium with  $200 \mu\text{M}$   $\text{NH}_4\text{Cl}$  was added (arrow on the temporal axis). (A) Concentration of particulate carbon and residual nitrate ( $\mu\text{M}$ ) during the batch culture. (B) Relative mRNA abundance of *TINrt2.1*. (C) Relative mRNA abundance of *TINrt2.2*. (D) Relative mRNA abundance of *TINrt2.3*. (E) Relative mRNA abundance of *TINrt2.4*. Each value represents the mean  $\pm$  SE of three independent experiments.

under nitrogen starvation (Fig. 6A). Interestingly, under nitrite repletion, the mRNA abundance of *TINrt2.1* also decreased but quicker than under nitrate-repletion (0.2-fold at 2 h). Finally, under ammonium nitrate (AN)-repletion, the expression of *TINrt2.1* gene was rapidly and strongly repressed after 30 min.

After 2 h under nitrate repletion, the mRNA abundance of *TINrt2.3* decreased very slightly to 0.7-fold compared with the mRNA abundance under nitrogen-free

conditions. The slight decrease of *TINrt2.3* gene was minor compared with the decrease in *TINrt2.1* mRNA abundance. However, results also show that the *TINrt2.3* expression profile was quite similar to that of *TINrt2.1* in response to nitrite repletion and AN repletion (Fig. 6C). Indeed, after nitrite addition, the repression of the *TINrt2.3* gene was very strong compared with nitrogen-free conditions (0.1-fold). The minimal transcript level of *TINrt2.3* was observed 2 h



**Fig. 5.** Relative mRNA abundance of *TINrt2* genes vs the N/C cellular ratio (N-status) in the ammonium batch culture of *Tisochrysis lutea*. The initial condition (nitrogen-starved) is figured by a filled symbol and the timeline of the culture is initiated by an arrow. Culture was enriched with 200  $\mu\text{M}$  ammonium immediately after the first sampling. The numbers represent the residual ammonium concentrations ( $\mu\text{M}$ ). N/C ratios were calculated by dividing the particulate N concentration by the particulate C concentration. (A) Relative mRNA abundance of *TINrt2.1* and *TINrt2.3* genes (B) *TINrt2.2* gene and (C) *TINrt2.4* gene vs the N/C cellular ratio.

after the addition of AN (no expression was observed after 2 h).

The expression of *TINrt2.2* gene was relatively constant throughout the experiment and seemed to be the same whatever the conditions of N repletion (Fig. 6B). Therefore, results confirmed that *TINrt2.2* is constitutively expressed in these conditions.

Unexpectedly, the expression profile of *TINrt2.4* gene under various N-substrate conditions was completely different from the other *TINrt2* genes (Fig. 6D). Indeed, under nitrate- and nitrite-repletion, the mRNA abundance of *TINrt2.4* decreased for at least 1 h, with a ratio of 0.3- and 0.2-fold the level of mRNA observed under nitrogen-starvation conditions. Under AN repletion, results showed an induction of *TINrt2.4* expression compared with the initial conditions (5.6-fold). Interestingly, at 2 h, a peak of *TINrt2.4* expression was observed whatever the nitrogen substrate, with ratios corresponding to 1.4-, 3- and 14-fold the mRNA abundance for the nitrate, nitrite and AN, respectively.

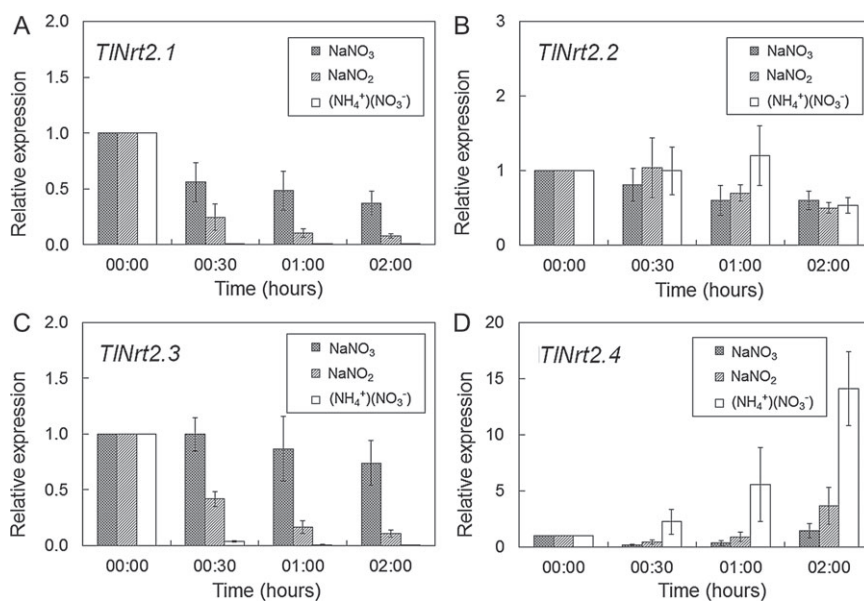
The addition of different nitrogen substrates involved in the nitrogen assimilation pathway allowed us to reveal the regulation kinetics of three *TINrt2* genes (*TINrt2.1*, *TINrt2.3* and *TINrt2.4*) and the absence of *TINrt2.2* gene regulation in these conditions.

## Discussion

To cope with the availability of nitrate in the environment, plants have transporters with different affinity for this substrate. A family of genes encoding high-affinity NRTs (NRT2) is involved in nitrate uptake when the external nitrate concentrations are very low ( $\mu\text{M}$ ). In recent years, several *Nrt2* genes have been identified in some land plants (Krapp et al. 1998, Orsel et al. 2002, Cai et al. 2008) and microalgae (Quesada et al. 1994, Koltermann et al. 2003, He et al. 2004). For instance, in the green algae *C. reinhardtii*, four members of the *Nrt2* gene family were identified (Galvan and Fernández 2001). More recently, in the diatom *T. pseudonana*, three putative NRT genes were reported (Song and Ward 2007). However, most studies in microalgae only describe the global expression profile of the *Nrt2* gene family and not the individual *Nrt2* gene expression (Hildebrand and Dahlin 2000, Kang et al. 2007, Song and Ward 2007). Among these reports, only two studies have investigated the Haptophyta phylum. In this article, we describe for the first time the individual *Nrt2* gene expression pattern under specific physiological conditions in the haptophyte *T. lutea*.

### In silico analyses reveal four genes encoding putative high-affinity NRTs (*TINrt2*) with original characteristics

We identified four genes encoding putative high-affinity NRTs in the marine microalgae *T. lutea*. The identification was performed from transcriptomic data (Carrier et al. 2014) using homology searches with NRT2 of other species. Interestingly, cloning of genomic sequences and their alignment with the cDNA sequences did not



**Fig. 6.** Effect of different N-substrates on transcript levels of *TINrt2* genes. After nitrogen starvation, *Tisochrysis lutea* cells were inoculated with different forms of nitrogenous nutrients (1 mM of total nitrogen). RNA extractions were performed at 0, 15, 30, 60 and 120 min. Graphs represent the expression profiles of each *TINrt2* gene under the different N-substrate conditions. Each value represents the mean  $\pm$  SE of three independent experiments.

reveal the presence of introns in putative *TINrt2* genes. Although the presence of introns in *Nrt2* genes appears to be very variable, the presence of at least two introns have been described in dicotyledonous plants and some microalgae (Orsel et al. 2002, Plett et al. 2010, Bhadury et al. 2011), whereas no intron was detected in grasses plants (Plett et al. 2010). In microalgae particularly, Song and Ward (2007) characterized *Nrt2* genes from several marine species and especially detected four introns in *Nrt2* gene sequence of another haptophyte *E. huxleyi*. Nevertheless, Bhadury et al. (2011) suggest that there are large variations in intron number and length in phytoplankton genomes.

In silico analyses showed that the four *TINRT2* deduced amino acid sequences are very similar to one another (95.7% similarity), but have fairly low similarities with *NRT2* of other phyla (land plants, green algae, fungi and yeast; Table S4). This can be explained by the fact that these species are relatively distant in terms of evolution, which is supported by the homology tree (Fig. 2). The distances shown by the tree confirm that the *Nrt2* genes from haptophytes cluster with the *Nrt2* genes from land plants and green algae and differ completely from other phyla. Nevertheless, our results also reveal that the Haptophyta *Nrt2* genes are distinct to the green lineage and form an independent group.

The full bioinformatic analyses reveal that the deduced *TINRT2* amino acid sequences have all the features of high-affinity *NRTs* described in literature (Forde 2000):

- (1) the 12 membrane-spanning domains separated by a central cytosolic loop as described in *MFS* members;
- (2) the *MFS* conserved domain and (3) the *NRT2* conserved motif. These results confirm that the four putative *TINRT2* belong to the *MFS* family and encode high-affinity *NRT* proteins. The alignment also reveals that the central cytosolic loop in *TINRT2* proteins is reduced (20–30 AA), as in land plants and microalgae, whereas this loop is much extended in yeast and fungi (90 AA) (Fig. 1). Furthermore, *TINRT2* proteins present an extended N-terminal domain (20–30 AA) and a large C-terminal domain (60–70 AA), as described in *NRT2* from green lineage species (Quesada et al. 1994, Trueman et al. 1996, Forde 2000). In fact, previous studies suggested that the cytosolic loop and the C-terminal domain may have a regulatory function (Katagiri et al. 1992, Due et al. 1995, Liu et al. 1995). Indeed, conserved protein kinase C recognition motifs (S/T-X-R/K) are present in the N- and C-terminal domains of plant and microalgal *NRT2* and in the central loop of the fungal *NRT2* (Fig. 1). The existence of these motifs could indicate that phosphorylation and dephosphorylation reactions play a part in the regulation of the activity of the *NRT2* proteins. However, the analyses reveal that these kinase C specific phosphorylation motifs were not present in *TINRT2* sequences and the lack of these conserved phosphorylation sites in *TINRT2* proteins could imply that high-affinity *NRTs* in *T. lutea* are regulated differently.

Interestingly, the presence of an atypical sequence of 100 amino acids length in TINRT2 sequences reveals an original specificity of the Haptophyta. The BLAST analysis results of this additional part with the non-redundant protein sequences (NCBI) fitted only with NRT2 sequences of another haptophyte *E. huxleyi* (data not shown). This unusual sequence forms an extracellular loop located between transmembrane domains 9 and 10. Many hypotheses could be formulated about the function of this atypical loop, especially that this additional sequence could be implicated in substrate binding or have a sensor function. These hypotheses could be supported by the fact that *Tisochrysis* NRT2 transporters may not need any NAR2 accessory proteins to function correctly in nitrate uptake, unlike to the majority of NRT2 proteins from land plants and microalgae. Indeed, no genes encoding accessory proteins (NAR2) were identified in *T. lutea*, despite many searches. It seems, therefore, that these accessory proteins are absent, suggesting that the *Tisochrysis* NRT2 could be a 'single component', as is the case in yeast and fungal species. This Haptophyta particularity will require further investigations to elucidate the effective role of this additional loop. To our knowledge, it is the first time that this feature has been described.

### Genes encoding high-affinity transporters present different expression levels

In concordance with the literature, *TINrt2* genes present different expression levels (Figs 3 and 4). Indeed, high expression was detected for the *TINrt2.1* gene, with a strong expression under nitrogen starvation but also under nitrate-sufficient conditions. The *TINrt2.3* is also strongly expressed in these conditions. Unlike the two latter genes, *TINrt2.4* gene was poorly expressed and did not reach the levels of expression of two other genes. The lowest expression level for *TINrt2* genes was observed for *TINrt2.2*, which has a very low expression in all conditions tested (Figs 3 and 4). This is in concordance with previous studies in plants and microalgae that described a specific role for each of the NRTs of the same family (Galván et al. 1996, Orsel et al. 2002).

### Experiments using $\text{NO}_3^-$ or $\text{NH}_4^+$ as nitrogen sources reveal the presence of inducible and constitutive systems in *T. lutea*

Previous studies reported the total mRNA abundance of *Nrt2* genes in several microalgae species during batch cultures, but without distinguishing the *Nrt2* genes individually (Kang et al. 2007, Song and Ward 2007). In this study, we monitored, for the first time, the individual

time-course of the expression of the four *Nrt2* genes in *T. lutea* depending on N source and N availability (Figs 3 and 4).

During the nitrate batch experiment, the transcript level of *TINrt2.1* increased when the residual nitrate reached  $30\ \mu\text{M}$  and peaked when the nitrate became undetectable in the medium (Fig. 3B). These results showed that *TINrt2.1* could be considered as inducible either by nitrate at low concentration or nitrogen starvation. This expression under nitrogen starvation can be considered as an adaptive strategy for facilitating the synthesis of NRT2 protein when nitrate is provided. Some microalgae have already demonstrated a high expression of *Nrt2* genes under nitrogen starvation (Kang et al. 2007, Song and Ward 2007). Moreover, this behavior is also observed in other transporter families that are strongly expressed in the absence of their substrates (Matsuda and Colman 1995, Chung et al. 2003, Li et al. 2006). Differently, the *TINrt2.3* expression was maximal at the beginning of the nitrate batch experiment, i.e. when the nitrate was sufficient in the medium (Fig. 3D). Later in this experiment, the mRNA abundance of *TINrt2.3* was slightly decreased, although remaining high, when the cells were in nitrogen-starvation conditions (Fig. 3D). These results show that *TINrt2.3* expression was induced in nitrogen-starved cells, but nitrate is required for its maximal expression. Although the expression pattern is not exactly the same, *TINrt2.1* and *TINrt2.3* genes belong to the inducible HATS system. In contrast to these observations, the abundance of *TINrt2.2* gene transcripts was stable throughout the nitrate batch culture (Fig. 3C). This expression pattern suggests that *TINrt2.2* belongs to the constitutive HATS component of the NRT2 family. Indeed, previous studies have shown that three genes encoding *Nrt2* in *A. thaliana* were characterized as constitutively expressed even under  $\text{NO}_3^-$ -starved conditions and the expression levels did not change substantially during  $\text{NO}_3^-$  exposure (Okamoto et al. 2003).

Many studies have found that ammonium addition can inhibit the expression of *Nrt2* genes in plants and microalgae (Quesada et al. 1994, Krapp et al. 1998, Hildebrand and Dahlin 2000, Vidmar et al. 2000, Koltermann et al. 2003, He et al. 2004). Therefore, to determine the ammonium-repressed transcript levels of *TINrt2* genes in *T. lutea*, the mRNA abundances were monitored during ammonium batch culture. As expected, the transcript levels of *TINrt2.1* and *TINrt2.3* genes decreased dramatically in presence of ammonium (Fig 4B, D) and showed that these genes are actively repressed by this substrate. Once the ammonium became undetectable, very high induction was detected for *TINrt2.1* and *TINrt2.3* genes, as previously observed under nitrogen starvation. These expression profiles during ammonium



batch culture are in concordance with a previous report that described not only a reduction of the total *Nrt2* mRNA abundance in the presence of ammonium, but also a strong increase when ammonium became undetectable in the medium in *I. galbana* (Kang et al. 2007). Considering the overall results, *TINrt2.1* and *TINrt2.3* genes not only present a typical inducibility by both nitrate and nitrogen starvation but also a downregulation in the presence of ammonium.

*TINrt2.2* expression remained stable during the ammonium batch culture (Fig. 4C), confirming that this gene belongs to the constitutive HATS system. Indeed, in *C. reinhardtii*, studies showed the existence of a nitrate transport system IV containing the *CrNrt2.4* gene, which is constitutively expressed and not repressed in the presence of ammonium (Rexach et al. 1999).

Our results on the *TINrt2.4* gene expression profile from all of our experiments will be discussed in its own specific section below.

### ***TINrt2* gene expression is differentially regulated by N metabolites**

Many reviews have reported the regulation of *Nrt2* gene expression by the accumulation of N metabolites in plant cells (Forde 2000, Miller et al. 2008). So, a short-term experiment was performed by adding high concentrations of different metabolizable nitrogen sources (1 mM) to the medium in order to generate intracellular N-metabolite accumulation.

The results showed that *TINrt2.1* and *TINrt2.3* gene expression was downregulated when nitrogen elements were provided at very high concentrations. A strong repression was observed after only 30 min of treatment with nitrate, nitrite and AN (Fig 6A, C). This repression continued for 1 h until reaching the maximal repression level. A variable kinetic of gene expression was also observed depending on the substrate ( $\text{NH}_4^+$ ,  $\text{NO}_2^-$  and  $\text{NO}_3^-$ ). In fact, the differential expression obtained with the different N substrates suggests that the rate of gene repression depends on the position of the substrate in the pathway of nitrate assimilation. These results support the idea that the intracellular N-metabolite accumulation coming from the nitrate assimilation pathway is involved in the regulation of *TINrt2.1* and *TINrt2.3* genes. In land plants, several studies have shown that the expression level of genes encoding NRT2 is quickly repressed by the metabolites generated through nitrate assimilation. In fact, ammonium and some amino acids supplied cause an inhibitory effect on nitrate transport. Krapp et al. (1998) showed a decrease of the *NpNrt2* gene expression level in *N. plumbaginifolia* in the presence of glutamine (Krapp et al. 1998). Similarly, in *A. thaliana*,

the addition of arginine to the medium resulted in a strong inhibition of *AtNrt2.1* expression (Zhuo et al. 1999). In the green microalga *C. reinhardtii*, previous studies showed the repression of three *CrNrt2* genes in the presence of ammonium (Quesada et al. 1998). Furthermore, Kang et al. (2009) reported that the inhibition of the GS/GOGAT enzymatic system removed the repression of total *Nrt2* genes in *I. galbana* (haptophyte) and *T. pseudonana* (diatom). Our experiment reveals a regulation system of *TINrt2.1* and *TINrt2.3* genes consistent with those already described in plants and some microalgae. As expected, expression of the constitutive gene *TINrt2.2* is not affected by this regulation system (Fig. 6B).

### ***TINrt2.4*: an atypical putative high-affinity NRT in *T. lutea***

In silico analysis of the TINRT2.4 protein revealed that this gene had some specificities that set it apart from other TINRT2 proteins (Fig. 1). Only TINRT2.4 harbored an atypical feature corresponding to the additional presence of 20 AA at the end of the C-terminal domain. Moreover, no protein kinase C recognition motif (conserved or not in NRT2 family) was predicted from its protein sequence. Nevertheless, the highly conserved motif found in all NRT2 transporters (NRT2 and MFS motif) was clearly identified in the TINRT2.4 protein and strengthens its status as belonging to the NRT2 family.

Very interestingly, the *TINrt2.4* expression pattern was totally unexpected. In contrast to other inducible *TINrt2* genes (*TINrt2.1* and *TINrt2.3*), the mRNA abundance of *TINrt2.4* was very weak during nitrogen starvation (Figs 3E and 4E). This result could indicate that the *TINrt2.4* gene is not directly implicated in the nitrogen-starvation response, contrary to *TINrt2.1* and *TINrt2.3*.

*TINrt2.4* expression was induced under nitrate-sufficient conditions (200  $\mu\text{M}$ ), like *TINrt2.1* and *TINrt2.3* genes, but its expression levels remained low compared with these other genes (Fig. 3E). In contrast, in a way surprisingly unlike *TINrt2.1* and *TINrt2.3*, the *TINrt2.4* expression level was induced under AN-sufficient conditions (Fig. 6D). Furthermore, Q-RT-PCR studies of the *TINrt2.4* gene revealed a slight yet significant expression during the ammonium batch experiment (Fig. 4E). This pattern contrasts with the repression of *Nrt2* genes by ammonium, which is well described in many species (land plants and microalgae) (Krapp et al. 1998, Forde 2000, Koltermann et al. 2003). Moreover, the *TINrt2.4* profile expression was inversely correlated with *TINrt2.1* and *TINrt2.3* transcriptional gene responses for almost all experiments.

Considering the atypical expression profile of *TINrt2.4* gene, a possible relation between its expression and the cell N status has been hypothesized. For this purpose, we observed the evolution of *TINrt2* gene expression vs the cell N/C quota during the ammonium batch culture (Fig. 5). The results exhibited three distinct patterns depending on the gene. *TINrt2.1* and *TINrt2.3* inducible genes were downregulated and upregulated according to the nitrogen depletion (total depletion occurred after the highest N/C ratio value) (Fig. 5A). As expected, the expression of the *TINrt2.2* constitutive gene was independent to both N/C ratios and residual nitrogen (Fig. 5B).

In contrast, the *TINrt2.4* gene was expressed irrespective of the presence of ammonium substrate (Fig. 5C). In fact, for both of these residual nitrogen levels, high *TINrt2.4* expression was observed when the cell quota was full. Conversely, expression of this gene was strongly repressed for an empty cell quota. This could mean that *TINrt2.4* expression would be linked to the cell N status with a significant threshold effect close to  $N/C = 0.11$  ( $P < 0.05$ ;  $n = 21$ ).

These results suggest that *TINrt2.4* has a different role in the nitrogen transport and/or metabolism pathway. Among several hypotheses, *TINRT2.4* could be involved in storage processes. This hypothesis would be supported by the presence of putative signal sorting in the C-terminal domain leading to a possibly different subcellular localization. Indeed, one study has even reported a storage function for the *AtNrt2.7* gene in *A. thaliana* seeds (Chopin et al. 2007). However, to date, none of the NRT2 proteins have been clearly localized in the intracellular compartment of microalgae. Alternatively, given its converse expression pattern, the *TINrt2.4* gene could be involved in a regulation system. Last the *TINrt2.4* gene could be a vestigial gene stimulated by N metabolism. Indeed, haptophytes, like other microalgae groups, are issued from secondary endosymbiosis, which implicates genomic rearrangement (McFadden 2001).

To our knowledge, this is the first time that this original expression profile for *Ntr2* genes has been described. Today, the function of *TINrt2.4* gene remains unclear and further investigations will be necessary for to improve our understanding of its involvement in the nitrogen metabolism of *T. lutea*.

## Conclusion

Due to its natural nutritional properties, the haptophyte *T. lutea* is commonly used as a feed in aquaculture. Recently, it has also been the subject of domestication for various applications (Cadoret et al. 2012). Beyond the obvious economic interest, there is also a

fundamental interest in the Haptophyta lineage, which is highly diverse and ecologically dominant in ocean euphotic zones. To date, our understanding of the nitrogen metabolism of *T. lutea* is limited. Accordingly, it would be of great interest to understand the biology of *T. lutea* in relation to nitrogen availability. This first study is an attempt to further knowledge in this direction.

Four genes, encoding putative high-affinity nitrate/nitrite transporters, were identified, cloned and sequenced in *T. lutea*. In silico analysis revealed that the *TINrt2* sequences did not contain introns, but had a unusual sequence of 100 AA forming an extracellular loop, whose function remains to be determined. This original additional sequence seems to be a particularity of the Haptophyta. The monitoring of individual *TINrt2* gene expression under different nitrogen sources highlights a differential expression profile that leads us to conclude that there are two inducible genes (*TINrt2.1* and *TINrt2.3*), one constitutive gene (*TINrt2.2*) and another gene characterized by an atypical expression profile (*TINrt2.4*). The expression of the *TINrt2.4* gene appears to be independent of the substrate used, while that of the other *TINrt2* genes seems to be related to the residual nitrogen. From this preliminary study, it is hazardous to speculate on the role of each gene in sensing and/or uptake of nitrogen substrates. Further investigations need to be done to reveal the true function of high-affinity nitrate/nitrite transporters in *T. lutea*. As for most microalgae of interest, the lack of genetic tools prevents us from using mutants to characterize the true function and localization [using green fluorescent protein (GFP)-chimeras] of these *TINrt2* genes in the cell.

Finally, this study contributes to an important topic of current research in plant nutrition via the analysis of nutrient transporter proteins, in our case those involved in nitrogen metabolism of microalgae. The understanding of microalgal nitrogen metabolism will not only provide us with fundamental knowledge but will also make a major contribution to the establishment of sustainable nitrogen management during biomass production with respect to the well-being of human populations.

## Author contributions

A. C. wrote the manuscript. All cell culture experiments and sampling were performed by A. C., J. B. B., F. F., A. F. C., C. R. and B. S. J. Gene expression analyses were carried out by A. C. and F. F. M. G. and J. B. B. helped with homology tree analysis and figure design, respectively. G. C. helped with bioinformatic analyses. Molecular analyses (cloning, sequencing, etc.) were performed

by A. C. and N. S. Elementary analyses (N, C) were done by E. L. G. B., A. C., J. B. B., J. P. C. and B. S. J. conceived the study and the project was coordinated by G. B. and B. S. J. All authors corrected and approved the final manuscript.

*Acknowledgements* – The authors are grateful to the anonymous reviewers for their critical comments that have greatly improved the manuscript. Thanks to Ms Deborah McCombie for the English reviewing of the manuscript. This work was supported by the French region of Pays de la Loire ('Nouvelles équipes, nouvelles thématiques' program) and the French Research Institute for Exploitation of the Sea (IFREMER). The nucleotide sequence reported in this article will be submitted to EMBL Data Library.

## References

- Ahmad I, Hellebust JA (1984) Nitrogen metabolism of the marine microalga *Chlorella autotrophica*. *Plant Physiol* 76: 658–663
- Aminot A, Kérouel R (2007) Dosage automatique des nutriments dans les eaux marines: méthodes en flux continu. Editions Quae, Versailles, France
- Bannai H, Tamada Y, Maruyama O, Nakai K, Miyano S (2002) Extensive feature detection of N-terminal protein sorting signals. *Bioinformatics* 18: 298–305
- Becker B (2007) Function and evolution of the vacuolar compartment in green algae and land plants (Viridiplantae). *Int Rev Cytol* 264: 1–24
- Bendif EM, Probert I, Schroeder DC, de Vargas C (2013) On the description of *Tisochrysis lutea* gen. nov. sp. nov. and *Isochrysis nuda* sp. nov. in the Isochrysidales, and the transfer of Dicrateria to the Prymnesiales (Haptophyta). *J Appl Phycol* 25: 1–14
- Bhadury P, Song B, Ward BB (2011) Intron features of key functional genes mediating nitrogen metabolism in marine phytoplankton. *Mar Genomics* 4: 207–213
- Blom N, Gammeltoft S, Brunak S (1999) Sequence and structure-based prediction of eukaryotic protein phosphorylation sites. *J Mol Biol* 294: 1351–1362
- Bougaran G, Le Déan L, Lukomska E, Kaas R, Baron R (2003) Transient initial phase in continuous culture of *Isochrysis galbana* affinis *Tahiti*. *Aquat Living Resour* 16: 389–394
- Brownlee AG, Arst HN (1983) Nitrate uptake in *Aspergillus nidulans* and involvement of the third gene of the nitrate assimilation gene cluster. *J Bacteriol* 155: 1138–1146
- Cadoret J-P, Garnier M, Saint-Jean B (2012) Microalgae, functional genomics and biotechnology. *Adv Bot Res* 64: 285–341
- Cai C, Wang J-Y, Zhu Y-G, Shen Q-R, Li B, Tong Y-P, Li Z-S (2008) Gene structure and expression of the high-affinity nitrate transport system in rice roots. *J Integr Plant Biol* 50: 443–451
- Carrier G, Garnier M, Le Cunff L, Bougaran G, Probert I, De Vargas C, Corre E, Cadoret J-P, Saint-Jean B (2014) Comparative transcriptome of wild type and selected strains of the microalgae *Tisochrysis lutea* provides insights into the genetic basis, lipid metabolism and the life cycle. *PLoS One* 9: e86889
- Chopin F, Orsel M, Dorbe M-F, Chardon F, Truong H-N, Miller AJ, Krapp A, Daniel-Vedele F (2007) The Arabidopsis ATNRT2.7 nitrate transporter controls nitrate content in seeds. *Plant Cell* 19: 1590–1602
- Chung C-C, Hwang S-PL, Chang J (2003) Identification of a high-affinity phosphate transporter gene in a prasinophyte alga, *Tetraselmis chui*, and its expression under nutrient limitation. *Appl Environ Microbiol* 69: 754–759
- Chung CC, Hwang SPL, Chang J (2005) Cooccurrence of ScDSP gene expression, cell death, and DNA fragmentation in a marine diatom, *Skeletonema costatum*. *Appl Environ Microbiol* 71: 8744–8751
- Collos Y, Vaquer A, Souchu P (2005) Acclimation of nitrate uptake by phytoplankton to high substrate levels. *J Phycol* 41: 466–478
- Crawford NM, Forde BG (2002) Molecular and developmental biology of inorganic nitrogen nutrition. *Arabidopsis Book* 1: e0011
- Crawford NM, Glass AD (1998) Molecular and physiological aspects of nitrate uptake in plants. *Trends Plant Sci* 3: 389–395
- Daniel-Vedele F, Filleur S, Caboche M (1998) Nitrate transport: a key step in nitrate assimilation. *Curr Opin Plant Biol* 1: 235–239
- de Angeli A, Monachello D, Ephritikhine G, Frachisse JM, Thomine S, Gambale F, Barbier-Brygoo H (2006) The nitrate/proton antiporter AtCLCa mediates nitrate accumulation in plant vacuoles. *Nature* 442: 939–942
- Dechorgnat J, Patrit O, Krapp A, Fagard M, Daniel-Vedele F (2012) Characterization of the *Nrt2.6* gene in *Arabidopsis thaliana*: a link with plant response to biotic and abiotic stress. *PLoS One* 7: e42491
- Dereeper A, Guignon V, Blanc G, Audic S, Buffet S, Chevenet F, Dufayard JF, Guindon S, Lefort V, Lescot M (2008) Phylogeny.fr: robust phylogenetic analysis for the non-specialist. *Nucleic Acids Res* 36: 465–469
- Due AD, Qu Z, Thomas JM, Buchs A, Powers AC, May JM (1995) Role of the C-terminal tail of the GLUT1 glucose transporter in its expression and function in *Xenopus laevis* oocytes. *Biochemistry* 34: 5462–5471
- Fernandez E, Galvan A (2007) Inorganic nitrogen assimilation in *Chlamydomonas*. *J Exp Bot* 58: 2279–2287
- Fernandez E, Galvan A (2008) Nitrate assimilation in *Chlamydomonas*. *Eukaryot Cell* 7: 555–559
- Forde BG (2000) Nitrate transporters in plants: structure, function and regulation. *Biochim Biophys Acta* 1465: 219–235

- Galvan A, Fernández E (2001) Eukaryotic nitrate and nitrite transporters. *Cell Mol Life Sci* 58: 225–233
- Galván A, Quesada A, Fernández E (1996) Nitrate and nitrite are transported by different specific transport systems and by a bispecific transporter in *Chlamydomonas reinhardtii*. *J Biol Chem* 271: 2088–2092
- Glass ADM, Shaff JE, Kochian LV (1992) Studies of the uptake of nitrate in barley. IV. Electrophysiology. *Plant Physiol* 99: 456–463
- He Q, Qiao D, Zhang Q, Li Y, Xu H, Wei L, Gu Y, Cao Y (2004) Cloning and expression study of a putative high-affinity nitrate transporter gene from *Dunaliella salina*. *J Appl Phycol* 16: 395–400
- Hildebrand M, Dahlin K (2000) Nitrate transporter genes from the diatom *Cylindrotheca fusiformis* (Bacillariophyceae): mRNA levels controlled by nitrogen sources and by the cell cycle. *J Phycol* 36: 702–713
- Hofmann K, Stoffel W (1993) TMBASE – A database of membrane spanning protein segments. *Biol Chem Hoppe Seyler* 374: 166
- Horton P, Park K-J, Obayashi T, Fujita N, Harada H, Adams-Collier CJ, Nakai K (2007) WoLF PSORT: protein localization predictor. *Nucleic Acids Res* 35: W585–W587
- Kang L-K, Hwang SPL, Gong GC, Lin HJ, Chen PC, Chang J (2007) Influences of nitrogen deficiency on the transcript levels of ammonium transporter, nitrate transporter and glutamine synthetase genes in *Isochrysis galbana* (Isochrysidales, Haptophyta). *Phycologia* 46: 521–533
- Kang L-K, Hwang SPL, Lin HJ, Chen PC, Chang J (2009) Establishment of minimal and maximal transcript levels for nitrate transporter genes for detecting nitrogen deficiency in the marine phytoplankton *Isochrysis galbana* (Prymnesiophyceae) and *Thalassiosira pseudonana* (Bacillariophyceae). *Phycologia* 45: 864–872
- Katagiri H, Asano T, Ishihara H, Tsukuda K, Lin JL, Inukai K, Kikuchi M, Yazaki Y, Oka Y (1992) Replacement of intracellular C-terminal domain of GLUT1 glucose transporter with that of GLUT2 increases Vmax and Km of transport activity. *J Biol Chem* 267: 22550–22555
- Koltermann M, Moroni A, Gazzarini S, Nowara D, Tischner R (2003) Cloning, functional expression and expression studies of the nitrate transporter gene from *Chlorella sorokiniana* (strain 211-8 k). *Plant Mol Biol* 52: 855–864
- Krapp A, Fraiser V, Scheible WR, Quesada A, Gojon A, Stitt M, Caboche M, Daniel-Vedele F (1998) Expression studies of *Nrt2:1 Np*, a putative high-affinity nitrate transporter: evidence for its role in nitrate uptake. *Plant J* 14: 723–731
- Léran S, Varala K, Boyer JC, Chiurazzi M, Crawford N, Daniel-Vedele F, David L, Dickstein R, Fernandez E, Forde B, Gassmann W, Geiger D, Gojon A, Gong JM, Halkier BA, Harris JM, Hedrich R, Limami AM, Rentsch D, Seo M, Tsay YF, Zhang M, Coruzzi G, Lacombe B (2014) A unified nomenclature of NITRATE TRANSPORTER 1/PEPTIDE TRANSPORTER family members in plants. *Trends Plant Sci* 1: 5–9
- Li Q, Gao X, Sun Y, Zhang Q, Song R, Xu Z (2006) Isolation and characterization of a sodium-dependent phosphate transporter gene in *Dunaliella viridis*. *Biochem Biophys Res Commun* 340: 95–104
- Liu H, Xiong S, Shi Y, Samuel SJ, Lachaal M, Jung CY (1995) ATP-sensitive binding of a 70-kDa cytosolic protein to the glucose transporter in rat adipocytes. *J Biol Chem* 270: 7869–7875
- Liu KH, Huang CY, Tsay YF (1999) CHL1 is a dual-affinity nitrate transporter of Arabidopsis involved in multiple phases of nitrate uptake. *Plant Cell* 11: 865–874
- Matsuda Y, Colman B (1995) Induction of CO<sub>2</sub> and bicarbonate transport in the green alga *Chlorella ellipsoidea*. II Evidence for induction in response to external CO<sub>2</sub> concentration. *Plant Physiol* 108: 253–260
- McFadden GI (2001) Primary and secondary endosymbiosis and the origin of plastids. *J Phycol* 37: 951–959
- Miller AJ, Fan X, Shen Q, Smith SJ (2008) Amino acids and nitrate as signals for the regulation of nitrogen acquisition. *J Exp Bot* 59: 111–119
- Okamoto M, Vidmar JJ, Glass ADM (2003) Regulation of NRT1 and NRT2 gene families of *Arabidopsis thaliana*: responses to nitrate provision. *Plant Cell Physiol* 44: 304–317
- Orsel M, Krapp A, Daniel-Vedele F (2002) Analysis of the NRT2 nitrate transporter family in Arabidopsis. Structure and gene expression. *Plant Physiol* 129: 886–896
- Orsel M, Chopin F, Leleu O, Smith SJ, Krapp A, Daniel-Vedele F, Miller AJ (2006) Characterization of a two-component high-affinity nitrate uptake system in Arabidopsis. Physiology and protein-protein interaction. *Plant Physiol* 142: 1304–1317
- Plett D, Toubia J, Garnett T, Tester M, Kaiser BN, Baumann U (2010) Dichotomy in the NRT gene families of dicots and grass species. *PLoS One* 5: e15289
- Quesada A, Galvan A, Fernandez E (1994) Identification of nitrate transporter genes in *Chlamydomonas reinhardtii*. *Plant J* 5: 407–419
- Quesada A, Hidalgo J, Fernández E (1998) Three *Nrt2* genes are differentially regulated in *Chlamydomonas reinhardtii*. *Mol Gen Genet* 25: 373–377
- Rexach J, Montero B, Fernández E, Galván A (1999) Differential regulation of the high affinity nitrite transport systems III and IV in *Chlamydomonas reinhardtii*. *J Biol Chem* 274: 27801–27806
- Rexach J, Llamas A, Fernández E, Galván A (2002) The activity of the high-affinity nitrate transport system I (NRT2;1, NAR2) is responsible for the efficient signalling of nitrate assimilation genes in *Chlamydomonas reinhardtii*. *Planta* 215: 606–611

- Siddiqi MY, Glass ADM, Ruth TJ, Rufty TW (1990) Studies of the uptake of nitrate in barley. *Plant Physiol* 93: 1426–1432
- Song B, Ward BB (2007) Molecular cloning and characterization of high-affinity nitrate transporters in marine phytoplankton. *J Phycol* 43: 542–552
- Steiner HY, Naider F, Becker JM (1995) The PTR family: a new group of peptide transporters. *Mol Microbiol* 16: 825–834
- Tong Y, Zhou JJ, Li Z, Miller AJ (2005) A two-component high-affinity nitrate uptake system in barley. *Plant J* 41: 442–450
- Trueman LJ, Richardson A, Forde BG (1996) Molecular cloning of higher plant homologues of the high-affinity nitrate transporters of *Chlamydomonas reinhardtii* and *Aspergillus nidulans*. *Gene* 175: 223–231
- Tsay YF, Chiu CC, Tsai CB, Ho CH, Hsu PK (2007) Nitrate transporters and peptide transporters. *FEBS Lett* 581: 2290–2300
- Ullrich WR (1983) Uptake and Reduction of Nitrate: Algae and Fungi. *Encyclopedia of Plant Physiology*, Vol. 15. Springer, Berlin, Heidelberg, pp 376–397
- Unkles SE, Hawker KL, Grieve C, Campbell EI, Montague P, Kinghorn JR (1991) *crnA* encodes a nitrate transporter in *Aspergillus nidulans*. *Proc Natl Acad Sci USA* 88: 204–208
- Vidmar JJ, Zhuo D, Siddiqi MY, Schjoerring JK, Touraine B, Glass ADM (2000) Regulation of high-affinity nitrate transporter genes and high-affinity nitrate influx by nitrogen pools in roots of barley. *Plant Physiol* 123: 307–318
- Walne P (1966) Experiments in the Large-Scale Culture of the Larvae of *Ostrea edulis* L. H. M. Stationery Office, London
- Wang R, Liu D, Crawford NM (1998) The Arabidopsis CHL1 protein plays a major role in high-affinity nitrate uptake. *Proc Natl Acad Sci USA* 95: 15134–15139
- Zhuo D, Okamoto M, Vidmar JJ, Glass ADM (1999) Regulation of a putative high-affinity nitrate transporter (*Nrt2;1At*) in roots of *Arabidopsis thaliana*. *Plant J* 17: 563–568
- Zhou JJ, Trueman LJ, Boorer KJ, Theodoulou FL, Forde BG, Miller AJ (2000) A high affinity fungal carrier with two transport mechanisms. *J Biol Chem* 275: 39894–39899

### Supporting Information

Additional Supporting Information may be found in the online version of this article:

**Table S1.** List of primers used for *TINrt2* gene cloning.

**Table S2.** List of Q-RT-PCR primers used for *TINrt2* gene expression.

**Table S3.** Comparative analyses of *TINrt2* sequences.

**Table S4.** Comparison of the amino acid sequences of TINRT2 with NRT2 sequences from *Aspergillus nidulans*, *Hansenula polymorpha*, *Arabidopsis thaliana*, *Oryza sativa*, *Chlamydomonas reinhardtii* and *Dunaliella salina*.

**Fig. S1.** Proteomic identification of the atypical sequence in *Tisochrysis lutea*.



## Chapitre II :

Les bases moléculaires de *Tisochrysis lutea*. Analyses transcriptomiques comparatives.

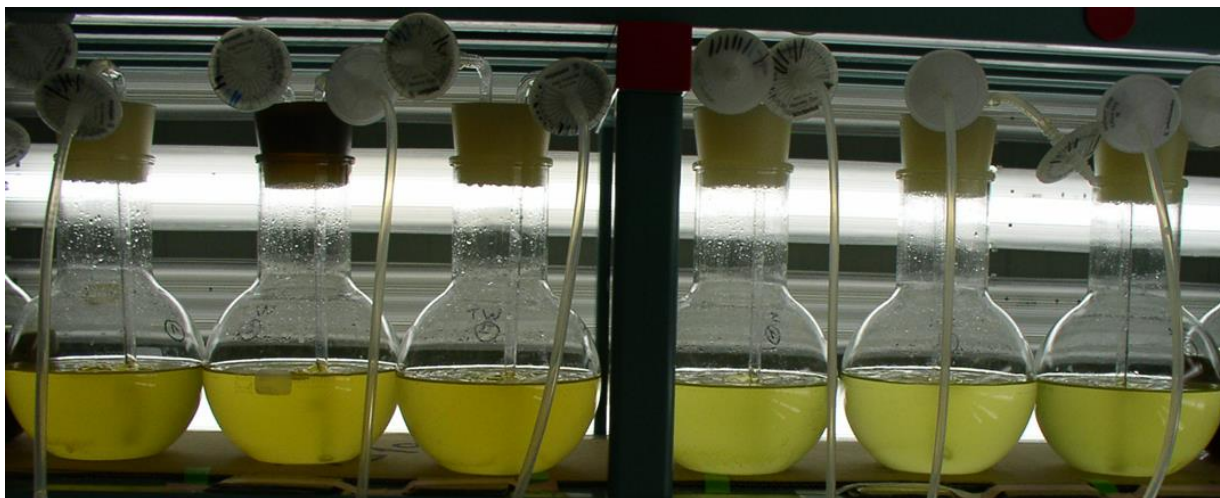


Figure Cultures batch de *T. lutea* limitées par l'azote.

Les 3 ballons à gauche et droite correspondent à la souche WT à la souche S2M2 respectivement.

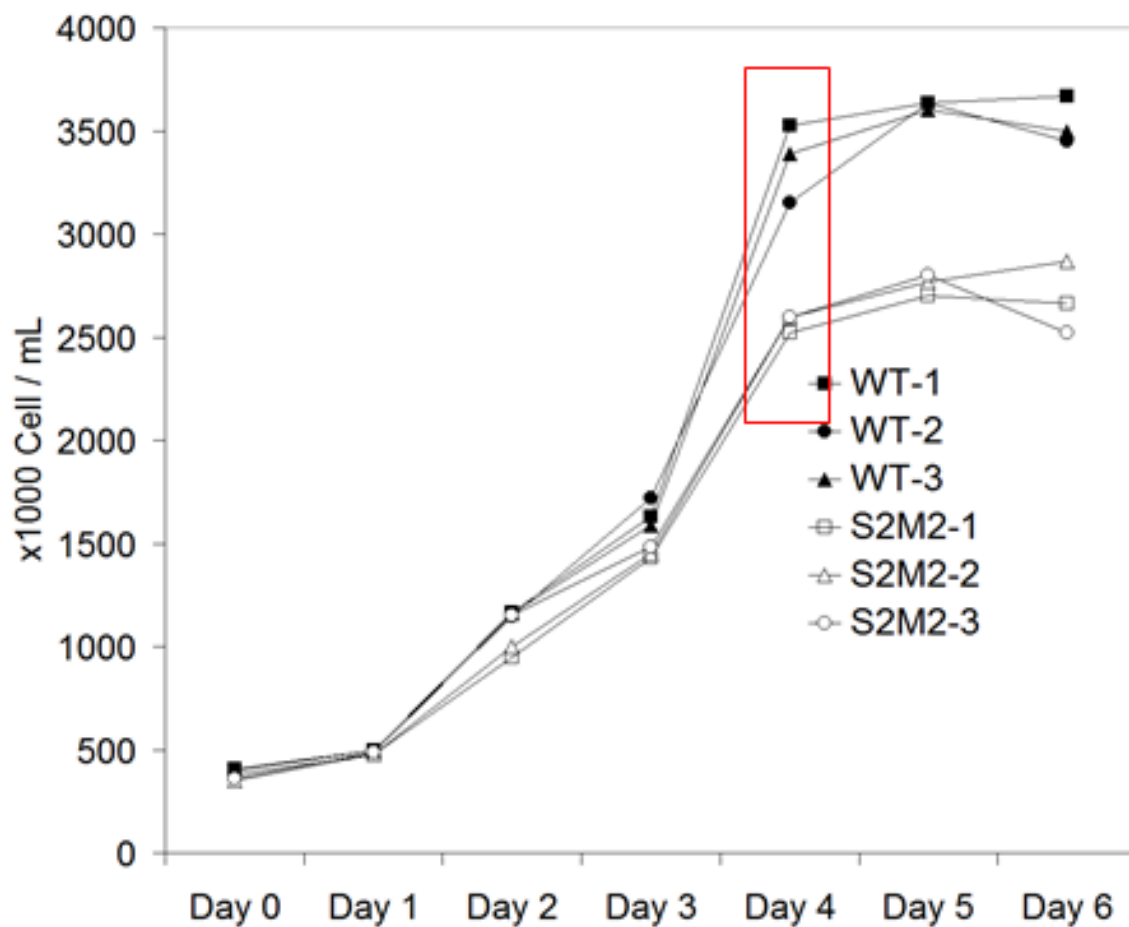


Figure Suivi des cultures batch des souches WT et S2M2.

Les échantillons prélevés pour les analyses transcriptomiques sont encadrés en rouge.



## Chapitre II : Les bases moléculaires de *Tisochrysis lutea*. Analyses transcriptomiques comparatives entre la souche sauvage (WT) et souche mutante hyper-lipidique S2M2 en carence azotée.

---

### 1 Introduction

Les mécanismes impliqués dans l'accumulation lipidique des haptophytes sont encore très mal connus, et le manque de données moléculaires limite très fortement l'avancée des connaissances sur le métabolisme des microalgues. *Tisochrysis lutea* est une haptophyte qui accumule de fortes quantités de lipides de réserve lors de la carence azotée. Une souche mutante S2M2 a été sélectionnée pour sa capacité à accumuler deux fois plus de lipides de réserve (Bougaran et al., 2012). Ce chapitre a pour objectif de caractériser ces différentes souches (WT et S2M2) afin de comprendre pourquoi la souche S2M2 accumule davantage de lipides neutres que la souche sauvage (WT). Pour répondre à cette question, 3 hypothèses de travail concernant cette suraccumulation lipidique ont été émises :

- 1) Les gènes codant des enzymes de la synthèse des lipides sont surexprimés chez la souche sauvage.
- 2) Les gènes codant des enzymes du catabolisme lipidique sont sous-exprimés
- 3) Les gènes codant des enzymes des voies métaboliques centrales sont différenciellement régulés pour orienter le carbone vers la synthèse des lipides au détriment des autres métabolites.

Aucune des expériences du laboratoire n'ayant montré de différences concernant la quantité de carbone séquestré entre les deux souches, l'hypothèse d'un plus fort rendement photosynthétique chez la souche S2M2 n'a pas été retenue dans un premier temps.

Pour valider les différentes hypothèses, nous nous sommes donné comme objectifs d'acquérir les bases moléculaires de *T. lutea* permettant d'initier des approches de génomique fonctionnelle pour l'étude de cette espèce et d'identifier les gènes impactés chez la souche mutante.

Les deux souches ont été cultivées en mode batch (**Figure 37**) limité par l'azote et analysées en début de phase stationnaire (**Figure 38**). Une approche de RNAseq a été privilégiée car permettant

d'acquérir non seulement des données moléculaires à haut débit sur les gènes exprimés, mais également des informations sur les niveaux d'expression et sur le polymorphisme allélique au sein d'une population. Les transcriptomes des deux souches carencées en azote ont été séquencés sur séquenceur illumina. Un transcriptome de référence a été reconstruit et la fonction putative des protéines codées par chacun des transcrits a été inférée par annotation automatique. Les données brutes de séquençage des deux transcriptomes ont ensuite été alignées sur le transcriptome de référence. Le polymorphisme intrinsèque à chaque souche et le polymorphisme entre les deux souches ont été analysés pour identifier les allèles sélectionnés dans la souche mutante. Les gènes différentiellement exprimés entre les 2 souches (WT et S2M2) dans les conditions écophysiologiques testées ont également été identifiés.

## 2 Résultats principaux et perspectives

Les résultats principaux de ces travaux ont été publiés dans un article en 2014, présenté en fin de ce chapitre (Carrier et al., 2014).

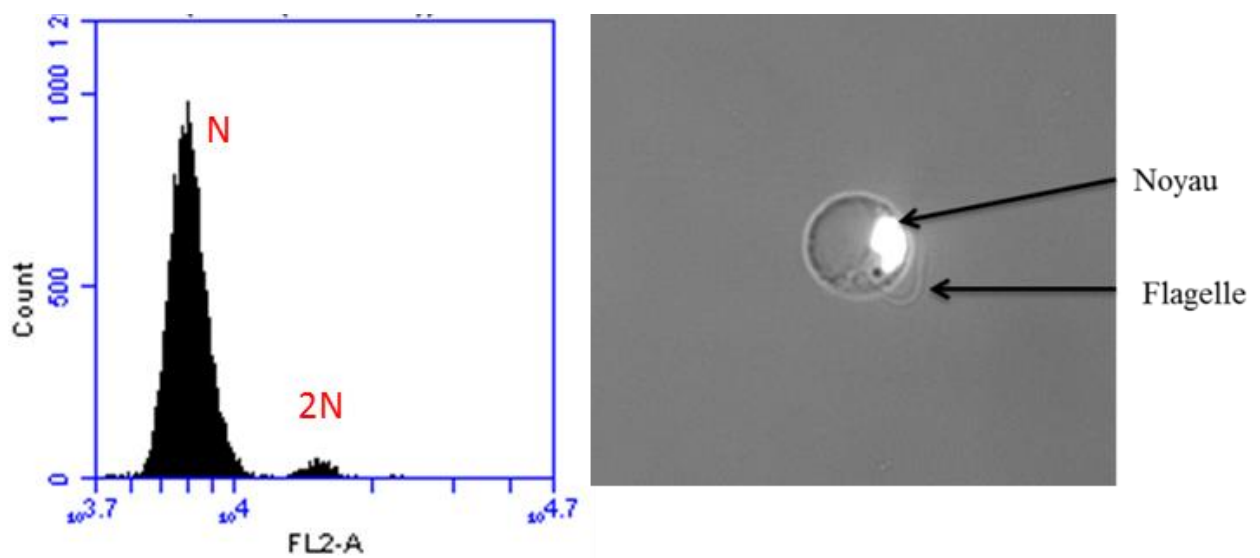
Ce transcriptome est le premier transcriptome d'haptophyte publié après celui d'*E. huxleyi* en 2009 (von Dassow et al., 2009). La fonction putative de 43 % des 34 074 transcrits a été identifiée (voir fig. 1 de Carrier et al., 2014) et une grande partie des gènes principaux du métabolisme semble avoir été identifié.

L'étude du polymorphisme génétique entre les deux souches a permis de sélectionner 8 gènes avec une forte signature de sélection allélique. Deux d'entre eux codent pour des protéines contenant un domaine « zinc finger », et qui pourraient être des facteurs de transcription. Un gène code pour un transporteur de sodium et la fonction des quatre derniers est encore inconnue. Les analyses d'expression ont permis d'identifier 291 gènes différentiellement exprimés entre les deux souches et de sélectionner 3 gènes pouvant être impliqués dans la suraccumulation lipidique de la souche S2M2. Le premier code pour un facteur de transcription potentiel et est fortement surexprimé chez la souche S2M2. Le second gène est fortement sous-exprimé chez la souche S2M2 et code pour une putative « long chain fatty acid synthase », enzyme impliquée dans l'élongation des acides gras à 14 ou 16 carbones. La sous-expression de ce gène suggère des différences de composition en acides gras entre les deux souches mais des analyses biochimiques antérieures ont cependant montré des compositions similaires (Bougaran et al., 2012). Enfin, le troisième gène est fortement sous-exprimé chez la souche S2M2 et code pour une « GDSL lipase », enzyme impliquée dans le catabolisme lipidique. La sous-expression de ce gène suggère que la baisse du catabolisme lipidique pourrait être une des causes de la suraccumulation lipidique observée chez la souche mutée S2M2. Deux autres

gènes codant des GDSL lipase ont également été identifiés dans le transcriptome mais aucune différence d'expression n'a été observée entre les deux souches. Les substrats de cette famille de protéines étant très variés, nous ne disposons d'aucune information sur les types de lipides qui pourraient être dégradés par ces trois enzymes.

Par ailleurs, différents indices suggèrent que certains facteurs de transcriptions ont été impactés dans la souche S2M2. L'identification des facteurs de transcription de *T. lutea*, l'étude de leur expression en fonction de conditions azotées, et la recherche des gènes cibles liés à l'azote permettra une meilleure connaissance des mécanismes de régulation transcriptionnelle liés au métabolisme lipidique. Ces travaux sont en cours au laboratoire et ont déjà fait l'objet d'une première publication (Thiriet-Rupert et al., 2016).

En marge des objectifs strictement liés à ce travail de thèse, cette étude a permis d'étudier le polymorphisme des deux souches et de révéler une conservation de l'amplitude de la diversité génétique au cours du programme de sélection. De manière inattendue en début de ce projet, les résultats d'analyses de polymorphismes ont permis d'avancer l'hypothèse que, comme de nombreuses haptophytes, *T. lutea* suivait un cycle de vie haplodiplophasique. Contrairement aux coccolithophores, ce cycle est vraisemblablement monomorphe car un seul morphotype cellulaire est connu à ce jour chez cette espèce. La durée de chacune des phases haploïde et diploïde, les signaux à l'origine des événements de méiose et de fécondation sont encore totalement inconnus. Des études ont été initiées lors de cette thèse pour étudier le niveau de ploïdie de cette espèce. Un protocole de coloration à l'Iodure de Propidium a été adapté à *T. lutea* et des premières analyses de ploïdie par cytométrie en flux ont été réalisées sur des cellules synchronisées par la lumière. Cependant, ces travaux préliminaires n'ont pas permis de déterminer clairement le niveau de ploïdie de *T. lutea* (**Figure 39**). De futures analyses devront être mises en œuvre pour confirmer la présence de ce cycle haplodiplophasique chez *T. lutea*.



**Figure 3 Analyse de la ploïdie chez *T. lutea*:**

Analyse cytométrique d'une population et observation au microscope à épifluorescence de *T. lutea* cultivée en batch et colorée à l'iodure de propidium. La population N correspond aux cellules haploïdes, et la population 2N à des cellules diploïdes, ou à des individus haploïdes en cours de mitose. Aucune population 4N, spécifique d'individus 2N en cours de mitose n'a été observée.

Cette étude a permis de poser les bases moléculaires de *T. lutea* qui ont permis par la suite 1) d'engager des analyses ciblées par RT-QPCR tels que les transporteurs d'azote (Voir Chapitre I), 2) d'engager des analyses protéomiques (Voir Chapitre III et IV) ; 3) d'annoter le génome de *T. lutea* qui sera prochainement séquencé. D'une manière générale, force est de constater que la quasi-totalité des 291 gènes différentiellement exprimés entre les deux souches ainsi que les 8 gènes à forte signature de sélection présentent une fonction soit inconnue, soit une fonction difficile à interpréter au regard du métabolisme du carbone et des lipides. L'annotation experte des gènes de fonction non identifiée, par recherche de motifs ou domaines protéiques, permettra d'avancer des hypothèses concernant les fonctions des gènes de *T. lutea*. Ce travail sera initié dans les chapitres suivants. Dans ce chapitre, une seule condition physiologique a été étudiée pour identifier les gènes différentiellement exprimés entre les deux souches. Etant donné la forte relation entre limitation azotée et accumulation lipidique, les chapitres suivant intégreront différentes conditions de limitation et de carence azotée pour identifier les mécanismes impliqués dans l'accumulation lipidique.



# Comparative Transcriptome of Wild Type and Selected Strains of the Microalgae *Tisochrysis lutea* Provides Insights into the Genetic Basis, Lipid Metabolism and the Life Cycle

Gregory Carrier<sup>1</sup>, Matthieu Garnier<sup>1</sup>, Loïc Le Cunff<sup>3</sup>, Gaël Bougaran<sup>1</sup>, Ian Probert<sup>2</sup>, Colombar De Vargas<sup>2</sup>, Erwan Corre<sup>4</sup>, Jean-Paul Cadoret<sup>1</sup>, Bruno Saint-Jean<sup>1\*</sup>

**1** IFREMER-PBA, Nantes, France, **2** CNRS-UPMC, UMR 7144, Station Biologique de Roscoff, Roscoff, France, **3** UMT Geno-Vigne<sup>®</sup>, Montpellier, France, **4** CNRS-UPMC, ABIMS, Station Biologique de Roscoff, Roscoff, France

## Abstract

The applied exploitation of microalgae cultures has to date almost exclusively involved the use of wild type strains, deposited over decades in dedicated culture collections. Concomitantly, the concept of improving algae with selection programs for particular specific purposes is slowly emerging. Studying since a decade an economically and ecologically important haptophyte *Tisochrysis lutea* (Tiso), we took advantage of the availability of wild type (Tiso-Wt) and selected (Tiso-S2M2) strains to conduct a molecular variations study. This endeavour presented substantial challenges: the genome assembly was not yet available, the life cycle unknown and genetic diversity of Tiso-Wt poorly documented. This study brings the first molecular data in order to set up a selection strategy for that microalgae. Following high-throughput Illumina sequencing, transcriptomes of Tiso-Wt and Tiso-S2M2 were *de novo* assembled and annotated. Genetic diversity between both strains was analyzed and revealed a clear conservation, while a comparison of transcriptomes allowed identification of polymorphisms resulting from the selection program. Of 34,374 transcripts, 291 were differentially expressed and 165 contained positional polymorphisms (SNP, Indel). We focused on lipid over-accumulation of the Tiso-S2M2 strain and 8 candidate genes were identified by combining analysis of positional polymorphism, differential expression levels, selection signature and by study of putative gene function. Moreover, genetic analysis also suggests the existence of a sexual cycle and genetic recombination in *Tisochrysis lutea*.

**Citation:** Carrier G, Garnier M, Le Cunff L, Bougaran G, Probert I, et al. (2014) Comparative Transcriptome of Wild Type and Selected Strains of the Microalgae *Tisochrysis lutea* Provides Insights into the Genetic Basis, Lipid Metabolism and the Life Cycle. PLoS ONE 9(1): e86889. doi:10.1371/journal.pone.0086889

**Editor:** María Mar Abad-Grau, University of Granada - Q1818002F, Spain

**Received:** June 18, 2013; **Accepted:** December 17, 2013; **Published:** January 29, 2014

**Copyright:** © 2014 Carrier et al. This is an open-access article distributed under the terms of the Creative Commons Attribution License, which permits unrestricted use, distribution, and reproduction in any medium, provided the original author and source are credited.

**Funding:** This work was partly funded by region of Pays de Loire "Nouvelle équipes, nouvelles thématique" program and by the Agence National de la Recherche, Facteur 4 project. There are no non-financial competing interests. The funders had no role in study design, data collection and analysis, decision to publish, or preparation of the manuscript.

**Competing Interests:** The authors have declared that no competing interests exist.

\* E-mail: Bruno.Saintjean@ifremer.fr

## Introduction

Interest in microalgae as a potential source of economic benefit is booming [1]. Applications are envisaged in very different domains such as human or animal alimentation due to their high nutritional value [2], bio-remediation such as water purification [3], and pigment production for the cosmetic industry, for food-processing or for human health [4]. In the last decade new biotechnological applications have emerged [5]. The use of microalgae as cell factories would offer numerous advantages for the production of safe and complex recombinant pharmaceutical proteins [6–8]. Recently, several research projects have focused on the use of microalgae for biofuel production [9], citing very attractive biomass and oil productivities compared to oleaginous land plants. Mass production of microalgae would not enter into competition with agricultural food production as they can be cultivated on non-arable land, saline or wastewater sources [10]. In the context of the energy crisis, certain concepts of production of biofuels from algal oils are currently at the demonstration stage.

However, the production of microalgae is currently not sufficiently economically efficient compared to the use of fossil fuels to be envisioned at a large scale [7].

Among the very large diversity of microalgae, a culture strain originally isolated from Tahiti and designated as *Isochrysis affinis galbana* but recently renamed *Tisochrysis lutea* (Tiso) [11] has been historically extensively studied due to its widespread use in aquaculture as a feedstock for shellfish and shrimps that reflects an attractive fatty acid content [12]. However, the lack of molecular data for this strain has limited investigation of aspects such as the metabolism and life cycle of this microalga. Rapid developments in Next Generation Sequencing (NGS) technologies now make it relatively easy to conduct large-scale genotyping of species for which full genome sequences are not yet available [13].

Beyond the obvious economic interest of Tiso, it is also of significant fundamental interest as a member of a microalgal lineage (the division Haptophyta) which is diverse and often ecologically dominant in the planktonic photic realm [14]. Tiso is a member of the haptophyte order Isochrysidales that comprises two families, the

Isochrysidaceae and the Noëlaerhadaceae. Members of the Noëlaerhadaceae exhibit a heteromorphic haplo-diploid life cycle in which the diploid phase produces calcified plates (coccoliths) and the haploid phase is non-calcifying [14]. The best-known member of this family is *Emiliana huxleyi*, which is by far the most abundant coccolithophore in modern oceans and consequently an extremely important actor in global carbon cycling. By contrast, isochrysidaceans such as Tiso have only one known non-calcifying morphological form. No information about sexual reproduction or ploidy levels are available for this family [16,17].

Sophisticated selection programs like those implemented in terrestrial agriculture will probably play an important role in the future exploitation of microalgal resources [18]. Domestication of plants and animals by long-term selection programs led to the rise of modern agriculture. For example, the yield of wheat culture has increased 16-fold in 1200 years through directed selection of highly productive strains [11]. By comparison, domestication of microalgae is in its infancy. Recent studies in this domain have focused, for example, on production of the pigment prodigiosin in the rhodophyte *Hahella chejuensis* [19], carotenoid production in *Dunaliella salina* [20], and lipid production in *Nannochloropsis* sp. [21] and in Tiso [22]. Until recently, all these selection programs of microalgae consisted to identify and select the best individuals among a population. To date, microalgal selection programs generally start without prior knowledge of the natural diversity of the taxon in question. A number of studies have reported high levels of intra-specific genetic or metabolic diversity in different microalgal species [23–25]. In this study, we estimated the genetic diversity in a Tiso culture strain, this being a requirement for conception of improved selection programs [18]. Life cycles of microalgae are generally poorly known and consequently breeding programs have yet to be initiated, despite several real advances in the knowledge of certain microalgal groups such as diatoms [18].

In our laboratory, a selection program was performed starting from a wild type strain of *Tisochrysis lutea* (Tiso-Wt). This wild type strain consists in one ecotype (Tahiti) and is presumed to be composed of several genotypes characterizing a population of Tiso with an unknown diversity. A sequential mutation-selection procedure was performed from this wild type strain, involving: i) UVc treatment to induce mutations and thus increase the genetic (and metabolic) diversity of the strain, and ii) selection of the 10% of cells with the highest lipid content. This resulted in selection of a new certificate strain [26] (Tiso-S2M2) that accumulates twice the amount of neutral lipids in nitrogen limited culture conditions compared to the Tiso-Wt strain [22].

In context of algae selection program, this study using RNAseq approach, brings the first molecular data for an economically and ecologically important microalgae *Tisochrysis lutea*. Here, we describe the impact of a selection program on the genetic repertoire and gene expression of a selected strain. Comparison of transcriptomes of wild type and selected strains allowed identification of positional polymorphism and differentially expression levels. Analysis of polymorphisms generated as a result of the selection program provides detailed information on the genomic-level impact of the program, and notably identification of candidate genes that could account for lipid over-accumulation, as well as providing insights into the putative life cycle of this species.

## Results

### De novo sequencing and annotation of Tiso transcriptomes

Transcriptomes of two Tiso strains, the reference strain (Tiso-Wt) and a selected strain (Tiso-S2M2), were sequenced with

Illumina HiSeq 2000 technology. Read pairs obtained for each strain were filtered and assembled into 44,983 and 44,564 transcripts for Tiso-Wt and Tiso-S2M2, respectively (Table 1). These two datasets were clustered to obtain a final consensus transcriptome of 46,687 transcripts. Of these, 34,374 were unique, representing a total length of 44.4 Mb. At least two isoforms were detected for the remaining (12,313) transcripts. The origin of these non-unique transcripts could be the sequencing of mature and non-mature RNA, alternatively spliced or the sequencing of duplicated genes [27]. The consensus transcriptome was annotated and 14,790 transcripts were associated with at least one Gene Ontology (GO) term. These transcripts with putative function were sorted according to cellular functions (Figure 1). Globally, enzymes of all major metabolic pathways such as nitrogen, photosynthesis or sugar metabolisms were represented and among those, 2,010 transcripts were assigned at least one known universal KEGG pathway (Kyoto Encyclopedia of Genes and Genomes, <http://www.genome.jp/kegg/>). Specifically, all the major enzymes of lipid metabolism were identified in the Tiso transcriptome and match in the universal KEGG lipid pathway (Figure S1). However, no putative function was identified for 57% of transcripts (19,584).

### Comparison of Tiso transcriptomes with reference microalgal transcriptomes

The consensus Tiso transcriptome was compared with transcriptomes from eight reference microalgal taxa chosen for their diverging phylogenetic position (2 chlorophytes, 2 diatoms, 1 rhodophyte, 1 glaucophyte, 1 dinoflagellate and 1 haptophyte). For each algae transcriptome, we considered only the coding transcripts known to produce a putative protein in order to avoid biases due to the existence of non-coding transcripts. The number of transcripts in each transcriptome and the number of homologous genes between Tiso and these reference microalgae are shown in Figure 2. Tiso has many more putative unique transcripts (more than 30,000) with the most closely related species in the list, *Emiliana huxleyi*, than with the other reference microalgae. Unsurprisingly, *E. huxleyi* possesses the highest proportion (25%) of genes that are homologous with those of Tiso, the proportion being less than 11% with the reference microalgae from other lineages. Finally, only 750 genes that were homologous between all of these algae were identified. The high diversity and very ancient divergence of these reference algae [28] explains this low number of homologous genes. Indeed, 66% (22,664) of Tiso genes have not homologous from these microalgae.

Codon usage bias and transcriptomic G+C content were also compared between the reference algae (Figures S2 and S3). The codon usage bias refers to differences in the frequency of occurrence of synonymous codons. Generally, the codon preference reflects a balance between mutations and natural selection for translational optimization [29]. The G+C content in coding DNA is variable between species and is known to play a role in the codon usage bias [30]. Our results indicate that the codon usage bias of Tiso is similar to that of the other haptophyte *E. huxleyi*, but also to that of the dinoflagellate *Alexandrium ostenfeldii* (Figure S3). Surprisingly, Tiso has a transcriptomic G+C content (60.2%) more similar to that of the dinoflagellate *A. ostenfeldii* (58.3%) than that of *E. huxleyi* (Figure S2).

**Impact of the selection program on the transcriptome of Tiso-S2M2.** The Tiso wild type strain is monospecific, but is presumed not to be a clonal strain but composed of several genotypes characterizing a population. During the selection program [22], diversity of Tiso-Wt was not explored. The



**Table 1.** Tiso transcriptome characteristics.

| Libraries | Read pairs, raw data | Read pairs produced with good quality | Assembly transcripts | Consensus transcripts between the libraries | Read pairs aligned on unique <i>loci</i> | Read pairs aligned on multi <i>loci</i> | Read pairs not aligned |
|-----------|----------------------|---------------------------------------|----------------------|---|--|---|------------------------|
| Wt        | 177 M                | 140 M (79.1%)                         | 44,983               | 46,687 among them                           | 100 M (71.6%)                            | 30 M (21.7%)                            | 9 M (6.7%)             |
| S2M2      | 189 M                | 156 (82.4%)                           | 44,564               | 34,374 unique                               | 115 M (73.7%)                            | 30 (19.3%)                              | 6 M (4.0%)             |

The table summarizes the different steps in building the Tiso transcriptome using RNAseq data obtained from Illumina HiSeq technology.  
doi:10.1371/journal.pone.0086889.t001

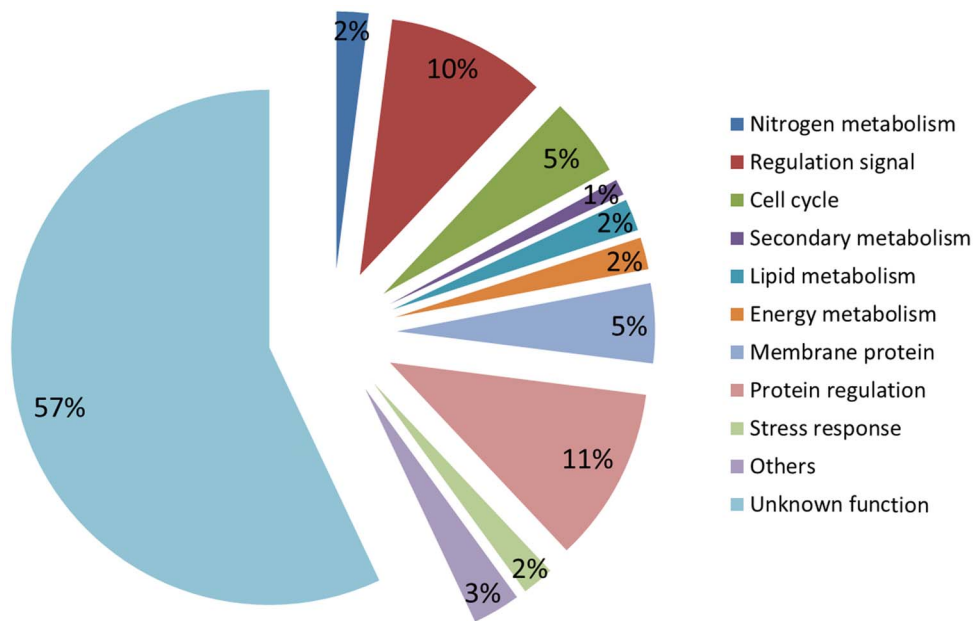
identification of transcriptome polymorphisms gives some light concerning the molecular diversity of this strain. Moreover, the selection program applied to Tiso was accomplished in closed conditions [22]. Therefore, the polymorphism observed between Tiso-Wt and Tiso-S2M2 was generated only by mutation and/or within-strain selection effects and not by allele flux from the environment. In these conditions, the impact of the selection program on the genetic diversity of Tiso-S2M2 could be studied.

We first investigated the molecular diversity in each strain at the transcriptome level and its evolution during the selection program. Polyallelic *loci* were identified and analyzed in the transcriptome of each strain (Figure 3) to estimate the molecular diversity. For SNPs, 925 and 883 biallelic *loci* were detected for Tiso-Wt and Tiso-S2M2, respectively. As for the indels, 782 and 784 biallelic *loci* were detected, respectively. These results confirm that both strains are composed of several genotypes. Allelic frequency of polymorph *loci* was compared between both strains to look for the evolution of the genetic diversity during selection program. Only transcripts without differentially expression level were considered, in each population. A Jost's D genetic index [31] was used and a score of 0.161 was estimated between both strains showing a high conservation of genetic diversity between the populations. Indeed, the majority of polyallelic *loci* detected in Tiso-Wt, i.e. 798 (86%) SNPs and 762 (97%) indels, were conserved in Tiso-S2M2. For each conserved polyallelic *locus*, the differential allelic frequency between the two strains was measured (Figure 4). On average, the differential allelic frequency per *locus* was 15.6% for SNPs and 8.5% for indels confirm a global conservation of genetic diversity at the end of the selection program. 92 SNPs and 20 indels were *loci* with a differential allele frequency greater than 35% (Figure 4), reflecting selection events during the selection program. Five transcripts containing more than five polyallelic *loci* with a differential allele frequency are of particular interest, these being considered as transcripts with a clear selection signature.

Thereafter, we focused on the positional polymorphisms and differentially expression levels generated during the selection program. For positional polymorphisms, 241 SNP and 22 indel polymorphisms were detected between the strains. SNP and indel polymorphisms were distributed among 146 and 19 transcripts, respectively (Figure S4). The large majority of these transcripts (124/165) contained only one polymorphism. However, seven hot spots of polymorphism with more than five polymorphisms in a specific region of one transcript were identified (frequency superior to 1 polymorphism per 100 bases). Among these seven hot spots, four were localized in UTR regions and three in coding regions.

Concerning differential gene expression levels, 84 transcripts were over-expressed and 207 under-expressed in Tiso-S2M2 compared to Tiso-Wt. Of these, 32 had a high expression difference (>100 fold) and 18 transcripts showed a specific expression in only one strain (Table S1). More precisely, eleven transcripts were specifically expressed in Tiso-S2M2 and seven transcripts were specific to Tiso-Wt. These results show that expression of some genes was clearly affected as a result of the selection program.

**Origin of polymorphisms.** The origin of polymorphisms (mutation or selection events) was identified to evaluate the evolution strength producing from the selection program. The selection program was conducted in closed conditions and consequently the 241 SNP and 22 indel polymorphisms between the strains could be sorted into different classes (Table 2). Class 1 comprises the polymorphisms for which there was one allele in Tiso-Wt and two alleles in Tiso-S2M2 (Figure 3). This class refers to polymorphisms generated by mutation events occurring during



**Figure 1. Annotation of Tiso transcriptome.** Transcripts were annotated by BLAST in the NCBI nr database. Transcripts were sorted among identified major cell functions from Gene Ontology.  
doi:10.1371/journal.pone.0086889.g001

the selection program (85 SNPs and 12 indels; Table 2). Class 2 comprises polymorphisms for which there were two alleles in Tiso-Wt, only one of which was conserved in Tiso-S2M2 (Figure 3). This implies a loss of one allele by selection pressure (126 SNPs and 10 indels; Table 2). Finally, class 3 comprises polymorphisms for which there was one allele in Tiso-Wt and a different allele in Tiso-S2M2 (Figure 3). This refers to polymorphisms appearing as a result of mutation followed by selection (30 SNPs and 0 indels; Table 2).

**Annotation and selection of candidate genes for lipid over-accumulation.** Transcripts with position polymorphism or differentially expressed between Tiso-Wt and Tiso-S2M2 were manually annotated and sorted according to metabolic pathways (Figure 5). A large number of differentially expressed transcripts involved in stress responses, protein signal regulation and membrane proteins (transporters and structural proteins) were identified. Few genes were classed as being involved in energy, lipid or nitrogen metabolism.

The selected strain Tiso-S2M2 is characterized by an over-accumulation of lipids in nitrogen-limited culture conditions and we focused on this aspect. Candidate genes were identified by a combined analysis of polymorphism between the strains. Firstly, transcripts with a selection signature generated by the impact of the selection program could be interesting candidates. Among positional polymorphisms, three hot spots located in coding regions of *TisoTranscripts-291*, *TisoTranscripts-227* and *TisoTranscripts-46* were detected (21, 7 and 6 SNPs were identified for each transcripts respectively). These hot spots contain polymorphisms only produced by selection effects and consequently are considered as transcripts with a selection signature. Moreover, some polymorphisms (12, 3 and 1 for *TisoTranscripts-291*, *TisoTranscripts-227* and *TisoTranscripts-46* respectively) were non synonymous and could induce a change of protein activities. Annotation of these candidate genes revealed a putative Na<sup>+</sup> solute transporter (*TisoTranscripts-291*) and two proteins with zinc finger domains (*TisoTranscripts-227* and *TisoTranscripts-46*). One homologous gene of *TisoTranscripts-291* was exclusively identified in *E. huxleyi* (*Emihu-*

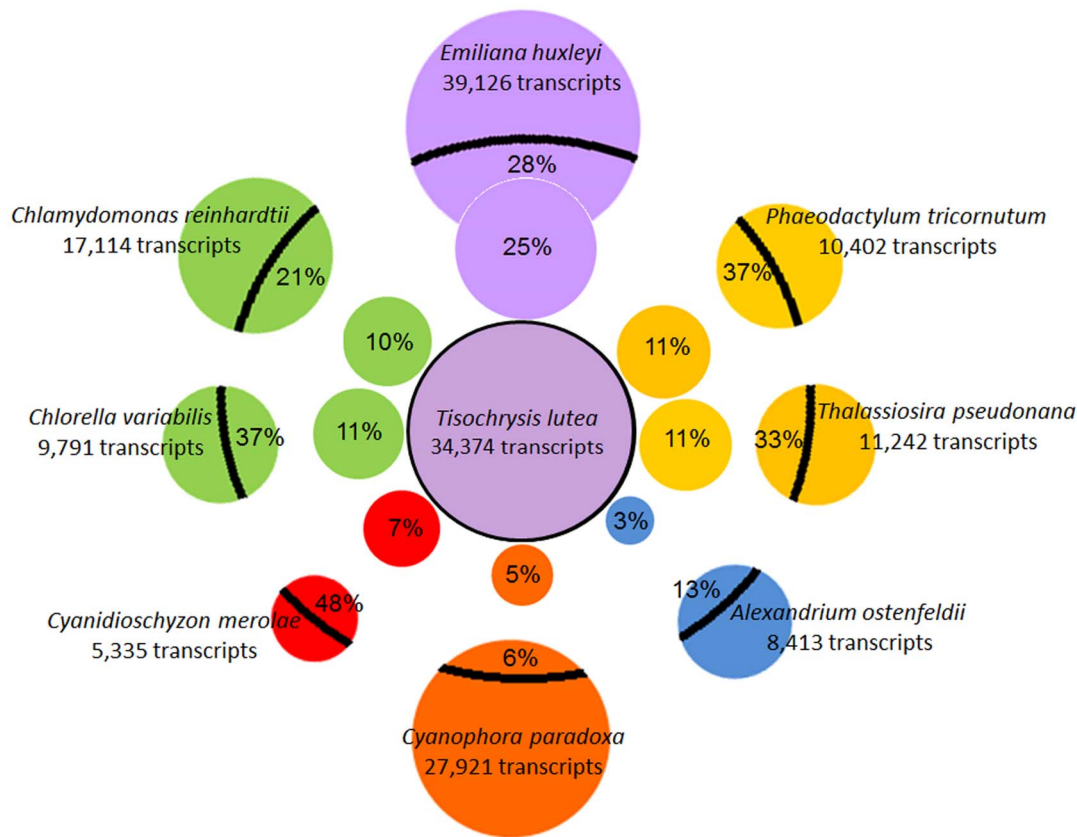
*233786*) suggesting a haptophyte specific gene. Five transcripts with hot spots of *loci* with differential allelic frequency were also detected (*TisoTranscripts-440*, *TisoTranscripts-441*, *TisoTranscripts-442*, *TisoTranscripts-443* and *TisoTranscripts-444*), but no function was found for these candidate genes bearing a selection signature.

In the same ecophysiological conditions, a total of 298 transcripts were differentially expressed between the two strains. Gene expression was therefore clearly affected by the selection program and this could explain lipid over-accumulation in Tiso-S2M2. A total of 18 transcripts were expressed specifically in only one strain (Table S1) and these were considered as promising candidate genes for further studies. The putative annotation of only three of these genes was possible. *TisoTranscripts-9* was positively assigned as a putative transcription factor, *TisoTranscripts-57* as an ankyrin protein-like and *TisoTranscripts-59* a Glycosyl-Phosphatidylinositol protein-like (GPI protein). No homologous genes of these candidates were identified in reference microalgae suggesting that these candidates are specific to Tiso.

Because the selected Tiso-S2M2 strain is characterized by lipid over-accumulation, the transcripts with a putative function linked to lipid metabolism and with positional polymorphism or differential gene expression were considered as good candidates. *TisoTranscripts-288* and *TisoTranscripts-160*, annotated as a long chain fatty acid ligase and a GDSL lipase respectively, showed differential expression (under expressed 53- and 24-fold in TisoS2M2, respectively). Their respective expression was confirmed by a RT-qPCR experiment (Data S1) and we consider them as excellent candidates for future studies. Moreover, homologous gene of *TisoTranscripts-288* was identified in *E. huxleyi* (*Emihu-456684*), *P. tricornutum* (*Phatr-45510*) and *C. merolae* (*CMG-147C*). However, *TisoTranscripts-160* was only one homologous identified in *E. huxleyi* (*Emihu-213608*).

## Discussion

The haptophyte *Isochrysis affinis galbana* is a species of major economic importance in aquaculture with good potential for biofuel

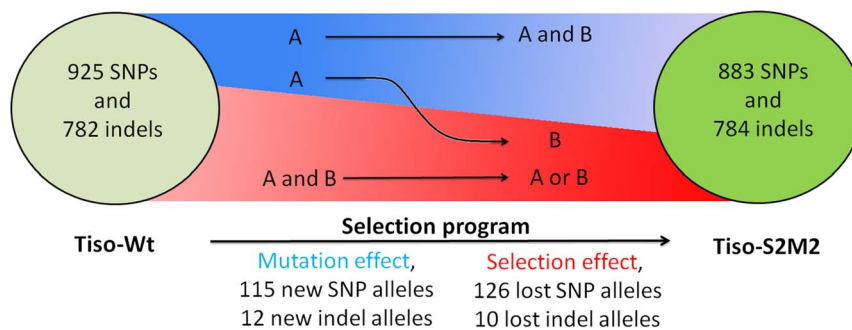


**Figure 2. Comparative analysis of consensus Tiso transcriptome with those of reference microalgae.** The size of circles represents transcript number. Color coding: green circle for chlorophytes, red for rhodophyte, orange for glaucophyte, blue for dinoflagellate, yellow for diatoms and purple for haptophyte. The number in each peripheral circles show proportion (%) homologous genes with Tiso. The number in each inner circles show proportion (%) homologous genes with reference microalgae. doi:10.1371/journal.pone.0086889.g002

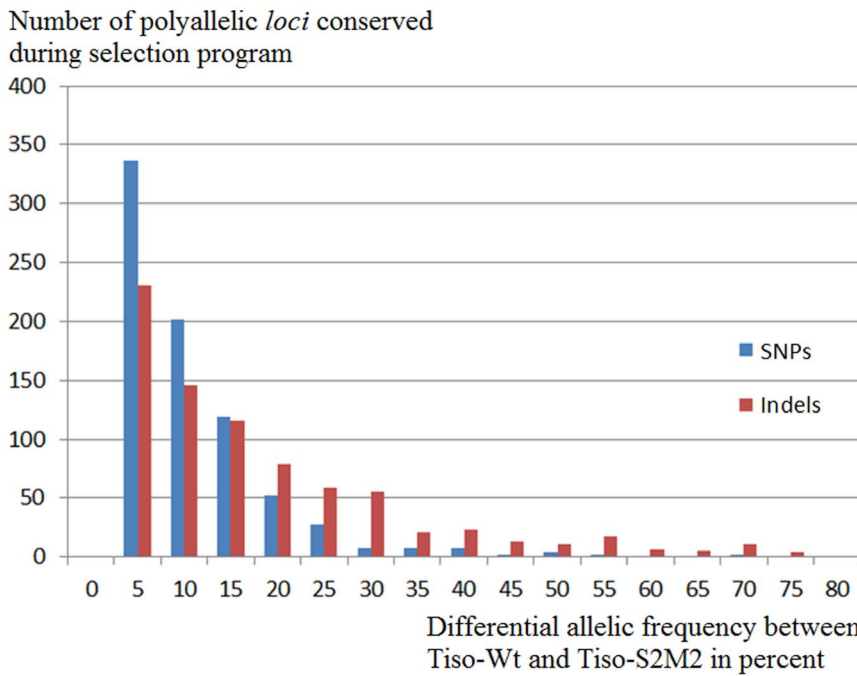
production [12]. A laboratory selection program was developed and a strain obtained (Tiso-S2M2) that accumulates more lipid in nitrogen-limiting conditions than the wild type [22]. Molecular evolution of Tiso-Wt resulting from the selection program was studied and this allowed us to establish a list of candidate genes that could play a role in lipid over-accumulation. Moreover, fine-scale analysis of the transcriptomes of the wild type and selected strains provides new insights concerning the life cycle of Tiso.

### First molecular knowledge of Tiso

In this study, transcriptomic data was produced for Tiso for the first time using high-throughput sequencing. The transcriptomes were annotated and all major metabolic pathways were identified. Annotation of these major pathways is usually relatively easy because they contain highly conserved protein domains [32]. However, no putative function was found for 57% of transcripts. To date, the number of genes with known function is very low for



**Figure 3. Impact of the selection program on the Tiso transcriptome.** This figure is a schematic representation of the selection program. The number in each circle represents genetic diversity for each strain. Between these circles, evolutionary origins of polymorphisms between strains are illustrated: in red, polymorphism generated by loss of alleles (selection events), the narrower of area represent a reduction of diversity; in blue, new alleles (mutation events) the top of the area represents an increase of diversity; the arrow from blue to red, new and selected alleles (mutation and selection events). doi:10.1371/journal.pone.0086889.g003



**Figure 4. Distribution of differential allelic frequency between Tiso-Wt and Tiso-S2M2.** This histogram represents the number of polymorph loci (SNP and indel) following their conservation rate through the selection program. Conservation rate defined as percent represents the differential allelic frequency between Tiso-Wt and Tiso-S2M2. doi:10.1371/journal.pone.0086889.g004

microalgae and the high diversity of microalgae makes annotation difficult [14].

The consensus transcriptome of Tiso was compared with eight other transcriptomes from reference microalgae. These microalgae were chosen because of their phylogenetic position and the availability of transcriptomic data. We compared the total number of transcripts and homologous genes, the transcriptomic G+C content and the codon usage bias. In general and as expected, these results confirmed that Tiso is genetically very closely related to *Emiliania huxleyi*, which is a member of the same haptophyte order, the Isochrysidales. Surprisingly, the codon usage bias and transcriptomic G+C content of Tiso were more similar to those of the dinoflagellate *Alexandrium ostenfeldii* than to those of *E. huxleyi*. Although these characteristics are not significant in an evolutionary sense, they reflect a high level of genomic speciation since the divergence between Tiso and *E. huxleyi*, estimated around 120 Mya [33,34].

**Table 2. Genotype class of polymorphic loci between wild type Tiso-Wt and selected Tiso-S2M2.**

| Class | Tiso-Wt   | Tiso-S2M2       | Polymorphism number |
|-------|-----------|-----------------|---------------------|
| 1     | Locus A   | => Locus A/B    | 85 SNPs             |
| 2     | Locus A/B | => Locus A or B | 126 SNPs            |
| 3     | Locus A   | => Locus B      | 30 SNPs             |

Class 1 shows polymorphisms generated by a mutation event. Wild allele (A) and mutated allele (B) were observed in Tiso-S2M2. Class 2 shows polymorphisms generated by selection events only. Only one allele, (A) or (B) was observed in Tiso-S2M2 strain, whereas the two alleles were found in Tiso-Wt strain. Class 3 shows polymorphisms generated by both mutation and selection events. Only the allele (B) was detected in Tiso-S2M2. doi:10.1371/journal.pone.0086889.t002

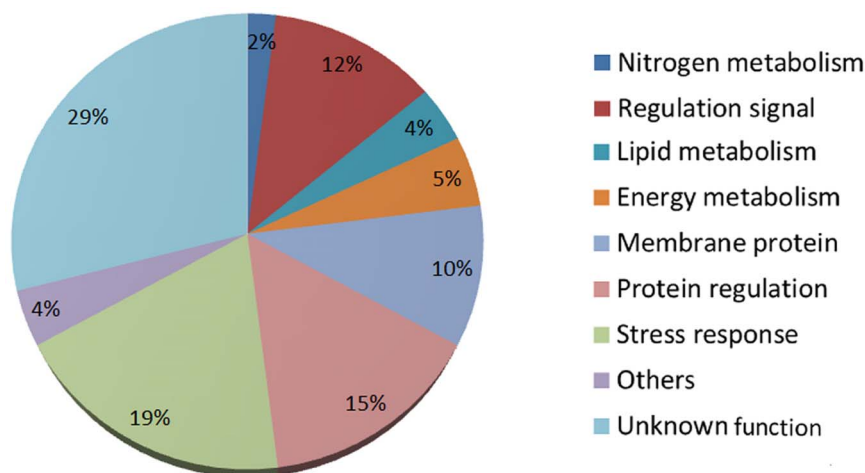
### Transcriptome evolution as a result of the selection program

The lipid over-accumulating selected strain Tiso-S2M2 was obtained from the wild type strain by a selection program [22]. This selection program consisted of increasing the genetic diversity by UVc exposition followed by selection of lipid-rich cells by flow cytometry.

In this study, we measured and analyzed the molecular modifications produced by the selection program on the population of Tiso-Wt at transcriptome level. These results could help to refine future selection programs. To measure the impact of this selection program, the genetic diversity of Tiso-Wt and Tiso-S2M2 was evaluated and compared at the transcriptome level. Polyallelic loci identified for both strains confirm the non-clonal character of Tiso-Wt and Tiso-S2M2. Interestingly, polyallelic loci detected in Tiso-Wt were mostly conserved in Tiso-S2M2 and their allele frequency did not change significantly after the selection program.

RNAseq strategy allowed us to analyze the gene expression and the positional polymorphism. Differential gene expression level observed for almost any cell functions reveals important modifications in all metabolism pathways. Studies of the inter-genic regions and the large polymorph insertions (requiring genome sequencing approaches) are underway. In turn, positional polymorphisms on coding region were observed between both strains. Among these polymorphisms, SNP mutations were more frequently detected than indels (i.e: 242 SNPs and 22 indels). This could be explained by a stronger selection pressure on indels than SNPs. Indeed, it is known that indel polymorphism has a stronger impact on phenotype because indel mutations are more harmful [35].

The selection program was undertaken in non-clonal strain in closed conditions and consequently the polymorphism observed between the strains was generated only by mutation or selection



**Figure 5. Expert annotations of transcripts containing polymorphisms or differential gene expression between Tiso-Wt and Tiso-S2M2.** Transcripts were sorted according to major cell function. doi:10.1371/journal.pone.0086889.g005

[22]. We sorted polymorphisms (Figure 3) according to whether they were: (i) new alleles generated by mutation events (class 1 and class 3, Table 2); (ii) loss of alleles in Tiso-S2M2 by a selection effect (class 2, Table 2). It is noteworthy that the numbers of new and lost alleles were approximately equal. This suggests that mutation and selection strengths were balanced [36,37]. The selection program was thus characterized by maintenance of genetic diversity [38], which has the theoretical advantage of producing a strain with higher capacity to adapt to environmental variability compared to a clonal strain [39]. The lipid over-accumulating phenotype in Tiso-S2M2 has been conserved in the absence of selective pressure about lipid contents for more than two years [22]. This could be explained by the selected trait being more easily maintained in a population with high genetic diversity [40,41].

The clonal diversity of Tiso-S2M2 will be used in a next program to further select lipid accumulating Tiso strains. Two selection strategies will be investigated: One will be to select the best clone for lipid content from the Tiso-S2M2 population. However, conservation of clonal strains is usually risky on a long term basis and cryopreservation could be the solution [42]. Another selection strategy could call for a different mutagenesis methods and higher selection pressure.

#### List of candidate genes for lipid over-accumulation in the selected Tiso strain (Tiso-S2M2)

The selection program modified globally all cell functions (Figure 5). The selection of lipid trait generated large modifications in cells. These large modifications could be explained by selection program not affecting only lipid trait but, for example, selection of cells with UVc tolerance. Furthermore, the lipid metabolism is in relationship with all other metabolisms and a weak modification can affect entire cells. We focused on the lipid metabolism as biofuel production by microalgae is considered as one of the most promising sources for future energy production [9]. Identification of genes or alleles that play roles in lipid over-accumulation could be of great interest for future selection and metabolic engineering programs. A combined approach was used to produce a list of candidate genes that included: (i) transcripts with a selection signature; (ii) transcripts with specific expression in only one of the strains; (iii) transcripts with a putative function in lipid metabolism and with a positional polymorphism or differential gene expression.

In this study, eight transcripts with a clear selection signature were detected. Of these, only three could be annotated. Two of these genes (*TisoTranscripts-227* and *TisoTranscripts-46*) encode proteins with zinc finger domains which are known to play an important role in the regulation of gene expression [43]. The target genes of these two candidates are not currently known, but their selection signatures imply a role in increasing the fitness of Tiso-S2M2 in terms of lipid accumulation or UVc tolerance. No homologous genes were identified in reference microalgae suggesting a specific regulation of Tiso. According to the annotation, the third transcript (*TisoTranscripts-291*) is a Na<sup>+</sup> solute transporter-like. The most closely related protein domain that we could identify is the SLC5 family [44]. This family of co-transporters is known to exchange Na<sup>+</sup> solutes with different substrates such as glucose, urea or amino acids [45]. Allele selection of this gene could allow Tiso-S2M2 to optimize the transport of a molecule involved in the resistance to the selection program. A functional study of these genes would be of great interest to understand their role in the Tiso-S2M2 phenotype and specifically in lipid metabolism.

Gene expression was affected by the selection program. Of the 34,374 transcripts of Tiso, 291 exhibited differential expression between the strains. This differential gene expression could have several origins, such as mutations in regulation regions or epigenetic variations. Of these transcripts, 18 were specifically expressed in Tiso-Wt or Tiso-S2M2. With the highest differential expression, these are considered as serious candidates to explain the selection result. Other genes with differential expression could also be good candidates, but their differential expression need to be confirmed by a qRT-PCR approach [46]. Among the 18 main differentially expressed candidates, a putative function was found for only three genes. These candidates as well have no homologous genes in reference microalgae. *TisoTranscripts-9* encodes a putative transcription factor. Differential expression of this type of gene is known to modify expression of target genes and thus metabolic pathways. *TisoTranscripts-57* codes for an ankyrin protein-like. The ankyrin domain is considered to be the most common location for protein-protein interactions [47] and can play a role in several cellular functions. *TisoTranscripts-59* was identified as a GPI protein-like, a category of proteins known for their roles in communication between cells [48]. Given their putative functions, a potential implication of these latter two genes in the lipid over-

accumulation observed in Tiso-S2M2 is not obvious, but they should be kept in mind for further studies.

The targeted phenotypic character of the selected strain is lipid over-accumulation and we therefore focused on the annotated genes of lipid pathways. Transcripts with putative annotation linked to lipid metabolism and containing a positional polymorphism or differential expression level were selected. Two candidate genes were identified (*TisoTranscripts-288* and *TisoTranscripts-160*) with differential expression between the strains. These published results rely on RNAseq dataset and because the implementation of this technique is however rather new, we confirmed the results using the well-established RT-qPCR technique (data S1) in a biological replicates. *TisoTranscripts-288* was identified as encoding a putative long chain fatty acid ligase (ACLS, EC: 6.2.1.3). This enzyme family is known to esterify free fatty acids containing C14/C20 carbon chains into fatty acyl-coenzyme A (acyl-CoA) [49,50]. Esterification into fatty acyl-CoA is a key step in numerous lipid metabolism pathways, in particular those involved in lipid catabolism. Analysis of the Tiso transcriptome revealed that *TisoTranscripts-288* was the only transcript annotated as coding for ACLS proteins. Consequently, the under-expression of this enzyme in Tiso-S2M2 may suggest a defect in lipid catabolism causing the lipid over-accumulation phenotype. Functional study of this enzyme is under way and will allow testing this hypothesis. The other candidate gene (*TisoTranscripts-160*) is assigned as a putative GDSL lipase. This family is composed of hydrolytic enzymes with multifunctional properties such as broad substrate and region specificities [51]. Two other GDSL lipase transcripts were identified in the Tiso transcriptome, but these were not differentially expressed. Functional study of the under-expressed GDSL lipase is also required to determine whether it is implicated in lipid catabolism. Surprisingly, the expression of known and identified genes involved in either fatty acid or triacylglycerol biosynthesis was similar between the two strains. In contrast, these candidate genes (*TisoTranscripts-288* and *TisoTranscripts-160*) showed the catabolic pathway related to fatty acid oxidation and hydrolytic lipase activity appears to have been affected.

### Insights into the life cycle of Tiso

Many haptophytes, including *Emiliania huxleyi*, are known to undergo dimorphic haplo-diplontic life cycles, in which both haploid and diploid phases are capable of independent asexual division [15]. Ploidy level and sexual stages have never been reported for Tiso, or for any other member of the Isochrysidaceae. In culture, isochrysidaceans have a single non-calcifying morphotype that resembles the haploid phase of noelhaerhabdaceans (i.e. non-calcifying, usually flagellate). Diploid phase calcification is thought to have evolved only once at the origin of coccolithophores, and was thus apparently lost early in the evolutionary history of the Isochrysidaceae [52]. It is not clear whether this reflects a complete loss, or reduction, of the diploid phase in these species (i.e. clonal or haplontic life cycle, respectively), or whether they undergo a haplo-diplontic life cycle like other haptophytes, but with isomorphic non-calcifying haploid and diploid stages.

Knowledge of ploidy level is the basis for the understanding of genetics of species [53] and knowledge of the life cycle of this microalga could allow addition of breeding steps during the selection program [18]. This type of information would enable, for example, the study of heritability, gene functions or regulation, and allele interactions. Study of the evolution of genetic diversity resulting from the selection program and observation of evolutionary origin for positional polymorphisms provides insights into the life cycle of Tiso in laboratory conditions.

Selection events typically generate a loss of genetic diversity in populations [54]. Numerous (136) alleles present in Tiso-Wt were selected in Tiso-S2M2 (class 2, Table 2) and several (30) new alleles that appeared as a result of mutation were also selected in Tiso-S2M2 (class 3, Table 2). The majority of genetic diversity observed in Tiso-Wt was conserved in Tiso-S2M2. The conservation of the observed diversity despite the selection strength necessarily suggests allelic recombination during the selection program. We suggest that this allelic recombination implies a sexual step during our selection program. In other microalgae, such as diatoms [55], sexual reproduction has also been observed in response to particular environmental conditions [56,57]. Observation and physiological conditions of the fertilization step in Tiso will be confirmed in future studies.

Evolutionary origins of positional polymorphisms were analyzed to determine the ploidy of Tiso. Polymorphisms were sorted into three classes (Table 2). Because we observed multiallelic *loci* in both strains, the first proposed hypothesis is that Tiso is diploid. In this case, class 1 and class 2 polymorphisms (Table 2) could be explained by a mutation event on one allele (class 1) or selection events which had selected one of the two alleles in Tiso-Wt (class 2). However, for the third class, the origin of polymorphisms is, in this case, difficult to explain. The first possibility is a mutation event on each allele at the same *locus* and selection of both mutations in TisoS2M2. The probability of a mutation impacting the two alleles at the same *locus* is near null ( $P = 1/(\text{number of nucleotides in genome})^2$ ). Consequently, this hypothesis is not conceivable. A second possibility is that a mutation appears on one allele and this individual undergoes self-fertilization. A part of this progeny is homozygote for the new allele and can be selected. However, in this case a high loss of genetic diversity in Tiso-S2M2 would be expected, which was not the case. These considerations lead us to suggest that Tiso is not diploid during the major stage of its life cycle, but rather that the Tiso-Wt and Tiso-S2M2 strains are composed of haploid cells. This latter hypothesis is attractive because it can explain the presence of polymorphisms in the third class by one mutation and one selection event.

The Tiso strains appear thus to be haploid in our culture conditions and capable of sexual reproduction, which means they either have a haplontic or a haplo-diplontic life cycle. Isolation and crossing of clonal haploid cultures could therefore be feasible in the context of development of a breeding program.

### Conclusion

This study brings molecular basis of *Tisochrysis lutea* in a perspective of intensive selection program but complementary studies such as genome sequencing project or large study of genetic diversity will be conducting. Here, we added value to a previous program by analyzing at the genetic level the events provoked by the mutation/selection procedure. This analysis shows that balanced selection led to production of a strain that over-accumulates lipids. A comparative analysis of polymorphisms in the strains allowed identification of 8 genes that are candidates for involvement in provoking this phenotypic difference. These are promising targets for functional studies in the perspective of developing marker-assisted selection and genetic engineering protocols.

### Materials and Methods

#### Microalgae strains and culture conditions

*Isochrysis affinis galbana* recently renamed *Tisochrysis lutea* clone Tahiti (Tiso) [11] was provided by the Culture Centre of Algae

and Protozoa (CCAP 926/14). This Tiso wild type strain is monospecific and was isolated by Haines in the late 70s and kept in algae bank until today. Tiso wild type strain has been used in the selection program previously realized in our laboratory [22] and is considered as the reference strain in this study (Tiso-Wt). The selection program allowed to acquire a new strain (Tiso-S2M2) with higher lipid content than Tiso-Wt in nitrogen starved conditions [22]. This selected strain was certificate (IFR 32B85, [26]). Strains were grown in 2 L flasks containing modified Conway medium [57] with a modified nitrate concentration of 0.12 mM and bubbled with 0.22  $\mu\text{m}$  filtered-air. Cultures were maintained at a constant temperature of 21°C and under constant irradiance of 100  $\mu\text{mol m}^{-2} \text{s}^{-1}$ . The harvesting of microalgae was undertaken at the same time of day for both strains at the onset of nitrogen starvation when Tiso-S2M2 over-accumulated more lipids than Tiso-Wt (Figure S5).

### RNA extraction, cDNA library construction and sequencing

Total RNA was extracted from each strain (Tiso-Wt and Tiso-S2M2) using the TRIZOL reagent (Invitrogen, USA) according to the manufacturer's instructions. DNase treatment (DNase RQ1, Promega) was used to remove residual genomic DNA. The quality and quantity of purified total RNA were determined by measurement of absorbance (260 nm/280 nm) using a Nanodrop ND-1000 spectrophotometer (LabTech, USA). Poly(A) mRNA was isolated from total RNA using oligo(dT) magnetic beads (MicroPoly(A)Purist™ Kit, Ambion) according to the manufacturer's instructions. The first and second-strand cDNA synthesis was performed on purified mRNA using the SuperScript Double-Stranded cDNA Synthesis Kit (Invitrogen, USA) according to the manufacturer's protocol. The two cDNA libraries were constructed and sequenced with an Illumina HiSeq 2000 sequencer (Illumina Corporation Inc.). Approximately 4–5  $\mu\text{g}$  of cDNA were used for library construction, undertaken by the Genoscope platform (<http://www.genoscope.cns.fr>). Sequencing was performed using the paired-ends method with a read length of 100 bases, producing an average of 183 Million of read pairs per transcriptome. Read pairs obtained were analyzed with FastQC software developed by S. Andrews in the Babraham Institute ([www.bioinformatics.bbsrc.ac.uk](http://www.bioinformatics.bbsrc.ac.uk)) in order to validate run qualities (read number, quality score of nucleotide sequenced in Q-phred scale [58], composition of reads). We sequenced 35 and 37 Gb for Tiso-Wt and Tiso-S2M2 cDNA libraries respectively (Table 1) with a mean sequencing quality score per read at Q35. Sequence data for this article have been deposited in the National Center for Biotechnology Information and are accessible in: SRR823264 for Tiso-S2M2 and SRR824147 for Tiso-Wt.

### Construction of the reference transcriptome for Tiso

Read pairs obtained for each sample were filtered to select only read pairs with the correct quality to be assembled. First, reads containing Illumina sequencing adapter and Illumina control sequences were eliminated with CutAdapt software [59]. In a second step, reads were filtered on a quality score of the last nucleotides for each read because quality of sequencing decreases proportionally with read length [60,61]. The last nucleotides were eliminated until detection of a nucleotide with a quality score of Q25. In a third step, reads were filtered on their length. Reads inferior to 75 bp were eliminated. In a final step, reads were filtered on a mean quality score of all nucleotides. Reads with a quality score inferior to Q25 were eliminated. After these different screens, 79.1% and 82.4% total read pairs for Tiso-Wt and Tiso-S2M2 respectively were conserved (Table 1).

Read pairs of each library were assembled with the Trinity pipeline [62] with the parameters advised by Zhao Q-Y *et al.*, [63]. The putative transcripts assembled for each library were clustered with CD-hit-EST software with 90% identity [64] to obtain the consensus transcripts considered as the reference transcriptome of Tiso (Table 1). Transcriptome datasets of each strain (Tiso-Wt and Tiso-S2M2) were aligned using the reference transcriptome with MosaikAssembler software (Wan-Ping Lee and Michael Strömberg, Marth lab). On average, 72.7% ( $\sigma = 1.4$ ) read pairs were aligned on unique *locus*, 20.5% ( $\sigma = 1.6$ ) aligned on multiple *loci* and 5.4% ( $\sigma = 1.9$ ) were not aligned (Table 1). Transcripts composed at 90% of reads aligned in multiple *loci* were considered as genes with 2 or more isoforms.

### Research of homologous genes from several reference microalgae and comparison of codon bias

Transcriptome data from Tiso were compared with data from 8 other reference microalgae. Data for 5 of these (the haptophyte *Emiliana huxleyi* [65], the diatoms *Phaeodactylum tricoratum* [66] and *Thalassiosira pseudonana* [67], the chlorophytes *Chlorella variabilis* [68] and *Chlamydomonas reinhardtii* [69]) were produced by the US Department of Energy Joint Genome Institute (JGI <http://www.jgi.doe.gov/>) and are publically available in the web site. The other reference microalga used were the dinoflagellate *Alexandrium ostenfeldii* [70], the glaucophyte *Cyanophora paradoxa* [71] and the rhodophyte *Cyanidioschyzon merolae* [72]. Homologous transcripts were detected by BLAST analysis [73] between the transcriptome data of reference microalgae and Tiso (tblastx with alignment length greater than 100 amino acids and identity score greater than 30%). Codon usage bias was calculated with the Sequence Manipulation Suite software [74] on coding regions of each reference taxon. For Tiso, the putative coding regions of each transcript were identified with ORF-predictor [75]. A similarity tree of codon bias was built from correlation scores obtained between microalgae and drawn with the Darwin software (<http://darwin.cirad.fr/>) using the hierarchical clustering method WPGMA [76].

### Annotation of Tiso transcriptome

Research of putative function was undertaken by BLAST analysis [73] on the NCBI database (nr bank; blastx with alignment length greater than 100 amino acids and identity score greater than 30%). Transcripts were sorted automatically for major cell functions. For the transcripts showing a polymorphism between Tiso-Wt and Tiso-S2M2, expert annotation was done. A second BLAST on SwissProt database (v. May2012) and functional domain was performed with InterProScan [77]. Consensus of annotation results was manually attributed for putative function for each transcript.

### Differential expression analysis

After read alignment for each strain on the reference transcriptome, to search differential expression we normalized the libraries themselves as a function of mean depth per putative transcript (324 $\times$  for Tiso-Wt and 389 $\times$  for Tiso-S2M2). The number of read pairs aligned per transcript was compared between strains. Differential expression was considered if the difference between the 2 strains was up to 20-fold (log2) and if for both the depth was superior to 50 reads. Differential expressions were also confirmed with the recent GFOLD algorithm [78] with the p-value fixed at 0.001.

### Positional polymorphism identification and estimation of genetic diversity

Positional polymorphisms, i.e. Single Nucleotide Polymorphism (SNP) and short insertion/deletions (indel), were identified between transcripts of Tiso-Wt and Tiso-S2M2. We used Freebayes software (Erik Garrison, Marth lab) and validated polymorphisms if depth was superior to 50× for each individual and if a minority of alleles had a depth superior to 10×.

Genetic diversity was measured for each strain (Tiso-Wt and Tiso-S2M2). Polyallelic *loci* were detected in transcriptomes of each strain. A *locus* was considered polyallelic if the depth of reads was greater than 50×. For each polyallelic *locus*, frequency of each allele was measured (number of alleles divided by sum of total alleles). Comparison of global genetic diversity between the both strains was estimated with D of Jost [31] using SPADE program [79].

Sequence data for this article have been deposited in the National Center for Biotechnology Information and are accessible in: SRR823264 for Tiso-S2M2 and SRR824147 for Tiso-Wt.

### Supporting Information

#### Data S1 Methods and results of RT-qPCR approach for the candidates *TisoTranscripts-288* and *TisoTranscripts-160*.

(DOC)

**Figure S1 Enzymes of lipid pathways identified in universal KEGG.** Each enzyme with a colour corresponds to a transcript annotated in KEGG. Figure A corresponds at lipid synthesis and Figure B catabolism of lipid.

(TIF)

**Figure S2 Comparison of G+C content in transcriptomes of Tiso and reference microalgae.** Colour code: green for chlorophytes, red for rhodophyte, orange for glaucophyte, blue for dinoflagellate, yellow for diatoms and purple for haptophytes.

(TIF)

### References

- Spolaore P, Joannis-Cassan C, Duran E, Isambert A (2006) Commercial applications of microalgae. *Journal of Bioscience and Bioengineering* 101: 87–96. doi:10.1263/jbb.101.87.
- Sili C, Torzillo G, Vonshak A (2012) *Arthrospira* (Spirulina). In: Whitton BA, editor. *Ecology of Cyanobacteria II*. Springer Netherlands, pp. 677–705.
- Gong N, Shao K, Feng W, Lin Z, Liang C, et al. (2011) Biototoxicity of nickel oxide nanoparticles and bio-remediation by microalgae *Chlorella vulgaris*. *Chemosphere* 83: 510–516. doi:10.1016/j.chemosphere.2010.12.059.
- Campo JAD, García-González M, Guerrero MG (2007) Outdoor cultivation of microalgae for carotenoid production: current state and perspectives. *Appl Microbiol Biotechnol* 74: 1163–1174. doi:10.1007/s00253-007-0844-9.
- Cadoret J-P, Garnier M, Saint-Jean B (2012) Chapter Eight - Microalgae, Functional Genomics and Biotechnology. In: Gwenaél Piganeau, editor. *Advances in Botanical Research*. Academic Press, Vol. Volume 64, pp. 285–341. Available: <http://www.sciencedirect.com/science/article/pii/B9780123914996000086>.
- Saei A, Ghanbari P, Barzegari A (2012) Haematococcus as a promising cell factory to produce recombinant pharmaceutical proteins. *Mol Biol Rep* 39: 9931–9939. doi:10.1007/s11033-012-1861-z.
- Cadoret J-P, Bernard O (2008) Lipid biofuel production with microalgae: potential and challenges. *Journal de la Société de Biologie* 202: 201–211. doi:10.1051/jbio:2008022.
- Cadoret J-P, Bardor M, Lerouge P, Cabiglieri M, Henriques V, et al. (2008) Les microalgues : Usines cellulaires productrices de molécules commerciales recombinantes. *Medecine Science* 24: 375–382.
- Wijffels RH, Barbosa MJ (2010) An Outlook on Microalgal Biofuels. *Science* 329: 796–799.
- Larkum AWD, Ross IL, Kruse O, Hankamer B (2012) Selection, breeding and engineering of microalgae for bioenergy and biofuel production. *Trends in Biotechnology* 30: 198–205. doi:10.1016/j.tubtech.2011.11.003.

**Figure S3 Codon bias analysis.** Figure 3A shows codon bias of Tiso and 3B shows comparison of codon bias between reference microalgae. The tree was built using a correlation score matrix of codon bias between microalgae with the hierarchical clustering method WPGMA. Color code: green for chlorophytes, red for rhodophyte, orange for glaucophyte, blue for dinoflagellate, yellow for diatoms and purple for haptophytes.

(TIF)

**Figure S4 Distribution of positional polymorphisms (SNPs and indels) between Tiso-Wt and Tiso-S2M2 per transcripts.**

(TIF)

**Figure S5 Growth of Tiso strains and lipid accumulation.** Cells were counted with a Malassez counting cell and image analysis (SAMBA software). Lipid accumulation was estimated by measurement of Nile Red fluorescence by spectrofluorimetry as described by Bougaran *et al.*, [22]. Red color for Tiso-Wt and black color for Tiso-S2M2. The yellow color shows sampling events.

(TIF)

**Table S1 List of transcripts contained polymorphism identified between Tiso-Wt and Tiso-S2M2.**

(XLSX)

### Acknowledgments

Christophe Caron from the ABiMS platform and Laure Quintric from IFREMER-Caparmor platform for the bioinformatic server maintenance. We acknowledge the Genoscope platform for the sequencing.

### Author Contributions

Conceived and designed the experiments: JPC MG GC GB BSJ. Performed the experiments: GC MG BSJ. Analyzed the data: GC. Contributed reagents/materials/analysis tools: EC IP CDV LLC. Wrote the paper: GC MG BSJ JPC LLC EC IP.



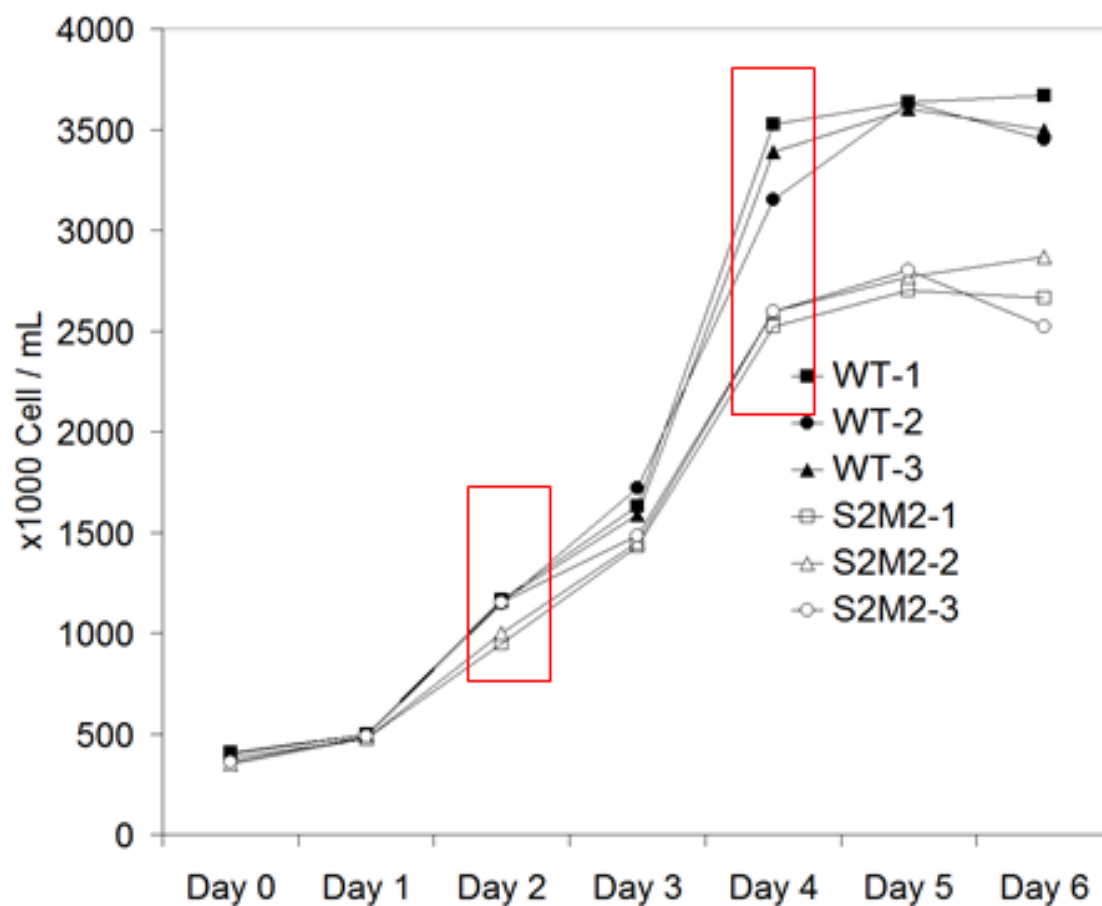
20. Mendoza H, De la Jara A, Freijanes K, Carmona L, Ramos AA, et al. (2009) Characterization of *Dunaliella salina* strains by flow cytometry: a new approach to select carotenoid hyperproducing strains.
21. Doan TTY, Obbard JP (2012) Enhanced intracellular lipid in *Nannochloropsis* sp. via random mutagenesis and flow cytometric cell sorting. *Algal Research* 1: 17–21. doi:10.1016/j.algal.2012.03.001.
22. Bougaran G, Rouxel C, Dubois N, Kaas R, Grouas S, et al. (2012) Enhancement of neutral lipid productivity in the microalga *Isochrysis affinis Galbana* (T-Iso) by a mutation-selection procedure. *Biotechnol Bioeng*. doi:10.1002/bit.24560.
23. Mendoza Guzmán H, Jara Valido A, Freijanes Presmanes K, Carmona Duarte L (2012) Quick estimation of intraspecific variation of fatty acid composition in *Dunaliella salina* using flow cytometry and Nile Red. *J Appl Phycol* 24: 1237–1243. doi:10.1007/s10811-011-9768-y.
24. Evans KM, Chepuron VA, Sluiman HJ, Thomas SJ, Spears BM, et al. (2009) Highly Differentiated Populations of the Freshwater Diatom *Sellaphora capitata* Suggest Limited Dispersal and Opportunities for Allopatric Speciation. *Protist* 160: 386–396. doi:10.1016/j.protis.2009.02.001.
25. Evans KM, Kühn SF, Hayes PK (2005) High levels of genetic diversity and low levels of genetic differentiation in north sea pseudo-nitzschia pungens (bacillariophyceae) populations. *Journal of Phycology* 41: 506–514. doi:10.1111/j.1529-8817.2005.00084.x.
26. Rouxel C, Bougaran G, Doulin Grouas S, Dubois N, Cadoret J-P (2011) novel *isochrysis* sp. Tahitian clone and uses therefore. *EP* 11006712.1
27. Wang Z, Gerstein Mark, Snyder Michael (2009) RNA-Seq: a revolutionary tool for transcriptomics. *Nat Rev Genet* 10: 57–63.
28. Cracraft J, Donoghue MJ (2004) *Assembling the Tree of Life*. Oxford University Press. 594 p.
29. Fox JM, Erill I (2010) Relative Codon Adaptation: A Generic Codon Bias Index for Prediction of Gene Expression. *DNA Res* 17: 185–196. doi:10.1093/dnares/dsq012.
30. Wuitschick JD, Karrer KM (1999) Analysis of Genomic G+C Content, Codon Usage, Initiator Codon Context and Translation Termination Sites In *Tetrahymena Thermophila*. *Journal of Eukaryotic Microbiology* 46: 239–247. doi:10.1111/j.1550-7408.1999.tb05120.x.
31. Chao A, Jost L, Chiang SC, Jiang Y-H, Chazdon RL (2008) A Two-Stage Probabilistic Approach to Multiple-Community Similarity Indices. *Biometrics* 64: 1178–1186. doi:10.1111/j.1541-0420.2008.01010.x.
32. Misra N, Panda PK, Parida BK, Mishra BK, Misra N, et al. (2012) Phylogenomic Study of Lipid Genes Involved in Microalgal Biofuel Production-Candidate Gene Mining and Metabolic Pathway Analyses. *Evolutionary Bioinformatics* 8: 545. doi:10.4137/EBO.S10159.
33. Bendif EM, Probert I, Hervé A, Billard C, Goux D, et al. (2011) Integrative Taxonomy of the Pavlovophyceae (Haptophyta): A Reassessment. *Protist* 162: 738–761. doi:10.1016/j.protis.2011.05.001.
34. Sáez AG, Probert I, Geisen M, Quinn P, Young JR, et al. (2003) Pseudo-cryptic speciation in coccolithophores. *Proceedings of the National Academy of Sciences* 100: 7163–7168.
35. Hamblin MT, Di Rienzo A (2000) Detection of the Signature of Natural Selection in Humans: Evidence from the Duffy Blood Group Locus. *The American Journal of Human Genetics* 66: 1669–1679. doi:10.1086/302879.
36. Singh RS, Krimbas CB (2000) *Evolutionary Genetics: From Molecules to Morphology*. Cambridge University Press. 736 p.
37. Hermisson J, Redner O, Wagner H, Baake E (2002) Mutation–Selection Balance: Ancestry, Load, and Maximum Principle. *Theoretical Population Biology* 62: 9–46. doi:10.1006/tpbi.2002.1582.
38. Reed DH (2009) When it comes to inbreeding: slower is better. *Molecular Ecology* 18: 4521–4522. doi:10.1111/j.1365-294X.2009.04367.x.
39. Jump AS, Marchant R, Peñuelas J (2009) Environmental change and the option value of genetic diversity. *Trends in Plant Science* 14: 51–58. doi:10.1016/j.tplants.2008.10.002.
40. Kristensen TN, Sørensen AC, Sørensen D, Pedersen KS, Sørensen JG, et al. (2005) A test of quantitative genetic theory using *Drosophila*— effects of inbreeding and rate of inbreeding on heritabilities and variance components. *Journal of Evolutionary Biology* 18: 763–770. doi:10.1111/j.1420-9101.2005.00883.x.
41. Demontis D, Pertoldi C, Loeschcke V, Mikkelsen K, Axelsson T, et al. (2009) Efficiency of selection, as measured by single nucleotide polymorphism variation, is dependent on inbreeding rate in *Drosophila melanogaster*. *Molecular Ecology* 18: 4551–4563. doi:10.1111/j.1365-294X.2009.04366.x.
42. Taylor R, Fletcher RL (1998) Cryopreservation of eukaryotic algae – a review of methodologies. *Journal of Applied Phycology* 10: 481–501. doi:10.1023/A:1008094622412.
43. Klug A (2010) The Discovery of Zinc Fingers and Their Applications in Gene Regulation and Genome Manipulation. *Annual Review of Biochemistry* 79: 213–231. doi:10.1146/annurev-biochem-010909-095056.
44. Wright EM, Turk E (2004) The sodium/glucose cotransport family SLC5. *Pflugers Arch - Eur J Physiol* 447: 510–518. doi:10.1007/s00424-003-1063-6.
45. Wright EM, Loo DDF, Hirayama BA (2011) Biology of Human Sodium Glucose Transporters. *Physiol Rev* 91: 733–794. doi:10.1152/physrev.00055.2009.
46. Fang Z, Cui X (2011) Design and validation issues in RNA-seq experiments. *Brief Bioinformatics* 12: 280–287. doi:10.1093/bib/bbr004.
47. Al-Khodori S, Price CT, Kalia A, Abu Kwaik Y (2010) Functional diversity of ankryrin repeats in microbial proteins. *Trends in Microbiology* 18: 132–139. doi:10.1016/j.tim.2009.11.004.
48. Müller A, Klöppel C, Smith-Valentine M, Van Houten J, Simon M (2012) Selective and programmed cleavage of GPI-anchored proteins from the surface membrane by phospholipase C. *Biochimica et Biophysica Acta (BBA) - Biomembranes* 1818: 117–124. doi:10.1016/j.bbame.2011.10.009.
49. Groot PH, Scholte HR, Hülsmann WC (1976) Fatty acid activation: specificity, localization, and function. *Adv Lipid Res* 14: 75–126.
50. Watkins PA (1997) Fatty acid activation. *Prog Lipid Res* 36: 55–83.
51. Akoh C, Lee G, Liaw Y, Huang T, Shaw J (2004) GDSL family of serine esterases/lipases. *Prog Lipid Res* 43: 534–552. doi:10.1016/j.plipres.2004.09.002.
52. Kroeker KJ, Kordas RL, Crim RN, Singh GG (2010) Meta-analysis reveals negative yet variable effects of ocean acidification on marine organisms. *Ecology Letters* 13: 1419–1434. doi:10.1111/j.1461-0248.2010.01518.x.
53. Morgan TH (1917) The Theory of the Gene. *The American Naturalist* 51: 513–544. doi:10.2307/2456204.
54. Darwin C (1859) On the origin of species by means of natural selection, or the preservation of favoured races in the struggle for life.
55. Chepuron VA, Mann DG, Sabbe K, Vyverman W (2004) Experimental Studies on Sexual Reproduction in Diatoms. *International Review of Cytology*. Academic Press, Vol. Volume 237. pp. 91–154. Available: <http://www.sciencedirect.com/science/article/pii/S0074769604370038>.
56. Mouget J-L, Gastineau R, Davidovich O, Gaudin P, Davidovich NA (2009) Light is a key factor in triggering sexual reproduction in the pennate diatom *Haslea oostreae*. *FEMS Microbiology Ecology* 69: 194–201. doi:10.1111/j.1574-6941.2009.00700.x.
57. Walne P (1966) Experiments in the large-scale culture of the larvae of *Ostrea edulis* L. 2. (London): Minist. Agric. Fish. Invest., Vol. 25. p. 53970. Available: [http://openlibrary.org/b/OL5568472M/Experiments\\_in\\_the\\_large-scale\\_culture\\_of\\_the\\_larvae\\_of\\_Ostrea\\_edulis\\_L](http://openlibrary.org/b/OL5568472M/Experiments_in_the_large-scale_culture_of_the_larvae_of_Ostrea_edulis_L).
58. Ewing B, Green P (1998) Base-Calling of Automated Sequencer Traces Using Phred. II. Error Probabilities. *Genome Res* 8: 186–194. doi:10.1101/gr.8.3.186.
59. Martin M (2011) Cutadapt removes adapter sequences from high-throughput sequencing reads. *EMBnetjournal*; Vol 17, No 1: Next Generation Sequencing Data Analysis. Available: <http://journal.embnet.org/index.php/embnetjournal/article/view/200>.
60. Carrier G, Le Cunff L, Dereeper A, Legrand D, Sabot F, et al. (2012) Transposable Elements Are a Major Cause of Somatic Polymorphism in *Vitis vinifera* L. *PLoS ONE* 7: e32973. doi:10.1371/journal.pone.0032973.
61. Dohm JC, Lottaz C, Borodina T, Himmelbauer H (2008) Substantial biases in ultra-short read data sets from high-throughput DNA sequencing. *Nucleic Acids Research* 36: e105–e105.
62. Grabherr MG, Haas BJ, Yassour M, Levin JZ, Thompson DA, et al. (2011) Full-length transcriptome assembly from RNA-Seq data without a reference genome. *Nat Biotech*: 1087–1056.
63. Zhao Q-Y, Wang Y, Kong Y-M, Luo D, Li X, et al. (2011) Optimizing de novo transcriptome assembly from short-read RNA-Seq data: a comparative study. *BMC Bioinformatics* 12: S2. doi:10.1186/1471-2105-12-S14-S2.
64. Fu L, Niu B, Zhu Z, Wu S, Li W (2012) CD-HIT: accelerated for clustering the next generation sequencing data. *Bioinformatics*. Available: <http://bioinformatics.oxfordjournals.org/content/early/2012/10/11/bioinformatics.bts565.abstract>.
65. Puerta MVS, Bachvaroff TR, Delwiche CF (2004) The Complete Mitochondrial Genome Sequence of the Haptophyte *Emiliania huxleyi* and its Relation to Heterokonts. *DNA Research* 11: 1–10. doi:10.1093/dnares/11.1.1.
66. Bowler C, Allen AE, Badger JH, Grimwood J, Jabbari K, et al. (2008) The *Phaeodactylum* genome reveals the evolutionary history of diatom genomes. *Nature* 456: 239–244. doi:10.1038/nature07410.
67. Armbrust EV, Berges JA, Bowler C, Green BR, Martinez D, et al. (2004) The Genome of the Diatom *Thalassiosira pseudonana*: Ecology, Evolution, and Metabolism. *Science* 306: 79–86.
68. Blanc G, Duncan G, Agarkova I, Borodovsky M, Gurion J, et al. (2010) The *Chlorella variabilis* NC64A Genome Reveals Adaptation to Photosymbiosis, Coevolution with Viruses, and Cryptic Sex. *The Plant Cell Online* 22: 2943–2955.
69. Merchant SS, Prochnik SE, Vallon O, Harris EH, Karpowicz SJ, et al. (2007) The *Chlamydomonas* Genome Reveals the Evolution of Key Animal and Plant Functions. *Science* 318: 245–250.
70. Jaecisch N, Yang I, Wohrlab S, Glöckner G, Kroymann J, et al. (2011) Comparative Genomic and Transcriptomic Characterization of the Toxicogenic Marine Dinoflagellate *Alexandrium ostenfeldii*. *PLoS ONE* 6: e28012. doi:10.1371/journal.pone.0028012.
71. Nozaki H, Maruyama S, Matsuzaki M, Nakada T, Kato S, et al. (2009) Phylogenetic positions of Glaucophyta, green plants (Archaeplastida) and Haptophyta (Chromalveolata) as deduced from slowly evolving nuclear genes. *Molecular Phylogenetics and Evolution* 53: 872–880. doi:10.1016/j.ympev.2009.08.015.
72. Matsuzaki M, Misumi O, Shin-i T, Maruyama S, Takahara M, et al. (2004) Genome sequence of the ultrasmall unicellular red alga *Cyanidioschyzon merolae* 10D. *Nature* 428: 653–657. doi:10.1038/nature02398.

73. Altschul SF, Gish W, Miller W, Myers EW, Lipman DJ (1990) Basic local alignment search tool. *Journal of Molecular Biology* 215: 403–410. doi:10.1016/S0022-2836(05)80360-2.
74. Stothard P (2000) The sequence manipulation suite: JavaScript programs for analyzing and formatting protein and DNA sequences. *BioTechniques* 28. Available: <http://view.ncbi.nlm.nih.gov/pubmed/10868275>.
75. Min XJ, Butler G, Storms R, Tsang A (2005) OrfPredictor: predicting protein-coding regions in EST-derived sequences. *Nucleic Acids Research* 33: W677–W680.
76. Perrier X, Flori A, Bonnot F (2003) Data analysis methods. Genetic diversity of cultivated tropical plants. Enfield, Science Publishers. p. pp 43–76.
77. Hunter S, Jones P, Mitchell A, Apweiler R, Attwood TK, et al. (2012) InterPro in 2011: new developments in the family and domain prediction database. *Nucleic Acids Research* 40: D306–D312.
78. Feng J, Meyer CA, Wang Q, Liu JS, Liu XS, et al. (2012) GFOLD: a generalized fold change for ranking differentially expressed genes from RNA-seq data. *Bioinformatics* 28: 2782–2788. doi:10.1093/bioinformatics/bts515.
79. Chao A, Shen T-J (2010) SPADE (Species Prediction And Diversity Estimation).

Chapitre III :

Effets de la carence azotée chez

*Tisochrysis lutea*



**Figure 4** : Suivi des cultures batch des souches WT et S2M2.

Les échantillons prélevés pour les analyses protéomiques sont encadrés en rouge.

## Chapitre III : Effets de la carence azotée chez *Tisochrysis lutea*. Analyses protéomiques comparatives entre la souche sauvage (WT) et une souche mutante hyper lipidique (S2M2) sous différentes conditions de disponibilité en azote.

---

### 1 Introduction

Il est désormais admis que l'expression d'un gène et l'abondance de la protéine ne sont pas nécessairement corrélées car de nombreux mécanismes de régulation post-transcriptionnelle peuvent intervenir et limiter ou activer la traduction d'un gène exprimé. Les protéines étant les constituants principaux de la machinerie cellulaire nous avons mis en place une approche protéomique pour identifier les mécanismes impliqués dans l'accumulation des lipides chez *T. lutea*. Nous avons émis les hypothèses que la suraccumulation des lipides de réserve chez la souche S2M2 était non constitutive et donc liée à une limitation azotée, et que les protéines dont l'abondance est à la fois spécifique de la souche S2M2 et de la limitation azotée pourraient être de bons candidats pour expliquer le phénotype hyper-lipidique observé. Les objectifs de notre travail ont donc été de :

- 1) Identifier les protéines impactées par la carence azotée.
- 2) Identifier les protéines différentiellement accumulées entre les deux souches WT et S2M2 en phase exponentielle de croissance et en début de phase stationnaire.
- 3) Identifier les protéines dont le niveau d'accumulation est spécifique de la souche S2M2 et de la limitation azotée.

Les souches multiclonales WT et S2M2 ont été cultivées en mode batch limité par l'azote. Au cours de ces cultures, les cellules ont été caractérisées par cytométrie en flux, et l'accumulation des lipides de réserve a été estimée par coloration des vésicules lipidiques au rouge du Nile. Des prélèvements pour analyses protéomiques ont été effectués lors de la phase exponentielle de croissance, en absence de limitation azotée, et en tout début de phase stationnaire, soit en début de carence (**Figure 40**). Les protéines ont été extraites, purifiées et séparées par électrophorèse bidimensionnelle (2-DE) (pH4-7; 12% acrylamide). Cette technique, développée en 1975 par O'farrell (O'Farrell, 1975) consiste à séparer les protéines en fonction de leurs propriétés physicochimiques (point isoélectrique et poids moléculaire). Elle permet ainsi de séparer non seulement les protéines en fonction de leur structure primaire, mais aussi les différents isoformes d'une même protéine. Les

conditions d'électrophorèses ont été optimisées au préalable pour visualiser le maximum de spots sur un même gel. Notons que lors de cette étude, les protéines basiques avec un point isoélectrique supérieur à sept n'ont pas été étudiées. Les spots protéiques différentiellement colorés en fonction des souches ou en fonction de la phase de croissance ont été sélectionnés par analyse d'image et analyses statistiques avec le logiciel Samespot®(TotalLab). Les protéines contenues dans les spots sélectionnés ont ensuite été identifiées par spectrométrie de masse sur la plateforme BIBS (INRA Nantes - Genopole Ouest). Brièvement, la méthodologie consiste à : 1) Digérer les protéines avec une endo-peptidase (la trypsine dans ce cas); 2) Séparer les peptides issus de la digestion par chromatographie liquide (LC) ; 3) Ioniser les peptides et mesurer la masse de chaque peptide ionisé (MS) ; 4) Fragmenter chaque peptide ionisé et mesurer les masses des résidus pour reconstruire la séquence de chaque peptide (MS/MS); 5) Comparer les profils de masse identifiés à des profils de masse générés *in silico* à partir de bases de données protéiques pour identifier les protéines.

## 2 Résultats principaux

Les résultats principaux ont été publiés dans un article en 2014 et présenté en fin de ce chapitre (Garnier et al., 2014)

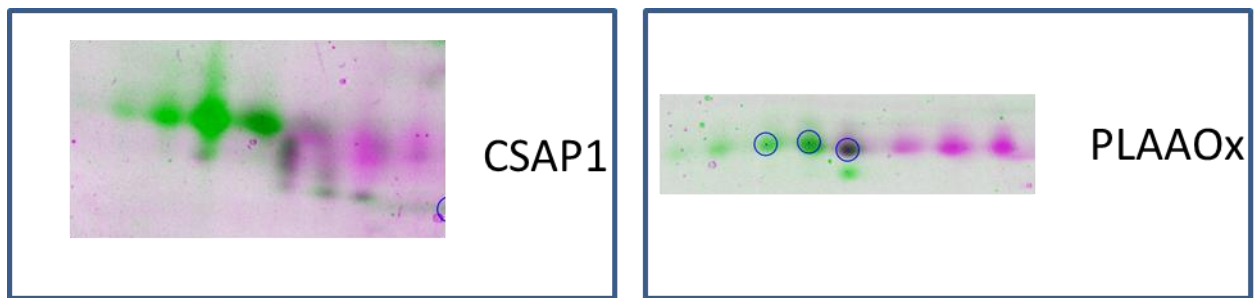
Les mesures d'accumulation lipidique au cours des cultures batch ont permis de montrer que la souche S2M2 ne sur-accumulait pas de lipides de réserve en absence de limitation azotée (correspondant à la phase exponentielle de croissance) confirmant ainsi l'hypothèse que la suraccumulation des lipides par la souche S2M2 était fortement liée à la limitation azotée (voir fig. 1 de Garnier et al., 2014). Les analyses de cytométrie en flux ont montré de nombreuses différences morphologiques et pigmentaires entre les deux souches suggérant que de nombreuses voies métaboliques ont été impactées chez la souche mutée S2M2. Ces différents résultats phénotypiques soulignent les difficultés à identifier les mécanismes liés au seul phénotype hyper-lipidique chez la souche S2M2 et donc l'intérêt d'étudier ces souches sous différentes conditions physiologiques azotées pour révéler les mécanismes spécifiques aux lipides et à l'azote.

Ces analyses protéomiques ont permis d'identifier 17 protéines dont l'abondance est impactée par la carence azotée chez *T. lutea* WT (voir tableaux 2 et 3 de Garnier et al., 2014). Nos résultats montrent notamment que chez *T. lutea*, la carence azotée induit la sous-accumulation de la petite sous-unité de la Rubisco, de plusieurs protéines intervenant dans la synthèse protéique et de protéines impliquées dans la synthèse de la chlorophylle. Ces résultats, renforcent les précédentes études sur les effets du stress azoté chez les microalgues. Ils montrent que la baisse de l'absorption du carbone

et la baisse de l'activité traductionnelle en réponse à la carence azotée est un comportement partagé entre les haptophytes et les autres espèces de microalgues étudiées. Nos travaux montrent également que la carence azotée induit la sous-accumulation de la  $\beta$ -ketoacyl-ACP réductase (FabG), protéine impliquée dans la synthèse *de novo* des acides gras. Ce résultat suggère ainsi que l'anabolisme des lipides est faiblement impliqué dans l'accumulation des lipides en carence azotée chez *T. lutea* WT. D'autre part, la carence azotée induit la très forte suraccumulation de la CSAP, protéine de fonction très mal connue et potentiellement impliquée dans l'homéostasie du carbone et de la PLAAOx, protéine potentiellement impliquée dans les phénomènes de reminéralisation de l'azote organique.

De plus, ces analyses protéomiques ont également permis d'identifier 37 protéines différenciellement accumulées entre les deux souches (voir tableaux 4 et 5 de Garnier et al., 2014). Notons que les gènes codant pour ces protéines accumulées n'ont pas été observés comme différenciellement exprimés lors de la précédente étude transcriptomique. D'une manière générale, ces protéines sont impliquées dans la réponse au stress, dans la respiration, dans la photosynthèse, dans la glycolyse et dans la dégradation des sucres de réserve. Ces résultats suggèrent que l'ensemble du métabolisme du carbone est impacté dans la souche mutée S2M2. Plus précisément, la suraccumulation chez la souche S2M2 de la glycoside hydrolase GH16 pourrait provoquer une réorientation du carbone des sucres vers les lipides de réserve.

De façon intéressante, alors que la carence azotée aboutit à une sous accumulation de la protéine FabG et à une très forte suraccumulation des protéines CSAP et PLAAOx chez la souche WT, leurs abondances protéiques respectives ne varient pas chez la souche S2M2 (voir table 6 de Garnier et al., 2014). Ces résultats suggèrent que la régulation par l'azote ne se fait pas de manière similaire entre les deux souches Wt et S2M2. Par conséquent, ces 3 protéines se révèlent être de bons candidats pour des analyses ciblées concernant le lien entre carence azotée et accumulation des lipides. Les protéines CSAP et PLAAOx feront l'objet d'une analyse ciblée dans le chapitre VI de ce document.



**Figure 1 :** Modifications post-traductionnelles observées sur gel 2D-E.

Alignement *in silico* de portions de gels bidimensionnels présentant des différences de modifications post-traductionnelles pour les protéines CSAP1 et PLAAOx en fonction des souches. Les protéines de la souche WT sont colorées virtuellement en vert et les protéines de S2M2 virtuellement en rose. L'ensemble des spots majoritaires visualisés correspondent à la même protéine CSAP1 dans l'encart de gauche et à la PLAAOx dans l'encart de droite.



### 3 Résultats complémentaires : Etude des kinases et phosphatases mutées.

Les analyses par électrophorèse bidimensionnelle montrent pour certaines protéines des profils de migration différents entre la souche WT et la souche S2M2. Ces différences peuvent s'expliquer par des différences de modifications post-traductionnelles (phosphorylation, glycosylations, glutathionylation, etc.) ou des clivages protéiques (Rabilloud, 2002). Les modifications post-traductionnelles (MPT) jouent un rôle crucial dans la régulation de l'activité enzymatique, dans l'adressage aux compartiments cellulaires, dans l'ancrage aux membranes, dans certaines cascades de signalisation et dans la reconnaissance par les systèmes de dégradation protéique. Les MPTs les plus courantes sont sans doute les phosphorylations qui régulent un très grand nombre de voies de signalisation et voies métaboliques. Chaque phosphorylation modifie de 79.98 Da le poids moléculaire d'une protéine et de 0 à 1 son point isoélectrique. Elle impacte donc sensiblement la migration des protéines sur gel 2-DE (Halligan, 2009). Dans cette étude, les différences de migration observées pour certaines protéines pourraient correspondre à des différences de phosphorylations (**Figure 41**). Des analyses complémentaires par marquage phospho-spécifique ou par analyses de masse seraient nécessaires pour valider cette hypothèse (Doll and Burlingame, 2015). Nous avons néanmoins suggéré que certaines kinases ou phosphatases pourraient être impliquées dans ces modifications car plusieurs travaux sur des modèles animaux ou plantes montrent des différences de profils 2-DE après mutation de protéines kinases ou phosphatases (Kernec et al., 2001; Wan et al., 2007; Candido et al., 2014).

Parmi les 315 gènes codant des phosphatases, un gène muté a été identifié (Tiso\_gene\_13163). Ce gène code pour une serine thréonine phosphatase de 391 acides aminés (*Tisochrysis\_lutea*\_Proteine\_9678) contenant un domaine catalytique PP2Cc très conservé (Serine/thréonine phosphatases, family 2C, catalytic domain). Enfin, 9 autres serine thréonine phosphatases PP2Cc ont été identifiées chez *T. lutea*. Cette famille de protéine dont le rôle physiologique est encore mal connu présente une large spécificité de substrats (Wenk et al., 1992). L'analyse structurale d'une serine thréonine phosphatases PP2Cc humaine a été réalisée et les analyses de séquences suggèrent une forte conservation des structures tridimensionnelles de cette famille de protéines (Das et al., 1996). Le gène muté chez la souche S2M2 contient un codon stop en position 169 à la place d'un codon codant la glutamine. Cette mutation est localisée dans le domaine fonctionnel PP2Cc (**Figure 42**). La protéine tronquée qui en résulte est donc vraisemblablement non fonctionnelle. Aucun paralogue à cette protéine n'a été identifié dans le transcriptome de *T. lutea*. En

conséquence, il serait intéressant d'évaluer son rôle dans la déphosphorylation de protéines cibles observées sur gel 2-DE.

>Tisochrysis\_lutea\_Proteine\_9678

```
MGNACAKPVNTQSLPDKESTSGGSVIPASAPVEGGSLDSKAKTFRDRRLSVAQKPPPEAVRRSRRLSVYGGAGGP
QSDPSTPIPPVTSCGAQSIAGLEPVPGGAVQKINQDRAIAIYPFNGDKACFLGGVFDGHGRAGEKVSQYVIDTLP
EELASHPSIKEDPGEALRQTFMSVDASLADHVDA SVSGTTAVACLVRGNHIWLANS GDSRAIMCRQKPKSNKLVA
HDLTVDQKPDTPAEMKRILSLGGHVTPAGANGSPARVWHNLRGLAMARSIGDHAAATVGVIAEPEVTEYDIMDDD
VCLIIASDGVWELLTSQQVVDVVADVPNLDPMTICNNIVAQASHEWKMEEGDYRDDITVVVLTFFPWLDSEYDGLT
EAPTSKSNVDIPKIAA
```

> Tisochrysis\_lutea\_Proteine\_9678 muté

```
MGNACAKPVNTQSLPDKESTSGGSVIPASAPVEGGSLDSKAKTFRDRRLSVAQKPPPEAVRRSRRLSVYGGAGGP
QSDPSTPIPPVTSCGAQSIAGLEPVPGGAVQKINQDRAIAIYPFNGDKACFLGGVFDGHGRAGEKVSQYVIDTLP
EELASHPSIKEDPGEALR*TFMSVDASLADHVDA SVSGTTAVACLVRGNHIWLANS GDSRAIMCRQKPKSNKLVA
HDLTVDQKPDTPAEMKRILSLGGHVTPAGANGSPARVWHNLRGLAMARSIGDHAAATVGVIAEPEVTEYDIMDDD
VCLIIASDGVWELLTSQQVVDVVADVPNLDPMTICNNIVAQASHEWKMEEGDYRDDITVVVLTFFPWLDSEYDGLT
EAPTSKSNVDIPKIAA
```

Parmi les 764 gènes codant des kinases, un gène muté a été identifié (Tiso\_gene\_13163). Il code pour une Cycline Dépendant protéine Kinase (CDK) de 301 acides aminés (*Tisochrysis\_lutea\_Proteine\_9678*) qui présente plus de 60 % d'identité avec les CDK2 humaine. Cette famille multigénique de protéines est très conservée et impliquée essentiellement dans la régulation du cycle cellulaire. Leur activité est contrôlée par l'expression de cyclines (Brown et al., 1999). La mutation en position 16 de la protéine est très proche de la poche ATP qui confère l'activité kinase aux CDKs (**Figure 43**). Elle aboutit à l'expression d'un acide aminé polaire (serine) à la place d'un acide aminé apolaire (glycine). Cette mutation modifie donc vraisemblablement la fonction de cette CDK2.

>P182.01 Tiso\_gene\_4902

```
PPMEKYQKIEKIGEGTYGVVYKAKDRGSGELVALKKIRLEAEDEGIPSTAIRESILKELQHPNIVRLHDVIHTE
KKLTLVFEYLDQDLKKYLDSCPDGADARMIKRALLQLLKGVAFCCHDRRVLHRDLKQPONLLINKHGELKLADFGLA
RAFGIPVRSYTHEVVTLWYRAPDVLMSGSRKYSTPVDLWSVGCIFGEMASGRPLFPGTSDHDQVVRIFKVLGTPTE
ETWPSMIDLPEYKADWPKYEPVALQSIAPSLDELGIDLLSRMLQYEPSRRI SAKDALDHDY LKGVAAEEWARERAG
A
```

>P182.01 Tiso\_gene\_4902\_muté

```
PPMEKYQKIEKIGEGTYSVVYKAKDRGSGELVALKKIRLEAEDEGIPSTAIRESILKELQHPNIVRLHDVIHTE
KKLTLVFEYLDQDLKKYLDSCPDGADARMIKRALLQLLKGVAFCCHDRRVLHRDLKQPONLLINKHGELKLADFGLA
RAFGIPVRSYTHEVVTLWYRAPDVLMSGSRKYSTPVDLWSVGCIFGEMASGRPLFPGTSDHDQVVRIFKVLGTPTE
ETWPSMIDLPEYKADWPKYEPVALQSIAPSLDELGIDLLSRMLQYEPSRRI SAKDALDHDY LKGVAAEEWARERAG
A
```

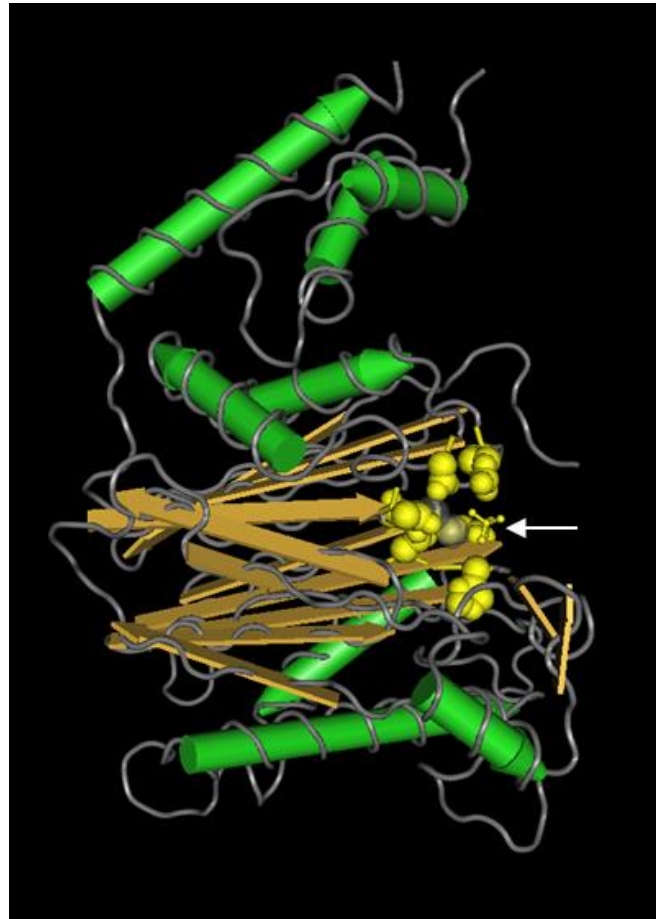


Figure Structure tridimensionnelle d'une serine thréonine phosphatases PP2C humaine.

La flèche indique l'emplacement de la mutation chez la protéine homologue de la souche S2M2

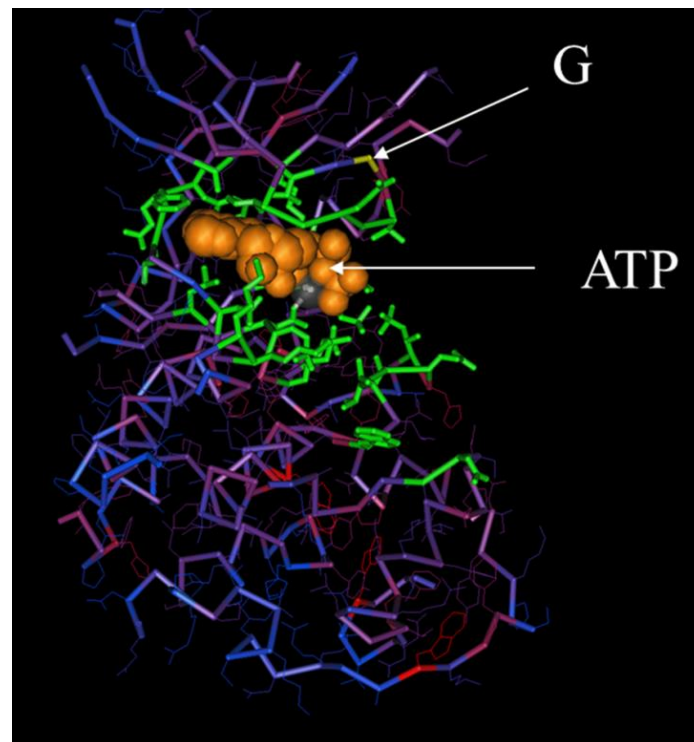


Figure Structure tridimensionnelle de la Cycline Dependante Kinase 2 humaine.

La flèche notée G indique l'emplacement de la mutation chez la protéine homologue de la souche S2M2.

Ces résultats suggèrent que la mutation de certaines enzymes impliquées dans la phosphorylation des protéines pourrait conduire à des différences de régulations post-traductionnelles entre les souches WT et S2M2. Ces résultats devront être confortés et enrichis par des analyses de phosphoprotéomiques pour mieux évaluer l'impact de la sélection sur les régulations post-traductionnelles de type phosphorylation. Par ailleurs, il serait intéressant d'étudier d'autres types de modifications post-traductionnelles (glycosylations, sumoylations, ubiquitinations) qui interviennent dans la régulation des protéines. Ainsi, nos résultats ouvrent de nouveaux champs d'investigation qui permettront une connaissance approfondie des régulations protéiques chez les microalgues haptophytes.

#### **4 Bilan et perspectives**

Les travaux présentés dans ce chapitre ont permis 1) de mieux caractériser le phénotype des souches S2M2 et WT cultivées dans une culture batch limitée par l'azote, et 2) d'identifier des protéines différentiellement accumulées en fonction de la souche et /ou de la carence azotée. 3) d'identifier des protéines mutées et impliquées dans les régulations post-traductionnelles. L'ensemble des résultats montre que de nombreuses fonctions cellulaires et moléculaires ont été affectées dans la souche S2M2 qui pourtant conserve des capacités de croissance similaires à la souche sauvage. Nous avons montré que différents niveaux de régulation (transcriptionnelle, traductionnel et post-traductionnel) étaient impactés par la carence azotée en fonction de la souche étudiée. La fonction de nombreux gènes (60 % des transcrits) reste encore indéterminée. Ces travaux ouvrent donc de nombreux champs d'investigations fonctionnelles qui permettront d'étendre les connaissances sur la fonction des gènes des microalgues encore insuffisantes.

Enfin, nos résultats discréditent l'hypothèse selon laquelle la suraccumulation lipidique est le fruit d'une augmentation du métabolisme anabolique des lipides. Ils suggèrent plutôt que la suraccumulation lipidique chez la souche S2M2 est une conséquence d'une réallocation du carbone intracellulaire, impliquant des voies métaboliques situées en amont de la synthèse des lipides. D'autre part, les travaux sur l'effet de la carence azotée suggèrent des différences entre les deux souches concernant la réponse à la limitation azotée. Dans le chapitre suivant, nous avons tenté par des approches protéomiques haut débit de décrire le comportement dynamique des deux souches face à des variations fines de limitation azotée impliquant des métabolismes anaboliques et cataboliques des lipides.

Available online at [www.sciencedirect.com](http://www.sciencedirect.com)

ScienceDirect

[www.elsevier.com/locate/jprot](http://www.elsevier.com/locate/jprot)

# Comparative proteomics reveals proteins impacted by nitrogen deprivation in wild-type and high lipid-accumulating mutant strains of *Tisochrysis lutea*☆



M. Garnier<sup>a,\*</sup>, G. Carrier<sup>a</sup>, H. Rogniaux<sup>b</sup>, E. Nicolau<sup>a</sup>, G. Bougaran<sup>a</sup>,  
B. Saint-Jean<sup>a</sup>, J.P. Cadoret<sup>a</sup>

<sup>a</sup>Laboratoire BRM-PBA Ifremer, Nantes, France

<sup>b</sup>INRA, UR1268 Biopolymers Interactions Assemblies, F-44316 Nantes, France

## ARTICLE INFO

Available online 28 February 2014

### Keywords:

Microalgae  
Biotechnology  
Lipid  
Nitrogen  
Proteomic  
Selection

## ABSTRACT

Understanding microalgal lipid accumulation under nitrogen starvation is of major interest for biomass feedstock, food and biofuel production. Using a domesticated oleaginous algae *Tisochrysis lutea*, we performed the first comparative proteomic analysis on the wild type strain and a selected lipid over-accumulating mutant. 2-DE analysis was made on these strains cultured in two metabolic conditions, with and without nitrogen deprivation, which revealed significant differences in proteomes according to both strain and nitrogen availability. Mass spectrometry allowed us to identify 37 proteins that were differentially expressed between the two strains, and 17 proteins regulated by nitrogen starvation concomitantly with lipid accumulation. The proteins identified are known to be involved in various metabolic pathways including lipid, carbohydrate, amino acid, energy and pigment metabolisms, photosynthesis, protein translation, stress response and cell division. Four candidates were selected for possible implication in the over-accumulation of lipids during nitrogen starvation. These include the plastid beta-ketoacyl-ACP reductase protein, the coccolith scale associated protein and two glycoside hydrolases involved in biosynthesis of fatty acids, carbon homeostasis and carbohydrate catabolism, respectively. This proteomic study confirms the impact of nitrogen starvation on overall metabolism and provides new perspectives to study the lipid over-accumulation in the prymnesiophyte haptophyte *T. lutea*.

### Biological significance

This paper study consists of the first proteomic analysis on *Tisochrysis lutea*, a non-model marine microalga of interest for aquaculture and lipids production. Comparative proteomics revealed proteins putatively involved in the up-accumulation of neutral lipids in a mutant strain during nitrogen starvation. The results are of great importance for future works to improve lipid accumulation in microalgae of biotechnological interest for biofuel production. This article is part of a Special Issue entitled: Proteomics of non-model organisms.

© 2014 Elsevier B.V. All rights reserved.

☆ This article is part of a Special Issue entitled: Proteomics of non-model organisms.

\* Corresponding author at: IFREMER BRM-PBA, rue de l'île d'Yeu, B.P. 21105, 44311 Nantes Cedex 03, France. Tel.: +33 2 40 37 43 36; fax: +33 2 40 37 40 01.

E-mail address: [mgarnier@ifremer.fr](mailto:mgarnier@ifremer.fr) (M. Garnier).

## 1. Introduction

The metabolism of lipids in microalgae has attracted new interest over the last few years because of the energetic potential offered by these photosynthetic microorganisms [1]. Algal lipids are also of interest for human health as they include the long chain polyunsaturated fatty acids (PUFAs) arachidonic, eicosapentenoic and docosahexenoic acid, which are transferred via the food chain and protect humans against cardiovascular diseases [2–4]. Moreover, some species can produce high amounts of neutral lipids such as triacylglycerols (TAGs) that can be used to produce 3rd generation biofuel [5], although cost effectiveness of such methods remains in question [6,7].

Enhancement of TAGs in most microalgae is known to be triggered by stress and nutrient deprivation, particularly nitrogen deprivation [2,8]. TAGs accumulate in lipid droplets and play roles in carbon and energy storage, as a source of long chain PUFAs, and in photooxidation prevention [8]. Because the increase of lipid production is of great biotechnological interest, one of the current important research objectives is to understand the molecular mechanisms that govern lipid accumulation under nitrogen starvation.

*Chlamydomonas reinhardtii* is the most commonly used algae model. The availability of starchless mutants that overaccumulate neutral lipids has facilitated investigations on lipid metabolism [1,4,9–13]. Although de novo FA biosynthesis and TAG build-up have been quite well described, the regulation of lipid biosynthesis remains poorly understood in this model species. In oleaginous algae, many fundamental biological questions relating to the biosynthesis and regulation of lipids need to be answered in order to allow more efficient lipid management. Post genomics has been shown to be a good way to develop biotechnology of microalgae including non-model species (for review see [14]). Thereby, transcriptomics has been used to study the effects of nitrogen starvation in the chlorophyceae *Micractinium pisillum*, the eustigmatophyceae *Nannochloropsis* sp. and the diatom *Phaeodactylum tricorutum* [15–18]. The results suggest that the carbon sources for neutral lipid accumulation could be largely derived from carbohydrates and that the acetyl-CoA metabolism would play an important role in driving carbon flow into TAG biosynthesis. In *Nannochloropsis gaditana* transcripts of a few genes involved in lipid biosynthesis were increased significantly during rapid nitrogen deprivation [19]. Proteomics allows us to study the changes of the final products of gene regulation, namely the proteins, from transcription until post-translational modifications. This approach, in complement to transcriptomic analysis, was implemented to examine the responses of *Nannochloropsis oceanica* to long-term nitrogen starvation [20]. Proteomics analysis of the chlorophyceae *Chlorella vulgaris* in response to nitrogen starvation revealed the up-regulation of proteins involved in de novo fatty acid biosynthesis and in the build-up of TAGs [21]. Moreover, the authors suggested that post-transcriptional regulation of key enzymes was important in the regulation of fatty acid synthesis. This highlights the interest of proteomic approaches for understanding lipid metabolism in neutral lipid-rich microalgae.

*Tisochrysis lutea* (*T. lutea*), previously named *Isochrysis* aff. *galbana* (Clone Tahiti) [22] is a small uncalcified prymnesiophyte haptophyte. Numerous ecophysiological studies have focused on haptophytes because of their extensive use as feeds in aquaculture. Isochrysidales naturally contain large amount of fatty acids and PUFAs and under nitrogen starvation they accumulate high amounts of polyunsaturated long-chain (C37–39) alkenes and alkenones (PULCA) rather than TAGs [23–27]. Recently, our laboratory implemented one of the first domestication strategies based on successive rounds of UV mutation and cell sorting. This non-GMO (Genetic Modified Organism) selection approach allowed us to obtain a *T. lutea* strain (*T. lutea*-S2M2) that accumulates twice the amount of neutral lipids under nitrogen starvation, with no decrease in growth rate compared to the wild type strain (WT) [28]. In order to maximize the yield of lipid products from microalgae, it is vital to improve our understanding of the mechanisms involved in the over-accumulation of lipids in selected mutants. Because homemade transcriptome is available for *T. lutea* and because a high lipid-accumulating mutant (S2M2) was selected, we proposed to use the *T. lutea* WT and S2M2 strains as models to study lipid metabolism in haptophytes in relation to nitrogen starvation.

Therefore, in this work, we applied a comparative proteomics study to learn more about the molecular mechanisms affected, firstly by selection and secondly by nitrogen starvation. Two-dimensional gel electrophoresis (2D-E) was performed, coupled with mass spectrometry analysis (MS) of spots displaying differential abundance. Similar approaches had been previously used to successfully determine the effects of breeding selection in plants and, very recently, in the non-oleaginous microalgae *C. reinhardtii* [29,30]. In our study, we identified proteins whose abundance was regulated by nitrogen starvation and whose abundance was different between the S2M2 mutant strain and the WT strain. By compiling these results, we were able to select a set of proteins that is regulated by nitrogen starvation in different way between the two strains. These proteins are good candidates to conduct further investigations.

## 2. Materials and methods

### 2.1. Strains and growth conditions

*T. lutea* CCAP 927/14 wild type strain (WT) was purchased from the Culture Center of Algae and Protozoa (CCAP, Oban, Scotland). A mutant strain accumulating twice the amount of neutral lipids (S2M2) (CCAP926/14) was previously obtained after two steps of UV mutation and cytometric selection [28]. Axenic WT and S2M2 strains were maintained in photoautotrophic batch cultures in Walne's medium [31]. Starter cultures were grown in the same broth with continuous illumination ( $100 \mu\text{mol} \pm 5 \text{ photons m}^{-2} \text{ s}^{-1}$ ) to medium growth phase ( $C = 12.6 \pm 1 \times 10^6 \text{ cell.mL}^{-1}$ ). For each strain, three flasks containing 1.5 L of  $0.2 \mu\text{M}$  filtered autoclaved sea water were inoculated at  $0.3 \times 10^6 \text{ cell.mL}^{-1}$ . Nutritive elements consisted of modified Walne's medium with a nitrate concentration of 0.12 mM instead of 1.2 mM. Growth in batch mode was conducted at  $20^\circ\text{C}$ , with a constant continuous

light irradiance of  $100 \mu\text{mol}\cdot\text{m}^{-2}\cdot\text{s}^{-1}$  and  $\text{CO}_2$ -enriched bubble aeration. All experiments were carried out in triplicate.

Algae concentrations were measured daily by cell count in a Malassez counting chamber. Particulate Nitrogen (QN) and Carbon (QC) were estimated by filtering a given volume of cells on precombusted 25 mm GF/C filters (Whatman,  $1.2 \mu\text{m}$ ). The filters were then dried for 24 h at  $70^\circ\text{C}$  and further analyzed by using a CN Elemental Analyzer (Flash 2000, ThermoScientific). Residual N and P in filtrates were assayed by DIONEX ion-chromatography (AS9-HC column).

## 2.2. Lipid accumulation

Lipid accumulation was analyzed by the Nile red staining method [32]. One mL of culture was stained with  $2 \mu\text{L}$  of Nile red diluted at  $250 \mu\text{g}\cdot\text{mL}^{-1}$  in acetone. The mix was vortexed and incubated for 5 min. Stained algae cells were excited at 480 nm and their total fluorescence intensity detected at the 525–580 nm emission waveband using a Tecan Saphir II TM spectrofluorimeter (Tecan Austria GmbH, Grödig, Salzburg, Austria). Indices of relative fluorescence per cell were calculated to estimate cell lipid concentration.

A flow cytometric analysis after Nile red staining was conducted on a BD Accuri™ C6 Flow Cytometer. For each culture, 30,000 events were analyzed daily and Nile red staining was analyzed on FL2 (488–585 nm) detector. An Olympus BH2-RFCA microscope equipped with an Olympus light source for excitation was used to observe cells after Nile red staining. Native and fluorescence images were acquired by using a CCD camera (Qimaging RETIGA 2000R).

## 2.3. Protein extraction

For the proteomic study, 400 mL of mid-exponential phase (Day 2) and 400 mL of end growth phase (Day 5) cultures were centrifuged at  $2500 \times g$  for 20 min at  $5^\circ\text{C}$ . Pellets were pooled and washed in 0.3 M sucrose then quickly frozen at  $-80^\circ\text{C}$ .

For each condition, total proteins were extracted from frozen cell pellets by using a modified version of the protocol by Lee et al. [33]. Briefly, 1 mL Trizol reagent was added to the pellets and pulse sonicated using a Vibra-Cell® 75022 sonicator (Bioblock, Illkirch, France) in an ice bath for 3 min in the presence of a protease inhibitor (cOmplete tablets, Roche Diagnostics, Mannheim, Germany). Then,  $200 \mu\text{L}$  of chloroform was added to the cell lysate before shaking and centrifugation at  $12,000 \times g$  for 10 min at  $4^\circ\text{C}$ . The hydrophilic phase was removed and  $300 \mu\text{L}$  ethanol was added to dissolve the reddish bottom layer. The mixtures were centrifuged at  $16,000 \times g$  for 10 min and the supernatants mixed with one volume of 20% trichloroacetic acid (TCA) and 0.14%  $\beta$ -mercaptoethanol, in cold acetone. After being left overnight, proteins were precipitated at  $-20^\circ\text{C}$ , the mixtures were centrifuged at  $16,000 \times g$  for 10 min at  $4^\circ\text{C}$ . The pellets were washed with cold acetone then resuspended in buffer containing 6 M urea, 2 M thio-urea, 4% CHAPS and 2% Bio-Lyte 3/10.

## 2.4. 2-Dimensional electrophoresis (2-DE)

Each extract was analyzed on analytic 2-DE gels by using the adapted O'Farrell protocol [34]. A pH gradient of 4–7 was chosen

for isoelectric focusing (IEF). The second-dimension electrophoresis was performed on 12% SDS polyacrylamide gels to optimize the separation of proteins with a molecular weight ranging from 10 to 120 kDa. Aliquots containing  $30 \mu\text{g}$  of protein for analytic gels and  $300 \mu\text{g}$  for preparative gels were purified with a 2D Clean-up kit (GE Healthcare) and resuspended in  $330 \mu\text{L}$  rehydration buffer containing 6 M urea, 2 M thio-urea, 4% CHAPS, 2% Bio-Lyte 3/10, 0.01% bromophenol blue, 3.3 mM tributylphosphine, and 5% DTT. After 18 h of active rehydration of dry immobilized pH gradient (IPG) strips, linear pH 4–7 (Bio-Rad, Marnes-la-Coquette, France), at 50 V, IEF was performed by using the Bio-Rad Protean IEF Cell at 66,000 V.h. The strips were next treated with buffer containing 6 M urea, 2% SDS, 0.05 M Tris-HCl pH 8.8, 30% glycerol and supplemented with 2% DTT and 3.3 mM tributylphosphine, and then again with the same buffer containing 4% iodoacetamide. Finally, proteins were visualized by the silver staining method for analytic gels and Bio-Safe colloidal Coomassie blue (Bio-Rad, Marnes la Coquette, France) for preparative gels. Two technical replicates were made for each of the twelve extracts.

## 2.5. Image and statistical analysis

Images of analytic gels were recorded on a Bio-Rad GS800 densitometer. Gels were analyzed with the Progenesis SameSpots, version 3.0, software (Nonlinear Dynamics Ltd., Newcastle, United Kingdom). The quality of the gels was verified by using the quality control (QC) of the software. The vector alignment tool of SameSpots Workflow was employed for an automatic pixel level geometric alignment of the gels, followed by manual corrections. The background-corrected abundance of each spot was calculated, and the abundance ratio was determined by dividing the sample abundance by the reference abundance. Spot volumes were normalized to calibrate data between different sample runs, and normalized spots were then analyzed statistically by using the statistics module in SameSpots. Principal component analysis (PCA) was used to separate the gels according to variations in the normalized volume of the spots. ANOVAs were performed to assess significant differences between the strains and the phases (exponential and stationary on Fig. 5). Significant over-abundant spots were detected at a 5% significance level ( $p$ -value  $<0.05$ ). Finally, these spots were refined by using a  $q$ -value  $<0.05$  to discard false positives, a power  $>0.8$  to ensure reproducibility among gels of with the same conditions and a fold number  $>2$  for the biological significance.

## 2.6. LC-MS/MS

Selected spots were excised manually, washed with  $100 \mu\text{L}$  25 mM  $\text{NH}_4\text{HCO}_3$ , followed by  $100 \mu\text{L}$  of 50% acetonitrile in 25 mM  $\text{NH}_4\text{HCO}_3$ . Proteins were then reduced by incubation with 10 mM DTT (1 h,  $57^\circ\text{C}$ ), and alkylated with 55 mM iodoacetamide (45 min at room temperature). Gel spots were further washed as described above. The proteins were digested overnight at  $37^\circ\text{C}$  by addition of 10–20  $\mu\text{L}$  trypsin ( $12.5 \text{ ng}\cdot\mu\text{L}^{-1}$  in 25 mM  $\text{NH}_4\text{HCO}_3$ ; modified trypsin purchased from Promega, Madison, WI). The resulting peptide mixture was acidified by the addition of  $1 \mu\text{L}$  of an aqueous

solution of formic acid (1% vol), stored at  $-20^{\circ}\text{C}$  and used for analysis without any further preparation.

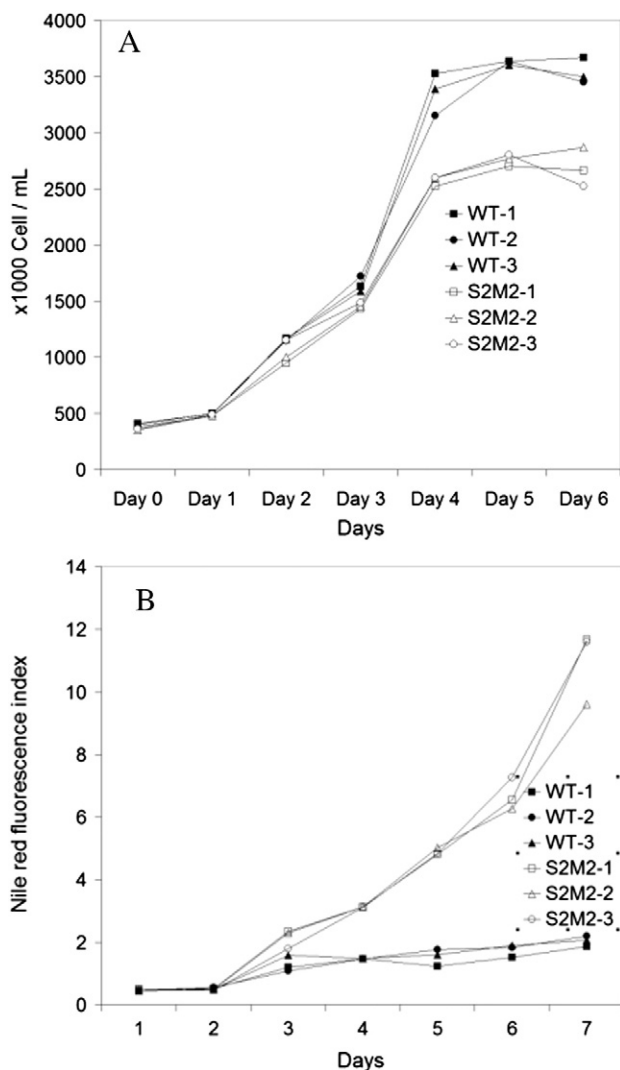
Nanoscale capillary liquid chromatography–tandem mass spectrometry analyses of the digested proteins were performed by using an Ultimate 3000 RSLC system (Dionex) coupled with a LTQ-Orbitrap VELOS mass spectrometer controlled by the X-Calibur version 2.1 software (Thermo Scientific). Chromatographic separation was conducted on a reverse-phase capillary column (Acclaim Pepmap C18 2  $\mu\text{m}$  100A, 75- $\mu\text{m}$  i.d.  $\times$  15-cm length, Thermo-Scientific) at a flow rate of 300  $\text{nL}\cdot\text{min}^{-1}$ . Mobile phase A was composed of 99.9% water and 0.1% formic acid; mobile phase B of 90% acetonitrile and 0.08% formic acid. The gradient consisted of a linear increase from 4% to 45% of B in 30 min followed by a rapid increase to 70% within 1 min.

Full MS scans were acquired at high resolution (FWMH 30,000) on the Orbitrap analyzer, while collision-induced dissociation (CID) MS/MS spectra were recorded on the five most intense ions in the linear LTQ traps. Dynamic exclusion

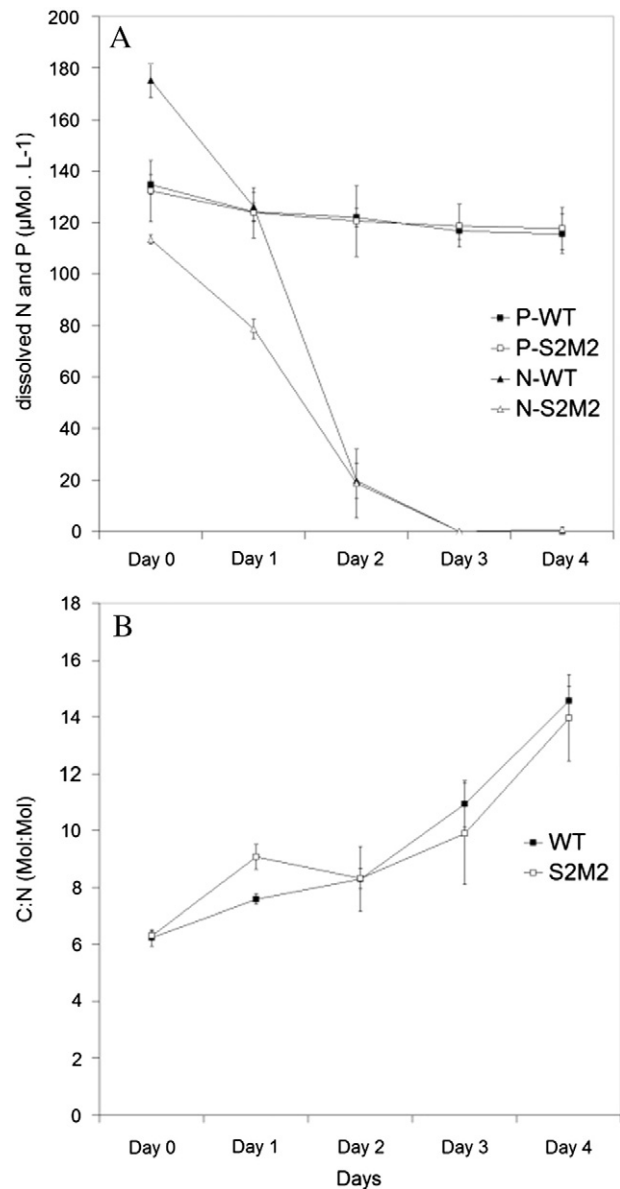
was employed within 60 s to prevent repetitive selection of the same peptide.

## 2.7. Database searches

Raw data collected during LC–MS/MS analyses were processed into MGF (Mascot Generic Format) files by using Proteome Discoverer version 1.7 (Thermo Scientific) and further searched against databases by using MASCOT Server version 2.2 (Matrix Science). One search was performed against a concatenated algae database (99898 sequences) built from UniProt release 2012\_01 (January 21, 2012) after restriction to the following taxonomies: *Isochrysis*, *Emiliania huxleyi*, *P. tricornutum*,



**Fig. 1 – (A) Growth and (B) neutral lipid accumulation of *Tisochrysis lutea* WT and S2M2 strains in a batch culture limited by nitrogen. Cultures were done in triplicate. Cell concentrations and Nile red fluorescence index per cell were calculated daily.**



**Fig. 2 – (A) Dissolved inorganic nitrogen and phosphorus in WT and S2M2 cultures. (B) C:N ratio was calculated from particulate carbon and nitrogen analysis. Means and standard errors were calculated from biological replicates and indicated on the graphs.**



*Thalassiosira pseudonana*, *C. reinhardtii*, *Ostreococcus tauri*, *Ostreococcus lucimarinus*, *Chlorella*, *Volvox carteri*, *Aureococcus*, *Micromonas* sp. A second database search was done against the six-frame translated de novo assembled *T. lutea* transcriptome. This transcriptome was recently obtained and assembled from raw data accessible in SRR824147 in the National Center for Biotechnology Information [35]. One missed trypsin cleavage was allowed. Carbamidomethylation of cysteines was set as a fixed modification, and oxidation of methionine as a variable modification. The mass tolerances in MS and MS/MS were set to 5 ppm and 0.5 Da respectively. Protein identifications were validated when a minimum of two unique peptides were matched in their sequence, with a MASCOT individual ion score above the threshold corresponding to a *p*-value of 0.05. The exponentially modified protein abundance index (emPAI) was calculated for each scoring protein [35] and the highest emPAI was selected as the most abundant protein of the spot.

The coding sequence (CDS) that contained peptides identified by MS was blasted (BLAST-X) against non-redundant protein sequences database (nr) from NCBI with “algae” as the filter. Molecular weight and pI were computed on the EXPASY website ([http://web.expasy.org/compute\\_pi](http://web.expasy.org/compute_pi)). Domains and motifs were sought by using Conserved Domain Database [36] and PRODOM [37] software, successively. The presence of signal peptides and location of membrane domains were predicted by Phobius [38] and SOSUI [39] software.

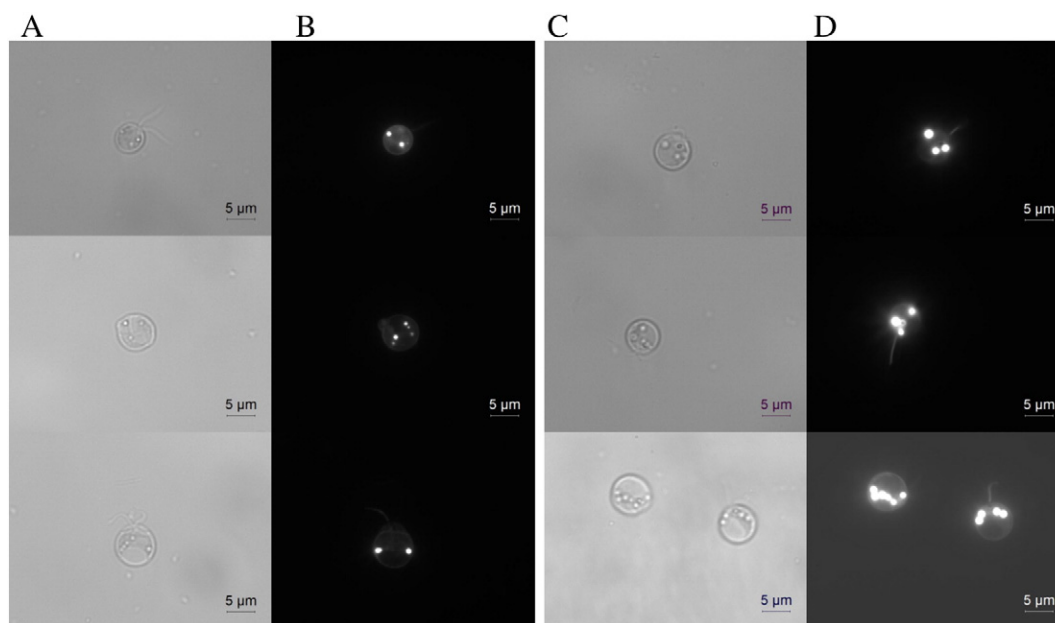
### 3. Results & discussion

#### 3.1. Growth and lipid accumulation

In most microalgae, the amount of neutral lipids increases under nitrogen starvation [40–43]. Neutral lipids accumulate in lipid droplets, whose size and number increase under

nitrogen starvation [23,44–48]. In this study, the detailed time course of growth and neutral lipid accumulation were assessed in nitrogen-limited batch cultures of *T. lutea* wild type and the mutant strain S2M2, selected for lipid over-accumulation. To obtain nitrogen-limiting conditions, a broth poor in nitrogen was used. The growth patterns of the two strains showed some similarity (Fig. 1). The stationary phase was reached in 4 days, and maximal cell concentrations were quite different between the strains ( $3.7 \times 10^6$  cell.mL<sup>-1</sup> for WT, and  $3.0 \times 10^6$  cell.mL<sup>-1</sup> for S2M2) (Fig. 1). Dissolved nitrogen (N) and phosphorus (P) concentrations in the extra-cellular medium were monitored over the first 5 days of the culture (Fig. 2). They constitute the two major substrates for microalgae. While the amount of P decreased slightly, the amount of N decreased drastically to reach 0 μmol.L<sup>-1</sup> at Day 3. The C:N ratios of cells increased from Day 2 to Day 4 (Fig. 2) confirming the nitrogen limitation [49].

Overall lipid accumulation was followed by using Nile red fluorescence. In both strains, total Nile red fluorescence increased until Day 6 (see supplementary data). In order to take account the increase of cell concentration, the index of fluorescence per cell was calculated. After 2 days, it increased in both strains until the end of the experiment (Fig. 1). This confirms that the increase of neutral lipid accumulation was correlated with nitrogen limitation, as previously shown for *I. galbana* [50]. Surprisingly, this increase did not continue so highly in the wild-type strain during the stationary phase, unlike in the S2M2 strain, where the amount of neutral lipids continued to increase until the end of the experiment. At Day 2, the mean of Nile red fluorescence index of S2M2 culture was 1.6-fold higher than that of WT, by Day 4 it was 3.2-fold higher and by Day 6 it was 5.4-fold higher. Cytometric analysis was performed to measure the individual cellular Nile red fluorescence of samples of 30,000 cells. The averages of cells fluorescence suggested an increase of lipid concentration



**Fig. 3 – Microscopic observations of *Tisochrysis lutea* WT (columns A and B) and S2M2 (C and D) strains. Cells were observed by transmissive optic microscopy and epifluorescence microscopy after Nile red staining. Sizes and number of lipid droplets were revealed by Nile red coloration of neutral lipids.**

per cell during the experiment for both strains. In addition, the averages of cell fluorescence inside each population were greater in S2M2 than in WT strain. These results are in accordance with the results of overall fluorescence measured with the spectrophotometer (see above). On other point, the distributions of Nile red fluorescence per cell measured by flow cytometry were analyzed on density histograms (see supplementary data). They revealed that WT and S2M2 populations followed normal distributions of Nile red fluorescence. This indicates that lipid accumulation is homogenous inside each one of both populations. In other words, the differences of lipid accumulation are not caused by the effect of a sub-population but concern the entire populations. Microscopic observations of cells after Nile red staining at Day 5 showed that the number of lipid droplets (LD) was about two per cell in WT cells and between 3 and 6 in S2M2 cells (Fig. 3). Droplet sizes appeared larger in S2M2 cells than in WT cells. These results are in accordance with the spectrofluorometric and cytometric analysis that showed higher Nile red fluorescence in S2M2 strain. Because the effect of nitrogen starvation on lipid accumulation is greater in strain S2M2, we propose that this S2M2 strain would make a good model to study the metabolism and accumulation of neutral lipids in *T. lutea* in the same manner as a starchless mutant was used for the study of lipid accumulation in *C. reinhardtii* [13,47].

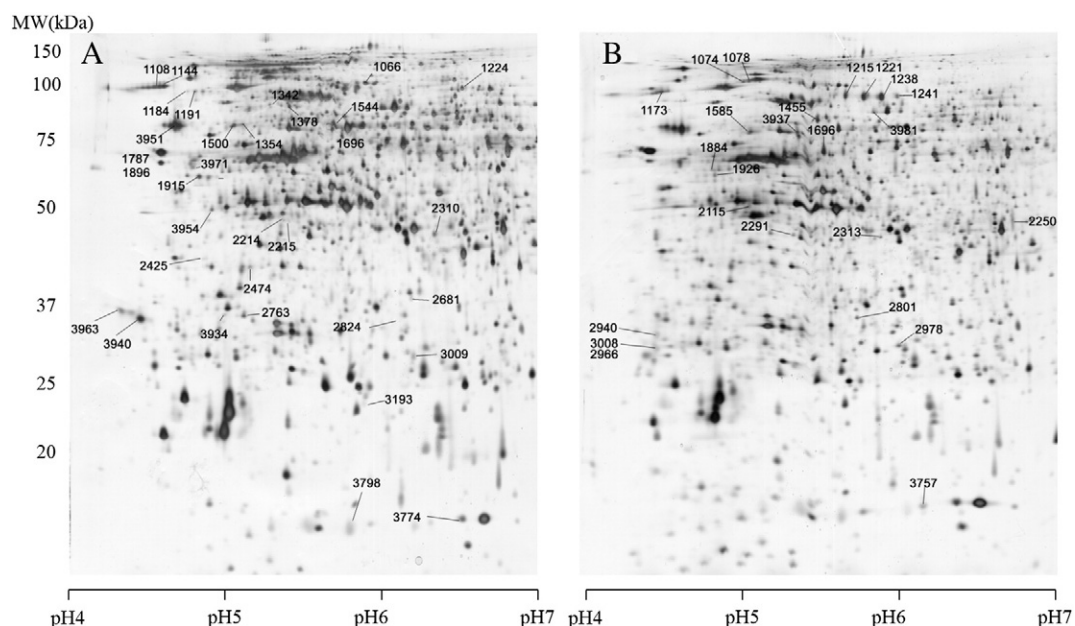
### 3.2. Comparative proteomics and functional classification

Proteomics was applied for the two strains (WT and S2M2) i) at exponential phase (Day 2) when neutral lipid accumulation was low and dissolved nitrogen still available, ii) at the beginning of stationary phase (Day 5) when neutral lipid accumulation was high and absence of dissolved nitrogen limited the growth. The

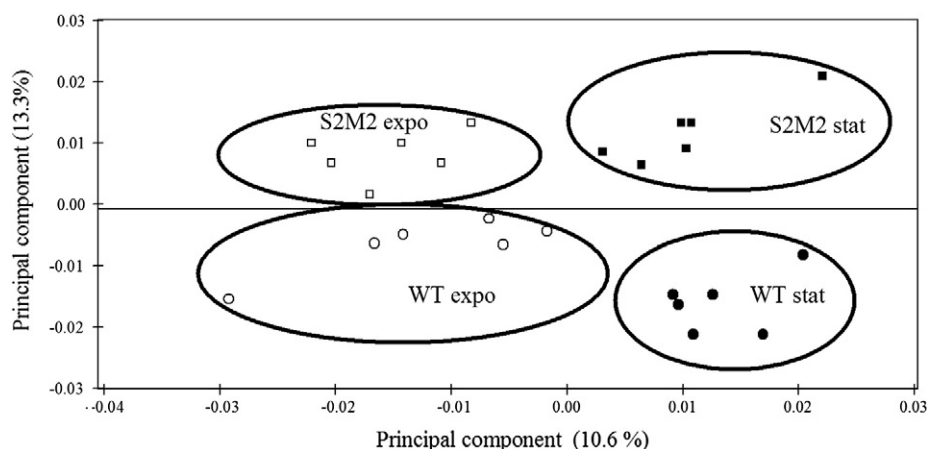
aim was to reveal the proteins whose abundance is regulated by nitrogen starvation, and the proteins whose abundance is different between the two strains. Two-dimensional electrophoresis analyses were performed. This robust technique was described as a valuable tool to separate with good resolution and quantify in the same time major proteins in non-model species. For each of the four conditions, biological triplicates and technical duplicates were performed. About 1850 spots were visualized on each of the 2-DE gels (Fig. 4). Principal component analysis of the complete dataset (24 gels) clearly showed four distinct clusters of gels corresponding to the four experimental conditions (Fig. 5). This suggests a modification of the proteome of the mutant strain, as well as induction of specific proteomes for both strains during N-limited batch stationary phase.

Statistical analysis of normalized volume of each spot on each gel was performed to select spots with difference in spot volume ( $p$  value  $< 0.05$ ). Considering the large number of tests (1850 spots), false discovery rate (FDR) was measured and significant positives were selected with a FDR  $q$ -value threshold of 5%. In the WT strain, 19 spots were up-accumulated at Day 5 (vs. Day 2) and 33 were down accumulated. In the S2M2 strain, 4 spots were up-accumulated at Day 5 (vs. Day 2) and 24 were down accumulated. In addition, 42 spots have a difference of intensity between the two strains at Day 2 (18 down and 24 up-expressed in S2M2 vs WT) and 73 at Day 5 (39 down and 34 up-expressed in S2M2 vs WT).

57 spots showing significant differences on analytical gels (Fig. 4) were sufficiently concentrated for been visualized on preparative gels stained with Coomassie blue. They were picked and analyzed by MS. Whereas searching against Uniprot databases only allowed the identification of six spots,



**Fig. 4** – 2-DE of whole cell proteoms of *Tisochrysis lutea* WT (A) and S2M2 (B) strains at early stationary phase of nitrogen limited batch cultures. Proteins of both strains at exponential and early stationary phases were extracted. Biological triplicates and technical duplicates were 30  $\mu$ g of whole cell proteins were separated on pH 4–7 gradient and 12% polyacrylamide SDS gel, and revealed by silver staining. 24 gels were included for image and statistical analysis. Identified spots by MS–MS are localized on the gels.



**Fig. 5 – Principal component analysis performed on the complete data set of the 24 2-DE gels according to variations in the normalized volume of the 1850 spots.**

searching against the *T. lutea* transcriptome led to the identification of 48 spots corresponding to 40 different single transcripts. This difference arose because sometimes more than one spot was affiliated to the same transcript; a result consistent with the observations of Guarnieri et al. [21]. The identification of proteins by comparing the mass profiles with in silico data could be done much more efficiently by using the homemade transcriptome of *T. lutea* than by using public data on other algae species. Nine spots failed to produce any unambiguous MS identification.

Manual annotation of translated transcripts was performed to obtain functional insights on identified sequences. BLAST-X and domain research allowed assignment of putative functions for 27 proteins, classified into nine metabolic groups (Table.1). Six other proteins had a homolog in other algae species but their function remains unknown (Table.1). They were named “conserved unknown proteins”. Among these six proteins, one has a MORN-repeat domain and three have a NAD-Rossmann-fold domain including one that has a FabG domain. To date, seven proteins have no homolog in public databases. Although a C1-peptidase domain could be found for one of them and a methyltransferase (MTase) domain was found for another, their functions remain unknown. For transcripts whose CDS was clearly identified, theoretical molecular weight and pI (MW/pI) were quite similar to experimental MW/pI on 2-DE gels (Table.1).

### 3.3. Proteins affected by nitrogen starvation

About 2.5% of the analyzed WT proteome was affected by nitrogen starvation. Numerous metabolic pathways were affected, but the abundance of the stress proteins identified in this study (SuperOxide Dismutase (SOD), Protein Disulfide Isomerase (Pdi), Clp protease and Heat Shock Protein Hsp60) was not affected. This may be because the sampling under nitrogen starvation corresponded to an early step of stationary phase when the growth was limited by nitrogen starvation, but cells had not yet triggered a stress response. This suggests that the comparative proteomic analysis shows the effects of a halt in growth due to nitrogen starvation but not the response to the stress that could occur later in the stationary phase.

Thirteen proteins identified in this study were less abundant during nitrogen starvation (Table 2). These include three plastid ribosomal proteins, the CF1 beta subunit of ATP synthase and the two subunits of rubisco (RuBisCo Large subunit and Small subunit (RBCL and RBCS)) involved in the first major step of carbon fixation. RBCL and RBCS co-accumulated in the same way during nitrogen starvation and their ORFs were located on the same transcript of *T. lutea*. These two ORFs are located on the same operon in prymnesiophyte plastids [51]. This suggests that transcriptional regulation of the whole operon could occur, leading to the regulation of protein abundance during stationary phase. Three enzymes involved in the pigment biosynthetic process were also down-accumulated at stationary phase including (1) uroporphyrinogen decarboxylase (fold = 3.1) and coproporphyrinogen III oxidase (fold = 2.1), successively involved in the porphyrin and chlorophyll metabolic pathways; and (2) geranylgeranyl pyrophosphate synthetase (GGPP synthase) (fold = 2.4), which plays a role in the level of carotenogenesis. Two proteins of lipid metabolism were down-accumulated by nitrogen starvation, including the plastid beta-ketoacyl-ACP reductase (FabG) (fold = 2.5) and the “FabG domain-containing conserved unknown protein” (fold = 4.7) (Table. 6). FabG catalyzes the NADPH-dependent reduction of beta-ketoacyl-ACP substrates to beta-hydroxyacyl-ACP products, the first reductive step in the elongation cycle of fatty acid biosynthesis. The “FabG domain-containing conserved unknown protein” was down-accumulated in the same manner but its function remains more uncertain.

To resume, nitrogen deprivation induced a decrease of proteins involved in: i) carbon fixation (RBCL and RBCS), ii) the pigment biosynthetic process (GGPP synthase, UPIII decarboxylase and CPIII oxidase), iii) energetic metabolism (ATP synthase), and iv) translation processes (3 ribosomal proteins) and v) fatty acid metabolism (FabG and FabG domain-containing conserved unknown protein). These results are in good agreement with previous transcriptomic and proteomic studies on the chlorophyceae *C. reinhardtii* [11,48,52–54], in the eustigmatophyte *Nannochloropsis* sp., the chlorophyte *Micractinium pusillum*, and the diatom *P. tricornutum* [15–18,52,55]. All these results suggest that a halt in growth in response to nitrogen starvation causes similar decreases in

Table 1 – MS identification of spots.

| Class                              | No spot | Mr (kDa)/PI experimental | Mr (kDa)/PI theoretical | Unique peptide matched | Hypothetical function  | NCBI accession number   |          |
|------------------------------------|---------|--------------------------|-------------------------|------------------------|--|---|----------|
| Lipid metabolism                   | 1224    | 90/6.5                   | 78/5.9                  | 50                     | acetyl-CoA/propionyl-CoA carboxylase                         | KF233705  |          |
| Carbohydrate catabolism            | 3009    | 35/6.2                   | 30/8.5                  | 18                     | FabG   | KF233706  |          |
|                                    | 1074    | 110/5.2                  | 99/4.5                  | 35                     | Glycoside hydrolase family                                   | KF233707  |          |
|                                    | 1078    | 110//5.3                 |                         | 30                     | GH30   |   |          |
|                                    | 1215    | 90/5.8                   | 81/6.1                  | 58                     | Glycoside hydrolase family                                   | KF233708  |          |
|                                    | 1221    | 90/6.0                   |                         | 163                    | GH16   |   |          |
|                                    | 1238    | 90/6.1                   |                         | 106                    |  |   |          |
| Amino acid metabolism              | 1241    | 90/6.2                   |                         | 37                     |  |   |          |
|                                    | 1108    | 105/4.6                  | 108/4.4                 | 30                     | Periplasmic L-amino acid oxidase                             | KF233709  |          |
|                                    | 1144    | 105/4.7                  |                         | 74                     |  |   |          |
|                                    | 1173    | 100/4.7                  |                         | 88                     |  |   |          |
| Energy metabolism; photosynthesis. | 3981    | 90/5.85                  | 78/5.7                  | 141                    | Glutamine synthetase III                                     | KF233710  |          |
|                                    | 1787    | 65/4.6                   | 54/5.9                  | 19                     | RBCL   | KF233711  |          |
|                                    | 3774    | 10/6.6                   | 9.2/4.7                 | 15                     | RBCS   | KF233712  |          |
|                                    | 3798    | 10/5.7                   |                         | 26                     |  |   |          |
|                                    | 3971    | 65/4.8                   | 51/4.6                  | 72                     | ATP synthase CF1 beta subunit                                | KF233713  |          |
|                                    | 1926    | 60/4.9                   | 54/5                    | 23                     | Ubiquinol: Cytochrome c oxidoreductase 50 kDa core 1 subunit | KF233714  |          |
|                                    | 1884    | 60/4.95                  |                         | 44                     |  |   |          |
|                                    |         | 1544                     | 60/5.6                  | 66/5.1                 | 150  | ATP synthase  | KF233715 |
|                                    |         | 2310                     | 42/6.4                  | 50/5.6                 | 38   | Chloroplast ferredoxin NADP(+) reductase                        | KF233716 |
|                                    |         | 1354                     | 75/5.1                  | 77/6.6                 | 31   | Ferredoxin  | KF233717 |
|                                    |         | 2250                     | 40/6.7                  | 36/5.9                 | 12   | GAPDH   | KF233718 |
|                                    |         | 1696                     | 65/5.7                  | 37/4.9                 | 61   | GAPDH   | KF233719 |
| Translation                        | 3937    | 73/5.5                   |                         | 14                     |  |   |          |
|                                    | 2474    | 40/5.2                   | 37.4/4.4                | 20                     | 30S Plastidal ribosomal protein S1                           | KF233720  |          |
|                                    | 3193    | 22/5.8                   | 20/9.8                  | 14                     | 30S Plastidal ribosomal protein S15                          | KF233721  |          |
| Pigment biosynthesis process       | 3954    | 47/4.9                   | 34/5.0                  | 34                     | 30S Plastidal ribosomal protein S1                           | KF233722  |          |
|                                    | 2214    | 42/5.2                   | 37/4.4                  | 44                     | Uroporphyrinogen decarboxylase, chloroplast precursor        | KF233723  |          |
|                                    |         | 2215                     | 42/5.3                  | 41/5.2                 | 23   | Chloroplast coproporphyrinogen III oxidase                      | KF233724 |
|                                    |         | 2425                     | 40/4.7                  | 34/4.5                 | 6  | Geranylgeranyl pyrophosphate synthetase                         | KF233725 |
|                                    |         | 3757                     | 13/6.3                  | 14/6                   | 9  | Superoxide dismutase Ni-type (SOD)                              | KF233726 |
| Stress                             | 1585    | 75/6                     | 51/4.6                  | 8                      | Protein disulfide isomerase (Pdi)                            | KF233727  |          |
|                                    | 1066    | 115/5.8                  | 90/5.4                  | 131                    | Clp protease ATP binding subunit                             | KF233728  |          |
|                                    | 1342    | 90/5.3                   | 135/4.5                 | 47                     | HSP60  | KF233729  |          |
|                                    | 1184    | 100/4.7                  | 72/7.9                  | 53                     | Luminal binding HSP70  | KF233730  |          |
|                                    | 1191    | 100/4.8                  |                         | 71                     |  |   |          |
| Cell division                      | 2801    | 32/5.8                   | 30/5.1                  | 37                     | Septum-site determining protein                              | KF233731  |          |
| Conserved unknown proteins         | 2313    | 42/5.9                   | 34/5.0                  | 10                     | MORN repeat domain containing conserved unknown protein      | KF233732  |          |
|                                    |         | 3951                     | 75/5                    | 70/4.7                 | 106  | Coccolith scale associated protein-1                            | KF233733 |
|                                    |         | 2681                     | 37/6.1                  | 31/5.7                 | 22   | FabG domain containing conserved unknown protein                | KF233734 |
|                                    |         | 1500                     | 75/5.0                  | 58/4.8                 | 41   | NAD-Rossmann-fold domain containing conserved unknown protein 1 | KF233735 |
|                                    |         | 2291                     | 40/5.5                  | 43/5.4                 | 15   | NAD-Rossmann-fold domain containing conserved unknown protein 2 | KF233736 |
|                                    |         | 2978                     | 27/6.0                  | 27/6.2                 | 106  | Conserved unknown protein 28404                                 | KF233737 |
|                                    |         | 2824                     | 30/6.2                  | 25/5.1                 | 20   | Unknown protein 18353   | KF233738 |
|                                    |         | 3934                     | 30/5.0                  | 27/4.4                 | 33   | Unknown protein 27667   | KF233739 |
|                                    |         | 2763                     | 30/5.1                  | 27/4.5                 | 24   | Unknown protein 36678   | KF233740 |
|                                    |         | 1378                     | 90/5.5                  | 58/5.1                 | 35   | C1 Peptidase domain-containing unknown protein 34982            | KF233741 |
| Unknown proteins                   | 1455    | 80/5.6                   |                         | 21                     |  |   |          |
|                                    | 3973    |                          | 37/4.8                  | 21                     | Unknown protein 1821   | KF233742  |          |
|                                    | 1915    | 55/4.8                   |                         | 25                     |  |   |          |
|                                    | 2115    | 48/5.2                   |                         | 16                     |  |   |          |
|                                    | 1896    | 65/4.6                   | 45/4.7                  | 9                      | Methyltransferase domain containing unknown protein 30039    | KF233743  |          |

Table 1 (continued)

| Class            | No spot | Mr (kDa)/PI experimental | Mr (kDa)/PI theoretical | Unique peptide matched | Hypothetical function | NCBI accession number |
|------------------|---------|--------------------------|-------------------------|------------------------|-----------------------|-----------------------|
| Unknown proteins | 2940    | 26/4.6                   | 25/4.7                  | 10                     | Unknown protein 27017 | KF233744              |
|                  | 2966    | 24/4.6                   |                         | 4                      |                       |                       |
|                  | 3008    | 25/4.6                   |                         | 10                     |                       |                       |
|                  | 3940    | 29/4.2                   |                         | 14                     |                       |                       |
|                  | 3963    | 30/4.3                   |                         | 12                     |                       |                       |

Table 2 – Protein down accumulated in WT and S2M2 strains during nitrogen starvation.

| Hypothetical function                                 | WT   |                      | S2M2 |                      | No spot | Class                             |
|---|------|----------------------|------|----------------------|---------|-----------------------------------|
|   | Fold | ANOVA (p)            | Fold | ANOVA (p)            |         |                                   |
| FabG  | 2.5  | 8.069e <sup>-8</sup> | 1.2  | 0.02                 | 3009    | Lipid metabolism                  |
| FabG domain-containing conserved unknown protein      | 4.7  | 2.524e <sup>-8</sup> | 1.5  | 0.025                | 2681    | Conserved unknown proteins        |
| RBCL  | 3.0  | 0.002                | 2.0  | 0.0054               | 1787    | Energy metabolism; photosynthesis |
| RBCS  | 3.3  | 2.426e <sup>-5</sup> | 2.6  | 0.339e <sup>-3</sup> | 3774    |                                   |
|   | 2.8  | 1.793e <sup>-5</sup> | 2.2  | 6.14e <sup>-5</sup>  | 3798    |                                   |
| ATP synthase CF1 beta subunit                         | 2.4  | 5.457e <sup>-4</sup> | 2.0  | 0.049                | 3971    | Translation                       |
| 30S Plastidal ribosomal protein S1                    | 2.0  | 5.479e <sup>-7</sup> | 1.8  | 0.168e <sup>-3</sup> | 2474    |                                   |
| 30S Plastidal ribosomal protein S15                   | 2.5  | 7.272e <sup>-5</sup> | 2.1  | 0.287e <sup>-3</sup> | 3193    |                                   |
| 30S Plastidal ribosomal protein S1                    | 2.6  | 4.852e <sup>-6</sup> | 1.8  | 0.929e <sup>-3</sup> | 3954    |                                   |
| Uroporphyrinogen decarboxylase, chloroplast precursor | 3.1  | 2.913e <sup>-9</sup> | 2.1  | 4.22e <sup>-5</sup>  | 2214    | Pigment biosynthetic process      |
| Chloroplast coproporphyrinogen III oxidase            | 2.1  | 8.939e <sup>-7</sup> | 1.6  | 1.44e <sup>-3</sup>  | 2215    | Unknown proteins                  |
| Geranylgeranyl pyrophosphate synthetase               | 2.4  | 2.478e <sup>-5</sup> | 1.5  | 2.88e <sup>-3</sup>  | 2425    |                                   |
| Unknown protein 18353                                 | 4.4  | 3.530e <sup>-9</sup> | 2.5  | 5.54e <sup>-5</sup>  | 2824    |                                   |
| Unknown protein 27667                                 | 3.0  | 5.557e <sup>-7</sup> | 1.9  | 3.19e <sup>-5</sup>  | 3934    |                                   |
| Unknown protein 36678                                 | 4.4  | 1.246e <sup>-7</sup> | 1.5  | 4.85e <sup>-3</sup>  | 2763    |                                   |

several biological activities in most microalgae. Longworth et al. interpreted these biological responses as an entry into a type of dormancy of the microalgae [52].

Three proteins up-accumulating during nitrogen starvation were identified (Table. 3). These include acetyl-CoA/propionyl-CoA carboxylase (ACCase) (fold = 2.9), which plays a major role in the first steps of fatty acid biosynthesis by catalyzing the carboxylation of acetyl-CoA to produce malonyl-CoA. Its role in fatty acid regulation has been demonstrated for the *Isochrysidales* [26,27]. Another of the proteins has a strong homology with the coccolith scale associated protein (CSAP1) of *Pleurochrysis carterae* and with an unknown predicted protein of *P. tricornutum*. To our knowledge, the function of this protein is unknown, but PRODOM software identified a pyridoxal-phosphate-dependent decarboxylase domain

specific to group II decarboxylase, which includes aromatic-L-amino-acid decarboxylases, tyrosine decarboxylase and histidine decarboxylase. Four isoforms of CSAP-1 of the same size increased by 6.2-fold in relative abundance during nitrogen starvation (spot 3951 on Fig. 4). CSAP-1 contains a DDC-GAD-HDC-YDC decarboxylase domain and could be involved in the decarboxylation of aromatic-L-amino-acid tyrosine or histidine. However, its function remains unclear. Homologs were found in the prymnesiophyte *P. carterae* transcriptome and in the *P. tricornutum* genome, but not in other algae species, even in other prymnesiophyte transcriptomes. RNAseq analysis of *P. tricornutum* showed an up-regulation of this protein under nitrogen starvation and Valenzuela et al. speculated that this protein might play a role in inorganic carbon homeostasis [18]. Because this protein is among those that are most up-

Table 3 – Protein up accumulated in WT and S2M2 strains during nitrogen starvation.

| Hypothetical function                         | WT   |                      | S2M2 |                     | No spot | Class                      |
|---|------|----------------------|------|---------------------|---------|----------------------------|
|   | Fold | ANOVA (p)            | Fold | ANOVA (p)           |         |                            |
| Acetyl-CoA/propionyl-CoA carboxylase          | 2.9  | 0.003                | 1.6  | 0.196               | 1224    | Lipid metabolism           |
| Periplasmic L-amino acid oxidase              | 8.2  | 7.794e <sup>-7</sup> | 1.2  | 0.44                | 1108    | Amino acid metabolism      |
|   | 4.3  | 1.160e <sup>-6</sup> | 1.2  | 0.277               | 1144    |                            |
| Coccolith scale associated protein-1 (CSAP-1) | 6.2  | 2.802e <sup>-6</sup> | 2.4  | 2.22e <sup>-3</sup> | 3951    | Conserved unknown proteins |

**Table 4 – Protein down accumulated in S2M2 strain.**

| Hypothetical function   | Exponential phase |                      | Stationary phase |                      | No spot | Class                              |
|---|-------------------|----------------------|------------------|----------------------|---------|------------------------------------|
|   | Fold              | ANOVA (p)            | Fold             | ANOVA (p)            |         |                                    |
| Glutamine synthetase III  | 1.8               | 0.066                | 1.8              | 0.005                | 3981    | Amino acid metabolism              |
| Periplasmic L-amino acid oxidase                                | 1.3               | 0.294                | Off              | 7.794e <sup>-5</sup> | 1108    |                                    |
|   | 1.4               | 0.014                | off              | 1.160e <sup>-4</sup> | 1144    |                                    |
| ATP synthase  | 1.9               | 0.017                | 2.5              | 6.6e <sup>-5</sup>   | 1544    | Energy metabolism; photosynthesis. |
| Chloroplast ferredoxin NADP(+) reductase                        | 2.0               | 0.221e <sup>-3</sup> | 2.2              | 0.33e <sup>-3</sup>  | 2310    |                                    |
| Ferredoxin  | Off               | 1.49e <sup>-5</sup>  | Off              | 3.339e <sup>-5</sup> | 1354    |                                    |
| Clp protease ATP binding subunit                                | 1.7               | 0.013                | 2.3              | 4.11e <sup>-4</sup>  | 1066    | Stress                             |
| HSP60   | 1.5               | 0.019                | Off              | 5.08e <sup>-5</sup>  | 1342    |                                    |
| Luminal binding HSP70   | Off               | 0.652e <sup>-3</sup> | Off              | 0.027                | 1184    |                                    |
|   | Off               | 0.026                | Off              | 0.009                | 1191    |                                    |
| Coccolith scale associated protein-1                            | 1.2               | 0.557                | 2.1              | 0.017                | 3951    | Conserved unknown proteins         |
| NAD-Rossmann-fold domain containing conserved unknown protein 1 | Off               | 1.04e <sup>-7</sup>  | Off              | 9.504e <sup>-5</sup> | 1500    |                                    |
| Unknown protein   | 2.1               | 7.95e <sup>-4</sup>  | 1.4              | 0.073                | 2763    | Unknown proteins                   |
| Unknown protein   | 1.2               | 0.358                | 2.9              | 0.019                | 3973    |                                    |
| Methyltransferase domain containing unknown protein             | 1.6               | 0.7e <sup>-2</sup>   | 2.1              | 0.0054               | 1896    |                                    |
| C1_Peptidase domain containing unknown protein                  | 4.1               | 1.08e <sup>-5</sup>  | Off              | 1.06e <sup>-5</sup>  | 1378    |                                    |
| Unknown protein 1821  | Off               | 2.73e <sup>-5</sup>  | Off              | 3.5e <sup>-4</sup>   | 1915    |                                    |
| Unknown protein 27017   | Off               | 7.83e <sup>-5</sup>  | Off              | 1.23e <sup>-5</sup>  | 3940    |                                    |
|   | Off               | 8.57e <sup>-4</sup>  | Off              | 6.91e <sup>-5</sup>  | 3963    |                                    |

accumulated under nitrogen deprivation, a functional analysis should be made to identify its molecular and cellular functions. Four isoforms of Coccolith Scale Associated Protein-1 (CSAP1) of same size were increased by 6.2-fold in relative abundance during nitrogen starvation (spot 3951 on Fig. 4). They probably correspond to different post-translational forms of the same protein. Two closed isoforms of the periplasmic L-amino acid oxidase (PAAOx) of the same size increased by 8.2- to 4.3-fold in relative abundance with nitrogen deprivation (spots 1108 and 1144 on Fig. 4 A) (Table. 3). Vallon et al. defined PAAOx as a scavenger of ammonium from extracellular amino acids in *C. reinhardtii* [56]. In silico analysis of the coding region revealed the presence of a signal peptide and transmembrane region. This suggests that this enzyme is anchored to the membrane and transported to the plasma membrane. This protein could be involved in the access of extracellular organic nitrogen in response to nitrogen deprivation.

### 3.4. Proteins affected by strain selection

The abundances of 33 spots identified by MS were found to differ between the two strains, whatever the phase of culture (Table. 4 and Table. 5). Five proteins involved in stress response were identified. The ATP-binding subunit of Clp protease and the two chaperones Hsp60 and Hsp70 were less abundant in the S2M2 strain, whereas superoxide dismutase Ni-type (SOD) and disulfide isomerase (Pdi) were more abundant. Because UV mutations and cytometric sorting generate cellular stress, we suggest that there was selection for cells acclimated to stress in the S2M2 population. Five identified proteins involved in respiration, photosynthesis and glycolysis were affected by N deprivation, suggesting an overall reorganization of the energetic metabolism in the selected S2M2 strain: two

glyceraldehyde 3-phosphate dehydrogenases (GAPDH), which are key enzymes of glycolysis, and the core 1 subunit of ubiquinol:cytochrome c oxidoreductase involved in the mitochondrial respiratory chain were up-accumulated in S2M2 strain. One ATP synthase and two proteins of photosynthesis (the chloroplast ferredoxin NADP reductase and the ferredoxin) were less abundant. The ferredoxin is the last protein of photosystem I and serves as a substrate for the chloroplast ferredoxin NADP reductase.

Finally, two Glycoside Hydrolases including GH16 (spots 1221, 1238, 1241 and 1215 on Fig. 4) and GH30 (spots 1074 and 1078 in Fig. 4) were abundant in the S2M2 strain, but were not detected in the WT strain (Table. 6). For these two proteins, several spots with the same molecular weight were identified, suggesting post-translational modifications. The analysis of coding regions revealed a trans-membrane region for each one of these enzymes and a signal peptide for GH30, suggesting that it had a specific cellular localisation. Glycoside hydrolases are a widespread group of enzymes that hydrolyze the glycosidic bond between two or more carbohydrates or between a carbohydrate and a non-carbohydrate moiety [57]. The GH16 and GH30 families are responsible for the degradation of many substrates and are well described on the carbohydrate-active enzymes (CAZy) database (<http://www.cazy.org>). Enzyme activities currently assigned within GH30 family include  $\beta$ -glucosidase,  $\beta$ -xylosidase and endo- $\beta$ -1,6-glucanase [57,58]. Enzyme activities currently assigned within GH16 family include enzymes involved in the hydrolysis of storage carbohydrates, such as laminarinases, beta-agarase and endo-1,3-beta-glucanases. To our knowledge, the nature of storage and cell wall carbohydrates in *T. lutea* has never been clearly identified and the substrates of these two enzymes should be identified for more accurate conclusions. However, we suggest that the

**Table 5 – Protein up accumulated in S2M2 strain.**

| Hypothetical function   | Exponential phase |                      | Stationary phase |                      | No spot | Class                      |                                    |
|---|-------------------|----------------------|------------------|----------------------|---------|----------------------------|------------------------------------|
|   | Fold              | ANOVA (p)            | Fold             | ANOVA (p)            |         |                            |                                    |
| FabG  | 1.1               | 0.55                 | 2.5              | 7.37e <sup>-5</sup>  | 3009    | Lipid metabolism           |                                    |
| Glycosyl hydrolase family GH30                                  | On                | 9.25e <sup>-6</sup>  | On               | 1.331e <sup>-6</sup> | 1074    | Glucide catabolism         |                                    |
|   | On                | 9.12e <sup>-6</sup>  | On               | 2.60e <sup>-4</sup>  | 1078    |                            |                                    |
|   | On                | 1.93e <sup>-5</sup>  | On               | 2.1e <sup>-5</sup>   | 1221    |                            |                                    |
| Glycosyl hydrolase family GH16                                  | On                | 1.73e <sup>-7</sup>  | On               | 4.07e <sup>-7</sup>  | 1238    |                            |                                    |
|   | On                | 5.36e <sup>-5</sup>  | On               | 8.0e <sup>-5</sup>   | 1241    |                            |                                    |
|   | 2.1               | 0.002                | 1.3              | 0.135                | 1215    |                            |                                    |
|   | 1.4               | 0.16                 | 2.3              | 8.42e <sup>-7</sup>  | 2801    |                            | Cell division                      |
|   | On                | 8.15e <sup>-6</sup>  | 1.3              | 0.118                | 1884    |                            | Energy metabolism; photosynthesis. |
| Septum-site determining protein                                 | On                | 9.5e <sup>-8</sup>   | On               | 8.59e <sup>-5</sup>  | 1926    |                            |                                    |
| Ubiquinol:cytochrome c oxidoreductase                           | 1.3               | 0.211                | 2.5              | 3.46e <sup>-4</sup>  | 2250    |                            |                                    |
| 50 kDa core 1 subunit   | 2.0               | 2.72e <sup>-5</sup>  | 2.2              | 1.97e <sup>-4</sup>  | 1696    |                            |                                    |
| GAPDH   | 2.0               | 1.52e <sup>-4</sup>  | 3.2              | 2.38e <sup>-7</sup>  | 3937    |                            |                                    |
| GAPDH   | 1.2               | 0.565                | 2.0              | 2.0e <sup>-4</sup>   | 3757    | Stress                     |                                    |
| Superoxide dismutase Ni-type (SOD)                              | 2.6               | 7.67e <sup>-5</sup>  | 1.6              | 0.0016               | 1585    |                            |                                    |
| Protein disulfide isomerase (Pdi)                               | On                | 9.23e <sup>-6</sup>  | On               | 0.0017               | 2291    | Conserved unknown proteins |                                    |
| NAD-Rossmann-fold domain containing conserved unknown protein 2 | 1.2               | 0.206                | 4.7              | 2.524e <sup>-5</sup> | 2681    |                            |                                    |
| FabG domain-containing conserved unknown protein                | 1.5               | 0.039                | 2.1              | 3.43e <sup>-5</sup>  | 2313    |                            |                                    |
| MORN repeat domain containing conserved unknown protein         | 1.3               | 0.027                | 2.0              | 4.27e <sup>-5</sup>  | 2978    |                            |                                    |
| Conserved unknown protein                                       | On                | 8.97e <sup>-5</sup>  | On               | 0.179                | 2115    | Unknown proteins           |                                    |
| Unknown protein 1821  | On                | 0.004                | On               | 1.19e <sup>-4</sup>  | 2940    |                            |                                    |
| Unknown protein 27017   | On                | 9.632e <sup>-5</sup> | On               | 0.016                | 3008    |                            |                                    |
| Unknown protein 27017   | 3.1               | 3.91e <sup>-4</sup>  | 2.5              | 4.96e <sup>-6</sup>  | 1455    |                            |                                    |
| C1 Peptidase domain-containing unknown protein                  | 2.7               | 6.77e <sup>-5</sup>  | 3.4              | 3.35e <sup>-5</sup>  | 2966    |                            |                                    |

up-regulation of these two glycoside hydrolases would lead to a better availability of hydrolysable carbohydrates for glycolysis. Interestingly, two glyceraldehyde 3-phosphate dehydrogenase (GAPDHs) enzymes known to be mainly involved in glycolysis were more abundant in the S2M2 strain than the WT. Glycolysis is an important source of acetyl-CoA. Studies of starchless mutants of the green algae *C. reinhardtii* strongly suggested that the carbon flux between the biosynthesis of starch and triacylglycerides is interrelated and that the carbon sources for TAG biosynthesis could be largely derived from carbohydrates and acetyl-CoA metabolism [13]. In the same way, our results suggest that the metabolism upstream of de novo fatty acid biosynthesis (carbohydrate catabolism and glycolysis) are determinant for the over production of lipids in S2M2 strain. Thus, like *C. reinhardtii*, lipid accumulation in *T. lutea* could be closely related to carbohydrate metabolism [13].

### 3.5. Proteins impacted by strain selection and nitrogen starvation

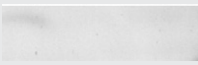
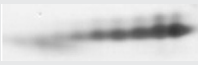
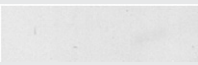
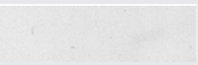

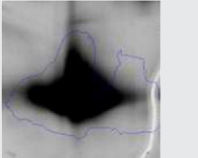
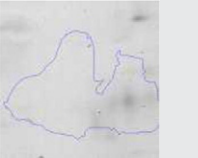
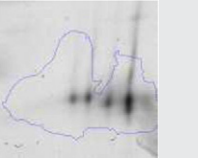
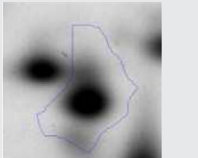

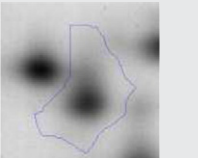
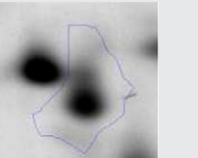
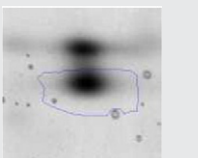
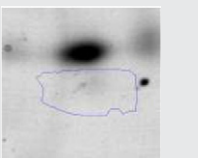
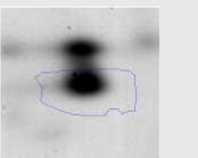





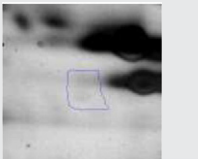
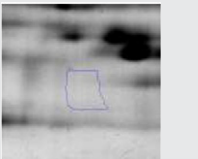
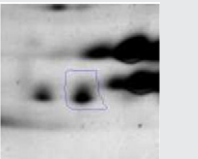
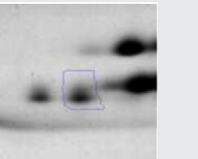
We focused on six proteins whose abundance was similar between strains during exponential phase (i.e. when lipid accumulation was the same) and whose abundance was different at early stationary phase, when lipid accumulation was much higher in strain S2M2 than WT.

The two spots identified as a FabG (spot 3009) and “FabG domain-containing conserved unknown protein” (spot 2681) were down-accumulated in the WT strain upon nitrogen starvation, while their relative abundance remained constant

in the S2M2 strain, suggesting the absence of regulation of these proteins here (Table.6). The involvement of the “FabG domain-containing conserved unknown protein” in the fatty acid metabolism remains speculative but, surprisingly, this protein was regulated like FabG. 3-oxoacyl-(acyl-carrier-protein) reductase (FabG) catalyzes the first reduction step of de novo fatty acid elongation. This process involves condensation of C18:1-CoA with malonyl-CoA to form 3-ketoacyl-CoA, reduction of this 3-ketoacyl-CoA, dehydration of the resulting 3-hydroxyacyl-CoA and, finally, reduction of the trans-2,3-enoyl-CoA. Because the amount of neutral fatty acid increases in strain S2M2 at stationary phase but not in WT, we assume that the down-expression of these proteins could be connected to the halt in of lipid accumulation in the WT strain. In strain S2M2, neutral lipid accumulation continues during stationary phase, when these proteins are not down-expressed. Because the regulation of protein spots was similar for both enzymes, this suggests that regulation mechanisms could be at the same step for both homologs. In *C. reinhardtii*, some genes involved in the build-up of TAGs were up-regulated during nitrogen starvation and perhaps driven by the transcription factor identified by Boyle et al. [11]. In *T. lutea*, regulation of FabG and “FabG domain-containing conserved unknown protein” should be explored at transcriptional level.

PLAAOx (spots 1108 and 1144 on Fig. 4) was strongly up-accumulated in the WT strain under nitrogen starvation (fold = 8.2 and 4.3) but not detected in the S2M2 strain (Table. 6). As previously stated, PLAAOx is involved in the access to

**Table 6 – Selected differentially accumulated spots of the identified proteins.**

| Hypothetical function                                  | No spot             | WTstrain   |   | S2M2 strain  |  |
|--|---------------------|--|---|--|--|
|  |                     | expo   | stat  | expo   | stat   |
| PLAAOx   | 1108–1144           |   |   |   |   |
| CSAP1  | 3951                |   |   |   |   |
| FabG   | 3009                |   |   |   |   |
| FabG domain containing<br>concerned unknown<br>protein | 2681                |   |   |   |   |
| Glycosyl hydrolase<br>family GH16                      | 1215 1221 1238 1241 |   |   |   |   |
| Glycosyl hydrolase<br>family GH30                      | 1074–1078           |  |  |  |  |

extra-cellular organic nitrogen [56]. The lower abundance of this protein under nitrogen starvation in strain S2M2 could lead to a reduction of its capacity to access nitrogen from dissolved organic nitrogen. In this study, no difference in nitrogen accumulation was observed between the two strains until Day 5. It would be interesting to examine the C:N ratio during the last days of stationary phase. The involvement of PLAAOx in lipid accumulation remains speculative, however.

CSAP1 (spot 3951 for CSAP1 in Fig. 4) was strongly up-accumulated in the WT strain under nitrogen starvation (fold = 6.2), but was only slightly up-accumulated in the S2M2 strain and was much less abundant there than in the WT strain (fold = 6.0) (Table. 6). This observation could suggest that the mechanisms regulating the overproduction of this protein and PLAAOx during nitrogen starvation are partially reduced in the S2M2 strain. The function of CSAP1 in neutral lipid accumulation remains unclear and should be explored. However, this protein is probably involved in carbon homeostasis [18]. As mentioned above, the orientation of carbon into acetyl-CoA upstream of de novo fatty acid biosynthesis appears to be crucial for lipid metabolism. A difference in carbon homeostasis between the two strains during nitrogen starvation could lead to a reallocation of carbon for lipid metabolism. Like the two glycoside hydrolases previously identified in this study, the CSAP1 provides a good candidate for further investigations into lipid accumulation under nitrogen starvation.

#### 4. Conclusion

To our knowledge, this paper is the first comparative proteomic analysis in a microalgae of biotechnological interest that makes a comparative analysis of nitrogen stress between a wild type strain and a selected mutant. Mutant and wild type strains of *T. lutea* were analyzed during growth phase and during early stationary phase in batch cultures limited by nitrogen. The results highlight proteins differentially expressed between the two strains and regulated during nitrogen starvation. A set of proteins was selected for having been potentially involved directly or indirectly in the up-accumulation of lipids in the selected strain. This group notably includes proteins involved in carbon homeostasis, fatty acid biosynthesis and carbohydrate catabolism.

#### Acknowledgments

We are very grateful to Mathilde Joint and Marija Pavlovic (INRA, UR1268 - BIBS platform, Nantes) for their excellent technical assistance with the mass spectrometry analysis, and Ewa Lukomska for CN Elemental and ion-chromatography analysis. This work was partly funded by a region of Pays de Loire “Nouvelle équipes, nouvelles thématique” program and by



the Agence National de la Recherche, Facteur 4 project. There are any non-financial competing interests.

## Appendix A. Supplementary data

Supplementary data to this article can be found online at <http://dx.doi.org/10.1016/j.jprot.2014.02.022>.

## REFERENCES

- [1] Khozin-Goldberg I, Cohen Z. Unraveling algal lipid metabolism: recent advances in gene identification. *Biochimie* 2011;93:91–100.
- [2] Guschina IA, Harwood JL. Lipids and lipid metabolism in eukaryotic algae. *Prog Lipid Res* 2006;45:160–86.
- [3] Harwood JL, Guschina IA. The versatility of algae and their lipid metabolism. *Biochimie* 2009;91:679–84.
- [4] Moellering ER, Miller R, Benning C. Molecular genetics of lipid metabolism in the model green alga *Chlamydomonas reinhardtii*. *Lipids Photosynth* 2010:139–55.
- [5] Hu Q, Sommerfeld M, Jarvis E, Ghirardi M, Posewitz M, Seibert M, et al. Microalgal triacylglycerols as feedstocks for biofuel production: perspectives and advances. *Plant J Cell Mol Biol* 2008;54:621–39.
- [6] Lardon L, Hélias A, Sialve B, Steyer J-P, Bernard O. Life-cycle assessment of biodiesel production from microalgae. *Environ Sci Technol* 2009;43:6475–81.
- [7] Petkov G, Ivanova A, Iliev I, Vaseva I. A critical look at the microalgae biodiesel. *Eur J Lipid Sci Technol* 2012;114:103–11.
- [8] Solovchenko AE. Physiological role of neutral lipid accumulation in eukaryotic microalgae under stresses. *Russ J Plant Physiol* 2012;59:167–76.
- [9] Merchant SS, Kropat J, Liu B, Shaw J, Warakanont J. TAG, You're it! *Chlamydomonas* as a reference organism for understanding algal triacylglycerol accumulation. *Curr Opin Biotechnol* 2012;23:352–63.
- [10] Gardner RD, Lohman E, Gerlach R, Cooksey KE, Peyton BM. Comparison of CO<sub>2</sub> and bicarbonate as inorganic carbon sources for triacylglycerol and starch accumulation in *Chlamydomonas reinhardtii*. *Biotechnol Bioeng* 2013;110:87–96.
- [11] Boyle NR, Page MD, Liu B, Blaby IK, Casero D, Kropat J, et al. Three acyltransferases and a nitrogen responsive regulator are implicated in nitrogen starvation-induced triacylglycerol accumulation in *Chlamydomonas*. *J Biol Chem* 2012;287:15811–25.
- [12] Fan J, Yan C, Andre C, Shanklin J, Schwender J, Xu C. Oil accumulation is controlled by carbon precursor supply for fatty acid synthesis in *Chlamydomonas reinhardtii*. *Plant Cell Physiol* 2012;53:1380–90.
- [13] Li Y, Han D, Hu G, Dauvillee D, Sommerfeld M, Ball S, et al. *Chlamydomonas* starchless mutant defective in ADP-glucose pyrophosphorylase hyper-accumulates triacylglycerol. *Metab Eng* 2010;12:387–91.
- [14] Cadoret J-P, Garnier M, Saint-Jean B. Chapter eight — Microalgae, functional genomics and biotechnology. In: Piganeau Gwenaël, editor. *Adv. Bot. Res.*, Volume 64. Academic Press; 2012. p. 285–341.
- [15] Tran N, Park J, Lee C. Proteomics analysis of proteins in green alga *Haematococcus lacustris* (Chlorophyceae) expressed under combined stress of nitrogen starvation and high irradiance. *Enzym Microb Technol* 2009;45:241–6.
- [16] Liang C, Cao S, Zhang X, Zhu B, Su Z, Xu D, et al. De Novo Sequencing and Global Transcriptome Analysis of *Nannochloropsis* sp. (Eustigmatophyceae) Following Nitrogen Starvation. *BioEnergy Res* n.d.:1–12.
- [17] Li Y, Fei X, Deng X. Novel molecular insights into nitrogen starvation-induced triacylglycerols accumulation revealed by differential gene expression analysis in green algae *Micractinium pusillum*. *Biomass Bioenergy* 2012;42:199–211.
- [18] Valenzuela J, Mazurie A, Carlson RP, Gerlach R, Cooksey KE, Peyton BM, et al. Potential role of multiple carbon fixation pathways during lipid accumulation in *Phaeodactylum tricornutum*. *Biotechnol Biofuels* 2012;5:40.
- [19] Radakovits R, Jinkerson RE, Fuerstenberg SI, Tae H, Settlage RE, Boore JL, et al. Draft genome sequence and genetic transformation of the oleaginous alga *Nannochloropsis gaditana*. *Nat Commun* 2012;3:686.
- [20] Dong H-P, Williams E, Wang D, Xie Z-X, Hsia R, Jenck A, et al. Responses of *Nannochloropsis oceanica* IMET1 to long-term nitrogen starvation and recovery. *Plant Physiol* 2013;162:1110–26.
- [21] Guarnieri MT, Nag A, Smolinski SL, Darzins A, Seibert M, Pienkos PT. Examination of triacylglycerol biosynthetic pathways via de novo transcriptomic and proteomic analyses in an unsequenced microalga. *PLoS One* 2011;6:e25851.
- [22] Bendif EM, Probert I, Schroeder DC, de Vargas C, et al. On the description of *Tisochrysis lutea* gen. nov. sp. nov. and *Isochrysis nuda* sp. nov. in the Isochrysidales, and the transfer of *Dicrateria* to the Prymnesiales (Haptophyta). *J Appl Phycol* 2013;2:1763–76.
- [23] Eltgroth ML, Watwood RL, Wolfe GV. Production and cellular localization of neutral long chain lipids in the haptophyte algae *Isochrysis galbana* and *Emiliania huxleyi*. *J Phycol* 2005;41:1000–9.
- [24] Feng D, Chen Z, Xue S, Zhang W. Increased lipid production of the marine oleaginous microalgae *Isochrysis zhangjiangensis* (Chrysophyta) by nitrogen supplement. *Bioresour Technol* 2011;102:6710–6.
- [25] Flynn K, Garrido J, Zapata M, Öpik H, Hipkin C. Changes in fatty acids, amino acids and carbon/nitrogen biomass during nitrogen starvation of ammonium- and nitrate-grown *Isochrysis galbana*. *J Appl Phycol* 1992;4:95–104.
- [26] Livne A, Sukenik A. Lipid synthesis and abundance of acetyl CoA carboxylase in *Isochrysis galbana* (Prymnesiophyceae) following nitrogen starvation. *Plant Cell Physiol* 1992;33:1175–81.
- [27] Sukenik A, Livne A. Variations in lipid and fatty acid content in relation to acetyl CoA carboxylase in the marine prymnesiophyte *Isochrysis galbana*. *Plant Cell Physiol* 1991;32:371–8.
- [28] Bougaran G, Rouxel C, Dubois N, Kaas R, Grouas S, Lukomska E, et al. Enhancement of neutral lipid productivity in the microalga *Isochrysis affinis galbana* (T-Iso) by a mutation-selection procedure. *Biotechnol Bioeng* 2012;109:2737–45.
- [29] Devouge V, Rogniaux H, Nési N, Tessier D, Guéguen J, Larré C. Differential proteomic analysis of four near-isogenic *Brassica napus* varieties bred for their erucic acid and glucosinolate contents. *J Proteome Res* 2007;6:1342–53.
- [30] Choi Y-E, Hwang H, Kim H-S, Ahn J-W, Jeong W-J, Yang J-W. Comparative proteomics using lipid over-producing or less-producing mutants unravels lipid metabolisms in *Chlamydomonas reinhardtii*. *Bioresour Technol* 2013;145:108–23.
- [31] Walne PR. Experiments in the large scale culture of the larvae of *Ostrea edulis*. L. Fish Invest Ministr; 1996.
- [32] Greenspan P, Mayer E, Fowler S. Nile Red — a selective fluorescent stain for intracellular lipid droplets. *J Cell Biol* 1985;100:965–73.

- [33] Lee F, Lo S. The use of Trizol reagent (phenol/guanidine isothiocyanate) for producing high quality two-dimensional gel electrophoretograms (2-DE) of dinoflagellates. *J Microbiol Methods* 2008;73:26–32.
- [34] O'Farrell PH. High resolution two-dimensional electrophoresis of proteins. *J Biol Chem* 1975;250:4007–21.
- [35] Carrier G, Garnier M, Le Cunf L, Bougaran G, Probert I, de Vargas C, et al. Comparative transcriptome of wild type and selected strains of the microalgae *Tisochrysis lutea* provides insights into the genetic basis, lipid metabolism and the life cycle. *PLoS One* 2014;9:e86889.
- [36] Marchler-Bauer A, Lu S, Anderson JB, Chitsaz F, Derbyshire MK, DeWeese-Scott C, et al. CDD: a Conserved Domain Database for the functional annotation of proteins. *Nucleic Acids Res* 2011;39:D225–9.
- [37] Corpet F, Gouzy J, Kahn D. The ProDom database of protein domain families. *Nucleic Acids Res* 1998;26:323–6.
- [38] Käll L, Krogh A, Sonnhammer ELL. A combined transmembrane topology and signal peptide prediction method. *J Mol Biol* 2004;338:1027–36.
- [39] Hirokawa T, Boon-Chieng S, Mitaku S. SOSUI: classification and secondary structure prediction system for membrane proteins. *Bioinformatics* 1998;14:378–9.
- [40] Markou G, Angelidaki I, Georgakakis D. Microalgal carbohydrates: an overview of the factors influencing carbohydrates production, and of main bioconversion technologies for production of biofuels. *Appl Microbiol Biotechnol* 2012;96:631–45.
- [41] Shifrin N, Chisholm S. Phytoplankton lipids — interspecific differences and effects of nitrate, silicate and light–dark cycles. *J Phycol* 1981;17:374–84.
- [42] Reitan KI, Rainuzzo JR, Olsen Y. Effect of nutrient limitation on fatty acid and lipid content of marine Microalgae.1. *J Phycol* 1994;30:972–9.
- [43] Griffiths M, van Hille R, Harrison S. Lipid productivity, settling potential and fatty acid profile of 11 microalgal species grown under nitrogen replete and limited conditions. *J Appl Phycol* 2012;24:989–1001.
- [44] Liu CP, Lin LP. Ultrastructural study and lipid formation of *Isochrysis* sp. CCMP1324. *Bot Bull Acad Sin* 2001;42:207–14.
- [45] Wang ZT, Ullrich N, Joo S, Waffenschmidt S, Goodenough U. Algal lipid bodies: stress induction, purification, and biochemical characterization in wild-type and starch-less *Chlamydomonas reinhardtii*. *Eukaryot Cell* 2009;8:1856–68.
- [46] Cooper MS, Hardin WR, Petersen TW, Cattolico RA. Visualizing “green oil” in live algal cells. *J Biosci Bioeng* 2010;109:198–201.
- [47] Work V, Radakovits R, Jinkerson R, Meuser J, Elliott L, Vinyard D, et al. Increased lipid accumulation in the *Chlamydomonas reinhardtii* sta7-10 starchless isoamylase mutant and increased carbohydrate synthesis in complemented strains. *Eukaryot Cell* 2010;9:1251–61.
- [48] Miller R, Wu G, Deshpande R, Vieler A, Gartner K, Li X, et al. Changes in transcript abundance in *Chlamydomonas reinhardtii* following nitrogen deprivation predict diversion of metabolism. *Plant Physiol* 2010;154:1737–52.
- [49] Droop M. Vitamin-B<sub>12</sub> and Marine Ecology.4. The kinetics of uptake, growth and inhibition in *Monochrysis lutheri*. *Curr Contents Agric Biol Environ Sci* 1985:16–16.
- [50] Lin YH, Chang FL, Tsao CY, Leu JY. Influence of growth phase and nutrient source on fatty acid composition of *Isochrysis galbana* CCMP 1324 in a batch photoreactor. *Biochem Eng J* 2007;37:166–76.
- [51] Fujiwara S, Tsuzuki M, Kawachi M, Minaka N, Inouye I. Molecular phylogeny of the Haptophyta based on the *rbcL* gene and sequence variation in the spacer region of the RUBISCO operon. *J Phycol* 2001;37:121–9.
- [52] Longworth J, Noirel J, Pandhal J, Wright PC, Vaidyanathan S. HILIC- and SCX-based quantitative proteomics of *Chlamydomonas reinhardtii* during nitrogen starvation induced lipid and carbohydrate accumulation. *J Proteome Res* 2012;11:5959–71.
- [53] Msanne J, Xu D, Konda AR, Casas-Mollano JA, Awada T, Cahoon EB, et al. Metabolic and gene expression changes triggered by nitrogen deprivation in the photoautotrophically grown microalgae *Chlamydomonas reinhardtii* and *Coccomyxa* sp. C-169. *Phytochemistry* 2012;75:50–9.
- [54] James GO, Hocart CH, Hillier W, Chen H, Kordbacheh F, Price GD, et al. Fatty acid profiling of *Chlamydomonas reinhardtii* under nitrogen deprivation. *Bioresour Technol* 2011;102:3343–51.
- [55] Allen AE, LaRoche J, Maheswari U, Lommer M, Schauer N, Lopez PJ, et al. Whole-cell response of the pennate diatom *Phaeodactylum tricornutum* to iron starvation. *Proc Natl Acad Sci* 2008;105:10438–43.
- [56] Vallon O, Bulté L, Kuras R, Olive J, Wollman F-A. Extensive accumulation of an extracellular l-amino-acid oxidase during gametogenesis of *Chlamydomonas reinhardtii*. *Eur J Biochem* 1993;215:351–60.
- [57] Cantarel BL, Coutinho PM, Rancurel C, Bernard T, Lombard V, Henrissat B. The Carbohydrate-Active EnZymes database (CAZy): an expert resource for glycogenomics. *Nucleic Acids Res* 2009;37:D233–8.
- [58] St John FJ, González JM, Pozharski E. Consolidation of glycosyl hydrolase family 30: a dual domain 4/7 hydrolase family consisting of two structurally distinct groups. *FEBS Lett* 2010;584:4435–41.

## Chapitre IV :

Limitation azotée et allocation du  
carbone chez *Tisochrysis lutea*.

Approche intégrative appliquée en  
Chémostat.



## Chapitre IV : Limitation azotée et allocation du carbone chez *Tisochrysis lutea*. Approche intégrative appliquée en chémostat.

---

### 1 Introduction

Les précédents résultats de protéomique comparative réalisées sur les souches WT et S2M2 (2X) en cultures batch limitées par l'azote suggèrent que la suraccumulation des lipides de réserve observée chez la souche mutante, durant la carence azotée, est une conséquence d'une altération notable du métabolisme carboné (altération vraisemblablement présente en partie amont de la synthèse des lipides) et d'une modification de sa régulation *via* la disponibilité en azote (Garnier *et al.*, 2014). L'accumulation des lipides de réserve en fonction de la limitation azotée semble obéir à des modèles linéaires chez *T. lutea* (Mairet *et al.*, 2011) et les mécanismes de signalisation aboutissant à l'expression d'enzymes métaboliques en réponse à la raréfaction de l'azote sont encore très mal connus chez les microalgues.

Nous avons décidé d'étudier métabolisme du carbone chez *T. lutea* pour identifier les voies métaboliques liées à l'accumulation des lipides, et de comprendre comment les souches sauvages et mutantes réagissent à des variations fines de limitation azotée. Nous avons plus particulièrement cherché à :

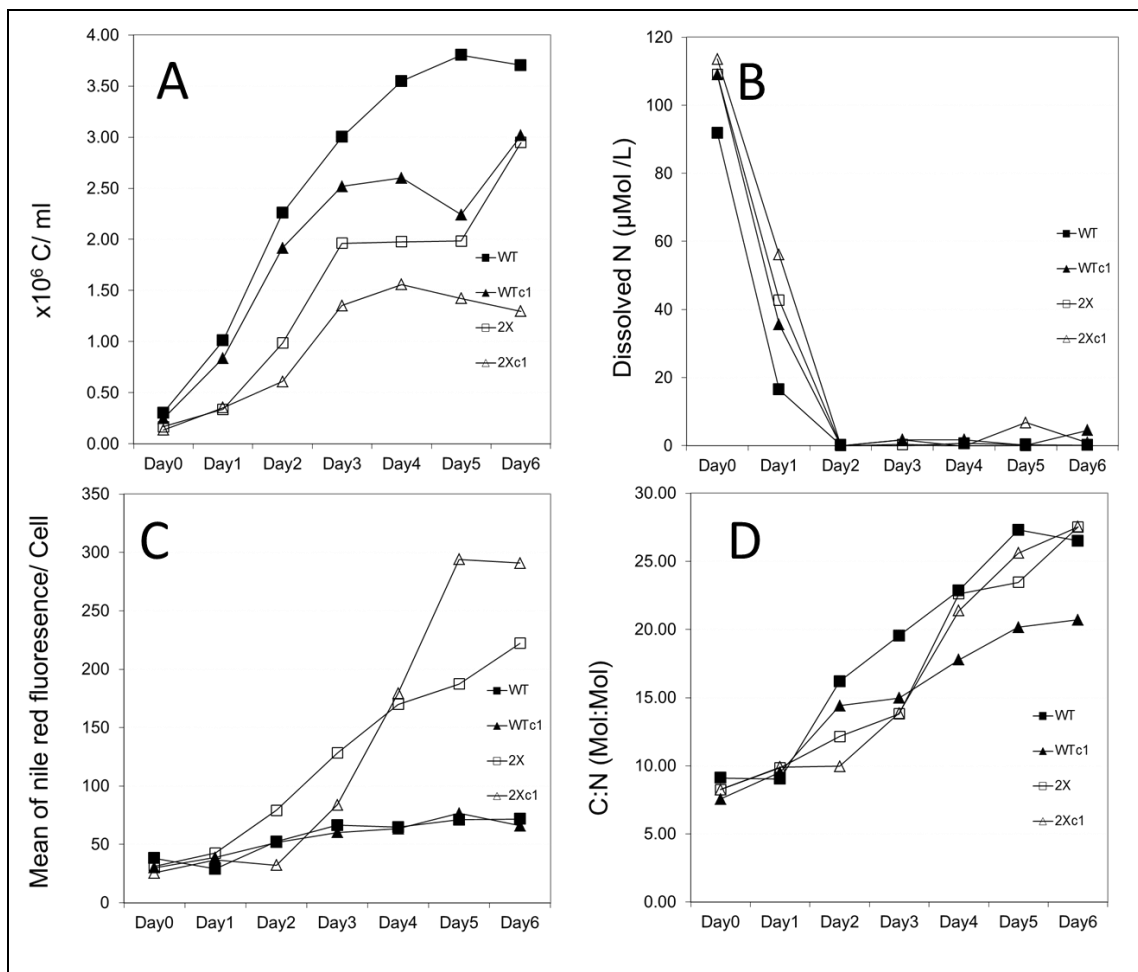
- ✓ Identifier les dynamiques d'accumulation et de dégradation des lipides de réserve, lors de transitions entre des états de limitation à des états de réplétion et de déplétion azotée.
- ✓ Identifier l'allocation du carbone au sein de la cellule, entre lipides de réserve, lipides membranaires, sucres et protéines, ceci en fonction des niveaux de limitation azotée.
- ✓ Identifier les voies métaboliques du carbone et les étapes impactées chez la souche mutée lors de la limitation azotée.
- ✓ Etudier les différents niveaux de régulations (gènes, protéines) mis en place par les souches étudiées *via* l'intégration des analyses transcriptomiques et protéomiques.

Dans cette étude, des souches clonales ont été utilisées pour limiter les risques de variabilité génétique au sein des populations. Ces souches clonales ont été caractérisées dans un premier temps dans des cultures en mode batch. Nous avons ensuite émis, sur la base de modèles

écophysiologiques, des hypothèses de comportement métaboliques lorsque les souches sont cultivées dans des cultures en chémostat limitées par l'azote et soumises à des injections discrètes de nitrates (« spike »). L'objectif était d'atteindre des états écophysiologiques parfaitement identifiés et associés à un métabolisme lipidique d'accumulation ou de dégradation des lipides de réserve. Nous avons ensuite testé ces hypothèses sur chacune des deux souches cultivées dans des photobioréacteurs dédiés, et évalué les différences de sensibilité à l'azote et d'allocation du carbone entre les deux souches. Nous avons alors analysé le protéome de *T. lutea* par une approche haut débit et identifié les protéines différentiellement accumulées entre les deux souches lors de la limitation azotée. Enfin nous avons étudié l'expression des protéines identifiées au niveau génique par RNAseq et comparé les résultats d'analyses transcriptomiques et protéomiques.

## 2 Caractérisation des souches clonales en culture batch

Des souches clonales (WTc1 et 2Xc1) ont été préalablement isolées par cyométrie en flux à partir des souches polyclonales WT (CCAP927/14) et S2M2 (2X, CCAP926/14) respectivement. Ces deux souches clonales ainsi que les deux souches multiclonales ont été cultivées en mode batch limité par l'azote dans des conditions identiques à celles précédemment décrites dans le chapitre II. Les souches clonales présentent des caractéristiques écophysiologiques et phénotypiques similaires aux souches polyclonales WT et S2M2 (**Figure 44**). Nous avons tenté de savoir si la réduction de la diversité des populations permettait de réduire le nombre de protéines candidates, c'est à dire différentiellement accumulées entre les deux souches et potentiellement impliquées dans la suraccumulation lipidique de la souche mutante. Pour ce faire, nous avons analysé les protéomes des souches clonales en début de phase stationnaire dans la même condition écophysiologique et selon la même démarche expérimentale que dans le chapitre II. Les résultats montrent que l'utilisation de souches clonales ne permet pas de réduire le nombre de protéines différentiellement accumulées entre souche mutante et souche sauvage. Les protéines sélectionnées dans le chapitre II pour leur implication potentielle dans la suraccumulation lipidique sont également différentiellement accumulées dans les souches clonales sauvage et mutante. La suite de l'étude est réalisée sur les souches clonales pour limiter les risques de dérive génétiques liés à des phénomènes de sélection au sein des populations.



**Figure 44** Suivi de croissance en mode batch limité par l'azote des souches multiclones WT et 2X (=S2M2) et des souches clones WTc1 et 2Xc1.

(A) Comptage cellulaire ; (B) Azote dissous, (C) Quantité de lipides neutres estimé par coloration au rouge du Nil et mesuré par cytométrie en flux ; (D) Rapport C/N des cellules.

### 3 Hypothèses et modèles écophysologiques.

L'hypothèse émise initialement dans cette étude est basée sur les modèles écophysologiques de croissance (Droop, 1985) et d'accumulation lipidique (Mairet *et al.*, 2011). Ces modèles sont basés sur deux principes qui sont que la croissance algale est une relation hyperbolique du quota d'azote cellulaire (**Figure 14**) et que l'accumulation de lipides de réserve est intimement liée à ce même quota. Sur la base de ces modèles, une expérience en chémostat a été envisagée pour obtenir différentes physiologies liées au métabolisme lipidique. Dans une culture en chémostat limitée par l'azote, l'injection discrète d'une quantité d'azote déterminée (spike) impose des déséquilibres écophysologiques et aboutit selon les modèles à trois états métaboliques distincts (**Figure 45**):

- ✓ Dans un chémostat à l'équilibre limité par l'azote, l'ensemble de l'azote absorbé est assimilé par les microalgues. Le taux d'absorption de l'azote (défini par  $\rho$ , en  $\text{molN.molC}^{-1} \text{ j}^{-1}$ ) est alors égal au produit du taux de croissance ( $\mu$ , en  $\text{j}^{-1}$ ) et du quota d'azote ( $Q$ , en  $\text{molN.mol C}^{-1}$ ):  $\rho = \mu \cdot Q$ . La relation  $\mu \cdot Q$  est définie comme représentant les besoins nécessaires aux algues pour maintenir leur croissance. Dans cet état d'équilibre, l'ensemble des paramètres écophysologiques, dont le rapport N/C, reste constant. Les cellules accumulent des sucres et lipides de réserve à un niveau qui dépend du niveau de limitation imposé par le taux de dilution.
- ✓ Suite à un ajout ponctuel d'azote, le taux d'absorption ( $\rho$ ) est alors supérieur aux besoins de l'algue ( $\rho > \mu \cdot Q$ ) du fait de la disponibilité en azote. Dans cet état physiologique, les algues sont dites « réplétées » en azote. Ainsi, le rapport N/C des algues augmente et les lipides et sucres de réserve sont catabolisés pour fournir les métabolites carbonés primaires nécessaires à l'augmentation de la croissance algale ( $\mu$ ). Lors de cette phase, il est possible d'étudier les mécanismes liés au catabolisme des lipides de réserve.
- ✓ Enfin, lorsque l'ensemble de l'azote injecté est absorbé, les algues ne peuvent maintenir leur croissance que sur l'azote apporté en continu. Les besoins en azote sont alors supérieurs à l'absorption spécifique de l'azote par les algues ( $\rho < \mu \cdot Q$ ). Les algues puisent alors dans leur quota N interne pour assurer leur croissance. En conséquence, le rapport N/C décroît. Cet état de déplétion azotée conduit ainsi à l'accumulation de sucres et lipides de réserve.



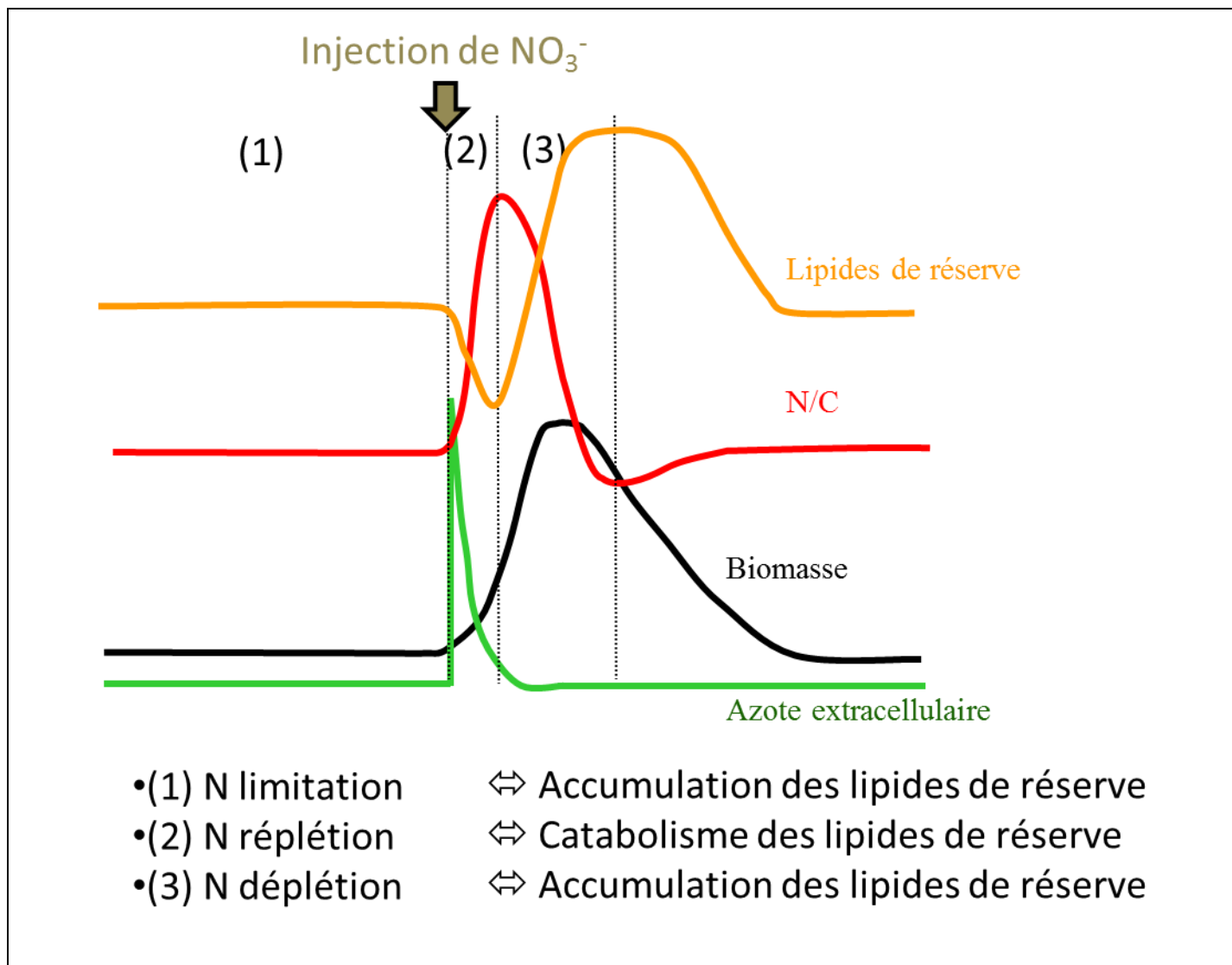


Figure 45 Représentation schématique des cinétiques des paramètres dans un chémostat limité par l'azote et soumis à une injection de nitrate selon les modèles écophysiologiques.

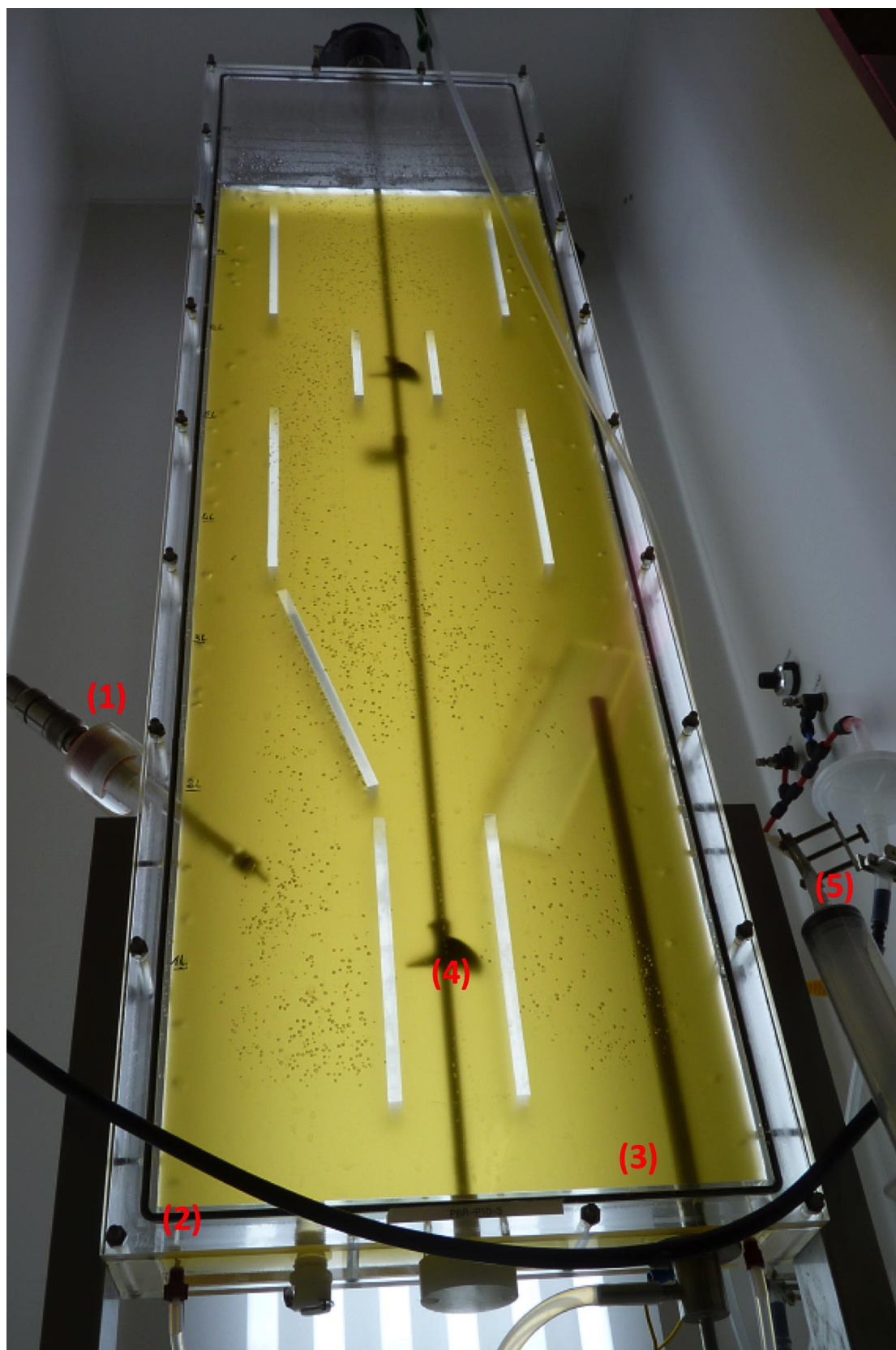
#### 4 Validation des hypothèses: Etude dynamique de la limitation azotée et de l'allocation du carbone.

Pour valider ces hypothèses et étudier les mécanismes d'accumulation et de dégradation des lipides de réserve, les souches clonales WTc1 et 2Xc1 ont été étudiées dans des cultures en chémostat limitées par l'azote et soumises à des injections discrètes d'azote afin d'imposer des déséquilibres écophysologiques ciblés.

Les méthodologie et résultats de ces travaux ont été présentés dans une première partie d'une publication proposée au journal *Algal Research* en janvier 2016 : «Use of a lipid rich strain reveals mechanisms of nitrogen limitation and carbon partitioning in the haptophyte *Tisochrysis lutea* ». Cette publication est intégrée en fin de ce chapitre.

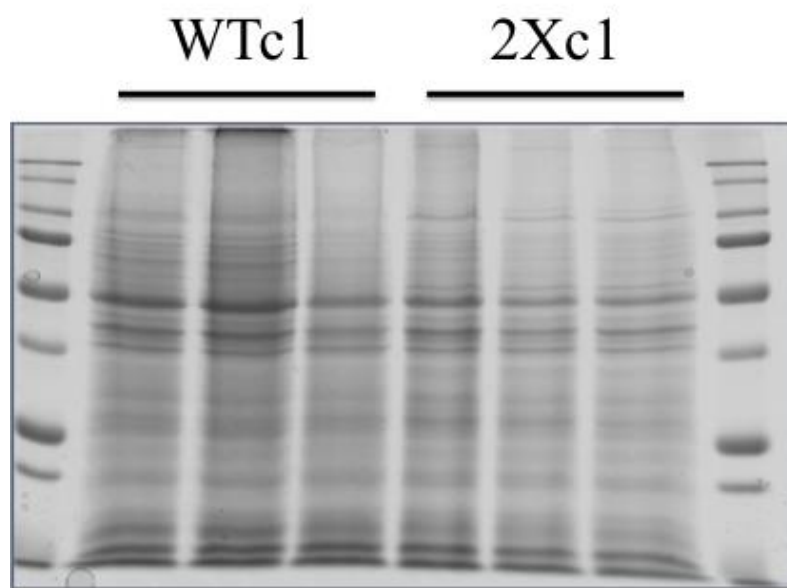
Les souches WTc1 et 2Xc1 ont été cultivées en chémostat limité par l'azote pendant 3 mois, chacune dans un photobioréacteur de 10L conçu au laboratoire PBA et dédié aux études écophysologiques (**Figure 46**). Des injections discrètes de nitrate de sodium ont été effectuées dans chaque réacteur (spike) pour provoquer les déséquilibres écophysologiques modélisés ci-dessus. Ces injections ont été réalisées trois fois sur les mêmes cultures pour évaluer la robustesse des résultats obtenus. Les paramètres écophysologiques ont été analysés au cours du temps pour valider les hypothèses initiales (voir Fig. 1 de Garnier *et al.*, soumise).

Alors que les résultats obtenus avec la souche mutante 2Xc1 sont conformes avec les hypothèses énoncées, ces hypothèses ne sont confirmées que de manière partielle chez la souche sauvage. En effet, alors que les variations du régime azoté provoquent la remobilisation des sucres chez les deux souches, l'accumulation et la dégradation des lipides de réserve n'a été observée que chez la souche mutante (voir Fig. 2 de Garnier *et al.*, soumise). Ces résultats montrent une plus grande plasticité du phénotype lipidique de la souche 2Xc1 et suggèrent une plus grande sensibilité de la souche 2Xc1 aux variations du régime azoté. L'absence de variations lipidiques chez la souche sauvage peut être expliquée de deux manières. 1) Les variations de contenus lipidiques chez la souche WTc1 sont trop faibles pour être mesurées par HPTLC et par mesure de coloration des vésicules lipidiques au rouge du Nile. 2) Les mécanismes de signalisation aboutissant à un changement du contenu lipidique lors de variations de la limitation azotée ne sont pas activés chez cette souche et dans les conditions de cette expérience. Il existerait alors des seuils de limitation en deçà desquels la souche WTc1 ne modifie pas son contenu lipidique.



**Figure 46 Photobioréacteur de 10L utilisé pour les cultures en chemostat.**

(1) sonde pH ; (2) régulation pH par bullage d'air enrichi en CO<sub>2</sub> ; (3) Régulation de la température par courant d'eau thermostatée dans un doigt de gant. ; (4) agitation mécanique ; (5) seringue de prélèvement.



**Figure 47** Protéomes des souches WTc1 et 2Xc1 analysés sur gel SDS-Page 12%.

Chaque protéome sera ensuite fractionné par découpage de 18 bandes de tailles identiques qui seront analysées par LC/MS-MS après digestion trypsique.

Alors que les modèles d'allocation carbonée sont basés sur des relations linéaires entre limitation azotée et accumulation des sucres et lipides de réserve, nous avançons donc l'hypothèse que des mécanismes de signalisation de la limitation azotée pourraient être impliqués et seraient plus sensiblement activés chez la souche 2Xc1 que chez la souche WTc1.

Les analyses d'allocation du carbone montrent que les sucres sont les premiers éléments, avant les lipides, mis à contribution lors de changement de régime azoté et que le carbone alloué aux lipides de réserve ne représente qu'une faible part du carbone total de la cellule, ceci contrairement aux cultures carencées par l'azote (voir Tableau 1 de Garnier *et al.*, soumise). Néanmoins, lors de la limitation azotée, ce carbone alloué aux lipides de réserve est deux à trois fois plus abondant chez la souche 2Xc1 que chez la souche WTc1. Les résultats d'analyse de classes lipidiques suggèrent que les lipides de réserve peuvent être remobilisés pour la synthèse de lipides membranaires lors de la réplétion azotée et inversement lors de la déplétion azotée.

## 5 Identification du protéome de *T. lutea* et analyses comparatives.

- **Méthodologie**

Pour chaque souche, trois échantillons ont été prélevés à plusieurs semaines d'intervalle dans les chémostat à l'équilibre lors de la limitation azotée. Une approche protéomique à haut débit a été développée pour identifier le protéome de *T. lutea* et les voies métaboliques impactées chez la souche mutante. A chaque étape de la démarche expérimentale, un effort particulier a été porté pour optimiser la profondeur des analyses.

Les protéines de chacun des 6 échantillons ont été extraites et purifiées avec le protocole développé dans le chapitre III. Les protéines ont ensuite été séparées sur gel SDS-PAGE 12% (**Figure 47**). Les protéomes de chacune des 6 pistes ont été fractionnés en 18 bandes pour améliorer la profondeur des analyses. Les protéines contenues dans chacune des 108 bandes ont été identifiées par spectrométrie de masse sur la plateforme BIBS (INRA Nantes - Biogenouest). Brièvement, la méthodologie consiste à : 1) Digérer les protéines à la trypsine; 2) Séparer les peptides issus de la digestion par chromatographie liquide (LC). Des tests préliminaires ont été réalisés pour améliorer la profondeur des analyses et ont montré que l'utilisation de capillaires de chromatographie liquide de 50cm au lieu de 30cm permettait d'augmenter de 30 % la quantité de protéines finalement identifiées (résultats non montrés); 3) Ioniser les peptides et mesurer la masse de chaque peptide ionisé (MS); 4) Fragmenter chaque peptide ionisé et mesurer les masses des résidus pour

reconstruire la séquence de chaque peptide (MS/MS); 5) Comparer les profils de masse identifiés à des profils de masse générés *in silico* à partir de bases de données protéiques pour identifier les protéines ; 6) Quantifier chaque peptide et chaque protéine. La méthode de quantification des peptides utilisée lors de cette étude est basée sur l'aire des pics MS des ions précurseurs détectés par LC-MS-MS. Le logiciel MassChroq a été utilisé pour aligner et normaliser les différentes analyses, et quantifier chaque peptide dans chaque échantillon (Valot *et al.*, 2011). Une méthode d'analyse a été développée sur logiciel R au cours de ce travail pour quantifier les protéines à partir de données MassChroq issues de protéomes préfractionnés sur gel.

- **Résultats principaux**

Les méthodologie et résultats de ces travaux ont été présentés dans la seconde partie de la publication : «Use of a lipid rich strain reveals mechanisms of nitrogen limitation and carbon partitioning in the haptophyte *Tisochrysis lutea* ».

Grâce à l'optimisation du protocole d'analyse protéomique, et notamment au préfractionnement avant analyses de masses, le protéome de *T. lutea* a été identifié avec une très bonne profondeur puisque 4332 protéines ont été détectées, soit vingt-cinq pour-cent des gènes identifiés chez *T. lutea*. Une fonction putative a pu être inférée à 2 155 protéines sur la base d'homologie de séquence ou de la présence de domaines fonctionnels. 254 réactions enzymatiques ont été identifiées à travers la fonction des protéines. La plupart des enzymes du métabolisme central du carbone (cycle de Calvin, glycolyse, cycle de Krebs, cycle du glyoxylate, voie des pentoses phosphates) ont été identifiées (voir Fig. 4 de Garnier *et al.*, soumise). Cependant, certaines voies métaboliques ayant trait avec le métabolisme du carbone restent incomplètes et nos analyses permettent d'émettre des hypothèses de recherche. Voici quelques exemples : 1) Bien que les enzymes du métabolisme des lipides soient généralement bien conservées chez les microalgues, certaines enzymes clé de la voie de Kennedy pour l'assemblage des TAGs, pourtant bien identifiées dans le transcriptome de ces souches, n'ont pas été détectées dans le protéome de *T. lutea*. Ces résultats suggèrent qu'il existe probablement des voies métaboliques parallèles encore non identifiées chez les haptophytes. 2) Les mécanismes de biosynthèse des lipides à très longue chaîne de type alkenones sont encore inconnus et l'étude fonctionnelle d'une « long chain fatty acid syntase » identifiée lors de ces travaux présente une première piste de recherche. 3) Les enzymes impliquées dans la biosynthèse de la chrysolaminarine chez les haptophytes sont mal connues et l'identification d'une protéine

potentiellement impliquée dans cette voie semble prometteuse. D'autre part, les quatre enzymes du cycle du mannitol décrites chez *Ectocarpus silliculosus* ont été identifiées dans le protéome de *T. lutea* et une d'entre elles est très fortement sous-accumulée chez la souche mutante (**Figure 4**). La quantification du mannitol dans les différentes souches et dans les différentes conditions physiologique permettra de mieux évaluer le rôle de stockage carboné de ce composé chez *T. lutea*.

Les analyses protéomiques comparatives entre les deux souches ont permis d'identifier 205 protéines sur-accumulées dans la souche 2Xc1 et 608 protéines sous accumulées (voir Fig. 3 de Garnier *et al.*, soumise). La fonction de 66 % et 48 % des protéines sur-accumulées et sous-accumulées respectivement demeure encore inconnue. Les protéines identifiées sont impliquées dans de nombreuses fonctions moléculaires et cellulaires (voir tableaux 2 et 3 de Garnier *et al.*, soumise). Ces résultats, en accord avec les travaux réalisés par électrophorèse bidimensionnelle, confirment la grande variété des métabolismes impactés dans la souche mutante 2Xc1.

Nos résultats montrent que de nombreuses enzymes du métabolisme azoté sont différentiellement accumulées entre les deux souches ce qui suggère que la souche 2Xc1 remobilise différemment l'azote intracellulaire. De nombreuses protéines impliquées dans le greffage des acides aminés sur les ARNs de transferts sont fortement sous accumulées ce qui suggère que la synthèse protéique est fortement impactée chez la souche 2Xc1. Par la suite, nous avons concentré nos efforts sur les enzymes impliquées dans le métabolisme central du carbone (voir fig.4 de Garnier *et al.*, soumise). Ces résultats suggèrent que: 1) la souche 2Xc1 préserve mieux ses lipides de réserve en limitant l'abondance des protéines du catabolisme lipidique et 2) la souche 2Xc1 limite la remobilisation de l'acétyl-CoA en limitant l'abondance de protéines impliquées dans le cycle du glyoxylate, le cycle de Krebs et la chaîne respiratoire. Ainsi, l'activité mitochondriale semble affectée dans la souche 2Xc1. Ce comportement est globalement similaire à celui d'une microalgue carencée par l'azote alors que les souches sont simplement limitées par l'azote.

D'autre part, nos résultats montrent une suraccumulation de protéines impliquées dans le cycle de Calvin et dans la photosynthèse, suggérant ainsi que contrairement à une algue carencée, la souche 2Xc1 poursuit son activité d'absorption et d'assimilation du carbone. Cet état lui assure une bonne croissance en condition de limitation azotée (voir fig.4 de Garnier *et al.*, soumise). Ces approches protéomiques permettent donc d'avancer des hypothèses pour expliquer pourquoi *T. lutea* 2Xc1 accumule plus de lipides de réserve tout en conservant un bon taux de croissance. Les travaux similaires sur les phases de réplétion azotée permettraient de mettre en évidence les voies

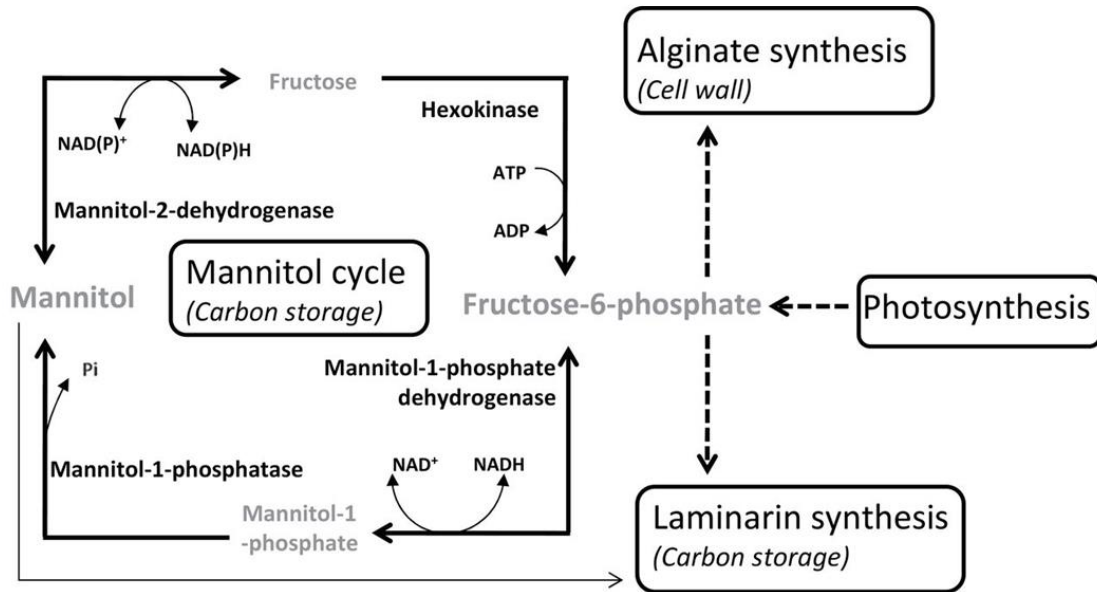


Figure 48 Cycle du Mannitol chez *E. siliculosus*. (Source : Groisillier et al., 2014)

Les quatre enzymes principale intervenant dans le cycle du Mannitol ont été identifiées dans le protéome de *T. lutea*. La Mannitol 1-phosphate dehydrogenase est fortement sous-accumulée dans la souche 2Xc1 par comparaison à la souche WTc1.

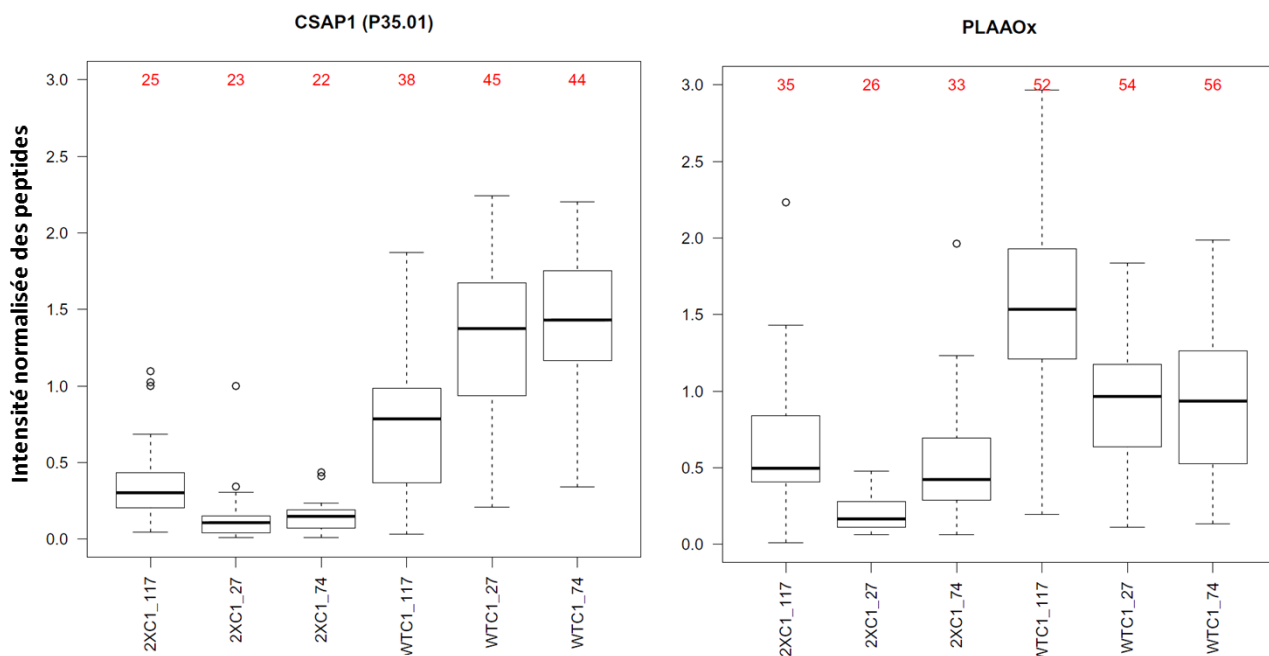


Figure 49 Abondance relative des protéines CSAP et PLAAOx chez les souches WTc1 et 2Xc1 en limitation azotée.

Distribution des intensités peptidiques normalisées. Le nombre de peptides identifiés est indiqué en rouge. Les données proviennent des analyses protéomiques réalisées sur 3 échantillons à l'équilibre dans un chemostat dont les cellules sont limitées par l'azote (Pt 27, Pt 74 et Pt 117) (Chapitre IV).



métaboliques impliquées lors du catabolisme des lipides. Des échantillons sont désormais disponibles pour ces analyses.

Alors que les cinétiques des teneurs en lipides de réserve suggèrent que des mécanismes de signalisation pourraient être plus sensiblement activés chez la souche 2Xc1 lors de variations de la limitation azotée, les résultats d'analyses protéomique montrent que des mécanismes de signalisations calcique impliquant des « calcium/calmodulin-dependent protein kinases » (CAMPK) sont fortement sous-accumulées chez la souche 2Xc1. Ces mécanismes de signalisation sont à ce jour très mal connus chez les microalgues mais deux études récentes font état de l'implication de la signalisation calcique dans l'accumulation des lipides de réserve chez les chlorophycées (Chen *et al.*, 2014; Chen *et al.*, 2015). Nous avançons donc l'hypothèse que les mécanismes de signalisation calciques pourraient être impliqués dans la plus grande sensibilité aux variations de régime azoté de la souche 2Xc1.

Enfin, deux protéines de fonction mal connus mais potentiellement impliqués conjointement dans le métabolisme du carbone et de l'azote (CSAP et PLAAOx), ont montré des différences d'abondance significatives entre la souche 2Xc1 et WT (**Figure 4**). L'identification de la fonction de ces protéines et de leur régulation permettra de mieux comprendre le métabolisme de l'azote et du carbone chez les microalgues.

## 6 Expression génique des protéines identifiées

- **Méthodologie**

L'expression génique des 4 332 protéines identifiées a été mesurée par RNAseq pour chacune des deux souches à l'équilibre du chémostat. Deux échantillons ont été analysés (Pt27 et Pt117). Les ARNs ont été extraits et purifiés, les ARNs messagers enrichis et les bibliothèques d'ADN complémentaire ont été produites comme précédemment présenté (Carrier et al., 2014). Les bibliothèques ont ensuite été séquencées par méthodologie « paired-end » (2x100b) sur séquenceur Illumina<sup>®</sup>. Pour chaque échantillon les données brutes ont été filtrées pour ne garder que des séquences de qualité satisfaisante pour la suite des analyses. Dans un premier temps, les séquences contenant des adaptateurs Illumina résiduels ont été supprimées (« Cutadapt » version 1.6 (Martin, 2011)). Dans un second temps, les séquences contenant une trop grande quantité de base mal séquencée (qualité score inférieur à 30) ont également été écartées (« Reads quality filter » Script produit dans le laboratoire). La qualité finale des séquences a été validée en utilisant le logiciel « FastQC » ([www.bioinformatics.bbsrc.ac.uk](http://www.bioinformatics.bbsrc.ac.uk)). Les séquences ont ensuite été alignées sur le « traductome » de *T. lutea*, généré depuis les analyses transcriptomiques et ne contenant que les CDS des protéines identifiées par spectrométrie de masse. Le logiciel Tophat2 (version 2.0) (Trapnell et al 2009) a été ensuite utilisé pour l'alignement des « reads » et le logiciel htseq-count (version 3.0) pour mesurer les niveaux d'expression normalisée. L'expression de chaque gène est exprimée en nombre de fragments par kilobase et par million de séquences alignées (FPKM) puis converti en log2. Le rapport d'expression entre la souche 2Xc1 et la souche WTc1 à chacun des deux points analysés (Pt27 et Pt117) a été calculé. Les gènes différentiellement exprimés ont été sélectionnés selon les conditions suivantes :  $\log_2(\text{rapport d'expression}) > 2$  ou  $\log_2(\text{rapport d'expression}) < -2$ .

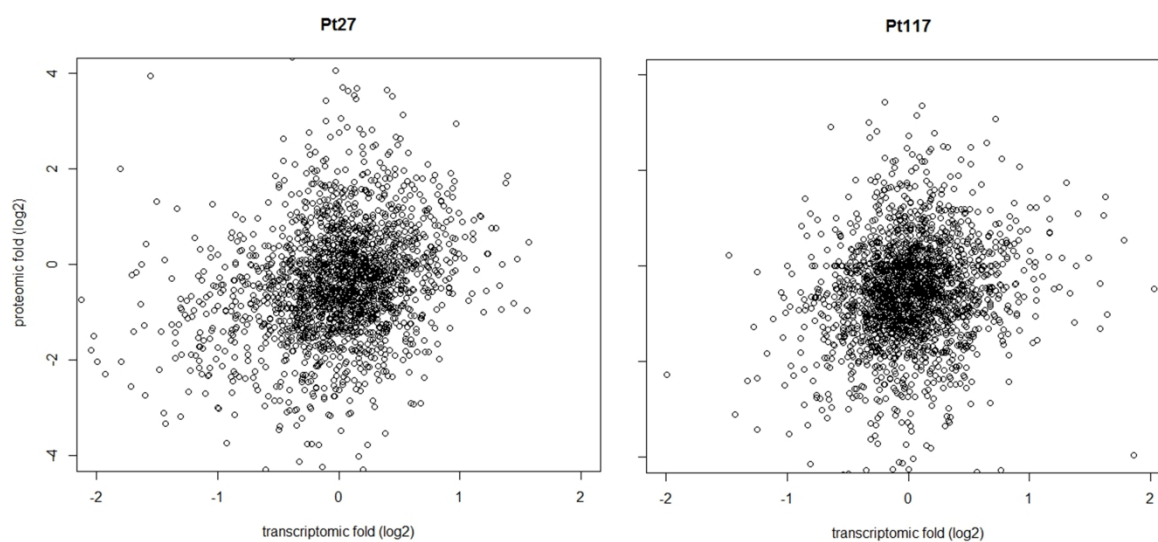
- **Résultats**

Les analyses ont permis de sélectionner 28 gènes différentiellement exprimés entre les deux souches en phase stationnaire du chémostat et présentés dans le tableau ci-dessous. .

**Tableau 1 Bilans des gènes différentiellement exprimés entre la souche 2Xc1 et la souche WTc1. nda : Non différentiellement accumulée.**

| Protéine ID | Fonction                               | Différentiel d'accumulation protéique 2Xc1 vs WTc1 | Différentiel de régulation (RNAseq) 2Xc1 vs WTc1 |
|-------------|--|--|--|
| P1789.01    | Concerved Unknown Function Protein     | sous-accumulée                                     | sous-exprimé                                     |
| P3801.01    | Concerved Unknown Function Protein     | sous-accumulée                                     | sous-exprimé                                     |
| P1639.01    | Malate synthase                        | sous-accumulée                                     | sous-exprimé                                     |
| P15.03      | Unknown Function Protein               | sous-accumulée                                     | sous-exprimé                                     |
| P2305.01    | Unknown Function Protein               | sous-accumulée                                     | sous-exprimé                                     |
| P2394.01    | Unknown Function Protein               | sous-accumulée                                     | sous-exprimé                                     |
| P460.01     | Unknown Function Protein               | sous-accumulée                                     | sous-exprimé                                     |
| P1066.01    | COP9 signalosome complex subunit 7     | nda  | sous-exprimé                                     |
| P1046.01    | DEAD-box ATP-dependent RNA helicase 50 | nda  | sous-exprimé                                     |
| P2049.01    | Uncharacterized protein C824.09c       | nda  | sous-exprimé                                     |
| P1995.01    | Unknown Function Protein               | nda  | sous-exprimé                                     |
| P2325.01    | Unknown Function Protein               | nda  | sous-exprimé                                     |
| P3564.01    | Unknown Function Protein               | nda  | sous-exprimé                                     |
| P2544.01    | NAD/NADP-dependent betaine aldehyde    | sous-accumulée                                     | surexprimé                                       |
| P1567.01    | Unknown Function Protein               | sous-accumulée                                     | surexprimé                                       |
| P2296.01    | Unknown Function Protein               | sous-accumulée                                     | surexprimé                                       |
| P55.03      | ATP:dAMP phosphotransferase            | nda  | surexprimé                                       |
| P2473.01    | Concerved Unknown Function Protein     | nda  | surexprimé                                       |
| P2134.01    | Peptidyl-prolyl cis-trans isomerase C  | nda  | surexprimé                                       |
| P1205.01    | Uncharacterized protein C216.04c       | nda  | surexprimé                                       |
| P1043.01    | Unknown Function Protein               | nda  | surexprimé                                       |
| P1117.01    | Unknown Function Protein               | nda  | surexprimé                                       |
| P1946.01    | Unknown Function Protein               | nda  | surexprimé                                       |
| P2496.01    | Unknown Function Protein               | nda  | surexprimé                                       |
| P2685.01    | Unknown Function Protein               | nda  | surexprimé                                       |
| P3577.01    | Unknown Function Protein               | nda  | surexprimé                                       |
| P672.01     | Unknown Function Protein               | nda  | surexprimé                                       |
| P312.01     | uroporphyrinogen decarboxylase         | sous-accumulée                                     | surexprimé                                       |

La fonction de la plupart des gènes différentiellement exprimés est inconnue. La sous-expression de sept gènes a été validée par les analyses protéomiques qui montrent la sous-accumulation des protéines traduites dans la souche 2Xc1 (Tableau 1 ; surlignage jaune). Parmi ces gènes, six protéines ont une fonction inconnue et un gène code pour la malate synthase, protéine clé du cycle du glyoxylate. Ce résultat suggère que la remobilisation du carbone dans la cellule *via* le cycle du glyoxylate est impactée au niveau transcriptomique dans la souche 2Xc1. Dans l'ensemble, l'interprétation des résultats issus des analyses RNAseq est fortement limitée par le manque de connaissance sur la fonction réelle des gènes différentiellement exprimés. De plus, la Figure 50 montre également une absence de corrélation entre les résultats d'expression génique par RNAseq et d'abondance protéiques par LC-MS/MS.



**Figure 50** Corrélation entre les analyses RNAseq et la quantification protéique par spectrométrie de masse.

Les rapports d'expression transcriptomique et d'abondance protéique entre la souche 2Xc1 et WTc1 ont été calculés pour chacun des deux prélèvements Pt27 et Pt117.

De tels résultats sont couramment observés dans la littérature. A titre d'exemple, chez la levure *Saccharomyces cerevisiae*, des coefficients de corrélation ( $r_p$ ) de 0.36 à 0.66 ont été rapportés dans les différentes études (lire pour revue Maier et al.(2009)). Dans notre analyse, les  $r_p$  calculés sont de 0.28 et de 0.35 pour les points de prélèvement Pt-27 et Pt-117 respectivement. Chez les microalgues *Aureococcus anophagefferens* et *Thalassiosira pseudonana*, de très faibles corrélations ont été également observées (Wurch et al., 2011 ; Dyhrman et al., 2012). Les raisons pouvant expliquer ces différences entre les résultats transcriptomiques et protéomiques sont multiples et sont résumées dans l'article de Maier et al. en 2009. Par exemple, des différences de conformations des molécules d'ARNs (« riboswitch »), des interactions ARN – protéines, ou l'action de micro-ARNs (miRNAs) ou de petits ARNs interférents (siRNAs) peuvent réguler le recrutement des ARNs messagers par les ribosomes. D'autre part, les vitesses de traduction peuvent également différer en fonction de l'occupation ribosomale (ribosome occupancy), des mécanismes d'initiation de la traduction ou de la quantité d'ARNs de transfert. Enfin, l'abondance d'une protéine dans une cellule dépend non seulement de la vitesse à laquelle elle est synthétisée mais également de sa durée de vie dans la cellule. Cette durée de vie, dépend entre autre de sa stabilité intrinsèque, des mécanismes de protéolyse et des mécanismes de sécrétion dans le milieu extracellulaire. Nous avons montré dans l'article Garnier et al (soumise) que de nombreuses protéines impliquées dans la traduction et la synthèse d'ARNt étaient sous-accumulées dans la souche 2Xc1. Or, des travaux chez la levure ont montré que près d'un tiers des gènes sont régulés en phase de carence nutritive au niveau traductionnel (Ingolia et al., 2009). Ces différences de régulations au niveau traductionnel pourraient donc expliquer partiellement les faibles corrélations entre analyses RNAseq et analyses protéomiques. Ces résultats suggèrent ainsi que différents niveaux de régulation post-transcriptionnelle pourraient intervenir. Par ailleurs, les analyses protéomiques ont aussi montré que certaines protéases étaient différentiellement accumulées entre les deux souches suggérant ainsi que les différences d'abondances protéiques mesurées entre les deux souches pourraient être en partie liées à des systèmes de protéolyse différents.

Enfin, les résultats d'analyses transcriptomiques suggèrent que différents niveaux de régulations géniques ont été impactés chez la souche 2Xc1. Des analyses RNAseq sur l'ensemble des gènes ont d'ores et déjà été entreprises au laboratoire, ceci sur chacune des deux souches et à différents états de limitation azotée (phases 1, 2 et 3 **Figure 45**). Les études de co-régulation génique sont en cours et permettront d'identifier les réseaux de gènes spécifiques de conditions physiologiques en lien à la fois avec la disponibilité en azote et avec l'accumulation des lipides de réserve.



# Title: Use of a lipid rich strain reveals mechanisms of nitrogen limitation and carbon partitioning in the haptophyte *Tisochrysis lutea*

## Authors:

Matthieu Garnier<sup>1\*</sup>, Gael Bougaran<sup>1</sup>, Marija Pavlovic<sup>2</sup>, Jean-Baptiste Berard, Gregory Carrier<sup>1</sup>, Aurélie Charrier<sup>1</sup>, Fabienne Le Grand<sup>3</sup>, Ewa Lukomska<sup>1</sup>, Catherine Rouxel<sup>1</sup>, Nathalie Schreiber<sup>1</sup>, Jean-Paul Cadoret<sup>1</sup>, Hélène Rogniaux<sup>2</sup>, Bruno Saint-Jean<sup>1</sup>.

<sup>1</sup>IFREMER. Physiology and Biotechnology of Algae, Nantes, France

<sup>2</sup>INRA, UR1268 Biopolymers Interactions Assemblies F-44316 Nantes, France

<sup>3</sup>LEMAR, UMR6539 Marine Environmental Sciences Laboratory, Brest France

## Abstract

Haptophytes are a diverse monophyletic group with a worldwide distribution, known to be significantly involved in global climate regulation in their role as a carbon sink. Because nitrogen is a major limiting macronutrient for phytoplankton in oceans and for cultures of microalgae, understanding the involvement of nitrogen availability in haptophyte carbon partitioning is of global and biotechnological importance. Here, we made an ecophysiological study coupled with comprehensive large scale proteomic analysis to examine differences of behavior in reaction to nitrogen availability changes between a wild type strain of *Tisochrysis lutea* (WTc1) and a mutant strain (2Xc1) known to accumulate more storage lipids. Strains were grown in chemostats and studied under different ecophysiological conditions including N limitation, N repletion and N depletion. Whereas short time N repletion triggered consumption of carbohydrates in both strains, storage lipid degradation and accumulation during changes of ecophysiological status were only recorded in 2Xc1, suggesting a higher sensitivity to nitrogen changes in the lipid-rich strain. After 3 months of continuous culture, 2Xc1 exhibited an unexpected increase of carbon sequestration ability (+50%) by producing twofold more carbohydrates for the same nitrogen availability. Deep proteomic analysis by LC-MS/MS identified and compared the abundance of 4332 proteins, *i.e.* the deepest coverage of a microalgal proteome obtained to date. Results revealed that storage lipid accumulation is favored by an overall reorganization of carbon partitioning in 2Xc1 cells that increases the metabolism of carbon and energy acquisition, and decreases mitochondrial activity and metabolic conversion of storage lipids to phosphoenolpyruvate before gluconeogenesis.

## 1. Introduction

Photosynthetic eukaryotes make a significant contribution to major global processes, such as oxygen production, carbon fixation and CO<sub>2</sub> sequestration and nutrient recycling, thereby sustaining the life of most other aquatic organisms. Because of their photo-autotrophic abilities, microalgae behave as sunlight-driven cellular factories that convert CO<sub>2</sub> into energy-rich storage compounds such as polymeric carbohydrates and lipids [1]. Hence they have received a considerable amount of attention as possible sources of next-generation energy feedstock, animal feeds, food and high valuable compounds [2,3]. The sequestration of atmospheric CO<sub>2</sub> by microalgae and their in-cell carbon partitioning is relevant both on a global level and to biotechnological innovation [4]. In oceans, nitrogen is the main nutrient likely to limit growth of phytoplankton [5,6]. Moreover,

nitrogen availability is one of the main drivers of carbon storage and partitioning in microalgae. The overall metabolism and molecular mechanisms of storage lipid accumulation following nitrogen deprivation have been documented in detail in the model green alga *Chlamydomonas reinhardtii* grown mixotrophically using CO<sub>2</sub> and acetate as carbon sources [7–9]; [10–12]; [13]. Other studies deal with autotrophically grown microalgae and concern *C. reinhardtii* [14], as well as diatoms of ecological interest, such as *Phaeodactylum tricorutum* [15–18], and species used in biotechnological applications, such as the eustigmatophyceae *Nannochloropsis oceanica* [19,20]. A general finding of these functional genomics studies has been that lipid accumulation is connected to changes in the expression of the core enzymes of the central carbon metabolism [21]. Remarkably, changes in the enzymes of lipid metabolism are rarely observed during TAG accumulation, indicating the existence of other control points for the process of lipid accumulation. Species and physiological specificity (mixotrophy vs autotrophy; short term N

CHAPITRE IV : Limitation azotée et allocation du carbone. Approche intégrative en chémostat.

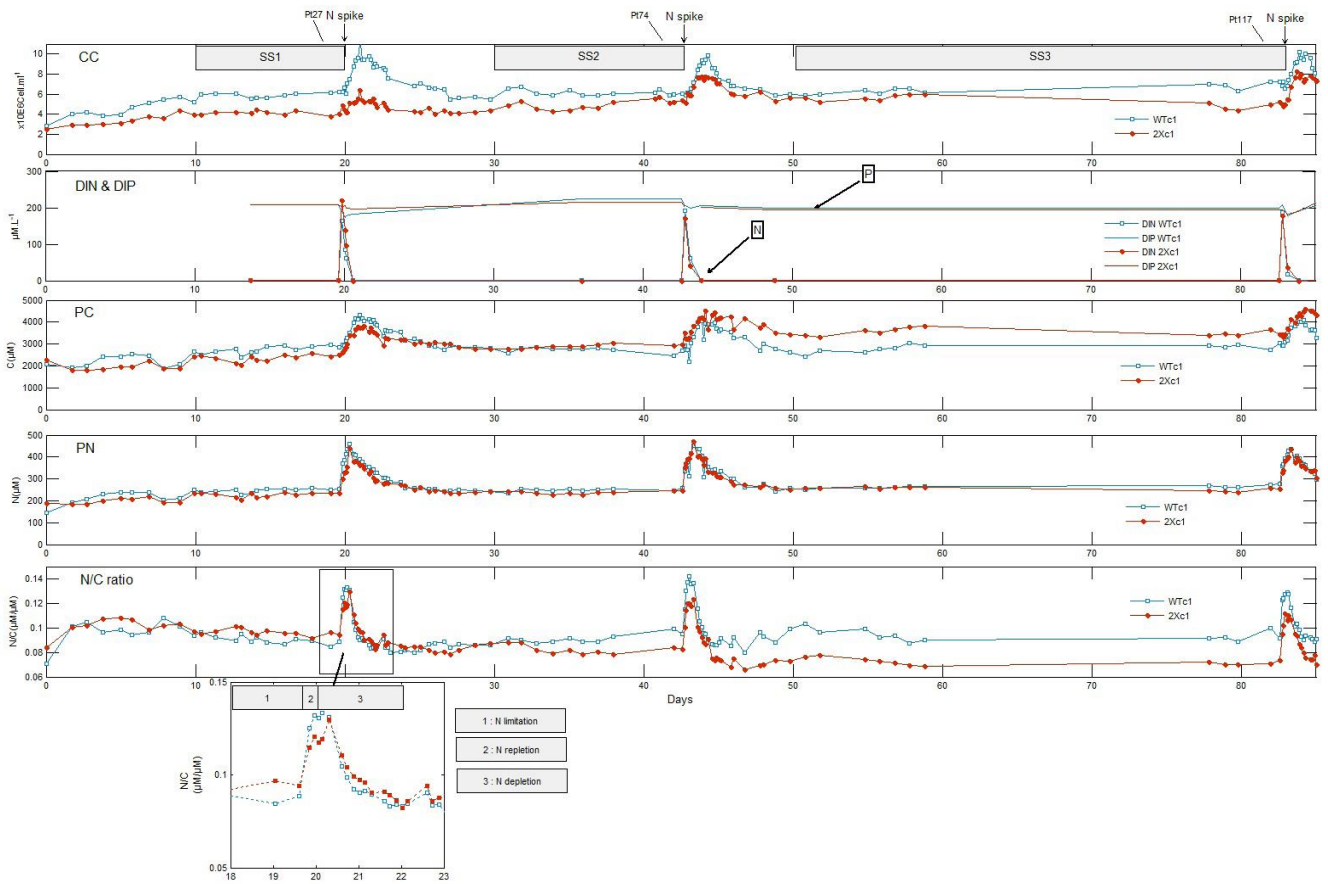


Fig. 1: Computed ecophysiological parameters. WTc1 and 2Xc1 strains were cultured for 85 days in nitrogen limited chemostats subjected to three nitrogen spikes. Cell Concentration (CC), Dissolved Inorganic Nitrogen (DIN) (squares) and Dissolved Inorganic Phosphorus (DIP) (no square), Particulate Carbon (PC), Particulate Nitrogen (PN), and particulate N/C ratio were calculated. Three steady states were delimited. SS1: Day 10→D20, SS2: D30→D43, and SS3: D50→D80. N/C ratio computed after the first N spike zooms in on the bottom square. Three phases were delimited: (1) N limitation, (2) N repletion and (3) N depletion.



deprivation vs long term deprivation) were revealed and but regulatory mechanisms remain poorly understood. Experimental approaches using mutant and complemented strains have enabled an assessment of the role of genes in lipid metabolism and deciphered carbon partitioning between carbohydrates and lipids in several species including *Chlorella sorokiniana*, *C. reinhardtii* and *P. tricornutum* [22–29]. However, although knowledge on the metabolic pathways of model species *C. reinhardtii* and *P. tricornutum* has improved, numerous papers attest that metabolic pathways and carbon storage can differ a great deal between different lineages of algae [30–32].

The haptophyte *T. lutea* is a mobile non-calcified species that produces a high amount of docosahexanoic acid (DHA) and storage lipids, of interest for nutritional and energy applications, respectively [33,34]. *T. lutea* is widely used to feed mollusk larvae in aquaculture. It produces alkenones, which are long-chain unsaturated methyl and ethyl n-ketones (C37 and C38), exclusive to haptophytes, and widely used as biomarkers for the reconstruction of marine paleoclimatology [35,36,37]. Haptophytes constitute a diverse monophyletic group that originated from secondary endosymbiosis of a red alga into a non-photosynthetic eukaryotic host. The group includes calcified and non-calcified morphotypes depending on sex and species. Haptophytes are distributed worldwide and participate greatly in global climate regulation as a carbon sink [38]. For these reasons, it is used as a biological model for studies on microalgal ecophysiology, lipid metabolism, nutrition, and toxicology. Understanding mechanisms of carbon partitioning in haptophytes is also of ecological and biotechnological relevance. Carbon partitioning and flows toward macromolecules have been described in the blooming coccolithophore *Emiliania huxleyi* [39,40]. The impact of nitrogen and phosphorus availability on carbon accumulation and partitioning was modeled in *T. lutea* [41–43]. However, very little is known about the metabolic pathways and regulations of carbon partitioning in *T. lutea*.

A lipid over-accumulating mutant strain (*T. lutea* S2M2) was obtained through a domestication process [44]. Forward genomics on lipid accumulating strains by comparative genomics would identify the potential metabolic controller that promotes carbon accumulation. Previous proteomic and transcriptomic analysis reveals that wild type and mutant strains behave differently during the early phases of nitrogen starvation and suggest that proteins involved in carbon homeostasis, lipid metabolism and carbohydrate catabolism are likely involved in lipid accumulation [45,46]. These studies focused on the effect of nitrogen starvation, but very little is yet known about nitrogen limitation or short-term nitrogen repletion. The objective of the current study was to characterize the ability of *T. lutea* WT and S2M2 to accumulate carbon or consume stored carbon following fine-tuned changes of nitrogen availability and to identify the molecular mechanisms involved in strain-specific metabolism. To compare strain with similar genetic diversity, this study was done with clones isolated from each strain (WTc1 from WT and 2Xc1 from S2M2). They were grown for 3 months in chemostats with nitrogen limitation and subjected to three nitrogen spikes. On the basis of growth limitation and lipid accumulation models [42,47], our hypothesis was that each nitrogen spike would lead to three successive physiological states including: 1) state of nitrogen limitation at the steady state phase before N spike and leading to storage

lipid accumulation, 2) state of nitrogen repletion after N spike and leading to storage lipid consumption, and 3) state of nitrogen depletion when all the nitrogen is consumed and leading to storage lipid accumulation. The physiology and carbohydrates and lipid profiles of the two strains were studied during the experiment. A previous qualitative proteomic analysis revealed that proteomic changes may be related to carbon partitioning in S2M2. In the present study, a large-scale quantitative proteomics approach was used to identify the proteins differentially accumulated in the mutant strain of *T. lutea* subjected to the aforementioned conditions of nitrogen supply. The data collected offer the most comprehensive view of the proteome of a microalga obtained to date, and provide new mechanistic insights into lipid accumulation and carbon partitioning in haptophytes.

## 2. Results

### 2.1 Physiology in chemostat cultures

WTc1 and 2Xc1 strains were cultured for 90 days in nitrogen-limited chemostats, which were subjected to three nitrogen spikes. Cell Concentration (CC), Particulate Carbon (PC), Particulate Nitrogen (PN), particulate N/C ratio, Dissolved Inorganic Nitrogen (DIN) and Dissolved Inorganic Phosphorus (DIP) were sampled at high frequency throughout the course of the experiment (Fig. 1). Three phases of steady state (SS) were delimited, each of which had calculated coefficients of variation (CVs) less than 5% for PN, PC and N/C. This confirmed the low variability of algal physiology within each SS and the appropriateness of using samples taken during these phases to obtain high-quality reproducible data. CC was lower in 2Xc1 than WTc1 all during the experiment for similar PN and PC concentrations, indicating the larger size of 2Xc1 cells, as previously observed [45] (Fig. 1).

During the dynamic phase after N spikes, CC, DIP, DIN, PC, PN and N/C ratio showed similar profiles both between the strains and for the three spikes (Fig. 1). DIN decreased quickly from 200  $\mu\text{M}$  to a non-detectable concentration ( $< 0.5\mu\text{M}$ ) in 24 hours, which was correlated with an increase of 200  $\mu\text{M}$  in PN and a 30 to 35% increase of N/C ratio. This indicates a rapid N uptake by strains whose growth is limited by nitrogen. After each spike, biomass estimated by PC and CC increased drastically during the first 24 hours, demonstrating the limitation by nitrogen during SS. Then, CC and PC maintained a high level for 36 hours and decreased slightly until a new steady state was reached within 10 days. Following N/C evolution, three physiological states were observed: nitrogen limitation at steady state; nitrogen repletion during about 24 H, when N/C ratio increased; and nitrogen depletion, when N/C ratio decreased (Fig. 1).

Computed growth rate was 0.5  $\text{d}^{-1}$  at steady state and increased for 48 hours up to 0.75  $\text{d}^{-1}$  after each N spike, then decreased over 48 hours to a minimum of 0.4  $\text{d}^{-1}$  and reached steady state within 10 days (Supp mat 1).

CHAPITRE IV : Limitation azotée et allocation du carbone. Approche intégrative en chémostat.

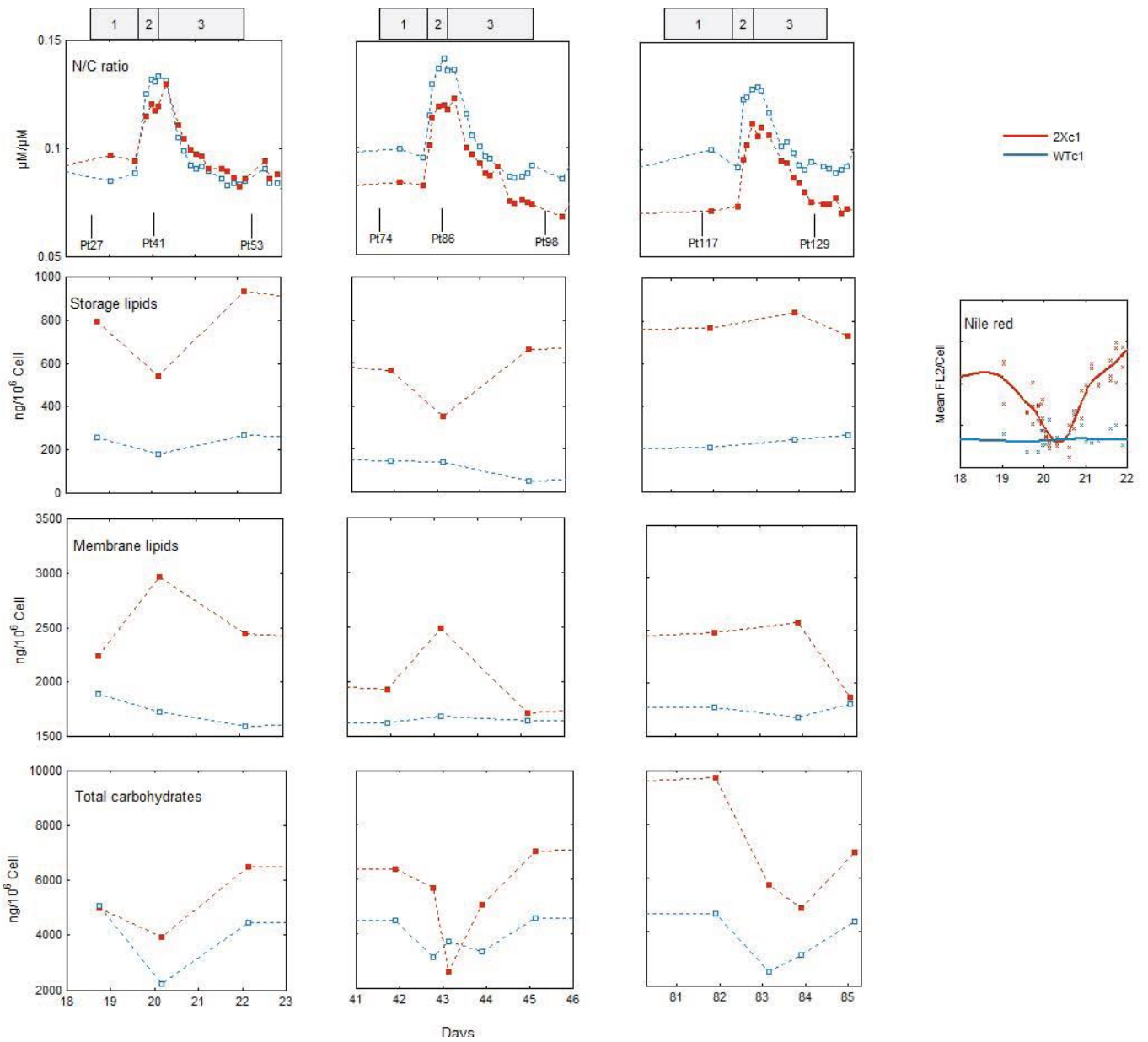


Fig. 2: Lipid and carbohydrate analysis during different phases before and after each N spike. (1) N limitation, (2) N repletion and (3) N depletion. Computing of N/C ratios, storage and membrane lipids by HPTLC, and total carbohydrates. Computing of storage lipids by Nile red fluorescence after the first N spike is given in the right-hand box.

## CHAPITRE IV : Limitation azotée et allocation du carbone. Approche intégrative en chémostat.

### 2.2 Carbon partitioning

Carbon partitioning between storage lipids, membrane lipids, carbohydrates, proteins and chlorophyll for the three nitrogen physiological states has been studied on the basis of conversion factors of gram carbon by gram of compound proposed by [48] (Tab. 1). Up to 10.7% and 27.5% of the carbon were not recorded in WTc1 and 2Xc1 respectively. This may partially be due to bias in the conversion factor and the absence of

measurement of other organic carbon compounds such as small metabolites and/or mineral carbon. As was generally found in this experiment, carbon was mainly allocated to proteins, carbohydrates and membrane lipids, and at a lower level to storage lipids. Throughout the experiment, proteins were 1.4 to 1.9-fold higher in WTc1 than in 2Xc1, chlorophyll was 1.2 to 1.8-fold higher in WTc1 and storage lipids were more than twofold higher in 2Xc1 (0.6 to 3.9% of carbon in WTc1 and 3.7 to 9.3% in 2Xc1). Membrane lipid (ML) content was quite similar in the two strains.

**Table 1: Carbon partitioning in percentage of carbon in the three nitrogen physiological states.** Pt 27, 41 and 117 corresponding to the state of nitrogen limitation, Pt 41 and 74 corresponding to the state of nitrogen repletion and Pt 53, 98 and 119 corresponding to the state of nitrogen depletion (see figure 2). *nd* is calculated part of carbon that miss for 100% final.

| Sample                  | Nitrogen state | N/C  |      | Storage lipids |      | Membrane lipids |      | Carbohydrates |      | Proteins |      | Chlorophyll a |      | <i>nd</i> |      |
|-------------------------|----------------|------|------|----------------|------|-----------------|------|---------------|------|----------|------|---------------|------|-----------|------|
|                         |                | WTc1 | 2Xc1 | WTc1           | 2Xc1 | WTc1            | 2Xc1 | WTc1          | 2Xc1 | WTc1     | 2Xc1 | WTc1          | 2Xc1 | WTc1      | 2Xc1 |
| Pt27                    | limitation     | 0.09 | 0.1  | 3.4            | 8.4  | 25.1            | 23.7 | 35.2          | 27.8 | 39.2     | 27.3 | 1.04          | 0.7  | 0         | 12.1 |
| Pt41                    | repletion      | 0.13 | 0.12 | 2.5            | 4.8  | 23.5            | 26.3 | 16.2          | 18.3 | 45.9     | 27.2 | 1.43          | 0.9  | 10.5      | 22.5 |
| Pt53                    | depletion      | 0.08 | 0.09 | 3.8            | 8.1  | 22.7            | 21.3 | 33.4          | 29.7 | 34.5     | 22.9 | 1.07          | 0.6  | 4.5       | 17.4 |
| Pt74                    | limitation     | 0.09 | 0.08 | 1.9            | 5.8  | 21.5            | 19.9 | 31.1          | 34.7 | 42.2     | 24.8 | 0.79          | 0.7  | 2.5       | 14.1 |
| Pt86                    | repletion      | 0.14 | 0.12 | 1.9            | 3.7  | 23              | 26.3 | 26.7          | 14.4 | 40.2     | 26.6 | 1.46          | 1.3  | 6.7       | 27.7 |
| Pt98                    | depletion      | 0.09 | 0.07 | 0.6            | 7    | 21              | 18.1 | 30.9          | 38.9 | 39.3     | 24.1 | 0.87          | 0.7  | 7.3       | 11.2 |
| Pt117                   | limitation     | 0.09 | 0.07 | 3.2            | 6.4  | 27.1            | 20.7 | 37.7          | 42.7 | 37.7     | 21.4 | 0.91          | 0.5  | 0         | 8.3  |
| Pt129                   | depletion      | 0.1  | 0.09 | 3.9            | 9.3  | 26.8            | 28.4 | 26.6          | 28.4 | 36.2     | 23.9 | 1.08          | 0.9  | 5.4       | 9.1  |
| R <sup>2</sup> with N/C |                |      |      | 0.06           | 0.21 | 0               | 0.56 | 0.56          | 0.96 | 0.35     | 0.63 | 0.78          | 0.58 |           |      |

Principal Component Analysis of the different variables of the Tab. 1 indicated that the N/C ratio was correlated with the allocation of carbon to chlorophyll a and protein and inversely correlated with carbohydrates in the first dimension of the PCA (70% of the observed variability) (Supp mat 2). The storage lipids (SL) at steady states were mainly composed of triacylglycerols (TAG) (72 to 85 % of SL in WTc1 and 95-98 % in 2Xc1) (Supp mat 3). In WTc1, 9 to 28 % of the storage lipids were alkenones, whereas alkenones were very low (<2% of SL) in 2Xc1. After the N spikes, cell storage lipid content, followed by Nile Red (NR) fluorescence and High Performance Thin Layer Chromatography (HPTLC), decreased in 2Xc1 during all phases of nitrogen repletion and increased during nitrogen depletion (Fig. 2). HPTLC analysis showed that membrane and storage lipids of 2Xc1 cells evolve in opposite directions, suggesting that a transfer of fatty acids could occur from membrane to lipid droplets colored with Nile red. Lipid content in WT cells did not change after an N spike. Our results indicate that 2Xc1 accumulates more storage lipids than WT strain as previously reported [44] and is more sensitive to changes in nitrogen limitation.

During the dynamic phase after N spikes, carbohydrate content (CH) decreased drastically in cells of both strains during nitrogen repletion, then increased during nitrogen depletion (Fig. 2). Moreover, by comparing the

three steady states, two PC increases were observed in 2Xc1 for the same PN (+20% from SS1 to SS2; + 22% from SS2 to SS3), causing a decrease in N/C ratio (Fig. 1). This suggests an increase of intracellular pool carbon in 2Xc1 strain during the experiment. According to these results, carbohydrate content was similar in the two strains at SS1, but a 100% increase was observed from SS1 to SS3 in 2Xc1 (Fig. 2). As a result, carbohydrate content in 2Xc1 was twofold higher in 2Xc1 at SS3. Moreover, for the same PN a 50% increase of PC was measured in 2Xc1 from the first SS to the third SS (+20% from SS1 to SS2; + 22% from SS2 to SS3) related to a decrease of N/C ratio. This suggests an increase of carbon accumulation capacity of the 2Xc1 strain during the experiment due to an increase of cell carbohydrate content.

### 2.3 First comprehensive proteome analysis of *Tisochrysis lutea* reveals large differences between mutant and wild type strains

Proteomes were analyzed on samples taken during the steady states of the chemostats. Three biological samples (Pt27, Pt74 and Pt117 on Fig. 2) were used as biological replicates for each of the three steady states. A large-scale proteomics analysis of the two strains and three replicates led to the identification of 4,332 proteins by testing 45,032 peptides for matching on

## CHAPITRE IV : Limitation azotée et allocation du carbone. Approche intégrative en chémostat.

the *T. lutea* database. The coverage of proteins by peptides ranged from 2 to 96 peptides per protein, with a median of 6 peptides per protein (Supp mat 4). The identified proteome represents 25% of the *in silico* predicted proteome. Yet, the function of 2,177 proteins remains unknown due to the lack of BLAST results from the Uniprot database and absence of clear functional domain annotation. Of these unknown proteins, 1,530 have homologies with proteins of unknown function in other microalgae, including 1,415 with the haptophyte *E. huxleyi*, 427 with the diatom *P. tricornutum* and 301 with the chlorophyceae *C. reinhardtii*. This reveals the lack of functional knowledge on proteins of *T. lutea* although their study may have significance for the study of haptophyte and model species metabolism. The proteins whose putative function has been inferred represent all functional categories of the cell. The most represented categories are central metabolism & energy and transcription & translation, with 322 and 313 identified proteins, respectively. Of the 254 unique EC numbers identified, 206 were classified as belonging to major metabolic pathways. Almost all of the essential reactions involved in the major energetic and metabolic pathways were identified in this proteome: Calvin cycle, glycolysis, gluconeogenesis, tricarboxylic acid (TCA) cycle, glyoxylate cycle, and pentose phosphate pathway (Fig. 3C). The high protein coverage (median = 6 peptides per protein), the comprehensiveness of the identified proteome (4,332 proteins), and the identification of key enzymes underlines the quality of the data, meaning we can have confidence in the subsequent exploitation of these data for quantitative comparison of the protein expression profiles between the two strains.

Results of peptide normalization, protein quantification and functional annotation are available as supplementary data (Supp mat 5). Principal component analysis on the whole proteome clearly showed two distinct clusters corresponding to the two strains, with 45.4% of the differences observed on the first dimension and 26.5% on the second (Fig. 3A). This shows strain specificities of the proteomes and justifies comparative analysis. In terms of abundance, 19% of the proteins therefore differed between the strains, with 205 up-accumulated and 608 down-accumulated proteins in 2Xc1, as visualized on the volcano plot in Fig. 3B. The function of 66% of the up-accumulated proteins and 48% of the down-accumulated proteins remains unknown. Yet, the results of the present paper indicate that proteins whose functional annotation could be retrieved and whose abundance is altered between strains are involved in numerous functional categories. The results of functional classification, fold changes and p values are reported in Tab. 2 for up-accumulated proteins and Tab. 3 for down-accumulated proteins.

Observed differences in the proteome profile between WT and 2Xc1 strains are discussed below, according to the functional category of the proteins.

CHAPITRE IV : Limitation azotée et allocation du carbone. Approche intégrative en chémostat.

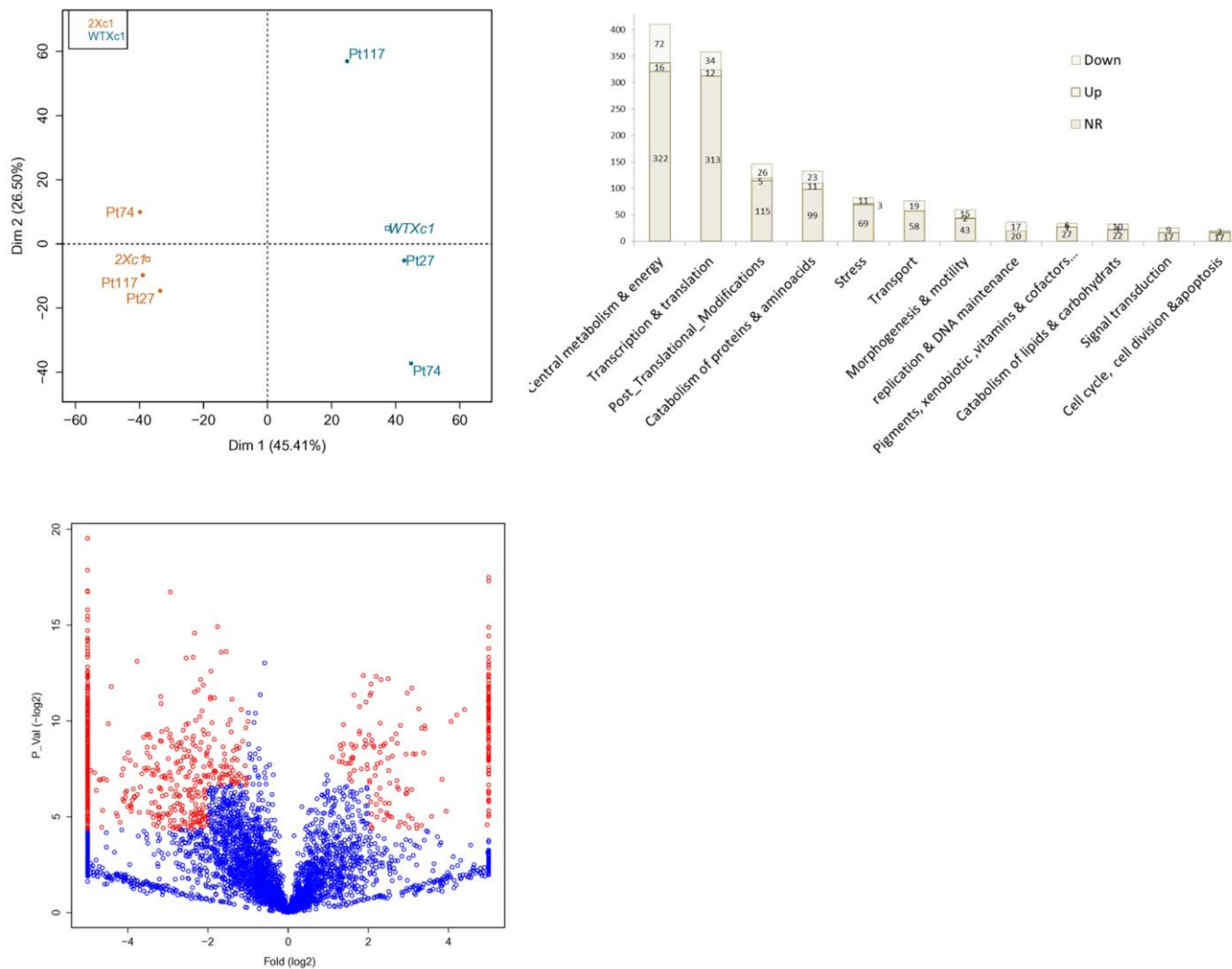


Fig. 3: Proteomic analysis: (A) Principal Component Analysis performed on the complete data set of the abundances of 4332 proteins on the 6 biological samples. Individual representation. (B) Volcano plot showing comparative proteomic data between 2Xc1 strain and WTc1 strain at steady state during nitrogen limitation. The red spots indicate proteins selected for being differentially accumulated. On the left side are the down accumulated proteins and on the right side the up-accumulated proteins. (C) Functional classification of the proteome of *T. lutea* and of proteins differentially accumulated between 2Xc1 strain and WTc1. Only proteins with identified functions are reported here.

### 2.4 2Xc1 strain increases its carbon accumulation.

Three proteins of the Calvin cycle were up-accumulated in 2Xc1, including GAPDH(NADP<sup>+</sup>), PPK, and two of the three identified FBPA (Tab. 2). Two components of photosystem II (PSBP and PSBU) were up-accumulated as well as three components of the photosynthetic electron transport (cyc6 and FNR1), indicating increased cyclic phosphorylation (Tab. 2). Conversely, two components of the photosystem I (PSAA and PSAB) were down-accumulated (Tab. 3), while components of cytochrome B6F complex were not differentially accumulated. Altogether, these results suggest an increase of the protein pool involved in carbon acquisition mechanisms (Fig. 4).

### 2.5 Mitochondrial machinery differs strongly between strains

The multi-enzyme complex pyruvate dehydrogenase (PDH) converts pyruvate into acetyl-CoA. It consists of three main enzymes: pyruvate dehydrogenase (PDC-E1) composed of 2 subunits ( $\alpha$  and  $\beta$ ), dihydrolipoamide S-acetyltransferase (PDC-E2), and dihydrolipoamide dehydrogenase (PDC-E3). All components and two isoforms for E1 and E2 were identified in *T. lutea* proteome including the chloroplastic and mitochondrial isoforms. The mitochondrial isoform of PDC-E2 was 2.7-fold down-accumulated in 2Xc1 (Tab. 3). Moreover, the mitochondrial pyruvate dehydrogenase kinase (PDHK), an inhibitor of PDH, was 3.8-fold up-accumulated (Tab. 2). In photoautotrophic cells, the PDH pathway can be shunted by the decarboxylation of pyruvate by pyruvate decarboxylase followed by the decarboxylation of acetaldehyde by ALDH and the conversion of acetate to acetyl-CoA by acetyl-coenzyme A synthetase (ACS). ALDH and ACS were both strongly down-accumulated in 2Xc1 (Tab. 3). We thus conclude there was a decrease of pyruvate-related hub enzymes and AcCoA synthesis in mitochondria in 2Xc1 (Fig. 4).

AcCoA is the main entry of the TCA cycle and can be shunted by pyruvate carboxylase (PCr) that converts pyruvate into oxaloacetate. PCr was also 2.8-fold down-accumulated in 2Xc1 (Tab. 2). Proteins involved in the first three successive reactions of the TCA cycle (Aco, IDH and OGDC) were down-accumulated (Tab. 2) (Fig. 4). These results suggest a possible reduction of energy in the form of ATP generated through the oxidation of acetate derived from carbohydrates lipids and proteins. The pool of NADH and precursors of certain amino acids from malate and oxaloacetate could be affected.

In parallel to the down-accumulation of TCA cycle proteins, we observed a strong down-accumulation of three components of the NADH dehydrogenase complex (NADHDH p1, p2 and p10) that catalyzes the transfer of electrons from NADH produced by the TCA cycle and consists in the first reaction of oxidative phosphorylation (Tab. 2 & Fig. 4). An element of the second reaction complex (FR(NADH)) was also down-accumulated (Tab. 2). This enzyme reduces the fumarate in succinate and interacts with the TCA cycle. Other proteins of oxidative phosphorylation were not differentially accumulated except for one of the two gamma subunits of ATP synthase identified, which was twofold down-accumulated (Tab. 2). These results suggest a decrease of oxygenic respiration concomitant with a decrease of the TCA cycle.

Two mitochondrial import receptor subunits (TOM40 and TOM70) and five non-differentially accumulated mitochondrial import inner membrane translocase subunits (TIMs) were identified in the proteome. Whereas the TIMs were not differentially accumulated, the two TOM subunits were strongly down-accumulated in 2Xc1 (Tab. 2). In plants, TIMs and TOMs are involved in protein-import apparatus of mitochondria [49]. This suggests a decrease of mitochondrial protein import activity at receptor level. 2.6 Lipid metabolism differs at the catabolic level and the conversion of lipids to carbohydrates is drastically affected

All the enzymes for fatty acid biosynthesis from acetyl-coA were identified in the present proteome survey (Fig 5). No difference in the expression of these enzymes was observed between the two strains. Most studies on haptophytes suggest that carbon is mainly stored in the form of triacylglycerides (TAGs) or alkenones, accumulated in lipid droplets [50]. The most frequently described route to triglycerides biosynthesis is the Kennedy pathway that occurs in the endoplasmic reticulum. The four enzymes (GPAT, LPAT, PAP and DGAT) of the Kennedy pathway have been identified in the genome of *T. lutea*, but only GPAT and LPAT were detected in the proteome (Fig. 5). We recorded the strong down-accumulation of the LPAT in the 2Xc1 strain. We identified a PDAT that, in the green microalgae *Chlamydomonas reinhardtii*, catalyzes the TAGs via transacylation of diacylglycerol (DAG) with acyl groups from phospholipids, galactolipids or phosphatidylcholine (PC) [51]. These authors suggest that “PDAT-mediated membrane lipid turnover is essential for membrane lipid degradation with concomitant production of TAG”. The absence of DGAT detection and the presence of PDAT suggests that the transfer of acyl groups from membrane lipids to DAG have a predominant role to produce TAGs. The biosynthesis of alkenones is poorly described. In the proteome of *Tisochrysis lutea* we identified a very-long-chain 3-oxoacyl-CoA reductase (Kcr), potentially involved in this biosynthesis. This protein was 2.2-fold down-accumulated in 2Xc1, which accordingly presents very low alkenone abundance (Tab. 3).

Numerous proteins involved in lipid catabolism were down-accumulated in 2Xc1 (Tab. 2). These included TAGH, 3 LACS, 2 HCDH and one ACAA, all involved in the major steps of  $\beta$ -oxidation (Fig. 4). These results suggest a strong decrease of TAG and fatty acid hydrolysis machinery. The glyoxylate cycle uses acetyl-CoA from  $\beta$ -oxidation for biosynthesis of carbohydrates by neoglucogenesis. We showed a twofold down-accumulation of ACO and the strong down-accumulation of MALSH, the key enzyme of the glyoxylate cycle (Tab. 3). This protein, identified by 13 peptides in the WTc1 strain, was never detected in the 2Xc1 strain. All these results suggest that the conversion of lipid to carbohydrates is drastically altered in 2Xc1 in this experiment compared with the wild type strain.

### 2.7 Carbohydrate metabolism

None of the unidirectional enzymes specifically involved in glycolysis or in gluconeogenesis were affected in terms of abundance in this study. In haptophytes, recent studies showed that carbohydrates can be stored in the form of polysaccharides and  $\beta$ -1,3-glucans known as chrysolaminarin [52].

CHAPITRE IV : Limitation azotée et allocation du carbone. Approche intégrative en chémostat.

Table 2. Proteins up-accumulated in 2Xc1

| Protein ID | Functional classification                                   | Pathways                                    | Protein Name  | Synonym                                | EC  | peptides | Log2(fold change) | p-value |
|------------|---|---|---|--|---|----------|-------------------|---------|
| P196.01    |   |   | Cytochrome c6   | CyC6                                   |   | 10       | 1.38              | 0.00    |
| P3303.01   |   |   | Cytochrome c6   | CyC6                                   |   | 2        | 5.00              | 0.00    |
| P31.04     |   | Photosynthesis                              | Ferredoxin--NADP reductase  | FNR                                    | 1.18.1.2  | 14       | 1.36              | 0.02    |
| P1680.01   |   |   | Ferredoxin  | Fd                                     |   | 8        | 3.26              | 0.00    |
| P2343.01   |   |   | PsbP domain containing unknown conserved protein                      | PsbP                                   |   | 5        | 1.30              | 0.01    |
| P235.01    |   |   | Photosystem II 12 kDa extrinsic protein                               | PsbU                                   |   | 13       | 1.83              | 0.01    |
| P64.01     |   |   | Phosphoribulokinase   | PPK                                    | 2.7.1.1.9   | 30       | 1.88              | 0.00    |
| P9.01      |   | Calvin cycle & glycolysis /<br>glucogenesis | glyceraldehyde-3-phosphate dehydrogenase (NADP+)                      | GAPDH(NAD P+)                          | 1.2.1.1.3   | 50       | 1.37              | 0.00    |
| P1109.01   | Central metabolism &<br>energy                              |   | Fructose-bisphosphate aldolase  | FBPA                                   | 4.1.2.1.3   | 11       | 3.57              | 0.03    |
| P2730.01   |   | Fructose-bisphosphate aldolase              | FBPA  | 4.1.2.1.3                              | 6   | 2.01     | 0.02              |         |
| P4005.01   |   | Polysaccharides                             | Callose synthase  |  |   | 3        | 5.00              | 0.01    |
| P1607.01   |   | Pyruvate metabolism                         | Pyruvate dehydrogenase kinase (mitochondrial)                         | PDHK                                   |   | 10       | 3.18              | 0.00    |
| P3289.01   |   | Oxidative phosphorylation                   | NADH dehydrogenase [ubiquinone] 1 alpha subcomplex assembly factor 5  | NADHHDH-p5                             | 1.6.5.3   | 4        | 1.94              | 0.00    |
| P748.01    |   | Biosynthesis of sterol<br>compounds         | Cycloartenol-C-24-methyltransferase 1                                 |  |   | 14       | 2.75              | 0.04    |
| P2525.01   |   | L-alanine biosynthesis                      | Cysteine desulfurase  | NIFS                                   | 2.8.1.7   | 6        | 1.53              | 0.01    |
| P1015.01   |   | Aminoacyl-tRNA biosynthesis                 | Phenylalanine--tRNA ligase  | PheRS                                  | 6.1.1.2.0   | 11       | 2.51              | 0.01    |
| P3826.01   |   | Pyrimidine metabolism                       | ATP:CMF phosphotransferase  | ATCM                                   | 2.7.4.1.4   | 3        | 5.00              | 0.00    |
| P3380.01   |   |   | Aminomethyltransferase  |  | 2.1.2.1.0   | 2        | 5.00              | 0.00    |
| P1056.01   | Catabolism of lipids &<br>carbohydrates                     | Beta-oxidation                              | Short-chain 3-hydroxyacyl-CoA dehydrogenase                           | HCDH                                   | 1.1.1.3.5   | 11       | 5.00              | 0.00    |
| P3630.01   | Replication and DNA<br>maintenance                          | DNA repair                                  | UV excision repair protein  | RAD23                                  |   | 2        | 5.00              | 0.00    |
| P49.07     |   | RNA helicase                                | Unknown conserved ATP-dependent RNA helicase                          |  |   | 1        | 5.00              | 0.00    |
| P4096.01   |   | Transcription regulation                    | Histone deacetylase   | Hdac                                   | 3.5.1.9.8   | 2        | 5.00              | 0.03    |
| P4013.01   |   |   | Uncharacterized RNA pseudouridine synthase Mb1738                     |  |   | 3        | 5.00              | 0.00    |
| P2856.01   |   |   | Ribosomal protein L11 methyltransferase                               | L11 Mtase                              |   | 4        | 2.19              | 0.00    |
| P3113.01   |   | Ribosomal proteins                          | 40S ribosomal protein S21-1   |  |   | 3        | 2.08              | 0.05    |
| P2012.01   |   |   | 40S ribosomal protein S28 gi  |  |   | 4        | 2.96              | 0.01    |
| P2188.01   |   |   | 50S ribosomal protein L28, chloroplastic                              |  |   | 5        | 2.91              | 0.04    |
| P1378.01   | Transcription & translation                                 |   | Ribosome biogenesis regulatory protein homolog                        |  |   | 11       | 1.97              | 0.01    |
| P3863.01   |   |   | Ribosome biogenesis   | Ribosome production factor 1           |   |          | 2                 | 5.00    |
| P2702.01   |   | tRNA  | Aminoacyl tRNA synthase complex-interacting multifunctional protein 1 |  |   | 6        | 1.98              | 0.01    |
| P1310.01   |   |   | 5'-3' exoribonuclease   |  |   | 10       | 1.61              | 0.00    |
| P2691.01   |   |   | RNA binding domain containing conserved unknown protein               |  |   | 5        | 5.00              | 0.00    |
| P4101.01   |   |   | C3H   |  | 2   | 5.00     | 0.00              |         |
| P3717.01   |   |   | TFIIF alpha sub-unit  |  | 4   | 5.00     | 0.02              |         |
| P2870.01   | Pigments, xenobiotic<br>,vitamins & cofactors<br>metabolism | Biosynthesis of steroids                    | 2-C-methyl-D-erythritol 2,4-cyclodiphosphate synthase                 | MCS                                    | 4.6.1.1.2   | 5        | 3.08              | 0.01    |
| P348.01    |   | Porphyrin and chlorophyll<br>metabolism     | porphobilinogen synthase  | PPBNGS                                 | 4.2.1.2.4   | 29       | 1.64              | 0.00    |
| P143.01    |   |   | Geranylgeranyl diphosphate reductase                                  |  |   | 31       | 2.50              | 0.00    |
| P3176.01   |   | Amino-acid catabolism                       | 2-oxoisovalerate dehydrogenase subunit alpha                          | BCKDHA                                 | 1.2.4.4   | 4        | 5.00              | 0.00    |
| P775.01    |   |   | KDEL-tailed cysteine endopeptidase CEP1                               | AtCP56                                 |   | 15       | 2.80              | 0.04    |
| P2807.01   |   |   | Proline iminopeptidase  | PIP                                    | 3.4.11.5  | 7        | 2.42              | 0.00    |
| P4106.01   | Catabolism of proteins &<br>amino acids                     | Protease / peptidase                        | Serine carboxypeptidase-like 10                                       | SAT                                    |   | 2        | 5.00              | 0.00    |
| P3693.01   |   |   | Tripeptidyl-peptidase 1   | TPP-1                                  |   | 3        | 5.00              | 0.00    |
| P1222.01   |   |   | Carboxyl-terminal-processing protease                                 |  |   | 13       | 2.46              | 0.03    |
| P3417.01   |   |   | Carboxyl-terminal-processing protease                                 |  |   | 4        | 5.00              | 0.00    |
| P2725.01   |   |   | Protease Do-like 1, chloroplastic                                     |  |   | 8        | 2.72              | 0.00    |
| P3664.01   |   |   | Putative tyrosinase-like protein tyr-3                                |  |   | 3        | 5.00              | 0.00    |
| P1106.01   |   |   | Unknown conserved signal peptidase                                    |  |   | 12       | 1.97              | 0.00    |
| P3685.01   |   |   | Signal transduction   | Regulation of intracellular<br>calcium | Calcium/calmodulin-dependent protein kinase type II delta chain | CAMPK    |                   | 3       |
| P3333.01   | EF-hand calcium-binding domain-containing conserved protein |   |   |  | 4   | 5.00     | 0.00              |         |
| P3142.01   | Cell cycle, cell division &<br>apoptosis                    | Cell cycle                                  | Cyclin-dependent kinase C-2   | CDK2                                   |   | 4        | 5.00              | 0.00    |
| P2261.01   |   | Cycle circadien                             | Cryptochrome DASH, chloroplastic/mitochondrial                        |  |   | 9        | 2.09              | 0.05    |
| P3799.01   |   | Protein isomerisation                       | Peptidyl-prolyl cis-trans isomerase FKBP53                            | PPiase FKBP53                          | 5.2.1.8   | 3        | 5.00              | 0.00    |
| P3486.01   | Post Traductional<br>Modifications                          |   | Unknown conserved Peptidylprolyl isomerase                            |  |   | 3        | 5.00              | 0.01    |
| P3514.01   |   |   | 8 ankyrin repeat domain containing unknown protein                    |  |   | 3        | 2.01              | 0.00    |
| P1287.01   |   |   | Hsp70 nucleotide exchange factor FES1                                 |  |   | 8        | 1.51              | 0.00    |
| P840.01    |   |   | DnaJ homolog subfamily B member 3                                     | DNAJ-B3                                |   | 19       | 2.17              | 0.01    |
| P4113.01   | Morphogenesis & motility                                    |   | ADP-ribosylation factor GTPase-activating protein 1                   | ARF GAP 1                              |   | 2        | 5.00              | 0.00    |
| P3257.01   |   |   | Dynein light chain 2, cytoplasmic                                     |  |   | 4        | 5.00              | 0.01    |

## CHAPITRE IV : Limitation azotée et allocation du carbone. Approche intégrative en chémostat.

Little information is available on the chrysolaminarin biosynthetic pathway. We identified several potential components of chrysolaminarin biosynthetic pathway including PGI, PGCM, UDPGP and KRE6. The degradation of chrysolaminarin is potentially catalyzed by the identified laminarinase-like protein (enzyme of the GH16 family), by the seven identified betaglucosidases and/or by seven other glucosidases. The glucose end-product would be subsequently phosphorylated by a glucokinase (GK) before entering glycolysis. These proteins were not differentially accumulated except one lysosomal beta glucosidase, which was strongly down-accumulated in 2Xc1 (Tab. 3). Furthermore, we identified a callose synthase presumably involved in *T. lutea* cell wall polysaccharide synthesis, which was strongly up-accumulated in 2Xc1 (Tab. 3).

### 2.8 Metabolism of nitrogen is differs strongly in strain 2Xc1

Nitrogen uptake includes several steps before incorporation into carbon skeletons. Nitrogen is mainly taken up in two forms: nitrate and/or ammonium (which is less costly in terms of energy). This nitrogen uptake across the plasma membrane is achieved by low or high affinity nitrate transporters (NRT) or by ammonium transporters (AMT). Nitrate is reduced to nitrite in the cytoplasm by nitrate reductase (NR). Nitrite is transported into the chloroplasts by a nitrite transporter (NAR1) for reduction to ammonia by nitrite reductase (NiR). AMT1, NRT2, NR, NAR1 and NiR were all identified in the present proteomics study. Four isoforms of NRT2 were identified in the transcriptome of *Tisochrysis lutea*, but the set of 23 peptides assigned to NRT2 does not allow discrimination between these four isoforms [53]. NRT2 and AMT1 were down-accumulated in 2Xc1 (Tab. 3).

Twenty-two proteins of the catabolism of proteins, peptides and amino-acids were down-accumulated and ten were up-accumulated (Tab. 2 and 3). We observed the strong up-accumulation of BCKDHA, a component of the branched-chain alpha-keto acid dehydrogenase complex involved in the second major step of the catabolism of the branched-chain amino acids (Tab. 2). The major protein periplasmic L-amino acid oxidase (PLAAX) identified with 56 peptides was 2.2-fold down-accumulated in *T. lutea* 2Xc1 (Tab. 3). This down-accumulation was previously reported in nitrogen-starved cells from batch cultures of *T. lutea* [45]. Twenty-eight proteins involved in protein degradation (proteases, peptidases and proteins of proteasome complexes, ubiquitination) were differentially accumulated between the two strains. An ornithine-urea cycle (OUC) driven by mitochondrial carbamoylphosphate synthase (CPS) was previously suggested in haptophytes [30]. In diatoms, the OUC is known to contribute to carbon and nitrogen repackaging in response to changes of nitrogen availability [30]. Based on the analysis of Allen et al., we identified most of the enzymes of OUC in the proteome of *Tisochrysis lutea*, including CPS, OTC, Asus and AsL. Arginase, reported by Allen et al. 2011, was not identified in the proteome. Proteins of OUC were not affected in 2Xc1 but the identified urease was twofold down-accumulated in 2Xc1, suggesting a decrease of urea catabolism capacity (Tab. 3). Thirteen out of the 41 identified aminoacyl-tRNA synthetases (aa-RS) were strongly down-accumulated in 2Xc1 (Tab. 3), suggesting a strong decrease in protein synthesis machinery.

The purpose of the Pentose Phosphate pathway (PP pathway) aims to produce ribulose-5-phosphate for the synthesis of purines and pyrimidines and erythrose-4-phosphate for the synthesis of aromatic amino acids. All enzymes of the pathway were identified in this proteome (Fig. 4). PGCM, which catalyzes the first step, was 2.3-fold down-accumulated in 2Xc1 and RPPK, an essential component for the synthesis of purines and pyrimidine was strongly down-accumulated (Tab. 3). These results suggest that the synthesis of nucleotides and aromatic amino acids is affected in 2Xc1.

### 2.9 DNA replication and maintenance differ significantly between strains'

The nucleotide excision repair protein RAD23 was strongly up-accumulated in *T. lutea* 2Xc1, whereas the double-strand-break repair protein RAD21 and three Structural Maintenance of Chromosomes protein (SMCs) were strongly down-accumulated. This suggests a large impact on DNA structure in 2Xc1. Twelve of the 23 identified proteins involved in replication were down-accumulated in the 2Xc1 strain (Tab. 3). This notably included the four identified DNA Replication Licensing Factors (MCM2; MCM4; MCM5; MCM6) involved in the initiation of replication.

### 2.10 From DNA to functional protein

More than a hundred proteins involved in transcription and splicing were identified, and the abundance of 26 was affected in 2Xc1 (Tab. 2&3). Five out of 69 initiation and transcription factors were affected in abundance in the 2Xc1 strain. Two transcription factors were strongly up-accumulated and three others were down-accumulated. This suggests that differences of transcriptional regulation level could occur between the two strains. The four identified subunits of CCR4-NOT transcription complex were down-accumulated. This protein is linked to various cellular processes including bulk mRNA degradation, miRNA-mediated repression, translational repression during translational initiation, and general transcription regulation (Zheng, 2012). Nine RNA helicase and polymerases out of the 28 identified were also affected in abundance in the 2Xc1 strain. Only one splicing factor of the 15 identified proteins was down-accumulated and one RNA binding protein out of the 15 identified. These results suggest that transcription is weakly affected in the 2Xc1 strain. However, the difference of accumulation of five transcription factors can be a key element in gene regulation.

Close to 200 proteins involved in translation and splicing were identified and 20 were affected in abundance in 2Xc1 (Tab. 2&3). Four of the 123 identified ribosomal proteins were up-accumulated and six were down-accumulated. Six of the 22 initiation factors and three of the elongation factors were down-accumulated.

Among the 151 proteins involved in folding and post translational modifications, we identified 36 differentially accumulated proteins, including two strongly up-accumulated isomerases, and three other up-accumulated proteins (Tab. 2&3). We also identified three down-accumulated chaperones, five down-accumulated phosphatases, one down-accumulated glucosyltransferase, six down-accumulated isomerases, and two down-accumulated proteins of ubiquitination, nine down-accumulated



CHAPITRE IV : Limitation azotée et allocation du carbone. Approche intégrative en chémostat.

Table 3. Proteins down-accumulated in 2Xc1

| Protein ID | Functional classification                      | Pathways   | Protein name  | Synonym                                    | EC              | peptides | Log2(fold change) | p-value |      |
|------------|--|--|---|--|-----------------|----------|-------------------|---------|------|
| P3313.01   |  | CCM  | Carbonic anhydrases   | CA   | 4.2.1.1         | 2        | -1.44             | 0.00    |      |
| P1924.01   |  | Photosynthesis   | Photosystem I P700 chlorophyll a apoprotein                       | PsaA                                       |                 | 8        | -4.00             | 0.02    |      |
| P1724.01   | Photosystem I P700 chlorophyll a apoprotein A2 |  | PsaB  |  | 9               | -4.29    | 0.03              |         |      |
| P1833.01   |  |  | Phosphoglucomutase  | PGCM                                       | 5.4.2.2         | 8        | -2.32             | 0.01    |      |
| P2352.01   |  | Glycolysis / Gluconeogenesis / Fructose and Mannose metabolism | 6-phosphofructo-2-kinase/fructose-2, 6-bisphosphatase             | PFK-2                                      | 2.7.1.105       | 9        | -5.00             | 0.00    |      |
| P3407.01   |  |  | 6-phosphofructo-2-kinase/fructose-2, 6-bisphosphatase             | PFK-2                                      | 2.7.1.105       | 5        | -5.00             | 0.00    |      |
| P500.01    |  |  | 2-isopropylmalate synthase, chloroplast                           | IPPSH                                      | 2.3.3.13        | 14       | -2.55             | 0.00    |      |
| P1538.02   |  | Pyruvate & AcCoA metabolism                                    | Acetyl-coenzyme A synthetase                                      | ACS  | 6.2.1.1         | 4        | -5.00             | 0.01    |      |
| P183.01    |  |  | Pyruvate Dehydrogenase Complex E2 (mitochondrial)                 | PDC-E2                                     | 2.3.1.12        | 19       | -2.69             | 0.01    |      |
| P1839.01   |  |  | Acetaldehyde dehydrogenase  | ALDH                                       | 1.2.1.10        | 11       | -4.6              | 0.02    |      |
| P7.01      |  |  | Pyruvate carboxylase  | PCr  | 6.4.1.1         | 79       | -2.73             | 0.05    |      |
| P25.01     |  | TCA & glyoxylate cycles  | Aconitate hydratase 2 (Aconitase)                                 | ACO  | 4.2.1.3         | 70       | -1.98             | 0.00    |      |
| P1639.01   |  |  | Malate synthase G   | MALSH                                      | 2.3.3.9         | 13       | -5.00             | 0.00    |      |
| P78.01     |  |  | Isocitrate dehydrogenase [NADP]                                   | IDH  | 1.1.1.42        | 41       | -2.03             | 0.00    |      |
| P198.01    |  |  | 2-oxoglutarate dehydrogenase-E1                                   | OGDC-E1                                    | 1.2.4.2         | 31       | -4.83             | 0.01    |      |
| P3745.01   |  |  | ATPase  |  | 3.6.3.14        | 4        | -5.00             | 0.00    |      |
| P246.01    |  |  | ATP synthase subunit gamma (chloroplastic)                        | ATPaseG                                    | 3.6.3.14        | 16       | -1.97             | 0.00    |      |
| P306.01    |  |  | NADH-dependent fumarate reductase                                 | FR (NADH)                                  | 1.3.1.6         | 30       | -1.84             | 0.00    |      |
| P306.02    |  |  | NADH-dependent fumarate reductase                                 | FR (NADH)                                  | 1.3.1.6         | 20       | -2.32             | 0.01    |      |
| P744.01    |  | Oxidative phosphorylation                                      | NADH dehydrogenase [ubiquinone] flavoprotein                      | NADHDP-<br>p1                              | 1.6.5.3         | 15       | -3.45             | 0.00    |      |
| P4035.01   |  |  | NADH dehydrogenase  | NADHDP-<br>p10                             | 1.6.5.3         | 3        | -5.00             | 0.01    |      |
| P3286.01   |  |  | NADH-quinone oxidoreductase subunit B                             | NADHOR-<br>p2                              | 1.6.5.3         | 7        | -5.00             | 0.01    |      |
| P2511.01   |  | Pentose phosphate pathway                                      | D-Ribulose-5-Phosphate 3-Epimerase                                | RPEh                                       | 5.1.3.1         | 3        | -2.76             | 0.05    |      |
| P3320.01   |  |  | Ribose-phosphate pyrophosphokinase                                | RPPK                                       | 2.7.6.1         | 5        | -5.00             | 0.00    |      |
| P1375.01   |  |  | Transaldolase   | TAL  | 2.2.1.2         | 9        | -3.86             | 0.01    |      |
| P1961.01   |  | Mannitol   | Mannitol 1-phosphate dehydrogenase                                | M1PDH                                      | 1.1.1.17        | 9        | -4.93             | 0.01    |      |
| P173.01    | Central metabolism & energy                    | Nitrogen uptake & assimilation                                 | High affinity nitrate transporter 2.5                             | NRT2                                       |                 | 23       | -4.19             | 0.04    |      |
| P173.02    |  |  | High affinity nitrate transporter 2.5                             | NRT2                                       |                 | 12       | -4.60             | 0.01    |      |
| P652.01    |  |  | Ammonium transporter 1 member 2                                   | AMT1                                       |                 | 6        | -3.71             | 0.03    |      |
| P3974.01   |  | Cyanate decomposition  | Cyanate hydratase   | Cyanase                                    |                 | 3        | -5.00             | 0.00    |      |
| P191.01    |  | Urea   | Urease  | Urease                                     | 3.5.1.5         | 36       | -2.01             | 0.00    |      |
| P1355.01   |  |  | Pyrraline-5-carboxylate reductase                                 |  | 1.5.1.2         | 9        | -2.49             | 0.00    |      |
| P2137.01   |  |  | Cysteine transaminase   | CYSTAm                                     | 2.6.1.3         | 7        | -2.95             | 0.04    |      |
| P2544.01   |  |  | NAD/NADP-dependent betaine aldehyde dehydrogenase                 | BADH                                       |                 | 7        | -1.68             | 0.00    |      |
| P2985.01   |  |  | Glycine C-acetyltransferase                                       |  | 2.3.1.29        | 4        | -5.00             | 0.00    |      |
| P780.01    |  |  | Histidinol-phosphatase, chloroplast                               | HPh  | 3.1.3.15        | 10       | -1.27             | 0.00    |      |
| P3501.01   |  | Amino-acid metabolism  | Threonine dehydratase   | AtSR                                       | 4.3.1.19        | 5        | -5.00             | 0.01    |      |
| P395.01    |  |  | Methionine synthase   | MatH                                       | 2.1.1.13        | 38       | -5.00             | 0.02    |      |
| P3539.01   |  |  | Kynurenine 3-monooxygenase and related flavoprotein monooxygenase |  |                 | 4        | -5.00             | 0.00    |      |
| P193.01    |  |  | Aspartate aminotransferase  | AST  | 2.6.1.1         | 27       | -2.66             | 0.03    |      |
| P969.01    |  |  | Phosphoserine aminotransferase                                    | PSAT                                       | 2.6.1.52        | 13       | -1.03             | 0.01    |      |
| P3849.01   |  |  | Branched-chain-amino-acid aminotransferase-like protein           |  |                 | 2        | -5.00             | 0.00    |      |
| P3817.01   |  |  | Cysteine--tRNA ligase, cytoplasmic                                | CysRS                                      | 6.1.1.16        | 4        | -5.00             | 0.00    |      |
| P170.01    |  |  | Alanine--tRNA ligase  | AlaRS                                      | 6.1.1.7         | 39       | -3.23             | 0.02    |      |
| P341.02    |  |  | Aspartate--tRNA ligase  | AspRS                                      | 6.1.1.12        | 18       | -3.08             | 0.01    |      |
| P549.01    |  |  | Cysteine--tRNA ligase   | CysRS                                      | 6.1.1.16        | 23       | -2.50             | 0.01    |      |
| P846.01    |  | Aminoacyl-tRNA biosynthesis                                    | Glutamine--tRNA ligase  | GlnRS                                      | 6.1.1.18        | 20       | -2.39             | 0.00    |      |
| P956.01    |  |  | Probable glutamate--tRNA ligase                                   | GlurS                                      | 6.1.1.17        | 17       | -2.45             | 0.01    |      |
| P1725.01   |  |  | Histidine--tRNA ligase  | HisRS                                      | 6.1.1.21        | 11       | -3.76             | 0.01    |      |
| P2809.01   |  |  | Isoleucine--tRNA ligase   | IleRS                                      | 6.1.1.5         | 7        | -5.00             | 0.01    |      |
| P2276.01   |  |  | Leucine--tRNA ligase  | LeuRS                                      | 6.1.1.4         | 11       | -5.00             | 0.05    |      |
| P2821.01   |  |  | Leucine--tRNA ligase  | LeuRS                                      | 6.1.1.4         | 6        | -4.11             | 0.01    |      |
| P609.01    |  |  | Proline--tRNA ligase  | ProRS                                      | 6.1.1.15        | 18       | -2.31             | 0.02    |      |
| P2501.01   |  |  | Valine--tRNA ligase   | ValRS                                      | 6.1.1.9         | 7        | -5.00             | 0.01    |      |
| P36.02     |  |  | Serine--tRNA ligase   | SerRS                                      | 6.1.1.11        | 34       | -1.99             | 0.01    |      |
| P446.01    |  |  | Threonine--tRNA ligase  | THRrs                                      | 6.1.1.3         | 23       | -5.00             | 0.00    |      |
| P2211.01   |  |  | Tyrosine--tRNA ligase   | TyrRS                                      | 6.1.1.1         | 9        | -5.00             | 0.02    |      |
| P960.01    |  | Pyrimidine metabolism  | thioredoxin-disulfide reductase, cytosol                          | TDSR                                       | 1.8.1.9         | 14       | -2.23             | 0.01    |      |
| P3196.01   |  | Purine metabolism  | Bifunctional purine biosynthesis protein                          |  | 3.4.24          | 5        | -5.00             | 0.00    |      |
| P2028.01   |  |  | nucleoside-triphosphate phosphatase                               |  |                 | 9        | -3.31             | 0.02    |      |
| P335.02    |  |  | Glycolipid transfer protein                                       | GLTP                                       |                 | 9        | -2.15             | 0.00    |      |
| P2580.01   |  | Carbohydrate catabolism  | Lysosomal beta glucosidase  | GH3  | 3.2.1.21        | 9        | -5.00             | 0.00    |      |
| P3802.01   |  |  | Mannosyl-oligosaccharide glucosidase GCS1                         | GH63                                       | 3.2.1.106       | 4        | -5.00             | 0.02    |      |
| P2632.01   |  |  | Lysophosphatidic acid-acyltransferase                             | LPAT                                       | 2.3.1.51        | 8        | -5.00             | 0.00    |      |
| P1115.01   |  | Very long chain Fatty acid biosynthesis                        | Very-long-chain 3-oxoacyl-CoA reductase 1                         | Kcr  | 1.1.1.330       | 11       | -2.22             | 0.02    |      |
| P815.01    |  | Glycerophospholipid metabolism                                 | Phosphatidylglycerophosphatase                                    |  | 3.1.3.27        | 8        | -1.42             | 0.01    |      |
| P514.01    |  | Isoprenoid metabolism  | Methylcrotonoyl-CoA carboxylase subunit alpha                     | Mccase                                     | 6.4.1.4         | 23       | -4.53             | 0.01    |      |
| P351.01    | Lipids & carbohydrates                         | Beta-oxidation   | Long chain acyl-CoA synthetase                                    | LACS                                       | 6.2.1.3         | 21       | -2.80             | 0.01    |      |
| P3689.01   |  |  |   | Long chain acyl-CoA synthetase             | LACS            | 6.2.1.3  | 3                 | -5.00   | 0.00 |
| P518.02    |  |  |   | Long chain acyl-CoA synthetase             | LACS            | 6.2.1.3  | 4                 | -3.91   | 0.02 |
| P2895.01   |  |  |   | 3-ketoacyl-CoA thiolase                    | ACAA            | 2.3.1.16 | 7                 | -5.00   | 0.02 |
| P59.01     |  |  |   | Long chain 3-hydroxyacyl-CoA dehydrogenase | HCDH            | 1.1.1.35 | 39                | -1.37   | 0.00 |
| P621.01    |  |  |   | 3-hydroxyacyl-CoA dehydrogenase            | HCDH            | 1.1.1.35 | 20                | -3.05   | 0.01 |
| P23.01     |  |  | Membrane lipid metabolism   | Glycerol-3-phosphate dehydrogenase (NAD+)  | G3PDH(N<br>AD+) | 1.1.1.8  | 32                | -1.23   | 0.01 |
| P383.01    |  |  |   | Glycerol-3-phosphate dehydrogenase         | G3PDH-M         | 1.1.1.8  | 24                | -2.47   | 0.01 |
| P1738.01   |  |  | Lysophospholipase   | LPL  |                 | 6        | -3.11             | 0.05    |      |
| P4043.01   |  | Triacylglycerol catabolism                                     | Triacylglycerol hydrolase   | TAGH                                       | 3.1.1.3         | 2        | -5.00             | 0.18    |      |
| P380.01    |  |  | 3-isopropylmalate dehydratase, 3-Carboxy-2-hydroxy-4-             |  | 4.2.1.33        | 24       | -2.70             | 0.01    |      |

CHAPITRE IV : Limitation azotée et allocation du carbone. Approche intégrative en chémostat.

|          |  | methylpentanoate forming                                    |   |  |       |          |       |       |
|----------|--|---|---|--|-------|----------|-------|-------|
| P2762.01 | Amino-Acid catabolism                        | Unknown conserved glutaminase                               |   | 5  | -5.00 | 0.00     |       |       |
| P24.01   |  | Periplasmic L-aminoacid oxydase                             | PLAAOX                                      | 56   | -2.22 | 0.05     |       |       |
| P3880.01 |  | 3-hydroxyanthranilate 3,4-dioxygenase                       | 3HOA  | 1.13.11.6                                    | 4     | -5.00    | 0.00  |       |
| P2841.01 |  | Probable Xaa-Pro aminopeptidase P                           | AMPP  |  | 3     | -2.62    | 0.00  |       |
| P3629.01 |  | Probable Xaa-Pro aminopeptidase P                           | AMPP  |  | 3     | -5.00    | 0.00  |       |
| P476.01  |  | Presequence protease 1                                      | AtPreP1                                     |  | 30    | -3.35    | 0.04  |       |
| P2736.01 |  | 26S proteasome non-ATPase regulatory subunit 1 homolog B    | AtRPN2b                                     |  | 9     | -5.00    | 0.04  |       |
| P713.01  |  | Ubiquitin carboxyl-terminal hydrolase 12                    | AtUBP12                                     |  | 27    | -3.92    | 0.02  |       |
| P588.01  |  | Ubiquitin carboxyl-terminal hydrolase 7                     | AtUBP7                                      |  | 16    | -2.40    | 0.00  |       |
| P912.01  | Catabolism of proteins & amino acids         | Proteasome subunit beta type-6                              | DAPS-1                                      |  | 14    | -2.35    | 0.01  |       |
| P3296.01 |  | Protease / peptidase  | Glutamate carboxypeptidase 2                | FGCP   |       | 4        | -5.00 | 0.00  |
| P268.01  |  |   | Puromycin-sensitive aminopeptidase          | PSA  |       | 37       | -2.92 | 0.02  |
| P3967.01 |  |   | E3 ubiquitin-protein ligase UPL3            |  |       | 3        | -5.00 | 0.01  |
| P1878.01 |  |   | ATP-dependent protease subunit HslV         |  |       | 6        | -3.15 | 0.01  |
| P3704.01 |  |   | Presequence protease                        |  |       | 4        | -5.00 | 0.00  |
| P1819.01 |  |   | Probable aminopeptidase NPEPL1              |  |       | 8        | -1.52 | 0.01  |
| P776.01  |  |   | Probable cytosolic oligopeptidase A         |  |       | 21       | -2.09 | 0.00  |
| P3924.01 |  |   | Protease 2                                  |  |       | 2        | -5.00 | 0.00  |
| P820.01  |  |   | Ubiquitin carboxyl-terminal hydrolase 5     |  |       | 21       | -2.78 | 0.00  |
| P2831.01 |  |   | Ubiquitin-like modifier-activating enzyme 1 |  |       | 5        | -2.43 | 0.04  |
| P541.01  |  |   | Uncharacterized peptidase y4nA              |  |       | 21       | -2.06 | 0.02  |
| P3901.01 |  |   | Unknown conserved peptidase                 |  |       | 3        | -5.00 | 0.00  |
| P187.01  |  |   | ND  | Methylmalonyl-CoA mutase                     | mcm   | 5.4.99.2 | 26    | -2.54 |
| P693.01  | Chaperones and HSP                           |   | T-complex protein 1 subunit alpha           | TCP-1-alpha                                  |       | 21       | -3.11 | 0.03  |
| P263.01  |  | T-complex protein 1 subunit gamma                           | TCP-1-gamma                                 |  | 28    | -2.12    | 0.05  |       |
| P18.01   |  | ATP-dependent Clp protease ATP-binding subunit clpA         | ClpC  |  | 56    | -2.07    | 0.03  |       |
| P108.01  |  | HSP_90  |   |  | 51    | -1.23    | 0.01  |       |
| P3961.01 |  | Heat shock protein sti1 homolog                             | HSP   |  | 3     | -5.00    | 0.01  |       |
| P100.01  |  | Heat shock Protein 70                                       | HSP70                                       |  | 45    | -4.71    | 0.01  |       |
| P17.01   |  | Heat shock protein 90-1                                     | HSP90                                       |  | 62    | -2.07    | 0.02  |       |
| P18.02   |  | Chaperone protein ClpB                                      | ClpB  |  | 25    | -2.43    | 0.03  |       |
| P18.04   |  | Chaperone protein ClpC1, chloroplastic                      |   |  | 17    | -4.03    | 0.01  |       |
| P3552.01 |  |   | Glucuronokinase 1                           | AtGlcAK1                                     |       | 6        | -5.00 | 0.04  |
| P4033.01 | Phosphorylation                              | Probable protein phosphatase 2C 48                          | OsPP2C48                                    |  | 2     | -5.00    | 0.00  |       |
| P2745.01 |  | Unknown phosphatase   |   |  | 5     | -5.00    | 0.01  |       |
| P3904.01 |  | Protein phosphatase 1 regulatory subunit pprA               |   |  | 3     | -5.00    | 0.00  |       |
| P2312.01 |  | Serine/threonine-protein phosphatase 4 regulatory subunit   |   |  | 9     | -5.00    | 0.00  |       |
| P1341.01 |  | Serine/threonine-protein phosphatase 4 regulatory subunit 1 |   |  | 8     | -1.46    | 0.01  |       |
| P2078.01 | Post translational modifications             | Glycosylation   |   | UDP-glucose:glycoprotein glucosyltransferase | 15    | -5.00    | 0.05  |       |
| P1316.01 |  | Protein disulfide-isomerase 5-3                             | AtPDIL5-3                                   |  | 14    | -2.94    | 0.00  |       |
| P2457.01 |  | Peptidyl-prolyl cis-trans isomerase B                       | PPIase B                                    | 5.2.1.8                                      | 6     | -1.39    | 0.01  |       |
| P4138.01 |  | Peptidyl-prolyl cis-trans isomerase CYP18-4                 | PPIase CYP18-4                              | 5.2.1.8                                      | 1     | -5.00    | 0.00  |       |
| P3888.01 |  | Peptidyl-prolyl cis-trans isomerase cyp3                    | PPIase cyp3                                 | 5.2.1.8                                      | 2     | -5.00    | 0.00  |       |
| P862.01  |  | Peptidyl-prolyl cis-trans isomerase FKBP62                  | PPIase FKBP62                               | 5.2.1.8                                      | 15    | -1.92    | 0.00  |       |
| P3749.01 |  | Peptidyl-prolyl cis-trans isomerase FKBP65                  | PPIase FKBP65                               | 5.2.1.8                                      | 5     | -5.00    | 0.01  |       |
| P386.01  |  | Ubiquitination  | U-box domain-containing protein 12          | OsPUB12                                      |       | 23       | -1.28 | 0.00  |
| P4022.01 |  |   | SUMO-activating enzyme subunit 2            |  |       | 2        | -5.00 | 0.00  |
| P3596.01 |  | Oxidative stress response                                   | Peptide methionine sulfoxide reductase      | MSRA   |       | 3        | -5.00 | 0.00  |
| P3784.01 | Alpha N-terminal protein methyltransferase 1 |   |   |  | 2     | -5.00    | 0.00  |       |
| P1851.01 | Glutathione S-transferase theta-2            |   | GST   |  | 7     | -2.14    | 0.04  |       |
| P2339.01 | Thioredoxin domain-containing protein 5      |   | ER protein 46                               |  | 4     | -1.17    | 0.00  |       |
| P977.01  | Thioredoxin                                  |   | Trx   |  | 8     | -1.14    | 0.00  |       |
| P1715.01 | Thioredoxin-like protein slr0233             |   |   | 8  | -1.35 | 0.01     |       |       |
| P3797.01 |  | Lon Protease  |   |  | 3     | -5.00    | 0.00  |       |
| P3526.01 | Chromosome structure                         | Structural maintenance of chromosomes protein 1             | SMC 1                                       |  | 6     | -5.00    | 0.01  |       |
| P3485.01 |  | Structural maintenance of chromosomes protein 3             | SMC 3                                       |  | 5     | -5.00    | 0.00  |       |
| P2789.01 |  | Structural maintenance of chromosomes protein 5             | SMC 5                                       |  | 7     | -5.00    | 0.00  |       |
| P1802.01 |  | DNA topoisomerase 2   | DNA topo-2                                  | 5.99.1.3                                     | 8     | -3.76    | 0.00  |       |
| P3972.01 | Replication & DNA maintenance                | DNA replication licensing factor mcm2                       | MCM2  |  | 2     | -5.00    | 0.01  |       |
| P3931.01 |  | DNA replication licensing factor mcm4                       | MCM4  |  | 2     | -5.00    | 0.00  |       |
| P3174.01 |  | DNA replication licensing factor MCM5                       | MCM5  |  | 7     | -5.00    | 0.00  |       |
| P4028.01 |  | DNA replication licensing factor mcm6                       | MCM6  |  | 2     | -5.00    | 0.01  |       |
| P3646.01 |  | Replication factor C subunit 3                              | RFC-3                                       | 3.6.1.15                                     | 3     | -5.00    | 0.00  |       |
| P2418.01 |  | Replication factor C subunit 5                              | RFC-5                                       | 3.6.1.15                                     | 6     | -2.24    | 0.00  |       |
| P2713.01 |  | Replication protein A 70 kDa DNA-binding subunit            | RPA1  |  | 5     | -2.75    | 0.02  |       |
| P3709.01 |  | Replication protein A 70 kDa DNA-binding subunit C          | RPA1  |  | 3     | -5.00    | 0.00  |       |
| P3299.01 |  | Mitochondrial DNA replication protein YHM2                  | YHM2  |  | 4     | -5.00    | 0.00  |       |
|          |  | DNA repair  | Double-strand-break repair protein rad21    | RAD21  |       | 2        | 5.00  | 0.00  |
| P3279.01 |  | Polyribonucleotide nucleotidyltransferase                   | PNPase                                      |  | 6     | -5.00    | 0.01  |       |
| P33.01   | ND   | 14-3-3-like protein F                                       |   |  | 47    | -1.03    | 0.01  |       |
| P805.01  |  | Putative chromatin-remodeling complex ATPase chain          |   |  | 16    | -3.17    | 0.01  |       |
| P2287.01 | RNA helicase                                 | ATP-dependent RNA helicase dbp9                             |   |  | 5     | -2.38    | 0.02  |       |
| P1784.01 |  | DEAD-box ATP-dependent RNA helicase 21                      |   |  | 8     | -2.22    | 0.04  |       |
| P4124.01 |  | DEAD-box ATP-dependent RNA helicase 52B                     |   |  | 2     | -5.00    | 0.01  |       |
| P3574.01 |  | Unknown conserved ATP-dependent RNA helicase                |   |  | 3     | -5.00    | 0.00  |       |
| P3443.01 |  | DNA-directed RNA polymerase II subunit rpb1                 | RNA pol                                     |  | 7     | -5.00    | 0.00  |       |
| P4131.01 | RNA polymerases                              | DNA-directed RNA polymerases I, II, and III subunit RPABC1  | RNA pol                                     |  | 2     | -5.00    | 0.01  |       |
| P3804.01 |  | Non-canonical poly(A) RNA polymerase PAPD7                  | TUTase 5                                    |  | 4     | -5.00    | 0.00  |       |
| P441.01  |  | Mediator of RNA polymerase II transcription subunit 36a     |   |  | 16    | -1.29    | 0.00  |       |
| P1273.01 | RNA-binding protein                          | SRP72 RNA-binding domain containing unknown protein         |   |  | 11    | -3.94    | 0.00  |       |

CHAPITRE IV : Limitation azotée et allocation du carbone. Approche intégrative en chémostat.

|          |  |   |   |         |         |       |       |      |
|----------|--|---|---|---------|---------|-------|-------|------|
| P3062.01 |  | Splicing  | Pre-mRNA-splicing factor                    |         | 5       | -5.00 | 0.01  |      |
| P2007.01 |  | Transcription factors                                 | HB-other                                    |         | 7       | -3.15 | 0.00  |      |
| P3527.01 | HB-other   |   |   | 4       | -5.00   | 0.00  |       |      |
| P1797.01 | MYB (2R)   |   |   | 9       | -2.08   | 0.01  |       |      |
| P420.01  |  | Elongation  | Elongation factor 3                         | EF-3    | 21      | -3.21 | 0.03  |      |
| P773.01  | Elongation factor P  |   | EF-P  | 12      | -1.22   | 0.00  |       |      |
| P2355.01 | Elongation factor G  |   | EFG   | 12      | -5.00   | 0.01  |       |      |
| P1185.01 |  | initiation factor                                     | Eukaryotic translation initiation factor 2D | eIF2d   | 12      | -2.19 | 0.01  |      |
| P3325.01 | Eukaryotic translation initiation factor 3 subunit A                       |   | eIF3a                                       | 3       | -5.00   | 0.02  |       |      |
| P888.01  | Eukaryotic translation initiation factor 3 subunit B                       |   | eIF3b                                       | 14      | -2.84   | 0.02  |       |      |
| P3469.01 | Probable translation initiation factor eIF-2B subunit epsilon              |   |   | 3       | -5.00   | 0.01  |       |      |
| P701.01  |  |   | Translation initiation factor IF-2          |         | 22      | -2.80 | 0.04  |      |
| P4009.01 |  | Ribosomal proteins                                    | 30S ribosomal protein S1 homolog A          |         | 2       | -5.00 | 0.01  |      |
| P3890.01 | 4 ankyrin repeat domain containing unknown protein                         |   |   | 3       | -5.00   | 0.00  |       |      |
| P188.01  | 40S ribosomal protein S3-3   |   |   | 12      | -2.15   | 0.03  |       |      |
| P3936.01 | 5'-3' exoribonuclease  |   |   | 2       | -5.00   | 0.00  |       |      |
| P3746.01 | 3-hydroxyisobutyryl-CoA hydrolase  |   | 3.1.2.4                                     | 2       | -5.00   | 0.00  |       |      |
| P3499.01 | 6 ankyrin repeat domain containing Serine/threonine-protein phosphatase    |   |   | 3       | -5.00   | 0.00  |       |      |
| P2411.01 | 60S ribosomal protein L15-1  |   |   | 2       | -2.49   | 0.05  |       |      |
| P292.01  | 60S ribosomal protein L9   |   |   | 15      | -2.59   | 0.03  |       |      |
| P2340.01 | CCR4-NOT transcription complex subunit 8                                   |   | CALIFp                                      | 6       | -2.18   | 0.01  |       |      |
| P811.01  | Pre-mRNA-processing factor 6   |   |   | 16      | -4.25   | 0.03  |       |      |
| P3625.01 | CCR4-NOT transcription complex subunit 1                                   |   | 4   | -5.00   | 0.19    |       |       |      |
| P4108.01 | CCR4-NOT transcription complex subunit 11                                  |   | 2   | -5.00   | 0.19    |       |       |      |
| P1732.01 | CCR4-NOT transcription complex subunit 3                                   |   | 9   | -1.86   | 0.05    |       |       |      |
| P2668.01 | m7GpppX diphosphatase  | 3.6.1.59  | 7   | -2.15   | 0.02    |       |       |      |
| P1897.01 | Transcription elongation factor SPT6                                       |   | 10  | -3.84   | 0.02    |       |       |      |
| P3487.01 | Unknown NAD+ ADP-ribosyltransferase  |   | 4   | -5.00   | 0.02    |       |       |      |
| P1800.01 |  | Pigments, xenobiotic ,vitamins & cofactors metabolism | 1-deoxy-D-xylulose-5-phosphate synthase     | DXS     | 2.2.1.7 | 9     | -4.05 | 0.01 |
| P1228.01 | 6-thioxanthine 5'-monophosphate:L-glutamine amidoligase                    |   |   | 6.3.5.2 | 12      | -3.58 | 0.01  |      |
| P1114.01 | Inositol hexakisphosphate and diphosphoinositol-pentakisphosphate kinase 1 |   |   | 16      | -4.65   | 0.05  |       |      |
| P110.01  | Fucoxanthin-chlorophyll a-c binding protein E                              |   |   | 11      | -1.81   | 0.01  |       |      |
| P175.01  | Fucoxanthin-chlorophyll a-c binding protein E                              |   |   | 23      | -1.40   | 0.00  |       |      |
| P2310.01 | Cyanuric acid amidohydrolase   |   | 3.5.2.15                                    | 8       | -3.51   | 0.00  |       |      |
| P4099.01 | Purple acid phosphatase 21   |   |   | 2       | -5.00   | 0.00  |       |      |
| P2930.01 | Calcium/calmodulin-dependent protein kinase type II delta chain            |   | CAMPK                                       | 8       | -5.00   | 0.03  |       |      |
| P1830.01 | Calcium/calmodulin-dependent protein kinase type 1                         | CAMPK   | 8   | -1.06   | 0.00    |       |       |      |
| P305.01  | Calcium/calmodulin-dependent protein kinase type 1D                        | CAMPK   | 19  | -2.34   | 0.00    |       |       |      |
| P2539.01 | EF-hand calcium-binding domain-containing conserved protein                |   | 8   | -2.04   | 0.00    |       |       |      |
| P3233.01 | EF-hand calcium-binding domain-containing conserved protein                |   | 4   | -5.00   | 0.00    |       |       |      |
| P1366.01 | EF-hand domain-containing family member C2                                 |   | 11  | -3.40   | 0.03    |       |       |      |
| P3307.01 | Phototropin  |   | 4   | -5.00   | 0.00    |       |       |      |
| P305.02  | Extracellular signal-regulated kinase 2                                    | ERK2  | 8   | -2.79   | 0.00    |       |       |      |
| P1163.01 | Glycogen synthase kinase-3 beta  | GSK-3 beta  | 5   | -2.94   | 0.00    |       |       |      |
| P3480.01 | Signal recognition particle receptor subunit alpha                         | SR-alpha  | 2   | -2.21   | 0.04    |       |       |      |
| P1279.01 | TNF receptor-associated protein 1 homolog, mitochondrial                   |   | 13  | -3.13   | 0.01    |       |       |      |
| P1942.01 | Mitochondrial import receptor subunit TOM40-1                              | TOM40   | 7   | -3.52   | 0.00    |       |       |      |
| P2928.01 | Mitochondrial import receptor subunit tom70                                | TOM70   | 6   | -5.00   | 0.00    |       |       |      |
| P2151.01 | COP9 signalosome complex subunit 4   | AtS4  | 12  | -5.00   | 0.04    |       |       |      |
| P1437.01 | Signal recognition particle subunit SRP68                                  | SRP68   | 11  | -2.96   | 0.00    |       |       |      |
| P3203.01 | Serine/threonine-protein phosphatase 2A 65 kDa regulatory subunit A        | PP2RA   | 8   | -5.00   | 0.01    |       |       |      |
| P3530.01 | Cytoskeleton-associated AAA family ATPase                                  |   | 4   | -5.00   | 0.00    |       |       |      |
| P2822.02 | Interferon-induced guanylate-binding protein                               |   | 4   | -5.00   | 0.00    |       |       |      |
| P2690.01 | Microtubule-associated protein   |   | 5   | -2.69   | 0.00    |       |       |      |
| P2787.01 | Myosin   |   | 7   | -5.00   | 0.00    |       |       |      |
| P2115.01 | Myosin and Kinesin motor domain containing unknown protein                 |   | 6   | -2.35   | 0.00    |       |       |      |
| P1242.01 | Myosin-6   |   | 20  | -3.80   | 0.00    |       |       |      |
| P1808.01 | Parafibromin   |   | 5   | -1.61   | 0.01    |       |       |      |
| P3433.01 | Vesicle-fusing ATPase  |   | 5   | -5.00   | 0.00    |       |       |      |
| P1376.01 | Cortactin-binding protein 2  | CortBP2   | 8   | -2.53   | 0.00    |       |       |      |
| P3772.01 | Dynactin subunit 1   | DP-150  | 2   | -5.00   | 0.01    |       |       |      |
| P117.01  | ADP-ribosylation factor 1  |   | 13  | -2.06   | 0.03    |       |       |      |
| P1614.01 | ADP-ribosylation factor 1  |   | 7   | -3.48   | 0.03    |       |       |      |
| P124.01  | Alpha-actinin A  |   | 46  | -2.44   | 0.04    |       |       |      |
| P2672.01 | Flagellar protein  |   | 8   | -5.00   | 0.03    |       |       |      |
| P276.01  | V-type proton ATPase subunit A   | V-ATPase  | 3.6.3.14                                    | 22      | -2.87   | 0.05  |       |      |
| P3519.01 | Coatomer subunit alpha-2   | Alpha-COP 2   |   | 5       | -5.00   | 0.01  |       |      |
| P142.01  | ADP,ATP carrier protein  | ANT   |   | 18      | -3.03   | 0.03  |       |      |
| P1037.01 | Coatomer subunit epsilon-1   | Epsilon-COP 1   |   | 9       | -2.41   | 0.03  |       |      |
| P3447.01 | Transportin-1  | MIP   |   | 4       | -2.64   | 0.02  |       |      |
| P3030.01 | Vacuolar iron transporter 1.2  | OsVIT1.2  |   | 2       | -3.15   | 0.03  |       |      |
| P3490.01 | Vesicle transport v-SNARE protein  | V-SNARE   |   | 4       | -5.00   | 0.00  |       |      |
| P2670.01 | ABC transporter B  |   | 7   | -5.00   | 0.01    |       |       |      |
| P3813.01 | ADP-ribosylation factor  |   | 2   | -5.00   | 0.00    |       |       |      |
| P3819.01 | ADP-ribosylation factor  |   | 3   | -5.00   | 0.00    |       |       |      |
| P3054.01 | Calcium-transporting ATPase 1, endoplasmic reticulum-type                  |   | 5   | -5.00   | 0.05    |       |       |      |
| P2466.01 | Translocation protein SEC63 homolog  |   | 8   | -5.00   | 0.00    |       |       |      |
| P3175.01 | Vacuolar protein sorting-associated protein 52 A                           |   | 6   | -5.00   | 0.00    |       |       |      |
| P2285.01 | Vacuolar protein sorting-associated protein 45                             |   | 8   | -2.63   | 0.01    |       |       |      |
| P3995.01 | AP-1 complex subunit mu  |   | 2   | -5.00   | 0.02    |       |       |      |

## CHAPITRE IV : Limitation azotée et allocation du carbone. Approche intégrative en chémostat.

heat shock proteins and six down-accumulated proteins involved in oxidative stress response. These results suggest that regulation at the post translational level could strongly impact the metabolism of *T. lutea* strain 2Xc1.

### 2.11 Calcium signaling pathways are affected.

Six proteins containing the EF-hand calcium-binding domain were identified in the proteome. This conserved domain can be found in calcium binding proteins, or in proteins involved in the regulation of intracellular calcium level, such as calmodulin. The accumulation of all these proteins was impacted in accumulation in the 2Xc1 strain, including two up- and four down-accumulated proteins (Tab. 2&3). In parallel, four of the five calcium/calmodulin-dependent protein kinases (CAMPK) identified in the proteome were down-accumulated (Tab. 2). In plants, these proteins are mediators of calcium signaling and involved in numerous biological functions in response to environment changes. In chlorophyceae, calcium signaling is involved in neutral lipid accumulation [54,55]. These results suggest differences in calcium homeostasis and regulation pathways mediated by calcium between both strains.

## 3. Discussion

### 3.1 Strategy

The aim of this work was to understand the molecular mechanisms by which microalgae up-accumulate storage carbon. Most studies done until now have focused on the effect of nitrogen deficiency, which causes an accumulation of carbohydrates and then lipid storage, but also a halt in cell division that blurs the messages of metabolic analysis. In this study, we compared under identical ecophysiological conditions two strains of *T. lutea* that differ in their ability to accumulate storage lipids, without this affecting growth. The following discussion will consider the relevance of this strategy, the original behavior of strain 2Xc1 for carbon accumulation, and the strongly altered metabolism of this mutant strain revealed by our large-scale proteomics study.

We initially focused our efforts on the physiological responses of strains to nitrogen limitation at steady state, to nitrogen repletion when N/C ratio increased, and to nitrogen depletion when N/C decreased. Unlike batch cultures, continuous cultures lead to steady ecophysiological states of great interest to study tight physiological and molecular differences in microorganisms [56]. Such cultures are very appropriate for transcriptomic, proteomic and metabolomic analysis in prokaryotes and unicellular eukaryotes [57]. In our N-limited chemostat, nitrogen was continuously supplied to the photobioreactor to thereby maintain the dynamics of cell division. The high reproducibility of ecophysiological parameters at steady states and after the three spikes confirms the appropriateness of using continuous cultures to facilitate the acquisition of responsive, high-quality and reproducible data on microalgae. However, during the experiment we observed an unexpected increase of carbon assimilation capacity at steady state in the mutant strain, due to a 100% increase of carbohydrate content

after 90 days of culture at 0.5 d<sup>-1</sup> (i.e. ~ 65 generations). In addition, the two strains show differences of storage lipid content at steady state, and differences in lipid degradation and accumulation kinetics in response to changes in nitrogen availability. These results are discussed below.

The proteomes of the two strains were studied to identify the differences of behavior, especially in the accumulation of storage lipids. A large number (4,332) of proteins were identified and their abundance compared between the strains. This is the first published proteome of a member of the isochrysidales and the second of a haptophyte, following the proteome of *Emiliania huxleyi* [58]; [59]. To our knowledge, this is the most complete proteome of a microalga published to date.

### 3.2 2Xc1: a plastic strain that accumulates carbohydrates and storage lipids.

Studies on chemostat are based on the principle that the growth rate is driven by the most limiting nutrient [47,60]. In such a paradigm, and without any other limitation occurring, the ability of carbon acquisition is determined by the amount of the limiting nutrient. However, when applied to long-term experiments, it does not consider the possible evolution of the studied organism. In our study, for identical limiting nitrogen quotas, a 50% increase in carbon quotas and a twofold increase of carbohydrate were measured in 2Xc1 after 3 months of continuous culture, revealing the high plasticity of this strain. The reasons that may explain such plasticity are numerous and may involve adaptation and acclimation mechanisms. Similar increases of glucose content were observed in bacteria after 280 generations of glucose-limited growth in a chemostat, and was associated with multiple and stable mutations [61]. In *C. reinhardtii*, 149 single nucleotide polymorphisms resulting in amino acid substitutions were observed after 1,880 generations, leading to changes of growth capacities and differences in gene regulation [62]. After 65 generations, the occurrence of mutations or other genomic reordering could have occurred in the 2Xc1 culture, leading to the increase of carbohydrate content. Rad21 and Rad23, involved in DNA maintenance and reparation, were differentially accumulated in both strains, and the among the four SMCs, involved in chromatin structure, three were strongly down-accumulated.. The consequences could be a higher genomic plasticity of the mutant strain. One drawback of the higher plasticity could be the loss of this hyper-lipidic character that gives this strain its high biotechnological potential. However, no such effect was observed since the isolation of this strain in 2009, which tends to demonstrate the permanent character of the lipid over-accumulation in laboratory culture conditions [44].

The nature of the carbohydrates in *T. lutea* and the involvement of the different classes of carbon storage are poorly known. Identified carbohydrates of *T. lutea* such as chrysolaminarin can have biotechnological interest [52, 63]. We observed the up-accumulation of Callose synthase in 2Xc1, suggesting that polysaccharides could be related to the increase of total carbohydrates. Previous papers showed that, compared to the WT strain, the mutant strain over-accumulates storage lipids in batch cultures as soon as nitrogen becomes limiting [45]. At steady state of this experiment in chemostat, the mutant strain limited by nitrogen accumulates 2 to 3-fold more storage lipids than the WT strain and

## CHAPITRE IV : Limitation azotée et allocation du carbone. Approche intégrative en chémostat.

membrane lipid were quite similar. Alkenones were very low in the mutant strain as previously observed [64]. The 2.2-fold down-accumulated in 2Xc1 of the Very-long-chain 3-oxoacyl-CoA, putatively involved alkenone biosynthesis, could have led to the lower concentration detected. The physical properties of alkenones are poorly suited to use as a biofuels but, nonetheless, represent an renewable carbon feedstock [37, 65].

### 3.3 Early response to changes of nitrogen

The dynamic model of microalgal lipid production under nitrogen limitation proposed by Mairet et al. (2011) was used as the basis of our original hypothesis. As proposed by the model, we observed the consumption of carbohydrate and lipid storage in the mutant strain during nitrogen repletion and the accumulation of storage carbohydrate and lipids during nitrogen depletion. In many species, carbohydrates are impacted in priority, rather than storage lipids, as sources of allocated energy. In most of studied microalgae, lipid accumulation occurs either at the same time or with a slight delay compared to the accumulation of carbohydrates. As consequence, they likely compete for metabolite precursors [66]. Even if carbon allocated to lipids varies between 0.6 and 3.9% in WTc1 strain and 3.7 to 9.3% in 2Xc1 strain, the carbon allocated to carbohydrates varies between 16.2 and 37.7 % in WTc1 strain and 27.8 and 42.7% in 2Xc1 strain. This clearly reveals that in the conditions of the experiment, carbohydrates rather than storage lipids are the major and the most dynamic sink for carbon allocation in *T. lutea*. The overall measured carbohydrates are affected by changes of nitrogen availability. Conversely, the analysis of the different classes of lipids in the mutant strain suggests not a dynamic of total lipids, but rather a retroactive switch from membrane lipids to storage lipids in lipid droplets. It seems that N/C variations were too low or too short to trigger the *de novo* biosynthesis of lipids and lead to a simple initiation of storage lipid accumulation and degradation. The behavior of WTc1 was similar to 2Xc1 for carbohydrates but, surprisingly, we did not observe the same dynamic of lipid composition: (i) storage lipid accumulation was not observed in the WT strain; (ii) *de novo* biosynthesis of lipids did not seem to be activated, but changes of lipid class instead appeared from membrane lipids to lipid bodies; (iii) carbohydrate changes were observed in both strains; (iv) physiological conditions are fairly distinct from nitrogen starvation. We therefore hypothesize that what we are likely seeing is the very early stages of lipid metabolism changes in response to nitrogen availability in contrast to the previous batch experiments for proteomic and transcriptomic analysis [45, 46].

In microalgae, storage lipids may serve as an internal buffer that can rapidly provide specific acyl groups for new synthesis of cell membranes after N recovery [67]. TAGs appear to be synthesized from the breakdown of plastid and endoplasmic reticulum membranes as well as from *de novo* synthesis [68]. In *C. reinhardtii* and *Isochrysis zhangjiangensis*, TAG accumulation occurs soon after nitrogen depletion, whereas the accumulation of total fatty acids occurs only after chronic nitrogen starvation [13, 69]. In *I. zhangjiangensis*, on the basis of oleic acid incorporation into TAG, authors suggested that TAG were mainly derived from freshly synthesized acyl groups. The time period of this short term response of N deprivation defined by the authors (four days of nitrogen depletion) is longer than the very early short term response of this study. In

*T. lutea* 2Xc1 strain, storage lipid biosynthesis is swiftly induced upon sudden changes in nutrient availability and membrane recycling and turnover seems to be the main source of FA for TAG assembly. In other words, we suggest that in the conditions of the study, TAGs are mainly synthesized from breakdown of membranes, as suggested by the conversion from membrane lipids to storage lipids after changes of nitrogen availability. This is supported by the non-detection of LPAT and PAP involved in *de novo* TAG synthesis and by the identification of PDAT that mediates membrane lipid turnover and TAG synthesis. Recently, Schmollinger et al (2014) pinpointed the significance of recycling existing thylakoid membranes for TAG production in *Chlamydomonas sp.* during nitrogen starvation. Surprisingly, we did not observe a change of storage lipids in the WT strain. In the conditions of this experiment, the N/C ratio varies from 0.8 to 0.13 whereas in the study by Mairet et al., lower N/C (from 0.06 to 0.09) resulted in storage lipid accumulation and degradation. These results suggest that a threshold of N/C ratio likely triggers accumulation and consumption of storage lipids at different levels for the two strains.

### 3.4 How is nitrogen limitation mediated?

The relationship between nitrogen stress and carbon metabolism has been studied mainly in the chlorophyceae *Chlamydomonas reinhardtii* and the diatom *Phaeodactylum tricorutum*. Nitrogen metabolism constitutes the major sink for carbon, and N deprivation increases carbon availability for carbohydrate and lipid accumulation [13]. Although carbon reorientation mechanisms are fairly well defined in model microalgae, the signal transduction mechanisms that trigger metabolic changes in response to nitrogen limitation are very poorly understood. As previously observed by Lacour et al. [43], we recorded a clear negative linear correlation between nitrogen limitation of *T. lutea* grown in chemostat and carbohydrate content (Fig. 3). This suggests a quite direct signal transduction between nitrogen availability and carbohydrate metabolism. However, the differences of lipid behavior after nitrogen availability changes suggest that links between N availability and lipid metabolism are less direct and that the signalization mechanisms that differ between the strains are probably more complex. In a recent study, authors showed that Ca<sup>2+</sup>-mediated signaling pathway plays a role in lipid accumulation in response to nitrogen limitation in the green algae *Chlorella sp.* [54]. Ca<sup>2+</sup> is a ubiquitous intracellular second messenger in the signal transduction of environmental stimuli in plants [70]. The abundance of numerous proteins involved in Ca<sup>2+</sup> signaling is strongly impacted in 2Xc1. Previous papers revealed that Ca<sup>2+</sup> signaling in *C. reinhardtii* and *Chlorella sp.* regulates N starvation-induced neutral lipid by increasing calmodulin activity [54,55]. We suggests that Ca<sup>2+</sup> signal transduction participates in lipid accumulation in haptophytes.

It has been shown that N partitioning in cells, associated mainly with protein/RNA ratio, is driven by the N/C ratio and triggers lipid accumulation [71]. There is evidence for the remobilization and redistribution of intracellular nitrogen in 2Xc1 because of its lower content of proteins and chlorophyll (Tab. 1), the differential accumulation of

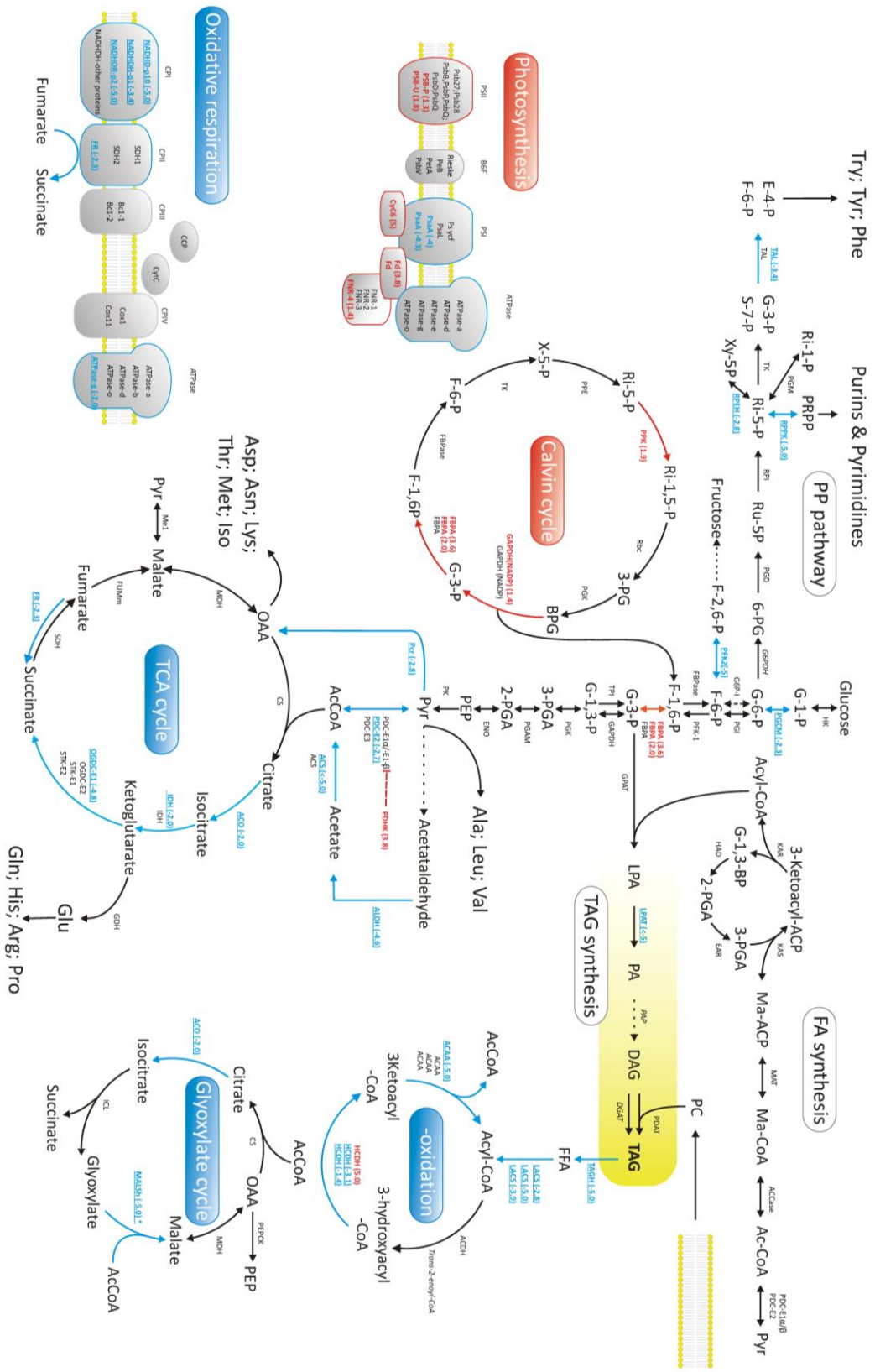


Fig. 4: Simplified representation of the central metabolism of *T. lutea* and of affected pathways in strain 2Xc1. Up-accumulated proteins are highlighted in red and down-accumulated ones in blue. The fold changes are indicated in brackets when a difference of accumulation was recorded. Proteins identified in the genome but not in the present proteome are indicated in italics. {Citation}

## CHAPITRE IV : Limitation azotée et allocation du carbone. Approche intégrative en chémostat.

proteins involved in nitrogen ammonium and protein transport, in translation, in biosynthesis of purine and pyrimidine, in urea catabolism and in protein degradation. This behavior resembles that of *C. reinhardtii* and *P. tricornutum* when subjected to nitrogen starvation [10,11,17,72]. In 2Xc1, we observed a decline in activity of protein biosynthesis with the significant decline of aminoacyl-tRNA biosynthesis and also a decrease in protein and amino acid degradation. These results are similar to the effects of nitrogen stress in *P. tricornutum* [73,74]. We suggest that 2Xc1 limits nitrogen transfers between compartments to save energy for other pathways. Nevertheless, the two strains have same kinetics of nitrogen uptake after nitrogen spikes. Since the accumulation of carbohydrates is strongly correlated with the N/C ratio and is identical between the two strains, the mechanisms of accumulation and degradation of carbohydrates appear correlated with the amount of total nitrogen in the cell. This reinforces the hypothesis above of mediation between nitrogen availability and carbohydrates. With regard to lipids, the 2Xc1 is more responsive to changes in N/C ratios than WTc1. Differences in nitrogen partitioning, suggested by the differences of abundance of proteins involved in nitrogen metabolism, could be related to the differences of lipid accumulation behavior. Furthermore, the periplasmic L-amino acid oxidase (PLAAX), and the coccolith scale associated protein (CSAP1) belonged to the major proteins in abundance in the proteome of *Tisochrysis lutea* WTc1 and were down-accumulated in 2Xc1. In *T. lutea* WT, these proteins are known for being co-regulated and up-accumulated during nitrogen starvation [45]. The function of these proteins stays unclear and would be related to aminoacid degradation and carbon homeostasis. One or both of these proteins were also up-regulated at transcript or protein level in *C. reinhardtii* and *P. tricornutum* during nitrogen starvation [10,15,72]. We suggest that these proteins could participate in lipid accumulation feedback repression during nitrogen starvation and could participate to the control of carbon and nitrogen partitioning.

### 3.5 Lipid biosynthesis plays only a minor role in storage lipid up-accumulation

Enzymes of *de novo* fatty acid and TAG biosynthesis were not up-accumulated in 2Xc1. The strong down-regulation of LPAT in the 2Xc1 strain and the absence of two major enzymes of the Kennedy pathway suggest the presence of alternative pathways to produce TAGs in *T. lutea*. Several papers report the little or no changes in abundance of transcripts of proteins involved in fatty acid and lipid metabolism during nitrogen deprivation [7,10,13,75]. In photoautotrophically grown cells of *C. reinhardtii*, precursors of fatty acid synthesis may be scarce, and are likely derived in part from the recycling of previously assimilated carbon [13]. Similarly, in heterotrophically grown cells, it is carbon precursor supply rather than the enzymes involved in fatty acid synthesis that is the limiting factor in oil synthesis under N starvation. The regulation of lipid synthesis and storage during nitrogen deprivation occurs by biochemical mechanisms dependent upon substrate levels and post-translational modifications [10]. In *P. tricornutum*, the build-up of precursors of the acetyl-CoA carboxylases may play a more significant role in TAG synthesis than the abundance of enzymes of *de novo* biosynthesis [15]. In *Isochrysis galbana*, in vitro activity of ACCase decreased during N starvation and increased during N recovery [76]. This suggests that the accumulation of storage lipid

in cells of *Isochrysis galbana* during N starvation is more the result of the absence of cell division than the increase of lipid biosynthesis. In addition, several attempts to over-express the relevant ACCase gene in the diatoms *Cyclotella cryptica* and *Navicula saprofila*, failed to improve lipid storage, showing that lipid storage accumulation is poorly constrained by *de novo* fatty acids biosynthesis [77,78]. In *T. lutea* 2Xc1, therefore, the up-accumulation of TAG is the consequence of numerous changes of metabolism upstream or downstream of lipid biosynthesis.

### 3.6 Carbon partitioning optimizes TAG accumulation in 2Xc1.

In 2Xc1, proteins of TAG degradation and  $\beta$ -oxidation were shut down and the consequences of this bottleneck at TAGs are likely one of the main reasons for the up-accumulation of TAG in *T. lutea* 2X (Fig. 5). A previous attempt at knockdown of a multifunctional lipase / phospholipase / acyltransferase increased lipid yields in *Thalassiosira pseudonana*, without affecting the growth of this alga [79]. Additionally, mutants for peroxysomal proteins of  $\beta$ -oxidation retain oil bodies and accumulate fatty acids in early seedling development in *Arabidopsis thaliana* [80]. In microalgae as in plants it is logical that blocking lipid degradation increases their accumulation. In 2Xc1 the decrease of lipid degradation may lead to a decrease of new acetyl-CoA provision.

In parallel, our results suggest that a decrease of acetyl-CoA should also arise from the decrease of mitochondrial oxidation of pyruvate and acetate by PDC, ACS and ALDH (Fig. 5). Plants and green algae possess a mitochondrial PDC isoform involved in supplying acetyl-CoA for the TCA cycle, and another chloroplastic PDC isoform involved in supplying acetyl-CoA for several reactions including fatty acid *de novo* synthesis (see[81] for review). In oleaginous plants, Acetyl-CoA destined for fatty acid *de novo* synthesis is mainly produced by the PDC. On the basis of sequence homology, the conversion of pyruvate into Acetyl-CoA in *T. lutea* 2Xc1 chloroplasts appears unaffected, unlike in mitochondria; this ensures a supply of Acetyl-CoA for *de novo* biosynthesis of fatty acids..

In strictly photoautotrophic conditions, CO<sub>2</sub> fixation by photosynthesis is the only source of carbon for the metabolic precursors synthesis.. In *C. reinhardtii*, the requirements for high amounts of energy (ATP) and reducing power (NADPH) for synthesis of storage compounds are mainly provided by photosynthetic electron transport [9]. In *T. lutea* 2X, several photosynthesis proteins were up-accumulated and could thus satisfy the energetic and reducing power needs of carbon assimilation. In relation to photosynthesis, carbon acquisition by the Calvin cycle appears to be up-activated in the 2Xc1 strain. Carbon availability is a key metabolic factor controlling oil biosynthesis and carbon partitioning between carbohydrates and oil. Under nitrogen limitation, *T. lutea* 2Xc1 increases its potential for lipid accumulation by increasing carbon and energy availability rather than by increasing lipid biosynthesis.

In the paper of Song et al (2013), the authors reported that in the haptophyte *Isochrysis galbana* “the glycolytic pathway and citrate transport system might be the main routes for lipid anabolism in N-deprived *I. galbana*, and that the tricarboxylic acid (TCA) cycle, glyoxylate cycle and sulfur assimilation system might be the major pathways involved in lipid catabolism” [82]. In 2Xc1, acetate and pyruvate metabolisms were impaired

## CHAPITRE IV : Limitation azotée et allocation du carbone. Approche intégrative en chémostat.

concomitant to the shutdown of  $\beta$ -oxidation (Fig. 5). This may lead to a decrease of acetyl-CoA, which is the precursor for TCA and glyoxylate cycles and fatty acid *de novo* biosynthesis. In fact, the key enzymes of the TCA and glyoxylate cycles were strongly down-accumulated in the 2Xc1 strain. In the diatom *P. tricornutum*, genes coupled to  $\beta$ -oxidation and the TCA cycle are co-regulated in the same way as observed in 2Xc1 [83]. The TCA cycle is the crossroad of several central metabolic pathways. It allows the adjusted reallocation of carbon skeletons as cell requirements. A reduction of TCA cycle activity results in a lower conversion from lipids to carbohydrates and proteins. The pool of NADH and precursors of certain amino acids from malate and oxaloacetate could be affected and could be the cause of changes in nitrogen metabolism.

On the basis of a decrease in abundance of the proteins involved in acetyl-CoA synthesis, in the TCA cycle in mitochondrial protein import machinery and in the first reactions of oxidative phosphorylation, we hypothesize there is an overall decrease of mitochondrial activity in the 2Xc1 strain grown in light (Fig. 5). In *P. tricornutum*, oxidation of FAs most likely provides acetyl-CoA for the TCA cycle during dark periods [83].

In the model species *C. reinhardtii* and *P. tricornutum*, nitrogen starvation leads to restructuring of carbon metabolism through the down-regulation of the Calvin cycle and up-regulation of glycolysis, TCA cycle, and pyruvate metabolism [10,12,18]. This would support the basic cellular functions during a halt in growth. It should now be asked why the cells store energy-rich lipids. According to Alipanah et al. (2015), this would lead to a funneling of lipid metabolism to carbon sources. Under nitrogen limitation conditions, compared with the wild strain, 2Xc1 tended to increase the Calvin cycle and limit mitochondrial activity and pyruvate metabolism (Fig. 5). TCA cycle allows the optimization of carbon resources and has the adaptive ability to change carbon and energy sources. We hypothesize that nitrogen-limited 2Xc1 inhibits lipid catabolism and mitochondrial activity to preserve acetyl-CoA for lipid anabolism and to limit carbon transfers from lipid compartments.

Moreover, our results show that the glyoxylate cycle in *T. lutea* 2X is shunted via the shutdown at both transcriptomic and proteomic levels of the Malate synthase G. The glyoxylate cycle converts acetyl-CoA to succinate for the biosynthesis of carbohydrates via neoglucogenesis (Fig. 5). It is the main pathway for the synthesis of carbohydrates from fatty acid oxidation. It bypasses the two reactions of the TCA cycle where four carbon molecules are lost, and produces oxaloacetate which is readily utilized by gluconeogenesis for carbohydrate synthesis. In *C. reinhardtii*, nitrogen deprivation results in the rapid depression of glyoxylate, resulting in more available acetyl-CoA for fatty-acid biosynthesis, and sets the stage for TAG biosynthesis initiation [10,7,11]. Conversely, a lipid-accumulating strain of *C. reinhardtii* up-accumulates proteins of glyoxylate [72]. As a result the behavior of the glyoxylate cycle of 2Xc1 resembles that of a nitrogen-starved alga. The shunt of glyoxylate cycle is likely one of the main reason of lipid up-accumulation and high sensitivity to nitrogen environment changes.

### 3.7 Conclusions

This study shows that the strain *T. lutea* 2Xc1 is not only very sensitive to nitrogen variations in the environment, but can also increase its capacity to accumulate carbohydrates. The in-depth proteomic analysis identified several mechanisms, from DNA maintenance to central metabolism, that likely participate in this behavior. By comparison with nitrogen starvation, which triggers TAG accumulation in algae, the lipid accumulating strain seems to behave similarly to a nitrogen-starved alga for  $\text{Ca}^{2+}$  signaling, nitrogen metabolism, glyoxylate cycle and lipid biosynthesis.

As the main result, the conversion from TAG to carbohydrates is impeded at all levels. However, in contrast to nitrogen-starved algae, in the absence of a halt in growth, 2Xc1 appears to increase photosynthesis and carbon fixation to adjust to lipid anabolism and changes in nitrogen availability. It also appears to impair mitochondrial activity to support the shutdown of lipid catabolism. The key mechanisms that trigger this metabolism should occur at the transcriptomic level but probably mainly occur at translational and post translational levels. To conclude, this study provides significant insights into mechanisms of carbon partitioning in haptophytes.

## 4. Material and Methods

### 4.1 Strains and cultures

*Thioschrysis lutea* CCAP 927/14 wild type (WT) and mutant CCAP 927/14 (S2M2) strains previously described [44] were purified by one-cell isolation (WTc1 and 2Xc1) and maintained by batch culture in Walne's medium [84]. Both strains were grown for 85 days in chemostat at a  $0.5\text{ j}^{-1}$  dilution rate in modified Walne's medium containing  $125/125\mu\text{M}$  N:P ratios in 10-L photobioreactors ( $1000 \times 400 \times 250$  mm) illuminated with continuous light ( $150\mu\text{mol}\cdot\text{m}^{-3}\cdot\text{s}^{-1}$ ) and maintained at  $27^\circ\text{C}$  and pH 7.3. The dilution rate was periodically checked by weighing the outcoming medium. Three nitrogen spikes were made at days 20, 43 and 83. Each spike consisted in the injection of 3,500  $\mu\text{moles}$  of  $\text{NaNO}_3$  in the 10 L of culture.

### 4.2 Analysis

Cell Concentration (CC), Particulate Carbon (PC), Particulate Nitrogen (PN), particulate N/C ratio, Dissolved Inorganic Nitrogen (DIN) and Dissolved Inorganic Phosphorus (DIP) were assessed at high frequency (from every 2 hours to daily) throughout the course of the experiment. PC and PN were measured on a CHN-elemental analyzer. The Matlab Curve fitting toolbox was used to perform smoothing spline fitting of computed PC. A fitted model was used to calculate growth rate during the experiment. Chemical analyses of residual DIN and DIP concentrations were carried out on a DIONEX ion-chromatography system (AS9-HC column). CC was measured on a Malassez hemocytometer. Cell lipid storage per cell was estimated on the FL2 detector (488 to 585 nm) of a BD Accuri™ C6 Flow Cytometer after Nile red staining [85].

For lipid analysis,  $150 \times 10^6$  cells were filtered on  $450^\circ\text{C}$  precombusted GF/C glass-fiber filters. Lipids were extracted in 6 mL chloroform/methanol (2/1, v/v) according to the method of Folch et al. [86] and stored at  $-20^\circ\text{C}$  under nitrogen. Neutral (NL) and polar lipids (PL) were analyzed separately by HPTLC on  $5\mu\text{l}$  of lipid extract. Neutral lipids



## CHAPITRE IV : Limitation azotée et allocation du carbone. Approche intégrative en chémostat.

were analyzed following the method described by Da Costa et al (2015). Six NL classes were identified / free fatty acids, sterol esters, alcohols, triacylglycerides (TAG), alkenones and free sterols : Three different HPTLC analyses were necessary to separate microalgae PL classes, These analyses followed the method used for NL but with different solvent systems / (1) methyl acetate/isopropanol/chloroform/methanol/KCl 0.25% (10/10/10/4/3.6, v/v/v/v/v), (2) methyl acetate/isopropanol/chloroform/methanol/KCl 0.25% (25/ 25/25/10/4, v/v/v/v/v) and (3) chloroform/methanol/ammonium (65/30/4, v/v/v). The first method allowed the separation of cardiolipin, lysophosphatidylcholine, phosphatidylcholine, phosphatidylserine, phosphatidylinositol, monogalactosyldiacylglycerol and digalactosyldiacylglycerol (DGDG) but phosphatidylethanolamine (PE) was co-eluted with sufoquinovosyldiacylglycerol (SQDG) and phosphatidylglycerol (PG). The second method allowed isolating SQDG, whereas PE + PG were co-eluted. The third method allowed the isolation of PG whereas PE + SQDG + DGDG were co-eluted. For both NL and PL, authentic standards allowed the identification and the quantification of lipid classes. Results were expressed as the quantity of membrane lipids (PL + free sterols) and of storage lipids (NL - free sterols) per cell and per carbon.

Protein, lipid, carbohydrate and chlorophyll a measurements were converted to % of total carbon using the following conversion factors: 0.53 g carbon / g proteins; 0.4 g carbon / g carbohydrates; 0.76 g carbon / g lipids; 0.74 g carbon / g chlorophyll a [48].

### 4.3 Proteomics analysis

In each one of both chemostats, sampling were done for proteomic analysis before each one of the 3 nitrogen spikes (Pt27, Pt74, Pt117 on Fig. 1). Culture samples of 50 mL were briefly centrifuged at  $2,000\times g$  for 5 min at  $5^{\circ}\text{C}$  and the pellet quickly frozen in liquid nitrogen and conserved at  $-80^{\circ}\text{C}$  for protein extractions. Total proteins were extracted and purified in the presence of protease inhibitors (Complete tablets, Roche Diagnostics, Mannheim, Germany). TRizol® reagent protocol was used following supplier's recommendations (Hummon et al, 2007). For each extract, 80  $\mu\text{g}$  proteins were pre-fractionated by 10% acrylamide SDS-PAGE. Each lane was cut into 18 bands of identical size.

Gel bands were excised and further processed into peptides as previously described [45]. Resulting peptide mixtures (18 bands  $\times$  2 strains  $\times$  3 biological replicates) were analyzed separately by nanoscale capillary liquid chromatography-tandem mass spectrometry (LC-MS/MS) using an Ultimate 3000 RSLC system (Thermo-Fisher Scientific), coupled with an LTQ-Orbitrap VELOS mass spectrometer (Thermo-Fisher Scientific). Chromatographic separation was conducted on a reverse-phase capillary column (Acclaim Pepmap C18  $2\ \mu\text{m}$  100A,  $75\text{-}\mu\text{m}$  i.d.  $\times$  50-cm length, Thermo-Fisher) at a flow rate of  $300\text{nL}\cdot\text{min}^{-1}$ . The percentage of acetonitrile in the mobile phase was linearly raised from 2% up to 70% in 56 min. Upon elution of the peptides, full MS scans were acquired at high resolution (FWMH 60,000) in an Orbitrap analyzer (mass-to-charge ratio (m/z): 400 to 2,000), while collision-induced dissociation (CID) spectra were recorded on the eighth most intense ions in the linear LTQ traps.

Raw data collected during the LC-MS/MS runs were converted into the mzXML standard format using the Msconvert tool available at <http://proteowizard.sourceforge.net/tools.shtml>. Protein identification was performed by comparing the LC-MS/MS data against a non-redundant protein database of *Tisochrysis lutea*. This database was obtained from *de novo* assembled transcriptomics data [46] as well as from *in silico* derived proteome from the *T. lutea* genome; some common contaminants including human keratins and trypsin were added to this databank (hits against these contaminants were thus discarded). The databank search engine was X!tandem (GPL v.3) embedded in the X!tandemPipeline available at <http://pappso.inra.fr/bioinfo/> [87]. Enzymatic cleavage was considered as a tryptic digestion with one possible missed cleavage event. Fixed modifications of cysteine residues by iodoacetamide as well as possible oxidation of methionines were considered. Precursor mass and fragment mass tolerance were set at 5 ppm and 0.5 Da, respectively. The search results for each LC-MS/MS run were then filtered as follows: peptide-to-spectrum matches were filtered out with a p-value of 0.01, protein identifications were considered as valid when at least two peptides matched the sequence according to the above peptide requirements, and an additional threshold of protein e-value was set at  $10\text{e-}4$ .

### 4.4 Functional Annotation

Proteins were functionally annotated by (1) using BLAST-P against Uniprot protein databases, (2) protein domain identification using InterProScan and NCBI Conserved Domain Database (CDD), and (3) expert curation. A search for homologs in other microalgae was done by BLAST-P on *in silico* proteomes of the haptophyte *Emiliania huxleyi*, the diatom *Phaeodactylum tricoratum* and the chlorophyceae *Chlamydomonas reinhardtii*.

### 4.5 Quantitative proteomic analysis

Relative quantification of identified proteins was done by comparing the intensity (peak area) measured in MS for the precursor ions corresponding with the peptides assigned to a given protein. This was achieved through XIC comparison (extracted ion chromatogram) using the MassChroQ program [88]. For each strain and each row excised from the gel lanes (1 to 18), one LC-MS/MS run among the 3 runs corresponding to the three biological replicates was chosen as the "reference" for the alignment of the related peptide features. The "reference" run was that exhibiting the highest number of identified peptides. The area derived for each peptide was further normalized by the total ion current of the run, to reduce technical variability (Supp mat 6). When the same peptides were identified in different bands of SDS-PAGE lanes, their normalized areas were summed (Sum of Normalized Peptide Area). To reduce the dominance of highly ionisable peptides while keeping the variability between the samples, the SNPA of each peptide was normalized by the mean of SNPAs in biological samples. The quantity of each protein in each sample was estimated as the sum of the normalized SNPAs of its assigned peptides.

The three biological samples taken from the cultures at steady states for each strain were statistically analyzed. ANOVA were performed on  $\log_2$  transformed data. The difference of protein quantity between the 2 samples was expressed as the  $\log_2$  fold of the means.

## CHAPITRE IV : Limitation azotée et allocation du carbone. Approche intégrative en chémostat.

( $\text{Log}_2(\text{mean}(2Xc1)/\text{mean}(WTc1))$ ). The effect was considered significant when  $p < 0.01$  and [ $\log_2\text{fold} > 1$  or  $< -1$ ] or  $p < 0.05$  and [ $\log_2\text{fold} > 2$  or  $< -2$ ].

### References

- [1] R. Sayre, Microalgae: The Potential for Carbon Capture, *BioScience*. 60 (2010) 722–727. doi:10.1525/bio.2010.60.9.9.
- [2] O. Pulz, W. Gross, Valuable products from biotechnology of microalgae, *Appl. Microbiol. Biotechnol.* 65 (2004) 635–648. doi:10.1007/s00253-004-1647-x.
- [3] P. Spolaore, C. Joannis-Cassan, E. Duran, A. Isambert, Commercial applications of microalgae, *J. Biosci. Bioeng.* 101 (2006) 87–96. doi:10.1263/jbb.101.87.
- [4] W. Klinthong, A Review: Microalgae and Their Applications in CO<sub>2</sub> Capture and Renewable Energy, *Aerosol Air Qual. Res.* (2015). doi:10.4209/aaqr.2014.11.0299.
- [5] M. Davey, G.A. Tarran, M.M. Mills, C. Ridame, R.J. Geider, J. LaRoche, Nutrient limitation of picophytoplankton photosynthesis and growth in the tropical North Atlantic, *Limnol. Oceanogr.* 53 (2008) 1722–1733. doi:10.4319/lo.2008.53.5.1722.
- [6] T.J. Browning, H.A. Bouman, C.M. Moore, C. Schlosser, G.A. Tarran, E.M.S. Woodward, et al., Nutrient regimes control phytoplankton ecophysiology in the South Atlantic, *Biogeosciences*. 11 (2014) 463–479. doi:10.5194/bg-11-463-2014.
- [7] R. Miller, G. Wu, R. Deshpande, A. Vieler, K. Gartner, X. Li, et al., Changes in Transcript Abundance in *Chlamydomonas reinhardtii* following Nitrogen Deprivation Predict Diversion of Metabolism, *PLANT Physiol.* 154 (2010) 1737–1752. doi:10.1104/pp.110.165159.
- [8] D.Y. Lee, J.-J. Park, D.K. Barupal, O. Fiehn, System Response of Metabolic Networks in *Chlamydomonas reinhardtii* to Total Available Ammonium, *Mol. Cell. Proteomics*. 11 (2012) 973–988. doi:10.1074/mcp.M111.016733.
- [9] J. Fan, C. Yan, C. Andre, J. Shanklin, J. Schwender, C. Xu, Oil accumulation is controlled by carbon precursor supply for fatty acid synthesis in *Chlamydomonas reinhardtii*, *Plant Cell Physiol.* 53 (2012) 1380–1390. doi:10.1093/pcp/pcs082.
- [10] N. Wase, P.N. Black, B.A. Stanley, C.C. DiRusso, Integrated Quantitative Analysis of Nitrogen Stress Response in *Chlamydomonas reinhardtii* Using Metabolite and Protein Profiling, *J. Proteome Res.* 13 (2014) 1373–1396. doi:10.1021/pr400952z.
- [11] J.-J. Park, H. Wang, M. Gargouri, R.R. Deshpande, J.N. Skepper, F.O. Holguin, et al., The response of *Chlamydomonas reinhardtii* to nitrogen deprivation: a systems biology analysis, *Plant J.* 81 (2015) 611–624. doi:10.1111/tpj.12747.
- [12] L. Valledor, T. Furuhashi, L. Recuenco-Muñoz, S. Wienkoop, W. Weckwerth, System-level network analysis of nitrogen starvation and recovery in *Chlamydomonas reinhardtii* reveals potential new targets for increased lipid accumulation, *Biotechnol. Biofuels*. 7 (2014) 171. doi:10.1186/s13068-014-0171-1.
- [13] J. Msanne, D. Xu, A.R. Konda, J.A. Casas-Mollano, T. Awada, E.B. Cahoon, et al., Metabolic and gene expression changes triggered by nitrogen deprivation in the photoautotrophically grown microalgae *Chlamydomonas reinhardtii* and *Coccomyxa* sp. C-169, *Phytochemistry*. 75 (2012) 50–59. doi:10.1016/j.phytochem.2011.12.007.
- [14] S. Schmollinger, T. Mühlhaus, N.R. Boyle, I.K. Blaby, D. Casero, T. Mettler, et al., Nitrogen-Sparing Mechanisms in *Chlamydomonas* Affect the Transcriptome, the Proteome, and Photosynthetic Metabolism[W], *Plant Cell*. 26 (2014) 1410–1435. doi:10.1105/tpc.113.122523.
- [15] J. Valenzuela, A. Mazurie, R.P. Carlson, R. Gerlach, K.E. Cooksey, B.M. Peyton, et al., Potential role of multiple carbon fixation pathways during lipid accumulation in *Phaeodactylum tricoratum*, *Biotechnol. Biofuels*. 5 (2012) 40. doi:10.1186/1754-6834-5-40.
- [16] J. Valenzuela, R.P. Carlson, R. Gerlach, K. Cooksey, B.M. Peyton, B. Bothner, et al., Nutrient resupplementation arrests bio-oil accumulation in *Phaeodactylum tricoratum*, *Appl. Microbiol. Biotechnol.* 97 (2013) 7049–7059. doi:10.1007/s00253-013-5010-y.
- [17] Z.-K. Yang, Y.-H. Ma, J.-W. Zheng, W.-D. Yang, J.-S. Liu, H.-Y. Li, Proteomics to reveal metabolic network shifts towards lipid accumulation following nitrogen deprivation in the diatom *Phaeodactylum tricoratum*, *J. Appl. Phycol.* 26 (2014) 73–82. doi:10.1007/s10811-013-0050-3.
- [18] L. Alipanah, J. Rohloff, P. Winge, A.M. Bones, T. Brembu, Whole-cell response to nitrogen deprivation in the diatom *Phaeodactylum tricoratum*, *J. Exp. Bot.* (2015) erv340. doi:10.1093/jxb/erv340.
- [19] H.-P. Dong, E. Williams, D. Wang, Z.-X. Xie, R. Hsia, A. Jenck, et al., Responses of *Nannochloropsis oceanica* IMET1 to Long-Term Nitrogen Starvation and Recovery, *Plant Physiol.* 162 (2013) 1110–1126. doi:10.1104/pp.113.214320.
- [20] D. Simionato, M.A. Block, N.L. Rocca, J. Jouhet, E. Maréchal, G. Finazzi, et al., The Response of *Nannochloropsis gaditana* to Nitrogen Starvation Includes De Novo Biosynthesis of Triacylglycerols, a Decrease of Chloroplast Galactolipids, and Reorganization of the Photosynthetic Apparatus, *Eukaryot. Cell*. 12 (2013) 665–676. doi:10.1128/EC.00363-12.
- [21] N. Shtaida, I. Khozin-Goldberg, S. Boussiba, The role of pyruvate hub enzymes in supplying carbon precursors for fatty acid synthesis in photosynthetic microalgae, *Photosynth. Res.* 125 (2015) 407–422. doi:10.1007/s11120-015-0136-7.
- [22] Y. Li, D. Han, G. Hu, D. Dauvillee, M. Sommerfeld, S. Ball, et al., *Chlamydomonas* starchless mutant defective in ADP-glucose pyrophosphorylase hyper-accumulates triacylglycerol, *Metab. Eng.* 12 (2010) 387–391.

## CHAPITRE IV : Limitation azotée et allocation du carbone. Approche intégrative en chémostat.

- [23] M. Siaux, S. Cuiné, C. Cagnon, B. Fessler, M. Nguyen, P. Carrier, et al., Oil accumulation in the model green alga *Chlamydomonas reinhardtii*: characterization, variability between common laboratory strains and relationship with starch reserves, *BMC Biotechnol.* 11 (2011) 7. doi:10.1186/1472-6750-11-7.
- [24] H. Vigeolas, F. Duby, E. Kaymak, G. Niessen, P. Motte, F. Franck, et al., Isolation and partial characterization of mutants with elevated lipid content in *Chlorella sorokiniana* and *Scenedesmus obliquus*, *J. Biotechnol.* (2012). doi:10.1016/j.jbiotec.2012.03.017.
- [25] I.K. Blaby, A.G. Glaesener, T. Mettler, S.T. Fitz-Gibbon, S.D. Gallaher, B. Liu, et al., Systems-level analysis of nitrogen starvation-induced modifications of carbon metabolism in a *Chlamydomonas reinhardtii* starchless mutant, *Plant Cell.* 25 (2013) 4305–4323. doi:10.1105/tpc.113.117580.
- [26] Y.-E. Choi, H. Hwang, H.-S. Kim, J.-W. Ahn, W.-J. Jeong, J.-W. Yang, Comparative proteomics using lipid over-producing or less-producing mutants unravels lipid metabolisms in *Chlamydomonas reinhardtii*, *Bioresour. Technol.* (2013). doi:10.1016/j.biortech.2013.03.142.
- [27] U. Goodenough, I. Blaby, D. Casero, S.D. Gallaher, C. Goodson, S. Johnson, et al., The Path to Triacylglyceride Obesity in the *sta6* Strain of *Chlamydomonas reinhardtii*, *Eukaryot. Cell.* (2014) EC.00013–14. doi:10.1128/EC.00013-14.
- [28] T. Li, M. Gargouri, J. Feng, J.-J. Park, D. Gao, C. Miao, et al., Regulation of starch and lipid accumulation in a microalga *Chlorella sorokiniana*, *Bioresour. Technol.* 180 (2015) 250–257. doi:10.1016/j.biortech.2015.01.005.
- [29] B.-H. Zhu, H.-P. Shi, G.-P. Yang, N.-N. Lv, M. Yang, K.-H. Pan, Silencing UDP-glucose pyrophosphorylase gene in *Phaeodactylum tricornutum* affects carbon allocation, *New Biotechnol.* (2015). doi:10.1016/j.nbt.2015.06.003.
- [30] A.E. Allen, C.L. Dupont, M. Oborník, A. Horák, A. Nunes-Nesi, J.P. McCrow, et al., Evolution and metabolic significance of the urea cycle in photosynthetic diatoms, *Nature.* 473 (2011) 203–207. doi:10.1038/nature10074.
- [31] A.E. Allen, A. Vardi, C. Bowler, An ecological and evolutionary context for integrated nitrogen metabolism and related signaling pathways in marine diatoms, *Curr Opin Plant Biol.* 9 (2006) 264–273. doi:10.1016/j.pbi.2006.03.013.
- [32] G. Michel, T. Tonon, D. Scornet, J.M. Cock, B. Kloareg, Central and storage carbon metabolism of the brown alga *Ectocarpus siliculosus*: insights into the origin and evolution of storage carbohydrates in Eukaryotes, *New Phytol.* 188 (2010) 67–81. doi:10.1111/j.1469-8137.2010.03345.x.
- [33] A. Sukenik, R. Wahnon, Biochemical Quality of Marine Unicellular Algae with Special Emphasis on Lipid-Composition .1. *Isochrysis-Galbana*, *Aquaculture.* 97 (1991) 61–72. doi:10.1016/0044-8486(91)90279-G.
- [34] M.L. Eltgroth, R.L. Watwood, G.V. Wolfe, Production and cellular localization of neutral long chain lipids in the haptophyte algae *Isochrysis galbana* and *Emiliana huxleyi*, *J. Phycol.* 41 (2005) 1000–1009. doi:10.1111/j.1529-8817.2005.00128.x.
- [35] E.M. Bendif, I. Probert, D.C. Schroeder, C. de Vargas, On the description of *Tisochrysis lutea* gen. nov. sp. nov. and *Isochrysis nuda* sp. nov. in the Isochrysidales, and the transfer of *Dicrateria* to the Prymnesiales (Haptophyta), *J. Appl. Phycol.* 25 (2013) 1763–1776. doi:10.1007/s10811-013-0037-0.
- [36] S. Theroux, W.J. D'Andrea, J. Toney, L. Amaral-Zettler, Y. Huang, Phylogenetic diversity and evolutionary relatedness of alkenone-producing haptophyte algae in lakes: Implications for continental paleotemperature reconstructions, *Earth Planet. Sci. Lett.* 300 (2010) 311–320. doi:10.1016/j.epsl.2010.10.009.
- [37] I.T. Marlowe, J.C. Green, A.C. Neal, S.C. Brassell, G. Eglinton, P.A. Course, Long chain (n-C37–C39) alkenones in the Prymnesiophyceae. Distribution of alkenones and other lipids and their taxonomic significance, *Br. Phycol. J.* 19 (1984) 203–216. doi:10.1080/00071618400650221.
- [38] H. Liu, I. Probert, J. Uitz, H. Claustre, S. Aris-Brosou, M. Frada, et al., Extreme diversity in noncalcifying haptophytes explains a major pigment paradox in open oceans, *Proc. Natl. Acad. Sci.* 106 (2009) 12803–12808. doi:10.1073/pnas.0905841106.
- [39] E. Fernández, E. Marañón, W.M. Balch, Intracellular carbon partitioning in the coccolithophorid *Emiliana huxleyi*, *J. Mar. Syst.* 9 (1996) 57–66. doi:10.1016/0924-7963(96)00016-4.
- [40] Y. Tsuji, M. Yamazaki, I. Suzuki, Y. Shiraiwa, Quantitative Analysis of Carbon Flow into Photosynthetic Products Functioning as Carbon Storage in the Marine Coccolithophore, *Emiliana huxleyi*, *Mar. Biotechnol.* 17 (2015) 428–440. doi:10.1007/s10126-015-9632-1.
- [41] G. Bougaran, O. Bernard, A. Sciandra, Modeling continuous cultures of microalgae colimited by nitrogen and phosphorus, *J. Theor. Biol.* 265 (2010) 443–454. doi:10.1016/j.jtbi.2010.04.018.
- [42] F. Mairet, O. Bernard, P. Masci, T. Lacour, A. Sciandra, Modelling neutral lipid production by the microalga *Isochrysis aff. galbana* under nitrogen limitation, *Bioresour. Technol.* 102 (2011) 142–149. doi:10.1016/j.biortech.2010.06.138.
- [43] T. Lacour, A. Sciandra, A. Talec, P. Mayzaud, O. Bernard, Neutral lipids and carbohydrate productivities as a response to nitrogen status in *Isochrysis* sp. (T-Iso, haptophyceae): Starvation versus limitation, *J. Phycol.* 48 (2012) 647–656. doi:10.1111/j.1529-8817.2012.01154.x.
- [44] G. Bougaran, C. Rouxel, N. Dubois, R. Kaas, S. Grouas, E. Lukomska, et al., Enhancement of neutral lipid productivity in the microalga *Isochrysis affinis Galbana* (T-Iso) by a mutation-selection procedure, *Biotechnol. Bioeng.* 109 (2012) 2737–2745. doi:10.1002/bit.24560.
- [45] M. Garnier, G. Carrier, H. Rogniaux, E. Nicolau, G. Bougaran, B. Saint-Jean, et al., Comparative proteomics reveals proteins impacted by nitrogen deprivation in wild-type and high lipid-accumulating mutant strains of *Tisochrysis lutea*, *J. Proteomics.* (2014). doi:10.1016/j.jprot.2014.02.022.
- [46] G. Carrier, M. Garnier, L. Le Cunff, G. Bougaran, I. Probert, C. De Vargas, et al., Comparative Transcriptome of Wild Type and Selected Strains of the Microalgae *Tisochrysis lutea* Provides Insights into the Genetic Basis, Lipid Metabolism and the Life Cycle, *PLoS ONE.* 9 (2014) e86889. doi:10.1371/journal.pone.0086889.
- [47] M.R. Droop, The nutrient status of algal cells in continuous culture, *J. Mar. Biol. Assoc. U. K.* 54 (1974) 825–855. doi:10.1017/S002531540005760X.
- [48] R. Geider, J. La Roche, Redfield revisited: variability of C:N:P in marine microalgae and its biochemical basis, *Eur. J. Phycol.* 37 (2002) 1–17. doi:10.1017/S0967026201003456.

## CHAPITRE IV : Limitation azotée et allocation du carbone. Approche intégrative en chémostat.

- [49] H.-P. Braun, U.K. Schmitz, The protein-import apparatus of plant mitochondria, *Planta*. 209 (1999) 267–274. doi:10.1007/s004250050632.
- [50] Q. Shi, H. Araie, R.K. Bakku, Y. Fukao, R. Rakwal, I. Suzuki, et al., Proteomic analysis of lipid body from the alkenone-producing marine haptophyte alga *Tisochrysis lutea*, *PROTEOMICS*. (2015) n/a–n/a. doi:10.1002/pmic.201500010.
- [51] K. Yoon, D. Han, Y. Li, M. Sommerfeld, Q. Hu, Phospholipid:diacylglycerol acyltransferase is a multifunctional enzyme involved in membrane lipid turnover and degradation while synthesizing triacylglycerol in the unicellular green microalga *Chlamydomonas reinhardtii*, *Plant Cell*. 24 (2012) 3708–3724. doi:10.1105/tpc.112.100701.
- [52] I. Sadvovskaya, A. Souissi, S. Souissi, T. Grard, P. Lencel, C.M. Greene, et al., Chemical structure and biological activity of a highly branched (1 → 3,1 → 6)-β-d-glucan from *Isochrysis galbana*, *Carbohydr. Polym.* 111 (2014) 139–148. doi:10.1016/j.carbpol.2014.04.077.
- [53] A. Charrier, J.-B. Bérard, G. Bougaran, G. Carrier, E. Lukomska, N. Schreiber, et al., High-affinity nitrate/nitrite transporter genes (Nrt2) in *Tisochrysis lutea*: identification and expression analyses reveal some interesting specificities of Haptophyta microalgae, *Physiol. Plant.* (2015). doi:10.1111/pp1.12330.
- [54] H. Chen, Y. Zhang, C. He, Q. Wang, Ca<sup>2+</sup> Signal Transduction Related to Neutral Lipid Synthesis in an Oil-Producing Green Alga *Chlorella* sp. C2, *Plant Cell Physiol.* 55 (2014) 634–644. doi:10.1093/pcp/pcu015.
- [55] H. Chen, J. Hu, Y. Qiao, W. Chen, J. Rong, Y. Zhang, et al., Ca<sup>2+</sup>-regulated cyclic electron flow supplies ATP for nitrogen starvation-induced lipid biosynthesis in green alga, *Sci. Rep.* 5 (2015) 15117. doi:10.1038/srep15117.
- [56] P.A. Hoskisson, G. Hobbs, Continuous culture – making a comeback?, *Microbiology*. 151 (2005) 3153–3159. doi:10.1099/mic.0.27924-0.
- [57] A.T. Bull, The renaissance of continuous culture in the post-genomics age, *J. Ind. Microbiol. Biotechnol.* 37 (2010) 993–1021. doi:10.1007/s10295-010-0816-4.
- [58] B.M. Jones, R.J. Edwards, P.J. Skipp, C.D. O'Connor, M.D. Iglesias-Rodriguez, Shotgun Proteomic Analysis of *Emiliana huxleyi*, a Marine Phytoplankton Species of Major Biogeochemical Importance, *Mar. Biotechnol.* (2010). doi:10.1007/s10126-010-9320-0.
- [59] B.A. McKew, S.C. Lefebvre, E.P. Achterberg, G. Metodieva, C.A. Raines, M.V. Metodiev, et al., Plasticity in the proteome of *Emiliana huxleyi* CCMP 1516 to extremes of light is highly targeted, *New Phytol.* 200 (2013) 61–73. doi:10.1111/nph.12352.
- [60] G.-Y. Rhee, Effects of N:P atomic ratios and nitrate limitation on algal growth, cell composition, and nitrate uptake 1, *Limnol. Oceanogr.* 23 (1978) 10–25. doi:10.4319/lo.1978.23.1.0010.
- [61] L. Notley-McRobb, T. Ferenci, The generation of multiple co-existing mal-regulatory mutations through polygenic evolution in glucose-limited populations of *Escherichia coli*, *Environ. Microbiol.* 1 (1999) 45–52. doi:10.1046/j.1462-2920.1999.00003.x.
- [62] M.-M. Perrineau, J. Gross, E. Zelzion, D.C. Price, O. Levitan, J. Boyd, et al., Using Natural Selection to Explore the Adaptive Potential of *Chlamydomonas reinhardtii*, *PLoS ONE*. 9 (2014) e92533. doi:10.1371/journal.pone.0092533.
- [63] Y. Sun, H. Wang, G. Guo, Y. Pu, B. Yan, The isolation and antioxidant activity of polysaccharides from the marine microalgae *Isochrysis galbana*, *Carbohydr. Polym.* 113 (2014) 22–31. doi:10.1016/j.carbpol.2014.06.058.
- [64] F. Da Costa, B. Petton, C. Mingant, G. Bougaran, C. Rouxel, C. Quéré, et al., Influence of one selected *Tisochrysis lutea* strain rich in lipids on *Crassostrea gigas* larval development and biochemical composition, *Aquac. Nutr.* (2015) n/a–n/a. doi:10.1111/anu.12301.
- [65] G.W. O'Neil, C.A. Carmichael, T.J. Goepfert, J.M. Fulton, G. Knothe, C.P.L. Lau, et al., Beyond Fatty Acid Methyl Esters: Expanding the Renewable Carbon Profile with Alkenones from *Isochrysis* sp., *Energy Fuels*. 26 (2012) 2434–2441.
- [66] H.-T. Wang, C.-H. Yao, J.-N. Ai, X.-P. Cao, S. Xue, W. Wang, Identification of carbohydrates as the major carbon sink of the marine microalga *Isochrysis zhangjiangensis* (Haptophyta) and optimization of its productivity by nitrogen manipulation, *Bioresour. Technol.* (2014). doi:10.1016/j.biortech.2014.08.090.
- [67] I. Khozin-Goldberg, P. Shrestha, Z. Cohen, Mobilization of arachidonyl moieties from triacylglycerols into chloroplastic lipids following recovery from nitrogen starvation of the microalga *Parietochloris incisa*, *Biochim. Biophys. Acta BBA - Mol. Cell Biol. Lipids*. 1738 (2005) 63–71. doi:10.1016/j.bbalip.2005.09.005.
- [68] M.T. Guarnieri, A. Nag, S.L. Smolinski, A. Darzins, M. Seibert, P.T. Pienkos, Examination of triacylglycerol biosynthetic pathways via de novo transcriptomic and proteomic analyses in an unsequenced microalga, *PLoS One*. 6 (2011) e25851. doi:10.1371/journal.pone.0025851.
- [69] H.-T. Wang, Y.-Y. Meng, X.-P. Cao, J.-N. Ai, J.-N. Zhou, S. Xue, et al., Coordinated response of photosynthesis, carbon assimilation, and triacylglycerol accumulation to nitrogen starvation in the marine microalgae *Isochrysis zhangjiangensis* (Haptophyta), *Bioresour. Technol.* 177 (2015) 282–288. doi:10.1016/j.biortech.2014.11.028.
- [70] N. Tuteja, S. Mahajan, Calcium Signaling Network in Plants, *Plant Signal. Behav.* 2 (2007) 79–85.
- [71] C. Adams, B. Bugbee, Nitrogen retention and partitioning at the initiation of lipid accumulation in nitrogen-deficient algae, *J. Phycol.* 50 (2014) 356–365. doi:10.1111/jpy.12167.
- [72] N. Velmurugan, M. Sung, S.S. Yim, M.S. Park, J.W. Yang, K.J. Jeong, Systematically programmed adaptive evolution reveals potential role of carbon and nitrogen pathways during lipid accumulation in *Chlamydomonas reinhardtii*, *Biotechnol. Biofuels*. 7 (2014) 117. doi:10.1186/s13068-014-0117-7.
- [73] T. Mock, M.P. Samanta, V. Iverson, C. Berthiaume, M. Robison, K. Holtermann, et al., Whole-genome expression profiling of the marine diatom *Thalassiosira pseudonana* identifies genes involved in silicon bioprocesses, *Proc. Natl. Acad. Sci. U. S. A.* 105 (2008) 1579–1584. doi:10.1073/pnas.0707946105.

## CHAPITRE IV : Limitation azotée et allocation du carbone. Approche intégrative en chémostat.

- [74] N.L. Hockin, T. Mock, F. Mulholland, S. Kopriva, G. Malin, The Response of Diatom Central Carbon Metabolism to Nitrogen Starvation Is Different from That of Green Algae and Higher Plants, *Plant Physiol.* 158 (2012) 299–312. doi:10.1104/pp.111.184333.
- [75] E. Moellering, C. Benning, RNA Interference Silencing of a Major Lipid Droplet Protein Affects Lipid Droplet Size in *Chlamydomonas reinhardtii*, *Eukaryot. CELL.* 9 (2010) 97–106. doi:10.1128/EC.00203-09.
- [76] A. Livne, A. Sukenik, Lipid Synthesis and Abundance of Acetyl CoA Carboxylase in *Isochrysis galbana* (Prymnesiophyceae) Following Nitrogen Starvation, *Plant Cell Physiol.* 33 (1992) 1175–1181.
- [77] T. Dunahay, E. Jarvis, S. Dais, P. Roessler, Manipulation of microalgal lipid production using genetic engineering, *Appl. Biochem. Biotechnol.* 57-8 (1996) 223–231.
- [78] J. Sheehan, T.G. Dunahay, J. Benemann, P. Roessler, A Look back at the U.S Department of Energy's Aquatic Species Program : Biodiesel from Algae pdf rapport, (1998).
- [79] E.M. Trentacoste, R.P. Shrestha, S.R. Smith, C. Glé, A.C. Hartmann, M. Hildebrand, et al., Metabolic engineering of lipid catabolism increases microalgal lipid accumulation without compromising growth, *Proc. Natl. Acad. Sci.* 110 (2013) 19748–19753. doi:10.1073/pnas.1309299110.
- [80] G. Cassin-Ross, J. Hu, Systematic Phenotypic Screen of Arabidopsis Peroxisomal Mutants Identifies Proteins Involved in  $\beta$ -Oxidation, *Plant Physiol.* 166 (2014) 1546–1559. doi:10.1104/pp.114.250183.
- [81] N. Shtaida, I. Khozin-Goldberg, S. Boussiba, The role of pyruvate hub enzymes in supplying carbon precursors for fatty acid synthesis in photosynthetic microalgae, *Photosynth. Res.* 125 (2015) 407–422. doi:10.1007/s11220-015-0136-7.
- [82] P. Song, L. Li, J. Liu, Proteomic Analysis in Nitrogen-Deprived *Isochrysis galbana* during Lipid Accumulation, *PLoS ONE.* 8 (2013) e82188. doi:10.1371/journal.pone.0082188.
- [83] A. Mühroth, K. Li, G. Røkke, P. Winge, Y. Olsen, M.F. Hohmann-Marriott, et al., Pathways of Lipid Metabolism in Marine Algae, Co-Expression Network, Bottlenecks and Candidate Genes for Enhanced Production of EPA and DHA in Species of Chromista, *Mar. Drugs.* 11 (2013) 4662–4697. doi:10.3390/md11114662.
- [84] P.R. Walne, Experiments in the large scale culture of the larvae of *Ostrea edulis*. L, FISH INVEST MINISTR, 1996.
- [85] P. Greenspan, E. Mayer, S. Fowler, Nile Red - a Selective Fluorescent Stain for Intracellular Lipid Droplets, *J. Cell Biol.* 100 (1985) 965–973. doi:10.1083/jcb.100.3.965.
- [86] J. Folch, M. Lees, G.H.S. Stanley, A Simple Method for the Isolation and Purification of Total Lipides from Animal Tissues, *J. Biol. Chem.* 226 (1957) 497–509.
- [87] R. Craig, R.C. Beavis, TANDEM: matching proteins with tandem mass spectra, *Bioinforma. Oxf. Engl.* 20 (2004) 1466–1467. doi:10.1093/bioinformatics/bth092.
- [88] B. Valot, O. Langella, E. Nano, M. Zivy, MassChroQ: A versatile tool for mass spectrometry quantification, *Proteomics.* 11 (2011) 3572–3577. doi:10.1002/pmic.201100120.

### Abbreviations

ACAA : 3-ketoacyl-CoA thiolase ; ACCase : Acetyl-CoA carboxylase ; ACO : Aconitase ; ACS : Acetyl-coenzyme A synthetase ; ALDH : Acetaldehyde dehydrogenase ; BC1-I : Cytochrome b-c1 complex subunit ; CCP : Cytochrome c peroxidase ; Cox : Cytochrome c oxidase ; CS : Citrate synthase ; CyC6 : Cytochrome c6 ; Cyt-c : Cytochrome c ; DGAT : Diacylglycerol O-acyltransferase ; EAR : Enoyl-[acyl-carrier-protein] reductase 1 ; ENO : Enolase ; FBPA : Fructose-bisphosphate aldolase ; FBPAse : Chloroplastic Fructose-1,6-bisphosphatase 1 ; Fd : Ferredoxin ; FNR : Ferredoxin--NADP reductase ; FR : Fumarate reductase ; FUM : Fumarase ; G6P-I : Putative glucose-6-phosphate 1-epimerase ; GAPDH : glyceraldehyde-3-phosphate dehydrogenase ; GDH : Glycine dehydrogenase ; GPAT : glycerol-3-phosphate acyltransferase ; HAD : 3-hydroxyacyl-[acyl-carrier-protein] dehydratase ; HCDH : 3-hydroxyacyl-CoA dehydrogenase ; HK : Hexokinase ; ICL : Isocitrate lyase ; IDH : Isocitrate dehydrogenase [NADP] ; KAR : 3-oxoacyl-[acyl-carrier-protein] reductase ; KASII : 3-oxoacyl-[acyl-carrier-protein] synthase ; LACS : Long chain acyl-CoA synthetase ; LPAAT : lysophosphatidic acid-acyltransferase ; MALsH : Malate synthase ; MAT : Malonyl-CoA-acyl carrier protein transacylase ; MDH : Malate dehydrogenase ; ME1 : NADP-dependent malic enzyme ; NADHDH : NADH dehydrogenase ; OGDC-E2 : 2-oxoglutarate dehydrogenase-E2 ; PAP : Phosphatidic acid phosphatase ; PCr : pyruvate carboxylase ; PDAT : phospholipid:diacylglycerol acyltransferase ; PDC : Pyruvate Deshydrogenase Complex PDC-E1-a/ $\beta$  ; PDHK : Pyruvate dehydrogenase kinase ; PeB : Cytochrome b6 ; PEPCCK : Phosphoenolpyruvate carboxykinase [ATP] ; PetA : Apocytocrome f ; PFK : 6-phosphofructokinase ; PGAM : 2,3-bisphosphoglycerate-dependent phosphoglycerate mutase ; PGCM : phosphoglucomutase ; PGD : 6-phosphogluconate dehydrogenase ; PGI : Glucose-6-phosphate isomerase ; PGK : Phosphoglycerate kinase ; PGM : Phosphoglucomutase ; PK : Pyruvate kinase ; PPE : Pentose-5-phosphate 3-épimérase ; PPK : Phosphoribulokinase ; PsaA : Photosystem I P700 chlorophyll a apoprotein ; PsaB : Photosystem I P700 chlorophyll a apoprotein A2 ; PsaL : Photosystem I reaction center subunit XI ; PsbB : Photosystem II protein ; PsYcf3 : Photosystem I assembly protein ; RbcS : Ribulose bisphosphate carboxylase small chain ; Rieske : Cytochrome b6-f complex iron-sulfur subunit ; RPEh : D-Ribulose-5-Phosphate 3-Epimerase ; RPI : Probable ribose-5-phosphate isomerase ; RPPK : Ribose-phosphate pyrophosphokinase ; SDH : Succinate dehydrogenase ; STK : succinyl-CoA ligase ; TAGH : Triacylglycerol hydrolase ; TAL : Transaldolase ; TK : Transketolase ; TPI : Triosephosphate isomerase.



## Chapitre V

CSAP & PLAAOX, deux protéines  
majeures régulées par l'azote.  
Annotation et étude de régulation.

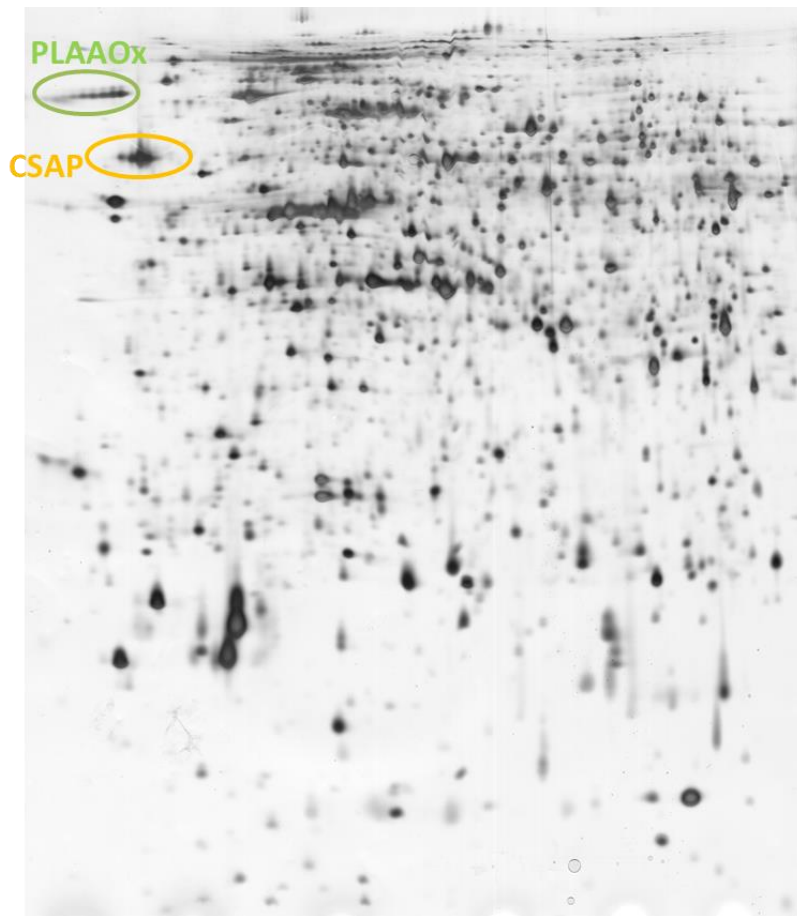


Figure 51 Protéome de *T. lutea* WT en carence azotée observé sur gel 2-DE (pH4-7, acrylamide 12%) coloré à l'argent.

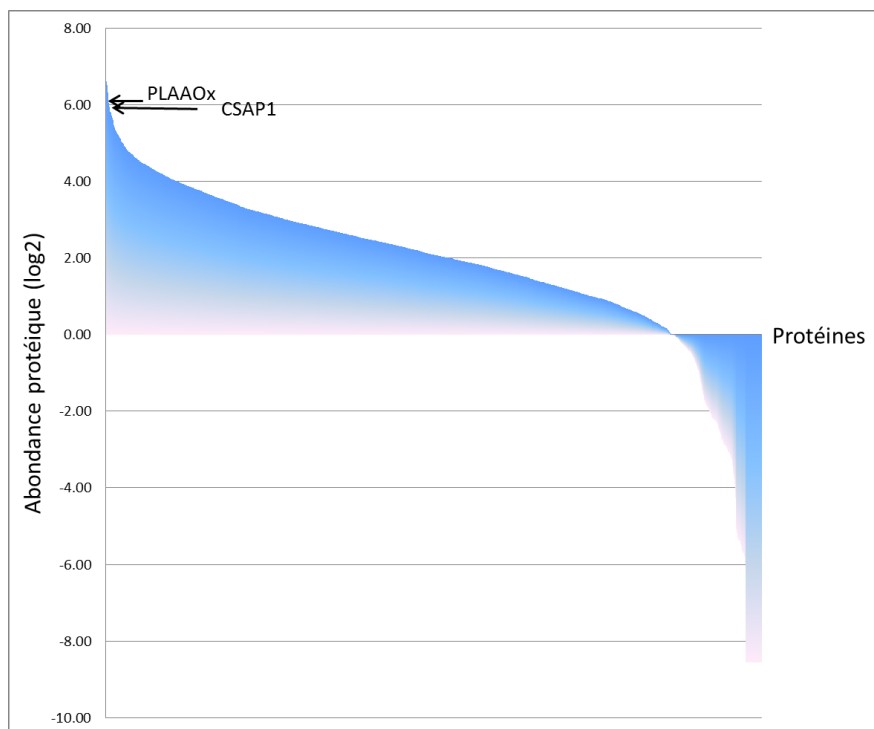


Figure 52 Distribution de l'abondance des 4332 protéines de *T. lutea* WTc1 identifiées par LC-MS/MS lors de la limitation azotée (Chapitre IV).



## Chapitre V : CSAP & PLAAOX, deux protéines majeures régulées par l'azote. Annotation et étude de leur régulation.

---

Les travaux présentés dans les chapitres précédents ont permis de montrer que l'accumulation des lipides chez l'haptophyte *Tisochrysis lutea* est vraisemblablement associée à une réallocation globale du carbone intracellulaire et à des mécanismes de signalisation encore mal identifiés chez les microalgues. Les analyses protéomiques et transcriptomiques ont mis en évidence des gènes régulés par l'azote, potentiellement impliqués dans la suraccumulation lipidique. Comme chez l'ensemble des microalgues séquencées, la fonction de nombreux gènes et protéines codées reste à ce jour mal connue. Parmi les protéines de fonction mal identifiée, les protéines annotées sous les noms de « Coccolite Scale Associated Protein » (CSAP) et « Periplamic L-Amino-acid Oxidase » (PLAAOx) ont montré des profils d'abondance particulièrement intéressants (Garnier et al., 2014). Chez *T. lutea* WT, la carence azotée induit la suraccumulation de ces deux protéines. Chez la souche S2M2, la carence azotée n'induit qu'une très faible accumulation des deux protéines. Ces résultats ont permis d'émettre l'hypothèse selon laquelle l'accumulation de ces deux protéines pourrait limiter l'accumulation lipidique chez *T. lutea* WT,(Garnier et al., 2014). Les différences d'accumulation protéique entre les deux souches, observées lors de la carence azotée, ont également été mesurées par analyses LC-MS/MS lors de la limitation azotée dans le chapitre IV (**Figure 49**). En revanche, les analyses RNAseq réalisées n'ont pas permis de confirmer ces résultats au niveau transcriptomique mais l'étude d'expression de ces gènes par RT-qPCR semble nécessaire pour valider ces résultats.

Les intensités des spots sur gels 2-DE suggèrent que ces protéines font partie des protéines les plus abondantes chez la souche WT lors de la carence azotée (**Figure 51**). Ces résultats ont été confirmés lors de la limitation azotée par les résultats d'analyses protéomiques haut débit (Chapitre IV) qui indiquent que la PLAAOx et la CSAP représentent la 15<sup>ème</sup> et la 29<sup>ème</sup> plus abondante des 4332 protéines identifiées respectivement (**Figure 52**). Les autres protéines qui partagent ce caractère d'abondance sont des protéines très conservées dans le monde du vivant et leurs fonctions sont bien connues. Pour l'essentiel ce sont des protéines chaperonnes, impliquées généralement dans la réponse au stress, des protéines du cycle cellulaire et quelques enzymes du métabolisme lipidique. A l'inverse des autres protéines majoritaires, les fonctions des protéines CSAP et PLAAOx restent mal déterminées. La CSAP a été annoté ainsi car, lors de son identification, la seule protéine homologue

dans les banques de données était la CSAP1 de l'haptophyte *Pleurochrysis carterae* (données non publiées). La sémantique suggère l'implication de cette protéine dans la synthèse des coccolites. Cependant, aucune donnée publiée ou accessible ne va dans ce sens et l'absence de coccolites chez *T. lutea* suggère que cette protéine semble davantage impliquée dans d'autres fonctions que la synthèse de coccolites. L'annotation de la protéine PLAAOx de *T. lutea* réside en la présence d'un domaine conservé amino-oxidase (Pfam 1593) et d'un fort pourcentage de similarité avec la Periplasmic L-amino acid oxydase de *Chrysochromulina sp.* (76.2 % de similarité dont 53.8 % d'identité pour 496 acides aminés). L'activité fonctionnelle et la localisation périplasmique de cette protéine n'a cependant jamais été vérifiée à notre connaissance. Le premier objectif de ce chapitre consiste à mieux caractériser la fonction de ces deux protéines. Des approches *in silico* seront employées pour émettre des hypothèses de fonction moléculaire et cellulaire. Le second objectif consiste à étudier les cinétiques d'expression des deux gènes chez chacune des deux souches et ceci lors de transitions entre différents états de limitation azotée. Dans ce but, des mesures d'expression par RT-qPCR ont été réalisées à différents états de limitation azotée (Chapitre IV).

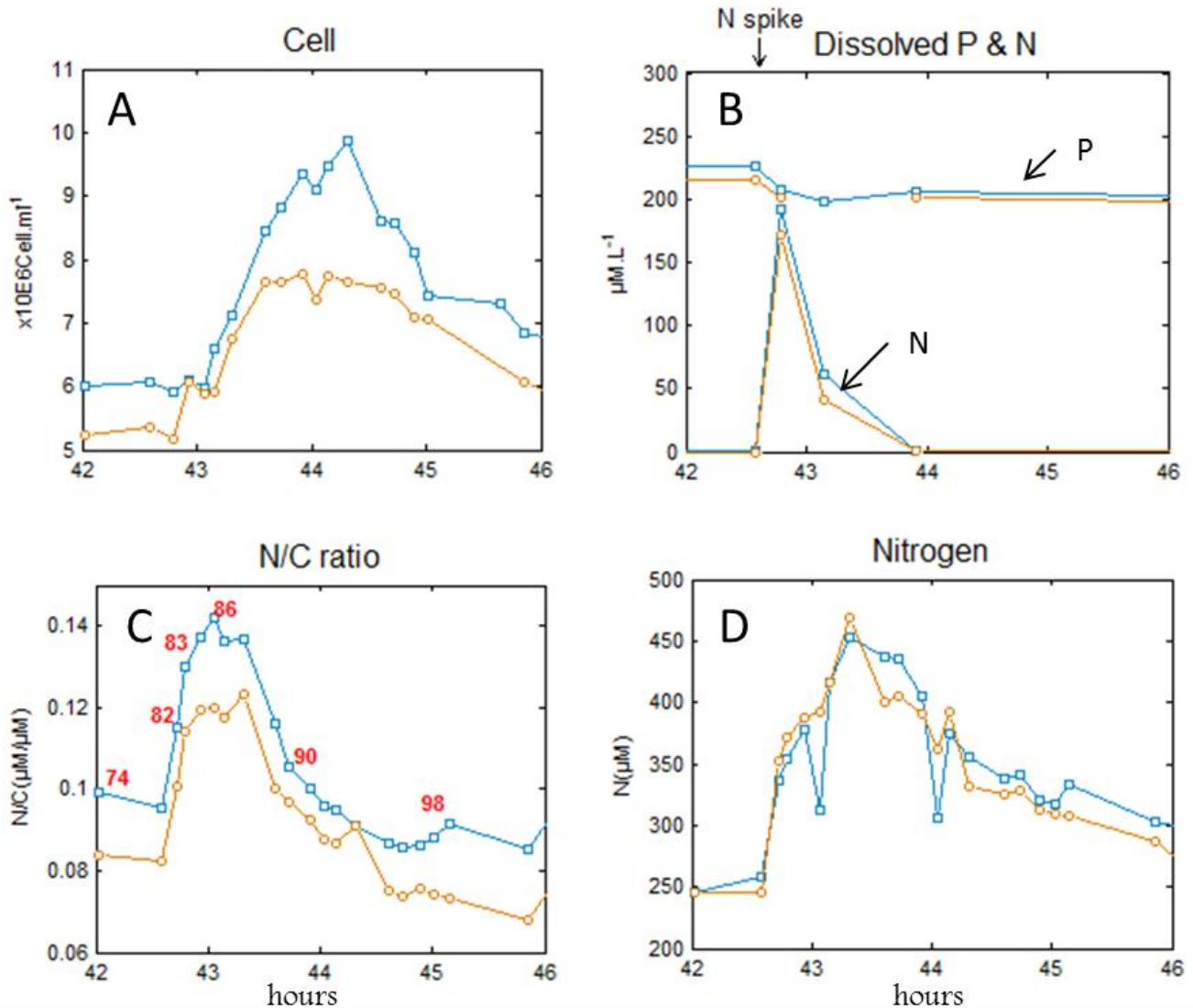
## 2 Matériel et méthodes

### Matériel biologique

Les échantillons biologiques proviennent des cultures en chemostat présentées dans le chapitre IV de ce document. Pour chacune des deux souches, six prélèvements ont été réalisés au cours des 3 jours suivant la seconde injection de nitrate (**Figure 53**). Le prélèvement Pt74 correspond à un état à l'équilibre de limitation azotée, les prélèvements Pt 82, Pt83, et Pt86 à des états successifs de réplétion azotée et les prélèvements Pt90 et Pt98 à des états de déplétion azotée. 50 ml de culture ont été centrifugés à 2 000 x g pendant 5 min à 5 ° C et le culot rapidement congelés dans de l'azote liquide et conservés à -80 ° C avant extraction des ARNs.

### Extraction des ARNs et production d'ADN complémentaire

Les ARNs ont été extraits dans 1 ml de TRIzol® (Invitrogen) et 200 µL de chloroforme, puis purifiés par traitement à l'ADNase (kit RQ1 RNase freeDNase Promega® : 1 u/µg d'ARN). Les ARNs ont été ensuite précipités à l'éthanol absolu, dilués dans 50 µL d'eau ultra pure et quantifiés par mesure de densité optique à 260 et 280 nm. L'intégrité des ARNs a été vérifiée au Bioanalyseur RNA 6000 nano d'Agilent technologies®. Les ARNs totaux ont été rétro-transcrits en ADN complémentaires à l'aide du kit « High capacity cDNA reverse transcription » de chez Applied Biosystems®.



**Figure 53** Caractérisation des échantillons pour la mesure de l'expression des gènes codant pour les protéines CSAP et PLAAOx.

Suivi de la concentration cellulaire (A), de l'azote et du phosphore dissous (B), du rapport N/C particulaire (C) et de l'azote particulaire (D) des souches WTc1 (bleu) et 2Xc1 (orange) en réponse à une injection de nitrate dans les chemostats pour lesquels les cellules sont limitées par l'azote. Ces figures sont issues des travaux réalisés dans le chapitre IV de ce document. Les prélèvements Pt74, Pt82, Pt83, Pt86, Pt90 et Pt98 indiqués en rouge sur le graphique C ont été analysés par RT-qPCR sur les gènes codants pour les protéines CSAP1 et PLAAOx.

### Clonage et séquençage des régions codantes.

Les régions codantes pour chacune des deux protéines ont été amplifiées par PCR à partir des ADNs complémentaires. Le mélange réactionnel de PCR contenait pour un volume final de 25  $\mu$ L : 7.5 unités de polymérase pFu (Promega®) et 1X final du tampon commerciale, 1  $\mu$ l de chaque amorce à 50  $\mu$ M, 0.5  $\mu$ l de dNTPs à 10mM, 1.5  $\mu$ M de MgCl<sub>2</sub> à 10mM et 5 ng d'ARN. Le programme d'amplification consiste en un cycle à 95 °C pendant 5 min, suivi de 30 cycles de 30 secondes à 95 °C, 30 secondes à 55 °C et 2 minutes à 55°C, et un cycle à 55°C pendant 5mn. Les gènes ont été amplifiés et clonés en deux fragments. Les couples d'amorces CSAP\_F3-CSAP\_R4 et CSAP\_F4-CSAP\_R3 (Tableau 2) ont été utilisés pour amplifier la région codante de la CSAP. Les couples d'amorces PLAAOx\_F4- PLAAOx\_R4 et PLAAOx\_F4- PLAAOx\_R7 (Tableau 2) ont été utilisés pour amplifier la région codante de la PLAAOx.

**Tableau 2** Amorces PCR utilisées pour le clonage des gènes CSAP et PLAAOx.

|           |                       |
|-----------|-----------------------|
| CSAP_F3   | CACCCCATCGCCGTA       |
| CSAP_R4   | GCCAGGAATGACATTGGTCT  |
| CSAP_F4   | CAACGGCATGATGATCAGC   |
| CSAP_R3   | ATGAATCAGGTGCATGGTTCG |
| PLAAOx_F3 | CTCCGCCGCTGAAGAGGG    |
| PLAAOx_R4 | GGGTGCGTCCTGAGAAGTCC  |
| PLAAOx_F4 | AGTGCAATGCGGACAAGAC   |
| PLAAOx_R7 | TTAGACAGAGTTGGCGACACG |

Les produits d'amplifications ont été clonés dans le vecteur pcr4TOPO® de chez Invitrogen® avant transformation dans les cellules TOP10® (Invitrogen®). Après extraction des plasmides par miniprep, les inserts ont été séquencés par la technique Sanger auprès d'un prestataire de service (GATC Biotech). Les séquences jointives de chacun des deux gènes ont ensuite été alignées pour définir les régions codantes complètes de chacune des deux protéines.

### Mesures d'expression

L'expression des gènes codant les protéines CSAP et PLAAOx a été mesurée par RT-qPCR. Le mélange réactionnel contient pour un volume final de 15 $\mu$ l : 12.5 $\mu$ l de SYBR Green PCR master mix 2X (Applied Biosystems®), 2.5 $\mu$ l de chacun des deux amorces à 1mM et 25ng d'ADN complémentaire. Le programme d'amplification consiste en 1 cycle à 95 °C pendant 10 min, suivi de 40 cycles de 30 secondes à 95 °C et 30 secondes à 60 °C. Chaque échantillon a été analysé en triplicat sur l'appareil Mx3000 qPCR system Agilent technologies (Santa Clara, Californie). Les deux gènes

GAPDH et EF1 ont été utilisés comme gènes de référence. Les amorces utilisées sont présentées dans le tableau ci-dessous.

**Tableau 3** Amorces utilisées pour les mesures d'expression de gènes par RT-qPCR.

|          |                      |
|----------|----------------------|
| CSAP1-F1 | CTGCCAACCATCACTTTCCC |
| CSAP1-R1 | ATGAACTTGCCACGTGAC   |
| AAOX-F2  | GACACACGATTTGGAGGACG |
| AAOX-R2  | TGAGATTGTGTCGAACGTGC |
| GAPDH-F  | CGGTGCTCAATGTAGTGGTT |
| GAPDH-R  | TAGTGATCATGCCCTTCTCG |
| EF1-F    | GTAGCGTGCCTTCTGTAGC  |
| EF1-R    | TAACTTCACCACTGCCATCC |

### Analyses bio-informatiques

La structure des gènes a été étudiée par alignement des régions codantes sur les séquences génomiques obtenues récemment au laboratoire. La région codante a été traduite *in silico*. La recherche de domaines fonctionnels a été effectuée sur les banques de données CDD v3.13-46918 PSSMs hébergée sur la plateforme NCBI, et ProDom (<http://prodom.prabi.fr>). La recherche de protéines homologues a été réalisée par BLASTP sur la base de données nr (non-redundant protein sequences) et sur le protéome *in silico* de *T. lutea*. Un score supérieur à 200 sur les résultats de BLASTP a été choisi pour sélectionner les protéines homologues. Les identités et similarités protéiques ont été mesurées avec le logiciel LALIGN (<http://www.ebi.ac.uk/Tools/psa/lalign/>). Les domaines transmembranaires ont été prédits avec l'outil TMHMM (<http://www.cbs.dtu.dk/services/TMHMM-2.0/>). Les masses moléculaires ont été prédites avec l'outil compute pi/Mw ([http://web.expasy.org/compute\\_pi/](http://web.expasy.org/compute_pi/)). La présence de sites potentiel de phosphorylation et glycosylation ont été étudiés avec les outils NetPhos 2.0 (<http://www.cbs.dtu.dk/services/NetPhos/>) et NetOGlyc 4.0 (<http://www.cbs.dtu.dk/services/NetOGlyc/>) respectivement.

### 3 Résultats

#### Clonage et séquençage

Les régions codantes des deux protéines ont été séquencées et traduites *in silico*. Ces séquences correspondent aux séquences protéiques obtenues précédemment par RNAseq et sont disponibles sur le site UNIPROT KB (PLAAOx : réf X5CW8 ; CSAP : réf X5DCM8)

```
>tr|X5DCM8|X5DCM8_9EUKA Cocolith scale associated protein 1 (Fragment)
OS=Tisochrysis lutea PE=2 SV=1
MLSISTQIILAQTPLGTTTCGAVKTFKENECCAPNQLGKELPMADGICPSVDLQISYPAKVGIIYTPCPSEEVVYE
FLDDNPVAPGYKGCVAEAGFDPCGWSDYYSYDAASGCSTDAASLTAIQTIRGGSPMSADMLRLTGEDFLPTITF
PMMPMSYPNVGSNPDDSEMQLDVTWTKFVIGYMGSGLDLSDFEQYPTYGAEQGMVLSVATKVLEMARTTCNRNFY
AFLEAPAYGYDWTQAVAWVDSRASSFYEDESCSCFAAGTCKSAGIVTISQRGWAPEMPLPAMPFAEADNGMMYQPN
STDANSPWFQTNVPIGNPIGRFGPCHTPRERCLCDGVYWPYVGFVAPDHTLSDIKCYSWAFSITKIYSARMRAGIM
FVMDTPDAASAARSMVGGALSANGLYSHMQIQGQMLMNMKIMEKPFSDATSWLHAMAMAQYKWDVMYDAFSTC
QAAGIARITPEQPKYFGAYIFSYPYLLPDYQGLAVNVGGSSSDFFLAVVGYNHFNYNWGWGREDPMNYGNGIDPSKV
TVQDFTRTHLFRGLVAYQEEARMKLVCGDLARATPSTLTVNEWVALRQADRRRRRRRLEDGPISSHARALEVQE
VAPRMKLLINALKFAMETDPRKLEWEYGMPRDMADVQ
```

```
>tr|X5CW8|X5CW8_9EUKA PLAAOx OS=Tisochrysis lutea PE=2 SV=1
MIRLALALTLVNAARAATSTCGELREAFLSGECNAADETPVAFGEMLPPPPSSPPALMPPPPSPSPTPSPT
VASPPPIPVPSNYTGCDITIAAGGAGGLYSAYRLAKDVGNGATICIFEADTRFGGRIYSIRGMGPMGDTVLDMG
GYRTFDTISPRTQFLITERLGLSLGCDPISCLGKVIIVDGEENRIGFVTFLEKMLEEITELGVRYFPGHAVTSLE
RAGEDYLVNVAALPFPIAASRVILAVPQYPLQQILRASPTVEVGDDLYTAIHSLQPVHAVKFFLYYEDAWWITKL
GLEEGGFTAEGNAVSPPLEGRYHDGDIKCNADKTSCHGWLQTYFWDGRTQNYFARFQKSRDSPVTMMSEISD
GAKAIADVHAKVLQYHNLSPQEVPPPIEGALVTWNLATPFANTGWHYWDATKVNLDLQQLSDQRLHLVNEAFSA
TPSWAEGAILMADTMIEDLFGIPPHDVPDYLARNYISETWADAPQSAGFPDICENTCTRIDTGEFPFPGFVNGA
CNDGGEGSSVIQVCEYGTDCADCGPRSMAGGPGGAVAEDPACFLGNARLLLADDSRIPISEAKVGMRVKSSFGVG
TITEVLKHPHIDYVRRFRRLPTEHGHVLTLDHPIFVDGRWLEAGEAHREGHLPKMQVEYEIVDYFVNLEVDGSAA
EGESHAYDVNGVTVSGLDNPRNLAIYQRQNAFKATPAAVAMSDSPVLSDAKLETRGITSGATTVHIAAVFTPV
LDLNTPPHNMKRCPAWDHIADGSQTCGSKVQWMMNAYRYDIERAMLAVSQRFRCASCRIPTNAPATAPMSMPMPR
SITLSESNATSRRRIQAGSCTVESLCPSPSPPTSDTSCDDAICGGEDDECDEYLCGDDVDECDEYLCGDDVDEC
DEYLCGDDGDCDAALCDPEPPLVVVAHPPSPSPNAEVSPPTAPAPKVESSPPAPVDIEAAAASRSLLPVILPV
LLIAAVLLVAGLGAFFYLLKTHKAGSISVKSAAAVKAVDTPKADAPSTSGGDARVANSV
```

#### Analyses de séquence protéique

La CSAP est une protéine de 637 acides aminés et sa masse moléculaire est estimée à 70.7 kDa. Aucun domaine transmembranaire ni peptide signal n'a été détecté dans la séquence protéique de cette protéine suggérant une vraisemblable localisation dans le cytoplasme de la cellule. Un domaine pyridoxal décarboxylase s'étend sur 541 acides aminés. Ce domaine contient un domaine décarboxylases de type II (**Figure 54**) caractérisé par le motif suivant : S-[LIVMFYW]-x-{KG}-x(3)-K-[LIVMFYWG]-[LIVMFYWG]-x-{R}-x-[LIVMFYW]-{V}-[CA]-x(2)-[LIVMFYWQ]-{K}-x-[RK] (Sandmeier et al., 1994). Ce motif confère un rôle potentiel de décarboxylation des acides aminés, et plus spécifiquement des résidus tyrosine, histidine ou glutamate. Enfin, 39 sites potentiels de phosphorylation et 3 sites potentiels de glycosylation ont été identifiés chez cette protéine.

La PLAAOx est une protéine de 1033 acides aminés pour un poids moléculaire de 110.5 kDa. De même que pour la CSAP, une seule protéine de type amino-acid oxydase a été détectée dans le protéome de *T. lutea*. Cette protéine comprend en plus du domaine « amino-acide-oxydase », un domaine de liaison au coenzyme NAD (nicotinamide adénine dinucléotide) de type Rossmann retrouvé chez la plupart des déshydrogénases et un domaine Hedgehog/intein de la superfamille Hint (**Figure 54**). Les domaines Hedgehog/intein sont impliqués dans les régulations post-traductionnelles des protéines. Ces domaines permettent l'épissage et la maturation des protéines (Perler, 1998), mécanismes sont encore très mal connus chez les microalgues. La détection d'un peptide signal (site de clivage prédit entre les positions 18 et 19) suggère que cette protéine est acheminée *via* le système endomembranaire de sécrétion de la cellule. Cette protéine contient un domaine transmembranaire en amont de la région C-terminale. Selon les prédictions, la grande région N-terminal en amont du domaine transmembranaire serait apparemment externe. Néanmoins, nous n'avons aucun indice pouvant indiquer précisément la localisation finale de cette protéine. Sa localisation dans le périplasma reste encore hypothétique. De plus, la présence d'un domaine Hedgehog/intein entre le domaine catalytique et le domaine transmembranaire suggère la possibilité de localisations alternatives en fonction des modifications post-traductionnelles. D'autre part, 60 sites potentiels de phosphorylation et 25 sites potentiels de glycosylation ont été identifiés chez cette protéine.

### Recherche de protéines orthologues

Quatre protéines orthologues à la CSAP de *T. lutea* ont été identifiées. Ces protéines sont toutes issues de microalgues : trois d'entre elles sont présentes chez les haptophytes *Chrysochromulina sp.*, *Pleurochrysis carterae*, et *E. huxleyi* et la dernière a été identifiée chez la diatomée *P. tricornutum* (Tableau 4). La présence de cette protéine chez une diatomée indique que la CSAP n'est pas spécifique aux haptophytes. En revanche, aucun paralogue n'a été identifié dans le génome de *T. lutea* indiquant l'appartenance du gène à une famille mono-génique chez *T. lutea*.

**Tableau 4** Identité et similarité des protéines homologues à La CSAP de *T. lutea*.

| Espèce       | <i>E. huxleyi</i>       | <i>Chrysochromulina sp.</i> | <i>Chrysochrysis carteri</i> | <i>P. tricornutum</i>   |
|--------------|-------------------------|-----------------------------|------------------------------|-------------------------|
| Orthologue   | Unnamed protein product | CSAP1                       | CSAP1                        | Unnamed protein product |
| Identité     | 39%                     | 50%                         | 36%                          | 34%                     |
| similarité   | 55%                     | 75%                         | 60%                          | 59%                     |
| Recouvrement | 971                     | 728                         | 712                          | 592                     |

Concernant la protéine PLAAOx, 5 protéines orthologues ont été identifiées : 2 présentes chez les haptophytes *Chrysochromulina sp.* et *E. huxleyi* ; 1 identifiée chez la Chromerida *Vitrella brassicaformis*, 1 identifiée chez la diatomée *P. tricornutum* et la dernière présente chez la chlorophycée *C. reinhardtii* (Tableau 5).

**Tableau 5 Identité et similarité des protéines homologues de la PLAAOx de *T. lutea*.**

| Espèce       | <i>E. huxleyi</i>    | <i>Chrysochromulina sp.</i>      | <i>V. brassicaformis</i> | <i>C. reinhardtii</i> | <i>P. tricornutum</i>   |
|--------------|----------------------|----------------------------------|--------------------------|-----------------------|-------------------------|
| Orthologue   | L amino acid oxydase | Periplasmic L amino acid oxidase | Unnamed protein product  | LAO1                  | Unnamed protein product |
| Identité     | 54%                  | 53%                              | 33.8%                    | 32.5%                 | 36.0%                   |
| similarité   | 74%                  | 76%                              | 59%                      | 60%                   | 60%                     |
| Recouvrement | 809                  | 496                              | 485                      | 461                   | 683                     |

### Structures génomiques

Les séquences codant les deux protéines ont été alignées sur les séquences génomiques pour étudier la structure des gènes. Le gène de la CSAP est constitué de trois exons de 298, 717 et 899 paires de bases séparés par deux introns de 76 et 84 paires de bases (**Figure 55**). Concernant le gène de la PLAAOx, celui-ci est constitué de deux exons de 774 et 2 328 paires de bases séparés par un seul intron de 124 paires de bases (**Figure 55**).

De manière intéressante, les deux gènes ont été identifiés sur le même « scaffold » (n°1920 ; 15 323 paires de bases) localisé sur le génome nucléaire de *T. lutea*. Le gène codant la CSAP est situé en position 2 692 – 4 763 et le gène codant la PLAAOx en position 5 147 – 8 372. Ces deux gènes sont voisins et orientés en sens opposé (**Figure 55**). La présence de régions non séquencées dans la région intergénique empêche cependant de définir la distance exacte séparant ces deux gènes.

Chez *E. huxleyi*, les orthologues à ces deux gènes sont également co-localisés sur le scaffold 247 de la version V1.0 (positions 121 552-123 444 pour la CSAP et 125 371-127 110 pour la PLAAOx) du génome et donc séparés par 1 927 paires de bases. Une localisation génomique similaire a été montrée chez la diatomée *P. tricornutum*. Les gènes orthologues de la CSAP et de la PLAAOx sont également co-localisés sur le chromosome 21 (positions 1 430 002-146 480 pour la CSAP et 147 314-15 014 pour la PLAAOx) et séparés de 834 paires de bases.



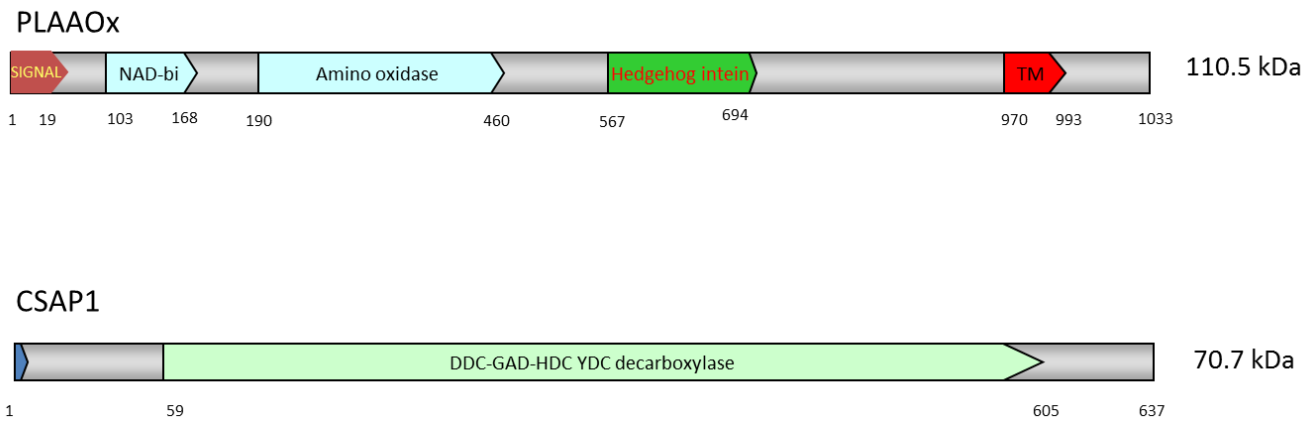


Figure 54 Structure primaire des protéines PLAAOx et CSAP1 de *T. lutea*.

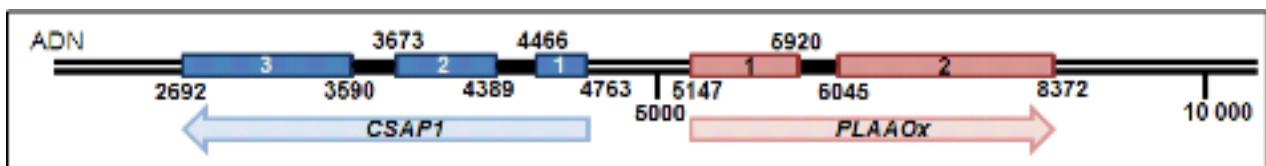
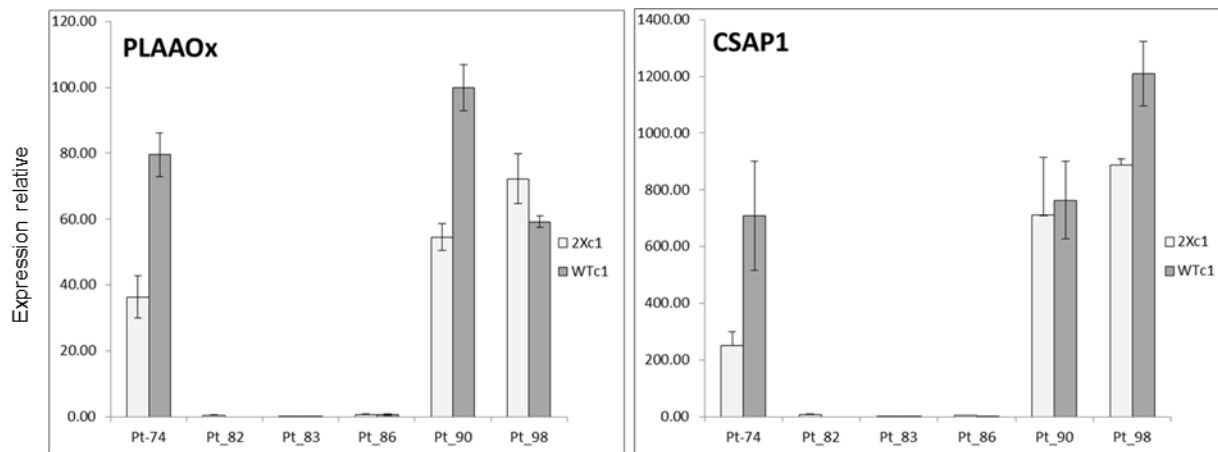


Figure 55 Représentation schématique du scaffold 1920 du génome de *T. lutea*.

Les exons ainsi que leurs positions relatives sur le scaffold sont représentés en bleu pour le gène CSAP1, en rouge pour le gène PLAAOx et les introns en noir. Les flèches indiquent l'orientation des gènes sur le scaffold. La barre verte indique une partie non séquencée du scaffold.



**Figure 56** Cinétique d'expression relative des gènes PLAAOx et CSAP1 après injection d'azote.

L'expression des deux gènes a été mesurée par RT-qPCR et normalisée avec l'expression du gène GAPDH.

### Régulation transcriptionnelle

Les mesures d'expression relative ont donné des résultats similaires avec les gènes de référence GAPDH et EF1. Les résultats d'expression par rapport à la GAPDH sont présentés sur la **Figure 56**. Ces résultats montrent que lors de la phase d'équilibre, en condition d'azote limitant (Pt-74), les deux gènes sont deux à trois fois moins exprimés dans la souche 2Xc1 que dans la souche WTc1. Des résultats identiques non présentés ont été obtenus pour les trois prélèvements à l'équilibre présentés dans le précédent chapitre (Pt-27, Pt-74 et Pt 117). Ces résultats suggèrent ainsi que les différences d'abondance protéiques observées dans ces conditions physiologiques sont dues à des différences d'expression des gènes et donc à des différences de régulation au niveau transcriptionnel. Ces deux gènes n'ayant pas été sélectionnés sur la base des résultats RNAseq, ces résultats confirment ainsi la meilleure sensibilité des approches ciblées par RT-qPCR pour mesurer l'expression génique de gènes cibles.

Enfin, les résultats présentés sur la **Figure 56** montrent également que les deux gènes sont totalement inhibés en absence de limitation azotée (N réplétion : Pt82, Pt83 et Pt 86) et cela pour les deux souches WTc1 et 2Xc1. En revanche, dès que l'azote est de nouveau limitant (N déplétion : Pt90 et Pt96) les deux gènes sont à nouveau exprimés. Ces résultats montrent ainsi une très forte corrélation entre la limitation azotée et l'expression de ces deux gènes. Ils suggèrent également des mécanismes de co-régulation des protéines au niveau transcriptionnel.

## 4 Discussion

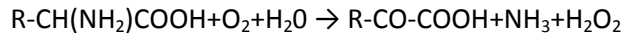
PLAAOx et CSAP sont deux protéines fortement accumulées lors de la carence azotée chez *T. lutea* WT et dans cette étude, nous avons montré que les gènes codant ces deux protéines étaient exprimés en azote limitant et fortement réprimés dès lors que du nitrate est ajouté dans le milieu. Les mécanismes de signalisations impliqués dans cette régulation sont à ce jour inconnu. Deux études récentes montrent que chez *C. reinhardtii*, LAO1, protéine homologue à la PLAAOx, est surexprimée et sur-accumulée lors d'une carence azotée (Aksoy et al., 2014; Wase et al., 2014). Chez la diatomée *P. tricornutum*, Valenzuela et al ont montré la surexpression d'une protéine homologue à la CSAP lors d'une carence azotée (Valenzuela et al., 2012). A notre connaissance, aucune étude ne fait mention de la régulation concomitante par l'azote de ces deux protéines. Par ailleurs, des tests d'activité de dégradation des acides aminés extracellulaires réalisés sur des cellules de *P. tricornutum* ont montré que l'activité amino-oxidase était inhibée en présence d'azote minérale (Rees and Allison, 2006). En supposant que cette activité de dégradation résulte en partie de l'activité d'une protéine homologue à la PLAAOx, alors ces deux protéines pourraient également être régulées par la disponibilité en azote chez *P. tricornutum*.

Chez *T. lutea*, la structuration des gènes au sein d'un même îlot génomique ainsi que la co-régulation par l'azote des deux gènes suggèrent également la présence d'un promoteur bidirectionnel situé entre les deux gènes inversement orientés. Chez les mammifères et les plantes, environ 11 % des gènes sont bi-directionnellement appariés et co-régulés par des promoteurs bidirectionnels (Trinklein et al., 2004; Wang et al., 2009a). Les gènes co-régulés ont généralement des fonctions liées l'une à l'autre (Adachi and Lieber, 2002) et des promoteurs bidirectionnels co-régulant des gènes impliqués dans concentration du carbone ont été identifiés chez la microalgue *C. reinhardtii* (Brueggeman et al., 2012). Les informations chez les microalgues restent cependant très parcellaires à ce jour. Or, nous avons montré que la synténie des deux gènes était conservée chez l'haptophyte *E. huxleyi* mais aussi chez la diatomée *P. tricornutum*. Ceci laisse à penser que ces gènes sont vraisemblablement co-régulés dans ces différents *phyla* de microalgues et que les deux protéines codées puissent avoir des rôles métaboliques complémentaires. L'étude des régions intergéniques sera une des voies à privilégier pour étudier les mécanismes de régulation par l'azote de ces deux gènes.

Les analyses sur gel d'électrophorèse bidimensionnelle (Garnier et al., 2014) indiquent que ces deux protéines subissent de nombreuses modifications post traductionnelles dont le rôle dans l'activité des protéines est à ce jour inconnu. La CSAP migre à environ 140kDa sur les gels alors que la taille estimée lors de cette étude est de 70.7kDa. De la même manière, la PLAAOx migre à une taille supérieure à celle calculée. La taille des protéines estimée sur gel 2-DE est difficile à estimer précisément, notamment pour des protéines de grande taille comme la PLAAOx et la CSAP. Mais dans tous les cas, cette inadéquation entre taille théorique et taille estimée sur gel 2-DE suggère que ces protéines forment des complexes, soit avec elle-même pour former des dimères, soit avec d'autres protéines partenaires. D'autre part, les trains de spots observés pour chacune des protéines suggèrent que ces protéines subissent des phosphorylations ou glycosylations. Or, les résultats d'analyses *in silico* dénotent la présence de nombreux sites potentiels de phosphorylation et glycosylation. Cependant, les outils de prédiction utilisés ne tiennent pas compte de la structure tridimensionnelle des protéines et surestiment donc le nombre de sites accessibles aux kinases, phosphatases et enzymes de glycosylation. L'utilisation de marqueurs spécifiques de protéines phosphorylées ou glycosylées pourra à l'avenir permettre d'identifier les types de modifications post-traductionnelles observées sur gels 2-DE.

Enfin, les analyses *in silico* suggèrent que ces deux protéines sont vraisemblablement toutes deux impliquées dans la dégradation des acides aminés. La PLAAOx intervient vraisemblablement dans la désamination par oxydation et la CSAP dans la décarboxylation. Les L-amino-acid-oxydases sont des

enzymes ubiquistes qui catalysent la désamination oxydative des acides aminés (L) et produisent l'  $\alpha$ -cétoacide correspondant, du peroxyde d'hydrogène et de l'ammonium, ceci selon la réaction suivante :



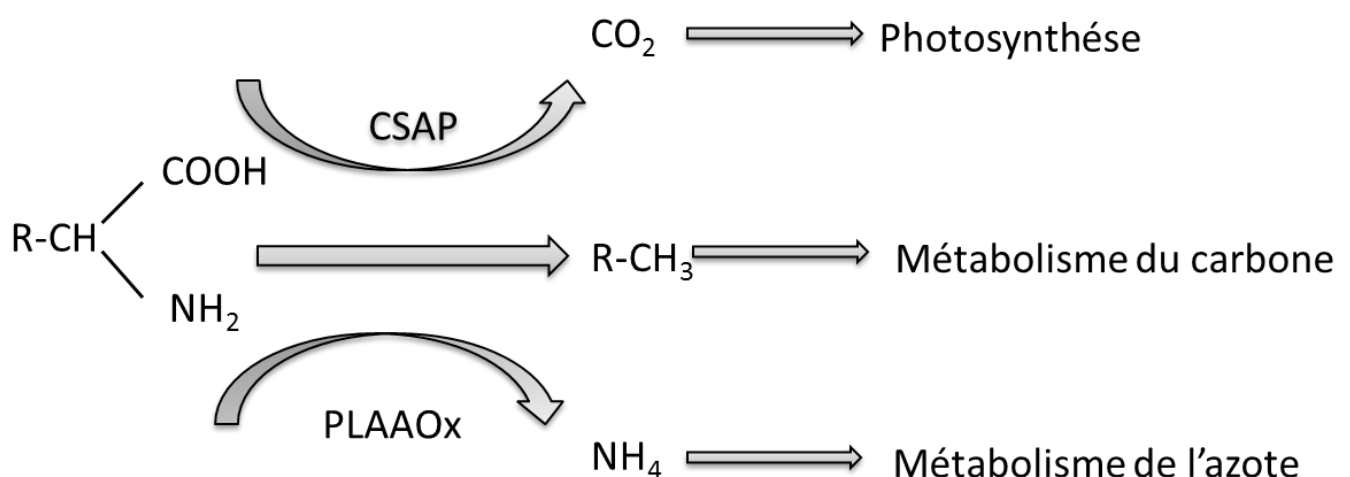
Ces enzymes peuvent être localisées à l'intérieur des cellules, sécrétées ou ancrées à la membrane externe des cellules. Elles interviennent dans la reminéralisation de l'azote mais également dans les interactions entre organismes (lire pour revue (Hossain et al., 2014)). Chez *T. lutea*, lors de la limitation azotée, nous suggérons que la PLAAOx intervient principalement dans la remise à disposition d'ammonium pour pallier à raréfaction de l'azote minérale. La localisation cellulaire de la PLAAOx et la nature des acides aminés oxydés restent encore incertaines. Nous proposons les deux hypothèses suivantes :

La présence d'un peptide signal et d'un domaine transmembranaire à l'extrémité C-terminal de la séquence protéique de la PLAAOx suggère que cette protéine pourrait être transportée *via* le réticulum endoplasmique jusqu'à la surface des cellules et intervenir dans l'oxydation des acides aminés extracellulaires. Plusieurs études montrent que les microalgues sont capables d'oxyder les acides aminés extracellulaires et d'utiliser l'ammonium généré pour leur croissance (Palenik and Morel, 1990b; Pantoja and Lee, 1994; Mulholland et al., 2003; Stoecker and Gustafson, 2003; Hellio et al., 2004; Rees and Allison, 2006). En 1991, les travaux de Palenik et Morel montrent que l'apport d'acides aminés à une culture de *T. lutea* induit la production extracellulaire de peroxyde d'hydrogène ( $\text{H}_2\text{O}_2$ ), coproduit de l'oxydation des acides aminés par les amino-oxydases. De ce fait, les auteurs suggèrent la présence chez cette espèce d' amino-oxydases en périphérie des cellules (Palenik and Morel, 1991). Aucune autre amino-oxidase n'ayant été identifiée chez *T. lutea*, nous suggérons ainsi que la PLAAOx est vraisemblablement responsable de cette activité enzymatique détectée à la surface des cellules.

La seconde hypothèse est que la PLAAOx pourrait agir également à l'intérieur de la cellule et intervenir dans la remobilisation de l'azote intracellulaire lors de la limitation azotée. Chez *T. lutea* et chez la plupart des microalgues, la carence azotée induit une réallocation globale de l'azote au sein de la cellule et notamment un changement global du protéome (Garnier et al., 2014). Ceci implique l'activation d'une activité protéolytique pour dégrader les protéines non essentielles. Wase et al suggèrent que la suraccumulation de la protéine LAO1 chez *C. reinhardtii* permet la désamination des acides aminés générés par la protéolyse (Wase et al., 2014). Selon ces auteurs, l'ammonium généré serait ensuite transporté vers le chloroplaste et assimilé pour produire du glutamate et alimenter lors

de la carence azotée la synthèse de protéines essentielles. D'autre part, selon Lee et al. (2012) et Wase et al. (2014), la désamination par oxydation des acides aminés permettrait de remettre à disposition de la cellule des métabolites carbonés métabolisables et utilisables pour la synthèse de sucres et de lipides, et de l'ammonium pour la synthèse de glutamate dans le chloroplaste. La désamination finale du glutamate en cétooglutarate, métabolite clé du cycle de Krebs et du cycle du glyoxylate, permettrait d'alimenter les voies de biosynthèse des lipides et des sucres. Cette dernière hypothèse est étayée par la co-régulation de la CSAP, protéine vraisemblablement cytoplasmique, et dont l'activité potentielle de décarboxylation des acides aminés pourrait agir de concert avec la désamination par la PLAAOx. L'activité concomitante de la CSAP et de la PLAAOx permettrait donc la remobilisation du carbone pour la synthèse de sucres et de lipides, et de l'azote pour la production de composés azotés indispensables lors de la limitation azotée (**Figure 57**). Le couple PLAAOx –CSAP pourrait donc être une clé métabolique dans la remobilisation de l'azote et du carbone lors de la limitation azotée.

Pour conclure, nous suggérons que la poursuite des travaux sur ces deux protéines permettra de mieux comprendre les interactions entre le métabolisme azoté et le métabolisme du carbone chez les haptophytes et chez les diatomées.



**Figure 57** Hypothèse d'action conjointe de la CSAP et de la PLAAOx dans la remobilisation des acides aminés vers le métabolisme du carbone et de l'azote.

Conclusions générales et perspectives.





## Conclusions générales et perspectives.

### Des transporteurs d'azote identifiés

L'identification des différents transporteurs d'azote à haute affinité et leur caractérisation a permis de mieux comprendre comment les haptophytes s'adaptent aux variations de concentration en azote minéral dans le milieu. Nous avons montré que chez les haptophytes, les transporteurs à haute affinité nitrate/nitrite contiennent une boucle extra-membranaire spécifique qui pourrait être impliquée dans la liaison au substrat en remplacement de la protéine NAR2. Nos résultats d'analyse d'expression suggèrent des rôles différents en fonction des quatre transporteurs identifiés. Le premier (TiNRT2.2) assurerait l'absorption de l'azote dans toutes les conditions azotées. Deux autres transporteurs (TiNRT2.1 et TiNRT2.3) seraient mis à contribution pour l'absorption lors de la raréfaction de l'azote et leur expression semble régulée par l'intermédiaire des métabolites azotés intracellulaires provenant de la voie d'assimilation du nitrate. Le dernier transporteur (TiNRT2.4) présente un profil d'expression tout à fait original et pourrait être impliqué dans le stockage de l'azote dans la vacuole lorsque les concentrations d'azote minéral dans le milieu sont élevées.

### Vers la caractérisation fonctionnelle des transporteurs

Les travaux futurs consisteront à identifier le rôle spécifique de chacun des 4 transporteurs dans l'absorption et le stockage de l'azote. Des anticorps spécifiques à chacun de ces 4 protéines ont été produits et leur spécificité doit être validée sur des protéines TiNRTs en cours de production en système bactérien. Ces anticorps seront utilisés pour étudier l'expression des transporteurs au niveau protéique par Western Blot et valider les résultats d'expression génique obtenus précédemment. Le rôle des transporteurs est intimement lié à leur localisation cellulaire et nous avons émis l'hypothèse que TiNRT2.4 pourrait être impliqué dans le stockage de l'azote dans les vacuoles. Les anticorps seront donc utilisés pour localiser les protéines à l'intérieur des cellules par immunolocalisation. Des protocoles d'immunohistologie par marquage des anticorps à l'or et utilisés avec succès chez *C. reinhardtii* seront être testés pour localiser les transporteurs sur des coupes histologiques (Vallon et al., 1993; Morita et al., 1997). Enfin, ces anticorps pourront permettre d'identifier d'éventuels partenaires de fonction similaire à Nar2, protéine non identifiée chez *T. lutea*. Des expériences de co-immunoprécipitation couplées à de l'identification par spectrométrie de masse de partenaires seront alors réalisées. Par ailleurs, les protéines complètes et les protéines tronquées (*i.e.* comprenant exclusivement la boucle extra-membranaire) seront exprimées en

Conclusions générales et perspectives.

système hétérologue déficient en protéine NAR2 (œufs de xénope). De telles stratégies ont été utilisées avec succès pour caractériser les partenaires des transporteurs NRT2 chez les plantes (Kotur et al., 2012). Ceci permettra ainsi de valider la fonctionnalité de TiNRTs et de caractériser le rôle fonctionnel des boucles additionnelles spécifiques des haptophytes.

### **Les voies métaboliques principales : avancées et perspectives**

L'annotation fonctionnelle de données génomiques et protéomiques obtenues au cours de nos travaux a permis, entre autre, d'identifier la plupart des enzymes du métabolisme du carbone et de les positionner dans un réseau métabolique central. Un travail similaire sur les voies métaboliques de l'azote, initié lors de cette thèse devra être poursuivi. Si la plus grande partie des enzymes du métabolisme central du carbone a été identifiée, plusieurs enzymes impliquées dans la synthèse des TAGs n'ont cependant pas été détectées dans le protéome de *T. lutea*. Ceci suggère l'existence de voies métaboliques centrales encore inconnues et qui doivent mettre à contribution des enzymes de fonction non déterminée. Ce réseau a néanmoins permis d'étudier l'orientation métabolique du carbone chez la souche mutante hyper lipidique et sera employé dans de futurs travaux pour étudier l'impact de caractères biotiques et abiotiques sur l'allocation du carbone. Des travaux de modélisation des réseaux métaboliques sont d'ores et déjà en cours dans notre laboratoire en collaboration avec des laboratoires de l'INRIA. Ils permettront de mieux prédire l'impact des facteurs abiotiques tels que la limitation nutritive et la lumière sur l'orientation du carbone chez *T. lutea*.

Cependant, une des limites du réseau métabolique présenté dans ce travail est qu'il n'intègre pas la compartimentation des réactions. Or, il est admis que la localisation cellulaire des réactions enzymatiques peut varier fortement d'une espèce à l'autre (Moriyama et al., 2014). L'interprétation des données reste donc à prendre avec précaution, surtout lorsqu'il s'agit de réactions pouvant intervenir dans différents compartiments de la cellule. Les outils de prédiction *in silico* de localisation cellulaire mis en place pour d'autres *phyla* de microalgues sont mal adaptés pour les haptophytes (Tardif et al., 2012). Des expériences de fractionnement cellulaires couplés à des identifications par spectrométrie de masse des protéines spécifiques à chaque organelle pourraient permettre d'identifier les motifs d'adressage chez *T. lutea* et de mettre en place des outils d'annotation fonctionnelle de localisation pour mieux décrire la compartimentation des réactions enzymatiques et donc les voies métaboliques de cette espèce.

## Limitation azotée et orientation métabolique

Dans ce travail de thèse, différentes approches de génomique fonctionnelle ont été appliquées pour identifier les mécanismes impliqués dans la limitation azotée et dans la suraccumulation lipidique d'une souche mutante. Les souches de microalgues ont été cultivées dans différents modes de culture pour atteindre différentes conditions écophysologiques. Dans un premier temps, l'étude de l'impact de la carence azotée sur les protéomes des souches mutantes et sauvage montre que : 1) Les mécanismes impliqués dans la carence azotée chez les haptophytes sont globalement similaires aux autres phyla de microalgues (baisse de la fixation du carbone et de la synthèse de composés azotés, réorientation du carbone et de l'azote intracellulaire); 2) La suraccumulation lipidique chez la souche mutante est le fait d'un métabolisme impacté en amont de la synthèse lipidique, au niveau du catabolisme des sucres et au niveau de métabolisme central du carbone; 3) La carence azotée induit des différences de régulation protéiques entre les deux souches. D'autre part, l'étude dynamique de la limitation azotée dans les cultures en chemostat et l'analyse protéomique haut débit lors de la limitation azotée montrent que : 1) La souche mutante est plus sensible aux variations de limitation azotée, vraisemblablement sous l'effet de mécanismes de signalisation calcique ; 2) La suraccumulation des lipides de réserve chez la souche mutante lors de la limitation azotée est liée à une réorientation globale du métabolisme du carbone incluant une augmentation de l'abondance des enzymes intervenant dans la fixation du carbone, et une baisse de l'abondance des enzymes impliquées dans l'activité mitochondriale, le cycle du glyoxylate et le catabolisme lipidique. Or les analyses biochimiques montrent que le catabolisme lipidique est très rapidement activé dès lors que l'azote ne limite plus la croissance. La suraccumulation des lipides chez la souche mutante semble donc être le fruit d'une dérégulation de l'activité catabolique des lipides en lien avec la disponibilité en azote. Des analyses protéomiques en dynamique devront être envisagées sur les échantillons prélevés suite à l'injection d'azote pour étudier l'allocation du carbone à différents stades de limitation et notamment lors du catabolisme des lipides. Des mesures d'activité cellulaires (activité photosynthétique, activité mitochondriale, activité lipase) et des mesures d'activité enzymatique de protéines différenciellement accumulées telle que la malate synthase, impliquée dans le cycle du glyoxylate, permettront de valider les hypothèses basées sur les estimations d'abondance protéiques relatives. Par ailleurs, l'étude des mécanismes de signalisation calciques constitue également un champ de recherche encore inexploré chez les haptophytes et d'intérêt pour comprendre l'impact de ce type de signalisation dans le métabolisme azoté des microalgues.

## Les niveaux de régulation

L'ensemble des résultats transcriptomiques et protéomiques laisse à penser que la réponse à la limitation azotée et la suraccumulation de lipides de réserve chez la souche mutante impliquent des mécanismes de signalisation et de régulation qui agissent à différents niveaux. L'absence de corrélation entre analyses RNAseq et analyses protéomiques haut débit suggère des régulations post-transcriptionnelles et traductionnelles différentes entre les deux souches. Ces régulations post-transcriptionnelles et traductionnelles, non étudiées jusqu'à présent chez les haptophytes, peuvent faire intervenir différents mécanismes : les « riboswitchs », les interactions ARN – protéines, les ARNs interférents, le recrutement polysomal, les cinétiques de traduction et la disponibilité en ARNs de transferts. Les travaux sur les petits ARN interférents (ou siRNA pour small interfering RNA) et micro ARN (ou miRNA) de microalgues sont relativement récents et montrent, notamment chez la diatomée *P. tricornutum* une très grande variété de petits ARNs non codants qui agissent à différents niveaux : épigénétique et régulation post-transcriptionnelle (Cerutti et al., 2011 ; De Riso et al., 2009; Riso et al., 2009; Norden-Krichmar et al., 2011; Rogato et al., 2014). L'identification de petits ARNs non codants chez *T. lutea* pourra être entreprise par séquençage haut débit des petits ARNs et analyses bio-informatiques comme précédemment chez les diatomées (Norden-Krichmar et al., 2011; Rogato et al., 2014). Des études d'expression en fonction de la limitation azotée permettront d'initier des travaux originaux sur les régulations post-transcriptionnelles mis en place lors de la limitation azotée. D'autre part, les analyses protéomiques suggèrent que le greffage des acides aminés sur les ARNs de transferts est fortement impacté chez la souche hyper-lipidique S2M2. Des régulations, au niveau traductionnel, pourraient donc être impliquées dans les différences protéomiques observées entre la souche mutante et la souche sauvage. Afin d'étudier la régulation traductionnelle chez *T. lutea*, nous proposons de séquencer les ARNs messagers en cours de traduction après purification des fractions polysomales. Ces approches, couramment utilisées chez différents modèles animaux et plantes n'ont, à notre connaissance, jamais été appliquées chez les microalgues.

## Limitation azotée et métabolisme du carbone : Clés métaboliques

Deux protéines ont été sélectionnées pour leur potentiel rôle clé dans le lien entre métabolisme de l'azote et du carbone : CSAP et PLAAOx. Ces deux protéines, co-régulées chez *T. lutea*, sont très abondantes lors de la limitation azotée. Les gènes codant ces deux protéines sont co-localisés et inversement orientés sur les génomes des haptophytes *T. lutea* et *E. huxleyi* mais aussi chez la diatomée *P. tricornutum*. Nous suspectons alors la présence d'un promoteur bidirectionnel situé entre les deux gènes pour les différents *phyla*. De nombreux travaux sont encore nécessaires pour

## Conclusions générales et perspectives.

bien comprendre le rôle et la régulation de ces protéines. Très récemment, nous avons clonés chacun des deux gènes dans un vecteur d'expression et des tests de production ont été initiés. La surexpression et la purification de ces protéines permettra d'étudier l'activité amino-acid oxydase et décarboxylase de la PLAAOx et de la CSAP respectivement. A l'instar de travaux antérieurs sur les amino-oxydases, (Piedras et al., 1992; Yu et al., 2013) et décarboxylases (Médici et al., 2011), nous testerons les activités enzymatiques des deux protéines sur différents acides aminés. Des analyses structurales pourront, dans un second temps, être initiées après cristallisation des protéines pour mieux comprendre les interactions entre enzymes et substrats, les partenaires et les cofacteurs. La production en cours d'anticorps polyclonaux permettra d'envisager l'étude de la localisation subcellulaire de ces protéines par immunohistologie, et l'identification de potentiels partenaires par co-immunoprécipitation. En absence d'outils génétiques chez les haptophytes, l'inactivation des gènes orthologues à ces deux protéines pourra être envisagée *in vivo* chez *P. tricornutum* par des nouvelles techniques d'extinction de gènes pour mieux comprendre le rôle métabolique de ces deux protéines (De Riso et al., 2009; Weyman et al., 2015).

### Perspectives

D'une manière générale, l'interprétation des nombreuses données obtenues lors de ce travail est limitée par un manque cruel de connaissances sur la fonction de la plus grande majorité des gènes et protéines identifiés et parfois différentiellement exprimés en fonction des souches et des conditions écophysologiques. La connaissance des activités protéiques, chez *T. lutea* comme chez la plupart des espèces, est basée sur des homologies de séquence avec des protéines caractérisées auparavant chez des espèces modèles. Chez *T. lutea*, plus de la moitié de gènes n'ont aucune homologie de séquence avec les gènes connus et les fonctions des gènes identifiés sont généralement très spéculatives dès lors qu'il ne s'agit pas de protéines fortement conservées et/ou impliquées dans le métabolisme central. Ces problèmes sont habituellement rencontrés pour l'ensemble des espèces dites non modèles et pour lesquelles l'explosion des données de séquençage fournit une quantité colossale de données « poubelles » par manque de connaissances fonctionnelles. Nous proposons trois stratégies complémentaires pour pallier à ce problème

1 Les réseaux de gènes et les réseaux métaboliques: Les gènes co-régulés étant souvent fonctionnellement liés entre eux, nous proposons de multiplier les analyses protéomiques et transcriptomiques dans des conditions physiologiques différentes. L'étude des réseaux de gènes permettront de préciser plus clairement la fonction de certaines protéines. Par ailleurs, la construction et la modélisation de réseaux métaboliques permettra également d'identifier les

Conclusions générales et perspectives.

enzymes indispensables (encore non identifiées actuellement) à la production de métabolites identifiés chez l'espèce étudiée.

2 Les approches *in vivo*. A ce jour, *T. lutea* n'a jamais été transformée génétiquement et l'absence d'outils génétiques limite fortement les possibilités d'exploration fonctionnelle des gènes de cette espèce. Les seuls moyens de validation de fonction *in vivo* consistent à envisager des approches génétiques chez la diatomée *P. tricornutum* qui est génétiquement transformable et pour laquelle de nombreux outils génétiques existent déjà (système CRISPR/Cas9 par exemple). Ces approches sont certes prometteuses pour des gènes conservés mais restent encore limitées pour étudier les voies métaboliques spécifiques aux haptophytes. Une première publication de 2014 présente des résultats encourageant de transformation génétique de l'haptophyte *Isochrysis galbana* par *Agrobacterium tumefaciens* (Prasad et al., 2014). Très récemment, une souche de *Pleurochrysis carterae* a également été transformée par transformation chimique en présence de polyéthylène glycol (Endo et al., 2016). Les outils présentés dans ces publications seront testés chez *T. lutea*.

3 Les approches biochimiques : Enfin l'étude fonctionnelle des protéines par des approches ciblées *in vitro* (études enzymatiques, recherche de partenaires, analyses de structures tridimensionnelles, régulations post-traductionnelles etc.) et *in vivo* (immuno-localisation, fractionnement cellulaire etc.) présente un levier de recherche considérable pour l'exploitation des données « omic » chez les microalgues.

## Bilan

Finalement, cette thèse contribue à une meilleure connaissance du métabolisme des haptophytes non coccolithophores, microalgues impliquées de façon considérable dans les cycles biogéochimiques des océans. L'espèce modèle de ce travail est *Tisochrysis lutea*, microalgue traditionnellement cultivée dans les écloséries et nurseries aquacoles et au potentiel biotechnologique avéré. Enfin, ce travail apporte des informations moléculaires d'intérêt pour de nombreux domaines de recherche et permet d'éclaircir les connaissances sur les mécanismes d'absorption de l'azote chez les haptophytes, sur les mécanismes d'adaptation à la limitation azotée, et les mécanismes d'allocation du carbone.

## BIBLIOGRAPHIE.

## Bibliographie

- Adachi N, Lieber MR** (2002) Bidirectional Gene Organization: A Common Architectural Feature of the Human Genome. *Cell* **109**: 807–809
- Aksoy M, Pootakham W, Grossman AR** (2014) Critical Function of a *Chlamydomonas reinhardtii* Putative Polyphosphate Polymerase Subunit during Nutrient Deprivation. *Plant Cell* **26**: 4214–4229
- Alipanah L, Rohloff J, Winge P, Bones AM, Brembu T** (2015) Whole-cell response to nitrogen deprivation in the diatom *Phaeodactylum tricornutum*. *J Exp Bot* **erv340**
- Alkhamis Y, Qin JG** (2013) Cultivation of *Isochrysis galbana* in Phototrophic, Heterotrophic, and Mixotrophic Conditions. *BioMed Res Int* **2013**: e983465
- Allen AE, Dupont CL, Oborník M, Horák A, Nunes-Nesi A, McCrow JP, Zheng H, Johnson DA, Hu H, Fernie AR, et al** (2011) Evolution and metabolic significance of the urea cycle in photosynthetic diatoms. *Nature* **473**: 203–207
- Andersen RA** (2004) Biology and systematics of heterokont and haptophyte algae. *Am J Bot* **91**: 1508–1522
- Archibald JM** (2007) Nucleomorph genomes: structure, function, origin and evolution. *BioEssays* **29**: 392–402
- Archibald JM** (2012) The Evolution of Algae by Secondary and Tertiary Endosymbiosis. *Adv. Bot. Res.* Elsevier, pp 87–118
- Beardall J, Young E, Roberts S** (2001) Approaches for determining phytoplankton nutrient limitation. *Aquat Sci* **63**: 44–69
- Bendif EM** (2011) De la macroevolution à la microévolution chez le phytoplancton : Le cas des isochrysidales. phdthesis. Paris 6
- Bendif EM, Probert I, Schroeder DC, Vargas C de** (2013) On the description of *Tisochrysis lutea* gen. nov. *sp. nov.* and *Isochrysis nuda* *sp. nov.* in the Isochrysidales, and the transfer of Dicrateria to the Prymnesiales (Haptophyta). *J Appl Phycol* **25**: 1763–1776
- Blaby IK, Glaesener AG, Mettler T, Fitz-Gibbon ST, Gallaher SD, Liu B, Boyle NR, Kropat J, Stitt M, Johnson S, et al** (2013) Systems-level analysis of nitrogen starvation-induced modifications of carbon metabolism in a *Chlamydomonas reinhardtii* starchless mutant. *Plant Cell* **25**: 4305–4323
- Bonin P, Groisillier A, Raimbault A, Guibert A, Boyen C, Tonon T** (2015) Molecular and biochemical characterization of mannitol-1-phosphate dehydrogenase from the model brown alga *Ectocarpus sp.* *Phytochemistry* **117**: 509–520
- Bougaran G, Bernard O, Sciandra A** (2010) Modeling continuous cultures of microalgae colimited by nitrogen and phosphorus. *J Theor Biol* **265**: 443–454



- Bougaran G, Le Déan L, Lukomska E, Kaas R, Baron R** (2003) Transient initial phase in continuous culture of *Isochrysis galbana* affinis Tahiti. *Aquat Living Resour* **16**: 389–394
- Bougaran G, Rouxel C, Dubois N, Kaas R, Grouas S, Lukomska E, Le Coz J-R, Cadoret J-P** (2012) Enhancement of neutral lipid productivity in the microalga *Isochrysis affinis Galbana* (T-Iso) by a mutation-selection procedure. *Biotechnol Bioeng* **109**: 2737–2745
- Bowler C, Allen AE, Badger JH, Grimwood J, Jabbari K, Kuo A, Maheswari U, Martens C, Maumus F, Otilar RP, et al** (2008) The *Phaeodactylum* genome reveals the evolutionary history of diatom genomes. *Nature* **456**: 239–244
- Bowler C, Vardi A, Allen AE** (2010) Oceanographic and Biogeochemical Insights from Diatom Genomes. *Annu Rev Mar Sci* **2**: 333–365
- Boyd PW, Strzepek R, Fu F, Hutchins DA** (2010) Environmental control of open-ocean phytoplankton groups: Now and in the future. *Limnol Oceanogr* **55**: 1353–1376
- Boyle N, Casero D, Hong-Hermesdorf A, Kropat J, Liu B, Karpowicz S, Benning C, Pellegrini M, Merchant SS** (2011) Temporal transcriptomics of *Chlamydomonas reinhardtii* during triacylglycerol accumulation. *Abstr. Pap. Am. Chem. Soc.* 241:
- Boyle NR, Page MD, Liu B, Blaby IK, Casero D, Kropat J, Cokus SJ, Hong-Hermesdorf A, Shaw J, Karpowicz SJ, et al** (2012) Three acyltransferases and nitrogen-responsive regulator are implicated in nitrogen starvation-induced triacylglycerol accumulation in *Chlamydomonas*. *J Biol Chem* **287**: 15811–15825
- Browning TJ, Bouman HA, Moore CM, Schlosser C, Tarran GA, Woodward EMS, Henderson GM** (2014) Nutrient regimes control phytoplankton ecophysiology in the South Atlantic. *Biogeosciences* **11**: 463–479
- Brownlee C, Wheeler GL, Taylor AR** (2015) Coccolithophore biomineralization: New questions, new answers. *Semin Cell Dev Biol* **46**: 11–16
- Brown NR, Noble ME, Endicott JA, Johnson LN** (1999) The structural basis for specificity of substrate and recruitment peptides for cyclin-dependent kinases. *Nat Cell Biol* **1**: 438–443
- Brueggeman AJ, Gangadharaiah DS, Cserhati MF, Casero D, Weeks DP, Ladunga I** (2012) Activation of the Carbon Concentrating Mechanism by CO<sub>2</sub> Deprivation Coincides with Massive Transcriptional Restructuring in *Chlamydomonas reinhardtii*. *Plant Cell* **24**: 1860–1875
- Busi MV, Barchiesi J, Martín M, Gomez-Casati DF** (2014) Starch metabolism in green algae. *Starch - Stärke* **66**: 28–40
- Cadoret J-P, Bougaran G, Bérard J-B, Carrier G, Charrier A, Coulombier N, Garnier M, Kaas R, Le Déan L, Lukomska E, et al** (2014) Microalgae and Biotechnology. *In* A Monaco, P Prouzet, eds, *Dev. Mar. Resour.* John Wiley & Sons, Inc., pp 57–115
- Cadoret J-P, Garnier M, Saint-Jean B** (2012) Chapter Eight - Microalgae, Functional Genomics and Biotechnology. *In* Gwenaël Piganeau, ed, *Adv. Bot. Res.* Academic Press, pp 285–341

- Candido TDS, Gonçalves RD, Felício AP, Freitas FZ, Cupertino FB, Carvalho ACGVD, Bertolini MC** (2014) A protein kinase screen of *Neurospora crassa* mutant strains reveals that the SNF1 protein kinase promotes glycogen synthase phosphorylation. *Biochem J* **464**: 323–334
- Carrier G, Garnier M, Le Cunff L, Bougaran G, Probert I, De Vargas C, Corre E, Cadoret J-P, Saint-Jean B** (2014) Comparative Transcriptome of Wild Type and Selected Strains of the Microalgae *Tisochrysis lutea* Provides Insights into the Genetic Basis, Lipid Metabolism and the Life Cycle. *PLoS ONE* **9**: e86889
- Cavalier-Smith T** (2002) The phagotrophic origin of eukaryotes and phylogenetic classification of Protozoa. *Int J Syst Evol Microbiol* **52**: 297–354
- Cerutti H, Ma X, Msanne J, Repas T** (2011) RNA-Mediated Silencing in Algae: Biological Roles and Tools for Analysis of Gene Function. *Eukaryot Cell* **10**: 1164–1172
- Charrier A, Bérard J-B, Bougaran G, Carrier G, Lukomska E, Schreiber N, Fournier F, Charrier AF, Rouxel C, Garnier M, et al** (2015) High-affinity nitrate/nitrite transporter genes (Nrt2) in *Tisochrysis lutea*: identification and expression analyses reveal some interesting specificities of Haptophyta microalgae. *Physiol Plant*. doi: 10.1111/ppl.12330
- Chen H, Hu J, Qiao Y, Chen W, Rong J, Zhang Y, He C, Wang Q** (2015) Ca<sup>2+</sup>-regulated cyclic electron flow supplies ATP for nitrogen starvation-induced lipid biosynthesis in green alga. *Sci Rep* **5**: 15117
- Chen H, Zhang Y, He C, Wang Q** (2014) Ca<sup>2+</sup> Signal Transduction Related to Neutral Lipid Synthesis in an Oil-Producing Green Alga *Chlorella sp. C2*. *Plant Cell Physiol* **55**: 634–644
- Chopin F, Orsel M, Dorbe M-F, Chardon F, Truong H-N, Miller AJ, Krapp A, Daniel-Vedele F** (2007) The *Arabidopsis* ATNRT2.7 Nitrate Transporter Controls Nitrate Content in Seeds. *Plant Cell* **19**: 1590–1602
- Curtis BA, Tanifuji G, Burki F, Gruber A, Irimia M, Maruyama S, Arias MC, Ball SG, Gile GH, Hirakawa Y, et al** (2012) Algal genomes reveal evolutionary mosaicism and the fate of nucleomorphs. *Nature*. doi: 10.1038/nature11681
- Das AK, Helps NR, Cohen PT, Barford D** (1996) Crystal structure of the protein serine/threonine phosphatase 2C at 2.0 Å resolution. *EMBO J* **15**: 6798–6809
- von Dassow P, Ogata H, Probert I, Wincker P, Da Silva C, Audic S, Claverie J, de Vargas C** (2009) Transcriptome analysis of functional differentiation between haploid and diploid cells of *Emiliana huxleyi*, a globally significant photosynthetic calcifying cell. *GENOME Biol*. doi: 10.1186/gb-2009-10-10-r114
- Davey M, Tarran GA, Mills MM, Ridame C, Geider RJ, LaRoche J** (2008) Nutrient limitation of picophytoplankton photosynthesis and growth in the tropical North Atlantic. *Limnol Oceanogr* **53**: 1722–1733
- Davidi L, Katz A, Pick U** (2012) Characterization of major lipid droplet proteins from *Dunaliella*. *Planta*. doi: 10.1007/s00425-011-1585-7
- Delwiche CF** (1999) Tracing the Thread of Plastid Diversity through the Tapestry of Life. *Am Nat* **154**: S164–S177

- De Riso V, Raniello R, Maumus F, Rogato A, Bowler C, Falciatore A** (2009) Gene silencing in the marine diatom *Phaeodactylum tricornutum*. *Nucleic Acids Res* **37**: e96
- Dittami SM, Aas HTN, Paulsen BS, Boyen C, Edvardsen B, Tonon T** (2011) Mannitol in six autotrophic stramenopiles and Micromonas. *Plant Signal Behav* **6**: 1237–1239
- Dolch L-J, Maréchal E** (2015) Inventory of Fatty Acid Desaturases in the Pennate Diatom *Phaeodactylum tricornutum*. *Mar Drugs* **13**: 1317–1339
- Doll S, Burlingame AL** (2015) Mass spectrometry-based detection and assignment of protein posttranslational modifications. *ACS Chem Biol* **10**: 63–71
- Dong H-P, Williams E, Wang D, Xie Z-X, Hsia R, Jenck A, Halden R, Li J, Chen F, Place AR** (2013) Responses of *Nannochloropsis oceanica* IMET1 to Long-Term Nitrogen Starvation and Recovery. *Plant Physiol* **162**: 1110–1126
- Droop M** (1985) Vitamin-B12 and Marine Ecology .4. the Kinetics of Uptake, Growth and Inhibition in Monochrysis-Lutheri. *Curr ContentsAgriculture Biol Environ Sci* 16–16
- Droop MR** (1968) Vitamin B12 and Marine Ecology. IV. The Kinetics of Uptake, Growth and Inhibition in Monochrysis Lutheri. *J Mar Biol Assoc U K* **48**: 689–733
- Dunahay T, Jarvis E, Dais S, Roessler P** (1996) Manipulation of microalgal lipid production using genetic engineering. *Appl Biochem Biotechnol* **57-8**: 223–231
- Dyhrman ST, Jenkins BD, Ryneanson TA, Saito MA, Mercier ML, Alexander H, Whitney LP, Drzewianowski A, Bulygin VV, Bertrand EM, et al** (2012) The Transcriptome and Proteome of the Diatom *Oceanica pseudonana* Reveal a Diverse Phosphorus Stress Response. *PLoS ONE* **7**: e33768
- Eglinton TI, Eglinton G** (2008) Molecular proxies for paleoclimatology. *Earth Planet Sci Lett* **275**: 1–16
- Eltgroth ML, Watwood RL, Wolfe GV** (2005) Production and cellular localization of neutral long chain lipids in the haptophyte algae *Isochrysis galbana* and *Emiliana huxleyi*. *J Phycol* **41**: 1000–1009
- Endo H, Yoshida M, Uji T, Saga N, Inoue K, Nagasawa H** (2016) Stable Nuclear Transformation System for the Coccolithophorid Alga *Pleurochrysis carterae*. *Sci Rep* **6**: 22252
- Fan J, Andre C, Xu C** (2011) A chloroplast pathway for the de novo biosynthesis of triacylglycerol in *Chlamydomonas reinhardtii*. *FEBS Lett*. doi: doi: 10.1016/j.febslet.2011.05.018
- Fan J, Yan C, Andre C, Shanklin J, Schwender J, Xu C** (2012) Oil accumulation is controlled by carbon precursor supply for fatty acid synthesis in *Chlamydomonas reinhardtii*. *Plant Cell Physiol* **53**: 1380–1390
- Feng D, Chen Z, Xue S, Zhang W** (2011) Increased lipid production of the marine oleaginous microalgae *Isochrysis zhangjiangensis* (Chrysoophyta) by nitrogen supplement. *Bioresour Technol* **102**: 6710–6716
- Fernandez E, Galvan A** (2008) Nitrate Assimilation in *Chlamydomonas*. *Eukaryot Cell* **7**: 555–559

- Ferreira M, Maseda A, Fabregas J, Otero A** (2008) Enriching rotifers with “premium” microalgae. *Isochrysis* aff. *galbana* clone T-ISO. *Aquaculture* **279**: 126–130
- Field CB, Behrenfeld MJ, Randerson JT, Falkowski P** (1998) Primary production of the biosphere: integrating terrestrial and oceanic components. *Science* **281**: 237–240
- Finazzi G, Moreau H, Bowler C** (2010) Genomic insights into photosynthesis in eukaryotic phytoplankton. *Trends Plant Sci* **15**: 565–572
- Flynn K, Garrido J, Zapata M, Öpik H, Hipkin C** (1992) Changes in fatty acids, amino acids and carbon/nitrogen biomass during nitrogen starvation of ammonium- and nitrate-grown *Isochrysis galbana*. *J Appl Phycol* **4**: 95–104
- Forde BG** (2000) Nitrate transporters in plants: structure, function and regulation. *Biochim Biophys Acta BBA - Biomembr* **1465**: 219–235
- Fradique M, Batista AP, Cristiana Nunes M, Gouveia L, Bandarra NM, Raymundo A** (2013) *Isochrysis galbana* and *Diacronema vlikianum* biomass incorporation in pasta products as PUFA's source. *Lwt-Food Sci Technol* **50**: 312–319
- Frandsen GI, Mundy J, Tzen JTC** (2001) Oil bodies and their associated proteins, oleosin and caleosin. *Physiol Plant* **112**: 301–307
- Galvan A, Fernández E** (2001) Eukaryotic nitrate and nitrite transporters. *Cell Mol Life Sci CMLS* **58**: 225–233
- Gao C, Wang Y, Shen Y, Yan D, He X, Dai J, Wu Q** (2014) Oil accumulation mechanisms of the oleaginous microalga *Chlorella protothecoides* revealed through its genome, transcriptomes, and proteomes. *BMC Genomics* **15**: 582
- Gargouri M, Park J-J, Holguin FO, Kim M-J, Wang H, Deshpande RR, Shachar-Hill Y, Hicks LM, Gang DR** (2015) Identification of regulatory network hubs that control lipid metabolism in *Chlamydomonas reinhardtii*. *J Exp Bot* **66**: 4551–4566
- Garnier M, Carrier G, Rogniaux H, Nicolau E, Bougaran G, Saint-Jean B, Cadoret JP** (2014) Comparative proteomics reveals proteins impacted by nitrogen deprivation in wild-type and high lipid-accumulating mutant strains of *Tisochrysis lutea*. *J Proteomics* **105**: 107–120
- Ge F, Huang W, Chen Z, Zhang C, Xiong Q, Bowler C, Yang J, Xu J, Hu H** (2014) Methylcrotonyl-CoA Carboxylase Regulates Triacylglycerol Accumulation in the Model Diatom *Phaeodactylum tricornutum*. *Plant Cell Online tpc.114.124982*
- Geider RJ, Delucia EH, Falkowski PG, Finzi AC, Grime JP, Kana TM, La Roche J, Long SP, Osborne BA, Platt T, et al** (2001) Primary productivity of planet earth: biological determinants and physical constraints in terrestrial and aquatic habitats. *Glob. Change Biol.* **7**:
- Goepfert T** *Isochrysis* sp. and *Phaeodactylum tricornutum* lipid characterization and physiology studies.
- Gonzalez-Ballester D, Camargo A, Fernandez E** (2004) Ammonium transporter genes in *Chlamydomonas*: the nitrate-specific regulatory gene Nit2 is involved in Amt1;1 expression. *Plant Mol Biol* **56**: 863–878

- Goodson C, Roth R, Wang ZT, Goodenough U** (2011) Structural Correlates of Cytoplasmic and Chloroplast Lipid Body Synthesis in *Chlamydomonas reinhardtii* and Stimulation of Lipid Body Production with Acetate Boost. *Eukaryot Cell* **10**: 1592–1606
- Gouveia L, Coutinho C, Mendonça E, Batista AP, Sousa I, Bandarra NM, Raymundo A** (2008) Functional biscuits with PUFA- $\omega$ 3 from *Isochrysis galbana*. *J Sci Food Agric* **88**: 891–896
- Groisillier A, Shao Z, Michel G, Goulitquer S, Bonin P, Krahulec S, Nidetzky B, Duan D, Boyen C, Tonon T** (2014) Mannitol metabolism in brown algae involves a new phosphatase family. *J Exp Bot* **65**: 559–570
- Guiheneuf F, Stengel DB** (2013) LC-PUFA-Enriched Oil Production by Microalgae: Accumulation of Lipid and Triacylglycerols Containing n-3 LC-PUFA Is Triggered by Nitrogen Limitation and Inorganic Carbon Availability in the Marine Haptophyte *Pavlova lutheri*. *Mar Drugs* **11**: 4246–4266
- Guiry MD** (2012) How Many Species of Algae Are There? *J Phycol* **48**: 1057–1063
- Guo B, Jiang M, Wan X, Gong Y, Liang Z, Hu C** (2013) Identification and Heterologous Expression of a Delta 4-Fatty Acid Desaturase Gene from *Isochrysis sphaerica*. *J Microbiol Biotechnol* **23**: 1413–1421
- Guschina IA, Harwood JL** (2006) Lipids and lipid metabolism in eukaryotic algae. *Prog Lipid Res* **45**: 160–186
- Halligan BD** (2009) ProMoST: A tool for calculating the pI and molecular mass of phosphorylated and modified proteins on 2 dimensional gels. *Methods Mol Biol Clifton NJ* **527**: 283–ix
- Hayashi Y, Sato N, Shinozaki A, Watanabe M** (2015) Increase in peroxisome number and the gene expression of putative glyoxysomal enzymes in *Chlamydomonas* cells supplemented with acetate. *J Plant Res* **128**: 177–185
- Hellio C, Veron B, Le Gal Y** (2004) Amino acid utilization by *Chlamydomonas reinhardtii*: specific study of histidine. *Plant Physiol Biochem* **42**: 257–264
- Hemaiswarya S, Raja R, Ravi Kumar R, Ganesan V, Anbazhagan C** (2011) Microalgae: a sustainable feed source for aquaculture. *World J Microbiol Biotechnol* **27**: 1737–1746
- Hildebrand M, Dahlin K** (2000) Nitrate transporter genes from the diatom *Cylindrotheca fusiformis* (Bacillariophyceae): mRNA levels controlled by nitrogen source and by the cell cycle. *J Phycol* **36**: 702–713
- Hossain GS, Li J, Shin H, Du G, Liu L, Chen J** (2014) L-Amino acid oxidases from microbial sources: types, properties, functions, and applications. *Appl Microbiol Biotechnol* **98**: 1507–1515
- Hovde BT, Deodato CR, Hunsperger HM, Ryken SA, Yost W, Jha RK, Patterson J, Jr RJM, Barlow SB, Starkenburg SR, et al** (2015) Genome Sequence and Transcriptome Analyses of *Chrysochromulina tobin*: Metabolic Tools for Enhanced Algal Fitness in the Prominent Order Prymnesiales (Haptophyceae). *PLOS Genet* **11**: e1005469

- Huerlimann R, Steinig EJ, Loxton H, Zenger KR, Jerry DR, Heimann K** (2014a) Effects of growth phase and nitrogen starvation on expression of fatty acid desaturases and fatty acid composition of *Isochrysis aff. galbana* (TISO). *Gene*. doi: 10.1016/j.gene.2014.05.009
- Huerlimann R, Steinig EJ, Loxton H, Zenger KR, Jerry DR, Heimann K** (2014b) The effect of nitrogen limitation on acetyl-CoA carboxylase expression and fatty acid content in *Chromera velia* and *Isochrysis aff. galbana* (TISO). *Gene* **543**: 204–211
- Hu Q, Sommerfeld M, Jarvis E, Ghirardi M, Posewitz M, Seibert M, Darzins A** (2008) Microalgal triacylglycerols as feedstocks for biofuel production: perspectives and advances. *Plant J Cell Mol Biol* **54**: 621–639
- Ingolia NT, Ghaemmaghami S, Newman JRS, Weissman JS** (2009) Genome-Wide Analysis in Vivo of Translation with Nucleotide Resolution Using Ribosome Profiling. *Science* **324**: 218–223
- Jardillier L, Zubkov MV, Pearman J, Scanlan DJ** (2010) Significant CO<sub>2</sub> fixation by small prymnesiophytes in the subtropical and tropical northeast Atlantic Ocean. *Isme J* **4**: 1180–1192
- Johnson X, Alric J** (2012) Interaction between starch breakdown, acetate assimilation, and photosynthetic cyclic electron flow in *Chlamydomonas reinhardtii*. *J Biol Chem* **287**: 26445–26452
- Kaffes A, Thoms S, Trimborn S, Rost B, Langer G, Richter K-U, Koehler A, Norici A, Giordano M** (2010) Carbon and nitrogen fluxes in the marine coccolithophore *Emiliana huxleyi* grown under different nitrate concentrations. *J Exp Mar Biol Ecol* **393**: 1–8
- Kang L, Hwang S, Gong G, Lini H, Chen P, Chang J** (2007) Influences of nitrogen deficiency on the transcript levels of ammonium transporter, nitrate transporter and glutamine synthetase genes in *Isochrysis galbana* (Isochrysidales, Haptophyta). *PHYCOLOGIA* **46**: 521–533
- Kang L-K, Chang J** (2014) Sequence Diversity of Ammonium Transporter Genes in Cultured and Natural Species of Marine Phytoplankton. *J Mar Sci Technol-Taiwan* **22**: 89–96
- Keeling PJ** (2010) The endosymbiotic origin, diversification and fate of plastids. *Philos Trans R Soc B Biol Sci* **365**: 729–748
- Kernec F, Ünlü M, Labeikovskiy W, Minden JS, Koretsky AP** (2001) Changes in the mitochondrial proteome from mouse hearts deficient in creatine kinase. *Physiol Genomics* **6**: 117–128
- Khozin-Goldberg I, Cohen Z** (2011) Unraveling algal lipid metabolism: Recent advances in gene identification. *Biochimie* **93**: 91–100
- Klok AJ, Martens DE, Wijffels RH, Lamers PP** (2013) Simultaneous growth and neutral lipid accumulation in microalgae. *Bioresour Technol* **134**: 233–243
- Kotajima T, Shiraiwa Y, Suzuki I** (2014) Functional screening of a novel Delta 15 fatty acid desaturase from the coccolithophorid *Emiliana huxleyi*. *Biochim Biophys Acta-Mol Cell Biol Lipids* **1841**: 1451–1458

- Kotur Z, Mackenzie N, Ramesh S, Tyerman SD, Kaiser BN, Glass ADM** (2012) Nitrate transport capacity of the *Arabidopsis thaliana* NRT2 family members and their interactions with AtNAR2.1. *New Phytol* **194**: 724–731
- Kroth PG** (2008) A model for carbohydrate metabolism in the diatom *Phaeodactylum tricorutum* deduced from whole genome analysis and comparative genomic analyses with *Oceanica pseudonana* and other photoautotrophs. *PLoS One* **3**: e1426
- Lacour T, Sciandra A, Talec A, Mayzaud P, Bernard O** (2012) Neutral lipids and carbohydrate productivities as a response to nitrogen status in *Isochrysis* sp. (T-Iso, haptophyceae): Starvation versus limitation. *J Phycol* **48**: 647–656
- Lardon L, Hélias A, Sialve B, Steyer J-P, Bernard O** (2009) Life-Cycle Assessment of Biodiesel Production from Microalgae. *Environ Sci Technol* **43**: 6475–6481
- Lauersen KJ, Willamme R, Coosemans N, Joris M, Kruse O, Remacle C** (2016) Peroxisomal microbodies are at the crossroads of acetate assimilation in the green microalga *Chlamydomonas reinhardtii*. *Algal Res* **16**: 266–274
- Laws EA, Popp BN, Bidigare RR, Riebesell U, Burkhardt S, Wakeham SG** (2001) Controls on the molecular distribution and carbon isotopic composition of alkenones in certain haptophyte algae. *Geochem Geophys Geosystems* **2**: n/a–n/a
- Lee DY, Park J-J, Barupal DK, Fiehn O** (2012) System Response of Metabolic Networks in *Chlamydomonas reinhardtii* to Total Available Ammonium. *Mol Cell Proteomics* **11**: 973–988
- Lee J-M, Williams ME, Tingey SV, Rafalski JA** (2002) DNA array profiling of gene expression changes during maize embryo development. *Funct Integr Genomics* **2**: 13–27
- Li C, Yang G, Pan J, Zhang H** (2010a) Experimental studies on dimethylsulfide (DMS) and dimethylsulfoniopropionate (DMSP) production by four marine microalgae. *Acta Oceanol Sin* **29**: 78–87
- Li J, Han D, Wang D, Ning K, Jia J, Wei L, Jing X, Huang S, Chen J, Li Y, et al** (2014) Choreography of Transcriptomes and Lipidomes of *Nannochloropsis* Reveals the Mechanisms of Oil Synthesis in Microalgae. *Plant Cell Online tpc.113.121418*
- Li M, Ou X, Yang X, Guo D, Qian X, Xing L, Li M** (2012a) Cloning and identification of a novel C18-Delta 9 polyunsaturated fatty acid specific elongase gene from DHA-producing *Isochrysis galbana* H29. *Biotechnol Bioprocess Eng* **17**: 22–32
- Lin Y-H, Chang F-L, Tsao C-Y, Leu J-Y** (2007) Influence of growth phase and nutrient source on fatty acid composition of *Isochrysis galbana* CCMP 1324 in a batch photoreactor. *Biochem Eng J* **37**: 166–176
- Liu H, Probert I, Uitz J, Claustre H, Aris-Brosou S, Frada M, Not F, Vargas C de** (2009) Extreme diversity in noncalcifying haptophytes explains a major pigment paradox in open oceans. *Proc Natl Acad Sci* **106**: 12803–12808
- Li Y, Fei X, Deng X** (2012b) Novel molecular insights into nitrogen starvation-induced triacylglycerols accumulation revealed by differential gene expression analysis in green algae *Micractinium pusillum*. *Biomass Bioenergy* **42**: 199–211

- Li Y, Han D, Hu G, Dauvillee D, Sommerfeld M, Ball S, Hu Q** (2010b) *Chlamydomonas* starchless mutant defective in ADP-glucose pyrophosphorylase hyper-accumulates triacylglycerol. *Metab Eng* **12**: 387–391
- Lohr M, Schwender J, Polle JEW** (2012) Isoprenoid biosynthesis in eukaryotic phototrophs: A spotlight on algae. *Plant Sci* **185–186**: 9–22
- López García de Lomana A, Schäuble S, Valenzuela J, Imam S, Carter W, Bilgin DD, Yohn CB, Turkarslan S, Reiss DJ, Orellana MV, et al** (2015) Transcriptional program for nitrogen starvation-induced lipid accumulation in *Chlamydomonas reinhardtii*. *Biotechnol Biofuels* **8**: 207
- Lu Y, Chi X, Li Z, Yang Q, Li F, Liu S, Gan Q, Qin S** (2010) Isolation and characterization of a stress-dependent plastidial delta12 fatty acid desaturase from the Antarctic microalga *Chlorella vulgaris* NJ-7. *Lipids* **45**: 179–187
- Lu Y, Chi X, Yang Q, Li Z, Liu S, Gan Q, Qin S** (2009) Molecular cloning and stress-dependent expression of a gene encoding Delta(12)-fatty acid desaturase in the Antarctic microalga *Chlorella vulgaris* NJ-7. *Extrem Life Extreme Cond* **13**: 875–884
- Maeda Y, Sunaga Y, Yoshino T, Tanaka T** (2014) Oleosome-Associated Protein of the Oleaginous Diatom *Fistulifera solaris* Contains an Endoplasmic Reticulum-Targeting Signal Sequence. *Mar Drugs* **12**: 3892–3903
- Maier T, Güell M, Serrano L** (2009) Correlation of mRNA and protein in complex biological samples. *FEBS Lett* **583**: 3966–3973
- Mairet F, Bernard O, Masci P, Lacour T, Sciandra A** (2011) Modelling neutral lipid production by the microalga *Isochrysis* aff. *galbana* under nitrogen limitation. *Bioresour Technol* **102**: 142–149
- Marchetti J, Bougaran G, Jauffrais T, Lefebvre S, Rouxel C, Saint-Jean B, Lukomska E, Robert R, Cadoret JP** (2013) Effects of blue light on the biochemical composition and photosynthetic activity of *Isochrysis* sp. (T-iso). *J Appl Phycol* **25**: 109–119
- Martin M** (2011) Cutadapt removes adapter sequences from high-throughput sequencing reads. *EMBnet.journal* **17**: pp. 10–12
- Mausz MA, Pohnert G** (2015) Phenotypic diversity of diploid and haploid *Emiliania huxleyi* cells and of cells in different growth phases revealed by comparative metabolomics. *J Plant Physiol* **172**: 137–148
- McKew BA, Metodieva G, Raines CA, Metodiev MV, Geider RJ** (2015) Acclimation of *Emiliania huxleyi* (1516) to nutrient limitation involves precise modification of the proteome to scavenge alternative sources of N and P. *Environ Microbiol* **17**: 4050–4062
- Médici R, de María PD, Otten LG, Straathof AJJ** (2011) A High-Throughput Screening Assay for Amino Acid Decarboxylase Activity. *Adv Synth Catal* **353**: 2369–2376
- Medlin LK, Sáez AG, Young JR** (2008) A molecular clock for coccolithophores and implications for selectivity of phytoplankton extinctions across the K/T boundary. *Mar Micropaleontol* **67**: 69–86



- Meireles LA, Guedes AC, Malcata FX** (2003) Lipid class composition of the microalga *Pavlova lutheri*: eicosapentaenoic and docosahexaenoic acids. *J Agric Food Chem* **51**: 2237–2241
- Merchant SS, Kropat J, Liu B, Shaw J, Warakanont J** (2011) TAG, You're it! *Chlamydomonas* as a reference organism for understanding algal triacylglycerol accumulation. *Curr Opin Biotechnol*. doi: 10.1016/j.copbio.2011.12.001
- Michel G, Tonon T, Scornet D, Cock JM, Kloareg B** (2010) Central and storage carbon metabolism of the brown alga *Ectocarpus siliculosus*: insights into the origin and evolution of storage carbohydrates in Eukaryotes. *New Phytol* **188**: 67–81
- Miller R, Wu G, Deshpande R, Vieler A, Gartner K, Li X, Moellering E, Zauner S, Cornish A, Liu B, et al** (2010) Changes in Transcript Abundance in *Chlamydomonas reinhardtii* following Nitrogen Deprivation Predict Diversion of Metabolism. *PLANT Physiol* **154**: 1737–1752
- Milliman JD** (1993) Production and accumulation of calcium carbonate in the ocean: Budget of a nonsteady state. *Glob Biogeochem Cycles* **7**: 927–957
- Moellering E, Benning C** (2010) RNA Interference Silencing of a Major Lipid Droplet Protein Affects Lipid Droplet Size in *Chlamydomonas reinhardtii*. *Eukaryot CELL* **9**: 97–106
- Moellering ER, Miller R, Benning C** (2010) Molecular Genetics of Lipid Metabolism in the Model Green Alga *Chlamydomonas reinhardtii*. *Lipids Photosynth* 139–155
- Moore CM, Mills MM, Arrigo KR, Berman-Frank I, Bopp L, Boyd PW, Galbraith ED, Geider RJ, Guieu C, Jaccard SL, et al** (2013) Processes and patterns of oceanic nutrient limitation. *Nat Geosci* **6**: 701–710
- Moore TS, Du Z, Chen Z** (2001) Membrane lipid biosynthesis in *Chlamydomonas reinhardtii*. In vitro biosynthesis of diacylglyceryltrimethylhomoserine. *Plant Physiol* **125**: 423–429
- Morita E, Kuroiwa H, Kuroiwa T, Nozaki H** (1997) High localization of ribulose-1,5-bisphosphate carboxylase/oxygenase in the pyrenoids of *Chlamydomonas reinhardtii* (Chlorophyta), as revealed by cryofixation and immunogold electron microscopy. *J Phycol* **33**: 68–72
- Moriyama T, Sakurai K, Sekine K, Sato N** (2014) Subcellular distribution of central carbohydrate metabolism pathways in the red alga *Cyanidioschyzon merolae*. *Planta* **240**: 585–598
- Msanne J, Xu D, Konda AR, Casas-Mollano JA, Awada T, Cahoon EB, Cerutti H** (2012) Metabolic and gene expression changes triggered by nitrogen deprivation in the photoautotrophically grown microalgae *Chlamydomonas reinhardtii* and *Coccomyxa sp.* C-169. *Phytochemistry* **75**: 50–59
- Mühlroth A, Li K, Røkke G, Winge P, Olsen Y, Hohmann-Marriott MF, Vadstein O, Bones AM** (2013) Pathways of Lipid Metabolism in Marine Algae, Co-Expression Network, Bottlenecks and Candidate Genes for Enhanced Production of EPA and DHA in Species of Chromista. *Mar Drugs* **11**: 4662–4697
- Mulders KJM, Lamers PP, Martens DE, Wijffels RH** (2014) Phototrophic pigment production with microalgae: biological constraints and opportunities. *J Phycol* **50**: 229–242

- Mulholland MR, Gobler CJ, Lee C** (2002) Peptide hydrolysis, amino acid oxidation, and nitrogen uptake in communities seasonally dominated by *Aureococcus anophagefferens*. *Limnol Oceanogr* **47**: 1094–1108
- Mulholland MR, Lee C, Glibert PM** (2003) Extracellular enzyme activity and uptake of carbon and nitrogen along an estuarine salinity and nutrient gradient. *Mar Ecol-Prog Ser* **258**: 3–17
- Nalder TD, Miller MR, Packer MA** (2015) Changes in lipid class content and composition of *Isochrysis* sp. (T-Iso) grown in batch culture. *Aquac Int* **23**: 1293–1312
- Nguyen HM, Baudet M, Cuiné S, Adriano J-M, Barthe D, Billon E, Bruley C, Beisson F, Peltier G, Ferro M, et al** (2011) Proteomic profiling of oil bodies isolated from the unicellular green microalga *Chlamydomonas reinhardtii*: with focus on proteins involved in lipid metabolism. *Proteomics* **11**: 4266–4273
- Norden-Krichmar TM, Allen AE, Gaasterland T, Hildebrand M** (2011) Characterization of the small RNA transcriptome of the diatom, *Oceanica pseudonana*. *PLoS One* **6**: e22870
- O'Farrell PH** (1975) High resolution two-dimensional electrophoresis of proteins. *J Biol Chem* **250**: 4007–4021
- O'Hara P, Slabas AR, Fawcett T** (2002) Fatty acid and lipid biosynthetic genes are expressed at constant molar ratios but different absolute levels during embryogenesis. *Plant Physiol* **129**: 310–320
- Okauchi M** (1990) Food Value of *Isochrysis* aff *galbana* for the growth of pearl oyster Spat. *Nippon Suisan Gakkaishi* **56**: 1343–1343
- Paasche E** (2001) A review of the coccolithophorid *Emiliania huxleyi* (Prymnesiophyceae), with particular reference to growth, coccolith formation, and calcification-photosynthesis interactions. *Phycologia* **40**: 503–529
- Palenik B, Morel F** (1990a) Comparison of Cell-Surface L-Amino-Acid Oxidases from Several Marine-Phytoplankton. *Mar Ecol-Prog Ser* **59**: 195–201
- Palenik B, Morel F** (1991) Amine Oxidases of Marine-Phytoplankton. *Appl Environ Microbiol* **57**: 2440–2443
- Palenik B, Morel F** (1990b) Amino-Acid Utilization by Marine-Phytoplankton - a Novel Mechanism. *Limnol Oceanogr* **35**: 260–269
- Pantoja S, Lee C** (1994) Cell-surface oxidation of amino acids in seawater. *Limnol Oceanogr* **39**: 1718–1726
- Parkhill J-P, Maillet G, Cullen JJ** (2001) Fluorescence-Based Maximal Quantum Yield for Psii as a Diagnostic of Nutrient Stress. *J Phycol* **37**: 517–529
- Park J-J, Wang H, Gargouri M, Deshpande RR, Skepper JN, Holguin FO, Juergens MT, Shachar-Hill Y, Hicks LM, Gang DR** (2015) The response of *Chlamydomonas reinhardtii* to nitrogen deprivation: a systems biology analysis. *Plant J* **81**: 611–624

- Pereira SL, Leonard AE, Huang YS, Chuang LT, Mukerji P** (2004) Identification of two novel microalgal enzymes involved in the conversion of the omega 3-fatty acid, eicosapentaenoic acid, into docosahexaenoic acid. *Biochem J* **384**: 357–366
- Perez-Garcia O, Escalante FME, de-Bashan LE, Bashan Y** (2011) Heterotrophic cultures of microalgae: Metabolism and potential products. *Water Res* **45**: 11–36
- Perler FB** (1998) Protein Splicing of Inteins and Hedgehog Autoproteolysis: Structure, Function, and Evolution. *Cell* **92**: 1–4
- Petrie JR, Mackenzie AM, Shrestha P, Liu Q, Frampton DF, Robert SS, Singh SP** (2010) Isolation of three novel LC-PUFA  $\Delta 9$  elongases and the transgenic assembly of the entire Pavlova salina DHA pathway in *Nicotiana benthamiana*. *J Phycol* **46**: 917–925
- Piedras P, Pineda M, Muñoz J, Cárdenas J** (1992) Purification and characterization of an L-amino-acid oxidase from *Chlamydomonas reinhardtii*. *Planta* **188**: 13–18
- Prasad B, Vadakedath N, Jeong H-J, General T, Cho M-G, Lein W** (2014) Agrobacterium tumefaciens-mediated genetic transformation of haptophytes (*Isochrysis* species). *Appl Microbiol Biotechnol* **98**: 8629–8639
- Qi BX, Beaudoin F, Fraser T, Stobart AK, Napier JA, Lazarus CM** (2002) Identification of a cDNA encoding a novel C18-Delta(9) polyunsaturated fatty acid-specific elongating activity from the docosahexaenoic acid (DHA)-producing microalga, *Isochrysis galbana*. *FEBS Lett* **510**: 159–165
- Rabilloud T** (2002) Two-dimensional gel electrophoresis in proteomics: old, old fashioned, but it still climbs up the mountains. *Proteomics* **2**: 3–10
- Ramanan R, Kim B-H, Cho D-H, Ko S-R, Oh H-M, Kim H-S** (2013) Lipid droplet synthesis is limited by acetate availability in starchless mutant of *Chlamydomonas reinhardtii*. *FEBS Lett*. doi: 10.1016/j.febslet.2012.12.020
- Ramazanov A, Ramazanov Z** (2006) Isolation and characterization of a starchless mutant of *Chlorella pyrenoidosa* STL-PI with a high growth rate, and high protein and polyunsaturated fatty acid content. *Phycol Res* **54**: 255–259
- Read BA, Kegel J, Klute MJ, Kuo A, Lefebvre SC, Maumus F, Mayer C, Miller J, Monier A, Salamov A, et al** (2013) Pan genome of the phytoplankton *Emiliana* underpins its global distribution. *Nature* **499**: 209–213
- Rees TAV, Allison VJ** (2006) Evidence for an extracellular L-amino acid oxidase in nitrogen-deprived *Phaeodactylum tricornutum* (Bacillariophyceae) and inhibition of enzyme activity by dissolved inorganic carbon. *Phycologia* **45**: 337–342
- Reinfelder JR** (2011) Carbon Concentrating Mechanisms in Eukaryotic Marine Phytoplankton. *Annu Rev Mar Sci* **3**: 291 – 315
- Reinfelder JR, Kraepiel AM, Morel FM** (2000) Unicellular C4 photosynthesis in a marine diatom. *Nature* **407**: 996–999

- Reitan KI** (2011) Digestion of lipids and carbohydrates from microalgae (*Chaetoceros muelleri* Lemmermann and *Isochrysis* aff. *galbana* clone T-ISO) in juvenile scallops (*Pecten maximus* L.). *Aquac Res* **42**: 1530–1538
- Rexach J, Llamas A, Fernández E, Galván A** (2002) The activity of the high-affinity nitrate transport system I (NRT2;1, NAR2) is responsible for the efficient signalling of nitrate assimilation genes in *Chlamydomonas reinhardtii*. *Planta* **215**: 606–611
- Rieley G, Teece MA, Peakman TM, Raven AM, Greene KJ, Clarke TP, Murray M, Lettley JW, Campbell CN, Harris RP, et al** (1998) Long-chain alkenes of the haptophytes *Isochrysis galbana* and *Emiliana huxleyi*. *Lipids* **33**: 617–625
- Rismani-Yazdi H, Haznedaroglu BZ, Hsin C, Peccia J** (2012) Transcriptomic analysis of the oleaginous microalga *Neochloris oleoabundans* reveals metabolic insights into triacylglyceride accumulation. *Biotechnol Biofuels* **5**: 74
- Riso VD, Raniello R, Maumus F, Rogato A, Bowler C, Falciatore A** (2009) Gene silencing in the marine diatom *Phaeodactylum tricornutum*. *Nucleic Acids Res* **37**: e96–e96
- Rogato A, Richard H, Sarazin A, Voss B, Cheminant Navarro S, Champeimont R, Navarro L, Carbone A, Hess WR, Falciatore A** (2014) The diversity of small non-coding RNAs in the diatom *Phaeodactylum tricornutum*. *BMC Genomics* **15**: 698
- Rokitta SD, de Nooijer LJ, Trimborn S, de Vargas C, Rost B, John U** (2011) Transcriptome analyses reveal differential gene expression patterns between the life-cycle stages of *Emiliana huxleyi* (Haptophyta) and reflect specialization to different ecological niches. *J Phycol* **47**: 829–838
- Roleda MY, Slocombe SP, Leakey RJG, Day JG, Bell EM, Stanley MS** (2013) Effects of temperature and nutrient regimes on biomass and lipid production by six oleaginous microalgae in batch culture employing a two-phase cultivation strategy. *Bioresour Technol* **129**: 439–449
- Ruuska SA, Girke T, Benning C, Ohlrogge JB** (2002) Contrapuntal Networks of Gene Expression during *Arabidopsis* Seed Filling. *Plant Cell* **14**: 1191–1206
- Ryckebosch E, Bruneel C, Termote-Verhalle R, Goiris K, Muylaert K, Foubert I** (2014) Nutritional evaluation of microalgae oils rich in omega-3 long chain polyunsaturated fatty acids as an alternative for fish oil. *Food Chem* **160**: 393–400
- Sandmeier E, Hale TI, Christen P** (1994) Multiple evolutionary origin of pyridoxal-5'-phosphate-dependent amino acid decarboxylases. *Eur J Biochem FEBS* **221**: 997–1002
- Saoudihelis L, Dubacq J, Marty Y, Samain J, Gudin C** (1994) Influence of Growth-Rate on Pigment and Lipid-Composition of the Microalga *Isochrysis* Aff *Galbana* Clone T-Iso. *J Appl Phycol* **6**: 315–322
- Scanlan DJ, Ostrowski M, Mazard S, Dufresne A, Garczarek L, Hess WR, Post AF, Hagemann M, Paulsen I, Partensky F** (2009) Ecological Genomics of Marine Picocyanobacteria. *Microbiol Mol Biol Rev* **73**: 249–+
- Schmollinger S, Mühlhaus T, Boyle NR, Blaby IK, Casero D, Mettler T, Moseley JL, Kropat J, Sommer F, Strenkert D, et al** (2014) Nitrogen-Sparing Mechanisms in *Chlamydomonas* Affect the Transcriptome, the Proteome, and Photosynthetic Metabolism[W]. *Plant Cell* **26**: 1410–1435

- Sherr EB, Sherr BF** (2007) Heterotrophic dinoilagellates: a significant component of microzooplankton biomass and major grazers of diatoms in the sea. *Mar Ecol Prog Ser* **352**: 187–197
- Shifrin N, Chisholm S** (1981) Phytoplankton Lipids - Interspecific Differences and Effects of Nitrate, Silicate and Light-Dark Cycles. *J Phycol* **17**: 374–384
- Shiraiwa Y** (2003) Physiological regulation of carbon fixation in the photosynthesis and calcification of coccolithophorids. *Comp Biochem Physiol B Biochem Mol Biol* **136**: 775–783
- Shi T, Yu A, Li M, Ou X, Xing L, Li M** (2012) Identification of a novel C22-Delta 4-producing docosahexaenoic acid (DHA) specific polyunsaturated fatty acid desaturase gene from *Isochrysis galbana* and its expression in *Saccharomyces cerevisiae*. *Biotechnol Lett* **34**: 2265–2274
- Shtaida N, Khozin-Goldberg I, Solovchenko A, Chekanov K, Didi-Cohen S, Leu S, Cohen Z, Boussiba S** (2014) Downregulation of a putative plastid PDC E1 $\alpha$  subunit impairs photosynthetic activity and triacylglycerol accumulation in nitrogen-starved photoautotrophic *Chlamydomonas reinhardtii*. *J Exp Bot* **65**: 6563–6576
- Siaut M, Cuiné S, Cagnon C, Fessler B, Nguyen M, Carrier P, Beyly A, Beisson F, Triantaphylidès C, Li-Beisson Y, et al** (2011) Oil accumulation in the model green alga *Chlamydomonas reinhardtii*: characterization, variability between common laboratory strains and relationship with starch reserves. *BMC Biotechnol* **11**: 7
- Simionato D, Block MA, Rocca NL, Jouhet J, Maréchal E, Finazzi G, Morosinotto T** (2013) The Response of *Nannochloropsis gaditana* to Nitrogen Starvation Includes De Novo Biosynthesis of Triacylglycerols, a Decrease of Chloroplast Galactolipids, and Reorganization of the Photosynthetic Apparatus. *Eukaryot Cell* **12**: 665–676
- Slade R, Bauen A** (2013) Micro-algae cultivation for biofuels: Cost, energy balance, environmental impacts and future prospects. *Biomass Bioenergy* **53**: 29–38
- Solovchenko AE** (2012) Physiological role of neutral lipid accumulation in eukaryotic microalgae under stresses. *Russ J Plant Physiol* **59**: 167–176
- Song B, Ward BB** (2007) Molecular cloning and characterization of high-affinity nitrate transporters in marine phytoplankton. *J Phycol* **43**: 542–552
- Song P, Li L, Liu J** (2013) Proteomic Analysis in Nitrogen-Deprived *Isochrysis galbana* during Lipid Accumulation. *PLoS ONE* **8**: e82188
- Spoehr HA, Milner HW** (1949) The Chemical Composition of *Chlorella*; Effect of Environmental Conditions. *Plant Physiol* **24**: 120–149
- Stephenson PG, Moore CM, Terry MJ, Zubkov MV, Bibby TS** (2011) Improving photosynthesis for algal biofuels: toward a green revolution. *Trends Biotechnol* **29**: 615–623
- Stoecker D, Gustafson D** (2003) Cell-surface proteolytic activity of photosynthetic dinoflagellates. *Aquat Microb Ecol* **30**: 175–183

- Swift DG, Taylor WR** (1974) Growth of Vitamin B12-Limited Cultures: *Oceanica Pseudonana*, *monochrysis lutheri*, and *Isochrysis galbana*. *J Phycol* **10**: 385–391
- Tanaka R, Kikutani S, Mahardika A, Matsuda Y** (2014) Localization of enzymes relating to C4 organic acid metabolisms in the marine diatom, *Thalassiosira pseudonana*. *Photosynth Res* **121**: 251–263
- Tardif M, Atteia A, Specht M, Cogne G, Rolland N, Brugiere S, Hippler M, Ferro M, Bruley C, Peltier G, et al** (2012) PredAlgo: A New Subcellular Localization Prediction Tool Dedicated to Green Algae. *Mol Biol Evol* **29**: 3625–3639
- Thinh L** (1994) Potential Use of Aging Cultures of *Isochrysis Aff Galbana* (*Isochrysis* Tahitian, T-Iso) as Starter Cultures for Live Algal Food-Production in Tropical Aquaculture. *J Appl Phycol* **6**: 357–358
- Thiriet-Rupert S, Carrier G, Chénais B, Trottier C, Bougaran G, Cadoret J-P, Schoefs B, Saint-Jean B** (2016) Transcription factors in microalgae: genome-wide prediction and comparative analysis. *BMC Genomics* **17**: 282
- Tillmann U** (1998) Phagotrophy by a plastidic haptophyte, *Prymnesium patelliferum*. *Aquat Microb Ecol* **14**: 155–160
- Toney JL, Theroux S, Andersen RA, Coleman A, Amaral-Zettler L, Huang Y** (2012) Culturing of the first 37:4 predominant lacustrine haptophyte: Geochemical, biochemical, and genetic implications. *Geochim Cosmochim Acta* **78**: 51–64
- Tonon T, Harvey D, Qing R, Li Y, Larson TR, Graham IA** (2004) Identification of a fatty acid [Delta] 11-desaturase from the microalga *Oceanica pseudonana*1. *FEBS Lett* **563**: 28–34
- Trinklein ND, Aldred SF, Hartman SJ, Schroeder DI, Otilar RP, Myers RM** (2004) An Abundance of Bidirectional Promoters in the Human Genome. *Genome Res* **14**: 62–66
- Tsuji Y, Suzuki I, Shiraiwa Y** (2012) Enzymological Evidence for the Function of a Plastid-Located Pyruvate Carboxylase in the Haptophyte alga *Emiliania huxleyi*: A Novel Pathway for the Production of C-4 Compounds. *Plant Cell Physiol* **53**: 1043–1052
- Tzovenis I, DePauw N, Sorgeloos P** (1997) Effect of different light regimes on the docosaehaenoic acid (DHA) content of *Isochrysis-aff-galbana* (clone T-ISO). *Aquac Int* **5**: 489–507
- Vaezi R, Napier JA, Sayanova O** (2013) Identification and Functional Characterization of Genes Encoding Omega-3 Polyunsaturated Fatty Acid Biosynthetic Activities from Unicellular Microalgae. *Mar Drugs* **11**: 5116–5129
- Valenzuela J, Carlson RP, Gerlach R, Cooksey K, Peyton BM, Bothner B, Fields MW** (2013) Nutrient resupplementation arrests bio-oil accumulation in *Phaeodactylum tricornutum*. *Appl Microbiol Biotechnol* **97**: 7049–7059
- Valenzuela J, Mazurie A, Carlson RP, Gerlach R, Cooksey KE, Peyton BM, Fields MW** (2012) Potential role of multiple carbon fixation pathways during lipid accumulation in *Phaeodactylum tricornutum*. *Biotechnol Biofuels* **5**: 40

- Valledor L, Furuhashi T, Recuenco-Muñoz L, Wienkoop S, Weckwerth W** (2014) System-level network analysis of nitrogen starvation and recovery in *Chlamydomonas reinhardtii* reveals potential new targets for increased lipid accumulation. *Biotechnol Biofuels* **7**: 171
- Vallon O, Bulté L, Kuras R, Olive J, Wollman F-A** (1993) Extensive accumulation of an extracellular l-amino-acid oxidase during gametogenesis of *Chlamydomonas reinhardtii*. *Eur J Biochem* **215**: 351–360
- Valot B, Langella O, Nano E, Zivy M** (2011) MassChroQ: A versatile tool for mass spectrometry quantification. *Proteomics* **11**: 3572–3577
- Vargas CD, Aubry M-P, Probert I, Young J** (2007) Origin and Evolution of Coccolithophores: From Coastal Hunters to Oceanic Farmers. ResearchGate
- Vargas C de, Audic S, Henry N, Decelle J, Mahé F, Logares R, Lara E, Berney C, Bescot NL, Probert I, et al** (2015) Eukaryotic plankton diversity in the sunlit ocean. *Science* **348**: 1261605
- Vieler A, Brubaker SB, Vick B, Benning C** (2012) A Lipid Droplet Protein of *Nannochloropsis* with Functions Partially Analogous to Plant Oleosins1[W][OA]. *Plant Physiol* **158**: 1562–1569
- Wallis JG, Browse J** (2010) Lipid biochemists salute the genome. *Plant J* **61**: 1092–1106
- Wang D-Z** (2008) Neurotoxins from Marine Dinoflagellates: A Brief Review. *Mar Drugs* **6**: 349–371
- Wang H-T, Meng Y-Y, Cao X-P, Ai J-N, Zhou J-N, Xue S, Wang W** (2015) Coordinated response of photosynthesis, carbon assimilation, and triacylglycerol accumulation to nitrogen starvation in the marine microalgae *Isochrysis zhangjiangensis* (Haptophyta). *Bioresour Technol* **177**: 282–288
- Wang H-T, Yao C-H, Ai J-N, Cao X-P, Xue S, Wang W** (2014) Identification of carbohydrates as the major carbon sink of the marine microalga *Isochrysis zhangjiangensis* (Haptophyta) and optimization of its productivity by nitrogen manipulation. *Bioresour Technol*. doi: 10.1016/j.biortech.2014.08.090
- Wang Q, Wan L, Li D, Zhu L, Qian M, Deng M** (2009a) Searching for bidirectional promoters in *Arabidopsis thaliana*. *BMC Bioinformatics* **10**: S29
- Wang ZT, Ullrich N, Joo S, Waffenschmidt S, Goodenough U** (2009b) Algal Lipid Bodies: Stress Induction, Purification, and Biochemical Characterization in Wild-type and Starch-less *Chlamydomonas reinhardtii*. *Eukaryot Cell* EC.00272–09
- Wan L, Ross ARS, Yang J, Hegedus DD, Kermod AR** (2007) Phosphorylation of the 12 S globulin cruciferin in wild-type and *abi1-1* mutant *Arabidopsis thaliana* (thale cress) seeds. *Biochem J* **404**: 247–256
- Wase N, Black PN, Stanley BA, DiRusso CC** (2014) Integrated Quantitative Analysis of Nitrogen Stress Response in *Chlamydomonas reinhardtii* Using Metabolite and Protein Profiling. *J Proteome Res* **13**: 1373–1396
- Wenk J, Trompeter H-I, Pettrich K-G, Cohen PTW, Campbell DG, Mieskes G** (1992) Molecular cloning and primary structure of a protein phosphatase 2C isoform. *FEBS Lett* **297**: 135–138

- Weyman PD, Beeri K, Lefebvre SC, Rivera J, McCarthy JK, Heuberger AL, Peers G, Allen AE, Dupont CL** (2015) Inactivation of *Phaeodactylum tricornutum* urease gene using transcription activator-like effector nuclease-based targeted mutagenesis. *Plant Biotechnol J* **13**: 460–470
- Woese CR, Fox GE** (1977) Phylogenetic structure of the prokaryotic domain: the primary kingdoms. *Proc Natl Acad Sci U S A* **74**: 5088–5090
- Work V, Radakovits R, Jinkerson R, Meuser J, Elliott L, Vinyard D, Laurens L, Dismukes G, Posewitz M** (2010) Increased Lipid Accumulation in the *Chlamydomonas reinhardtii* sta7-10 Starchless Isoamylase Mutant and Increased Carbohydrate Synthesis in Complemented Strains. *Eukaryot CELL* **9**: 1251–1261
- Wurch LL, Bertrand EM, Saito MA, Van Mooy BAS, Dyhrman ST** (2011) Proteome Changes Driven by Phosphorus Deficiency and Recovery in the Brown Tide-Forming Alga *Aureococcus anophagefferens*. *PLoS ONE* **6**: e28949
- Xia S, Gao B, Li A, Xiong J, Ao Z, Zhang C** (2014) Preliminary Characterization, Antioxidant Properties and Production of Chrysolaminarin from Marine Diatom *Odontella aurita*. *Mar Drugs* **12**: 4883–4897
- Yan D, Dai J, Wu Q** (2012) Characterization of an ammonium transporter in the oleaginous alga *Chlorella protothecoides*. *Appl Microbiol Biotechnol* **97**: 919–928
- Yang Z-K, Ma Y-H, Zheng J-W, Yang W-D, Liu J-S, Li H-Y** (2014) Proteomics to reveal metabolic network shifts towards lipid accumulation following nitrogen deprivation in the diatom *Phaeodactylum tricornutum*. *J Appl Phycol* **26**: 73–82
- Yoon K, Han D, Li Y, Sommerfeld M, Hu Q** (2012) Phospholipid:diacylglycerol acyltransferase is a multifunctional enzyme involved in membrane lipid turnover and degradation while synthesizing triacylglycerol in the unicellular green microalga *Chlamydomonas reinhardtii*. *Plant Cell* **24**: 3708–3724
- Yu S, Liu S, Li C, Zhou Z** (2011) Submesoscale characteristics and transcription of a fatty acid elongase gene from a freshwater green microalgae, *Myrmecea incisa* Reisigl. *Chin J Oceanol Limnol* **29**: 87–95
- Yu Z, Zhou N, Zhao C, Qiu J** (2013) In-Gel Determination of L-Amino Acid Oxidase Activity Based on the Visualization of Prussian Blue-Forming Reaction. *PLoS ONE* **8**: e55548
- Zäuner S, Jochum W, Bigorowski T, Benning C** (2012) A Cytochrome b5-Containing Plastid-Located Fatty Acid Desaturase from *Chlamydomonas reinhardtii*. *Eukaryot Cell* **11**: 856–863
- Zeeman SC, Kossmann J, Smith AM** (2010) Starch: its metabolism, evolution, and biotechnological modification in plants. *Annu Rev Plant Biol* **61**: 209–234
- Zhang P, Liu S, Cong B, Wu G, Liu C, Lin X, Shen J, Huang X** (2010) A Novel Omega-3 Fatty Acid Desaturase Involved in Acclimation Processes of Polar Condition from Antarctic Ice Algae *Chlamydomonas* sp. ICE-L. *Mar Biotechnol* **13**: 393–401
- Zhu B-H, Shi H-P, Yang G-P, Lv N-N, Yang M, Pan K-H** (2015) Silencing UDP-glucose pyrophosphorylase gene in *Phaeodactylum tricornutum* affects carbon allocation. *New Biotechnol*. doi: 10.1016/j.nbt.2015.06.003





**Cadoret, J.-P., et al. "Microalgae and Biotechnology." *Development of Marine Resources* (2014): 57-115.**

2

---

## Microalgae and biotechnology

---

### 2.1. Microalgae

Microalgae are a group of heterogeneous, unicellular, photosynthetic, eukaryotic organisms<sup>1</sup>. The first event of endosymbiosis, at the origin of all photosynthetic eukaryotes goes back to 1.8 billion years ago [FIN 10], while terrestrial upright plants only separated from green algae 500 millions years ago [KEE 99]. The photosynthetic yield of microalgae is slightly greater than that of terrestrial plants [WIJ 10] and the fact that they evolve in an aqueous medium, which gives them direct access to their nutritional elements, explains in part a better productivity and a higher growth.

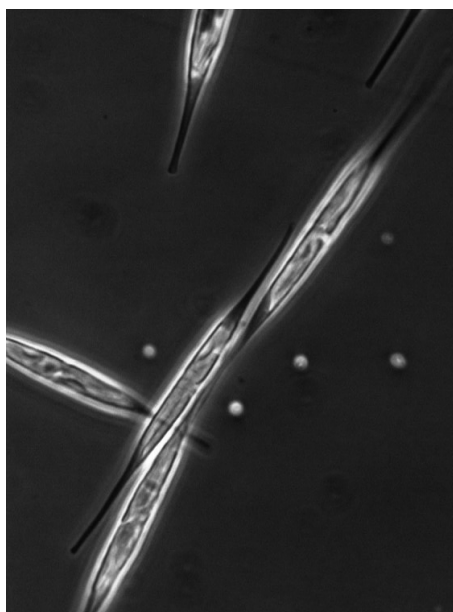
In function of the ambient conditions such as salinity, light, concentrations of nutrients, etc., the size and the appearance of microalgae can change greatly, making their identification difficult. A recent article [GUI 12] suggest a reasonable number of 72 000 estimated species. We can also find estimations going up to 40 000 and 60 000 known species, and assumptions on the number of non-described species is in the order of hundreds of thousands of species [ROS 10]. Microalgae are distributed over the surface of the globe, when in a marine, freshwater or brackish water environments. They have colonized all mediums, from polar ice to deserts or hot

---

Chapter written by Jean-Paul CADORET, Gaël BOUGARAN, Jean-Baptiste BÉRARD, Grégory CARRIER, Aurélie CHARRIER, Noémie COULOMBIER, Matthieu GARNIER, Raymond KAAS, Loïc LE DÉAN, Ewa LUKOMSKA, Elodie NICOLAU, Catherine ROUXEL, Bruno SAINT-JEAN and Nathalie SCHREIBER.

1. Photosynthetic prokaryotes such as *Prochlorococcus* or *Synechococcus* are of major importance at a global level, and are considered to be key actors. However, it would be ambitious to attempt to cover all of this photosynthetic aquatic world. This chapter is essentially oriented toward microalgae and therefore eukaryotes.

water sources. They have adapted themselves to extreme environments, living in salt marshes, acidic media, or even in very low-light conditions. They contribute toward 90 % of primary aquatic production and 50 % of global primary production (figure 2.1). They are at the bottom of the aquatic food chain. The annual ocean production is estimated to be at  $100 \cdot 10^9$  tons of dry matter [PAU 95]. Through their presence on the surface of the oceans, covering 70 % of the planet, they play a major role in global climate by turning  $\text{CO}_2$  into organic matter [RAV 99].



**Figure 2.1.** *Cylindrotheca closterium*, a benthic pennate diatom over around 100  $\mu\text{m}$  in length (photo Kaas/Ifremer)

This biological diversity, a result of excellent adaptability, would suggest a proportional richness in original molecules and therefore of applications in the field of biotechnologies. Twenty species of microalgae are the object of valorization for providing carotenoids, fatty acids and other polysaccharides. The systematic screening of known species and, in the future, of species to be discovered, will benefit from technological advances, allowing notably the low-cost sequencing of genomes and screening automation that Genopole or other private consortiums are becoming equipped with. A complementary path in this research for original molecules consists of transferring the genes of chosen molecules by genetic engineering and profit from all the advantages offered by unicellular microalgae.

The rise of petrol prices has put microalgae forward as sources of vegetal biomasses in the same league as terrestrial plants. Indeed, phytoplankton will play two major roles in the near future, both as an energy source but also as a source of precursor primary matter for polymers in the domain known as “green chemistry”. Microalgae do present singular characteristics that distinguish them advantageously from terrestrial plants. The following section describe these differences which are, for example, better growth, better yields per acre thanks to superior photosynthetic activity. In terms of energy, microalgae thus accede to the rank of third generation.

## **2.2. The potential value of microalgae**

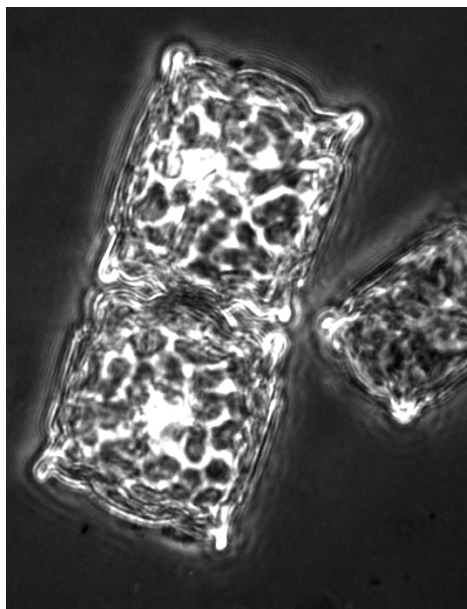
### **2.2.1. Human nutrition**

Certain Amerindian and African populations have long included spirulina in their diets, and insist on the not only nutritional values of these cyanobacteria, but also on their preventative capabilities against certain pathologies [JEN 01]. Without counting macroalgae (for which 19 species can be consumed as vegetables or condiments), the current market is dominated by spirulina and chlorella, and the only diatom to have received this approval in France is *Odontella aurita* (figure 2.2). At a global level, we can add the green microalgae *Dunalliella salina* for its  $\beta$ -carotene. Biscuits made from the microalgae *Tisochrysis lutea* rich in Omega 3 have, for example, also been made [GOU 08]. A large amount of investigation remains to be done for teams with enough energy to homologate other microalgae as foods [JEN 01]. However, the production costs do greatly hinder the applications in this domain [BEC 07].

### **2.2.2. Animal nutrition**

Microalgae represent an important source of food in animal production, outside of aquaculture. An estimated 30 % of the global algae production is for the feeding of terrestrial animals, representing a huge market. The most common species in this market are spirula, chlorella and *Scenedesmus* sp.

However, one of the first fields of application where algae found a place was in aquaculture. The production of phytoplankton remains an obligatory step in the farming of mollusks, whichever their stage of development, by particularly in the larvae stages, for which the food source must be living. While the plethora of microalgae concerned only represents some tens of species, only a dozen are commonly cultivated. Scientific studies showing the links between the choice of the cocktail of species making up the algal food and the quality of the farms still have not been carried out [RIC 06].



**Figure 2.2.** *Odontella aurita*: length of around 50  $\mu\text{m}$ , this large diatom is regularly cultivated in Vendée (photo Kaas/Ifremer)

Microalgae are also used to raise the first larval stages of some fish, but they could also represent an alternative to using fishmeal as feed for fish farming. In 2006, the aquaculture sector consumed a total of 62 % of the global production of fishmeal (or more than 32 million tons) and 88.5 % of the global fish oil production, or 835 000 tons [TAC 08]. In the context of the preservation of biodiversity and the problem of managing stocks of marine species, the total or partial replacement of fishmeal and fish oils by microalgae is of great economic and ecological importance. Thus, generally, the replacement of fish oils by algae is perfectly foreseeable [ABU 09], even if the economic dimension should not be underestimated. And, if it is possible to feed bass with dried microalgae [TUL 12], we can also incorporate 5 to 10 % of microalgae in chicken feed, with some effect on the coloration of the meat and of the yolk [BEC 07].

### **2.2.3. Health**

#### **2.2.3.1. Fatty acids**

Polyunsaturated fatty acids with a gamma-linolenic (GLA), arachidonic (AA), eicosapentaenoic (EPA) or docosahexaenoic (DHA) long chain, produced by

microalgae accumulate in most marine animals. Consumption of sufficient quantities of this type of fatty acid would have a positive impact on health: protective properties against cardiovascular diseases and cancers. The oil extracted for example from the microalgae *Schizochytrium* sp. (authorized as a food product) contains 35 to 45 % of DHA. As a comparison, the traditional oils richest in omega-3 (nut oil, colza oil, etc.) contain around 10 % of alpha-linolenic acid, a precursor of the omega-3 family. The main known sources of omega-3 in algae are *Cryptocodinium cohnii* and *Schizochytrium* sp.

#### 2.2.3.2. Pigments

Since the establishment of REACH (recording, evaluation and authorization of chemical), entrepreneurs have been led to take an interest in the replacement of synthetic molecules by molecules coming from resources said to be sustainable, such as pigments, which can intervene in the domain of human feeding as natural colorings.

Microalgae contain three big types of photosynthetic pigments: the phycobiliproteins, chlorophylls and carotenoids.

Phycobiliproteins are pigments mainly present in cyanobacteria, red algae and glaucophytes. They are water-soluble macromolecules, whose colors are different: red for phycoerythrin and blue for phycocyanine and allophycocyanine. These colorings can be used in the agro-alimentary industry to color food and drink products. Phycocyanine is the only natural blue coloring authorized in Europe. The natural products present the advantage of decreasing risks of allergens [MOR 12].

Chlorophyll is present in all photosynthetic organisms. It is mainly used as a green food coloring (E 140). As a photosensitive, or “photosensitizing”, pigment, chlorophyll can transfer its excitation energy toward its molecular environment to create reactive oxygen species (ROS). These molecules, which are highly reactive, initiate powerful oxidation mechanisms, whose effects at high doses can be noxious for a cell [ROB 09]. As a promoter of reactive oxidation chains, which can be controlled, chlorophyll and its derivatives allow for varied application: anti-bacterial action, scarring of tissue, studies of the oxidation of materials, oxidative cellular stress, etc. It was shown early on that it accelerates scarring of the skin [HOR 51], stimulates the growth of tissues and is used in the treatment of ulcers by reducing pain and improving the aspect of damaged tissue [CAD 48].

Carotenoids are the pigments with the greatest diversity amongst natural products. In 2004, more than 700 had been described [BRI 04]. The carotenoids are made of an unsaturated carbon chain (like alpha- and beta-carotene), while the xanthophylls (such as astaxanthine, lutein and zeaxanthine) are oxygenated derivatives. Most of the carotenoids are powerful antioxidants [CHR 13]. We shall

mention beta-carotene, referenced as E160a, whose rate in spirula is ten times greater than in the carrot, astaxanthine (E161j) used in the farming and coloring of salmon which is the only pigment fixed by the muscles of farm salmon, lutein (E161b) and zeaxanthine (E161h) added to foods to color the skin of chickens and increase the yellow color of yolks. Outside of their use in food, carotenoids also have potential applications in human health through their ability to isolate reactive oxygen species. Beta-carotene, or pro-vitamin A is a vital co-factor in preventative child health. Epidemiological studies have shown that intake of carotenoids decrease the prevalence of cancers and inflammatory diseases [GAG 12], particularly lycopene. Beta-carotene, astaxanthin, cantaxanthine and zeaxanthine all present anti-tumor activity in the liver. Lutein and zeaxanthine are the pigments responsible for the maintenance of normal vision in humans. These pigments are added as supplements in the diet of persons suffering from diseases of the retina such as age-related macular degeneration (ARMD). Preventatively, carotenoids prevent the skin from UV rays and are used with other anti-oxidants in sun protection products (see *infra*) [VIL 11], suggesting a wide fields of application for micro-algae.

#### 2.2.3.3. Polysaccharides

These polymers, essentially their sulfated forms, have antiviral and anti-proliferative capabilities, revealed in lines of cancer cells, but also in the rabbit during *in vivo* experiments. They are already extracted from chlorella and from the red microalgae *Porphyridium purpureum*. These compounds could appear in the formulation of hydrogels for bone reconstruction and in the vectorization of osteo-inducing vectors. EPS (exopolysaccharides) taken from microalgae and their applications are reviewed by [RAP 13].

#### 2.2.3.4. Antioxidants

The assimilation of oxygen by organism can lead to the creation of dangerous derivatives, including singlet oxygen and free radicals. These highly reactive forms of oxygen play an important role in various chronic (cancer atherosclerosis, arthritis, Parkinson's, etc.) or acute pathologies (inflammation, etc.). Like antioxidants, the superoxide dismutases (SOD) are of interest in protecting tissues. This SOD is one of the three catalysts involved in the conversion of the superoxide anion  $O_2^-$  into  $H_2O_2$ . The sequence of this metalloprotein (there are three classes: Cu/Zn, Mn or Fe) is known. The SOD are not however the only antioxidants used. In plants we can cite ascorbate peroxidase, monodehydroascorbate reductase, glutathione reductase, ascorbic acid, glutathione and the phenylpropanoid pathway. It is in chlorella that [KO12] describe the anti-oxidant properties of a peptide.

#### 2.2.3.5. Cellular factory

The controlled production of simple and complex molecules for industrial, nutraceutical and therapeutic use represents an extraordinary opportunity for the development of a market moving quickly forward (market estimated at several tens of billions of dollars) [SCH 04]. There are currently many systems for the production of recombinant proteins (bacteria, yeast, mammalian cells, plant) and allow the production of more or less complex molecules such as insulin, growth hormones, monoclonal antibodies, as well as other therapeutic proteins. However, all of these systems present advantages also several disadvantages such as production costs, regulation in terms of sanitary security (dissemination of GMOs, absence of pathogens such as viruses, prions), ease of extraction and purification of the proteins chosen. Apart from the growing interest in microalgae as natural sources of high value compounds (pigments, polyunsaturated fatty acids, polysaccharides, etc.), they also present many advantages as factories of the production of recombinant proteins used therapeutically [CAD 08]. This promising technology has for objective the simplification of production processes and the reduction of production costs. Compared with the current systems for the production of recombinant proteins, microalgae present many competitive advantages. Indeed, most microalgae are photoautotrophic organisms, depending only on water, light and base nutrients such as nitrogen and phosphorus and carbon present in the form of carbonic gas. These culture conditions are therefore much cheaper than the media used notably for mammalian cells. Finally, microalgae present high productivity levels (close to those of bacteria). The possibility of culturing them in confined and controlled media gets rid of the problems linked with the dissemination of genetically modified organisms into nature.

While no therapeutic protein from transgenic microalgae has yet been commercialized, several studies have shown the real potential of this genetic approach [CAD 08, CAD 12, HEM 11].

The use of microalgae as “cellular factories” requires the mastering of genetic modifications. It is currently difficult to make any comment on the number of microalgae, coming from different taxons, successfully genetically modified. Generally, two paths of transgenesis have been used in microalgae: the nuclear path and the chloroplastic path. This last one is used in particular in the green algae *Chlamydomonas reinhardtii*.

Currently, around twenty therapeutic recombinant proteins have been produced in the the chloroplast of the microalgae *C. reinhardtii*. The use of the chloroplastic path presents a considerable advantage of the nuclear path: it does not possess of gene-silencing after gene modification. This process of gene silencing is often at the origin of a small accumulation of recombinant proteins *via* the nuclear path



[POT 10], which explains why this path, unlike the chloroplastic path, is far less explored. The development of this production pathway is interesting for two reasons:

- being able to produce complex molecules requiring post-translational modifications;
- favoring secretion into the extracellular medium of proteins of interest, with the goal of minimizing the steps of extraction and purification of these proteins.

#### **2.2.4. Cosmetics**

Algae extracts are researched for use as emollients, incorporated into creams to prevent wrinkles, stimulate the synthesis of collagens, without forgetting research on UV protection. While most of the assertions made in the advertisements may seem slightly exaggerated, the commercial perspectives largely justify the interest that is given to it. The same algae are seen again, *Spirulina* and *Chlorella* in anti-aging products, regenerative products [SPO 06], or more originally, *Botryococcus braunii* [BUO 12].

#### **2.2.5. Industrial application**

The ability of some species of microalgae to accumulate molecules and physically elaborate structures in response to the biotopes that they colonize is a measurement of the diversity of the habitats previously mentioned.

##### **2.2.5.1. Silica and calcite**

The diatomite extracted from primary sedimentary rocks is largely used in filtration or even as an absorbent, a mortar, abrasive material, and complementary powder in horticulture. It has been shown that the silica extracted from cultivated diatoms had an exploitable surface 80 times larger than that of diatoms of geological origin [CSO 99]. Silica is produced by phytoplankton in a lace structure with unequalled precision. The mastering by genetic engineering of the architecture of the fixing of silicon on the frustules of diatoms is thus envisaged to obtain new generation electronic components [BAO 07]. All these applications have been reviewed by [GOR 09].

##### **2.2.5.2. Emulsifiers**

Emulsifiers are components used to mix two immiscible substances. The classic example is of water and oil and the applications are common in the food industry or in cosmetics. Research in this domain is still quite limited. There is however an increasing association of microalgae with this idea [SCH 13].

#### 2.2.5.3. Depollution

Microalgae are found to be associated with the treatment of urban effluents by wetpark. This technology, which remains fairly cheap, has been used for many years as a tertiary treatment system in the purification process. The improvement of the process, notably by the mixing of the lagoons, allows in certain cases an increase of both the polluting charge applied, initially smaller than in other systems, but also the efficiency of the purification. In these open basins, microalgae and bacteria work tightly together. By providing oxygen to the bacteria, the microalgae favor the decomposition and the assimilation of organic substances. In return, the bacteria provide the microalgae with the CO<sub>2</sub> necessary for their metabolism. This synergy presents the advantage of allowing the elimination of toxic compounds, all the while limiting the risks of dissemination in the form of aerosols, favored notably by mechanical aeration systems. The oxygen produced by the microalgae favors a reduction of the sizeable energy requirement that its continuous supply entails, as in the systems of “activated muds”. Several pilots are being trialed according to this strategy [ZHA 13].

#### 2.2.5.4. Assimilation of nitrogen and phosphorus

An important physiological characteristic of microalgae resides in a high intracellular concentration in proteins, and this for most species.

Also, the metabolic activity necessary for the synthesis of these molecules requires an important intake of nitrogen. The synthesis of membranes (in the form of phospholipids) and of nucleic acids (DNA and RNA) calls upon phosphorus residing in the medium. This physiological activity associated with rapid growth makes microalgae big consumers of nitrogen and of phosphorus. This characteristic can be observed notably massive efflorescence in the natural environment, where anthropic output of these elements is great.

#### 2.2.5.5. Fixing heavy metals

This aspect is one of the remarkable properties of these cells and is the object of numerous studies and publications (33 publications in 2012 with the key-words “microalgae + heavy metal”). To provide their needs in vital metallic elements they use two mains mechanisms. First of all, particular physico-chemical properties of their cell walls, which will allow the trapping of the metals to then move them into the cell, but also the synthesis of important amounts of exo-polysaccharides. The hydrophilic and polyanionic compounds form a gangue, retain water and trap the cations, allowing the cell to resist desiccation.

These properties of accumulation have pointed toward applications in environmental engineering *via* the detoxification of environments polluted by heavy metals (lead, arsenic, mercury, cadmium, chrome, etc.) [SOU 12] or even the

salvaging of metals of interest such as gold [LUA 11], and could be envisaged for uranium or even copper. For a more general review of this domain, under the name of biosorption, see [GAD 09].

### **2.2.6. Microalgae as fuel sources**

#### **2.2.6.1. Generalities**

As for other terrestrial biomasses, several paths of energetic valorization can be envisaged first of all. The production of a “gross” algal biomass, which can be integrated into the more classical areas of energetic valorization, such as for example organic matter made by terrestrial plants. These are essentially the processes of thermochemical conversion, liquefaction or even gasification. This biomass can thus be used as a substrate for the production of methane by anaerobic digestion, or for the production of ethanol by alcoholic fermentation. A second path looks more specifically at the molecules synthesized which present high energetic potential: hydrogen and lipids.

The production of hydrogen by microalgae was observed for the first time at the end of the 19<sup>th</sup> century. It was then and still is the object of intense research. The metabolic and molecular mechanisms involved are increasingly better understood. However, the problem of low productivity still needs to be solved, and makes this area difficult to exploit.

The idea of the use of microalgae to produce lipids for use in fuel is not a new one, even though the first proper advances only appeared in the 1970s, as illustrates the resulting report by the NREL of the US energy department covering the years 1978-1996 [SHE 98]. Just like superior oleaginous plants, microalgae have the ability in certain conditions to accumulate an important amount of lipids. But, compared with these, the present *a priori* a large number of additional advantages, which contribute along with others to their recent “popularity”, amongst which we will list:

- higher photosynthetic yield;
- no conflict with food supply;
- non-conflicting water management, if seawater culture;
- higher growth per acre;
- high metabolic plasticity;
- mastering of the cycles of nitrogen and phosphorus;
- possible coupling with an industrial source of CO<sub>2</sub>;

- possibility of continuous production;
- many valuable sub-products.

Several issues do, however, come tamper with this list of advantages. Whatever the productivity obtained, even if, as we shall see, this can be high, the surfaces of the necessary cultures must be very high and the productions must be significant. In terms of mass energy, microalgae with energetic vocations will fare better in countries with large non-cultivable spaces. A way of increase productivity per unit of space consists of exploiting the undeniable advantage of being able to cultivate microalgae in large volumes. This option is followed by an increase of the price of a liter of oil, already high.

The recent reviews are adding up, discussing, analyzing and critiquing all of the supposed advantages of microalgae. For a list of the prospective publications see <http://wwz.ifremer.fr/pba/Presentation>. For a list of the significant issues, one can look at the turquoise book, a collective work by the French specialization currently in creation:

[www.adebiotech.org/home/img/algues/LIVRE\\_TURQUOISE-V.screen.pdf](http://www.adebiotech.org/home/img/algues/LIVRE_TURQUOISE-V.screen.pdf)

The main factors influencing the production of lipids are linked to stress: low temperature, intense luminosity, low levels of nitrogen, severe phosphorus deficiency, lack of silica in the diatoms and alkalinity. All these parameters are not as important as each other, and analyses calling upon factorial planes allowing us to estimate the interactions between factors are then vital. The figures in the literature oscillate between 10 to 100 g.m<sup>-2</sup>.day<sup>-1</sup> of dry biomass. For comparison's sake, examples of cultures on the French Atlantic coast reach 10 g.m<sup>-2</sup>.day<sup>-1</sup> (36,5 T.ha<sup>-1</sup>.year<sup>-1</sup>), a conservative figure, meaning for an alga containing 50 % oil, the equivalent of 18 tons of oil.ha<sup>-1</sup>.year<sup>-1</sup>. This number is far from the 100 tons of oil from the Internet site "oilgae", but the improvement margins, as much in the production of biomass as in the selection of super-producing strains, or even in the metabolic orientation during the different phases of culture, remain important starting with such a pessimistic calculation.

#### 2.2.6.2. Energetic yields

A way of covering the energetic point of view is a theoretical approach of the transfer of solar energy by photosynthesis. Experiments in the laboratory [BEN 97] have shown that ten moles of photons (217 KJ.(mole photons)<sup>-1</sup>) are required for the fixing of a mole of carbon (475 KJ.(mole C)<sup>-1</sup>) by photosynthesis. The theoretical energetic limit is therefore 22 %. Only 45 % of the solar spectrum is exploitable by photosynthesis (Photosynthetically Active Radiation, PAR), which decreases the maximum conversion efficiency of solar energy by photosynthesis to a value of 10

%. In reality, the yields registered in experimental cultures are even lower, and it seems reasonable to retain an effective yield of around 3 %. Moreover, we can consider that the lipids represent around 30 % of the carbon fixed by photosynthesis, which leads to a photosynthetic yield for the synthesis of lipids of around 1 %.

Based on this hypothesis, [CAD 08] presents potentials for the production of lipids in the order of 30 to 100 T.ha<sup>-1</sup>.year<sup>-1</sup> in Southern Europe. These figures must be compared with the 6 T.ha<sup>-1</sup>.year<sup>-1</sup> of the oil produced by palm trees.

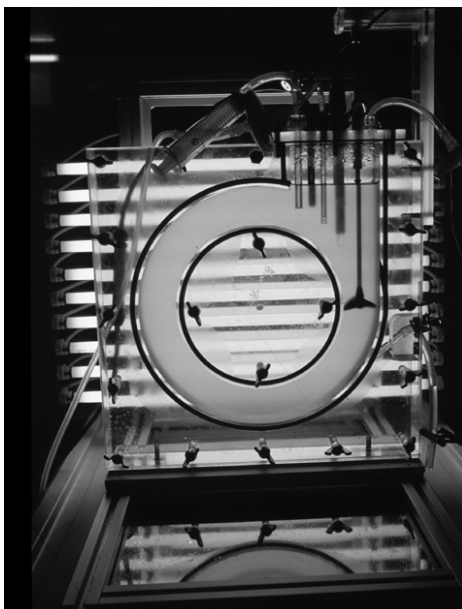
### **2.3. The culture of microalgae**

The use of microalgae in biotechnology underwent a net increase in interest in the 1990s [APT 99]. Today, most commercial production remains based on empirical knowledge. Information on the ecophysiological needs of species currently used or envisage to be used in certain applications are rarely available, or patchy in scientific literature. Surprisingly, while they are fundamental for the optimization of productions, base knowledge such as the influence on growth or the biochemical composition of light, temperature, of the availability of dissolved carbon or nutritional requirement are often yet to be acquired. In the same manner, despite a lot of research and development around culture systems [OGB 03], progress still needs to be made to improve the economy of phytoplankton production.

#### **2.3.1. *Ecophysiological needs***

##### *2.3.1.1. Light*

As mainly autotrophic organisms, microalgae are able to conduct photosynthesis. This process allows for the conversion of radiation energy, in this case light (figure 2.3), into exploitable carbon hydrate by the cell. Only 2 to 3 % of the incident energy is actually used by the vegetal biosynthesis pathways [MEL 09].



**Figure 2.3.** *Toric photobioreactor, with a geometry particularly adapted to studies of the effects of light on the growth of microalgae (photo Kaas/Ifremer)*

The reactions of this biosynthesis are carried out in two distinct phases.

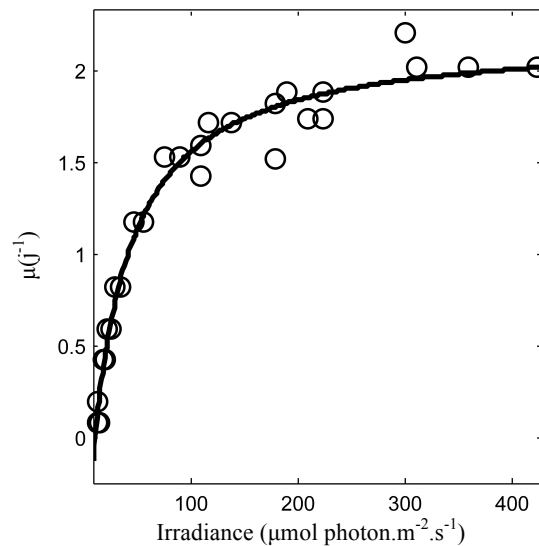
In the first phase, the light or photochemical phase, the photons are absorbed by the chlorophyll, which goes into an activated state and goes back to its initial state by releasing the captivated energy: this energy is used to carry out the photolysis of water which then releases  $H^+$  ions, oxygen and electrons. Two metabolic pathways recuperate the potential energy of the photons and of the electrons through series of transporters located in the membrane of the chloroplast. One produces energy directly available for use by the cell in the form of adenosine triphosphate (ATP) and the other produces reducing organic molecules [FAR 06].

In the second phase, the dark phase, the reduced organic molecules and part of the ATP formed during the light phase are used in the synthesis of phosphorylated sugars (pentose pathway). Variants of this photosynthetic cycle exist. In particular we can cite the C4 cycle of tropical poaceae and the cycle of succulent plants. The biosynthetic pathways of certain bacteria are also different. These mechanisms linked to  $CO_2$  have been identified in certain microalgae but their exact role and their level of activity remain debated [HAI 13].

The central molecule and precursor of the reactions of photosynthesis is chlorophyll, a tetrapyrrolic molecule with in its center an atom of magnesium. This is found associated with proteins included in lamellar structures, called thylacoid. These lamellar structures are organized into super-structures called *granum*, which are most often gathered together into chloroplasts [FAR 06].

In the natural environment microalgae live in the euphotic zone [KIR 94]. The ability of microalgae to become acclimatized and to adapt to this zone has allowed them to spread out according to their requirements of sunlight so as to obtain the best conditions to carry out photosynthesis. This depends directly on the incident luminous flux on the cell, whose power per unit of surface is expressed in  $W.m^{-2}$  (equivalent to  $J.s^{-1}.m^{-2}$ ). This flux is referred to as irradiance and is expressed in  $\mu mol.photons.m^{-2}.s^{-1}$ . Without the intervention of another phenomenon that would limit the physiology of the microalgae, irradiance directly determines its growth rate ( $\mu$ ) which, in function of the irradiance (I) (figure 2.4), follows a typical curve, whose optimum is dependent on the species. The growth rate increases rapidly for low irradiances, lower than a few hundred  $\mu mol.photons.m^{-2}.s^{-1}$ , then reaches an asymptotic optimum, and finally decreases as soon as the process of photoinhibition intervenes, as well as the oxidative stress that results from it.

Light is also defined by its spectrum, which is altered when it penetrates seawater. In solar electromagnetic radiation visible light is contained between 400 and 700 nm and represents 40 % of the incident energy. Thanks to the pigments that make up the Light Harvesting Complex (LHC) of the microalgae's photosystems, this domain of wavelengths is that in which photosynthetic activity takes place. It defines the PAR (Photosynthetically Active Radiation). It must be distinguished from the PUR (Photosynthetically Usable Radiation), which groups together all of wavelengths really usable by the microalgae and which depends on the pigment composition of a species in a given state. This composition determines the absorption efficiency of the photonic energy and of the electronic transfer of LHC as well as the aptitude of the LHC to dissipate excess illumination. The acclimation abilities of the microalgae with regards to the quality and the quantity of light is linked to the plasticity of the biosynthesis of pigment. This acclimation is more guided toward the optimization of photosynthetic activity than toward its maximization [MAC 02].



**Figure 2.4.** Variation of the growth rate ( $\mu$ ) of *Tisochrysis lutea* in function of the irradiance (data PBA-Ifremer)

Access to an optimal quantity of light for each of the cells of the microalgae is a classical problem met by the production systems of microalgae, as they need to obtain high levels of productivity, high biomasses, and this within sizeable volumes.

The more the concentration of a culture increases, the more the phenomenon of luminous attenuation accentuates. This is often represented by the optical law of Beer-Lambert: the auto-darkening of the cells generates a light gradient, with a rapid decrease of the irradiance in function of cellular depth and concentration [LEE 99]. In dark or thick cultures, this results in illuminated zones where photosynthesis dominates, and dark zones where respiration is the main phenomenon. The light gradient can therefore lead to significant losses of productivity.

To increase the light access of all the cells of a culture, the decrease of the thickness of the culture is a strategy for the optimization of the penetration of light, but this causes a decrease of the volume of the culture for a given surface. Another strategy involves the agitation of cultures. The various agitation devices available each have pros and cons, in terms of mixing efficiency, biological constraints and exploitation costs. The management of lighting is a key factor in the growth yields, notably in the case of controlled production areas like photobioreactors. This issue has experienced increased interest since the 1990s since the use of customized light is since then available thanks to light-emitting diodes (LED). These controllable lighting devices offer possibilities of biochemical orientation in controlled algal



productions, whether during growth or in the maturation process of the cells. The studies conducted up to present involve the metabolic effects of the wavelengths of lighting [MAR 13], of high values of irradiance (several thousand  $\mu\text{mol.photons.m}^{-2}.\text{s}^{-1}$ ) and irradiance frequencies [YEH 09].

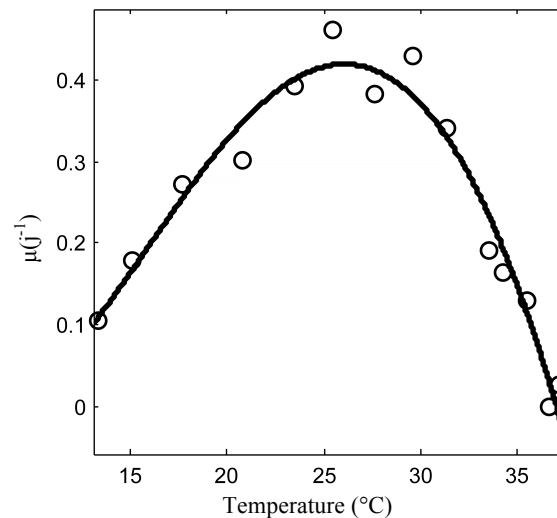
Research and development linked to light remains considerable: which spectrum/a to use to orient biology? How to manage mixes of wavelengths? What are limits of the scale transfer of LEDs? The technologies of light sources continue to evolve. The use of organic LEDs or polymer LEDs is promising, as is the use of flexible materials to take on the shape of the cultures receptacles so as to reduce light loss.

In the case of external productions, where the light is highly available in function of the latitudes, the natural phenomena of night/day cycles and of the climate are dynamic parameters that constantly modify the incident light. While these variations limit the access of outside cultures to the highest levels of productivity, the natural plasticity of the cells, the polymorphism and the genetic potential of a population of microalgae ensure a certain ability of acclimatization and of resilience. Outside, developments in light can involve the modification of the solar spectrum so as to control metabolism. The use of films or plastic greenhouses that filter some wavelengths is one example. Such setups, whose costs do need to be evaluated, can be a way of equally dealing with rainy episodes, evaporation and could be a potential way of helping with a better thermal management of cultures.

#### 2.3.1.2. *Temperature*

Whether the microalgae are cultivated outside or in controlled conditions, knowledge of the reactions of each species to the temperature is primordial. In the case of outside productions, it allows the choice of species that are particularly adapted or of a succession of species to accommodate for seasonal changes in conditions. In controlled conditions, the leading of cultures to their optimal temperature leads to an optimization of the productions.

Generally, microalgae that present a high temperature optimum have high growth rates. The sensitivity of a rate of growth to temperature is characterized by strong asymmetry: below the optimum, a drop in the temperature, a drop of temperature leads to a gradual decrease of the growth rate. Contrarily, temperatures above the optimum affect growth in an abrupt manner [EPP 72] (figure 2.5).



**Figure 2.5.** Variation of the growth rate ( $\mu$ ) of *Dunaliella salina* in function of the temperature (data from PBA-Ifremer)

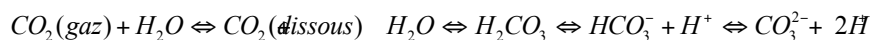
Beside the growth rate, temperature can affect other characteristics of the biomass and notably its composition. It is well known that the temperature of the culture influences the amount of pigment it contains [ZUC 01], notably of chlorophyll, with the appearance of phenomena of chlorosis (destruction of the chlorophyll) at low temperatures [GEI 87]. Lipid content and composition are also sensitive to temperature [CON 09], resulting in an increase of the lipid concentration and of the degree of unsaturation of the fatty acids for low temperatures. [ZHU] shows clearly in *Isochrysis galbana* the influence of a drop in temperature from 30 °C to 15 °C on the increase of the concentrations observed a 18:3(n-3) and 22:6(n-3). These two fatty acids depend on an omega-3 desaturase, whose expression is controlled by the temperature.

#### 2.3.1.3. pH and inorganic carbon

CO<sub>2</sub> is the main anthropic greenhouse gas. The capture of this CO<sub>2</sub>, coming mainly from thermal power stations, metal and cement production, is a major preoccupation for those involved in the industry.

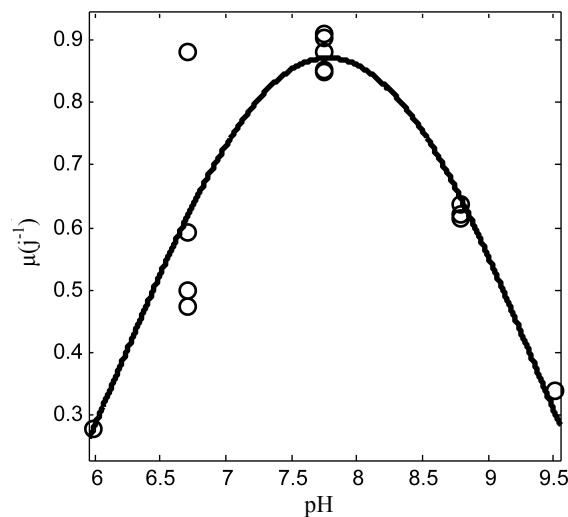
As opposed to terrestrial plants, which have direct access to atmospheric carbon dioxide CO<sub>2</sub>, microalgae must use dissolved inorganic carbon (DIC) in the aqueous medium, in the form of bicarbonate (HCO<sub>3</sub><sup>-</sup>) or of carbon dioxide. Especially in the marine environment, all other things being equal, pH is tightly linked to the amount of

inorganic carbon dissolved and governs the balance between the different forms of carbon [DIC 87]:



In surface marine waters, the pH is generally of 8.2. The dissolution of atmospheric carbon in the medium is the limiting step of this system. The fixing of carbon by the photosynthetic activity of the algal biomass can reduce the availability of the DIC at levels that mean that primary productivity is limited, resulting in a decrease of the rates of growth and of accumulation of carbon reserves. The photosynthetic activity of microalgae therefore results in a significant increase in the pH of the cultures, which can reach values greater than 10 at the end of the culture. Microalgae have therefore developed active carbon transport systems and specific enzymes (carbon anhydrases) that are released into the external medium, allowing them to efficiently access low ambient concentrations of carbon [BHA 02]. The sensitivity of microalgae to the pH of the medium is seen in a curve of the response of the growth rate in the shape of symmetrical convex bell (figure 2.6). Values of pH more acid than the optimum can lead to the excretion of part of the carbon fixed by the algae, while higher values of pH limit the fixing of the carbon. There are very few studies available on the influence of pH on the growth of microalgae. It would seem that for marine algae, the optimal pH is often located around the pH of seawater. However, it has been shown that *Tisochrysis lutea* (*Isochrysis affinis galbana*, clone T-Iso) has an optimal pH located around 7, a value which is significantly different from that of seawater [MAR 12].

From the point of view phytoplankton productions, these physic-chemical aspects have important repercussions on productivity. For this reason, it is advisable to regulate the pH of the cultures so as to ensure a constant availability of DIC. This regulation is classically carried out by injection of gaseous CO<sub>2</sub> or of bicarbonate into the cultures.



**Figure 2.6.** Variation of the growth rate ( $\mu$ ) of *Thalassiosira weissflogii* in function of the pH (data PBA-Ifremer)

It takes between 1.5 and 2 kg of  $CO_2$  to produce 1 kg of algal dry weight. Here again, the distinction must be made between the yields provided by open culture processes and productions carried out in photobioreactors. A prospective analysis carried out as part of the Shamash research project (a project supported by the National research agency) found a possible fixing of between 13 and 280 tons of  $CO_2$  per hectare and per year in an open system.

#### 2.3.1.4. Nutrition

Microalgae are generally considered to be photoautotrophic organisms, meaning that they are able to develop from the light energy from the sun and from nutrients. However, some species are also able to develop from the chemical energy contained in organic carbon, and are thus heterotrophic for carbon.

##### 2.3.1.4.1. Mineral nutrition

When they are “operating” in a photoautotrophic regime, microalgae take all the required mineral nutrients from their dissolved form in the medium. We can make the distinction between macronutrients and micronutrients depending on whether the quantitative needs of the microalgae are high or low. For the growth of marine microalgae, the essential macronutrients are carbon, nitrogen, and phosphorus. [RED 34] observed that these three elements are included in the elementary composition of phytoplankton in uniform proportions, statistically, and with a molar

ratio of 106:16:1, called the Redfield ratio. The micronutrients include elements (iron, cobalt, zinc, manganese, magnesium, etc.) that are vital for certain key enzyme activities as well as other intracellular functions.

Besides carbon, which makes up the carbon backbone of molecules, cellular nitrogen is found majorly and in equal proportion (around 30 %) in the nucleic acids (DNA and RNA) and proteins. Chlorophylls represent another significant stock, around 10 %, or intracellular nitrogen. In the same manner, a large part of intracellular phosphorus, around 40 % is involved in the composition of the two types of nucleic acid. Membrane phospholipids represent up to 20 % of cellular phosphorus [GEI 02]. Finally, while they only represent a small proportion of cellular phosphorus, the adenosine phosphates (ATP, ADP, AMP) and NADPH play a primordial role for the cell's energy and reductive powers.

As mentioned previously, carbon is absorbed by microalgae in the form of CO<sub>2</sub> or dissolved HCO<sub>3</sub><sup>-</sup>. Mineral phosphorus is bioavailable in the form of phosphate (PO<sub>4</sub><sup>3-</sup>). However, in the case of a strong limitation for the phosphate, microalgae can access organic phosphorus through the use of extracellular phosphatases [KUE 65]. The forms of mineral nitrogen accessible by microalgae are more diverse and comprise nitrates (NO<sub>3</sub><sup>-</sup>), nitrites (NO<sub>2</sub><sup>-</sup>) and ammonium (NH<sub>4</sub><sup>+</sup>). The most reduced forms are more readily assimilated due to smaller energy requirement. On the other hand, at high pH levels, the transformation of ammonium into ammoniac can generate high toxicity. In conditions of limitation by mineral nitrogen, microalgae are, like for phosphorus, able to absorb different forms of organic nitrogen: the use of urea and free amino acids in this way is well known [SOL 10].

Whichever the element concerned, microalgae possess very efficient absorption systems that allow them take elements from the medium, down to concentrations lower than a micromole per liter [FAL 75]. At these low concentrations, the transport systems involved are said to be active and as a result their operation requires energy provided by photosynthetic activity. While nitrogen transport systems are relatively well studied, with a diversity of transporters, more or less specific for one chemical species, and variable affinities and capabilities for their substrate [REX 02], studies on phosphate transporters remain uncommon.

Under the pressure of a limitation, microalgae are able to accumulate the nutrients present in excess in the medium, well beyond their needs, resulting in a phenomenon called "luxury consumption". Excess nitrogen can thus be stocked in the form of nitrates or of ammonium depending on the species [LOM 00], while reserves of phosphorus are held in the form of polyphosphate granules [EIX 05]. For example, in *Selenastrum minutum*, [ELR 85] showed maximal stocking capabilities in excess of sixteen times the requirements for growth, while for nitrogen, this capability is four times smaller.

The availability of nutrients conditions and limits the development of microalgae populations. Depending on whether the limiting factor modulates the growth rate or the maximal level of the population, this is either a Blackman limiting factor [BLA 05] or a Liebig limiting factor [LIE 55]. To understand the impact of nutritional limiting factors, Droop [DRO 68] proposed an increasing and hyperbolic relation between growth and cellular content of the limiting element (notion of cellular quota). This relation has been used successfully to describe microalgal growth as part of the concept of the law of the minimum [RHE 78], which postulates that the element that governs growth is the one whose availability is the smallest compared to need. More recently, the concept of co-limitation has partially questioned the paradigm of the law of the minimum [SAI 08]: in some situations, several nutritional elements, whether biochemically linked or not, can work together to limit growth at the same time. Varied examples of co-limitation involve substrates and co-enzymes of a particular enzyme path, like carbon and zinc in carbonic anhydrase [BUI 03]. The hypothesis of co-limitation phenomena that are comparable between nitrogen and phosphorus is today also proposed [BOU 10, PAH 09].

The notion of limitation by the nutrients has important implications for application. Nutritional limitation, linked to the strong metabolic plasticity of microalgae, can result in the accumulation of stocked carbon (sugars and lipids). This observation is largely used as part of research on the production by microalgae of energetic lipids for use in biodiesel [CAD 08].

This ability to use solar energy is by far the most used. The large global microalgae productions mainly call upon the photoautotrophic pathway.

The company Mera Pharmaceuticals, located in Hawaii, produces a biomass of 6.6 T.year<sup>-1</sup> thanks to use of a closed tubular photobioreactor. Similar systems are also used by the company Algatechnologies, in Israel, and Fuji Health Science, in Hawaii. However, due to the low rate of growth of *Haematococcus* and the production protocol that requires two steps, the astaxanthine produced using these methods is hardly competitive with synthetic pigment [GUE 03].

The production of  $\beta$ -carotene by *Dunaliella* sp. is also very important in the world. It represents a level of photoautotrophic production of 1.2 T.year<sup>-1</sup> globally. Two types of production coexist. The companies Betaten and Aquacaroten, located in Australia, cultivate this microalga in lagoons without agitation. Betaten lists annual productions of around thirteen tons of  $\beta$ -carotene for a culture surface of around 400 hectares. The associate production costs appear relatively low due to a favorable climate and the absence of energy consumption linked to more intense culture systems, like *raceway*. Several studies describe *Dunaliella* trials in closed photobioreactors. These trials, however, have not yet been conducted on an industrial scale [DEL 07].

Many small companies produce a variety of microalgae, cultured photoautotrophically for their high contents of polyunsaturated fatty acids like DHA (docosahexaenoic acid) and EPA (eicosapentaenoic acid). This is notably the case for the company Innovative Aquaculture Products Ltd, established in Canada, which produces the haptophyte *Tisochrysis lutea* or BlueBiotech InT in Germany or even Innoalg in France, which produces the diatom *Odontella aurita*, co-cultured with the microalga *Chondrus crispus*, intensively in *raceways* which surfaces of up to 1000 m<sup>2</sup>.

Finally, one of the biggest photobioreactors for the production of microalgae photoautotrophically is established in Hanover, Germany. With a total volume of 700 m<sup>3</sup>, this tubular photobioreactor, developed by [PUL 01] and recently acquired by the company Roquette, is capable of producing between 130 and 150 tons of dry microalgal matter per year.

#### 2.3.1.4.2. Organ nutrition

Heterotrophy is defined as being the ability of an organism to develop on the basis of organic carbon produced by other organism. A medium for heterotrophic culture is thus made up of the same mineral elements as those necessary for photoautotrophy, but also provides a source of organic carbon.

Work on the heterotrophic pathway in microalgae was started as early as the 1960s and showed that some species are able to develop on the basis of organic carbon substrates. Amongst all of the known species, only a small number demonstrated this ability [PER 11], and it would also seem that commonly cultivated marine microalgae present relatively undeveloped abilities for heterotrophy [UKE 76]. Since the 2000s, the heterotrophic pathway is the object of an increase of research activity, with a lot of work from Chinese teams [LIA 09] as part of the development of the production of algae oils.

The main advantages of heterotrophy relate to:

- possible productions in volume, in any kind of fermenter and no longer only on the surface like in the autotrophic systems;
- the reduction of production and maintenance costs [PER 11].

The advantage of this trophic pathway for industrial cultures aiming products with little added value – such as biofuels – must however be relativized because of the disadvantages it presents compared to the more classic autotrophic culture:

- the sizeable volumes involved in “biofuel” applications would required access to a cheaper resource of organic carbon;

– the respiratory activity of cells, linked to the degradation of organic carbon sources, generates CO<sub>2</sub>, which can be remedied in the autotrophic pathway;

– the heterotrophic path requires axenic conditions or at least very low contamination levels to avoid competition with bacterial communities that usually have higher growth rates than the microalgae. As underlines by [BUM 11], even the smallest microbial contamination introduced after inoculation can easily overtake the microalgal biomass in the competition for organic carbon. The maintenance of axenic conditions during the production period thus requires precautions of culture protocol and the use of particular materials. Heterotrophic productions should therefore be reserved for high-value markets.

Generally, species capable of heterotrophy show growth performances and maximal biomasses that are greatly superior to those recorded in photoautotrophy [LEE 97], by using a variety of organic substrates (glucose, glycerol, acetate, malate, lactate, glutamate, ethanol) depending on the metabolic capabilities of the species involved [BUM 11]. For example, high concentrations of biomass (45 g.L<sup>-1</sup>) and volume productivities of 20 g.L<sup>-1</sup>.day<sup>-1</sup> have been obtained thanks to heterotrophic *Nitzschia alba* cultures [GLA 94]. The direct consequences are lower production, maintenance and harvesting costs. Production by heterotrophy in a fermenter is well mastered in Japan and Korea, mainly for aquacole and nutraceutical applications [LEE 97]. The company Martake, in the USA, produces DHA (docosahexaenoic acid) with the help of heterotrophic *Cryptocodinium cohnii* cultures [MEN 09].

Quite surprisingly, some pigments are produced by microalgae, even in the absence of light [PER 11]. Thus, [SHI 00] obtained lutein contents between 68.42 and 83.81 mg.L<sup>-1</sup> in the heterotrophic *Chlorella protothecoides* cultures. [WAN 08] also carried out production of astaxanthine with *Chlorella zofingiensis* cultured on glucose. This study even suggests that the *maxima* of biomass and of astaxanthine production can be obtained simultaneously with the help of a single-step culture, instead of the two-step culture usually carried out for *Haematococcus* sp.

The mixotrophic pathway is an intermediary between strict heterotrophy and autotrophy; it allows the algae to benefit from both organic carbon and CO<sub>2</sub>, through photosynthesis [HER 11]. It appears as a more promising alternative to autotrophy than heterotrophy, inasmuch as it combines the advantages of each of the previous pathways, leading to synergic effects: the growth rates recorded for the species concerned are indeed greater than those from the heterotrophic pathway [SCA 10]. [YAN 00] obtained biomass yields, calculated on the basis of the energy provided, four times greater for *Chlorella pyrenoidosa* cultures produced in mixotrophy, compared to photoautotrophic cultures. They also showed that alternations between photoautotrophic phases and heterotrophic phases could lead to even higher yields than for true mixotrophy. [PUL 04] observed that the growth rate in mixotrophic cultures of *Chlorella vulgaris* and *Haematococcus pluvialis* was the sum of the



growth rates obtained in strict heterotrophy and strict photoautotrophy. Mixotrophy can therefore allow the overcoming of limitation caused by the availability of high-density light. [COM 94] underline that this mechanism is important in the case of *Scenedesmus obliquus* and it seems to be shared by many mixotrophic species.

Mixotrophy also provides an effective way of increasing the productivity of light-inducible metabolites. [STA 98] also obtained in *Galdieria partita* contents of chlorophyll a, carotenoids, phycocyanine and allophycocyanine that were greater in mixotrophy in comparison to the results obtained in heterotrophy. Analogous results are reported by [SHI 99] with lutein and chlorophyll contents in *Chlorella protothecoids* that are greater in mixotrophy.

Finally, mixotrophic activity, combining both respiration and photosynthesis, allows the consideration of neutral or positive carbon balances. However, as for heterotrophic cultures, the controlling competition with bacterial communities remains unstudied.

To a certain extent, microalgae cultures become independent or at least only slightly dependent on any source of light. This characteristic contributes to a smaller occupation of space, a decrease in the investment linked to production structures, a production rhythm independent of the nycthemeral cycle and, to a lesser extent, of the seasons. Moreover, the cultivation of microalgae on organic carbon substrates allows us to consider the purging of sources rich in organic carbon but also in nitrogen and phosphorus.

### **2.3.2. Productions and productivities**

#### *2.3.2.1. Modes of culture*

There are three different modes of production: the discontinuous mode, the semi-continuous mode and the continuous mode of cultures. In the case of discontinuous cultures, the various nutritional elements are only distributed at the start of the production, and the harvesting is carried out at the end of the cultivation period. Semi-continuous cultures are partially harvested at regular intervals, and also resupplied in the same manner with nutritive medium. Continuous cultures allow for the constant harvesting of cells, as the supplying of the medium nutritionally is ensured continuously. This method of production allows for stable culture parameters throughout the entirety of the length of production, and therefore allows for the production of a biomass of constant quality. It also reduces production costs by minimizing the amount of human work.

##### **2.3.2.1.1. The discontinuous mode [BAI 86]**

If the photobioreactor or the basin is only supplied with nutrients one, without any previous supply, the system functions discontinuously, called batch mode. The

inoculated cells experience a period of adaptation to the new environmental conditions, of various lengths, called latency phase, and then develop and express all of their potential when the amounts of nutritional salts and light are not yet limiting factors. During this period, called the exponential growth phase, the algae reach their highest specific growth speed in function of the conditions that imposed on them. If we call  $x$  the concentration of microalgae in the expressed culture volume (either in  $\text{g.L}^{-1}$  or in the number of cells per liter), we can define the volume speed of the culture as being the increase of the cellular concentration per unit of time [2.1]:

$$V_{vol} = \frac{\partial x}{\partial t} \text{ expressed in } \text{g.L}^{-1}.\text{h}^{-1} \text{ or in number of cells mL}^{-1}.\text{h}^{-1} \quad [2.1]$$

By dividing the volume speed by the amount of algae present at time  $t$ , we define the specific growth rate ( $\mu$ ), independent from the volume of the culture, which is an essential characteristic of cells in culture [2.2]:

$$\mu = \frac{V_{vol}}{x} = \frac{\partial x}{x \times \partial t} \text{ expressed in } \text{h}^{-1} \text{ or in days}^{-1} \quad [2.2]$$

The specific growth rate expresses the ability that possesses, for example a gram of algae, to produce  $\mu$  grams of algae per unit of time (in hours or in days), or the ability of cell to produce  $\mu$  cells per unit of time.

It comes naturally that:

$$\mu \times \partial t = \frac{\partial x}{x} \quad [2.3]$$

which we can integrate between  $t_0$  and  $t_1$  when the algal concentration passes from  $x_0$  to  $x_1$  [2.4]:

$$\mu(t_1 - t_0) = \ln(x_1) - \ln(x_0) \quad [2.4]$$

$$\mu = \frac{(\ln(x_1) - \ln(x_0))}{(t_1 - t_0)} \text{ expressed in } \text{h}^{-1} \text{ or in days}^{-1} \quad [2.5]$$

The generation time ( $t_g$ ) is another value that characterizes the abilities of these organisms in a determined situation. It represents the time that a population takes to double, either in weight, either in numbers. By going back to equation [2.4], we can replace  $x_1$  by  $2x_0$  and we obtain:

$$\mu = \frac{(\ln(2 \times x_0) - \ln(x_0))}{(t_2 - t_0)} = \frac{\ln(2)}{(t_2 - t_0)} \quad [2.6]$$

$$(t_2 - t_0) = \frac{\ln(2)}{\mu} = G \text{ is the generation time expressed in hours or in days} \quad [2.7]$$

#### 2.3.2.1.2. The continuous mode

If the bioreactor is permanently supplied with medium, the mode of culture is said to be continuous. For the volume present at any moment within the system to remain fixed, the charge introduced into the reactor is equivalent to volume removed. The continuous mode can be started either from a culture in discontinuous mode, either directly [BOU 03]. In function of the imposed culture conditions, the population of the cells will reach a level of equilibrium that is a function of the amount of light dispensed, of the nutrient content of the renewal rate imposed by pump bringing the culture medium. This state is not very stable, and any modification, even minimal, of the conditions governing the reactor will lead to a change of this equilibrium level. At equilibrium, the amount of algae produced per unit of time is equal to the amount exported by the flow of the pump [SCR 99]:

$$\mu \times x \times V = Q \times x \text{ with } V = \text{reactor volume (L) and } Q = \text{flow (L.h}^{-1}\text{)} \quad [2.8]$$

$$\mu = \frac{Q}{V} = D \text{ corresponds to the dilution rate of the reactor} \quad [2.9]$$

By imposing a determined flow, we are fixing the specific growth speed of the microalgae at equilibrium. If the dilution rate overtakes the maximal specific speed of the species in the conditions of the culture, the cells will be washed and the cellular concentration will irremediably decrease until there are no more cells in the culture volume [BAI 86].

It is possible to lead cultures continuously according to different principles, which at equilibrium provide the same results:

- the chemostat principle. In this operating mode, the culture is continuously supplied with nutritional medium with a pump whose flow rate is fixed at a certain value. By fixing the flow, the specific growth rate is imposed and the culture will be stabilized at equilibrium around a cellular concentration undetermined at the start;

- the turbidostat principle. The objective of this type of culture is to reach a determined cellular concentration by using the flow of the pump as a continuous measurement of the biomass or of the cellular concentration present in the reactor. This requires the use of a measurement system allowing us to consider the charge

present in the reactor. Often, optical measurement systems are used to link the cellular concentration to light absorption. By fixing an optical instruction, the optical system will dilute the culture when this value is overcome. After a certain amount of time has passed, and in function the hysteresis of the measurements, the pump will be controlled near-continuously according to a flow rate corresponding to a dilution rate equal to the specific growth speed of the cultivated algae.

### 2.3.2.1.3. The discontinuous supply mode, or *Fed Batch*

The discontinuous supplied mode is characterized by the addition, in a predetermined or controlled manner, of nutrients in the photobioreactor at certain periods. The addition of nutrients can thus be adapted to cellular concentration or the biomass present in the production area [BAI 86]. At the start of the culture, the reactor is only partially full, the new medium is brought gradually along with the development of the cells and the culture is usually finished when the reactor is full. This process is often used for bacterial or yeast productions as it allows the reaching of important levels of productivity. In the case of microalgae, the requirement of bringing light to allow the cells to grow significantly reduces the attraction of this type of production. Heterotrophic cultures can, however, benefit from this, and important levels of productivity can be reached. [BUM 11] report cellular concentrations in the order of 100 g.L<sup>-1</sup> for *Chlorella* sp., *Cryptocodinium* c. or *Galdieria* s. cultured heterotrophically.

In this case, the amount of algae produced per unit of time is linked both to the variation of the volume of the culture and to the concentration in algae:

$$\mu \times V = \frac{\partial(V \times x)}{\partial t} \quad [2.10]$$

$$\mu \times \partial t = \frac{\partial(V \times x)}{V} \quad [2.11]$$

By integrating between time  $t_0$  and  $t_1$  and the volume  $V_0$  and  $V_1$ , it results that:

$$\int_{t_0}^{t_1} \mu \times \partial t = \int_{V_0}^{V_1} \frac{\partial(V \times x)}{V} \quad [2.12]$$

$$\mu \times t = \ln \left( \frac{x \times V}{x_0 \times V_0} \right) \quad [2.13]$$

and the concentration at any moment within the reactor is an exponential function of time:

$$x \times V = x_0 \times V_0 \times e^{\mu \times t} \text{ expressed in number of cells} \quad [2.14]$$

### 2.3.2.2. The production systems

Currently, the techniques for the production of microalgae are split between large-scale cultures in an open medium, lagoon, continuous flow system (*raceway* or circular basin) and closed systems, photobioreactors, plastic bags, sheaths, pipes (figure 2.7). The choice between the different culture techniques is based on economic considerations, very much in favor of open systems, but which present risks linked to possible contamination and little amounts of control to counterbalance climate variations.



**Figure 2.7.** Photobioreactor JSP-120 for the automated production of microalgae in marine mollusk hatcheries (photo Kaas/Ifremer)

Most of the production of microalgae is carried out today in external basins [SPO 06].

The distinction must be made between production in controlled photobioreactors with artificial or natural lighting, which allows for very high levels of productivity,

with a circulating charge able to reach  $4 \text{ g.L}^{-1}$ , for a high cost in terms of both investment and operation (the reactors also allow to proceed with highly controlled productions for biotechnology and pharmaceuticals), from production in natural or tubular lagoons extensively with algal concentrations generally comprised between  $0,4\text{-}1 \text{ g.L}^{-1}$  and for which the yields and the costs are lower.

#### 2.3.2.2.1. Lagoons

One of the most important lagoon-based commercial productions of microalgae is carried out in Australia, where hundreds of hectares are used to cultivate *Dunaliella salina*. With a depth of 20 to 30 cm, they are only agitated by the wind and movements of convection. This extensive production is made possible by extreme conditions, notably very high salinity levels, which suit the growth of *Dunaliella salina* and limit the development of contaminants. This culture system also requires little land costs, due to the large surfaces required as well as the optimal climate conditions throughout the year. Moreover, seeing as productivity never exceeds  $1 \text{ g.m}^{-2}\text{.day}^{-1}$ , an efficient harvesting system is required [RIC 08].

#### 2.3.2.2.2. Raceways

*Raceways* are currently the most commonly used production systems used for the large-scale cultivation of microalgae. The choice of this system of culture is usually based on economics, as the investment and operating costs are not high. They are usually cement or dug basins, covered in plastic films with a water height that does not go over 40 to 50 cm, to ensure light access, and not below 20 cm to reduce temperature fluctuation problems. Impellers ensure the agitation to maintain the algae in suspension. Compared to closed systems, the levels of productivity reached are not very high. The difficulty comes partly from the low effectiveness of agitation, which does not allow access to the light and to optimal gas-liquid transfers, and partly due to the lack of control over the ambient conditions. The cultures are submitted to the randomness of the weather. For example, in the case of strong rain, the salinity of the culture is reduced, the nutrients and the biomass are diluted, reducing productivity, without forgetting an important risk of contamination by other microalgae, protozoa and bacteria.

Geographical positioning plays a vital role in the productivity, which is estimated in a *raceway* to be between  $10$  and  $25 \text{ g.m}^{-2}\text{.day}^{-1}$  [ROS 12], while the theoretical calculations would leave hope for up to  $60$  to  $198 \text{ g.m}^{-2}\text{.day}^{-1}$  [COO 11]. Average productivity levels observed for the diatom *Odontella aurita* by the Innovalg society in the "Pays de Loire" are of  $10 \text{ g.m}^{-2}\text{.day}^{-1}$ .

#### 2.3.2.2.3. Photobioreactors (PBR)

Photobioreactors are closed systems (figure 2.8), lit up by a light source that can be natural when the PBR are placed outside [GRO 03], or artificial (fluorescent tubes, LEDs).

They can be equipped with different probes so as to control the kinetics of the growth of the microalgae (temperature, pH, agitation speed, renewal rate, lighting). Many different types have been developed. Some correspond to specific study requirements, in particular in the domain of ecophysiology, while others have been established with the goal of optimizing the commercial production of biomass.

The PBRs allow us to work in condition of asepsis, ensuring the lack of contaminations such as the predators of microalgae, undesired opportunist species, and to limit the bacterial load. If they are built from inox, they can be sterilized with water vapor. This type of material is very costly, and as a result most PBR are made of synthetic matter such as PMMA (poly(methyl methacrylate)). Sterilization is then chemical (bleach or peroxyacetic acid).



**Figure 2.8.** Photobioreactor with instrumented turbine, used in ecophysiological studies in controlled conditions (photo Kaas/Ifremer)

As part of studies on the effect of lighting, as much in terms of quantity as of the nature of the spectrum, the use of planar PBRs of little thickness is favored. This arrangement allows the distribution of luminous energy homogeneously inside the PBR and the representative measurement of the light that really penetrates the area.

This type of PBR, equipped with an absorption probe that activates a sampling pump, provides the possibility of working in turbidostat mode. This allows the maintenance of a biomass concentration that is constant and low, no matter the quantity and the quality of the light, as the growth rate indirectly steers the operating frequency of the sampling pump. This type of arrangement means that, due to the fact the access to light is optimized, high levels of productivity can be achieved. However, these PBRs do not allow a volume increase. To conserve the benefit of the small thickness, and therefore of the access to light, but to increase the volume, either an increase in height is required, or an increase of the length of the PBR. For a planar PBR of 1000 liters and with a thickness of 6 cm of the curve number, 1.5 meters of height and 11 m of length would be needed. Moreover, the levels of productivity then achieved would be reached at the cost of a large amount of water, the elimination of which would add a significant cost.

To deal with this problem of space, the choice of cylindrical PBRs is required [TSY 01]. This type of reactor can be made up of one or several tubes.

Column-type cylindrical PBRs are largely used to produce microalgae in mollusk hatcheries. To have a sufficient culture volume to deal with the needs of the larvae, these PBR have a capacity of around 300 liters and a diameter in the order of 60 to 90 cm. The light parameter quickly becomes a limiting factor, as the cells of the microalgae limit the penetration of the photons in the PBR. Ring-type cylindrical PBRs partially overcome this problem of light access to the culture. They are made up of two concentric tubes of equal height. The lighting system is positioned in the central tube. The thickness of the water layers exposed to the lighting is less important and the biomass yield is therefore better.

Tubular cylindrical PBRs lead to a significant reduction of the light's access path. They can be made up of a long tube with a small diameter (between 1 and 5 cm), deployed in a serpentine form on the ground. The congestion of occupied surface is very high for a PBR of several hundred liters. They are therefore mostly reserved for outside use [TRE 98]. The other way to accommodate the long tube is to roll it around a support of up to several meters of diameter and of height [TRE 98]. The space occupied on the ground is then greatly reduced. These two types of tubular reactor are dedicated in priority to outside installations.

The last type of tubular PBR is more suited to inside production. They are made up of vertical tubes of 50 cm to 1.5 m, linked together by flanges so as to form a closed



loop [OLI 07]. These tubes with a diameter in the order of 6 cm can be deployed in a space on the ground and in areas of reduced height. For example, a PBR of 120 liters containing the microalgae *Tisochrysis lutea*, allows for a productivity of 20 to 30 g.m<sup>-2</sup>.day<sup>-1</sup> of dry matter in the laboratory. The moving of the culture, inside the PBR, can be ensured by an air injection device, or *airlift*, by an agitation mobile or by a pump. Depending on the fragility of the species cultivated, it is important to take into account the shearing forces induced by the agitation system and by the geometry of the PBR. Inasmuch as it constitutes a closed system, it is also necessary for the PBR to be equipped with a degassing system of the oxygen produced (in the order of 1 g.m<sup>-3</sup>.min<sup>-1</sup>), so that this does not reach concentrations that are toxic for microalgae. The supply of carbon and the controlling of the pH level can be ensured by the injection of CO<sub>2</sub>. This can be used for the measurement of the pH, or fixed so as to represent a constant percentage of the gaseous mix of air-CO<sub>2</sub>. Finally, these tubular systems, built on a larger scale, exist in some private companies over hundred of square meters of useful cultures.

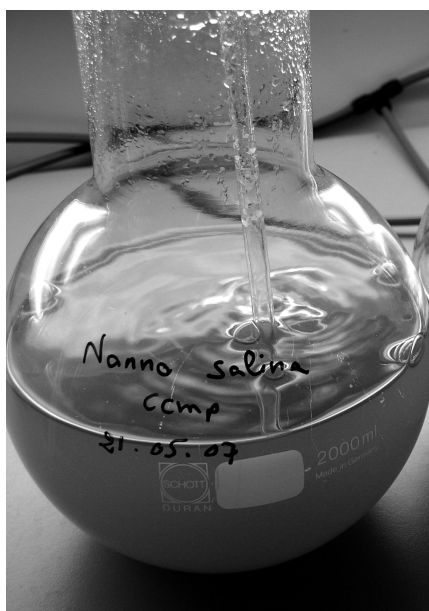
## 2.4. Research in support of the development of the branch

### 2.4.1. Omics

Like with research in the domains of plant biology for agronomy, or microbiology for biotechnology, the acquisition of knowledge on microalgae species, whether they are models or exploited allows the improvement of their use and the discovery of new fields of biotechnological applications. The rise of molecular biology in the second half of the 20<sup>th</sup> century, and the technological sequencing revolution that started in the 2000s, have transformed the world of biological research. Work on microalgae using genomic and post-genomic approaches majorly involved the species *Chlamydomonas reinhardtii*, a model chlorophyte species, of interest for its taxonomic proximity with upright plants [HAR 01]. The genome of this species has been sequenced [MER 07]. The numerous tools and molecular approaches (RNA chips, antibodies, RNA interference, RNA seq, proteomics, etc.) developed in this model unicellular species have allowed a better understanding of the metabolisms and cellular mechanisms of photosynthetic eukaryotic organisms. In 2013, 27 model microalgae models are entirely sequenced, over some biodiversity, including chlorophyceae, diatoms, a rhodophyceae, a cryptophyte and a haptophyte. See <http://wwz.ifremer.fr/pba>. The structures and the genic composition of the genomes of microalgae can prove to be complex. Their sizes vary strongly in function of the species: 12,6 Mpb for the chlorophyceae *Ostreococcus tauri*; 168 Mpb for the haptophyte *Emiliana huxleyi*; 10 000 Mpb estimated for the dynophyceae *Karenia brevis*. The genomic data obtained in these species are completed by many transcriptomes of species of phylogenomic and biotechnological interest, both published and in the middle of

being sequenced. All of the genomic data has led on the one hand to the better description of phenomena of endosymbiosis and evolution which give this extraordinary to microalgae, and on the other hand to establish a base of biological knowledge for ecological and functional studies.

The genomic analyses aimed at biotechnology mainly involve the exploitation of lipids and the secondary metabolites of microalgae. The exploration of the genomes and transcriptomes of species that produce polyunsaturated long chain fatty acids such as *Pseudochattonella farcimen*, *Myrmecia incisa* and *Nannochloropsis oceanica*, has led to the identification of the enzymes involved in the biosynthesis of these lipids of nutritional interest [YU 11]. In the same manner, many teams have set up genomic analyses to identify *in silico* genes of interest for the biosynthesis of secondary metabolites of high biotechnological potential such as phycotoxines, pigments or phycocolloids [ZHA 11]. The exploration of genomes is a promising strategy, not only for the identification of pathways for the biosynthesis of natural products of interest, but also to identify new bioactive compounds [WIN 11].



**Figure 2.9.** Culture of the microalgae *Nannochloropsis salina* in a round-bottom flask (photo Kaas/Ifremer)

Recently, in the face of the rising popularity of third generation biofuels, several research teams have developed genomic, transcriptomic and proteomic approaches to characterize metabolic pathways, and, more precisely, the biosynthetic pathways of

triacylglycerides in oleaginous microalgae such as *Dunaliella tertiolecta*, *Botryococcus braunii*, *Hematococcus pluvialis*, *Chlorolla vulgaris* or *Eustigmatos cf. polyphem* [WAN 12]. Generally speaking, the main metabolic pathways involved in the metabolism of lipids present homologies with upright plants, but certain pathways specific for microalgae have been identified [FAN 11]. Furthermore, the regulatory mechanisms of lipid synthesis are currently mostly unknown in microalgae.

To this day, the scientific community generates an explosion of genomic data, which constitutes a base for the optimization of the exploitation of microalgae and for the discovery of new biotechnological potential. Less than 50 % of the genes of microalgae studied can be identified as homologous with known genes of other organisms. The functions of most of them have never been confirmed. While efforts have been made in model algae, and notably in the chlorophyceae *C. reinhardtii*, the taxonomic distances between the different phyla limit the functional exploration of the genomes. The study of the function of genes and proteins and of the regulatory mechanisms at the levels of transcription, translation and post-translation is a promising perspective for the exploration of genomic data for biotechnology.

#### **2.4.2. Species improvement**

Microalgae represent a still largely unexplored world, and the few commercial cultures that exist rely on limited number of species. All of the species cultivated are “as discovered”, as the microalgae have never been selected, but only deposited in banks and transferred from tube to tube. As in the case of the strategies developed in agriculture, and depending on the biology of the species, the access to diversity and the mode of reproduction, the improvement methods that can be put into place are varied. Generally, four main selection strategies can be identified: 1) by genetic engineering, 2) by controlled crossing, 3) individual screening or 4) by artificial and controlled induction of genetic variability [MUR 07].

The genetic engineering approach consists of introducing a gene or an allele of interest coming from one organism into another, whether it is of the same species or not. This technique has the advantage of only introducing the gene or the allele of interest, in an already cultivated strain. In most cases, the transfer concerns one gene, three or four or more. In microalgae, this technique is largely used in fundamental research, and their applications have been reviewed [CAD 12] and are objects of several patents [BAR 10, CAD 09]. A large part of the families of microalgae now have transformed representatives. The diversity mentioned above makes adapting techniques necessary, in function, for example of the fragilities of membranes or of the specificity of gene-regulating sequences (promoters, GC content, etc.). In the context of the elaboration of complex pharmaceutical molecules, this strategy is already a reality and involves a few companies around the world [BAR 10, CAD 09, CAR 10, JON 12, LEJ 10, TRA 13]. In a context of

“biofuels”, some biosynthesis pathways are targeted and perfectly identified. Modifications in these labyrinths remain hypothetical and risky, but this choice has still been made by some of those in the industry who see this path as the most promising.

The strategy of improvement by crossing of individuals consists of choosing two parents for their aptitudes and exploiting their progeny as best possible. Different methods can be used to characterize and exploit this progeny according to the objective and the reproductive mode of the species (genealogical, backcrossing, etc.) [TES 10]. With regards to microalgae, the cycle and the modes of reproduction are still poorly understood, with the exception of some model species like *Chlamydomonas reinhardtii* [CHI 67], *Thalassiosira pseudonana* and *Phaeodactylum tricornutum* [CHE 11]. This lack of knowledge makes it difficult to use crosses as selection procedures in many microalgae and this selection strategy will be, in the future, very dependent on the elucidation of the varied reproductive cycles, specific for each group.

The birth of genetics in the 20<sup>th</sup> century, and more generally the birth of “omics” in the present day (genomics, transcriptomics, proteomics, etc.), enables the establishment of new tools such as marker-assisted selection [LAN 11]. Once a population demonstrating high diversity is found, a screening-based approach is usually carried out and consists of selecting one or several individuals with characteristics of interest observed in a population. In microalgae, these approaches concern some characteristics of the phenotype [BOU 12]. The difficulty of the establishment of high-speed phenotyping techniques currently limits the number of characteristics that can be screened for. New molecular marker screening methods (marker-assisted selection) have been developed. They could allow for the selecting of strains based on their genes/alleles of interest to avoid high-speeding phenotyping [COL 08]. This type of approach requires a relatively large amount of knowledge on the studied species [XU 08]. These last few years, the capabilities and the cost of genotyping have permitted the analysis of several hundred individuals at the same time for a large number of markers [VAR 09]. Several strategies have appeared to identify the markers linked to phenotypes (protein research, transcripts, genome regions (QTL), mutations (QTN), genes or alleles of interest [FOU 09] and could be, in part, transferable to microalgae. Currently 27 microalgae genomes have been sequenced as well as several dozen of transcriptomes [CAD 12], thus providing a considerable amount of data.

Like for plants, the exploitation of biodiversity requires the conducting of prospective campaigns, conservation strategies and the establishment of collections [ULU 11]. Currently, collections of microalgae exist but they usually only cover a small number of the strains present in each type of algae and look more at interspecies diversity (for example, The Roscoff Culture Collection ([www.sb-](http://www.sb-)

roscoff.fr/Phyto/RCC/index.php) or the *Australian National Algae Culture Collection* ([www.marine.csiro.au/algaedb/default.htm](http://www.marine.csiro.au/algaedb/default.htm)), the *Culture Collection of Algae and Protozoa* ([www.ccap.ac.uk/index.htm](http://www.ccap.ac.uk/index.htm)) or even the *National Center for Marine Algae and Microbiota* (<https://ncma.bigelow.org/>). However, the first studies on a small number of microalgae species show that there is a large amount of intra-species diversity, whether at the genetic level [EVA 09] and/or at the level of the phenotype [MEN 12]. The exploitation of biodiversity in microalgae therefore seems to be an attractive potential source of improvement.

Unlike the improvement of plants and animals, which started in Antiquity, the first programs for the selection of microalgae only started recently, but benefit from methods and tools developed in other organisms. This transfer of knowledge could allow for the retrieval of improved microalgae strains relatively quickly.

Methods based on isolation have already allowed for the effective selection of microalgae strains [MOL 95], knowing that the use of chemical mutagen agents or even UV rays can cause changes leading to higher performances [BON 11]. Even if this generated diversity remains limited compared to diversity obtained from crossing [GRA 05], [SHA 91] used UV irradiation to mutate and then select strains of *Dunaliella bardawil* that are rich in beta-carotene. By using a similar process, [ALO 96] managed to increase the EPA content of the diatom *Phaeodactylum tricorutum* by 37%. More recently, [MEI 03] succeeded in increasing the production of EPA and DHA by 33% in *Pavlova lutheri* by using UV rays. Chemical mutagenesis agents, such as EMS (*ethyl methane sulfonate*), have also been used successfully to improve the production of a variety of compounds. Thus, [CHA 06] increased the production of EPA in *Nannochloropsis oculata* and [MEN 08] selected a strain that hyperproduced carotenoids in *Dunaliella salina*. The selection of cells can be operated manually by limit dilution or by micromanipulation [VIG 12]. However, automatic sorting techniques are a lot quicker, resulting in an increase in the number of cell sorted and, as a result, in a quicker selection of the desired population. The combination of a fluorescent vital marker and sorting by flow cytometry has been described for the selection of high lipid contents in *Tetraselmis suecica* [MON 10], *Nannochloropsis* sp. [DOA 12]. The latter added a chemical mutation step (CMS), while the combination of “UV mutagenesis” with an automation of the sorting in the flow cytometer to select for lipid-producing cells has been seen in the isochrysis *Tisochrysis lutea* [BEN 13], commonly cultivated in aquaculture. This strategy has led to a doubling of the total fatty acid content in this microalgae [BOU 12], and this in a stable manner over several years. These works have led to a patent in France of the first improved microalgae strain, in 2011 [ROU 11].

## 2.5. Conclusion

Thousands of microalgae are on shelves around the world and thousands remain to be discovered. Some of the main algal libraries provide for the many research teams that specialize in all the domains of application cited above. These libraries are distributed over the globe (see *supra*). Despite this, the quest for new species is the object of many projects, of various sizes. Aside from the laboratories that isolate one species for particular characteristics, large and ambitious programs finance prospective campaigns all over the world. One of the first was led by Craig Venter: on the ship *Sorcerer II* during the expedition: *Global Ocean Sampling Expedition* (GOS) ([www.sorcerer2expedition.org/](http://www.sorcerer2expedition.org/)). The same idea is behind all of the Tara cruises (<http://oceans.taraexpeditions.org/>), recently completed by the Oceanomics program, which aims to understand the biocomplexity and the biotechnological potential of oceanic plankton (<http://oceans.taraexpeditions.org/fr/>). This leads to the notion of metagenomics, reflecting the global sequencing of masses of water, “blindly”, for which the assembly and the interpretation would be carried out *a posteriori in silico*.

The estimation of the number of species will become more accurate in this way. In the mean time, we can read the review by Michael Guiry [GUI 12] as the most informative and balanced, which bases itself significantly on the site Algaebase: [www.algaebase.org/](http://www.algaebase.org/).

Out of the thousands of species known currently, only a few dozen are exploited. Surprisingly, all of the species are “as discovered”, in the same state that they were in when discovered, sometimes dozens of years ago, and placed in a tube. In 2013 less than five publications were on structured works of selection attempting to imitate the world of terrestrial plants so as to improve performances.

In terms of the valorization of biotechnology, microalgae present a series of advantages that are reflected in the high levels of global investment. The yields of dry biomass per square meter and per day are higher than for many terrestrial plants. It is true that the surfaces that are needed for cultivation in no way need to be cultivatable lands, on the contrary it must be noted that industrial cultures of marine microalgae would preserve freshwater reserves.

As for all plants, the vital sources come from fertilizer and carbon. These fertilizers can be supplied by urban or agricultural effluents or administered chemically. This is also true for carbon. We can imagine the use of gas taken from the bottom of industrial chimneys or the provision of pure gas from bottles. The culture of microalgae would then fit into an industrial environment as a system for the fixation of nitrogen, phosphorus, CO<sub>2</sub> or even heavy metals, for later use or valorization.

We are currently at the dawn of the appropriation of an original, extraordinary diverse plant that is still very little exploited. This plant source will complement terrestrial stocks, and its exploitation will profit from modern agricultural knowledge.

## 2.6. Bibliography

- [ABU 09] ABUGHAZALEH A.A., POTU R.B., IBRAHIM S., « Short communication: The effect of substituting fish oil in dairy cow diets with docosahexaenoic acid-micro algae on milk composition and fatty acids profile », *Journal of Dairy Science*, 92, 6156-6159, 2009.
- [ALO 96] ALONSO D.L., SEGURA DEL CASTILLO C.I., MOLINA GRIMA E., COHEN Z., « First insight into improvement of eicosapentaenoic acid content in *Phaeodactylum tricoratum* (Bacillariophyceae) by induced mutagenesis », *Journal of Phycology*, 32, 339-345, 1996.
- [APT 99] APT K.E., BEHRENS P.W., « Commercial developments in microalgal biotechnology », *Journal of Phycology*, 35, 215-226, 1999.
- [BAI 86] BAILEY J.E., OLLIS D.F., *Biochemical engineering fundamentals*, McGraw-Hill, New York, 1986.
- [BAO 07] BAO Z., WEATHERSPOON M.R., SHIAN S., CAI Y., GRAHAM P.D., ALLAN S.M., AHMAD G., DICKERSON M.B., CHURCH B.C., KANG Z., ABERNATHY III H.W., SUMMERS C.J., LIU M., SANDHAGE K.H., « Chemical reduction of three-dimensional silica micro-assemblies into microporous silicon replicas », *Nature*, 446, 172-175, 2007.
- [BAR 10] BARDOR M., LOUVET R., SAINT-JEAN B., BUREL C., CARLIER A., CADORET J.P., LEROUGE P., N-Glycosylation in transformed *Phaeodactylum tricoratum*, brevet : WO2012013337A1, 2010.
- [BEC 07] BECKER W., « Microalgae in Human and Animal Nutrition », dans A. Richmond (dir.), *Handbook of Microalgal Culture: Biotechnology and Applied Phycology*, Blackwell Publishing, Oxford, 2007.
- [BEN 13] BENDIF E.M., PROBERT I., SCHROEDER D.C., VARGAS C., « On the description of *Tisochrysis lutea* gen. nov. sp. nov. and *Isochrysis nuda* sp. nov. in the Isochrysidales, and the transfer of Dicrateria to the Prymnesiales (Haptophyta) », *Journal of Applied Phycology*, 2013.
- [BEN 97] BENEMANN J.R., « CO<sub>2</sub> mitigation with microalgae systems », *Energy Conversion and Management*, 38, S475-S479, 1997.
- [BHA 02] BHATTI S., HUERTAS I.E., COLMAN B., « Acquisition of Inorganic Carbon by the Marine Haptophyte *Isochrysis Galbana* (prymnesiophyceae)1 », *Journal of Phycology*, 38, 914-921, 2002.
- [BLA 05] BLACKMAN F.F., « Optima and Limiting Factors », *Annals of Botany*, os-19, 281-296, 1905.

- [BON 11] BONENTE G., FORMIGHIERI C., MANTELLI M., CATALANOTTI C., GIULIANO G., MOROSINOTTO T., BASSI R., « Mutagenesis and phenotypic selection as a strategy toward domestication of *Chlamydomonas reinhardtii* strains for improved performance in photobioreactors », *Photosynthesis Research*, 108, 107-120, 2011.
- [BOU 10] BOUGARAN G., BERNARD O., SCIANDRA A., « Modelling continuous cultures of microalgae colimited by nitrogen and phosphorus », *Journal of Theoretical Biology*, 265, 443-454, 2010.
- [BOU 03] BOUGARAN G., LE DÉAN L., LUKOMSKA E., KAAS R., BARON R., « Transient initial phase in continuous culture of *Isochrysis galbana affinis* Tahiti », *Aquatic Living Resources*, 16, 389-394, 2003.
- [BOU 12] BOUGARAN G., ROUXEL C., DUBOIS N., KAAS R., GROUAS S., LUKOMSKA E., LE COZ J.R., CADORET J.P., « Enhancement of neutral lipid productivity in the microalga *Isochrysis affinis Galbana* (T-Iso) by a mutation-selection procedure », *Biotechnology Bioengineering*, n/a, 2012.
- [BRI 04] BRITTON G., LIAAEN-JENSEN S., PFANDER H.P., *Handbook of Carotenoids*, Springer, Vienne, 2004.
- [BUI 03] BUITENHUIS E.T., TIMMERMANS K.R., DE BAAR H.J., « Zinc-bicarbonate colimitation of *Emiliania huxley* », *Limnology and Oceanography*, 48, 1575-1582, 2003.
- [BUM 11] BUMBAK F., COOK S., ZACHLEDER V., HAUSER S., KOVAR K., « Best practices in heterotrophic high-cell-density microalgal processes: achievements, potential and possible limitations », *Applied Microbiology and Biotechnology*, 91, 31-46, 2011.
- [BUO 12] BUONO S., LANGELLOTTI A.L., MARTELLO A., BIMONTE M., TITO A., CAROLA A., APONE F., COLUCCI G., FOGLIANO V., « Biological activities of dermatological interest by the water extract of the microalga *Botryococcus braunii* », *Archives of Dermatological Research*, 304, 755-764, 2012.
- [CAD 08a] CADORET J.P., BARDOR M., LEROUGE P., CABIGLIERA M., HENRIQUEZ V., CARLIER A., « Les microalgues : Usines cellulaires productrices de molécules commerciales recombinantes », *Médecine/Sciences*, 24, 375-382, 2008.
- [CAD 08b] CADORET J.P., BERNARD O., « La production de biocarburant lipidique avec des microalgues: promesses et défis », *Journal Société Biologie*, 202, 201-211, 2008.
- [CAD 09] CADORET J.P., CARLIER A., BUREL C., MAURY F., BARDOR M., LEROUGE P., Production of glycosylated proteins in microalgae, PCT/EP/2009/051672, 2009.
- [CAD 12] CADORET J.P., GARNIER M., SAINT-JEAN B., « Chapter Eight: Microalgae, Functional Genomics and Biotechnology », dans G. Piganeau (dir.), *Advances in Botanical Research*, p. 285-341, Academic Press, New York, 2012.
- [CAD 48] CADY J.B., MORGAN W.S., « Treatment of chronic ulcers with chlorophyll: Review of a series of fifty cases », *American Journal of Surgery*, 75, 562-569, 1948.
- [CAR 10] CARLIER A., MICHEL R., DUFOURMANTEL N., CADORET J.P., LEJEUNE A., Production of high mannose glycosylated proteins stored in the plastid of microalgae, EP10016162.9, 2010.



- [CHA 06] CHATURVEDI R., FUJITA Y., « Isolation of enhanced eicosapentaenoic acid producing mutants of *Nannochloropsis oculata* using ethyl methane sulfonate induced mutagenesis techniques and their characterization at mRNA transcript level », *Phycological Research*, 54, 208-219, 2006.
- [CHE 11] CHEPURNOV V.A., CHAERLE P., ROEF L., MEIRHAEGHE A., VANHOUTTE K., « Classical Breeding in Diatoms: Scientific Background and Practical Perspectives », dans J. Seckbach, P. Kociolek (dir.), *Cellular Origin, Life in Extreme Habitats and Astrobiology*, p. 167-194, Springer, Amsterdam, 2011.
- [CHI 67] CHIANG K.S., SUEOKA N., « Replication of chromosomal and cytoplasmic DNA during mitosis and meiosis in the eucaryote *Chlamydomonas reinhardi* », *Journal of Cellular Physiology*, 70, 89-112, 1967.
- [CHR 13] CHRISTAKI E., BONOS E., GIANNENAS I., FLOROU-PANERI P., « Functional properties of carotenoids originating from algae », *Journal of the Science of Food and Agriculture*, 93, 5-11, 2013.
- [COL 08] COLLARD B.C., MACKILL D.J., « Marker-assisted selection : an approach for precision plant breeding in the twenty-first century », *Philosophical Transaction of the Royal Society B: Biological Science*, 363, 557-572, 2008.
- [COM 94] COMBRES C., LALIBERTÉ G., REYSSAC J.S., DE LA NOÛE J., « Effect of acetate on growth and ammonium uptake in the microalgae *Scenedesmus obliquus* », *Plant Physiology*, 91, 729-734, 1994.
- [CON 09] CONVERTI A., CASAZZA A.A., ORTIZ E.Y., PEREGO P., DEL BORGHI M., « Effect of temperature and nitrogen concentration on the growth and lipid content of *Nannochloropsis oculata* and *Chlorella vulgaris* for biodiesel production », *Chemical Engineering and Processing: Process Intensification*, 48, 1146-1151, 2009.
- [COO 11] COONEY M.J., YOUNG G., PATE R., « Bio-oil from photosynthetic microalgae: Case study », *Bioresource Technology*, 102, 166-177, 2011.
- [CSO 99] CSOGOR Z., MELGAR D., SCHMIDT K., POSTEN C., « Production and particle characterization of the frustules of *Cyclotella cryptica* in comparison with siliceous earth », *Journal of Biotechnology: Biotechnological Aspects of Marine Sponges*, 70, 71-75, 1999.
- [DEL 07] DEL CAMPO J.A., GARCÍA-GONZÁLEZ M., GUERRERO M.G., « Outdoor cultivation of microalgae for carotenoid production: current state and perspectives », *Applied Microbiology and Biotechnology*, 74, 1163-1174, 2007.
- [DIC 87] DICKSON A.G., MILLERO F.J., « A comparison of the equilibrium constants for the dissociation of carbonic acid in seawater media », *Deep Sea Research Part I: Oceanographic Research Papers*, 34, 1733-1743, 1987.
- [DOA 12] DOAN T.T.Y., OBBARD J.P., « Enhanced intracellular lipid in *Nannochloropsis* sp. via random mutagenesis and flow cytometric cell sorting », *Algal Research*, 1, 17-21, 2012.
- [DRO 68] DROOP M.R., « Vitamin B12 and Marine Ecology. IV. The Kinetics of Uptake, Growth and Inhibition in *Monochrysis Lutheri* », *Journal of the Marine Biological Association of the United Kingdom*, 48, 689-733, 1968.

- [EIX 05] EIXLER S., SELIG U., KARSTEN U., « Extraction and detection methods for polyphosphate storage in autotrophic planktonic organisms », *Hydrobiologia*, 533, 135-143, 2005.
- [ELR 85] ELRIFI I.R., TURPIN D.H., « Steady-state luxury consumption and the concept of optimum nutrient ratios: a study with phosphate and nitrate limited *selenastrum minutum* (chlorophyta) », *Journal of Phycology*, 21, 592-602, 1985.
- [EPP 72] EPPLEY R.W., « Temperature and phytoplankton growth in the sea », *Fish Bulletin*, 70, 1972.
- [EVA 09] EVANS K.M., CHEPURNOV V.A., SLUIMAN H.J., THOMAS S.J., SPEARS B.M., MANN D.G., « Highly Differentiated Populations of the Freshwater Diatom *Sellaphora capitata* Suggest Limited Dispersal and Opportunities for Allopatric Speciation », *Protist*, 160, 386-396, 2009.
- [FAL 75] FALKOWSKI P.G., « Nitrate Uptake in Marine Phytoplankton: Comparison of Half-Saturation Constants from Seven Species », *Limnology and Oceanography*, 20, 412-417, 1975.
- [FAN 11] FAN J., ANDRE C., XU C., « A chloroplast pathway for the de novo biosynthesis of triacylglycerol in *Chlamydomonas reinhardtii* », *FEBS Letters*, 23, 585(12), 1985-91, 2011.
- [FAR 06] FARINEAU J., MOROT-GAUDRY J.F., *La Photosynthèse : processus physiques, moléculaires et physiologiques*, Editions Quae, Versailles, 2006.
- [FIN 10] FINAZZI G., MOREAU H., BOWLER C., « Genomic insights into photosynthesis in eukaryotic phytoplankton », *Trends in Plant Science*, 15, 565-572, 2010.
- [FOU 09] FOURNIER-LEVEL A., LE CUNFF L., GOMEZ C., DOLIGEZ A., AGEORGES A., ROUX C., BERTRAND Y., SOUQUET J.M., CHEYNIER V., THIS P., « Quantitative Genetic Bases of Anthocyanin Variation in Grape (*Vitis vinifera* L. ssp. *sativa*) Berry: A Quantitative Trait Locus to Quantitative Trait Nucleotide Integrated Study », *Genetics*, 183, 1127-1139, 2009.
- [GAD 09] GADD G.M., « Biosorption: critical review of scientific rationale, environmental importance and significance for pollution treatment », *Journal of Chemical Technology and Biotechnology*, 84, 13-28, 2009.
- [GAG 12] GAGEZ A.L., THIERY V., PASQUET V., CADORET J.P., PICOT L., « Epoxycarotenoids and Cancer », *Review Current Bioactive Compounds*, 8, 109-141, 2012.
- [GEI 02] GEIDER R., LA ROCHE J., « Redfield revisited: variability of C:N:P in marine microalgae and its biochemical basis », *European Journal of Phycology*, 37, 1-17, 2002.
- [GEI 87] GEIDER R.J., « Light and Temperature Dependence of the Carbon to Chlorophyll a Ratio in Microalgae and Cyanobacteria: Implications for Physiology and Growth of Phytoplankton », *New Phytologist*, 106, 1-34, 1987.
- [GLA 94] GLADUE R.M., MAXEY J.E., « Microalgal feeds for aquaculture », *Journal of Applied Phycology*, 6, 131-141, 1994.
- [GOR 09] GORDON R., LOSIC D., TIFFANY M.A., NAGY S.S., STERRENBURG F.A.S., « The Glass Menagerie: diatoms for novel applications in nanotechnology », *Trends in Biotechnology*, 27, 116-127, 2009.

- [GOU 08] GOUVEIA L., COUTINHO C., MENDONCA E., BATISTA A.P., SOUSA I., BANDARRA N.M., RAYMUNDO A., « Functional biscuits with PUFA-omega 3 from *Isochrysis galbana* », *Journal of the Science of Food and Agriculture*, 88, 891-896, 2008.
- [GRA 05] GRAPPUTO A., KUMPULAINEN T., MAPPES J., PARRI S., « Genetic diversity in populations of asexual and sexual bag worm moths (Lepidoptera: Psychidae) », *BMC Ecology*, 5, 5, 2005.
- [GRO 03] GROBBELAAR J.U., KURANO N., « Use of photoacclimation in the design of a novel photobioreactor to achieve high yields in algal mass cultivation », *Journal of Applied Phycology*, 15, 121-126, 2003.
- [GUE 03] GUERIN M., HUNTLEY M.E., OLAIZOLA M., « *Haematococcus* astaxanthin: applications for human health and nutrition », *Trends in Biotechnology* 21, 210-216, 2003.
- [GUI 12] GUIRY M.D., « How many species of algae are there? », *Journal of Phycology*, 48, 1057-1063, 2012.
- [HAI 13] HAIMOVICH-DAYAN M., GARFINKEL N., EWE D., MARCUS Y., GRUBER A., WAGNER H., KROTH P.G., KAPLAN A., « The role of C<sub>4</sub> metabolism in the marine diatom *Phaeodactylum tricorutum* », *New Phytologist*, 197, 177-185, 2013.
- [HAR 01] HARRIS E.H., « *Chlamydomonas* as a Model Organism », *Annual Review of Plant Physiology and Plant Molecular Biology*, 52, 363-406, 2001.
- [HEM 11] HEMPEL F., LAU J., KLINGL A., MAIER U.G., « Algae as Protein Factories: Expression of a Human Antibody and the Respective Antigen in the Diatom *Phaeodactylum tricorutum* », *PLoS One*, 6, e28424, 2011.
- [HER 11] HEREDIA-ARROYO T., WEI W., RUAN R., HU B., « Mixotrophic cultivation of *Chlorella vulgaris* and its potential application for the oil accumulation from non-sugar materials », *Biomass Bioenergy*, 35, 2245-2253, 2011.
- [HOR 51] HORWITH B., « Role of chlorophyll in proctology », *American Journal of Surgery*, 81, 81-84, 1951.
- [JEN 01] JENSEN G.S., GINSBERG D., DRAPEAU C., « Blue-Green Algae as an Immuno-Enhancer and Biomodulator », *Journal of the American Nutraceutical Association*, 3, 24-30, 2001.
- [JON 12] JONES C.S., LUONG T., HANNON M., TRAN M., GREGORY J.A., SHEN Z., BRIGGS S.P., MAYFIELD S.P., « Heterologous expression of the C-terminal antigenic domain of the malaria vaccine candidate Pfs48/45 in the green algae *Chlamydomonas reinhardtii* », *Applied Microbiology and Biotechnology*, 97, 1987-1995, 2012.
- [KEE 99] KEELING P.J., DEANE J.A., HINK-SCHAUER C., DOUGLAS S.E., MAIER U.G., MCFADDEN G.I., « The secondary endosymbiont of the cryptomonad *Guillardia theta* contains Alpha-, Beta-, and Gamma-tubulin Genes », *Molecular Biology and Evolution*, 16, 1308-1313, 1999.
- [KIR 94] KIRK J.T.O., *Light and photosynthesis in aquatic ecosystems*, 2<sup>e</sup> édition, Cambridge University Press, Cambridge, 1994.

- [KO12] KO S.C., KIM D., JEON Y.J., « Protective effect of a novel antioxidative peptide purified from a marine *Chlorella ellipsoidea* protein against free radical-induced oxidative stress », *Food and Chemical Toxicology*, 50, 2294-2302, 2012.
- [KUE 65] KUENZLER E.J., PERRAS J.P., « Phosphatases of Marine Algae », *Biological Bulletin*, 128, 271-284, 1965.
- [LAL 93] LALIBERTÉ G., DE LA NOÛE J., « Auto-, hetero-, and mixotrophic growth of *chlamydomonas humicola* (cmloroimiyckak) on acetate1 », *Journal of Phycology*, 29, 612-620, 1993.
- [LAN 11] LANGRIDGE P., FLEURY D., « Making the most of “omics” for crop breeding », *Trends in Biotechnology*, 29, 33-40, 2011.
- [LEE 99] LEE C.G., « Calculation of light penetration depth in photobioreactors », *Biotechnology and Bioprocess Engineering*, 4, 78-81, 1999.
- [LEE 97] LEE Y.K., « Commercial production of microalgae in the Asia-Pacific rim », *Journal of Applied Phycology*, 9, 403-411, 1997.
- [LEJ 10] LEJEUNE A., MICHEL R., CADORET J.P., CARLIER A., Secretion of recombinant polypeptides in the extracellular medium of diatoms, EP10013808.0, 2010.
- [LIA 09] LIANG Y., SARKANY N., CUI Y., « Biomass and lipid productivities of *Chlorella vulgaris* under autotrophic, heterotrophic and mixotrophic growth conditions », *Biotechnology Letters*, 31, 1043-1049, 2009.
- [LIE 55] LIEBIG J.F. VON, *Principles of Agricultural Chemistry: With Special Reference to the Late Researches Made in England*, Walton & Maberly, Londres, 1855.
- [LOM 00] LOMAS M.W., GLIBERT P.M., « Comparisons of nitrate uptake, storage, and reduction in marine diatoms and flagellates », *Journal of Phycology*, 36, 903-913, 2000.
- [LUA 11] LUANGPIPAT T., BEATTIE I.R., CHISTI Y., HAVERKAMP R.G., « Gold nanoparticles produced in a microalga », *Journal of Nanoparticle Research*, 13, 6439-6445, 2011.
- [MAC 02] MACINTYRE H.L., KANA T.M., ANNING T., GEIDER R.J., « Photoacclimation of Photosynthesis Irradiance Response Curves and Photosynthetic Pigments in Microalgae and Cyanobacteria1 », *Journal of Phycology*, 38, 17-38, 2002.
- [MAR 13] MARCHETTI J., BOUGARAN G., JAUFFRAIS T., LEFEBVRE S., ROUXEL C., SAINT-JEAN B., LUKOMSKA E., ROBERT R., CADORET J.P., « Effects of blue light on the biochemical composition and photosynthetic activity of *Isochrysis* sp. (T-iso) », *Journal of Applied Phycology*, 25, 109-119, 2013.
- [MAR 12] MARCHETTI J., BOUGARAN G., LE DEAN L., MÉGRIER C., LUKOMSKA E., KAAS R., OLIVO E., BARON R., ROBERT R., CADORET J.P., « Optimizing conditions for the continuous culture of *Isochrysis affinis galbana* relevant to commercial hatcheries », *Aquaculture*, 326-329, 106-115, 2012.
- [MEI 03] MEIRELES L., GUEDES A.C., MALCATA F.X., « Increase of the yields of eicosapentaenoic and docosahexaenoic acids by the microalga *Pavlova lutheri* following random mutagenesis », *Biotechnology Bioengineering*, 81, 50-55, 2003.

- [MEL 09] MELIS A., « Solar energy conversion efficiencies in photosynthesis: Minimizing the chlorophyll antennae to maximize efficiency », *Plant Science*, 177, 272-280, 2009.
- [MEN 09] MENDES A., REIS A., VASCONCELOS R., GUERRA P., LOPES DA SILVA T., « *Cryptocodinium cohnii* with emphasis on DHA production: a review », *Journal of Applied Phycology*, 21, 199-214, 2009.
- [MEN 12] MENDOZA GUZMÁN H., JARA VALIDO A., FREIJANES PRESMANES K., CARMONA DUARTE L., « Quick estimation of intraspecific variation of fatty acid composition in *Dunaliella salina* using flow cytometry and Nile Red », *Journal of Applied Phycology*, 24, 1237-1243, 2012.
- [MEN 08] MENDOZA H., DE LA JARA A., FREIJANES K., CARMONA L., RAMOS A.A., DE SOUSA DUARTE V., VALERA J.C.S., « Characterization of *Dunaliella salina* strains by flow cytometry: a new approach to select carotenoid hyperproducing strains », *Electronic Journal Biotechnology*, 11, 1-13, 2008.
- [MER 07] MERCHANT S.S., « The *Chlamydomonas* genome reveals the evolution of key animal and plant functions », *Science*, 318, 245-250, 2007.
- [MOL 95] MOLINA GRIMA E., SANCHEZ PEREZ J.A., GARCIA CAMACHO F., MEDINA, A.R., GIMENEZ, ALONSO D.L., « The production of polyunsaturated fatty acids by microalgae: from strain selection to product purification », *Process Biochemistry*, 30, 711-719, 1995.
- [MON 10] MONTERO M., ARISTIZABAL M., GARCIA REINA G., « Isolation of high-lipid content strains of the marine microalga *Tetraselmis suecica* for biodiesel production by flow cytometry and single-cell sorting », *Journal of Applied Phycology*, 1-5, 2010.
- [MOR 12] MOREIRA I. DE O., PASSOS T.S., CHIAPINNI C., SILVEIRA G.K., SOUZA J.C., COCAVELLARDE L.G., DELIZA R., DE LIMA ARAÚJO K.G., « Colour evaluation of a phycobiliprotein-rich extract obtained from *Nostoc* PCC9205 in acidic solutions and yogurt », *Journal of the Science of Food and Agriculture*, 92, 598-605, 2012.
- [MUR 07] MURPHY D., *Plant Breeding and Biotechnology*, Cambridge University Press, Cambridge, 2007.
- [OGB 03] OGBONNA J.C., « Photobioreactors », *Recent Advance in Marine Biotechnology*, vol. 9, 315-348, 2003.
- [OLI 07] OLIVO E., Conception et étude d'un photobioréacteur pour la production en continu de microalgues en écloséries aquacoles, Université de Nantes, 2007.
- [PAH 09] PAHLOW M., OSCHLIES A., « Chain model of phytoplankton P, N and light colimitation », *Marine Ecology Progress Series*, 376 in file, 69-83, 2009.
- [PAU 95] PAULY D., CHRISTENSEN V., « Primary production required to sustain global fisheries », *Nature*, 374, 255-257, 1995.
- [PER 11] PEREZ-GARCIA O., ESCALANTE F.M.E., DE-BASHAN L.E., BASHAN Y., « Heterotrophic cultures of microalgae: Metabolism and potential products », *Water Research*, 45, 11-36, 2011.

- [POT 10] POTVIN G., ZHANG Z., « Strategies for high-level recombinant protein expression in transgenic microalgae: A review », *Biotechnology Advances*, 28, 910-918, 2010.
- [PUL 01] PULZ O., « Photobioreactors: Production systems for phototrophic microorganisms », *Applied Microbiology and Biotechnology*, 57(3), 287-293, 2001.
- [PUL 04] PULZ O., GROSS W., « Valuable products from biotechnology of microalgae », *Applied Microbiology and Biotechnology*, 65, 635-648, 2004.
- [RAP 13] RAPOSO M., DE MORAIS R., BERNARDO DE MORAIS A., « Bioactivity and applications of sulphated polysaccharides from marine microalgae », *Marine Drugs*, 11, 233-252, 2013.
- [RAV 99] RAVEN J.A., FALKOWSKI P.G., « Oceanic sinks for atmospheric CO<sub>2</sub> », *Plant Cell and Environment*, vol. 22, 741-755, 1999.
- [RED 34] REDFIELD A.C., On the proportions of organic derivatives in sea water and their relation to the composition of plankton, University Press of Liverpool, Liverpool, 1934.
- [REX 02] REXACH J., LLAMAS A., FERNANDEZ E., GALVAN A., « The activity of the high-affinity nitrate transport system I (NRT2;1, NAR2) is responsible for the efficient signalling of nitrate assimilation genes in *Chlamydomonas reinhardtii* », *Planta*, vol. 215, 606-611, 2002.
- [RHE 78] RHEE G.Y., « Effects of N:P atomic ratios and nitrate limitation on algal growth, cell composition, and nitrate uptake », *Limnology and Oceanography*, 23, 10-24, 1978.
- [RIC 08] RICHMOND A., *Handbook of Microalgal Culture: Biotechnology and Applied Phycology*, John Wiley, New York, 2008.
- [RIC 06] RICO-VILLA B., LE COZ J.R., MINGANT C., ROBERT R., « Influence of phytoplankton diet mixtures on microalgae consumption, larval development and settlement of the Pacific oyster *Crassostrea gigas* (Thunberg) », *Aquaculture*, 256, 377-388, 2006.
- [ROB 09] ROBERTSON C.A., EVANS D.H., ABRAHAMSE H., « Photodynamic therapy (PDT): A short review on cellular mechanisms and cancer research applications for PDT », *Journal of Photochemistry and Photobiology*, B 96, 1-8, 2009.
- [ROS 12] RÖSCH C., POSTEN C., « Challenges and Perspectives of Microalgae Production », *Technikfolgenabschätzung*, 5-16, 2012.
- [ROS 10] ROSELLO SASTRE R., POSTEN C., « Die vielfältige Anwendung von Mikroalgen als nachwachsende Rohstoffe », *Chemie Ingenieur Technik*, 82, 1925-1939, 2010.
- [ROU 11] ROUXEL C., BOUGARAN G., DOULIN-GROUAS S., DUBOIS N., CADORET J.-P., Novel isochrysis sp tahitian clone and uses therefore, EP 11006712.1, 2011.
- [SAI 08] SAITO M.A., GOEPFERT T.J., RITT J.T., « Some thoughts on the concept of colimitation: Three definitions and the importance of bioavailability », *Limnology and Oceanography*, 53, 276-290, 2008.
- [SCA 10] SCARSELLA M., BELOTTI G., DE FILIPPIS P., BRAVI M., « Study on the optimal growing conditions of *Chlorella vulgaris* in bubble column photobioreactors », *Chemical Engineering Transactions*, 20, 85-90, 2010.
- [SCH 04] SCHMIDT F.R., « Recombinant expression systems in the pharmaceutical industry », *Applied Microbiology and Biotechnology*, 65(4), 363-72. 2004

- [SCH 13] SCHWENZFEIER A., HELBIG A., WIERENGA P.A., GRUPPEN H., « Emulsion properties of algae soluble protein isolate from *Tetraselmis* sp. », *Food Hydrocolloids*, 30, 258-263, 2013.
- [SCR 99] SCRIBAN R., *Biotechnologie*, Lavoisier Tec.&Doc, Paris, 1999.
- [SHA 91] SHAISH A., BEN-AMOTZ A., AVRON M., « Production and selection of high beta-carotene mutants of *Dunaliella bardawil* (Chlorophyta) », *Journal of Phycology*, 27, 652-656, 1991.
- [SHE 98] SHEEHAN J., DUNAHAY T., BENEMANN J., ROESSLER P., « A Look Back at the U.S. Department of Energy's Aquatic Species program: Biodiesel from Algae », *Golden*, 1998.
- [SHI 99] SHI X.M., CHEN F., « Production and rapid extraction of lutein and the other lipid-soluble pigments from *Chlorella protothecoides* grown under heterotrophic and mixotrophic conditions », *Food Research*, 43, 109-113, 1999.
- [SHI 00] SHI X.M., ZHANG X.W., CHEN F., « Heterotrophic production of biomass and lutein by *Chlorella protothecoides* on various nitrogen sources. Enzyme Microb », *Enzyme and Microbial Technology*, 27, 312-318, 2000.
- [SOL 10] SOLOMON C.M., COLLIER J.L., MINE BERG G., GLIBERT P.M., « Role of urea in microbial metabolism in aquatic systems: a biochemical and molecular review », *Aquatic Microbial Ecology*, 59, 67-88, 2010.
- [SOU 12] SOUZA P.O., FERREIRA L.R., PIRES N.R., DUARTE F.A., PEREIRA C.M., MESKO M.F., « Algae of economic importance that accumulate cadmium and lead: a review », *Revista Brasileira de Farmacognosia*, 22, 825-837, 2012.
- [SPO 06] SPOLAORE P., JOANNIS-CASSAN C., DURAN E., ISAMBERT A., « Commercial applications of microalgae », *Journal of Bioscience and Bioengineering*, 101, 87-96, 2006.
- [STA 98] STADNICHUK I.N., RAKHIMBERDIEVA M.G., BOLYCHEVTSEVA Y.V., YURINA N.P., KARAPETYAN N.V., SELYAKH I.O., « Inhibition by glucose of chlorophyll a and phycocyanobilin biosynthesis in the unicellular red alga *Galdieria partita* at the stage of coproporphyrinogen III formation », *Plant Science*, 136, 11-23, 1998.
- [TAC 08] TACON A.G.J., METIAN M., « Global overview on the use of fish meal and fish oil in industrially compounded aquafeeds: Trends and future prospects », *Aquaculture*, 285, 146-158, 2008.
- [TES 10] TESTER M., LANGRIDGE P., « Breeding Technologies to Increase Crop Production in a Changing World », *Science*, 327, 818-822, 2010.
- [TRA 13] TRAN M., VAN C., BARRERA D.J., PETERSSON P.L., PEINADO C.D., BUI J., MAYFIELD S.P., « Production of unique immunotoxin cancer therapeutics in algal chloroplasts », *Proceedings of the National Academy of Sciences*, 110, E15-E22, 2013.
- [TRE 98] TREDICI M.R., ZITTELLI G.C., « Efficiency of sunlight utilization: Tubular versus flat photobioreactors », *Biotechnology Bioengineering*, 57, 187-197, 1998.
- [TSY 01] TSYGANKOV A.A., « Laboratory Scale Photobioreactors », *Applied Biochemistry and Microbiology*, 37, 333-341, 2001.

- [TUL 12] TULLI F., CHINI ZITTELLI G., GIORGI G., POLI B.M., TIBALDI E., TREDICI M.R., « Effect of the Inclusion of Dried *Tetraselmis suecica* on Growth, Feed Utilization, and Fillet Composition of European Sea Bass Juveniles Fed Organic Diets », *Journal of Aquatic Food Product Technology*, 21, 188-197, 2012.
- [UKE 76] UKELES R., ROSE W.E., « Observations on organic carbon utilization by photosynthetic marine microalgae », *Marine Biology*, 37, 11-28, 1976.
- [ULU 11] ULUKAN H., « The use of plant genetic resources and biodiversity in classical plant breeding », *Acta Agriculturae Scandinavica Section B – Soil and Plant Science*, 61, 97-104, 2011.
- [VAR 09] VARSHNEY R.K., NAYAK S.N., MAY G.D., JACKSON S.A., « Next-generation sequencing technologies and their implications for crop genetics and breeding », *Trends in Biotechnology*, 27, 522-530, 2009.
- [VIG 12] VIGEOLAS H., DUBY F., KAYMAK E., NIESSEN G., MOTTE P., FRANCK F., REMACLE C., « Isolation and partial characterization of mutants with elevated lipid content in *Chlorella sorokiniana* and *Scenedesmus obliquus* », *Journal of Biotechnology*, 162, 3-12, 2012.
- [VIL 11] VÍLCHEZ C., FORJÁN E., CUARESMA M., BÉDMAR F., GARBAYO I., VEGA J.M., « Marine Carotenoids: Biological Functions and Commercial Applications », *Marine Drugs*, 9, 319-333, 2011.
- [WAN 12] WAN L., HAN J., SANG M., LI A., WU H., YIN S., ZHANG C., « De Novo Transcriptomic Analysis of an Oleaginous Microalga: Pathway Description and Gene Discovery for Production of Next-Generation Biofuels », *PLoS ONE*, 7, e35142, 2012.
- [WAN 08] WANG Y., PENG J., « Growth-associated biosynthesis of astaxanthin in heterotrophic *Chlorella zofingiensis* (Chlorophyta) », *World Journal of Microbiology and Biotechnology*, 24, 1915-1922, 2008.
- [WIJ 10] WIJFFELS R.H., BARBOSA M.J., EPPINK M.H.M., « Microalgae for the production of bulk chemicals and biofuels », *Biofuels Bioproducts and Biorefining*, 4, 287-295, 2010.
- [WIN 11] WINTER J.M., BEHNKEN S., HERTWECK C., « Genomics-inspired discovery of natural products », *Current Opinion in Chemical Biology*, 15, 22-31, 2011.
- [XU08] XU Y., CROUCH J.H., « Marker-Assisted Selection in Plant Breeding: From Publications to Practice », *Crop Science*, 48, 391-407, 2008.
- [YAN 00] YANG C., HUA Q., SHIMIZU K., « Energetics and carbon metabolism during growth of microalgal cells under photoautotrophic, mixotrophic and cyclic light-autotrophic/dark-heterotrophic conditions », *Biochemical Engineering Journal*, 6, 87-102, 2000.
- [YEH 09] YEH N., CHUNG J.P., « High-brightness LEDs—Energy efficient lighting sources and their potential in indoor plant cultivation », *Renewable and Sustainable Energy Reviews*, 13, 2175-2180, 2009.
- [YU 11] YU S., LIU S., LI C., ZHOU Z., « Submesoscale characteristics and transcription of a fatty acid elongase gene from a freshwater green microalgae, *Myrmecia incisa* Reisingl », *Chinese Journal of Oceanology and Limnology*, 29, 87-95, 2011.



- [ZHA 13] ZHANG Y., WHITE M.A., COLOSI L.M., « Environmental and economic assessment of integrated systems for dairy manure treatment coupled with algae bioenergy production », *Bioresource Technology*, 130, 486-494, 2013.
- [ZHA 11] ZHAO R., CAO Y.U., XU H., LV L., QIAO D., CAO Y.I., « Analysis of Expressed Sequence Tags From The Green Alga *Dunaliella Salina* (Chlorophyta)1 », *Journal of Phycology*, 47, 1454-1460, 2011.
- [ZHU 97] ZHU C., LEE Y., CHAO T., « Effects of temperature and growth phase on lipid and biochemical composition of *Isochrysis galbana* TK1 », *Journal of Applied Phycology*, 9, 451-457, 1997.
- [ZUC 01] ZUCCHI M.R., NECCHI O., « Effects of temperature, irradiance and photoperiod on growth and pigment content in some freshwater red algae in culture », *Phycological Research*, 49, 103-114, 2001.



# Microalgae, Functional Genomics and Biotechnology

Jean-Paul Cadoret<sup>1,\*</sup>, Matthieu Garnier\*, and Bruno Saint-Jean\*

\*Ifremer, Laboratoire Physiologie et Biotechnologie des Algues, rue de l'île d'Yeu BP 21105 44311 Nantes cedex 3, France

<sup>1</sup>Corresponding author: E-mail: jean.paul.cadoret@ifremer.fr

## Contents

|  |     |
|--|-----|
| 1. Introduction  | 286 |
| 1.1. Microalgae  | 286 |
| 1.2. Applications of Microalgae  | 288 |
| 1.3. Genomics and Microalgae   | 290 |
| 2. Biotechnology and Microalgae  | 292 |
| 2.1. Microalgal Lipids as Biofuel and Food                                       | 295 |
| 2.1.1. <i>Algal Lipid Synthesis: The Contribution of Genomic Data</i>            | 295 |
| 2.1.2. <i>Algal Lipids as Biofuel</i>  | 296 |
| 2.1.3. <i>Algal Lipids as Feed and Food</i>                                      | 299 |
| 2.2. Bioactive Natural Products  | 299 |
| 2.3. Molecular Farming   | 301 |
| 2.3.1. <i>Transgenic Microalgae as a Platform for Biopharmaceutical Proteins</i> | 302 |
| 2.3.2. <i>Genomic Strategies for Optimising Recombinant Protein Expression</i>   | 311 |
| 3. Future Outlook  | 323 |
| 3.1. Domestication   | 323 |
| 3.2. Working Towards a New Algal Metabolism, Enzymes and Compounds               | 325 |
| 3.3. Algal Pathogens: Looking Towards the Future                                 | 326 |
| 4. Conclusions   | 328 |
| References   | 329 |

## Abstract

Microalgae have been studied for decades, but a new wave of research has recently begun as part of the search for renewable and sustainable energy sources. For economic optimization, microalgal biomass is being considered as a whole (main products and co-products) in an overall 'biorefinery' concept. Applications of microalgae cover a broad spectrum, including the food and (livestock) feed industries, bio-energy, cosmetics, healthcare and environmental restoration or protection. In the field of biotechnology, the access to genomic data is playing a growing role. As the cost of sequencing strategies has fallen, studies of gene function at the transcript, protein and biosynthesis pathway levels have multiplied. Notably, sequencing and mass spectrometry technologies are used to delineate the pathways of lipid synthesis, which will

be valuable for the future application of microalgae in the biotechnology and biofuel industries. Another field making an applied use of genomics is the 'cell factory' approach, which uses the cell to manufacture (express) natural or recombinant proteins for diverse purposes. In this chapter, we present a vision of the potential future of genomics in the biotechnology of microalgae from several points of view.



## 1. INTRODUCTION

Microalgae in biotechnology are presently the focus of an unprecedented surge in interest and investment worldwide. Over recent decades, research predicted the explosion of attention this field would attract following the U.S. Aquatic Species Program (Sheehan, Dunahay, Benemann, & Roessler, 1998), as microalgae can provide a new source of vegetal material. They offer complementary products to land plants and higher manipulability, but as the consequence of their large phylogenetic spread (reviewed in Chapter I of this volume), they have vast unknown metabolic potential because most species are, as yet, unexamined.

Driven by the giants of the energy industry, the race to develop mass microalgal production capacity started about 5 years ago, fuelled by hundreds of millions of U.S. dollars targeting the production of renewable biofuels. The challenges we face today are to adapt and improve existing methods, develop new processes and achieve a drastic reduction in costs. The objective is to use this green biomass in its entirety and not only for energy production. The potential is huge and the fields of study numerous, offering very high added value in the areas of new energy (oil, hydrogen and fermentation), healthcare (pigments, enzymes and secondary metabolites), food (human or animal), environmental management (depuration and assimilation mechanisms) and industry (recovery of silica, enzymes or pigments). Here, we have chosen to focus our presentation on the world of microalgae, their broad fields of application, the advances in genomics for biotechnologies and some of the bottlenecks that need to be overcome.

### 1.1. Microalgae

We use the term *microalgae* to cover a heterogeneous group of single-celled photosynthetic organisms, including photosynthetic eukaryotes and photosynthetic prokaryotes like *Prochlorococcus* and *Synechococcus*, which are of major global importance and considered as key players among phytoplanktonic organisms in oligotrophic oceanic areas. It would be vastly overambitious to attempt to cover the biotechnological potential of the

entire aquatic photosynthetic world in one book chapter, so this review will address only the genomics and biotechnology of eukaryotic microalgae.

Depending on environmental conditions such as salinity, light, temperature, pH and nutrient concentrations, the size and appearance of microalgae can change profoundly, making their identification difficult without molecular tools. The estimated number of described species ranges between 40,000 and 60,000, but estimations of the number of undescribed species range from hundreds of thousands to millions of species spread over the globe (Norton, Melkonian, & Andersen, 1996, Sastre & Posten, 2010). In comparison, only 250,000 land plant species have been recorded. Half of the world's oxygen is produced via microalgal photosynthesis. Microalgae contribute up to 50% of all aquatic productivity and 25% of global productivity (Raven & Falkowski, 1999). They are the foundation of the aquatic food chain and have colonized nearly all biotopes from the polar ice to deserts and hot springs. They have adapted to extreme environments, living in salt marshes, acidic environments or conditions with very low light. Through their presence on the surface of the oceans, which cover 70% of the earth, they play a major role in global climate regulation, as a machine that transforms CO<sub>2</sub> into organic matter (Raven & Falkowski, 1999).

Ancestors of the present day cyanobacteria invented photosynthesis as far back as 3.6 billion years ago (Gould, Waller, & McFadden, 2008) and the primary endosymbiotic event at the origin of all photosynthetic eukaryotes can be traced to 1.8 billion years ago (Finazzi, Moreau, & Bowler, 2010). The number and the diversity of algal species offer a whole new field of research when considering their potential commercial applications and biotechnology. Although progress still needs to be made on culture techniques, algal production systems on scales from a few litres up to cubic metre volumes, in photobioreactors or open ponds, are now a reality at the industrial level. Microalgae have clear advantages over land plants. Their photosynthetic yields are slightly better than those of land plants (Wijffels, Barbosa, & Eppink, 2010) and the fact that they live in an aqueous medium gives them direct access to their nutrients and explains why they display higher growth productivity. As an example, the productivity of classic crops in Europe is around 1–2 g/m<sup>2</sup>/day (dry weight), whereas the microalgae in small and medium-sized enterprises on the Atlantic coast produce around 10 g/m<sup>2</sup>/day. Additionally, aqueous cultures in marine water offer the advantage of using land unsuitable for food crops, avoiding the much-publicized dilemma between 'food and fuel'. Other differences between land plants and microalgae that could give microalgae the advantage include

the possibility of performing continuous cultures in photobioreactors with a high level of control, the potential to couple microalgal production with the disposal of effluents that provide nutritive components, the attractive idea of using industrial CO<sub>2</sub> sources and the saving of freshwater by cultivation of microalgae in seawater. The opportunity to cultivate in photobioreactors offers the additional possibility of adjusting and adapting culture conditions in real time, allowing growers to react instantaneously to the culture situation. The biological diversity of microalgae provides an exceptional range of adaptability and represents a vast potential as a source of food and feed, biomaterial, original molecules and applications in the broad field of biotechnology. Gene transfer of the means to produce selected molecules by genetic engineering will provide a complementary production method for novel compounds.

## 1.2. Applications of Microalgae

The current and forthcoming applications of microalgae are numerous and diverse, including food, feed, healthcare, industry and energy. Although the use of cyanobacteria in food dates back many hundreds of years, advances in this area were made in the 20th century (Habib, Huntington, & Hasan, 2008). The market for microalgae as food and food supplements is dominated by the Cyanobacteria *Spirulina platensis* (also called *Arthrospira platensis*), the Chlorophyta *Chlorella* sp., and in France, the diatom *Odontella aurita*. In addition, the green microalga *Dunaliella salina* is used for its beta-carotene, *Haematococcus pluvialis* for astaxanthin and the Cyanobacteria *Aphanizomenon flos-aquae* as a dietary supplement. Investigation is still needed on the use of other microalgae as food, requiring effort to be made for the acceptance of these alternative sources. For example, cookies made from the Haptophyta *Isochrysis galbana*, rich in omega-3, have already been produced (Gouveia *et al.*, 2008).

The area in which microalgae were first mass produced was aquaculture. Phytoplanktonic organisms are an essential food for the rearing of molluscs and fish, especially to feed the early life stages of bivalves, for which microalgae must be provided as live food. A large production capacity is devoted to this activity worldwide. Although around 40 microalgal species are used in this way, the number routinely grown is closer to a dozen. The technology and skills developed as part of this culture are important for the future of microalgal biotechnology. Microalgae could become an important source of land animal feed. The most common species used for this are

*Spirulina*, *Chlorella* and *Scenedesmus*. In chicken farming, it is reported that the incorporation of 5–10% microalgae in the diet has an effect on the colour of the meat and egg yolk (Becker, 2007). The potential substitution of fish oil with algae oil has also been discussed (AbuGhazaleh, Potu, & Ibrahim, 2009).

Algae also offer several benefits in the field of human healthcare. Land plants and animals lack the enzymes to synthesise polyunsaturated fatty acids (PUFAs) longer than 18 carbon atoms. Long-chain PUFAs like gamma-linolenic, arachidonic (AA), eicosapentaenoic (EPA) and docosahexaenoic acid (DHA), produced by microalgae, accumulate in most marine animals. Sufficient consumption of such fatty acids could have beneficial effects on human health. The oil from the stramenopile *Schizochytrium* sp. (permitted as a food ingredient) contains 35–45% DHA. In comparison, most conventional oils rich in omega-3 (walnut oil, canola oil) contain about 10% alpha-linolenic acid, the precursor of omega-3. The production of these PUFAs will undoubtedly be a major challenge in the coming years.

Algal pigments, such as carotenoids, are already commercially exploited but are also the subject of intensive research. The most popular among these are beta-carotene, alpha-carotene, lutein, lycopene and zeaxanthin. Even though the main supply of astaxanthin to colour salmon is 95% of synthetic origin, natural sources such as the green microalga *H. pluvialis* are authorized in Japan and Canada (Lorenz & Cysewski, 2000). Among other marine pigments of interest, the phycobiliproteins are a very unusual class identified in microalgae. First commercialized in clinical and immunological analysis, broader uses in industry and therapy are envisioned (Sekar & Chandramohan, 2008).

The uptake of oxygen by organisms can cause the formation of dangerous derivatives, including singlet oxygen and free radicals. These forms of highly reactive oxygen species (ROS) play an important role in various chronic diseases (cancer, atherosclerosis, osteoarthritis, Parkinson's, etc.) or acute reactions (inflammation, septic shock, etc.). However, ROS production can also be used as a means of therapy in human health. Indeed, photodynamic therapy (PDT) is an innovative discipline calling for photosensitive molecules with a tumour tropism that react to light and destroy the surrounding tissues by ROS production. Only a few drugs are presently in use for PDT. Less than a dozen molecules have been identified so far and none are, as yet, considered very efficient. It is, however, a promising field as our laboratory was able to identify a group of molecules from microalgae that is 30 times more efficient than the best commercial

gold standard (T. Patrice, J. P. Cadoret, L. Picot, R. Kaas, and J. B. Berard, unpublished work).

The polysaccharides extracted from the red microalga *Porphyridium purpureum* have been proven to have antiviral activity on cell lines as well as *in vivo* in rabbits (Huheihel, Ishanu, Tal, & Arad, 2002). Indeed, red algae have been studied for their polysaccharide contents both for health (Matsui, Muizzuddin, Arad, & Marenus, 2003) and industry applications (Gourdon *et al.*, 2008). Apart from structural polysaccharides, some microalgae synthesize exopolysaccharides. These polymeric compounds form a hydrophilic and polyanionic matrix, retain water and trap cations, allowing the microalgae to resist desiccation. These properties suggest that the algae could be useful for biotechnological applications in environmental fields through the detoxification of biotopes polluted by heavy metals (Pb, As, Hg, Cd) and in the recovery of some metals such as gold and uranium. The physico-chemical characteristics of polysaccharides—particularly their rheological, lubricant and flocculent properties—have been suggested for various applications.

A few hundred microalgae are classified as dangerous due to their toxin production. Among the 90 recorded species, 70 belong to the dinoflagellate group. The potential applications of these toxins in human healthcare have been reviewed by Camacho *et al.* (2006). Characteristics such as the anti-fouling properties of microalgae could be exploited produce a range of 'biogenic' products (Bhadury & Wright, 2004).

Some algal extracts are considered emollients and are incorporated into anti-aging creams to prevent wrinkles and stimulate collagen synthesis; their ultraviolet (UV) protection properties are also being researched. Although many of the marketing claims about algal bioproducts still need to be proven, business prospects justify the interest shown in this field. *Arthrospira* and *Chlorella* are again those involved in the anti-aging and regenerative products (Spolaore, Joannis-Cassan, Duran, & Isambert, 2006). However, while many applications of microalgae are already in existence, genomics is opening up still more opportunities.

### 1.3. Genomics and Microalgae

The rise of next-generation sequencing (NGS) technologies, accompanied by a sharp fall in their cost, has led to the acquisition of important genomic data on microalgae since the 1990s. The pace of the availability of microbial genomes is obviously increasing with NGS technologies and in addition to

the 14 nuclear genomes available (see Chapters II and III of this volume for a review), the gene repertoire of many additional species is now available through transcriptomics, as discussed below. Due to its phylogenetic proximity to land plants and because many molecular tools are available, the Chlorophyta *Chlamydomonas reinhardtii* was chosen as a model among photosynthetic organisms and the sequencing of its entire nuclear genome completed in 2007 (Merchant *et al.*, 2007). Comparative phylogenomic analyses have provided insight into the evolution of plants and animals, allowing genes to be associated with photosynthesis and flagellar functions, and links established between ciliopathy and the composition and function of flagellae (Umen & Olson 2012 in this volume). Over the past decade, many post-genomics and genetic tools have been used on this species, including microarrays, antibodies, RNA interference (RNAi) and genetic transformation. These approaches have enabled the exploration of metabolic pathways and biological processes such as responses to stress, the circadian clock (Matsuo & Ishiura, 2011), photosynthetic electron transport chains (Hermsmeier, Schulz, & Senger, 1994), mechanisms of carbon concentration (Yamano & Fukuzawa, 2009) and flagellar assembly (Iomini, Till, & Dutcher, 2009). In addition, proteomic studies have provided major research contributions in the areas of photosynthesis, molecular biology and evolution (Muhlhaus, Weiss, Hemme, Sommer, & Schroda, 2011; Rolland *et al.*, 2009). The other alga species sequenced were chosen due to their ecological role, phylogenetic distribution or harmful nature. Sequencing provided extensive information on the evolution of these species, helped to identify metabolic pathways and specific genes and clarified processes involved in the cycles of iron, calcium, silica, urea and nitrogen. In addition, sequence data provide essential references for matching with post-genomic investigations, including transcriptomic and proteomic analyses.

The gene content of microalgae is only beginning to be explored. Microalgal genomes can be structurally complex and sizes range from 12.6 Mbp for the Chlorophyta *Ostreococcus tauri* and 168 Mbp for the Haptophyta *Emiliania huxleyi* to an estimated 10,000 Mbp for the Dinophyta *Karenia brevis* (see Chapter XI for a discussion of genome size variations in algae). These large genome sizes can preclude full-genome sequencing, thus enforcing the use of transcriptome sequencing to build gene catalogues. Many authors have made this choice, although aware of the risk of neglecting non-transcribed sequences. Among the species studied in this way, we can mention the Ochrophyta *Pseudochattonella farcimen*, which is associated with fish mortalities (Dittami *et al.*, 2011), green microalgae



*Chlorella vulgaris* UTEX 395 (Guarnieri *et al.*, 2011), *D. salina* (Zhao *et al.*, 2011) and *Dunaliella tertiolecta* (Rismani-Yazdi, Haznedaroglu, Bibby, & Peccia, 2011) and the coccolithophore *E. huxleyi* (Von Dassow *et al.*, 2009). Transcriptomic data have been used for phylogenomics and opened the way for functional post-genomics approaches to the study of physiology, environmental adaptation, life cycles, metabolism and signal transduction pathways. Several major projects for transcriptome sequencing are currently underway (Table 8.1). One example is the ‘Marine Microbial Eukaryotic Transcriptome Project’, which aims to sequence the transcriptomes of approximately 750 samples expected to represent hundreds of species and strains with key ecological roles and evolutionary importance in the tree of microeukaryotes (<http://marinemicroeukaryotes.org/>). To date, 39 microbial algal transcriptomes have been sequenced (Table 8.1). In order to establish a reference database from ecologically and phylogenetically relevant photosynthetic protists for the ‘Tara Oceans expedition’, the ‘Prometheus project’ is proposing to sequence about 30 species of ecological or phylogenetic importance (<http://oceans.taraexpeditions.org>) (Karsenti *et al.*, 2011).

We can therefore hope, in a few months or years, to have a very large number of new transcriptomic and genomic data for algae. The development of genomics has already made a major contribution to fundamental research on photosynthetic eukaryotes in the fields of functional biology, global ecology and the evolution of organisms. These data will accelerate the commercialization of alga-derived compounds by providing a framework for hypothesis-based strain improvement programs built on an improved fundamental understanding of the specific pathways and regulation of networks. These studies are also the source of new biotechnologies that will be presented in the following sections.



## 2. BIOTECHNOLOGY AND MICROALGAE

For 2011, a search using the two keywords ‘microalgae’ and ‘biotechnology’ returned 51 publications in Web of Science database. More than a third of these were on energy and biofuels. In second position, around 20% of the papers deal with different cultivation and extraction techniques. Cell factories, i.e. the production of recombinant proteins, came in third position, with a number of technical advances in *Chlamydomonas* sp.

**Table 8.1** Ongoing Microalgae Transcriptomic Projects—cont'd

| Phylum       | Species                         | Strain     | Status                |
|--------------|---------------------------------|------------|-----------------------|
| Cryptophyta  | <i>Hemiselmis andersenii</i>    | CCMP644    | Sequencing            |
| Dinophyta    | <i>Alexandrium minutum</i>      | CCMP113    | Sequencing            |
| Dinophyta    | <i>Cryptothecodinium cohnii</i> | Seligo     | Sequencing            |
| Dinophyta    | <i>Karenia brevis</i>           | SP3        | Sequencing            |
| Dinophyta    | <i>Oxyrrhis marina</i>          | CCMP788    | Assembly & annotation |
| Dinophyta    | <i>Oxyrrhis marina</i>          | CCMP1795   | Sequencing            |
| Dinophyta    | <i>Symbiodinium kavagutii</i>   | CCMP2468   | Sequencing            |
| Euglenophyta | <i>Eutreptiella gymnastica</i>  | NIES-381   | Assembly & annotation |
| Haptophyta   | <i>Hyalolithus neolepis</i>     | TMR5       | Sequencing            |
| Ochrophyta   | <i>Dinobryon sp.</i>            | UTEXLB2267 | Assembly & annotation |
| Ochrophyta   | <i>Ochromonas sp.</i>           | CCMP 1393  | Assembly & annotation |
| Rhodophyta   | <i>Rhodorus marinus</i>         | 769        | Assembly & annotation |

Source: From [http://marinemicroeukaryotes.org/project\\_organisms](http://marinemicroeukaryotes.org/project_organisms).

## Annexes 2 Microalgae, Functional Genomics and Biotechnology

**Table 8.1** Ongoing Microalgae Transcriptomic Projects

| Phylum             | Species                           | Strain      | Status                |
|--------------------|-----------------------------------|-------------|-----------------------|
| Bacillariophyta    | <i>Asterionellopsis glacialis</i> | 1712        | Assembly & annotation |
| Bacillariophyta    | <i>Chaetoceros</i> sp.            |             | Assembly & annotation |
| Bacillariophyta    | <i>Corethron hystrix</i>          | 308         | Assembly & annotation |
| Bacillariophyta    | <i>Cylindrotheca closterium</i>   |             | Assembly & annotation |
| Bacillariophyta    | <i>Grammatophora oceanica</i>     | 410         | Assembly & annotation |
| Bacillariophyta    | <i>Melosira</i> sp.               | CCMP 2643   | Sequencing            |
| Bacillariophyta    | <i>Navicula transitans</i>        | 80          | Assembly & annotation |
| Bacillariophyta    | <i>Odontella</i> sp.              |             | Assembly & annotation |
| Bacillariophyta    | <i>Odontella sinensis</i>         | Grunow 1884 | Sequencing            |
| Bacillariophyta    | <i>Skeletonema costatum</i>       | 1716        | Sequencing            |
| Bacillariophyta    | <i>Stephanopyxis turris</i>       | CCMP 815    | Sequencing            |
| Chlorarachniophyta | <i>Lotharella oceanica</i>        | CCMP622     | Assembly & annotation |
| Chlorarachniophyta | <i>Lotharella globosa</i>         | LEX01       | Assembly & annotation |
| Chlorarachniophyta | <i>Lotharella amoebiformis</i>    | CCMP2058    | Assembly & annotation |
| Chlorarachniophyta | <i>Bigelowiella natans</i>        | CCMP 2755   | Assembly & annotation |
| Chlorophyta        | <i>Crustomastix stigmata</i>      | CCMP3273    | Sequencing            |
| Chlorophyta        | <i>Dolichomastix tenuilepis</i>   | CCMP3274    | Sequencing            |
| Chlorophyta        | <i>Micromonas</i> sp.             | CCMP2099    | Assembly & annotation |
| Chlorophyta        | <i>Nephroselmis pyriformis</i>    | CCMP717     | Assembly & annotation |
| Chlorophyta        | <i>Pyramimonas parkeae</i>        | CCMP725     | Assembly & annotation |
| Chlorophyta        | <i>Tetraselmis</i> sp.            | GSL018      | Sequencing            |
| Cryptophyta        | <i>Chroomonas mesostigmatica</i>  | CCMP1168    | Assembly & annotation |
| Cryptophyta        | <i>Cryptomonas paramecium</i>     | CCAP977/2a  | Assembly & annotation |
| Cryptophyta        | <i>Goniomonas pacifica</i>        | CCMP1869    | Sequencing            |
| Cryptophyta        | <i>Guillardia theta</i>           | CCMP2712    | Assembly & annotation |

(Continued)

## 2.1. Microalgal Lipids as Biofuel and Food

### 2.1.1. Algal Lipid Synthesis: The Contribution of Genomic Data

Compared with land plants, the lipid composition of algae shows great specificity, such as the presence of long-chain PUFAs or the species-specific absence of phosphatidylcholine and phosphatidylserine in the membranes, replaced by diacylglyceryltrimethylhomoserine (Guschina & Harwood, 2006). In addition, for many algal species, high-energy reserves of triacylglycerol (TAG) accumulate in large amounts in lipid droplets in response to different types of stress or nutrient deficiency. TAG represents >50% of the algal dry weight and serve for membrane synthesis or carbon storage (Hu *et al.*, 2008), making it possible to obtain oil yields 10 times higher per hectare than with land plant species. Recent soaring oil prices, diminishing world reserves and the environmental damage associated with fossil fuel consumption have led to increased interest in using algae as an alternative and renewable feedstock for fuel production. The development of the microalgal biodiesel industry depends primarily on the reduction of production costs and one strategy to achieve this is to increase lipid productivity. This explains the large investment being placed in such technology and demonstrates why most genomics work on algae is aimed at describing and orienting their lipid metabolism (Norsker, Barbosa, Vermue, & Wijffels, 2011).

Many studies have been conducted on land plants to understand their mechanisms of lipid synthesis and the development of reserves in their seeds. It was reported that environmental conditions (nutrients, salinity, light, etc.) affect microalgal fatty acid accumulation (for a review, see Hu *et al.*, 2008). However, molecular mechanisms that trigger and control the accumulation of storage lipids in microalgae are poorly understood. Genomic data have allowed the identification of new enzymes and helped to show how lipid pathways interrelate with energy and carbohydrate metabolism (Wallis & Browse, 2010). Until recently, the molecular mechanisms involved in regulatory pathways in algae were still poorly understood. With genomic data and genetic tools available for the green microalga *C. reinhardtii*, lipid metabolism has been mainly studied in this species and overviews of these findings can be found in several papers (Guschina & Harwood, 2006; Khozin-Goldberg & Cohen, 2011; Moellering & Benning, 2010). Many genes of *C. reinhardtii* involved in fatty acids and TAG metabolism have been identified based on their orthological relationships to fungi and land plants. In green microalgae, starch synthesis shares common carbon precursors with

lipid synthesis. In *C. reinhardtii*, it has been shown that shunting of carbon precursors from the starch synthesis pathway may facilitate carbon partitioning into the fatty acid synthesis pathway resulting in enhanced production of TAG (Li, Han, Hu, Dauvillee *et al.*, 2010). Identification of genes and biosynthetic pathways implicated in lipid biosynthesis is usually made using starchless mutants. With regard to the metabolism of TAGs, genomic data have shown conservation of the main biosynthetic pathways between microalgae and seed plants. Briefly, fatty acids are synthesized in the chloroplasts in which acetyl-CoA carboxylase (ACCase) provides the malonyl-CoA substrate for the biosynthesis of fatty acids thanks to the fatty acid synthase, a multifunctional enzymatic complex (Guschina & Harwood, 2006). Free fatty acids are then either used for the synthesis of membrane lipids or exported to the endoplasmic reticulum for the biosynthesis of TAGs. This synthesis involves the sequential transfer of acyl groups from acyl-CoA to different positions of glycerol-3-phosphate. Most acyl-transferases and a phosphatases involved have been identified in the genome of *C. reinhardtii* (Merchant, Kropat, Liu, Shaw, & Warakanont, 2011). Nevertheless, significant differences from land plants were observed in the TAG pathways of *C. reinhardtii*, such as the absence of the extra-plastidic lysophosphatidyl acyltransferase in the genome and the presence of new enzymes that are, as yet, poorly characterized (Hu *et al.*, 2008). Most recently, an alternative chloroplast pathway of TAG synthesis was identified in *C. reinhardtii* (Fan, Andre, & Xu, 2011). TAG accumulates in lipid droplets in which proteomics techniques revealed the importance of a major lipid droplet protein (MLDP). Miller *et al.* (2010) used 454 and Illumina technologies for transcriptomic analysis and showed how nitrogen deprivation redirects lipid metabolism. In brief, genomic and post-genomic data have allowed lipid metabolism pathways and regulation to be characterized in the Chlorophyta *C. reinhardtii*. However, this alga is not an oleaginous species. With the great diversity that exists among algae, specific studies are now being conducted on lipid-accumulating species in numerous laboratories around the world.

### 2.1.2. Algal Lipids as Biofuel

Very recently, several studies have used post-genomics to study the lipid metabolism of high-oil-content algae. This illustrates a real drive in the exploration of the functional metabolism of oleaginous algae. In 2011, Rismani-Yazdi *et al.* (2011) published the NGS and transcriptome annotation of a non-model member of the Chlorophyta: *D. tertiolecta*.

Genes-encoding key enzymes were identified by homology and metabolic pathways involved in the biosynthesis and catabolism of fatty acids, TAG and starch were reconstructed (Rismani-Yazdi *et al.*, 2011). A few months later, similar work was reported in a strain of the oil-producing green alga *Botryococcus braunii* (Baba, Ioki, Nakajima, Shiraiwa, & Watanabe, 2011). In parallel, proteomic approaches have identified new proteins involved in the storage of TAG in the lipid droplets of the Chlorophyta *H. pluvialis* (Peled *et al.*, 2011). Guarnieri *et al.* (2011) reported a comprehensive proteomic and transcriptomic investigation of lipid accumulation in the unsequenced green alga *C. vulgaris* UTEX 395. The authors presented the first utilization of a *de novo* assembled transcriptome as a search model for proteomic analysis. The regulation of fatty acid and TAG biosynthetic pathways was analyzed under nitrogen limitation. This oleaginous species is extensively studied due to its relatively fast growth rate, its value as both a food supplement and a potential biofuel feedstock and its ability to produce high-economic value molecules and to remediate heavy metals from wastewater. For these reasons, the genome of the Chlorophyta *Chlorella variabilis* NC64A was previously sequenced by Blanc *et al.* (2010). However, difficulties were encountered in identifying proteins by comparing data with strains of species from the same phylum. The researchers pointed out the importance of having unique sequence data to study species and strains of interest (Guarnieri *et al.*, 2011).

Although lipid biosynthesis pathways have been studied in several species, very few studies focus on the regulation of these pathways. Given the induction of TAG biosynthesis by different stresses, it is likely that the mechanisms for the regulation of TAG synthesis differ between algae and seed plants, as the latter produce oil during a specific phase of their life cycle and in specialized tissues. The means of regulation are presently of great interest, as these are the key to engineering algal crop production without causing weakening through nutrient stress. Although transcriptomics offer a wealth of information on gene expression, the processes of messenger RNA (mRNA) splicing, ribosome recruitment and post-translational regulations of proteins are not well understood in algae and transcriptomic analysis does not adequately define the control points for metabolic regulation.

By providing insight into the mechanisms underpinning lipid metabolic processes, results can be of use for the genetic manipulation of organisms to enhance the production of feedstock for commercial microalgal biofuels. By 1996, Dunahay and co-authors were able to overexpress ACCase in the

diatom *Cyclotella cryptica*, which is a key enzyme in the biosynthesis of fatty acids (Dunahay, Jarvis, Dais, & Roessler, 1996). However, no increase in the amount of lipid was observed. In expressing recombinant thioesterases to enhance the expression of shorter chain length fatty acids, Radakovits, Jinkerson, Darzins, & Posewitz (2010) were able to improve the level of lauric and myristic acids in the diatom *Phaeodactylum tricorutum*. This creates an advantage for biofuel feedstock because biodiesel made from saturated short or medium chain length fatty acids has a relatively low cloud point and is resistant to oxidation. In addition, several studies have shown metabolic shifts in starchless mutants of *C. reinhardtii* in favour of an overexpression of TAG (Moellering, Miller, & Benning, 2009; Li, Han, Hu, Sommerfeld, & Hu, 2010; Wang, Ullrich, Joo, Waffenschmidt, & Goodenough, 2009). In a starchless mutant, Moellering *et al.* (2010) inhibited the expression of MLDPs by RNAi, which not only increased the size of the lipid globules but also resulted in decreased growth. In contrast, the fatty acid content of a starchless selected mutant of *Chlorella pyrenoidosa* was doubled without detriment to its growth characteristics (Ramazanov & Ramazanov, 2006). This suggests that it is possible to improve the productivity of microalgae using lipid selection strategies. To date, the genomic data available on the selected species are still patchy, and reverse genetic tools are completely absent in these species. We also lack genetic information on the molecular mechanisms leading to these beneficial mutations. The exponential increase of genomic and post-genomic technology should enable biologists to acquire data, and reverse genetic tools should improve our understanding of the metabolism of these lipids and demonstrate ways in which these processes can be improved.

Recently, we put one of the first varietal selection strategies into action in our laboratory. We used successive rounds of UV mutation and cell sorting to improve the TAG production of the Haptophyta *I. galbana* affinis Tahiti (a strain related to the *I. galbana* strain), a species that offers numerous advantages for lipid production. This approach, which does not create genetically modified organisms (GMOs), allowed us to obtain a strain that accumulates twice the amount of neutral lipids as the original without affecting the growth rate (Rouxel, Bougaran, Doulin-Grouas, Dubois, & Cadoret, 2011). This strategy quickly improved the performance of an unsequenced selected species, so similar strategies will now be tried on other species and other valuable molecules. From now on, the acquisition of transcriptomic and proteomic data will be used to identify genes and molecular processes involved in the increase of lipid accumulation.

### 2.1.3. Algal Lipids as Feed and Food

Apart from the high importance of TAG from algae, the identification of enzymes involved in the synthesis of PUFAs, such as the long-chain PUFAs AA, EPA and DHA, is of great interest due to the health benefits they offer. Production of PUFAs involves a consecutive series of desaturations and elongations of the fatty acyl chain. Until recently, numerous authors isolated and characterized lipid metabolism and enzymes using biochemical technologies. These studies are reported in a review by [Guschina and Harwood \(2006\)](#). Over the past few years, authors have used genomic data to understand the biosynthetic pathways of PUFAs. Because of the putative role of PUFAs in the virulence of the fish pathogen *P. farcimien*, [Dittami](#) and co-authors analyzed the expressed sequence tags (ESTs) of this species. Focusing their attention on PUFA metabolic pathways, they identified new specific desaturases related to this virulence ([Dittami et al., 2011](#)). In the same way, the ESTs of *Myrmecea incisa*, a green coccoid freshwater microalga rich in AA, were analyzed and a putative new elongase was identified ([Yu, Liu, Li, & Zhou, 2011](#)). [Pan et al. \(2011\)](#) sequenced the genome of the high PUFA content species of Heterokonta *Nannochloropsis oceanica* using next-generation Illumina sequencing technologies. Sequence similarity-based investigation identified new elongase- and desaturase-encoding genes involved in the biosynthesis of long-chain PUFAs, which provide the genetic basis of its rich EPA content.

To date, major lipid primary metabolism has been well studied in model species, but regulation pathways, catabolism and secondary metabolic pathways of lipids are complex and rarely studied. Many metabolites of lipids have high biotechnological potential. The control of lipid metabolism, which is highly regulated, is of great interest as a means of increasing the lipid yields in culture. Furthermore, strategies using random mutations and strain selection have succeeded in increasing the lipid content of selected strains, but without a clear understanding of the mechanisms involved. This demonstrates that there are still many gaps in the knowledge that would help us to optimize lipid production from algae. Genomic and post-genomic studies on a variety of microalgae will provide the basis for identifying metabolic and signalling pathways.

## 2.2. Bioactive Natural Products

Commercial applications of microalgae include their use as natural sources of valuable macromolecules, such as carotenoids and phycocolloids. Due to



the exceptionally high diversity of the different groups and the low level of exploration carried out so far, algae are a burgeoning reservoir of high added value compounds. During the last decade, full genome analysis unveiled numerous new natural products in bacteria and fungi. Indeed, it appears that many of their genomes contain more gene clusters coding for the biosynthesis of natural products than natural products isolated from these same species (Winter, Behnken, & Hertweck, 2011). Similar results have been observed in microalgae. For example, *in silico* analysis of the Heterokonta *Aureococcus anophagefferens* genome revealed the presence of five berberine bridge enzymes involved in the synthesis of toxic isoquinoline alkaloids, although this type of alkaloid had never been previously identified in this harmful species (Gobler *et al.*, 2011). Genomic exploration of microalgae appears to be a promising way to discover new bioactive products. To date, the analysis of available genomes has aided the identification of pathways to known compounds, thereby greatly facilitating regulatory and functional investigations. The search for enzymes involved in the biosynthesis of polyketides, isoprenoids, non-ribosomal peptides, oxylipins and alkaloids was conducted *in silico* by looking for homologous genes of land plants in sequenced genomes of microalgae (for review, see Sasso, Pohnert, Lohr, Mittag, & Hertweck, 2011). Although some pathways have been elucidated, there are still many gaps in our knowledge of the metabolism of the secondary metabolites. For example, isoprenoids comprise numerous bioactive molecules such as sterols, phytohormones, phytol, prenylated quinones and carotenoids, which have numerous qualities of interest for biotechnology. While the common first steps of the synthesis of isoprenoid compounds have been well described (Lohr, Schwender, & Polle, 2012), very little is known about the biosynthesis of secondary isoprenoids except for the carotenoids. The genetic basis of the biosynthetic pathways of sterols and carotenoids in algae has been examined in detail by phylogenomics across several phyla of algae in order to gain insight into the evolution and diversity of photosynthetic eukaryotes (Cui, Wang, & Qin, 2011; Desmond & Gribaldo, 2009; Frommolt *et al.*, 2008) (see Archibald, 2012; De Clerck, Bogaret, & Leliaert, 2012; Not *et al.*, 2012, in this volume). This has led to the identification of genes in organisms where pathways had not been identified before and demonstrated the steps by which more new enzymes could be discovered. The induction and regulation of astaxanthin and carotenoid biosynthesis in Chlorophyta such as *Sphaerella lacustris* or *D. salina* has received considerable attention owing to the increasing use of

secondary carotenoids as a source of pigmentation for fish in aquaculture and their potential as free-radical quenching drugs in cancer prevention. In aiming to identify the proteins involved in the regulation and biosynthesis of astaxanthin, comparative proteomics and transcriptomics were applied to the chlorophytes *H. pluvialis* and *Haematococcus lacustris* (re-named *S. lacustris*) under nitrogen starvation and irradiance stress (Eom, Lee, & Jin, 2005; Kim *et al.*, 2006; Tran, Park, Hong, & Lee, 2009) and the regulated genes identified. These genes putatively play a role in signal transduction from stress to the cellular defence system and activate the biosynthesis of astaxanthin. Complementary in-depth analysis should confirm the significance of these results. These genes include potential targets to increase the expression of astaxanthin.

Overall, it is clear that our understanding of secondary metabolism and its regulation is still rudimentary. Secondary metabolites include a large number of natural bioactive products, many of which are unknown. *In silico* genome analyses are a key to the identification of new metabolic and signalling pathways. Post-genomics can be applied to identify physiological conditions that lead the expression of new pathways and so identify hitherto undetected metabolites.

### 2.3. Molecular Farming

The extraction of natural substances remains the main source of supply for a large number of pharmaceutical molecules. However, since it is possible to identify the genes responsible for building a protein molecule, they can be introduced into cultured cells, which then become cell factories, making millions of copies of the desired product. This strategy—the expression of molecules with high added value in recombinant cell systems—offers extraordinary opportunities for the development of a very promising biotechnology market (estimated to be worth up to several tens of billions of dollars, depending on the information source) (Gasdaska, Spencer, & Dickey, 2003; Schmidt, 2004). The production systems available are bacteria, yeasts and animal or plant cells, which are genetically modified to produce insulin, growth hormones, monoclonal antibodies and other therapeutic proteins. Each system has advantages and disadvantages relating to factors such as cost, production safety, ease of extraction, purification and complexity of producing the molecules. Some solutions, however, combine a number of benefits, putting them in a strong position for the future of this industry.

Microalgae have several advantages over other expression systems for the production of recombinant proteins, such as (1) a high growth rate (they commonly double their biomass within 24 h), (2) easy cultivation at a low production cost (they only require water and nutrients), (3) the possibility of performing post-transcriptional and post-translational modification as in other eukaryotic expression systems and (4) photobioreactor culture methodologies that prevent transgenes from escaping into the environment, which is a potential risk when using land plants (Janssen, Tramper, Mur, & Wijffels, 2003).

Several interesting reviews on transgenic tools describe the use of microalgae as a platform for production of recombinant proteins (Bozarth, Maier, & Zauner, 2009; Hallmann, Amon, Godl, Heitzer, & Sumper, 2007; Potvin & Zhang, 2010; Walker, Collet, & Purton, 2005). Here, we focus on recent progress and results on transgenic microalgae technology for the production of therapeutic recombinant proteins and discuss the contribution of genomic studies for the optimization of genetic manipulation in microalgae.

### **2.3.1. Transgenic Microalgae as a Platform for Biopharmaceutical Proteins**

In this section, we provide a review of biopharmaceutical proteins expressed in microalgae systems according to their intracellular cell localization (chloroplastic or nuclear). The interest in the N-glycosylation of pharmaceutical proteins will also be discussed.

Although no recombinant protein produced by transgenic algae is yet available on the market, some therapeutic proteins have been successfully produced using microalgae, mainly the Chlorophyta *C. reinhardtii* for which suitable transgenic tools and genomic data are available (for all three genomes: nuclear, chloroplastic and mitochondrial). Mayfield's group has done considerable work on the chloroplastic expression of recombinant protein in *C. reinhardtii* (Rasala & Mayfield, 2011). Indeed, the majority of microalgal therapeutic proteins have been produced by chloroplasts (Table 8.2). Recombinant protein can accumulate to much higher levels in the transgenic chloroplast than when expressed by the nuclear genome because plastids lack disadvantages such as gene-silencing mechanisms (Bock, 2007). Indeed, expression of foreign proteins remains very low for reasons that are not yet fully understood (Potvin & Zhang, 2010). The chloroplast of *C. reinhardtii* has been used to produce a range of recombinant proteins, including reporters such as glucuronidase, luciferase, green fluorescent

## Annexes 2 Microalgae, Functional Genomics and Biotechnology

**Table 8.2** Biopharmaceutical Proteins Expressed In Microalgae

| Gene Expressed | Function  | Host Species and Cell Localization             | Expression Level Achieved | Application                   | Source                        |
|----------------|---|--|---------------------------|-------------------------------|-------------------------------|
| HSV8-lsc       | Mammalian antibody  | <i>Chlamydomonas reinhardtii</i> , Chloroplast | Detectable                | Pharmaceutical                | Mayfield <i>et al.</i> (2003) |
| CTB-VP1        | Cholera toxin B subunit fused to foot and mouth disease VP1           | <i>Chlamydomonas reinhardtii</i> , Chloroplast | 3% TSP                    | Vaccine                       | Sun <i>et al.</i> (2003)      |
| HSV8-scFv      | Classic single-chain antibody   | <i>Chlamydomonas reinhardtii</i> , Chloroplast | 0.5% TSP                  | Pharmaceutical                | Mayfield <i>et al.</i> (2005) |
| hMT-2          | Human metallothionine-2   | <i>Chlamydomonas reinhardtii</i> , Chloroplast | Detectable                | Pharmaceutical, UV-protection | Zhang <i>et al.</i> (2006)    |
| hTRAIL         | Human tumor necrosis factor-related apoptosis-inducing ligand (TRAIL) | <i>Chlamydomonas reinhardtii</i> , Chloroplast | ~0.67% TSP                | Pharmaceutical                | Yang <i>et al.</i> (2006)     |
| M-SAA          | Bovine mammary-associated serum amyloid                               | <i>Chlamydomonas reinhardtii</i> , Chloroplast | ~5% TSP                   | Therapeutics, oral delivery   | Manuell <i>et al.</i> (2007)  |
| CSFV-E2        | Swine fever virus E2 viral protein                                    | <i>Chlamydomonas reinhardtii</i> , Chloroplast | ~2% TSP                   | Vaccine                       | He <i>et al.</i> (2007)       |
| hGAD65         | Diabetes-associated anutoantigen human glutamic acid decarboxylase 65 | <i>Chlamydomonas reinhardtii</i> , Chloroplast | ~0.3% TSP                 | Diagnostics and therapeutics  | Wang <i>et al.</i> (2008)     |

(Continued)

## Annexes 2 Microalgae, Functional Genomics and Biotechnology

**Table 8.2** Biopharmaceutical Proteins Expressed In Microalgae—cont'd

| Gene Expressed             | Function   | Host Species and Cell Localization             | Expression Level Achieved          | Application  | Source                        |
|----------------------------|--|--|------------------------------------|--------------|-------------------------------|
| 83K7C                      | Full-length IgG1 human monoclonal antibody against anthrax protective antigen 83                     | <i>Chlamydomonas reinhardtii</i> , Chloroplast | 0.01% dry algal biomass            | Therapeutics | Tran <i>et al.</i> (2009)     |
| IgG1                       | Murine and human antibodies (LC and HC)  | <i>Chlamydomonas reinhardtii</i> , Chloroplast | Detectable                         | Therapeutics | Tran <i>et al.</i> (2009)     |
| VP28                       | White spot syndrome virus protein 28   | <i>Chlamydomonas reinhardtii</i> , Chloroplast | ~10.5% TSP                         | Vaccine      | Surzycki <i>et al.</i> (2009) |
| CTB-D2                     | D2 fibronectin-binding domain of <i>Staphylococcus aureus</i> fused with the cholera toxin B subunit | <i>Chlamydomonas reinhardtii</i> , Chloroplast | 0.7% TSP                           | Oral vaccine | Dreesen <i>et al.</i> (2010)  |
| 10NF3, 14FN3               | Domains 10 and 14 of human fibronectin   | <i>Chlamydomonas reinhardtii</i> , Chloroplast | 14FN3: 3% TSP<br>10FN3: detectable | Therapeutics | Rasala <i>et al.</i> (2010)   |
| M-SAA-Interferon $\beta$ 1 | Multiple sclerosis treatment fused to M-SAA  | <i>Chlamydomonas reinhardtii</i> , Chloroplast | Detectable                         | Therapeutics | Rasala <i>et al.</i> (2010)   |
| Proinsulin                 | Blood sugar level-regulating hormone, type I diabetes treatment                                      | <i>Chlamydomonas reinhardtii</i> , Chloroplast | Detectable                         | Therapeutics | Rasala <i>et al.</i> (2010)   |
| VEGF                       |  |  | 2% TSP                             | Therapeutics | Rasala <i>et al.</i> (2010)   |

## Annexes 2 Microalgae, Functional Genomics and Biotechnology

|                  |   |  |                                     |                                |  |
|------------------|---|--|-------------------------------------|--------------------------------|--|
|                  | Human vascular endothelial growth factor isoform 121              | <i>Chlamydomonas reinhardtii</i> , Chloroplast |                                     |                                |  |
| HMGB1            | High mobility group protein B1                                    | <i>Chlamydomonas reinhardtii</i> , Chloroplast | 2.5% TSP                            | Therapeutics                   | Rasala <i>et al.</i> (2010)            |
| NP-1             | Rabbit neutrophil peptide-1                                       | <i>Chlorella ellipsoidea</i> , nuclear         | Detectable                          | Antimicrobial                  | Chen <i>et al.</i> (2001)              |
| ARS2-crEpo-his6  | Human erythropoietin fused to ARS2 export sequence w/6xhis tag    | <i>Chlamydomonas reinhardtii</i> , Nuclear     | 100 µg/L culture                    | Pharmaceutical, protein export | Eichler-Stahlberg <i>et al.</i> (2009) |
| CL4mAb and HBsAg | Human antibody CL4mAB and the Hepatitis B surface antigen (HBsAg) | <i>Phaeodactylum tricorutum</i> , Nuclear      | CL4mAb: 8.7% TSP<br>HBsAg: 0.7% TSP | Vaccine                        | Hempel, Lau <i>et al.</i> (2011)       |
| mEPO             | Murine Erythropoietin   | <i>Phaeodactylum tricorutum</i> , Nuclear      | 300 µg/L culture                    | Therapeutics                   | Carlier A (unpublished work)           |

TSP: Total Soluble Proteins.

Source: Modified from [Specht \*et al.\* \(2010\)](#). Recent successes in therapeutic protein production in algae.

protein (GFP), industrial enzymes, vaccines and therapeutic enzymes (Rasala & Mayfield, 2011).

The first therapeutic protein expressed by transgenic microalgae was produced at Mayfield's laboratory using chloroplast transformation in the green microalga *C. reinhardtii*. In the study of Mayfield, Franklin, & Lerner (2003), the entire immunoglobulin A heavy chain protein (HSV8-lcs) fused to the variable region of the light chain was expressed and accumulated as a soluble protein able to bind to the herpes virus protein. Nevertheless, the expression yield was too low (detectable only) for commercial use, even though several regulation sequences (promoters) were tested. Regulation sequence aspects will be examined in the next section. This previous study was completed by the chloroplastic expression of a single chain fragment variable antibody (HSV8-scFv) that accumulated to 0.25% of total soluble protein (TSP) (Mayfield & Franklin, 2005). In their next study, the same team successfully increased the accumulation of a bioactive mammalian protein, bovine mammary-associated serum amyloid A (M-SAA), to 5% of TSP with by chloroplasts using different promoter sequences and an interesting strategy consisting of replacing an endogenous gene by the expression cassette (Manuell *et al.*, 2007). Recently, a full-length human monoclonal antibody was expressed in the chloroplast of *C. reinhardtii*, proving that this eukaryotic green alga is capable of synthesising and assembling a full-length antibody in transgenic chloroplasts (Tran, Zhou, Pettersson, Gonzalez, & Mayfield, 2009). More recently, a study was conducted to examine the versatility of algal chloroplasts for the expression of seven different therapeutic proteins: human erythropoietin (EPO), the 10th and 14th human fibronectin type III domains (14FN3 and 10FN3), human interferon  $\beta$ 1, the human vascular endothelial growth factor isoform, the high mobility group protein (HMGB1) and the human proinsulin. Of the seven proteins tested, four were successfully expressed in transgenic chloroplasts to above 2% of TSP (Rasala *et al.*, 2010). However, no detectable expression was shown for EPO or interferon  $\beta$ 1. Like Mayfield's group, other research groups have successfully shown that the chloroplast of *C. reinhardtii* is a perfect platform to produce recombinant proteins at an economically viable cost (Wang *et al.*, 2008; Yang *et al.*, 2006; Zhang, Shen, & Ru, 2006). In addition to therapeutic proteins, some vaccines have been successfully produced in algal chloroplasts. Indeed, a fusion protein between the foot and mouth disease virus VP1 and the cholera toxin B subunit (as mucosal adjuvant) was reported to accumulate to 3% of TSP in transgenic algal chloroplasts (Sun *et al.*, 2003). This fusion protein retained both specific

ganglioside-binding affinity and antigenic function. A classical swine fever virus E2 recombinant protein was also successfully expressed in chloroplast to around 2% of TSP and observed to have immunological activity (He *et al.*, 2007). Surzycki *et al.* (2009) reported a strong expression of the white spot syndrome VP28 protein by chloroplasts to around 10.5% of TSP. Moreover, in this study, the authors attempted to determine factors affecting the level of recombinant protein expression, which will be covered in the next section. Recently, Dreesen, Charpin-El Hamri, & Fussenegger (2010) reported the oral immunization of mice by transgenic algae expressing (to 0.7% of TSP) the *Staphylococcus aureus* fibronectin-binding domain D2 fused to the cholera toxin B subunit.

It is important to reiterate that all these studies were carried out using transgenic chloroplasts of the green algae *C. reinhardtii*. To our knowledge, there are no reports of biopharmaceutical protein expression by transgenic chloroplasts in other microalgae.

Although it is estimated that most of the therapeutic human antibodies used in therapy do not require glycosylation, other therapeutic proteins require the correct glycosylation pattern to function properly (Dove, 2002). Nevertheless, nuclear expression of therapeutic proteins remains limited because of some problems in reducing yield expression (Potvin & Zhang, 2010). Transgenic microalgal technologies are still in their infancy and the therapeutic proteins expressed by the nuclear genome are still rare in microalgae.

Initial work has been done by Hawkins and Nakamura (1999) to produce human growth hormone in the extracellular medium of *Chlorella sorokiniana* and *C. vulgaris* C-27. In a subsequent study, growth hormone of sole was produced and expressed as a stable product in *C. ellipsoidea* (since renamed *Chloroidium ellipsoideum*). Soles fed with these transgenic microalgae increased in size by 25% (Kim *et al.*, 2002). Another research team has shown the efficient expression and biological activity of rabbit neutrophil peptide-1 in *C. ellipsoideum* cells (Chen, Wang, Sun, Zhang, & Li, 2001).

Recently, Dauvillée *et al.* (2010) expressed a nuclear protein corresponding to the *Plasmodium* antigens that fuse to granule-bound starch synthase (GBSS), a protein involved in the starch matrix of plants and algae. The C-terminal domains from apical major antigen (AMA1) or major surface protein (MSP1) fused to GBSS were both efficiently expressed in nuclear cells and targeted starch particles in the chloroplasts, taking advantage of the transit peptide on the GBSS protein. Although expressed in the nucleus, these fusion proteins directly targeted starch granules, avoiding



post-translation modification such as N-glycosylation. Immunogenicity tests for both fusion proteins were successfully performed in mice (Dauvillee *et al.*, 2010).

More recently, diatoms have also been used as cell factories to produce recombinant proteins. Diatoms are an algal group of great ecological importance (Mock & Medlin 2012). Their contribution to global CO<sub>2</sub> fixation represents around 40% of marine carbon production. Diatoms like *P. tricornutum* represent an interesting subject for a variety of biotechnological applications, and this species has become a model organism for the diatoms (Bowler *et al.*, 2008; Hempel, Bozarth *et al.*, 2011, Hempel, Lau, Klingl, & Maier, 2011; Siaut *et al.*, 2007). Indeed, its whole genome has been sequenced and molecular tools for functional genomics are available (Maheswari, Mock, Armbrust, & Bowler, 2009; Siaut *et al.*, 2011). To date, diatoms have not been employed for expression of any biopharmaceutical proteins, but a research team has recently reported the first stable expression of a full-length human antibody and the respective antigen in *P. tricornutum* (Hempel, Lau *et al.*, 2011). In this study, the antibody and respective antigen were both expressed and accumulated within the endoplasmic reticulum (ER) using the ER retention signal. Interestingly, while the same expression vector and molecular tools were used for the expression of both these recombinant proteins, different expression levels were observed for the antibody (7.8% of TSP) and antigen (0.7% of TSP). This result confirms that not all foreign proteins are equally expressed (Potvin & Zhang, 2010).

At our laboratory, we became interested by the potential of microalgae as a means to produce therapeutic proteins (Cadoret *et al.*, 2008). This interest led to the creation of a private company by our laboratory: Algenics. Algenics is the first privately owned European biotechnology company focusing on innovative uses of microalgae to produce recombinant biotherapeutics. Using microalgae as a platform for recombinant proteins, our laboratory filed a patent on the production of glycosylated proteins in microalgae (Cadoret *et al.*, 2009). Recently, as proof of the concept, we successfully produced another therapeutic protein, murine erythropoietin (mEPO), in the diatom *P. tricornutum* (A. Carlier, M. Bardor, P. Lerouge, P. Delavault, B. Saint-Jean, A. Gerard and J. P. Cadoret, unpublished work). The data show that recombinant mEPO accumulates to around of 0.05% of TSP (or 300 µg/L). This recombinant EPO is glycosylated and able to bind the human EPO receptor *in vitro* with the same affinity. These results, combined with Hempel's data, confirm the high potential of diatoms to express biopharmaceutical proteins.

This last result corroborates the expression specificity of some foreign proteins according to cell localization and/or algal taxon. Indeed, no detection of recombinant EPO has been reported in Chlorophyta *C. reinhardtii* transgenic chloroplasts (Rasala *et al.*, 2010). In contrast, Eichler-Stahlberg, Weisheit, Ruecker, & Heitzer (2009) observed a minor accumulation of recombinant EPO up to around 100 µg/L in nuclear expression by *C. reinhardtii* cells. Thus, EPO protein accumulates differently and at different expression levels according to cell localization or species.

To conclude, many efforts have been made to produce biopharmaceutical proteins at a level sufficient to be economically viable, but extensive research to optimize microalgae as cell factories still needs to be done. Recent success in microalgal transgenesis and input from genomic data will allow a response to the growing demand for biopharmaceutical molecules. However, microalgae can also provide compounds other than pharmaceutical proteins. Indeed, an interesting study has recently been reported that used microalgae to produce industrial products such as bioplastic: Hempel and co-workers (2011) expressed three prokaryotic enzyme genes in the diatom *P. tricornutum* to produce poly-3-hydroxybutyrate (PHB). These genes (i.e. a ketolase, an acetoacetyl-CoA reductase and a PHB synthase) are able to synthesize PHB from acetyl-CoA in diatom cells up to a level of 10.6% of algal dry weight.

Of the post-translational modifications encountered in eukaryotic proteins, N-glycosylation is the most prevalent of those that appear essential for biological functions (biological activity, short half-life). Moreover, glycosylation is of particular interest for biopharmaceutical proteins since more than 70% of biopharmaceuticals are glycoproteins. Glycosylation capability is an advantage for any system used to produce biopharmaceuticals. This pathway is currently well understood among the different production systems available today, such as cultured mammalian, yeast and plant cells. Plants have N-glycosylation capability similar to mammalian cells. However, N-glycosylation patterns processed in plant cells differ from those of humans and other mammals. In plants, N-linked glycans contain  $\beta(1,2)$ -xylose and  $\alpha(1,3)$ -fucose instead of the  $\alpha(1,6)$ -fucose found in mammals. These plant-specific glycans are considered to be potentially antigenic and/or allergenic epitopes (Bakker *et al.*, 2001). Several strategies have been studied to remove the antigenic potential of plant-specific glycans. One simple approach is aglycosylation to obtain recombinant protein with no N-glycosylation by mutating the N-glycosylation sites of

expressed genes (Conley, Mohib, Jevnikar, & Brandle, 2009). This approach is effective if the biological activity is not affected by aglycosylation.

Another approach consists of retaining the foreign protein in the ER using KDEL/HDEL (i.e Lys/His-Asp-Glu-Leu) polypeptide retention signals to avoid plant-specific glycan residues such as  $\beta$ -(1,2)-xylose and  $\alpha$ -(1,3)-fucose (Gomord *et al.*, 2004; Ko *et al.*, 2003; Petruccioli *et al.*, 2006). Indeed, glycosylation processing in the ER is conserved between the plant and animal kingdoms and restricted to high mannose-type N-glycans, whereas the further glycosylation process in the Golgi apparatus, where additional glycans are added for glycan maturation, is highly diverse. Another approach to eliminating plant-specific glycan residues is to knock out the gene expression of glycosyltransferases involving  $\beta$ -(1,2)-xylosylation and  $\alpha$ -(1,3)-fucosylation (Gomord *et al.*, 2004). However, in addition to eliminating plant-specific sugar, humanization of N-glycosylation is also essential for the production of authentic glycosylated recombinant proteins in plants. The strategy to humanize plant N-glycans consists of expressing mammalian glycosyltransferases, which would complete N-glycan maturation, in plants (Bakker *et al.*, 2001).

So far, little information regarding the glycosylation of microalgae is available and it is interesting, both from a purely scientific point of view and for biotechnological applications, to determine their capacity for this process. Our laboratory published the first *in silico* N-glycosylation study in microalgae. Using the genomic data available for *P. tricornutum*, we identified specific genes coding enzymes involved in the N-glycosylation pathway in diatoms (Baiet *et al.*, 2011). Moreover, by structural analyses of N-linked glycans, this study also demonstrated that *P. tricornutum* proteins carry mainly high mannose-type N-glycans. Interestingly, other recent biochemical studies have reported the existence of special glycosyltransferase and glycosylation pathways, unique to the red alga *Porphyridium* sp. (Levy-Ontman *et al.*, 2011).

The emergence of genomic data in microalgae will provide the opportunity to perform comparative genomic studies and to dissect biosynthetic pathways such as N-glycosylation.

Recently, we initiated new studies to evaluate the N-glycosylation pathway of microalgae representing different phyla: green and red microalgae, glaucophytes, alveolates, stramenopile and haptophytes. This study will help us to determine how this specific process evolved within the eukaryotes. Moreover, demonstrating that microalgae are a suitable alternative system for the production of biopharmaceuticals requires the demonstration of their N-glycosylation capability.

### 2.3.2. Genomic Strategies for Optimising Recombinant Protein Expression

In this section, we report three strategies commonly used to optimize recombinant protein accumulation in microalgae.

#### 2.3.2.1. Translation optimization by codon usage bias

Specific variations in codon usage are often cited as one of the major factors impacting protein expression level. The presences of rare codons that are correlated with low levels of their endogenous transfer RNA species in the cell can reduce the translation rate of target mRNA. The classical strategy to bypass this problem is to redesign genes to increase their expression level. For this, two approaches have been attempted, both of which require choosing from a vast number of possible DNA sequences. The first approach consists of assigning the most abundant codon of the host of a given amino acid in the target sequence. The second uses translation tables based on the frequency distribution of the codons in an entire genome or for a range of highly expressed genes. This approach was successfully used in *C. reinhardtii* to improve the expression level of foreign proteins such as GFP in the nucleus (a 5-fold increase) (Fuhrmann, Oertel, & Hegemann, 1999) and chloroplasts (increased up to 80-fold) (Franklin, Ngo, Efuot, & Mayfield, 2002). Similar studies using a codon-optimized human antibody gene or luciferase reporter gene confirmed that codon bias play an important role in protein accumulation in chloroplasts of *C. reinhardtii* (Mayfield & Schultz, 2004; Mayfield *et al.*, 2003).

The nuclear and chloroplastic genome of *C. reinhardtii* may exhibit different codon bias, and thus, adjustment of codons in foreign gene sequences is necessary to obtain a high rate of protein production. To overcome this issue, the codon adaptation index (CAI) is used as a quantitative tool to predict the expression level of transgenes based on their codon usage. Several molecular software programs are available to determine and optimize codon usage. A list of these programs is given in Villalobos, Ness, Gustafsson, Minshull, & Govindarajan (2006).

This approach, which consists of optimizing the codon usage of transgenes, was successfully used in the green alga *C. reinhardtii* and diatom *P. tricornutum*. Specific codon usage is a field that will benefit from the contribution of future microalgal genomic and transcriptomic sequences.

#### 2.3.2.2. Identification of promoter sequences

Genome data are also necessary to identify functional sequences such as promoter, 5' and 3'- untranslated region (UTR) sequences that regulate the

gene expression rate. These sequences are specific for each gene and microalgal strain. Due to the presence of plastid and nuclear genomes in microalgae, there are different types of promoter sequences according to cell localization. Plastid transgenes are expressed under the control of an endogenous promoter and 5' and 3'-UTR. Overall, promoter sequence control transcription and 5'-UTR mediate mRNA stability, and translation initiation and 3'-UTR regulate stability and act in the termination of transcription. The same sequences were found for nuclear promoters, but other regulated sequences such as intron sequences are also involved in the regulation of nuclear gene expression. Previous studies identified sequences within the 5'-UTR that were involved in RNA stability and used as a means to increase recombinant protein synthesis. For a comprehensive review of chloroplast translation regulation, see Marin-Navarro, Manuell, Wu, & Mayfield (2007).

Concerning chloroplastic transformation in microalgae, the green alga *C. reinhardtii* has been intensively studied. Among chloroplastic promoters for the expression of foreign proteins (Table 8.3), the endogenous *atpA*, *psbD*, *rbcL* and *psbA* promoters are generally used (Hallmann *et al.*, 2007; Specht, Miyake-Stoner, & Mayfield, 2010). An excellent study performed by Barnes *et al.* (2005) reported the effect of various promoters and UTRs on recombinant proteins in the chloroplast of *C. reinhardtii*. Using different combinations of chimeric proteins corresponding to the promoters and 5'-UTRs of chloroplast genes, *atpA*, *rbcL*, *psbA*, *psbD* and 16S rRNA, fused to the GFP reporter and followed by 3'-UTR of either gene, they observed different protein accumulation levels. Moreover, they showed that mRNA accumulation is, in general, proportional to protein accumulation. Also, according to chimeric construction, they observed that the 5'-UTR sequence had a significant impact on recombinant protein production, while 3'-UTR had little effect. The highest level of reporter protein was found using the *atpA* or *psbD* promoter and 5'-UTR, while a minor protein accumulation level was observed under control of *rbcL* and *psbA* and no expression was seen using the 16S rRNA promoter and 5'-UTR (Barnes *et al.*, 2005).

Interestingly, the *psbA* promoter fused with its 5'-UTR was actually the most used (Manuell *et al.*, 2007; Surzycki *et al.*, 2009). Recently, Rasala, Muto, Sullivan, & Mayfield (2011) reported a high recombinant protein expression level with the *psbA* promoter in comparison to the levels reached with the *atpA* promoter. It remains unclear why certain regulatory elements induce a high expression level in some genes but not in others

## Annexes 2 Microalgae, Functional Genomics and Biotechnology

**Table 8.3** Promoter Used For Microalgae Genetic Transformation

| Host Species of Microalgae       | Promoter of Gene and its Product                               | Cell Expression Localization | Source of Promoter               | Source  |
|----------------------------------|--|------------------------------|----------------------------------|---|
| <i>Chlamydomonas reinhardtii</i> | <i>arg7</i> , arginosuccinate lyase                            | Nuclear                      | <i>Chlamydomonas reinhardtii</i> | Debuchy, Purton, and Rochaix (1989)   |
|                                  | <i>35S</i> , cauliflower mosaic virus 35S                      | Nuclear                      | Cauliflower mosaic virus         | Brown, Sprecher, and Keller (1991)<br>Tang, Qiao, and Wu (1995)<br>Kumar <i>et al.</i> , 2004   |
|                                  | <i>RbcS2</i> , rubisco small subunit 2                         | Nuclear                      | <i>Chlamydomonas reinhardtii</i> | Auchincloss, Loroch, & Rochaix (1999)<br>Fuhrmann <i>et al.</i> (1999)<br>Sizova, Fuhrmann, and Hegemann (2001)<br>Stevens, Rochaix, and Purton (1996)<br>Nelson and Lefebvre (1995)<br>Kovar, Zhang, Funke and Weeks (2002)<br>Cerutti, Johnson, Gillham, and Boynton (1997)<br>Cordero <i>et al.</i> (2011) |
|                                  | <i>HSP70</i> , heat shock protein 70 (fused to other promoter) | Nuclear                      | <i>Chlamydomonas reinhardtii</i> | Schroda <i>et al.</i> (2000)<br>Eichler-Stahlberg <i>et al.</i> (2009)  |

(Continued)

## Annexes 2 Microalgae, Functional Genomics and Biotechnology

**Table 8.3** Promoter Used For Microalgae Genetic Transformation—cont'd

| Host Species of Microalgae | Promoter of Gene and its Product                      | Cell Expression Localization | Source of Promoter               | Source  |
|----------------------------|---|------------------------------|----------------------------------|---|
|                            | <i>Nos</i> , nopaline synthase                        | Nuclear                      | <i>Agrobacterium tumefaciens</i> | Hall, Taylor, and Jones (1993)  |
|                            | <i>Nit1</i> , nitrate assimilation 1                  | Nuclear                      | <i>Chlamydomonas reinhardtii</i> | Ohresser, Matagne, and Loppes (1997)<br>Llamas, Igeno, Galvan, and Fernandez (2002) |
|                            | <i>Cop</i> , chlamyopsin                              | Nuclear                      | <i>Chlamydomonas reinhardtii</i> | Fuhrmann <i>et al.</i> (1999)   |
|                            | <i>TubA1</i> , alpha-tubulin                          | Nuclear                      | <i>Chlamydomonas reinhardtii</i> | Kozminski, Diener, and Rosenbaum (1993)   |
|                            | $\beta 2$ -tubulin                                    | Nuclear                      | <i>Chlamydomonas reinhardtii</i> | Blankenship and Kindle (1992)<br>Berthold, Schmitt, and Mages (2002)                |
|                            | <i>CabII-1</i> , chlorophyl-ab binding                | Nuclear                      | <i>Chlamydomonas reinhardtii</i> | Blankenship and Kindle (1992)   |
|                            | <i>pcy1</i> , plastocyanin                            | Nuclear                      | <i>Chlamydomonas reinhardtii</i> | Quinn and Merchant (1995)   |
|                            | <i>atpC</i> , gamma-subunit of chloroplast ATPase     | Nuclear                      | <i>Chlamydomonas reinhardtii</i> | Quinn and Merchant (1995)   |
|                            | <i>psaD</i> , photosystem I complex protein           | Nuclear                      | <i>Chlamydomonas reinhardtii</i> | Fischer and Rochaix (2001)  |
|                            | <i>atpA</i> , alpha subunit of adenosine triphosphate | Chloroplast                  | <i>Chlamydomonas reinhardtii</i> | Sun <i>et al.</i> (2003)  |
|                            | <i>psbD</i> , photosystem II D1                       | Chloroplast                  | <i>Chlamydomonas reinhardtii</i> | Manuell <i>et al.</i> (2007)  |

## Annexes 2 Microalgae, Functional Genomics and Biotechnology

|                              |  |             |                                  |  |
|------------------------------|--|-------------|----------------------------------|--|
|                              | <i>RbcL</i> , ribulose biphosphate carboxylase large subunit | Chloroplast | <i>Chlamydomonas reinhardtii</i> | Dreesen <i>et al.</i> (2010)   |
| <i>Dunaliella salina</i>     | <i>psbA</i> , photosystem II <i>psbA</i>                     | Chloroplast | <i>Chlamydomonas reinhardtii</i> | Rasala, Muto <i>et al.</i> (2011)  |
|                              | <i>Ubi1-Ω</i> , ubiquitin- $\Omega$                          | Nuclear     | <i>Zea mays</i>                  | Geng, Wang, Wang, Li, and Sun (2003)   |
|                              | 35S, cauliflower mosaic virus 35S                            | Nuclear     | Cauliflower mosaic virus         | Tan, Qin, Zhang, Jiang, and Zhao (2005)<br>Sun <i>et al.</i> (2005)<br>Feng, Xue, Liu, and Lu (2009)<br>Wang, Xue <i>et al.</i> (2007) |
|                              | <i>NR</i> , Nitrate reductase                                | Nuclear     | <i>Dunaliella salina</i>         | Li <i>et al.</i> (2007)<br>Li <i>et al.</i> (2008)   |
|                              | <i>RbcS2</i> , rubisco small subunit                         | Nuclear     | <i>Dunaliella salina</i>         | Sun <i>et al.</i> (2005)   |
| <i>Dunaliella bardawil</i>   | 35S, cauliflower mosaic virus 35S                            | Nuclear     | Cauliflower mosaic virus         | Anila <i>et al.</i> (2011)   |
| <i>Chlorella ellipsoidea</i> | 35S, cauliflower mosaic virus 35S                            | Nuclear     | Cauliflower mosaic virus         | Jarvis and Brown (1991)  |
|                              | <i>Ubi1-Ω</i> , ubiquitin- $\Omega$                          | Nuclear     | <i>Zea mays</i>                  | Chen <i>et al.</i> (2001)  |
|                              | <i>RbcS2</i> , rubisco small subunit 2                       | Nuclear     | <i>Chlamydomonas reinhardtii</i> | Kim <i>et al.</i> (2002)   |
| <i>Chlorella sorokiniana</i> | <i>NR</i> , nitrate reductase                                | Nuclear     | <i>Chlorella</i> sp.             | Dawson, Burlingame, and Cannons (1997)   |

(Continued)



## Annexes 2 Microalgae, Functional Genomics and Biotechnology

**Table 8.3** Promoter Used For Microalgae Genetic Transformation—cont'd

| Host Species of Microalgae                                | Promoter of Gene and its Product                              | Cell Expression Localization | Source of Promoter                                  | Source   |
|---|---|------------------------------|---|--|
| <i>Chlorella vulgaris</i>                                 | 35S, cauliflower mosaic virus 35S                             | Nuclear                      | Cauliflower mosaic virus                            | Cha, Yee, and Aziz (2011)<br>Chow and Tung (1999)<br>Wang, Xue <i>et al.</i> (2007)              |
| <i>Platymonas subcodiformis</i><br>( <i>Tetraselmis</i> ) | NR, nitrate reductase<br>CMV, cytomegalovirus                 | Nuclear<br>Nuclear           | <i>Phaeodactylum tricornutum</i><br>Cytomegalovirus | Niu <i>et al.</i> (2011)<br>Cui <i>et al.</i> (2010)   |
| <i>Nannochloropsis sp</i>                                 | HSP70, heat shock protein 70 / RbcS2, rubisco small subunit 2 | Nuclear                      | <i>Chlamydomonas reinhardtii</i>                    | Chen <i>et al.</i> (2008)<br>Li and Tsai (2008)  |
|   | 35S, cauliflower mosaic virus 35S                             | Nuclear                      | Cauliflower mosaic virus                            | Cha, Chen <i>et al.</i> (2011)   |
|   | VCP, violaxanthin/ chlorophyl binding protein                 | Nuclear                      | <i>Nannochloropsis sp</i>                           | Kilian, Benemann, Niyogi, and Vick (2011)  |
| <i>Haematococcus pluvialis</i>                            | SV40, simian virus pds, phytoene desaturase                   | Nuclear                      | simian virus<br><i>Haematococcus pluvialis</i>      | Teng <i>et al.</i> (2002)<br>Steinbrenner and Sandmann (2006)<br>Kathiresan <i>et al.</i> (2009) |
|   | 35S, cauliflower mosaic virus 35S                             | Nuclear                      | Cauliflower mosaic virus                            |  |
| <i>Volvox carteri</i>                                     | NR, nitrate reductase   | Nuclear                      | <i>Volvox carteri</i>                               | Schiedlmeier <i>et al.</i> (1994)  |

## Annexes 2 Microalgae, Functional Genomics and Biotechnology

|   |   |         |   |  |
|---|---|---------|---|--|
| <i>Gonium pectorale</i>                           | <i>psD</i> , photosystem I complex protein / <i>HSP70</i> , heat shock protein 70                         |         | <i>Chlamydomonas reinhardtii</i>                              | Lerche and hallmann (2009)   |
| <i>Closterium peracerosum-strigosum littorale</i> | <i>HSP70</i> heat shock protein 70 / <i>Cab</i> , chlorophyl-ab binding Ch a/b-binding protein            |         | <i>Closterium peracerosum-strigosum littorale</i>             | Abe, Hiwatashi, Ito, Hasebe, and Sekimoto (2008)<br>Abe <i>et al.</i> (2011) |
| <i>Lotharella amoebiformis</i>                    | <i>RbcS2</i> , rubisco small subunit 2  | Nuclear | <i>Lotharella amoebiformis</i>                                | Hirakawa <i>et al.</i> (2008)  |
| <i>Cyclotella criptyca</i>                        | <i>Acc1</i> , acetylCoA carboxylase   | Nuclear | <i>Cyclotella criptyca</i>                                    | Dunahay <i>et al.</i> (1995)   |
| <i>Navicula saprophila</i>                        | <i>Acc1</i> , acetylCoA carboxylase   | Nuclear | <i>Cyclotella criptyca</i>                                    | Dunahay <i>et al.</i> (1995)   |
| <i>Phaeodactylum tricornutum</i>                  | <i>fcpA/B/C/E</i> , fucoxanthin chlorophyll   | Nuclear | <i>Phaeodactylum tricornutum</i>                              | Apt <i>et al.</i> (1996)   |
|   | <i>fcpF</i> , fucoxanthin chlorophyll   | Nuclear | <i>Phaeodactylum tricornutum</i>                              | Falciatore <i>et al.</i> (1999)  |
|   | <i>fcpA</i> , fucoxanthin chlorophyll   | Nuclear | <i>Phaeodactylum tricornutum</i>                              | Zaslavskaja and Lippmeier (2000)   |
| <i>Phaeodactylum tricornutum</i>                  | <i>cah</i> , carbonic anyhdrase   | Nuclear | <i>Phaeodactylum tricornutum</i>                              | Harada and Matsuda (2005)  |
|   | <i>CMV</i> , cytomegalovirus; <i>PRSV-LTR</i> , rous sarcoma virus; <i>35S</i> , cauliflower mosaic virus | Nuclear | Cytomegalovirus; Rous sarcoma virus; Cauliflower mosaic virus | Sakaue <i>et al.</i> (2008)  |

(Continued)

**Table 8.3** Promoter Used For Microalgae Genetic Transformation—cont'd

| Host Species of Microalgae       | Promoter of Gene and its Product                                       | Cell Expression Localization | Source of Promoter               | Source                                   |
|----------------------------------|--|------------------------------|----------------------------------|--|
|                                  | <i>fcpA</i> , fucoxanthin chlorophyll                                  | Nuclear                      | <i>Phaeodactylum tricornutum</i> | Coesel <i>et al.</i> (2009)              |
|                                  | <i>fcp</i> , fucoxanthin chlorophyll and <i>NR</i> , nitrate reductase | Nuclear                      | <i>Cylindrotheca fusiformis</i>  | Miyagawa <i>et al.</i> (2009)            |
| <i>Cylindrotheca fusiformis</i>  | $P\delta$ , frustulin $\alpha 3$                                       | Nuclear                      | <i>Cylindrotheca fusiformis</i>  | Fischer, Robl, Sumper, and Kroger (1999) |
| <i>Thalassiosira pseudonana</i>  | <i>NR</i> , nitrate reductase  | Nuclear                      | <i>Cylindrotheca fusiformis</i>  | Poulsen and Kroger (2005)                |
|                                  | <i>fcp</i> , fucoxanthin chlorophyll                                   | Nuclear                      | <i>Thalassiosira pseudonana</i>  | Poulsen <i>et al.</i> (2006)             |
| <i>Thalassiosira weissflogii</i> | <i>fcpB</i> , fucoxanthin chlorophyll                                  | Nuclear                      | <i>Thalassiosira pseudonana</i>  | Falciatore <i>et al.</i> (1999)          |
| <i>Chaetoceros sp.</i>           | <i>pTpNR</i> (nitrate reductase de <i>Thalassiosira pseudonana</i> )   | Nuclear                      | <i>Thalassiosira pseudonana</i>  | Miyagawa-Yamaguchi <i>et al.</i> (2011)  |

## Annexes 2 Microalgae, Functional Genomics and Biotechnology

|  |   |                    |  |   |
|--|---|--------------------|--|---|
| <i>Amphidinium spp.</i><br><i>Symbiodinium microadriaticum</i> | 35S, cauliflower mosaic virus 35S                                     | Nuclear            | Cauliflower mosaic virus   | Ten Lohuis and Miller (1998)  |
| <i>Cyanidioschyzon merolae</i>                                 | UMP synthase  | Nuclear            | <i>Cyanidioschyzon merolae</i>                                   | Minoda, Sakagami, Yagisawa, Kuroiwa, and Tanaka (2004)                              |
|  | $\beta$ -tubulin  | Nuclear            | <i>Cyanidioschyzon merolae</i>                                   | Ohnuma, Yokoyama, Inouye, Sekine, and Tanaka (2008)                                 |
|  | <i>cat</i> , catalase<br><i>apcC</i> , phycocyanin-associated protein | Nuclear<br>Nuclear | <i>Cyanidioschyzon merolae</i><br><i>Cyanidioschyzon merolae</i> | Ohnuma <i>et al.</i> (2009)<br>Watanabe, Ohnuma, Sato, Yoshikawa, and Tanaka (2011) |
| <i>Porphyidium sp.</i>   | <i>AHAS</i> , acetoxyacid synthase                                    | Nuclear            | <i>Porphyidium sp.</i>   | Lapidot, Raveh, Sivan, Arad, and Sapira (2002)                                      |
| <i>Euglena gracilis</i>  | <i>psbA</i> , photosystem II complex protein                          | Chloroplast        | <i>Euglena gracilis</i>  | Doetsch, Favreau, Kuscuoğlu, Thompson, and Hallick (2001)                           |

(Marin-Navarro *et al.*, 2007). The *psbA* promoter and 5'-UTR are the most studied but essentially require a *psbA*-deficient genetic background for high foreign protein accumulation (Rasala & Mayfield, 2011).

Other exogenous promoter sequences have been used in *C. reinhardtii* chloroplasts. Kato, Kolenic, & Pardini (2007) showed the functionality of the inducible system of the *lac* operon of *Escherichia coli* in *C. reinhardtii* chloroplasts. At the same time, a riboswitch was reported to act as a translational regulatory factor in *C. reinhardtii* (Croft, Moulin, Webb, & Smith, 2007). Finally, all the data suggest that the translation mechanism and mRNA accumulation are primarily controlled by the promoter and 5'-UTR and that the choice of these sequences is a critical factor to consider for each protein of interest in order to achieve high yields of recombinant proteins. On the other hand, to our knowledge, no chloroplast transformation has been reported for microalgae other than *C. reinhardtii* and the unicellular flagellate protist *Euglena gracilis*, leaving the way open for research to study this mechanism of expression in other microalgae.

Concerning nuclear promoters, several studies have been performed in different taxa of microalgae using endogenous, exogenous and synthetic promoters (Table 8.3). The most widely used constitutive promoter in the chlorophyte group is *RbcS* (RuBisCO small subunit). Interestingly, some endogenous promoters of *C. reinhardtii* can be used in other Chlorophyta algae. Indeed, the *C. reinhardtii* *RbcS* promoter has been successfully used in the green alga *D. salina* (Sun *et al.*, 2005), *C. ellipsoideum* formerly *Chlorella ellipsoidea* (Kim *et al.*, 2002), the Heterokonta *Nannochloropsis oculata* (Chen, Li, Huang, & Tsai, 2008; Li, Xue, Yan, Liu, & Liang, 2008) and the Chlorarachniophyta *Lotharella amoebiformis* (Hirakawa, Kofuji, & Ishida, 2008). A chimeric promoter using heat shock protein A (*HSP70A*) fused to *psaD* was also successfully used in *C. reinhardtii* (Fischer & Rochaix, 2001; Schroda, Blocker, & Beck, 2000) and more recently in the multicellular alga *Gonium pectorale* (Lerche & Hallmann, 2009). The same strategy, using *HSP70* fused to *CAb* (chlorophyll-binding protein), was reported in the charophyte *Closterium peracerosum* (Abe *et al.*, 2011). Usual plant promoters, such as the cauliflower mosaic virus 35S with *Ubiquitin-Q*, have been also tested in some microalgae (Chen *et al.*, 2001; Jarvis & Brown, 1991; Kumar, Misquitta, Reddy, Rao, & Rajam, 2004; Wang, Wang, Su, & Gao, 2007; Wang, Xue *et al.*, 2007), and recently, the 35S promoter demonstrated efficiency in the diatom *P. tricornutum* (Sakaue, Harada, & Matsuda, 2008), Chlorophytes *Haematococcus* sp. (Kathiresan, Chandrashekar, Ravishankar, & Sarada, 2009) and *Dunaliella bardawil* (Anila, Chandrashekar, Ravishankar, &

Sarada, 2011) and the Heterokonta *Nannochloropsis* sp. (Cha, Chen, Yee, Aziz, & Loh, 2011). Moreover, inducible promoters have been chosen for some algae. Indeed, the gene expression under the control of the nitrate reductase promoter is switched off when cells are grown in the presence of ammonium and becomes switched on when cells are transferred to a medium-containing nitrate. This approach was reported for the diatom *Cylindrotheca fusiformis* (Poulsen & Kroger, 2005) and recently in *C. vulgaris* (strain not reported) using the *NR* cassette (promoter and 5' and 3'-UTR of nitrate reductase) of the diatom *P. tricornutum* (Niu *et al.*, 2011). A similar strategy was applied in *P. tricornutum* using the endogenous *NR* cassette (Hempel, Bozarth *et al.*, 2011, Hempel, Lau *et al.*, 2011) and exogenous *NR* cassette from the diatom *Cylindrotheca fusiformis* (Miyagawa *et al.*, 2009). Miyagawa-Yamaguchi *et al.* (2011) reported the same approach in another diatom, *Chaetoceros* sp., using the *NR* cassette of the diatom *Thalassiosira pseudonana*. The study performed by Niu *et al.* (2011) is particularly interesting as the diatom *NR* cassette was shown to be functional in green algae, suggesting that this type of inducible promoter could be universally employed across diverse species of algae.

In contrast to plastid promoters, several studies have been performed on nuclear promoters in diatoms. So far, unlike in green algae, the RuBisCO small subunit gene of diatoms is encoded by the chloroplast genome and its promoter is not adapted for nuclear transformation. Other promoters were identified from genomic and transcriptomic data from diatoms. Early studies reported protein expression using the acetylCoA carboxylase (*Acc1*) promoter in diatoms *C. cryptica* and *Navicula saprophila* (Dunahay, Jarvis, & Roessler, 1995). Members of the family of light-inducible fucoxanthin chlorophyll (*Fcp*) promoters have also been used to produce foreign protein in diatoms *P. tricornutum* (Apt, Kroth-Pancic, & Grossman, 1996; Falciatore, Casotti, Leblanc, Abrescia, & Bowler, 1999; Zaslavskaja & Lippmeier, 2000) and *Thalassiosira* sp. (Falciatore *et al.*, 1999; Poulsen, Chesley, & Kroger, 2006). In contrast to the *NR* promoter, the *Fcp* promoter appears to be more specific to the host as, for example, the *Fcp* promoter of *P. tricornutum* is not functional in *Cylindrotheca fusiformis* (Poulsen & Kroger, 2005).

Some use of virus promoters other than 35S has also been reported in algae, such as mammalian cytomegalovirus *CMV* in *P. tricornutum* (Sakaue *et al.*, 2008), and recently in the Chlorophyta *Platymonas subcordiformis* (Cui, Wang, Jiang, Bian, & Qin, 2010), as well as the Rous sarcoma virus in the diatom *P. tricornutum* (Sakaue *et al.*, 2008).

Surprisingly, the use of microalgal virus sequences in algal expression constructs to enhance gene expression has still not been explored. To date, several algal viruses have been identified and their full genomes sequenced in some microalgal taxa, specifically chlorophytes, dinoflagellates, diatoms and haptophytes (for reports and reviews on this topic, see Nagasaki, 2008; Nissimov *et al.*, 2011; Schroeder, Oke, Malin, & Wilson, 2002; Van Etten & Dunigan, 2012; Wilson, Van Etten, & Allen, 2009). To date, algal viruses represent a largely unexplored source of genetic elements for engineering algae and land plants. This approach has previously been used in both monocotyledonous and dicotyledonous land plants as well as in bacteria (Mitra, Higgins, & Rohe, 1994). Another study reported the functionality of a translation enhancer element from the *Chlorella* virus in the plant *Arabidopsis thaliana* (Nguyen, Falcone, & Graves, 2009).

Another strategy to increase the yield of recombinant proteins consists of adding intronic sequences to the expression vector to act as an endogenous enhancer. Indeed, while regulation of gene expression occurs at the post-transcriptional level in the plastid, it appears that most regulation occurs both at the transcriptional and at the translational levels in the nucleus (Marin-Navarro *et al.*, 2007). The introns are non-encoding sequences but can affect the expression of genes by alternative splicing or through the regulation of transcription. In *C. reinhardtii*, Lumbreras and Purton (1998) reported that the insertion of endogenous introns from heterologous genes increases the expression level. Recently, a similar approach has been used to increase the expression level of the *Renilla*-luciferase gene reporter in *C. reinhardtii* (Eichler-Stahlberg *et al.*, 2009). However, the way in which the introns affect the expression level is still unclear.

### 2.3.2.3. The challenges of transgene silencing and proteolysis

Transgene silencing is another problem for high-yield recombinant protein expression in plants and algae, but different strategies exist to overcome this obstacle. Indeed, gene silencing can function as a protective system against pathogens or viruses (Specht *et al.*, 2010). Plant virus-encoded suppressors of RNA silencing are useful tools for counteracting silencing, but their wide application in transgenic plants is limited because their expression often causes harmful developmental effects. To our knowledge, this approach has not yet been attempted in microalgae. Recently, another strategy to prevent transgene silencing was reported in *C. reinhardtii* using a process of UV mutation and selection by antibiotic resistance on a selective medium (Neupert, Karcher, & Bock, 2009).

To date, most efforts to improve recombinant protein accumulation in plants or algae have focused on increasing protein expression. Moreover, proteolysis is also one of the factors that can affect the yield of recombinant protein accumulated and also lead to difficulties in purification due to degraded forms or non-functional protein (Doran, 2006; Surzycki *et al.*, 2009). However, proteolytic enzymes are essential for the degradation of misfolding or incorrectly processed endogenous proteins. Some strategies have been attempted to minimize foreign protein degradation in plants and microalgae, like producing recombinant proteins in other cell compartments that have an environment with less proteolytic activity. Indeed, for nuclear-expressed protein, the targeting of the ER using the HDEL or KDEL retention signal prevents the degradation of the foreign protein. A similar approach has been successfully used by our laboratory to express recombinant EPO in diatoms. Another approach used in plants consists of concomitantly producing protease inhibitor to neutralize endogenous protease (Doran, 2006).



### 3. FUTURE OUTLOOK

In this chapter, we tried to provide an overview of the principal applications of microalgae and show how genomics and post-genomics can improve their uses in biotechnology. Here, we mainly focused on some of the most popular applications. Without wishing to suggest that they are less important, we chose not to make a detailed review of other applications such as environmental biomarkers, silica synthesis from diatoms or hydrogen and methane production for energy. In any case, the future of microalgal biotechnology will depend on several steps, including domestication and a search for new intrinsic species characteristics, steps for which the contributions of ‘omics’ technologies will be invaluable.

#### 3.1. Domestication

A strategy comparable to that used for the domestication of crops is now making its way into the world of microalgae. This is a matter of selecting favourable mutations and finding markers that will help select the desired traits. In agriculture, the cross-breeding of species and selection of strains was conducted empirically for thousands of years before Mendel’s laws provided a scientific basis for species improvement. For sexual reproduction, considerable work remains to be done in microalgae. Knowledge of reproductive



strategies is of major importance for maintaining strains, cultivating them on a long-term basis in continuous culture or envisaging selection strategies. Some algal groups have become the subject of increased attention concerning their reproduction strategies and sexual behaviour, including the diatoms (Chepurnov, Chaerle, Roef, Meirhaeghe, & Vanhoutte, 2011). In the Coccolithophore *E. huxleyi*, different morphotypes associated with different forms of ploidy have been observed and studied by transcriptomic analysis. This work revealed mechanisms involved in functional differentiation without proving that sexual reproduction occurs (Von Dassow *et al.*, 2009). To date, there is too little knowledge to envisage the improvement of strains by cross-breeding and selection through sexual reproduction, so future studies in this direction will be of great interest.

Mutation followed by selection for favourable phenotypes has been used for crop plants, and some promising strategies are now beginning to emerge for algae. This domestication route calls for induced mutations and subsequent selection. Bonente, Formighieri, Morosinotto, and Bassi (2011) identified the major relevant points for the selection of H<sub>2</sub>-producing *Chlamydomonas* sp., namely a reduction of photosynthetic antenna size, an alteration of photosystem II to manipulate the oxygen concentration and a maximized electron flow towards hydrogenase. This strategy was thought to enhance carotenoid levels. Early studies involved *D. salina* and the selection of beta-carotene-rich strains (Shaish, Ben-Amotz, & Avron, 1991). These were followed by a search for hyperproductive variants sorted by flow cytometry (Mendoza *et al.*, 2008), and recently, there have been improvements in lutein production in the microalga *C. sorokiniana* (Cordero, Couso, Leon, Rodriguez, & Angeles Vargas, 2011). This strategy was implemented to enhance overall lipid contents or EPA and DHA, in particular, with the Haptophytes *I. galbana* (Molina Grima *et al.*, 1995) and *Pavlova lutheri* (Meireles, Guedes, & Malcata, 2003), the Heterokonta *N. oculata* (Chaturvedi & Fujita, 2006) or the chlorophyte *D. salina* (Mendoza *et al.*, 2008). In this context, the availability of a reliable marker, such as Nile Red or BODIPY for staining lipid bodies, greatly helps in the selection process. In the Haptophyte *I. galbana* affinis Tahiti, this strategy allowed our laboratory to select an improved strain that could stably produce twice the amount of TAG compared to its wild-type counterpart (Rouxel *et al.*, 2011).

We have reported that the improvement of microalgae for biotechnology uses will come through the domestication of strains and this approach has already been initiated. Far from being in conflict, the different approaches ('natural' vs. 'GMO') are complementary. Synthetic biology,

synthetic genomics and genome engineering are disruptive technologies. Indeed, the development of ‘GMO’ strategies is very promising for applications with very high added value such as the production of drugs or antibodies. However, taking into account the environmental risks arising with such transgenic species and societal pressure against their use, their culture will have to be performed in confined and controlled conditions. Their use for energy and food (large outdoor cultures) therefore seems somewhat inappropriate. The completely opposite point of view is that, given the immeasurable biodiversity of algae, the ideal alga for a given application is probably available in nature. Although this perspective is somewhat optimistic, the exploration of biodiversity was the source of the algae presently in use and will doubtless continue to be in the future. Screening this diversity will enable us to identify new, more efficient strains with new features, some of which may have uses that have not yet been imagined. This does not preclude subsequent domestication to improve these species for use in biotechnology.

### 3.2. Working Towards a New Algal Metabolism, Enzymes and Compounds

As seen earlier in this chapter, the implementation of genomic and post-genomic approaches is now largely underway in the world of microalgae. In parallel, ecological approaches in metagenomics have only been seen very recently. These will hopefully lead to the identification of a large number of presently unknown microalgae and, consequently, to new gene networks, enzymes and metabolic pathways. Due to the wide variety of microalgae and difficulties in cultivating certain of them, many metabolic pathways have remained out of our reach until the present. Metagenomics aims to analyze all the genomic data in a given ecosystem without a strain isolation and cultivation step. This allows access to unknown mechanisms of potential biotechnological interest. In this situation, the ‘sequencing campaigns’ on research cruises (Karsenti *et al.*, 2011) will offer new and valuable insight in the field of microalgal genomics. Chapter X of this volume provides a review on the power and challenges of metagenomics for microbial algae (Toulza, Blanc-Mathieu, Goubiere, & Piganeau 2012). Conversely, metagenomics will be greatly aided by new methods like single cell genome analysis (Ebenezer, Medlin, & Ki, 2011), which can improve methods of isolation and cultivation of new algae.

Among the wide variety of metabolic pathways conceivable across the diversity of microalgae, particular attention should be paid to metabolism from extremes environments. Like bacteria, although to a lesser extent, some microalgal species live under severe physicochemical pressures such as high salinity, extreme temperatures from below 0 °C to over 50 °C, alkaline or acidic waters or very high irradiance. Additionally, some strains have been isolated downstream from industrial sites such as acid mine drainage or in waters rich in contaminants such as metals (for review, see [Das \*et al.\*, 2009](#)). Extremophiles offer numerous advantages including (1) the absence of contaminants in open door cultures subjected to physico-chemical pressure, (2) their potential adaptation to industrial environments such as presence of toxins, radioactive elements or extreme pH and consequently their potential use for the biocatalysis of effluents and (3) their ability to produce enzymes with biotechnological applications. Proteomics have been carried out to highlight the adaptation mechanisms in the halophilic species *D. salina* ([Katz, Waridel, Shevchenko, & Pick, 2007](#); [Liska, 2004](#)) for which the genome sequence will soon be available. Transcriptomics and comparative genomics have dealt with the very high biochemical versatility of thermoacidophilic *Galdieria sulphuraria* ([Barbier \*et al.\*, 2005](#); [Weber \*et al.\*, 2004](#)). Psychrophilic species have been identified, such as *Fragilariopsis cylindrus*, *Xanthonema* sp., *Koliella antarctica* and *Chlamydomonas* sp. ICE-L. However, the culture of psychrophiles is far from being technically mastered, making post-genomic approaches difficult. In such cases, metagenomics would be an appropriate solution. Overall, efforts are still needed to isolate and cultivate extremophiles, and genomics will provide a source of new applications.

### 3.3. Algal Pathogens: Looking Towards the Future

Like land plants, phytoplankton are susceptible to diseases and parasitism, which impact their population dynamics and use in commercial industry. Interactions between bacteria and microalgae in the environment and in cultures are numerous, and bacteria can have beneficial or negative effects on the growth of microalgae. For a review, see [Fukami, Nishijima, and Ishida \(1997\)](#). Numerous algicidal bacteria have been identified in the ocean and their influence on algal bloom dynamics has been demonstrated ([Mayali & Azam, 2004](#)). Although they have not yet been associated with real economic losses in cultures, the experience in production of other marine species suggests that diseases will likely appear in parallel with the

expansion of the industry. Viruses are extremely abundant in seawater and are believed to be significant pathogens to photosynthetic protists. They are known to affect the regulation of eukaryotic phytoplankton population densities. Since the discovery of the very high abundance of viruses in the marine environment, researchers have highlighted their possible ecological significance. To date, more than 40 viruses infecting marine microalgae have been isolated and characterized to different extents (Nagasaki, 2008). Several studies have focused on the relationship between eukaryotic microalgae and their viruses (for review, see Nagasaki, 2008). Without going into great detail, it is interesting to note that most algae can use various strategies of resistance to their viruses, but the mechanisms involved are not yet clearly understood (Morin, 2008; Thomas *et al.*, 2011). The next chapter of this volume, 'Genomics of Algal Host-Virus Interactions', reviews algal host-virus interactions (Grimsley *et al.*, 2012). Finally, it will be interesting to compare the emergence of pathogens such as plant viruses during this new agricultural revolution and increase in demand for algal culture by industry. Microalgal cultivation remains a niche market in almost all countries, but the increasing interest in sustainable biofuel sources has triggered a high investment in culture facilities all over the world. Consequently, intensive algal aquaculture using open pond systems for the mass culture of microalgae might favour disease outbreaks. Gachon, Sime-*Ngando*, Strittmatter, Chambouvet, and Kim (2010) suggest that development towards intensive macroalgal production correlates with more damaging disease outbreaks. The best example is the case of edible red macroalgae *Porphyra* sp., which represents a very valuable industry in Asia. The market is estimated to be worth about \$1.5 billion worldwide and has reported losses of about 10% of annual production due to oomycete pathogens, although these outbreaks can even lead to losses of 25–40% in some cases. To overcome this problem, sea farmers can use chemical treatments, but their use in large doses could have a real impact on ecosystems as well as on production costs. A better understanding of the relationships between pathogens and microalgae would be useful to identify causes and possible solutions to overcome disease epidemics. Prophylactic and microbial flora management of cultures will probably be a key to the durability of production in the coming years. Varietal selection of microalgal strains for resistance to a large range of pathogens is one strategy that could increase the resistance of microalgal cultures. In any case, in the context of intensive microalgal production, we must anticipate future epidemics that will affect algal culture yields.



## 4. CONCLUSIONS

Due to the huge amount of diversity among microalgae, their applications have a very bright future. As seen in this chapter, the uses of microalgae are numerous and there is work for many research teams in many fields of specialization.

Genomics and post-genomics have led to new areas of research and development and to the modernization of our view of biology. The increase in sequencing capacities will soon face a data tsunami, a fantastic amount of data that will soon be generated by fast low-cost sequencing methods. However, storage, calculation power, annotations and access to this information now pose a limit to its optimal exploration. Data mining and conversion of data into biological knowledge will be an important challenge in coming years. The confirmation of all the *in silico* analyses and discoveries will require a return to experimental testing, and the association of molecular data with biological functions will become vital work in the future (Lopez, Casero, Cokus, Merchant, & Pellegrini, 2011).

The culture of microalgae for biomass production dates back to the 1940s when it started in the United States before spreading to Europe, Japan and Israel (Grobbelaar, 2010). Since then, work has continued all over the world at different speeds, with irregular publication rates. Some of the early work still forms the basis for the today's revival of the microalgal trend (Sheehan *et al.*, 1998). The dramatic increase in the world population concerns about the ecological equilibrium, pollution, the world energy demand and failing supplies of oil and coal have all led to a more 'bio'-orientated attitude, meaning a general increase in the attention paid to 'renewable' resources. From a global perspective, in the context of a demographic crisis, the major issues in the coming years will be to provide everyone with access to water, food, education and healthcare. In a world of limited resources (energy, clean water, arable land) and increasing anthropogenic pressure on the environment, the development of biotechnological processes to provide renewable energy, new molecules and molecular farming and cleaner industrial processes is one of the key challenges. Marine microalgae possess assets that make them suitable for some of these applications. While land plants are the subject of numerous programs aiming to use vegetal organisms for the so-called 'green chemistry', the algae, particularly microalgae, are expected to participate in this race in a complementary way. Although far less studied than their terrestrial counterparts, microalgae

offer an, as yet, untapped diversity and manipulability that explain the enthusiasm and investment from around the world. Phytoplankton research is being revisited and enriched by modern techniques like molecular biology and biocomputing, and the 'omics' technologies offer new insights into their biology. The young generation of students will have the chance, at the strictly scientific level, to be present when the majority of the genomes are still to be sequenced, the transcriptome is unknown and even the reproductive strategies or size of the genomes are undefined. The earth still hides a tremendous amount of original biology, including much that concerns microalgae. Their discovery, study, analysis and use will serve applications in all imaginable fields.

## REFERENCES

- Abe, J., Hiwatashi, Y., Ito, M., Hasebe, M., & Sekimoto, H. (2008). Expression of exogenous genes under the control of endogenous HSP70 and CAB promoters in the *Closterium peracerosum-strigosum-littorale* complex. *Plant and Cell Physiology*, *49*, 625–632.
- Abe, J., Hori, S., Tsuchikane, Y., Kitao, N., Kato, M., & Sekimoto, H. (2011). Stable nuclear transformation of the *Closterium peracerosum-strigosum-littorale* complex. *Plant and Cell Physiology*, *52*, 1676–1685.
- AbuGhazaleh, A. A., Potu, R. B., & Ibrahim, S. (2009). Short communication: The effect of substituting fish oil in dairy cow diets with docosahexaenoic acid-micro algae on milk composition and fatty acids profile. *Journal of Dairy Science*, *92*, 6156–6159.
- Anila, N., Chandrashekar, A., Ravishankar, G. A., & Sarada, R. (2011). Establishment of *Agrobacterium tumefaciens*-mediated genetic transformation in *Dunaliella bardawil*. *European Journal of Phycology*, *46*, 36–44.
- Apt, K. E., Kroth-Pancic, P. G., & Grossman, A. R. (1996). Stable nuclear transformation of the diatom *Phaeodactylum tricornutum*. *Molecular and General Genetics*, *252*, 572–579.
- Archibald, J. (2012). The evolution of algae by secondary and tertiary endosymbiosis. *Advances in Botanical Research*, *64*, 87–118.
- Auchincloss, A. H., Lorocho, A. I., & Rochaix, S. D. (1999). The argininosuccinate lyase gene of *Chlamydomonas reinhardtii*: Cloning of the cDNA and its characterization as a selectable shuttle marker. *Molecular and General Genetics*, *261*, 21–30.
- Baba, M., Ioki, M., Nakajima, N., Shiraiwa, Y., & Watanabe, M. M. (2011). Transcriptome analysis of an oil-rich race: A strain of *Botryococcus braunii* (BOT-88-2) by de novo assembly of pyrosequencing cDNA reads. *Bioresource Technology*, *109*, 282–286.
- Baïet, B., Burel, C., Saint-Jean, B., Louvet, R., Menu-Bouaouiche, L., Kiefer-Meyer, M. C., et al. (2011). N-glycans of *Phaeodactylum tricornutum* diatom and functional characterization of its N-acetylglucosaminyltransferase I enzyme. *The Journal of Biological Chemistry*, *286*, 6152–6164.
- Bakker, H., Bardor, M., Molthoff, J. W., Gomord, V., Elbers, I., Stevens, L. H., et al. (2001). Galactose-extended glycans of antibodies produced by transgenic plants. *Proceedings of the National Academy of Sciences of the United States of America*, *98*, 2899–2904.
- Barbier, G., Oesterhelt, C., Larson, M. D., Halgren, R. G., Wilkerson, C., Garavito, R. M., et al. (2005). Comparative genomics of two closely related unicellular thermo-

- acidophilic red algae, *Galdieria sulphuraria* and *Cyanidioschyzon merolae*, reveals the molecular basis of the metabolic flexibility of *Galdieria sulphuraria* and significant differences in carbohydrate metabolism of both algae. *Plant Physiology*, 137, 460–474.
- Barnes, D., Franklin, S., Schultz, J., Henry, R., Brown, E., Coragliotti, A., et al. (2005). Contribution of 5'- and 3'-untranslated regions of plastid mRNAs to the expression of *Chlamydomonas reinhardtii* chloroplast genes. *Molecular Genetics and Genomics*, 274, 625–636.
- Becker, W. (2007). Microalgae in human and animal nutrition. In A. Richmond (Ed.), *Handbook of microalgal culture. Biotechnology and applied phyecology* (pp. 312–351). Oxford: Blackwell Science.
- Berthold, P., Schmitt, R., & Mages, W. (2002). An engineered *Streptomyces hygroscopicus* *aph 7''* gene mediates dominant resistance against hygromycin B in *Chlamydomonas reinhardtii*. *Protist*, 153, 401–412.
- Bhadury, P., & Wright, P. C. (2004). Exploitation of marine algae: Biogenic compounds for potential antifouling applications. *Planta*, 219, 561–578.
- Blanc, G., Duncan, G., Agarkova, I., Borodovsky, M., Gurnon, J., Kuo, A., et al. (2010). The *Chlorella variabilis* NC64A genome reveals adaptation to photosymbiosis, coevolution with viruses, and cryptic sex. *The Plant Cell*, 22, 2943–2955.
- Blankenship, J. E., & Kindle, K. L. (1992). Expression of chimeric genes by the light-regulated Cabii-1 promoter in *chlamydomonas-reinhardtii*—A Cabii-1/Nit1 gene functions as a dominant selectable marker in a Nit1-Nit2-strain. *Molecular and Cellular Biology*, 12, 5268–5279.
- Bock, R. (2007). Plastid biotechnology: Prospects for herbicide and insect resistance, metabolic engineering and molecular farming. *Current Opinion in Biotechnology*, 18, 100–106.
- Bonente, G., Formighieri, C., Morosinotto, T., & Bassi, R. (2011). Domestication of wild unicellular algae for growth in photobioreactors. *FEBS Journal*, 278, 64–65.
- Bowler, C., Allen, A. E., Badger, J. H., Grimwood, J., Jabbari, K., Kuo, A., et al. (2008). The *Phaeodactylum* genome reveals the evolutionary history of diatom genomes. *Nature*, 456, 239–244.
- Bozarth, A., Maier, U. G., & Zauner, S. (2009). Diatoms in biotechnology: Modern tools and applications. *Applied Microbiology and Biotechnology*, 82, 195–201.
- Brown, L. E., Sprecher, S. L., & Keller, L. R. (1991). Introduction of exogenous DNA into *Chlamydomonas reinhardtii* by electroporation. *Molecular and Cellular Biology*, 11(4), 2328–2332.
- Cadoret, J.-P., Bardor, M., Lerouge, P., Cabiglieria, M., Henriquez, V., & Carlier, A. (2008). Les microalgues: Usines cellulaires productrices de molécules commerciales recombinantes. *Medecine Science*, 24, 375–382.
- Cadoret, J.-P., Carlier, A., Burel, C., Maury, F., Bardor, M., & Lerouge, P. (2009). *Production of glycosylated proteins in microalgae*. PCT/EP/2009/051672.
- Camacho, F. G., Rodríguez, J. G., Mirón, A. S., García, M. C. C., Belarbi, E. H., Chisti, Y., et al. (2006). Biotechnological significance of toxic marine dinoflagellates. *Biotechnology Advances*, 25, 176–194.
- Cerutti, H., Johnson, A. M., Gillham, N. W., & Boynton, J. E. (1997). A eubacterial gene conferring spectinomycin resistance on *Chlamydomonas reinhardtii*: Integration into the nuclear genome and gene expression. *Genetics*, 145, 97–110.
- Cha, T. S., Chen, C. F., Yee, W., Aziz, A., & Loh, S. H. (2011). Cinnamic acid, coumarin and vanillin: Alternative phenolic compounds for efficient *Agrobacterium*-mediated transformation of the unicellular green alga, *Nannochloropsis sp.* *Journal of Microbiological Methods*, 84, 430–434.

- Cha, T. S., Yee, W., & Aziz, A. (2011). Assessment of factors affecting *Agrobacterium*-mediated genetic transformation of the unicellular green alga, *Chlorella vulgaris*. *World Journal of Microbiology & Biotechnology*. doi: 10.1007/s11274-011-0991-0.
- Chaturvedi, R., & Fujita, Y. (2006). Isolation of enhanced eicosapentaenoic acid producing mutants of *Nannochloropsis oculata* ST-6 using ethyl methane sulfonate induced mutagenesis techniques and their characterization at mRNA transcript level. *Phycological Research*, 54, 208–219.
- Chen, Y., Wang, Y. Q., Sun, Y. R., Zhang, L. M., & Li, W. B. (2001). Highly efficient expression of rabbit neutrophil peptide-1 gene in *Chlorella ellipsoidea* cells. *Current Genetics*, 39, 365–370.
- Chen, H. L., Li, S. S., Huang, R., & Tsai, H. J. (2008). Conditional production of a functional fish growth hormone in the transgenic line of *Nannochloropsis oculata* (Eustigmatophyceae). *Journal of Phycology*, 44, 768–776.
- Chepurnov, V. A., Chaerle, P., Roef, L., Meirhaeghe, A., & Vanhoutte, K. (2011). Classical breeding in diatoms: scientific background and practical perspectives. In J. Seckbach, & P. Kociolek (Eds.), *The diatom world* (pp. 167–194). The Netherlands: Springer.
- Chow, K. C., & Tung, W. L. (1999). Electrotransformation of *Chlorella vulgaris*. *Plant Cell Reports*, 18, 778–780.
- Coesel, S., Mangogna, M., Ishikawa, T., Heijde, M., Rogato, A., Finazzi, G., et al. (2009). Diatom PtCPF1 is a new cryptochrome/photolyase family member with DNA repair and transcription regulation activity. *EMBO Reports*, 10, 655–661.
- Conley, A. J., Mohib, K., Jevnikar, A. M., & Brandle, J. E. (2009). Plant recombinant erythropoietin attenuates inflammatory kidney cell injury. *Plant Biotechnology Journal*, 7, 183–199.
- Cordero, B. F., Couso, I., Leon, R., Rodriguez, H., & Angeles Vargas, M. (2011). Enhancement of carotenoids biosynthesis in *Chlamydomonas reinhardtii* by nuclear transformation using a phytoene synthase gene isolated from *Chlorella zofingiensis*. *Applied Microbiology and Biotechnology*, 91, 341–351.
- Croft, M. T., Moulin, M., Webb, M. E., & Smith, A. G. (2007). Thiamine biosynthesis in algae is regulated by riboswitches. *Proceedings of the National Academy of Sciences of the United States of America*, 104, 20770–20775.
- Cui, Y. L., Wang, J. F., Jiang, P., Bian, S. G., & Qin, S. (2010). Transformation of *Platymonas (Tetraselmis) subcordiformis* (Prasinophyceae, Chlorophyta) by agitation with glass beads. *World Journal of Microbiology & Biotechnology*, 26, 1653–1657.
- Cui, H., Wang, Y., & Qin, S. (2011). Molecular evolution of lycopene cyclases involved in the formation of carotenoids in eukaryotic algae. *Plant Molecular Biology Reporter*, 29, 1013–1020.
- Das, B. K., Roy, A., Koschorreck, M., Mandal, S. M., Wendt-Potthoff, K., & Bhattacharya, J. (2009). Occurrence and role of algae and fungi in acid mine drainage environment with special reference to metals and sulfate immobilization. *Water Research*, 43, 883–894.
- Dauvillee, D., Delhaye, S., Gruyer, S., Slomianny, C., Moretz, S. E., d'Hulst, C., et al. (2010). Engineering the chloroplast targeted malarial vaccine antigens in *Chlamydomonas* starch granules. *PLoS ONE*, 5, e15424. doi: 10.1371/journal.pone.
- Dawson, H. N., Burlingame, R., & Cannons, A. C. (1997). Stable transformation of *Chlorella*: rescue of nitrate reductase-deficient mutants with the nitrate reductase gene. *Current Microbiology*, 35, 356–362.
- Debuchy, R., Purton, S., & Rochaix, J.-D. (1989). The arginosuccinate lyase gene of *Chlamydomonas reinhardtii*: an important tool for nuclear transformation and for correlating the genetic and molecular maps of the ARG7 locus. *EMBO Journal*, 8, 2803–2809.



- De Clerck, O., Bogaret, K., & Leliaert, F. (2012). Diversity and evolution of algae: primary endosymbiosis. *Advances in Botanical Research*, 64, 55–86.
- Desmond, E., & Gribaldo, S. (2009). Phylogenomics of sterol synthesis: insights into the origin, evolution, and diversity of a key eukaryotic feature. *Genome Biology and Evolution*, 1, 364–381.
- Dittami, S. M., Riisberg, I., John, U., Orr, R. J. S., Jakobsen, K. S., & Edvardsen, B. (2011). Analysis of expressed sequence tags from the marine microalga *Pseudochattonella farcimen* (Dictyochophyceae). *Protist*, 163, 143–161.
- Doetsch, N. A., Favreau, M. R., Kuscuoğlu, N., Thompson, M. D., & Hallick, R. B. (2001). Chloroplast transformation in *Euglena gracilis*: splicing of a group III twintron transcribed from a transgenic psbK operon. *Current Genetics*, 39, 49–60.
- Doran, P. M. (2006). Foreign protein degradation and instability in plants and plant tissue cultures. *Trends in Biotechnology*, 24, 426–432.
- Dove, A. (2002). Uncorking the biomanufacturing bottleneck. *Nature Biotechnology*, 20, 777–779.
- Dreesen, I. A. J., Charpin-El Hamri, G., & Fussenegger, M. (2010). Heat-stable oral alga-based vaccine protects mice from *Staphylococcus aureus* infection. *Journal of Biotechnology*, 145, 273–280.
- Dunahay, T. G., Jarvis, E. E., & Roessler, P. G. (1995). Genetic transformation of the diatoms *Cyclotella cryptica* and *Navicula saprophila*. *Journal of Phycology*, 31, 1004–1012.
- Dunahay, T., Jarvis, E., Dais, S., & Roessler, P. (1996). Manipulation of microalgal lipid production using genetic engineering. *Applied Biochemistry and Biotechnology*, 57(8), 223–231.
- Ebenezer, V., Medlin, L., & Ki, J.-S. (2011). Molecular detection, quantification, and diversity evaluation of microalgae. *Marine Biotechnology*, 14(2), 129–142.
- Eichler-Stahlberg, A., Weisheit, W., Ruecker, O., & Heitzer, M. (2009). Strategies to facilitate transgene expression in *Chlamydomonas reinhardtii*. *Planta*, 229, 873–883.
- Eom, H., Lee, C. G., & Jin, E. (2005). Gene expression profile analysis in astaxanthin-induced *Haematococcus pluvialis* using a cDNA microarray. *Planta*, 223, 1231–1242.
- Falcitore, A., Casotti, R., Leblanc, C., Abrescia, C., & Bowler, C. (1999). Transformation of nonselectable reporter genes in marine diatoms. *Marine Biotechnology*, 1, 239–251.
- Fan, J., Andre, C., & Xu, C. (2011). A chloroplast pathway for the de novo biosynthesis of triacylglycerol in *Chlamydomonas reinhardtii*. *FEBS Letters*, 585, 1985–1991.
- Feng, S. Y., Xue, L. X., Liu, H. T., & Lu, P. J. (2009). Improvement of efficiency of genetic transformation for *Dunaliella salina* by glass beads method. *Molecular Biology Reports*, 36, 1433–1439.
- Finazzi, G., Moreau, H., & Bowler, C. (2010). Genomic insights into photosynthesis in eukaryotic phytoplankton. *Trends in Plant Science*, 15, 565–572.
- Fischer, H., Robl, I., Sumper, M., & Kroger, N. (1999). Targeting and covalent modification of cell wall and membrane proteins heterologously expressed in the diatom *Cylindrotheca fusiformis* (Bacillariophyceae). *Journal of Phycology*, 35, 113–120.
- Fischer, N., & Rochaix, J. D. (2001). The flanking regions of PsalD drive efficient gene expression in the nucleus of the green alga *Chlamydomonas reinhardtii*. *Molecular Genetics and Genomics*, 265, 888–894.
- Franklin, S., Ngo, B., Efuot, E., & Mayfield, S. (2002). Development of a GFP reporter gene for *Chlamydomonas reinhardtii* chloroplast. *Plant Journal*, 30, 733–744.
- Frommolt, R., Werner, S., Paulsen, H., Goss, R., Wilhelm, C., Zauner, S., et al. (2008). Ancient recruitment by chromists of green algal genes encoding enzymes for carotenoid biosynthesis. *Molecular Biology and Evolution*, 25, 2653–2667.
- Fuhrmann, M., Oertel, W., & Hegemann, P. (1999). A synthetic gene coding for the green fluorescent protein (GFP) is a versatile reporter in *Chlamydomonas reinhardtii*. *Plant Journal*, 19, 353–361.

- Fukami, K., Nishijima, T., & Ishida, Y. (1997). Stimulative and inhibitory effects of bacteria on the growth of microalgae. *Hydrobiologia*, 358, 185–191.
- Gachon, C. M. M., Sime-Ngando, T., Strittmatter, M., Chambouvet, A., & Kim, G. H. (2010). Algal diseases: spotlight on a black box. *Trends in Plant Science*, 15, 633–640.
- Gasdaska, J. R., Spencer, D., & Dickey, L. (2003). Advantages of therapeutic protein production in the aquatic plant *Lemna*. *BioProcessing Journal*, 2(2), 49–56.
- Geng, D. G., Wang, Y. Q., Wang, P., Li, W. B., & Sun, Y. R. (2003). Stable expression of hepatitis B surface antigen gene in *Dunaliella salina* (Chlorophyta). *Journal of Applied Phycology*, 15, 451–456.
- Gobler, C. J., Berry, D. L., Dyhrman, S. T., Wilhelm, S. W., Salamov, A., Lobanov, A. V., et al. (2011). Niche of harmful alga *Aureococcus anophagefferens* revealed through ecogenomics. *Proceedings of the National Academy of Sciences of the United States of America*, 108, 4352–4357.
- Gomord, W., Sourrouille, C., Fitchette, A. C., Bardor, M., Pagny, S., Lerouge, P., et al. (2004). Production and glycosylation of plant-made pharmaceuticals: the antibodies as a challenge. *Plant Biotechnology Journal*, 2, 83–100.
- Gould, S. B., Waller, R. F., & McFadden, G. I. (2008). Plastid evolution. *Annual Review of Plant Biology*, 59, 491–517.
- Gourdon, D., Lin, Q., Oroudjev, E., Hansma, H., Golan, Y., Arad, S., et al. (2008). Adhesion and stable low friction provided by a subnanometer-thick monolayer of a natural polysaccharide. *Langmuir*, 24, 1534–1540.
- Gouveia, L., Coutinho, C., Mendonca, E., Batista, A. P., Sousa, I., Bandarra, N. M., et al. (2008). Functional biscuits with PUFA-omega 3 from *Isochrysis galbana*. *Journal of the Science of Food and Agriculture*, 88, 891–896.
- Grimsley, N., Thomas, R., Kegel, J., Jacquet, S., Moreau, H., & Desdevises, Y. (2012). Genomics of algal host-virus interactions. *Advances in Botanical Research*, 64, 343–378.
- Grobbelaar, J. (2010). Microalgal biomass production: challenges and realities. *Photosynthesis Research*, 106, 135–144.
- Guarnieri, M. T., Nag, A., Smolinski, S. L., Darzins, A., Seibert, M., & Pienkos, P. T. (2011). Examination of triacylglycerol biosynthetic pathways via de novo transcriptomic and proteomic analyses in an unsequenced microalga. *PLoS ONE*, 6, e25851. doi: 10.1371/journal.pone.0025851.
- Guschina, I. A., & Harwood, J. L. (2006). Lipids and lipid metabolism in eukaryotic algae. *Progress in Lipid Research*, 45, 160–186.
- Habib, M. A. B., Huntington, T., & Hasan, M. R. (2008). A review on culture, production and use of *Spirulina* as food for humans and feeds for domestic animals and fish. *FAO Fisheries and Aquaculture Circular*. No. 1034.
- Hall, L. M., Taylor, K. B., & Jones, D. D. (1993). Expression of a foreign gene in *Chlamydomonas reinhardtii*. *Gene*, 124, 75–81.
- Hallmann, A., Amon, P., Godl, K., Heitzer, M., & Sumper, M. (2007). Algal transgenics and biotechnology. *Transgenic Plant Journal*, 1, 81–98.
- Harada, H., & Matsuda, Y. (2005). Promoter analysis of two CO<sub>2</sub>-inducible carbonic anhydrases in the marine diatom *Phaeodactylum tricorutum*. *Plant and Cell Physiology*, 46, 88–89.
- Hawkins, R. L., & Nakamura, M. (1999). Expression of human growth hormone by the eukaryotic alga, *Chlorella*. *Current Microbiology*, 38, 335–341.
- He, D. M., Qian, K. X., Shen, G. F., Zhang, Z. F., Li, Y. N., Su, Z. L., et al. (2007). Recombination and expression of classical swine fever virus (CSFV) structural protein E2 gene in *Chlamydomonas reinhardtii* chloroplasts. *Colloids and Surfaces B-Biointerfaces*, 55, 26–30.
- Hempel, F., Bozarth, A. S., Lindenkamp, N., Klingl, A., Zauner, S., Linne, U., et al. (2011). Microalgae as bioreactors for bioplastic production. *Microbial Cell Factories*. doi: 10.1186/1475-2859-10-81.

- Hempel, F., Lau, J., Klingl, A., & Maier, U. G. (2011). Algae as protein factories: expression of a human antibody and the respective antigen in the diatom *Phaeodactylum tricorutum*. *PLoS ONE*, *6*, e28424. doi: 10.1371/journal.pone.0028424.
- Hermesmeier, D., Schulz, R., & Senger, H. (1994). Formation of light-harvesting complexes of photosystem II in *Scenedesmus*. 1. Correlations between amounts of photosynthetic pigments, Lhc messenger RNAs and LHC apoproteins during constitutional dark- and light-dependent Lhc-gene expression. *Planta*, *193*, 398–405.
- Hirakawa, Y., Kofuji, R., & Ishida, K. (2008). Transient transformation of a chlorarachniophyte alga, *Lotharella amoebiformis* (Chlorarachniophyceae), with uidA and egfp reporter genes. *Journal of Phycology*, *44*, 814–820.
- Hu, Q., Sommerfeld, M., Jarvis, E., Ghirardi, M., Posewitz, M., Seibert, M., et al. (2008). Microalgal triacylglycerols as feedstocks for biofuel production: perspectives and advances. *Plant Journal*, *54*, 621–639.
- Huheihel, M., Ishanu, V., Tal, J., & Arad, S. (2002). Activity of *Porphyridium* sp polysaccharide against herpes simplex viruses in vitro and in vivo. *Journal of Biochemical and Biophysical Methods*, *50*, 189–200.
- Iomini, C., Till, J. E., & Dutcher, S. K. (2009). *Cilia: Model organisms and intraflagellar transport*. *Methods in cell biology*, Vol. 93. Academic Press. p. 121.
- Janssen, M., Tramper, J., Mur, L. R., & Wijffels, R. H. (2003). Enclosed outdoor photobioreactors: light regime, photosynthetic efficiency, scale-up, and future prospects. *Biotechnology and Bioengineering*, *81*, 193–210.
- Jarvis, E. E., & Brown, L. M. (1991). Transient expression of firefly luciferase in protoplasts of the green alga *Chlorella ellipsoidea*. *Current Genetics*, *19*, 317–321.
- Karsenti, E., Acinas, S. G., Bork, P., Bowler, C., De Vargas, C., Raes, J., et al. (2011). A holistic approach to marine eco-systems biology. *PLoS Biology*, *9*, e1001177. doi: 10.1371/journal.pbio.1001177.
- Kathiresan, S., Chandrashekar, A., Ravishankar, G. A., & Sarada, R. (2009). *Agrobacterium*-mediated transformation in the green alga *Haematococcus pluvialis* (Chlorophyceae, Volvocales). *Journal of Phycology*, *45*, 642–649.
- Kato, T., Kolenic, N., & Pardini, R. S. (2007). Docosahexaenoic acid (DHA), a primary tumor suppressive omega-3 fatty acid, inhibits growth of colorectal cancer independent of p53 mutational status. *Nutrition and Cancer*, *58*, 178–187.
- Katz, A., Waridel, P., Shevchenko, A., & Pick, U. (2007). Salt-induced changes in the plasma membrane proteome of the halotolerant alga *Dunaliella salina* as revealed by blue native gel electrophoresis and nano-LC-MS/MS analysis. *Molecular and Cellular Proteomics*, *6*, 1459–1472.
- Khozin-Goldberg, I., & Cohen, Z. (2011). Unraveling algal lipid metabolism: recent advances in gene identification. *Biochimie*, *93*, 91–100.
- Kilian, O., Benemann, C., Niyogi, K., & Vick, B. (2011). High-efficiency homologous recombination in the oil-producing alga *Nannochloropsis* sp. *Proceedings of the National Academy of Sciences of the United States of America*, *108*, 21265–21269.
- Kim, D. H., Kim, Y. T., Cho, J. J., Bae, J. H., Hur, S. B., Hwang, I., et al. (2002). Stable integration and functional expression of flounder growth hormone gene in transformed microalga, *Chlorella ellipsoidea*. *Marine Biotechnology*, *4*, 63–73.
- Kim, J., Lee, W., Kim, B., & Lee, C. (2006). Proteomic analysis of protein expression patterns associated with astaxanthin accumulation by green alga *Haematococcus pluvialis* (Chlorophyceae) under high light stress. *Journal of Microbiology and Biotechnology*, *16*, 1222–1228.
- Ko, K., Tekoah, Y., Rudd, P. M., Harvey, D. J., Dwek, R. A., Spitsin, S., et al. (2003). Function and glycosylation of plant-derived antiviral monoclonal antibody. *Proceedings of the National Academy of Sciences of the United States of America*, *100*, 8013–8018.

- Kovar, J. L., Zhang, J., Funke, R. P., & Weeks, D. P. (2002). Molecular analysis of the acetolactate synthase gene of *Chlamydomonas reinhardtii* and development of a genetically engineered gene as a dominant selectable marker for genetic transformation. *Plant Journal*, *29*, 109–117.
- Kozminski, K. G., Diener, D. R., & Rosenbaum, J. L. (1993). High-level expression of nonacetylatable alpha-tubulin in *Chlamydomonas reinhardtii*. *Cell Motility and the Cytoskeleton*, *25*, 158–170.
- Kumar, S., Misquitta, R., Reddy, V., Rao, B., & Rajam, M. (2004). Genetic transformation of the green alga—*Chlamydomonas reinhardtii* by *Agrobacterium tumefaciens*. *Plant Science*, *166*, 731–738.
- Lapidot, M., Raveh, D., Sivan, A., Arad, S., & Sapira, M. (2002). Stable chloroplaste transformation of the unicellular red alga *Porphyridium* species. *Plant Physiology*, *129*, 7–12.
- Lerche, K., & Hallmann, A. (2009). Stable nuclear transformation of *Gonium pectorale*. *BMC Biotechnology*, *9*. doi: 10.1186/1472-6750-9-64.
- Levy-Ontman, O., Arad, S. M., Harvey, D. J., Parsons, T. B., Fairbanks, A., & Tekoah, Y. (2011). Unique N-glycan moieties of the 66-kDa cell wall glycoprotein from the red microalga *Porphyridium* sp. *Journal of Biological Chemistry*, *286*, 21340–21352.
- Li, H., Xue, L., Yana, H., Wang, L., Liu, L., Lu, Y., et al. (2007). The nitrate reductase gene-switch: a system for regulated expression in transformed cells of *Dunaliella salina*. *Gene*, *403*, 132–142.
- Li, J., Xue, L. X., Yan, H. X., Liu, H. T., & Liang, J. Y. (2008). Inducible EGFP expression under the control of the nitrate reductase gene promoter in transgenic *Dunaliella salina*. *Journal of Applied Phycology*, *20*, 137–145.
- Li, S. S., & Tsai, H. J. (2008). Transgenic microalgae as a non-antibiotic bactericide producer to defend against bacterial pathogen infection in the fish digestive tract. *Fish and Shellfish Immunology*, *26*, 316–325.
- Li, Y., Han, D., Hu, G., Sommerfeld, M., & Hu, Q. (2010). Inhibition of starch synthesis results in overproduction of lipids in *Chlamydomonas reinhardtii*. *Biotechnology and Bioengineering*, *107*, 258–268.
- Li, Y. T., Han, D. X., Hu, G. R., Dauvillee, D., Sommerfeld, M., Ball, S., et al. (2010). *Chlamydomonas* starchless mutant defective in ADP-glucose pyrophosphorylase hyperaccumulates triacylglycerol. *Metabolic Engineering*, *12*, 387–391.
- Liska, A. J. (2004). Enhanced photosynthesis and redox energy production contribute to salinity tolerance in *Dunaliella* as revealed by homology-based proteomics. *Plant Physiology*, *136*, 2806–2817.
- Llomas, A., Igeno, M. I., Galvan, A., & Fernandez, E. (2002). Nitrate signalling on the nitrate reductase gene promoter depends directly on the activity of the nitrate transport systems in *Chlamydomonas*. *Plant Journal*, *30*, 261–271.
- Lohr, M., Schwender, J., & Polle, J. E. W. (2012). Isoprenoid biosynthesis in eukaryotic phototrophs: a spotlight on algae. *Plant Science*, *185*, 9–22.
- Lopez, D., Casero, D., Cokus, S., Merchant, S., & Pellegrini, M. (2011). Algal functional annotation tool: a web-based analysis suite to functionally interpret large gene lists using integrated annotation and expression data. *BMC Bioinformatics*, *12*. doi: 10.1186/1471-2105-12-282.
- Lorenz, R. T., & Cysewski, G. R. (2000). Commercial potential for *Haematococcus* microalgae as a natural source of astaxanthin. *Trends in Biotechnology*, *18*, 160–167.
- Lumbreras, V., & Purton, S. (1998). Recent advances in *Chlamydomonas* transgenics. *Protist*, *149*, 23–27.
- Maheswari, U., Mock, T., Armbrust, E. V., & Bowler, C. (2009). Update of the diatom EST database: a new tool for digital transcriptomics. *Nucleic Acids Research*, *37*, 1001–1005.

- Manuell, A. L., Beligni, M. V., Elder, J. H., Siefker, D. T., Tran, M., Weber, A., et al. (2007). Robust expression of a bioactive mammalian protein in *Chlamydomonas* chloroplast. *Plant Biotechnology Journal*, *5*, 402–412.
- Marin-Navarro, J., Manuell, A. L., Wu, J., & Mayfield, S. P. (2007). Chloroplast translation regulation. *Photosynthesis Research*, *94*, 359–374.
- Matsui, M. S., Muizzuddin, N., Arad, S., & Marenus, K. (2003). Sulfated polysaccharides from red microalgae have antiinflammatory properties in vitro and in vivo. *Applied Biochemistry and Biotechnology*, *104*, 13–22.
- Matsuo, T., & Ishiura, M. (2011). *Chlamydomonas reinhardtii* as a new model system for studying the molecular basis of the circadian clock. *FEBS Letters*, *585*, 1495–1502.
- Mayali, X., & Azam, F. (2004). Algicidal bacteria in the sea and their impact on algal blooms. *The Journal of Eukaryotic Microbiology*, *51*, 139–144.
- Mayfield, S. P., Franklin, S. E., & Lerner, R. A. (2003). Expression and assembly of a fully active antibody in algae. *Proceedings of the National Academy of Sciences of the United States of America*, *100*, 438–442.
- Mayfield, S., & Schultz, J. (2004). Development of a luciferase reporter gene, luxCt, for *Chlamydomonas reinhardtii* chloroplast. *Plant Journal*, *37*, 449–458.
- Mayfield, S. P., & Franklin, S. E. (2005). Expression of human antibodies in eukaryotic micro-algae. *Vaccine*, *23*, 1828–1832.
- Meireles, L., Guedes, A. C., & Malcata, F. X. (2003). Increase of the yields of eicosapentaenoic and docosahexaenoic acids by the microalga *Pavlova lutheri* following random mutagenesis. *Biotechnology and Bioengineering*, *81*, 50–55.
- Mendoza, H., de la Jara, A., Freijanes, K., Carmona, L., Ramos, A. A., de Sousa Duarte, V., et al. (2008). Characterization of *Dunaliella salina* strains by flow cytometry: a new approach to select carotenoid hyperproducing strains. *Electron Journal of Biotechnology*, *11*, 1–13.
- Merchant, S. S., Prochnik, S. E., Vallon, O., Harris, E. H., Karpowicz, S. J., Witman, G. B., et al. (2007). The *Chlamydomonas reinhardtii* genome reveals the evolution of key animal and plant functions. *Science*, *318*, 245–250.
- Merchant, S. S., Kropat, J., Liu, B., Shaw, J., & Warakanont, J. (2011). TAG, You're it! *Chlamydomonas* as a reference organism for understanding algal triacylglycerol accumulation. *Current Opinion in Biotechnology*. doi: 10.1016/j.copbio.2011.12.001.
- Miller, R., Wu, G. X., Deshpande, R. R., Vieler, A., Gartner, K., Li, X. B., et al. (2010). Changes in transcript abundance in *Chlamydomonas reinhardtii* following nitrogen deprivation predict diversion of metabolism. *Plant Physiology*, *154*, 1737–1752.
- Minoda, A., Sakagami, R., Yagisawa, F., Kuroiwa, T., & Tanaka, K. (2004). Improvement of culture conditions and evidence for nuclear transformation by homologous recombination in a red alga, *Cyanidioschyzon merolae* 10D. *Plant and Cell Physiology*, *45*, 667–671.
- Mitra, A., Higgins, D. W., & Rohe, N. J. (1994). A *Chlorella* virus gene promoter functions as a strong promoter both in plants and bacteria. *Biochemical and Biophysical Research Communications*, *204*, 187–194.
- Miyagawa, A., Okami, T., Kira, N., Yamaguchi, H., Ohnishi, K., & Adachi, M. (2009). Research note: high efficiency transformation of the diatom *Phaeodactylum tricornutum* with a promoter from the diatom *Cylindrotheca fusiformis*. *Phycological Research*, *57*, 142–146.
- Miyagawa-Yamaguchi, A., Okami, T., Kira, N., Yamaguchi, H., Ohnishi, K., & Adachi, M. (2011). Stable nuclear transformation of the diatom *Chaetoceros* sp. *Phycological Research*, *59*, 113–119.
- Mock, T., & Medlin, L. K. (2012). Genomics and genetics of diatoms. *Advances in Botanical Research*, *64*, 245–289.

- Moellering, E. R., Miller, R., & Benning, C. (2009). Molecular genetics of lipid metabolism in the model green alga *Chlamydomonas reinhardtii*. In H. Wada, & N. Murata (Eds.), *Advances in photosynthesis and respiration. Lipids in photosynthesis: Essential and regulatory functions* (pp. 139–155). Springer.
- Moellering, E. R., & Benning, C. (2010). RNA interference silencing of a major lipid droplet protein affects lipid droplet size in *Chlamydomonas reinhardtii*. *Eukaryotic Cell*, *9*, 97–106.
- Molina Grima, E., Sanchez Perez, J. A., Garcia Camacho, F., Medina, A. R., Gimenez, A. G., & Alonso, D. L. (1995). The production of polyunsaturated fatty acids by microalgae: from strain selection to product purification. *Process Biochemistry*, *30*, 711–719.
- Morin, P. J. (2008). Sex as an algal antiviral strategy. *Proceedings of the National Academy of Sciences of the United States of America*, *105*, 15639–15640.
- Muhlhaus, T., Weiss, J., Hemme, D., Sommer, F., & Schroda, M. (2011). Quantitative shotgun proteomics using a uniform <sup>15</sup>N-labeled standard to monitor proteome dynamics in time course experiments reveals new insights into the heat stress response of *Chlamydomonas reinhardtii*. *Molecular and Cellular Proteomics*, *10*. doi: 10.1074/mcp.M110.004739.
- Nagasaki, K. (2008). Dinoflagellates, diatoms, and their viruses. *Journal of Microbiology*, *46*, 235–243.
- Nelson, J., & Lefebvre, P. (1995). Targeted disruption of the NIT8 gene in *Chlamydomonas reinhardtii*. *Molecular and Cellular Biology*, *15*, 5762–5769.
- Neupert, J., Karcher, D., & Bock, R. (2009). Generation of *Chlamydomonas* strains that efficiently express nuclear transgenes. *Plant Journal*, *57*, 1140–1150.
- Nguyen, P., Falcone, D. L., & Graves, M. V. (2009). The A312L 5'-UTR of *Chlorella* virus PBCV-1 is a translational enhancer in *Arabidopsis thaliana*. *Virus Research*, *140*, 138–146.
- Nissimov, J. I., Worthy, C. A., Rooks, P., Napier, J. A., Kimmance, S. A., Henn, M. R., et al. (2011). Draft genome sequence of the coccolithovirus *Emiliania huxleyi* virus 203. *Journal of Virology*, *85*, 13468–13469.
- Niu, Y. F., Zhang, M. H., Xie, W. H., Li, J. N., Gao, Y. F., Yang, W. D., et al. (2011). A new inducible expression system in a transformed green alga, *Chlorella vulgaris*. *Genetic Molecular Research*, *10*(4), 3427–3434.
- Norsker, N. H., Barbosa, M. J., Vermue, M. H., & Wijffels, R. H. (2011). Microalgal production: a close look at the economics. *Biotechnology Advances*, *29*, 24–27.
- Norton, T. A., Melkonian, M., & Andersen, R. A. (1996). Algal biodiversity. *Phycologia*, *35*, 308–326.
- Not, F., Siano, R., Kooistra, W. H. C. F., Simon, N., Vaulot, D., & Probert, I. (2012). Diversity and ecology of eukaryotic marine phytoplankton. *Advances in Botanical Research*, *64*, 1–53.
- Ohnuma, M., Yokoyama, T., Inouye, T., Sekine, Y., & Tanaka, K. (2008). Polyethylene glycol (PEG)-mediated transient gene expression in a red alga, *Cyanidioschyzon merolae* 10D. *Plant and Cell Physiology*, *49*, 117–120.
- Ohnuma, M., Misumi, O., Fujiwara, T., Watanabe, S., Tanaka, K., & Kuroiwa, T. (2009). Transient gene suppression in a red alga, *Cyanidioschyzon merolae* 10D. *Protoplasma*, *236*, 107–112.
- Ohresser, M., Matagne, R. F., & Loppes, R. (1997). Expression of the arylsulphatase reporter gene under the control of the nit1 promoter in *Chlamydomonas reinhardtii*. *Current Genetics*, *31*, 264–271.
- Pan, K., Qin, J. J., Li, S., Dai, W. K., Zhu, B. H., Jin, Y. C., et al. (2011). Nuclear monoploidy and asexual propagation of *Nannochloropsis oceanica* (Eustigmatophyceae) as revealed by its genome sequence. *Journal of Phycology*, *47*, 1425–1432.

- Peled, E., Leu, S., Zarka, A., Weiss, M., Pick, U., Khozin-Goldberg, I., et al. (2011). Isolation of a novel oil globule protein from the green alga *Haematococcus pluvialis* (Chlorophyceae). *Lipids*, *46*, 851–861.
- Petrucelli, S., Otegui, M. S., Lareu, F., Dinh, O. T., Fitchette, A. C., Circosta, A., et al. (2006). A KDEL-tagged monoclonal antibody is efficiently retained in the endoplasmic reticulum in leaves, but is both partially secreted and sorted to protein storage vacuoles in seeds. *Plant Biotechnology Journal*, *4*, 511–527.
- Potvin, G., & Zhang, Z. (2010). Strategies for high-level recombinant protein expression in transgenic microalgae: a review. *Biotechnology Advances*, *28*, 910–918.
- Poulsen, N., & Kroger, N. (2005). A new molecular tool for transgenic diatoms: control of mRNA and protein biosynthesis by an inducible promoter-terminator cassette. *FEBS Journal*, *272*, 3413–3423.
- Poulsen, N., Chesley, P., & Kroger, N. (2006). Molecular genetic manipulation of the diatom *Thalassiosira pseudonana* (Bacillariophyceae). *Journal of Phycology*, *42*, 1059–1065.
- Quinn, J. M., & Merchant, S. (1995). 2 Copper-responsive elements associated with the *Chlamydomonas* Cyc6 gene-function as targets for transcriptional activators. *The Plant Cell*, *7*, 623–638.
- Radakovits, R., Jinkerson, R. E., Darzins, A., & Posewitz, M. C. (2010). Genetic engineering of algae for enhanced biofuel production. *Eukaryotic Cell*, *9*, 486–501.
- Ramazanov, A., & Ramazanov, Z. (2006). Isolation and characterization of a starchless mutant of *Chlorella pyrenoidosa* STL-PI with a high growth rate, and high protein and polyunsaturated fatty acid content. *Phycological Research*, *54*, 255–259.
- Rasala, B. A., Muto, M., Lee, P. A., Jager, M., Cardoso, R. M. F., Behnke, C. A., et al. (2010). Production of therapeutic proteins in algae, analysis of expression of seven human proteins in the chloroplast of *Chlamydomonas reinhardtii*. *Plant Biotechnology Journal*, *8*, 719–733.
- Rasala, B. A., & Mayfield, S. (2011). The microalgae *Chlamydomonas reinhardtii* as a platform for the production of human protein therapeutics. *Bioengineered bugs*, *2*, 50–54.
- Rasala, B. A., Muto, M., Sullivan, J., & Mayfield, S. P. (2011). Improved heterologous protein expression in the chloroplast of *Chlamydomonas reinhardtii* through promoter and 5' untranslated region optimization. *Plant Biotechnology Journal*, *9*, 674–683.
- Raven, J. A., & Falkowski, P. G. (1999). Oceanic sinks for atmospheric CO<sub>2</sub>. *Plant, Cell and Environment*, *22*, 741–755.
- Rismani-Yazdi, H., Haznedaroglu, B. Z., Bibby, K., & Peccia, J. (2011). Transcriptome sequencing and annotation of the microalgae *Dunaliella tertiolecta*: pathway description and gene discovery for production of next-generation biofuels. *BMC Genomics*, *12*. doi: 10.1186/1471-2164-12-148.
- Rolland, N., Atteia, A., Decottignies, P., Garin, J., Hippler, M., Kreimer, G., et al. (2009). *Chlamydomonas* proteomics. *Current Opinion in Microbiology*, *12*, 285–291.
- Rouxel, C., Bougaran, G., Doulin-Grouas, S., Dubois, N., & Cadoret, J.-P. (2011). Novel *Isochrysis* sp tahitian clone and uses therefore. EP 11006712.1., EU.
- Sakaue, K., Harada, H., & Matsuda, Y. (2008). Development of gene expression system in a marine diatom using viral promoters of a wide variety of origin. *Physiologia Plantarum*, *133*, 59–67.
- Sasso, S., Pohnert, G., Lohr, M., Mittag, M., & Hertweck, C. (2011). Microalgae in the postgenomic era: a blooming reservoir for new natural products. *FEMS Microbiology*. doi: 10.1111/j.1574-6976.2011.00304.
- Sastre, R. R., & Posten, C. (2010). The variety of microalgae applications as a renewable resource. *Chemie Ingenieur Technik*, *82*, 1925–1939.
- Schiedlmeier, B., Schmitt, R., Muller, W., Kirk, M. M., Gruber, H., Mages, W., et al. (1994). Nuclear transformation of *Volvox-carteri*. *Proceedings of the National Academy of Sciences of the United States of America*, *91*, 5080–5084.

- Schmidt, F. R. (2004). Recombinant expression systems in the pharmaceutical industry. *Microbiology and Biotechnology*, 65, 363–372.
- Schroda, M., Blocker, D., & Beck, C. F. (2000). The HSP70A promoter as a tool for the improved expression of transgenes in *Chlamydomonas*. *Plant Journal*, 21, 121–131.
- Schroeder, D. C., Oke, J., Malin, G., & Wilson, W. H. (2002). Coccolithovirus (Phycodnaviridae): characterisation of a new large dsDNA algal virus that infects *Emiliania huxleyi*. *Archives of Virology*, 147, 1685–1698.
- Sekar, S., & Chandramohan, M. (2008). Phycobiliproteins as a commodity: trends in applied research, patents and commercialization. *Journal of Applied Phycology*, 20, 113–136.
- Shaish, A., Ben-Amotz, A., & Avron, M. (1991). Production and selection of high beta-carotene mutants of *Dunaliella bardawil* (Chlorophyta). *Journal of Phycology*, 27, 652–656.
- Sheehan, J., Dunahay, T., Benemann, J., & Roessler, P. (1998). A look back at the U.S. Department of Energy's Aquatic Species program: Biodiesel from algae. In "US Report NREL/TP-580-24190" (p. 323). Golden, USA: US Dpt of Energy.
- Siaut, M., Heijde, M., Mangogna, M., Montsant, A., Coesel, S., Allen, A., Manfredonia, A., Falciatore, A., & Bowler, C. (2007). Molecular toolbox for studying diatom biology in *Phaeodactylum tricornutum*. *Gene*, 406, 23–35.
- Siaut, M., Cuiné, S., Cagnon, C., Fessler, B., Nguyen, M., Carrier, P., et al. (2011). Oil accumulation in the model green alga *Chlamydomonas reinhardtii*: characterization, variability between common laboratory strains and relationship with starch reserves. *BMC Biotechnology*, 11. doi: 10.1186/1472-6750-11-7.
- Sizova, I., Fuhrmann, M., & Hegemann, P. (2001). A *Streptomyces rimosus* aphVIII gene coding for a new type phosphotransferase provides stable antibiotic resistance to *Chlamydomonas reinhardtii*. *Gene*, 277, 221–229.
- Specht, E., Miyake-Stoner, S., & Mayfield, S. (2010). Micro-algae come of age as a platform for recombinant protein production. *Biotechnology Letters*, 32, 1373–1383.
- Spolaore, P., Joannis-Cassan, C., Duran, E., & Isambert, A. (2006). Commercial applications of microalgae. *Journal of Bioscience and Bioengineering*, 101, 87–96.
- Steinbrenner, J., & Sandmann, G. (2006). Transformation of the green alga *Haematococcus pluvialis* with a phytoene desaturase for accelerated astaxanthin biosynthesis. *Applied and Environmental Microbiology*, 72, 7477–7484.
- Stevens, D. R., Rochaix, J. D., & Purton, S. (1996). The bacterial phleomycin resistance gene ble as a dominant selectable marker in *Chlamydomonas*. *Molecular & General Genetics*, 251, 23–30.
- Sun, M., Qian, K. X., Su, N., Chang, H. Y., Liu, J. X., & Chen, G. F. (2003). Foot-and-mouth disease virus VP1 protein fused with cholera toxin B subunit expressed in *Chlamydomonas reinhardtii* chloroplast. *Biotechnology Letters*, 25, 1087–1092.
- Sun, Y., Yang, Z. Y., Gao, X. S., Li, Q. Y., Zhang, Q. Q., & Xu, Z. K. (2005). Expression of foreign genes in *Dunaliella* by electroporation. *Molecular Biotechnology*, 30, 185–192.
- Surzycki, R., Greenham, K., Kitayama, K., Dibal, F., Wagner, R., Rochaix, J.-D., et al. (2009). Factors effecting expression of vaccines in microalgae. *Biologicals*, 37, 133–138.
- Tan, C., Qin, S., Zhang, Q., Jiang, P., & Zhao, F. (2005). Establishment of a micro-particle bombardment transformation system for *Dunaliella salina*. *Journal of Microbiology*, 43, 361–365.
- Tang, D., Qiao, S., & Wu, M. (1995). Insertion mutagenesis of *Chlamydomonas reinhardtii* by electroporation and heterologous DNA. *Biochemistry and Molecular Biology International*, 36, 1025–1035.
- Ten Lohuis, M. R., & Miller, D. J. (1998). Genetic transformation of dinoflagellates (*Amphidinium* and *Symbiodinium*): expression of GUS in microalgae using heterologous promoter constructs. *Plant Journal*, 13, 427–435.



- Teng, C., Qin, S., Liu, J., Yu, D., Liang, C., & Tseng, C. (2002). Transient expression of lacZ in bombarded unicellular green alga *Haematococcus pluvialis*. *Journal of Applied Phycology*, *14*, 495–500.
- Thomas, R., Grimsley, N., Escande, M. L., Subirana, L., Derelle, E., & Moreau, H. (2011). Acquisition and maintenance of resistance to viruses in eukaryotic phytoplankton populations. *Environmental Microbiology*, *13*, 1412–1420.
- Toulza, E., Blanc-Mathieu, R., Gourbiere, S., & Piganeau, G. (2012). Environmental genomics of microbial algae: power and challenges of metagenomics. *Advances in Botanical Research*, *64*, 379–423.
- Tran, N., Park, J., Hong, S., & Lee, C. (2009). Proteomics of proteins associated with astaxanthin accumulation in the green alga *Haematococcus lacustris* under the influence of sodium orthovanadate. *Biotechnology Letters*, *31*, 1917–1922.
- Tran, M., Zhou, B., Pettersson, P. L., Gonzalez, M. J., & Mayfield, S. P. (2009). Synthesis and assembly of a full-length human monoclonal antibody in algal chloroplasts. *Biotechnology and Bioengineering*, *104*, 663–673.
- Umen, J., & Olson, B. (2012). Genomics of volvocine algae. *Advances in Botanical Research*, *64*, 185–243.
- Van Etten, J. L., & Dunigan, D. D. (2012). Chloroviruses: not your everyday plant virus. *Trends in Plant Science*, *17*, 1–8.
- Villalobos, A., Ness, J. E., Gustafsson, C., Minshull, J., & Govindarajan, S. (2006). Gene designer: a synthetic biology tool for constructing artificial DNA segments. *BMC Bioinformatics*, *7*. doi: 10.1186/1472-2105-7-285.
- Von Dassow, P., Ogata, H., Probert, I., Wincker, P., Da Silva, C., Audic, S., et al. (2009). Transcriptome analysis of functional differentiation between haploid and diploid cells of *Emiliana huxleyi*, a globally significant photosynthetic calcifying cell. *Genome Biology*, *10*. doi: 10.1186/gb-2009-10-10-r114.
- Walker, T. L., Collet, C., & Purton, S. (2005). Algal transgenics in the genomic ERA. *Journal of Phycology*, *41*, 1077–1093.
- Wallis, J. G., & Browse, J. (2010). Lipid biochemists salute the genome. *Plant Journal*, *61*, 1092–1106.
- Wang, C. H., Wang, Y. Y., Su, Q., & Gao, X. R. (2007). Transient expression of the GUS gene in a unicellular marine green alga, *Chlorella* sp MACC/C95, via electroporation. *Biotechnology and Bioprocess Engineering*, *12*, 180–183.
- Wang, T. Y., Xue, L. X., Hou, W. H., Yang, B. S., Chai, Y. R., Ji, X. A., et al. (2007b). Increased expression of transgene in stably transformed cells of *Dunaliella salina* by matrix attachment regions. *Applied Microbiology and Biotechnology*, *76*, 651–657.
- Wang, X. F., Brandsma, M., Tremblay, R., Maxwell, D., Jevnikar, A. M., Huner, N., et al. (2008). A novel expression platform for the production of diabetes-associated auto-antigen human glutamic acid decarboxylase (hGAD65). *BMC Biotechnology*, *8*. doi: 10.1186/1472-6750-8-87.
- Wang, Z. T., Ullrich, N., Joo, S., Waffenschmidt, S., & Goodenough, U. (2009). Algal lipid bodies: stress induction, purification, and biochemical characterization in wild-type and starch-less *Chlamydomonas reinhardtii*. *Eukaryotic Cell*, *8*(12), 1856–1868.
- Watanabe, S., Ohnuma, M., Sato, J., Yoshikawa, H., & Tanaka, K. (2011). Utility of a GFP reporter system in the red alga *Cyanidioschyzon merolae*. *Journal of General and Applied Microbiology*, *57*, 69–72.
- Weber, A., Oesterhelt, C., Gross, W., Brautigam, A., Imboden, L., Krassovskaya, I., et al. (2004). EST-analysis of the thermo-acidophilic red microalga *Galdieria sulphuraria* reveals potential for lipid A biosynthesis and unveils the pathway of carbon export from rhodoplasts. *Plant Molecular Biology*, *55*, 17–32.
- Wijffels, R. H., Barbosa, M. J., & Eppink, M. H. M. (2010). Microalgae for the production of bulk chemicals and biofuels. *Biofuels, Bioproducts and Biorefining*, *4*, 287–295.

- Wilson, W. H., Van Etten, J. L., & Allen, M. J. (2009). The Phycodnaviridae: the story of how tiny giants rule the world. *Current topics in microbiology and immunology*, 328, 1–42.
- Winter, J. M., Behnken, S., & Hertweck, C. (2011). Genomics-inspired discovery of natural products. *Current Opinion in Chemical Biology*, 15, 22–31.
- Yamano, T., & Fukuzawa, H. (2009). Carbon-concentrating mechanism in a green alga, *Chlamydomonas reinhardtii*, revealed by transcriptome analyses. *Journal of Basic Microbiology*, 49, 42–51.
- Yang, Z. Q., Li, Y. N., Chen, F., Li, D., Zhang, Z. F., Liu, Y. X., et al. (2006). Expression of human soluble TRAIL in *Chlamydomonas reinhardtii* chloroplast. *Chinese Science Bulletin*, 51, 1703–1709.
- Yu, S., Liu, S., Li, C., & Zhou, Z. (2011). Submesoscale characteristics and transcription of a fatty acid elongase gene from a freshwater green microalgae, *Mymecia incisa* Reisigl. *Chinese Journal of Oceanology and Limnology*, 29, 87–95.
- Zaslavskaja, L., & Lippmeier, J. C. (2000). Transformation of the diatom *Phaeodactylum tricorutum* (Bacillariophyceae) with a variety of selectable marker and reporter genes. *Journal of Phycology*, 36, 379–386.
- Zhang, Y. K., Shen, G. F., & Ru, B. G. (2006). Survival of human metallothionein-2 transplastomic *Chlamydomonas reinhardtii* to ultraviolet B exposure. *Acta Biochimica Et Biophysica Sinica*, 38, 187–193.
- Zhao, R., Cao, Y., Xu, H., Lv, L., Qiao, D., & Cao, Y. (2011). Analysis of expressed sequence tags from the green alga *Dunaliella salina* (Chlorophyta). *Journal of Phycology*, 47, 1454–1460.

# Thèse de Doctorat

Matthieu GARNIER

Allocation du carbone et métabolisme azoté chez l'haptophyte  
*Tisochrysis lutea*.

Carbon allocation and nitrogen metabolism in the haptophyt  
*Tisochrysis lutea*.

## Résumé

L'objectif de cette thèse est d'identifier les mécanismes moléculaires impliqués dans la réponse à la limitation azotée et dans l'accumulation des lipides chez la microalgue haptophyte *Tisochrysis lutea*. La souche sauvage et une souche mutante hyper-lipidique ont été cultivées dans différentes conditions de nutrition azotée, et analysées par des approches de génomique fonctionnelle.

Quatre transporteurs d'azote à haute affinité (Nrt2) ont été identifiés et caractérisés pour comprendre les mécanismes impliqués dans l'absorption minérale chez cette espèce. Les transcriptomes des deux souches ont été séquencés et les protéines affectées par la carence azotée et différenciellement exprimées entre les deux souches ont été identifiées. Les résultats permettent d'identifier des fonctions régulées lors de la carence azotée et potentiellement impliquées dans l'accumulation des lipides de réserve. La réponse de chacune des deux souches à des fluctuations fines de limitation azotée a été étudiée. Les résultats d'analyses protéomiques haut débit suggèrent que la suraccumulation lipidique dans la souche mutante est la conséquence d'un métabolisme du carbone globalement impacté, ceci sous l'impulsion de mécanismes de signalisation encore mal définis. Deux protéines ont été étudiées plus spécifiquement car vraisemblablement impliquées dans la remobilisation du carbone et de l'azote issus des acides aminés lors de la limitation azotée.

L'ensemble de ce travail permet d'abonder les connaissances sur les haptophytes et de formuler des hypothèses sur les clés métaboliques impliquées dans la limitation azotée et l'allocation du carbone chez les microalgues.

## Mots clés

Microalgues ; métabolisme ; azote ; carbone ; lipides ; génomique fonctionnelle ; protéomique ; transcriptomique

## Abstract

The aim of this thesis is to improve knowledge on mechanisms involved in the response to nitrogen limitation and in lipid accumulation in the microalgae haptophyte *Tisochrysis lutea*. The wild type strain and a lipid accumulating mutant strain were grown under different nitrogen limitation and starvation and analyzed by functional genomics. Four genes of high-affinity nitrate/nitrite transporter (Nrt2) were identified and characterized to reveal the mechanisms involved in mineral absorption in this species. Transcriptomes of both strains were sequenced and proteins affected by nitrogen starvation and differentially expressed between the two strains were identified.

We so identified the functions regulated by nitrogen deficiency and potentially involved in the accumulation of storage lipids. The responses of both strains to thin variations of nitrogen limitation were studied. The results of high-throughput proteomic analyzes suggest that the lipid-accumulation in the mutant strain is the result of carbon metabolism impacted overall, this spurred on signaling mechanisms. Two proteins have been studied since probably involved in carbon and nitrogen remobilization from amino acids catabolism during nitrogen limitation.

This work increases knowledge on haptophytes, and brings assumptions on metabolic key involved in nitrogen limitation and carbon allocation in microalgae.

## Key Words

Microalgae; metabolism; nitrogen; carbon; lipids; functional genomics; proteomics; transcriptomics